The Dissertation Committee for Eric Patrick Koehler certifies that this is the approved version of the following dissertation:

Aggregates in Self-Consolidating Concrete

Committee:

David W. Fowler, Supervisor

John E. Breen

Kevin J. Folliard

Maria C.G. Juenger

Harovel G. Wheat

Aggregates in Self-Consolidating Concrete

by

Eric Patrick Koehler, B.S., M.S.

Dissertation

Presented to the Faculty of the Graduate School of

The University of Texas at Austin

in Partial Fulfillment

of the Requirements

for the Degree of

Doctor of Philosophy

The University of Texas at Austin

August 2007

Acknowledgements

Aggregates in Self-Consolidating Concrete

Publication No._____

Eric Patrick Koehler, Ph.D.

The University of Texas at Austin, 2007

Supervisor: David W. Fowler

Self-consolidating concrete (SCC) is an advanced type of concrete that can flow under its own mass without vibration, pass through intricate geometrical configurations, and resist segregation. SCC constituent materials and mixture proportions must be properly selected to achieve these flow properties. The effects of any changes in materials or mixture proportions on hardened concrete performance must be considered in evaluating SCC.

A research project was conducted to investigate the role of aggregates in SCC. The objectives of this research were to evaluate the effects of aggregate characteristics and mixture proportions on the workability and hardened properties of SCC, to identify favorable aggregate characteristics for SCC, and to develop guidelines for proportioning SCC with any set of aggregates.

The research indicated that although SCC can be proportioned with a wide range of aggregates, the selection of favorable aggregates can significantly enhance the economy and performance of SCC. The effects of aggregate grading; maximum size; shape, angularity, and texture; apparent clay content; and packing density were evaluated. The main effect of aggregates larger than approximately 75 μm was found to be on the minimum required paste volume for achieving SCC workability. It was found that dust-of fracture microfines, defined as mineral material finer than approximately 75 μm produced during the crushing of aggregates, could be an economical choice to comprise part of the paste volume.

Based on the results of this research, a mixture proportioning procedure for SCC was developed. The procedure is based on a consistent, rheology-based framework and was designed and written to be accessible and comprehensible for routine use. In the procedure, SCC is represented as a suspension of aggregates in paste. Aggregates are selected on the basis of grading, maximum size, and shape and angularity. The paste volume is set based on the aggregate characteristics in order to achieve workability requirements. The paste composition is established to achieve workability and hardened property requirements.

Table of Contents

Chapter 1: Introduction

Self-consolidating concrete (SCC) is an advanced type of concrete that can flow under its own mass without vibration, pass through intricate geometrical configurations, and resist segregation. The application of SCC has significant implications for the way concrete is specified, produced, and placed. The use of SCC can result in increased construction productivity, improved jobsite safety, and improved hardened properties; however, the material costs for SCC are generally higher than for conventionally placed concrete and the production of SCC may require greater technical expertise and quality control measures. The proper selection of constituents and mixture proportions for SCC is crucial to ensuring that the advantageous properties of SCC can be achieved economically. The effects of individual constituents and of changes in mixture proportions are often greater in SCC than in conventionally placed concrete. Well-established guidelines on the effects of constituent characteristics and mixture proportions on SCC performance are needed in order to design and control SCC more effectively. The research described in this dissertation focuses on the role of aggregates in SCC, including the effects of aggregates on the performance of SCC, the selection of optimal aggregates for SCC, and the proportioning of SCC with any set of aggregates. Although SCC can be proportioned with a wide range of aggregates, the selection of favorable aggregate characteristics can significantly enhance the economy and performance of SCC.

1.1 Background

SCC is defined, in large measure, by its workability. The three essential properties of SCC are its ability to flow under its own mass (filling ability), its ability to pass through congested reinforcement (passing ability), and its ability to resist segregation (segregation resistance). The American Concrete Institute defines SCC as a "highly flowable, non-segregating concrete that can spread into place, fill the formwork, and encapsulate the reinforcement without any mechanical consolidation." The Precast/Prestressed Concrete Institute (2003) defines SCC as "a highly workable concrete that can flow through densely reinforced or geometrically complex structural elements under its own weight and adequately fill voids without segregation or excessive bleeding without the need for vibration to consolidate it." Rheology, or the scientific study of the flow of matter, is commonly used to describe the

workability of SCC. (A full description of rheological properties is provided in Chapter 3 of this dissertation.)

The development of mixture proportions often requires more effort for SCC than for conventionally placed concrete. The exact choice of proportions depends on material availability and performance requirements. For instance, passing ability may be of little or no importance in some cases whereas segregation resistance is needed in all cases. SCC mixtures always include a high-range water-reducing admixture (HRWRA) to ensure concrete is able to flow under its own mass. In addition, the water-powder ratio is reduced or a viscosity modifying admixture (VMA) is used to ensure the concrete resists segregation. SCC mixture proportions, in comparison to conventionally placed concrete mixture proportions, typically exhibit some combination of higher paste volume, higher powder content, lower water-cementitious materials or water-powder ratio, finer combined aggregate grading, and smaller maximum aggregate size. Supplementary cementitious materials and mineral fillers are commonly utilized to decrease cost, improve workability, and improve hardened properties. Ozyildirim (2005) found that although SCC can often be made with local materials, shipping materials—even from long distances— may be cost effective for SCC. Proportioning methods for SCC have traditionally been classified into three general categories depending on the predominate change in mixture proportions. These categories include use of high powder content and low water-powder ratio (powder-type SCC); use of low powder content, high water-powder ratio and VMA (VMA-type SCC); and use of moderate powder content, moderate water-powder ratio, and moderate VMA (combination-type SCC).

SCC is highly sensitive to changes in material properties and proportions and, therefore, requires increased quality control. Further, the consequences of deviations in workability are more significant for SCC. For instance, a slight change in water content may have minimal effect on conventionally placed concrete but lead to severe segregation and rejected work in SCC.

The typical characteristics of SCC mixture proportions, which are necessary to ensure adequate fresh properties, can have significant consequences for hardened properties, including strength, stiffness, shrinkage, and durability. The same trends associated with conventionally placed concrete typically apply to SCC. The relatively low water-cementitious ratios, use of SCMs, and improved quality control measures can result in improved hardened properties. The

reduced coarse aggregate content and increased paste volume may result in changes such as increased shrinkage and heat of hydration and reduced modulus of elasticity and shear strength.

Although SCC is not right for every application, the technology required for SCC can be utilized to improve the properties of non-SCC mixtures (Szecsy 2005). Furthermore, with the difficulty of achieving compaction resolved, the availability of SCC can enable the development of new types of concrete systems with novel structural designs (Ouchi 1999; PCI 2003).

The advantages and disadvantages of SCC must be evaluated for each producer and application. In general, the advantages of SCC may include:

- Improved ability of concrete to flow into intricate spaces and between congested reinforcement.
- Improved form surface finish and reduced need to repair defects such as bug holes and honeycombing.
- Reduced construction costs due to reduced labor costs and reduced equipment purchase and maintenance costs.
- Increased construction speed due to fewer construction tasks.
- Faster unloading of ready mixed concrete trucks.
- Improved working conditions with fewer accidents due to elimination of vibrators.
- Improved durability and strength of the hardened concrete in some cases.
- Reduced noise generated by vibrators.

The disadvantages of SCC may include:

- Increased material costs, especially for admixtures and cementitious materials.
- Increased formwork costs due to possibly higher formwork pressures.
- Increased technical expertise required to develop and control mixtures.
- Increased variability in properties, especially workability.
- Increased quality control requirements.
- Reduced hardened properties—possibly including reduced modulus of elasticity and increased shrinkage—due to factors such as high paste volumes or low coarse aggregate contents.
- Delayed setting time in some cases due to the use of admixtures.
- Increased risk and uncertainty associated with the use of a new product.

3

It is generally accepted that SCC was originally developed in Japan in the 1980s in response to the lack of skilled labor and the need for improved durability. According to Ouchi (1999) the need for SCC was first identified by Okamura in 1986 and the first prototype was developed in 1988. Collepardi (2003), however, states that self-leveling concretes were studied as early as 1975 and used in commercial applications in Europe, the United States, and Asia in the 1980s. The use of SCC has gradually increased throughout the world since the 1980s, gaining particular momentum in the late 1990s. One of the first high profile applications of SCC was the Akashi Kaikyo bridge in Japan (Tanaka et al. 2003). Major international symposia on SCC were held in 1999, 2001, 2003, and 2005. Originally, the main application for SCC was in precast plants; however, the use of SCC in ready mixed concrete applications has grown.

1.2   Objectives

There three main objectives of the research described in this dissertation were to:

- Evaluate the effects of specific aggregate characteristics and mixture proportions on the workability and hardened properties of SCC.
- Identify favorable aggregate characteristics for SCC to assist in both the production and selection of aggregate for SCC.
- Develop guidelines for proportioning SCC for any set of aggregates.

Although aggregates comprise the majority of SCC volume, limited information is available on selecting aggregates for SCC. Much more information is available for selecting admixtures, cementitious materials, and mixture proportions. By improving the aggregate characteristics the economy, robustness, and performance of SCC can be enhanced significantly. In particular, this dissertation aims to answer the following questions:

- What are the effects of aggregate shape, angularity, texture and grading?
- What is the role of aggregate packing density?
- Can aggregate microfines be used effectively in SCC?
- What changes must be made to SCC mixture proportions when aggregate characteristics are changed?

Because SCC mixture proportioning is an engineering optimization problem that depends on the characteristics of all materials, the roles of both aggregates and other constituents in SCC are evaluated. The main focus of the research is for ready mixed concrete applications; however, the results are also applicable to precast concrete. The results of this research can be used not just by concrete producers, but also by aggregate producers to create improved aggregates for use in SCC.

1.3   Scope

To understand the behavior of SCC and to evaluate the role of aggregates, testing was conducted on paste, mortar, and concrete with a range of different materials. The paste measurements were conducted on a parallel plate rheometer at the National Institute of Standards and Technology (NIST). The purpose of the paste testing was to determine the effects of different cements, fly ashes, microfines, HRWRAs, and VMAs on rheological properties. Mortar measurements were conducted to evaluate the effects of fine aggregates, microfines, and mortar mixture proportions on workability and hardened properties. Concrete testing was conducted in two stages. In the first stage, the effects of fine aggregates, coarse aggregates, and microfines on workability and hardened properties were evaluated. In the second stage, the effects of mixture proportions and constituents other than aggregates on workability and hardened properties were evaluated. Based on this laboratory data, the behaviors of paste, mortar, and concrete were linked and specific guidelines for proportioning SCC were developed.

At the beginning of the research project in January 2005, many SCC workability test methods had been suggested in the literature; however, none had been standardized in the United States. Therefore, an analysis of available test methods was conducted to select the best test methods, to determine how each test should be performed, and to decipher the meaning of the test results.

Hardened property testing was performed to evaluate compressive strength, flexural strength, modulus of elasticity, drying shrinkage, chloride permeability, and abrasion resistance.

The materials used in the research were selected to represent a broad range of characteristics. In total, the materials used in the research included 12 fine aggregate, 7 coarse aggregates, 6 microfines, 4 fly ashes, 4 cements, 6 HRWRAs, and 2 VMAs.

This dissertation describes all aspects of this research, which was conducted as part of a Research Project 108 at the International Center for Aggregates Research (ICAR). In addition,

partial results from a separate research project conducted at the University of Texas at Austin are also included to support further the ICAR results (Koehler et al. 2007). This other project, TxDOT 0-5134, was sponsored by the Texas Department of Transportation and was focused on the early-age characteristics of SCC for precast, prestressed bridge girders in Texas. Chapters 2 through 5 present the literature review. The materials and material characterization techniques used in the research are described in Chapter 6. Target properties for SCC are defined and discussed in Chapter 7. The results of the paste and mortar testing are described in Chapters 8 and 9, respectively. The effects of aggregate characteristics on concrete properties are described in Chapter 10 and the effects of constituents other than aggregates are described in Chapter 11. Chapter 12 compares the results of the paste, mortar, and concrete test results. Guidelines for proportioning SCC mixtures based on aggregate characteristics are presented in Chapter 13. The evaluation of available workability test methods is presented in Chapter 14. Lastly, Chapter 15 summarizes the results of the entire research project and lists topics for further research.

Chapter 2: Materials for SCC Literature Review

Although SCC can be made with a wide range of materials, the proper selection of materials is essential to optimizing SCC. Compared to conventionally placed concrete, SCC is generally much more sensitive to changes in material properties. This chapter describes the characteristics of chemical admixtures, aggregates, cement, and supplementary cementitious materials needed for SCC production.

2.1 Chemical Admixtures

The key admixtures used to produce SCC are HRWRAs and, in some cases, VMAs. Other admixtures—including air-entraining admixtures and set-modifying admixtures—can also be used successfully in SCC.

2.1.1 High-Range Water Reducing Admixtures

SCC is most commonly produced with polycarboxylate-based HRWRAs, which represent an improvement over older sulfonate-based HRWRAs such as those based on naphthalene sulfonate formaldehyde condensate (NSFC) and melamine sulfonate formaldehyde condensate (MSFC). Although SCC can be made with NSFC-, MSFC-, and lignosulfonate-based HRWRAs (Lachemi et al 2003; Assaad, Khayat, and Meshab 2003a; Petersen and Reknes 2003), the introduction of polycarboxylate-based HRWRAs has facilitated the adoption of SCC (Bury and Christensen 2002). Compared to sulfonate-based HRWRAs, polycarboxylate-based HRWRAs require lower dosages, have a reduced effect on setting time, exhibit improved workability retention, and increase stability. In fact, polycarboxylate-based HRWRAs typically enable a 70 to 80% reduction in dosage compared to a typical NSFC- or MSFC-based HRWRAs, based on solids content as a percentage of cement mass (Jeknavorian et al. 2003).

Polycarboxylate-based HRWRAs differ from sulfonate-based HRWRAs in their structure and mode of action. Sulfonate-based HRWRAs consist of anionic polymers that adsorb onto cement particles and impart a negative charge, resulting in electrostatic repulsion. Polycarboxylate-based HRWRAs, by contrast, consist of flexible, comb-like polymers with a main polycarboxylic backbone and grafted polyethylene oxide side chains. The backbone, which includes ionic carboxylic or sulfonic groups, adsorbs onto a cement particle and the nonionic

side chains extend outward from the cement particle. The side chains physically separate cement particles, which is referred to as steric hindrance. Polycarboxylate-based HRWRAs may function by both electrostatic repulsion and steric hindrance (Bury and Christensen 2002; Yoshioka et al. 2002; Cyr and Mouret 2003; Li et al. 2005) or only by steric hindrance (Blask and Honert 2003; Li et al. 2005; Hanehara and Yamada 1999) depending on the structure of the polymer. The reduced significance of electrostatic repulsion is indicated by the less negative or near-zero zeta-potential measurements for cement pastes with polycarboxylate-based HRWRAs as compared to cement pastes with sulfonate-based HRWRAs (Blask and Honert 2003; Li et al. 2004; Collepardi 1998; Sakai, Yamada, and Ohta 2003). In fact, zeta-potential measurements are frequently insufficient to justify dispersion of cement particles by polycarboxylate-based HRWRAs on the basis of the DLVO theory for electrostatic repulsion (Sakai, Yamada, and Ohta 2004).

Compared to sulfonate-based HRWRAs, polycarboxylate-based HRWRAs generally produce rheological characteristics that are more favorable for the production of SCC. Polycarboxylate-based HRWRAs are able to reduce the yield stress to a greater degree than NSFC- and MSFC-based HRWRAs (Cyr and Mouret 2003). For a given decrease in yield stress, the reduction in plastic viscosity is less for polycarboxylate-based HRWRAs than for sulfonate-based HRWRAs (Golaszewski and Szwabowski 2004). Yamada et al. (2000) found that polycarboxylate-based HRWRAs reduce plastic viscosity at high water-cement ratios but result in only slight reductions in plastic viscosity at low water-cement ratios. Similarly, Golaszewski and Szwabowski (2004) found that differences in rheological performance between polycarboxylate-based and sulfonate-based HRWRAs were most pronounced at lower water-cement ratios. According to Hanehara and Yamada (1999), polycarboxylate-based HRWRAs begin to affect mortar mini-slump flow at lower dosages than NSFC-based HRWRAs; however, NSFC-based HRWRAs increase mortar mini-slump flow at a faster rate once they begin to have an effect. The relatively high plastic viscosities associated with polycarboxylate-based HRWRAs can make high-strength, low water-cement ratio concrete mixtures impractical (Sugamata, Sugiyama, and Ohta 2003; Golaszewski and Szwabowski 2004). As a consequence, Sugamata, Sugiyama, and Ohta (2003) developed a new polycarboxylate-based HRWRA that incorporated a new monomer in order to reduce plastic viscosity and thixotropy.

The unique structure of polycarboxylate-based HRWRAs contributes to their improved performance. Polycarboxylate-based HRWRAs can be designed at the molecular level for a

particular application by changing such characteristics as the length of the backbone, or the length, density, or type of the side chains (Bury and Christensen 2002; Schober and Mader 2003; Comparet et al. 2003; Sakai, Yamada, and Ohta 2003). These changes can affect water reduction, workability retention, setting time, and early strength development (Bury and Christensen 2002). As such, not all polycarboxylate-based HRWRAs are intended for SCC. Those intended for SCC typically provide a higher plastic viscosity for a similar slump flow and dosage (Berke et al. 2002). Velten et al. (2001) suggest blending multiple polycarboxylate-based polymers to create a single admixture that exhibits improved workability retention and reduced sensitivity to changes in cement characteristics.

Numerous studies have been published describing the development of polycarboxylate-based polymers to optimize water reduction, workability retention, setting time, and strength development. In general, water reduction can be increased by increasing the side chain length, reducing the side chain density, reducing the backbone length, or increasing the sulfonic group content (Yamada et al. 2000; Plank and Hirsch 2003; Sakai, Yamada, Ohta 2003; Schober and Mader 2003). In general, the workability retention for polycarboxylate-based HRWRAs is superior to that for sulfonate-based admixtures for two main reasons (Flatt and Houst 2001; Cerulli et al. 2003). First, the side chains of polycarboxylate-based polymers are active at longer distances away from the cement grain and are, therefore, not incorporated into hydration products as soon. Second, some polycarboxylate polymers can remain in aqueous solution and adsorb onto cement particles gradually over time as hydration progresses. Sakai, Yamada, and Ohta (2003) suggest that workability retention can be improved by increasing the side chain length while Schober and Mader (2003) and Yamada et al. (2000) suggest that workability retention can be increased by decreasing the side chain length. Schober and Mader (2003) suggest the improved workability retention for shorter side chains is due to the fact that shorter side chains require longer times to adsorb on cement surfaces. Sakai, Yamada, and Ohta (2003) further suggest that workability retention can be improved by reducing the backbone length or increasing the side chain density, while Yamada et al. (2000) found that reducing the backbone length had minimal effect on workability retention. Velten et al. (2001) found that reducing the ionic content of the backbone reduced the adsorption rate, allowing more polymer to remain in solution to be adsorbed at later times. The increase in setting time associated with HRWRAs can be decreased by increasing the side chain length, increasing the backbone length, or increasing the degree of polymerization in the backbone (Yamada et al. 2000). The improved strength gain

in polycarboxylate-based HRWRAs is the result of the hydrophilic side chains, which draw water to the cement particles, resulting in uniform hydration and rapid early strength gain (Jeknavorian et al. 2003).

The performance of polycarboxylate-based HRWRAs is strongly influenced by cement characteristics, including specific surface area, particle size distribution, sulfate type and content, C_3A content, alkali content, and the presence of grinding aids (Flatt and Houst 2001). Differences in performance of various cement-admixture combinations are typically more significant at lower water-cement ratios (Schober and Mader 2003). The action of polycarboxylate-based polymers added to concrete can be classified in one of three categories: the polymers may be consumed by intercalation, coprecipiation, or micellization, resulting in the formation of an organo-mineral phase; they may be adsorbed on cement particles; or they may remain dissolved in the aqueous phase (Flatt and Houst 2001). Because the performance of HRWRAs depends on the early-age reactions taking place in the first two hours, the initial reactivity of the cement is critical.

Cements with higher fineness and higher C_3A contents are more reactive and, therefore, require higher dosages (Sakai, Yamada, Ohta 2003; Yoshioka et al. 2002). Yoshioka et al. (2002) found that single synthetic phases of C_3A and C_4AF adsorbed significantly more superplasticizer than C_2S and C_3S; however, the ratio of superplasticizer adsorbed by C_3A to that adsorbed by C_3S was less for the two polycarboxylate-based admixtures considered than for the NSFC-based admixture. Plank and Hirsch (2003), however, found that the decrease in adsorption observed in cements with lower C_3A contents was more significant for the polycarboxylate-based admixtures than for the NSFC- or MSFC-based admixtures. It should be noted that other differences in the three cements tested by Plank and Hirsch (2003) could have contributed to the differences in performance. Although dispersion of cement particles generally increases with increasing HRWRA adsorption (Schober and Mader 2003), the preferential adsorption by C_3A necessitates a higher dosage for adsorption on other phases. Further, a portion of the HRWRA adsorbed on C_3A is consumed in early age hydration products (Schober and Madder 2003). It is also desirable to have some polycarboxylate-based polymer remaining in solution to provide dispersion over time (Burge 1999). Indeed, Schober and Mader (2003) found that cements with higher C_3A contents exhibited reduced workability retention unless the dosage was sufficiently high to provide polymer for delayed adsorption. The early hydration products such as ettringite increase specific surface area, requiring additional polycarboxylate-

based polymers to maintain dispersion (Schober and Madder 2003). Polycarboxylate-based polymers are not intercalated into ettringite, but can be intercalated into monosulfoaluminate, C-S-H, and possibly brucite-like phases (Flatt and Houst 2001; Plank and Hirsch 2003). Plank and Hirsch (2003) found that ettringite is the preferred phase for adsorption of NSFC-, MSFC-, and polycarboxylate-based polymers, but that calcium hydroxide and gypsum show no adsorption. Although the presence of HRWRAs does not affect the quantity of ettringite formed, the HRWRAs do reduce the size of the ettringite crystals formed, especially with sulfonate-based HRWRAs (Plank and Hirsch 2003). Cerulli et al. (2003) suggest that the rate of hydration and mechanical strength development are influenced by the difference in the morphological structures of the ettringite crystals.

The presence of sulfate ions in solution reduces the adsorption of polycarboxylate-based polymers because it is generally thought that sulfates compete with polycarboxylate-based polymers for adsorption on cement particles (Sakai, Yamada, Ohta 2003; Schober and Mader 2003). Whereas an optimum sulfate ion concentration exists for sulfonate-based HRWRAs, the sulfate ion concentration should be minimized for polycarboxylate-based HRWRAs (Flatt and Houst 2001; Yamada, Ogawa and Takahashi 2001). Comparet et al. (2003), however, found that the reduction in adsorption was not due to the increase in sulphate ion concentration but instead due to an increase in ionic strength, regardless of whether sodium sulphate or sodium chloride was used to change the ionic strength of a calcium carbonate model system. Ohno et al. (2001) state that the reduction in polycarboxylate performance may be due to an increase in sulphate ion concentration, an increase in ionic strength, or both. They point out that the ionic strength increases at lower water-cement ratios, which may further reduce cement dispersion. In evaluating the effects of sulfates, the source of sulfates should be considered. Sulfates are supplied by both alkali sulfates and calcium sulfates. The type of calcium sulfate matters, as hemihydrate supplies sulfate ions faster than gypsum (Sakai, Yamada, Ohta 2003). Schober and Mader (2003) suggest using low-alkali cements to reduce the availability of soluble sulfates. Hanehara and Yamada (1999) indicate that the content of alkali sulfates is responsible for the majority of the difference in performance between different cements and conclude that the presence of sulfate ions both reduce adsorption and reduce side chain length. Sakai, Yamada and Ohta (2003) suggest that changes in the performance of polycarboxylate-based polymers due to changes in sulfate ion concentration can be minimized most effectively by increasing the carboxylic group ratio in the backbone. As hydration progresses, the gradual decrease in sulfate

ion concentration allows any polycarboxylate-based polymer remaining in solution to be adsorbed on cement particles more readily, which helps to maintain or even increase workability (Sakai, Yamada and Ohta 2003). Yamada, Ogawa, and Takahashi (2001) suggest increasing the backbone length, side chain length, or carboxylic ratio to increase the resistance to changes in sulfate ion concentration and suggest blending polycarboxylate-based admixtures with different adsorbing abilities to ensure initial fluidity and long workability retention.

The performance of polycarboxylate-based HRWRAs is influenced by temperature. Yamada, Yanagisawa, and Hanehara (1999) found that at low temperatures, the initial fluidity was low but increased with time due to the slower increase in cement surface area, the high initial sulfate ion concentration and the faster decrease in sulfate ion concentration. At high temperatures, the fluidity decreased more rapidly because of the faster reaction rate for cement, which resulted in a faster increase in cement surface area and a slower reduction in sulfate ion concentration.

Polycarboxylate-based HRWRAs are less sensitive than sulfonate-based admixtures to the time of addition. Whereas the efficiency of sulfonate-based admixtures can be improved by delaying the addition of the admixture to the start of the dormant period, the time of addition has minimal effect for polycarboxylate-based admixtures (Blask and Honert 2003; Collepardi 1998; Golaszewski and Szwabowski 2004). Plank and Hirsch (2003) and Collepardi (1998) suggest that sulfonate-based admixtures have high adsorption rates during ettringite growth, resulting in the consumption of the admixture such that a lower concentration remains in solution for dispersion of C_3S and C_2S. Flatt and Houst (2001) suggest that sulfonate-based admixtures are consumed in the organo-mineral phase whereas the side chains in polycarboxylates extend beyond the organo-mineral phase.

Polycarboxylate-based HRWRAs are more sensitive than sulfonate-based HRWRA to the amount of mixing energy. Blask and Honer (2003) found that increasing the mixing energy dramatically reduced the shear resistance of cement pastes with polycarboxylate-based HRWRA but had only minimal effects on cement pastes with naphthalene sulfonate-based HRWRA. Takada and Walraven (2001) found that increasing the mixing energy for cement paste mixtures reduced plastic viscosity significantly but had no effect on yield stress. The difference was attributed to better dispersion of powder particles and to the generation of high air contents.

The presence of certain clays within aggregates can reduce the performance of polycarboxylate-based HRWRAs significantly. Jardine et al. (2002), Jeknavorian et al. (2003),

and Jardine et al. (2003) examined the use of polycarboxylate-based HRWRAs with aggregates containing swellable smectite clays. These clays expand when wetted by the mix water and adsorb polycarboxylate-based polymers, resulting in significantly higher dosage requirements and accelerated loss of workability. One solution to this problem was to change the mixing order so that the water, HRWRA, and part of the cement are mixed prior to the addition of the clay-bearing aggregate. This mixing procedure, however, was not considered practical. Another solution was to utilize a sacrificial agent that would adsorb and intercalate with clay minerals, would be compatible with other admixtures, and would not harm concrete properties. A suggested sacrificial agent was polyethylene glycol, although it was found that this agent did itself reduce workability. Third, a calcium salt such as calcium nitrate could be added prior to the addition of sand. A combination of these three methods could be used. An additional solution was to add a polyphosphate, which could be used independent of the order of addition.

2.1.2   Viscosity-Modifying Admixtures

Viscosity-modifying admixtures, also known as anti-washout admixtures, generally increase some or all of the following properties in concrete mixtures: yield stress, plastic viscosity, thixotropy, and degree of shear thinning. They can be used for SCC applications to improve segregation resistance, increase cohesion, reduce bleeding, allow the use of a wider range of materials such as gap-graded aggregates and manufactured sands, and mitigate the effects of variations in materials and proportions (Bury and Christensen 2002). They may be used as an alternative to increasing the powder content or reducing the water content of a concrete mixture. Berke et al. (2002) suggest that SCC should be produced without a VMA whenever possible, but that a VMA can be necessary in certain situations such as where aggregate moisture content cannot be controlled adequately or in mixtures with poorly graded aggregates or low powder content.

The VMAs used for SCC are typically water-soluble polymers; however, other materials such as precipitated silica can be used (Rols, Ambrose, and Pera 1999; Khayat and Ghezal 2003; Collepardi 2003). Water-soluble polymers for use as VMAs in concrete can be broadly classified as natural, semi-synthetic, and synthetic. Examples of each class are provided in Table 2.1. Common VMAs for concrete include cellulose derivatives—which contain nonionic cellulose ether with various substitutes in the ether—and welan gum—which is an anionic, high-

molecular weight, natural polysaccharide fermented under controlled conditions (Khayat 1998; Lachemi et al. 2004a; Lachemi et al. 2004b).

Table 2.1: Examples of Water-Soluble Polymers Used as VMA (Khayat 1998)

Natural	Semi-Synthetic	Synthetic

• starches
• guar gum
• locust bean gum
• alginates
• agar
• gum arabic
• welan gum
• xanthan gum
• rhamsan gum
• gellan gum
• plant protein
	• decomposed starch and its derivatives
	• cellulose-ether derivatives
	   o hydroxypropyl methyl cellulose (HPMC)
	   o hydroxyethyl cellulose (HEC)
	   o carboxy methyl cellulose (CMC)
	• electrolytes
	   o sodium alginate
	• propyleneglycol alginate
		• polymers based on ethylene
		   o polyethylene oxide
		   o polyacrylamide
		   o polyacrylate
		• polymers based on vinyl
		   o polyvinyl alcohol

VMAs based on water-soluble polymers typically affect the water phase of concrete. Khayat (1995) describes three modes of action by which VMAs function. First, the VMA polymers adsorb onto water molecules, which causes a portion of the water to become trapped and the polymers to expand. Second, the polymers themselves develop attractive forces and thereby block the motion of water. Third, the polymer chains intertwine at low shear rates but break apart at higher shear rates, resulting in shear-thinning behavior. This shear-thinning behavior is desirable because the high apparent viscosity at low shear rates ensures static stability while the lower apparent viscosity at high shear rates results in less energy needed for processes such as mixing, conveying, and consolidating. Bury and Christensen (2002) divide VMAs into two categories: thickening-type and binding-type. Thickening-type VMAs increase viscosity by thickening the concrete but do not significantly increase HRWRA demand. Binding-type VMAs, which are more potent than thickening-types, bind water and result in thixotropic properties and reduced bleeding.

The improvements in concrete properties when VMAs are used are mainly due to increases in viscosity and degree of shear thinning. The increase in yield stress typically must be offset with additional water or HRWRA. For example, the anionic nature of natural polymers may cause them to adsorb onto cement particles, thereby requiring additional HRWRA (Phyffereon et al. 2002). Even with this increase in HRWRA dosage, water content, or both, the concrete will still exhibit increased viscosity and a greater degree of shear thinning. The higher viscosity and greater degree of shear thinning can increase segregation resistance. Bleeding is

reduced due to the increase in viscosity and the reduction in free water. This reduction in bleeding, however, can increase the susceptibility to plastic shrinkage cracking (Khayat 1999). Top bar effect, or the reduction in bond between concrete and reinforcing bars higher in a structural element, is reduced due to the reduction in bleeding, segregation, and surface settlement (Khayat 1998).

Welan gum, one of the most common types of VMA, has been shown to increase yield stress, viscosity, and the degree of shear thinning (Khayat and Yahia 1997) while also mitigating the effects of changes in water content (Berke et al. 2002; Sakata, Maruyama, and Minami 1996). Whereas cellulose derivatives are incompatible with naphthalene-based HRWRAs, welan gum is compatible (Khayat 1995). Welan gum, xanthan gum, and guar gum are less affected by changes in temperature than are polyacrylate, methyl cellulose, and hydroxyl ethyl cellulose (Sakata, Maruyama, and Minami 1996). Whereas some cellulose derivates can entrap relatively large air volumes, thereby necessitating the use of a defoamer, welan gum does not generally affect the air void system (Khayat 1999). Phyffereon et al. (2002) found that diutan gum was slightly preferable to welan gum because it exhibited higher viscosity and a greater degree of shear thinning, was less affected by changes in cement characteristics, and exhibited a lower charge density so that less HRWRA was required for a constant flow. Despite the many advantages of welan gum, Lachemi et al. (2004a) suggests that the high cost of welan gum relative to other possible alternatives could make the use of welan gum impractical.

Welan gum and cellulose derivative VMAs may delay concrete setting times, while acrylic-type VMAs generally do not affect setting time (Khayat 1995; Khayat 1998). Not only do welan gum and cellulose derivative VMAs themselves increase setting time, the higher dosages of HRWRA required to maintain constant slump flow may further delay setting time. The use of VMA may require significantly higher dosages of air entraining agent due in part to the reduction of available free water (Khayat 1995). Nonetheless, Khayat (1995) found that adequate air void parameters could be achieved in mixtures with VMA.

The presence of VMAs can alter cement hydration, resulting in changes in hardened concrete properties. Khayat (1996) found that welan gum and hydroxypropyl methyl cellulose generally decreased compressive strength, flexural strength, and modulus of elasticity. The reductions in flexural and compressive strengths were more pronounced at lower water-cement ratios while the reduction in modulus of elasticity was more pronounced at higher water-cement ratios. On the basis of x-ray diffraction and scanning electronic microscopy, Khayat (1996)

speculated that VMAs interfere with hydration by limiting the water available to cement particles for hydration and reducing the rate of dissolution of cement. Mercury intrusion porosimetry measurements indicated that these VMAs increased the volume of coarse capillary pores for high water-cement ratios but had little effect on the pore size distribution at low water-cement ratios.

2.1.3   Air Entraining Admixtures

Air entraining admixtures (AEAs) can be used in SCC to achieve adequate air content, air bubble size, air bubble spacing, and freeze-thaw resistance (Khayat 2000; Khayat and Assaad 2002; Persson 2003; Ozyildirim 2005). Ozyildirim (2005) found that improper air void systems and poor freeze-thaw durability can occur in SCC, but added that these properties are not intrinsic to SCC. If the volume of paste is increased for SCC, the volume of air in the concrete may need to be increased to maintain the same percentage of air volume in the paste.

The potential use of SCMs and multiple chemical admixtures can increase the complexity of entraining an adequate air void system (Khayat and Assaad 2002). Indeed, Khayat (2000) reported using AEA in SCC at a considerably higher dosage than required for conventionally placed concrete. Khayat and Assaad (2002) found that increasing NFSC-based HRWRA dosage increased AEA demand; however, increasing the fluidity of mixtures by other means reduced AEA demand as more free water was available. Khayat and Assaad (2002) further found that the spacing factor increased with increased slump flow, possibly due to the tendency of air bubbles to coalesce. Increasing the binder content; however, decreased the spacing factor. Polycarboxylate-based admixtures may themselves entrain air; however, most commercially available admixtures include a defoamer to offset this effect.

Entrained air bubbles can reduce viscosity, which may reduce the stability of the concrete and necessitate other changes to the mixture such as the use of VMA or reduced water content (Khayat 2000). Similarly, low viscosity in concrete may reduce air void stability. Khayat and Assaad (2002) found that the air void system in SCC can remain stable even after agitation over time. They concluded that yield stress and plastic viscosity should not be too low, which would cause segregation and a loss of air, nor too high, which would increase the internal pressure in air bubbles and could result in a loss of air content.

2.2 Aggregates

SCC mixtures generally have some combination of lower total aggregate content, greater amount of fine aggregate relative to coarse aggregate, and smaller maximum aggregate size. Although SCC can be produced with a wide range of aggregate sources, the optimization of aggregate characteristics can result in improved flow properties and reduced demand for cementitious materials, water, and chemical admixtures. In selecting an aggregate source for SCC, key characteristics include but are not limited to shape, angularity, and texture; grading (including maximum aggregate size); and microfines characteristics. In predicting flow properties, these characteristics may be considered based on empirical or rheology-based models.

2.2.1 Description of Aggregate Properties

2.2.1.1 Shape, Angularity, and Texture

Shape, angularity, and texture are defined in a variety of ways. Shape generally describes geometrical characteristics at the coarsest scale, texture at the finest scale, and angularity at an intermediate scale. Shape, texture, and angularity are independent of each other, although they may be correlated for certain sets of particles (Ozol 1978). Shape, texture, and angularity are of great interest in many industrial applications and have been the focus of much research (Pons et al. 1999). Methods of describing shape, angularity, and texture may be classified as non-mathematical, mathematical but incomplete, and mathematical and reasonably complete (Erodgan 2005). Although particle descriptors can be based on two- or three-dimensional measurements, two-dimensional measurements can be biased—especially for materials with low sphericity (Garboczi et al. 2001).

Shape is frequently defined in terms of the three principle dimensions of a particle. For example, Powers (1968) defines a shape factor, which is shown in Equation (2.1):

$$\text{shape factor} = \frac{LS}{I^2} \tag{2.1}$$

where L is the longest principle dimension, S is the shortest principle dimension, and I is the intermediate principle dimension. A shape factor less than unity indicates a prolate shape while a shape factor greater than unity indicates an oblate shape. Shape may also be defined in terms of flatness and elongation, which are defined in Equations (2.2) and (2.3):

$$\text{flatness} = \frac{I}{S} \tag{2.2}$$

$$\text{elongation} = \frac{L}{I} \tag{2.3}$$

Sphericity, which represents how close the shape of a particle is to that of a sphere, is further used to describe shape (Powers 1968). It may be defined as the diameter of an equivalent sphere with the same surface area per unit volume as the actual particle divided by the diameter of a sphere with the same volume as the actual particle. Similarly, it may be defined as the surface area of an equivalent sphere with the same volume as the actual particle divided by the surface area of the actual particle. For a two-dimensional projection of a particle, it may be defined as the square root of the maximum inscribed circle divided by the minimum circumscribed circle. The Wadell sphericity factor is defined as the cube root of the actual volume of the particle divided by the volume of the circumscribing sphere (Ozol 1978). In terms of principle dimensions, the sphericity can be defined as shown in Equations (2.4) or (2.5) (Barrett 1980):

$$\text{Intercept Sphericity} = \left(\frac{IS}{L^2} \right)^{\frac{1}{3}} \tag{2.4}$$

$$\text{Maximum Projection Sphericity} = \left(\frac{S^2}{LI} \right)^{\frac{1}{3}} \tag{2.5}$$

Further definitions of particle shape are provided by Ozol (1978) and Barrett (1980). Similarly, equivalent shapes can be defined (Taylor 2002). The simplest and most widely used approach in concrete mixture proportioning is to assume spherical particles with the diameter derived from the sieve analysis (Bui, Akkaya, and Shah 2002; Schwartzentruber and Catherine 2000). Two-parameter ellipsoids can be generated using volume and surface area or volume and aspect ratio. Three-parameter ellipsoids or parallelepipeds can be generated with the principle dimensions or with equivalent principal moments of inertia.

Angularity describes the sharpness of the corners and edges of a particle. In qualitative terms, particles may be described as angular, sub-angular, sub-rounded, rounded, or well-rounded. Powers (1968) describes angularity as the reciprocal of the sphericity factor. Further, roundness may be defined in terms of Equation (2.6):

18

$$\text{roundness} = \frac{\text{average radius of curvature of corners and edges}}{\text{radius of maximum inscribed circle}} \tag{2.6}$$

Angularity may be described by comparing the particle area and convex area, which are defined in Figure 2.1. The convexity ratio is the divisor of the particle area and the convex area while the fullness ratio is the square root of this divisor. These ratios, however, do not describe fully the sharpness of the corners (Erdogan 2005).
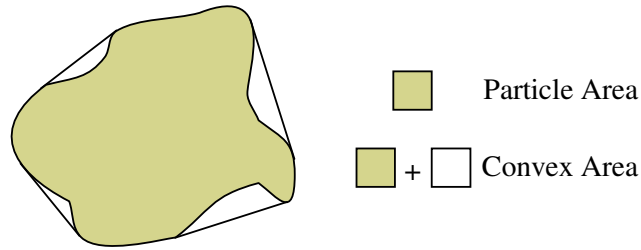
Figure 2.1: Definition of Particle Area and Convex Area

Texture describes the roughness of a particle on a scale smaller than that used for shape and angularity. For example, Bouwman et al. (2004) define roughness as a function of the perimeter measured with lower resolution (P_{smooth}) and higher resolution (P_{rough}), as shown in Equation (2.7).

$$\text{Roughness} = 1 - \frac{P_{smooth}}{P_{rough}} \tag{2.7}$$

Similarly, Ozol (1978) defines texture as either the degree of surface relief or the amount of surface area per unit of dimension or projected area and points out that texture depends on the amplitude and frequency of asperities.

Numerous other descriptors are available for shape, angularity, and texture. These descriptors vary in the sophistication of imaging techniques and mathematics required (Ozol 1978; Barrett 1980; Pons et al. 1999; Bouwman 2004).

Measurement techniques for shape, angularity, and texture range from simple and inexpensive to complex and expensive. Many variations on each approach have been attempted, as summarized by Ozol (1978). Simple methods involve visually observing the particles or manually measuring the principle dimensions of a particle. Coarse aggregate shape may be classified as flat, elongated, flat and elongated, or neither flat nor elongated in accordance with ASTM D 4791. In this method, the length, width, and thickness are measured with proportional calipers for 100 particles from each size fraction. Flatness and elongation ratios, which were

defined in Equations (2.2) and (2.3), are computed and compared to maximum specified values. The percentage of fractured faces in an aggregate sample may be determined in accordance with ASTM D 5821 by visually assessing aggregates one-by-one to count the number of fractured faces. A fractured surface must constitute at least one-quarter of an aggregate's cross sectional area to be considered a fractured face. If a particle has a certain number of fractured faces it is considered a fractured particle. The percentage of fractured particles within a sample is determined. The shape and texture characteristics of both fine and coarse aggregates can be further represented with a single particle index determined based on ASTM D 3398. This test is mainly intended for soil-aggregate and asphalt concrete mixtures, but has been applied successfully to concrete (Jamkar and Rao 2004). The test consists of placing three layers of aggregates in a cylindrical mold and compacting the aggregate with either 10 or 50 drops per layer. The percentage of voids are determined for the case of 10 drops per layer, V_{10}, and 50 drops per layer, V_{50}, and then used to calculate the particle index, I_a, indicated in Equation (2.8):

$$I_a = 1.25 V_{10} - 0.25 V_{50} - 32.0 \qquad (2.8)$$

The test is conducted for individual size fractions and the weighted average particle index is calculated based on the combined aggregate grading. Shape, angularity, and texture can be determined indirectly by measuring the uncompacted void content obtained by allowing aggregate to fall through a funnel at a known height and into a standard-size cylindrical container. The test is standardized as ASTM C 1252 for fine aggregate and AASHTO TP 56 for coarse aggregate. The test may be performed on the as-received grading, on three separate size fractions, or on a standard grading. Hudson (2003f) criticizes the test because it cannot distinguish between shape and texture and concludes that testing an aggregate in its as-received grading is of little value. The size of the container, the funnel opening size, and the drop height influence test results (Hudson 2003f). Other indirect methods include measuring settling velocity or the flow rate of water through aggregate (Jamkar and Rao 2004).

The more sophisticated methods involve using various sensors to acquire digital data on particle geometry, processing the data, and computing morphological parameters (Pons et al. 1999). Methods of acquiring the geometry data can involve digital external imaging, surface profilometry, or tomography (Taylor 2002). In digital external imaging, a camera is used to capture a two-dimensional image of the particle (Mora, Kwan, and Chan 1998; Kwan, Mora, and Chan 1999; Mora and Kwan 2000; Fernlund 2005; Browne et al. 2003). Depending on the sophistication of the device, information on shape, angularity, and texture can be obtained.

Several approaches are available to estimate three-dimensional data from these two-dimensional images. For example, Mora, Kwan, and Chan (1998), Kwan, Mora, and Chan (1999) and Mora and Kwan (2000) computed a single parameter for a given aggregate sample to relate area to volume measurements and to obtain flatness, elongation, sphericity, shape factor, convexity ratio, and fullness ratio measurements. Fernlund (2005) measured each particle from two positions—standing and lying—to determine the principle dimension of the particle. Chetana, Tutumluer, and Stefanski (2001) utilized cameras at three orthogonal directions to obtain three-dimensional information. Chandan et al. (2004) utilized a single camera but adjusted the focus to define the depth of each particle.

Surface profilometry consists of determining three-dimensional coordinates and can be accomplished with laser ranging, acoustic ranging, direct mechanical probing, or speckle interferometry (Taylor 2002). For example, the Laser-based Aggregate Scanning System (LASS) is an automated, on-line quality control system that captures and analyzes three-dimensional images of aggregate particles (Haas et al. 2002). A laser beam is used to illuminate aggregates and the resulting image is captured by a charge coupled device (CCD) camera. Although LASS does capture a three-dimensional image of each aggregate particle, it does not capture the underside of a particle, a problem known a self-occlusion. Software processes the image to determine traditional measurements such as grading (virtual sieve) and flatness and elongation ratios (virtual caliper). The software further characterizes the particle by calculating shape, angularity, and texture indices, which express quantitatively the deviation from a smooth, spherical particle. Other laser scanning devices with different resolutions and scan rates are available (Tolppanen et al. 1999).

Tomography can be accomplished with x-rays, gamma rays, magnetic resonance imaging, or acoustic imaging (Taylor 2002). X-ray computed tomography, which overcomes the problem of self-occlusion and provides true three-dimensional data, is accomplished by embedding aggregates in a medium, such as epoxy or mortar, and using x-rays to scan horizontal slices of this specimen. The slices are then reconstructed into a three-dimensional image, which can be processed by computer. One available approach to processing the digital images is spherical harmonics (Garboczi et al. 2001; Garboczi 2002). In this approach, an individual particle is identified, its center of mass is determined, and the surface of the particle is defined as a function of $r(\theta, \phi)$, where r is the distance from the center of mass to the surface in a direction specified by the polar coordinates θ and ϕ. The expansion of this function requires that a set of

coefficients be defined for each shape. These coefficients can be stored in a database and used to compute typical aggregate shape characteristics—such as volume, surface area, curvature or moment of inertia—or to generate actual aggregate shapes in computer models of concrete.

In concrete, the size, shape, and texture of aggregates affect the bulk voids and frictional properties of the aggregates (Hudson 2002). The void content in combined aggregate can vary as much as 8 to 9 percent due to variations in shape and texture, but in practice this range is typically much less (Ozol 1978). Hudson (2003c) suggests that shape and texture are more important than grading and asserts that the focus on grading is manly due to the historic use of natural sands, which do not vary in shape, texture, and angularity to the degree that manufactured sands do. Hudson (2003b) cites data indicating that mixtures with the same specific area but with different gradings had similar water requirement and compressive strength. Aggregates with cubical shapes are desirable; poorly shaped aggregate may require increased cement content (Hudson 2003e; Goldsworthy 2005). According to Hudson (2003f), texture becomes more important as particle size decreases because more surface area is available. Ozol (1978) indicates that angularity is more influential than shape for workability. Tattersall (1991) and Bager, Geiker, and Jensen (2001) found that texture had little effect on workability. Bager, Geiker, and Jensen (2001) found that increasing the aspect ratio of particles increased yield stress and plastic viscosity.

The shape of an aggregate particle is determined by the degree of anisotropy in the material, the original shape of the particle, and the effects of transport and abrasion of natural particles and of crushing and sizing of crushed particles (Ozol 1978). In the case of gravel, the original shape depends on large-scale structural features such as joints, fractures, and faults. For natural sands, the original shape of the particle is mainly a function of the mineral grain shape. The degree of rounding that occurs with natural particles depends on the hardness and toughness of the rock and the presence of cleavage or cracks, which induce fracturing. For crushed aggregates, the original shape formed by blasting is affected by large scale structural features in the bedrock as well as small-scale flaws and discontinuities. The effect of crushing depends on the degree of anisotropy of the rock, which results in flat and elongated particles, and the type of crushing. According to Aitcin (1998) and Ozol (1978), particles with impact crushers are preferable to compression crushers, such as jaw, gyratory, and cone crushers. Goldsworthy (2005) recommends rock-on-rock impact crushers to produce concrete aggregates with improved

shape, texture, and grading. The larger the reduction ratio of the crusher, the more flat and elongated the particles are likely to be (Ozol 1978).

2.2.1.2 Grading

The grading, or particle size distribution, of all materials in a concrete mixture—including aggregates, cementitious materials, and other additions—are highly relevant to concrete performance. A variety of techniques must be employed to characterize the full grading, which can range from the order of nanometers to tens of millimeters. In obtaining a specimen for grading analysis, proper sampling techniques are critical because of the tendency of granular materials to segregate by size. A sieve analysis, which is performed in accordance with ASTM C 136, is the most common method for measuring the grading of aggregates larger than 75 µm in size. Prior to performing this sieve analysis, the amount of aggregate finer than 75 µm in a particular sample is determined in accordance with ASTM C 117 by washing the sample over a 75 µm sieve. The grading of materials finer than 75 µm must be determined with more sophisticated methods, such as a sieve analysis with a sonic sifter, laser diffraction, particle counting in scanning electron microscope images, electrical zone sensing, or sedimentation based on the application of Stokes' law (Ferraris et al. 2002). Alternatively, a single number representing fineness can be obtained with the Blaine air permeability method (ASTM C 204), the Wagner Turbidimeter (ASTM C 115), or the nitrogen BET method. The use of a single number representing fineness, however, may not provide adequate information for predicting the performance of material finer than 75 µm (Stewart et al. 2006).

The measurement of a particular size for each aggregate particle is complicated by the irregularity of aggregate shapes, which raises the question of which dimension of the aggregate should be used to define size (Pons et al. 1999; Taylor 2002). In a sieve analysis, the measured size is typically related to the intermediate principle dimension because a particle can pass through the sieve opening in an orientation such that the long principle dimension is perpendicular to the plane of the sieve. The square shape of the sieve, however, means that a particle's intermediate dimension can be oriented diagonally across the sieve opening such that the intermediate dimension is larger than the nominal size of the sieve. Complications are also inherent with other measurements. For example, laser diffraction measurements and some sedimentation methods assume spherical particles.

For an aggregate source with certain shape, angularity, and texture characteristics, the grading can significantly influence the aggregate's performance in concrete. The importance of a well-graded aggregate with a wide range of particle sizes is well established for producing high-quality concrete. As an aggregate size gets smaller, its value to concrete increases because it becomes more costly to produce and its characteristics have a larger influence on concrete properties (Hudson 2002). Shape, angularity, and texture vary for each size fraction (Hudson 2003d). For coarse aggregate, the use of a large maximum aggregate size reduces fresh concrete water demand; however, the hardened properties can be affected negatively because of the increased interfacial transition zone thickness and the fact that larger particles tended to contain more internal defects that would otherwise be removed during crushing (Aitcin 1998). In general, it is desirable to use the largest particle practical to maximize the ratio of volume to surface area (Hudson 2003a). The intermediate size fraction, which approximately ranges from a No. 8 sieve to 13 mm, is known to affect workability, finishability, and shrinkage (Shilstone 1990; Hudson 2002). Bager, Geiker, and Jensen (2001) found that increasing the sand fineness increased the yield stress and plastic viscosity of self-consolidating mortars. For high-performance concrete, Aitcin (1998) suggests using coarse sands, with fineness moduli between 2.7 and 3.0, because the use of such sands decreases the amount of mixing water required and because sufficient fine particles are available from the cementitious materials. Hudson (2003d) suggests that sands should be made finer as angularity increases. Hudson (2003c) further suggests using a manufactured sand with the same grading and volume as the natural sand it is replacing but cautions that the ideal grading depends on shape, angularity, and texture, and must be selected independently for each sand. According to Ozol (1978), sphericity increases with size.

2.2.1.3 Microfines and Other Mineral Fillers

Mineral fillers—including dust-of-facture microfines—are generally defined as mineral material finer than 75 μm. Dust-of-fracture microfines are generated in the production of manufactured sands. It is estimated that 100 million tons of aggregate microfines are stockpiled or disposed of annually (Hudson 2002). Microfines are also present in natural sands, though typically in a smaller quantity. The other source of mineral filler is finely ground filler, which is not a byproduct but an intentionally produced product with specific intended applications. It is most commonly comprised of limestone.

Microfines may be included in the sand or added separately. ASTM C 150 allows up to 5% limestone to be added to cement, provided all other requirements of the standard are also met. The limestone added to cement must consist of at least 70% calcium carbonate. Like sand in general, the shape, angularity, texture, and grading of microfines are important. In addition, the potential presence of clays and other deleterious materials must be considered. Clays may adsorb water in freshly mixed concrete and expand. The resulting reduction in free water reduces workability (Yool, Lees, and Fried 1998). If the clays later dry and shrink, the resulting voids reduce strength and permeability (Hudson 2002). Further, clays may interfere with admixture performance (Jardine et al. 2002; Jardine et al. 2003). The effects of a given clay are a function of its fineness and activity (Yool, Leeds, and Fried 1998). Smectite (montmorillonite) adsorbs more water than illite or kaolinite (Stewart et al. 2006). Yool, Leeds and Fried (1998) found that mixtures with constant workability exhibited a 2% reduction in strength for each 1% addition of kaolinite by mass of cement and a 10% reduction in strength for each 1% addition of smectite by mass of cement. This reduction was mainly due to the increase in water content required to maintain constant workability. When the water-cement ratio was held constant, the strength was essentially unchanged, although the workability decreased.

A potentially severe durability problem when limestone mineral fillers are used in cold, sulfate-rich environments is the possibility for the thaumasite form of sulfate attack (TSA). Thaumasite ($CaSiO_3 \cdot CaCO_3 \cdot CaSO_4 \cdot 15H_2O$) typically forms from the reaction of sulfate ions, C-S-H, water, and either carbonate ions or carbon dioxide (Santhanam, Cohen, and Olek 2001). Thaumasite may form in a variety of ways (Bensted 2003). Ground limestone filler is a potential source for carbonate ions. Its small size makes it more reactive than larger limestone aggregates. Other sources of carbonate ions besides limestone aggregates include dolomite aggregates, seawater, and groundwater (Thomas et al. 2003; Sahu, Badger, and Thaulow 2003). Unlike traditional forms of sulfate attack that lead to expansion and cracking, TSA literally turns C-S-H to mush (Crammond 2003). Thaumasite is particularly threatening because it is limited only by the availability of sulfate and carbonate ions and can, in theory, continue until the depletion of all C-S-H (Macphee and Diamond 2003). Thaumasite is structurally similar to ettringite, but with silicate in place of aluminate and carbonate ions in place of sulfate ions. Thaumasite formation is generally associated with low temperatures (below approximately 15°C) and has been shown to form at faster rates at lower temperatures. Thaumasite has, however, been observed in warmer climates such as southern California (Diamond 2003; Sahu, Badger, and Thaulow 2003). The

increased use of limestone filler in cements around the world has increased the incidence of thaumasite formation (Irassar et al. 2005); however, thaumasite has also been identified in historic buildings (Collepardi 1999) and was identified in the United States as early as the 1960s (Stark 2003). Furthermore, the increased availability of analytical techniques has likely increased identification of thaumasite (Thomas et al. 2003).

The content of microfines is currently limited by some specifications. For manufactured sands essentially free of clay and shale, ASTM C 33 limits the content of dust-of-fracture microfines to 5% of the sand mass for concrete subjected to abrasion and 7% for all other cases. Other standards around the world allow higher percentages of microfines (Quiroga 2003).

The shape, angularity, and texture of aggregate microfines and other mineral fillers can be evaluated with methods such as micro-tomography and scanning electron microscopy (Erdogan 2005, Stewart et al. 2006). Particle size distribution can be evaluated with a sieve analysis with a sonic sifter, laser diffraction, particle counting in scanning electron microscope images, electrical zone sensing, or sedimentation based on the application of Stokes' law. Fineness can be measured with the Blaine air permeability apparatus, Wagner turbidimetner, or nitrogen BET measurements. The mineralogical composition can be determined with x-ray diffraction (Stewart et al. 2006).

The effects of microfines and other mineral fillers on workability—as influenced by factors such as shape, angularity, texture, and particle size distribution—can be evaluated by measuring the water demand of microfines. For example, the Vicat test can be used to determine the amount of water to reach normal consistency, as defined in ASTM C 187. In the single drop test (Bigas and Gallias 2002; Bigas and Gallias 2003), a 0.2 ml drop of water is placed on a bed of powder, resulting in the formation of an agglomerate. The powder bed may consist of only microfines, or some combination of microfines and cementitious materials. After 20 seconds, the agglomerate is removed from the bed and its mass is determined. The test must be performed 15 times for sufficient precision. The water-powder ratio is determined in both the Vicat and single drop tests. Bigas and Gallias (2002) found that both the single drop test and Vicat test for normal consistency differentiated between different fineness, particle shape, and texture for blends of cement with various mineral additions and for mineral additions tested independently.

The presence of clay and organic matter in microfines can be detected with differential thermal analysis, the sand equivalent value test, or the methylene blue value test. Differential thermal analysis is conducted by gradually heating a sample of microfines to 1200°C while

monitoring the change in mass. Mass changes at different temperatures may be associated with the presence of certain clays (Stewart et al. 2006). In the sand equivalent value test, a sample of fine aggregate is placed in a plastic graduated cylinder filled with flocculating solution. The contents or the cylinder are agitated with mechanical or manual shaking. Additional flocculating solution is added and the specimen is left undisturbed for a sedimentation period so that the sand will remain at the bottom of the cylinder and any clay will float to the top. The sand equivalent value is expressed as the ratio of the height of sand to the height of clay multiplied by 100.

The methylene blue test consists of determining the amount of methylene blue solution adsorbed by clays in an aggregate sample. The test measures the ability of clays to adsorb dye onto active surfaces, and therein provides an indication of cation exchange capacity and surface area (Yool, Lees, and Fried 1998). When performed in accordance with AASHTO TP57, a sample of fine aggregate is dried and sieved to obtain the portion passing the No. 200 sieve. The methylene blue solution is created by dissolving 5 mg of solid methylene blue ($C_{16}H_{18}ClN_3S$) per 1 ml of solution. A 10-g sample of the minus 75 μm material is placed into a beaker with 30 ml of distilled water. A magnetic mixer with a stir bar is used to form a slurry. Methylene blue solution is added to this slurry in 0.5 ml increments. After each addition, the slurry is stirred for 1 minute. A glass stirring rod is used to remove a drop of solution, which is placed on filter paper. The end point of the test is reached when a light blue halo forms around the drop. As long as the clays adsorb the dye, the drop consists of blue stained particles surrounded by a colorless ring of water. When the adsorption capacity of the clay is reached, the excess methylene blue results in the light blue halo. After this point, the slurry is stirred for five minutes and retested. With experience, more methylene blue can be added initially to speed up the test. The methylene blue value (MBV) is calculated as the mg of methylene blue per g of material, as shown in Equation (2.9):

$$MBV = \frac{CV}{W}$$
(2.9)

where C is the concentration of the methylene blue solution (mg of methylene blue per mL of solution), V is the volume of methylene blue solution required for titration (mL), and W is the mass of material (g).

The methylene blue test is not able to distinguish between different clays and does not provide results that are in proportion with the potential damage of clays (Yool, Lees, and Fried 1998). For instance, Yool, Lees, and Fried (1998) found that a smectite clay resulted in a

reduction in strength that was 5 times that for a kaolinite clay; however, the methylene blue value for the smectite clay was 34 times that of the kaolinite clay. This discrepancy could be corrected by adding a sufficient quantity of polyethylene glycol or using cartasol blue dye instead of methylene blue dye. More research is needed to determine what the methylene blue value test measures and whether other tests may be more appropriate.

Microfines and other mineral fillers have been used successfully in conventionally placed concrete and SCC. Research has indicated the concretes incorporating manufactured sands with high contents of dust-of-fracture microfines can perform equal to or better than concrete made with natural sands (Ahn 2000; Quiroga 2003). Hudson (2003a) likens the effect of microfines on workability to the lubricating effect of fly ash and adds that particles smaller than 75 µm densify the paste. The quality of the aggregates larger than 75 µm may influence the amount of microfines that can be used (Hudson 2002).

In evaluating the effects of microfines, two key experimental considerations are whether the material is used to replace sand or cement and whether the water-cement ratio or water-powder ratio is held constant. When microfines are used to replace sand, the water content usually must be increased due to the higher powder content. If microfines are used to replace cement, the water content may be reduced in many cases depending on the particle size distribution and shape characteristics of the microfines. If the water-cement ratio is held constant as microfines are added, the compressive strength may increase because of the improved packing density and the interaction of microfines with cement hydration. If the water-powder ratio is held constant as microfines are added, the compressive strength will likely decrease due to the higher water-cement ratio, although the decrease will be offset by improved packing density and interaction with cement hydration.

The majority of data in the literature regarding the use of mineral fillers is for ground limestone fillers, which are widely used in some parts of Europe (Zhu and Gibbs 2005) but not in the United States. The particle size distribution and fineness of ground limestone fillers vary widely by source. Not only does the particle size depend on variations in grinding, limestone fillers can be classified to produce a certain size range. Ground limestone fillers typically consist predominately calcium carbonate, with few other minerals present. Ground limestone filler, when used to replace cement at levels up to 50%, can improve the economy of SCC by reducing the amounts of portland cement and HRWRA (Ghezal and Khayat 2002).

The use of ground limestone filler as a replacement for cement can reduce water demand or superplasticizer demand. The improved workability is typically attributed to the improved particle size distribution, despite the higher fineness (Tsivilis et al. 1999; Nehdi, Mindess and Aitcin 1998; Zhu and Gibbs 2005). In terms of rheology, limestone filler has been shown to decrease both yield stress and plastic viscosity (Svermova, Sonebi, and Bartos 2003; Ghezal and Khayat 2002). Above a critical dosage, however, the addition of ground limestone filler can increase viscosity substantially (Yahia, Tanimura, and Shimoyama 2005). This critical dosage is related to the amount of free space within the solid skeleton and depends on the characteristics of the ground limestone filler, cementitious materials, and aggregates. Once the free space is filled with ground limestone filler, packing is no longer improved and interparticle friction is increased. Ground limestone filler can also increase static stability and reduce bleeding in SCC mixes (Ghezal and Khayat 2002).

Limestone powders can also accelerate hydration, resulting in increased compressive strength at early ages. The effects of ground limestone filler at later ages are less significant (Zhu and Gibbs 2005). Kadri and Duval (2002) found that later-age strengths can be reduced due to the lack of pozzolanic reaction. The individual particles can provide sites for heterogeneous nucleation (Kadri and Duval 2002). Limestone filler can also react with C_3A to form carboaluminate and with C_3S to form a calcium carbosilicate hydrate (Pera et al. 1999; Tsivilis et al. 1999). The quantity of monosufate can be reduced or eliminated (Pera et al. 1999). The dilution of alkali concentration can also contribute to hydration (Tsivilis et al. 1999). Research has also shown that the SO_4 ions in ettringite are replaced with CO_3 ions when ground limestone filler is present (Pera et al. 1999). Limestone filler increases the density of the paste, which is particularly important in improving the strength and transport properties in the interfacial transition zone. In cases where limestone filler reduces compressive strength, especially at relatively high cement replacement rates, the improvement in workability may permit the reduction in water content to offset the decrease in strength (Ghezal and Khayat 2002).

Aside from ground limestone filers, alternative ground materials have also been utilized. For instance, Zhu and Gibbs (2005) examined chalk powders, which were composed primarily calcium carbonate (approximately 90%) and some insoluble residue. The mixtures with ground chalk filler exhibited a smaller reduction in HRWRA demand and smaller increase in compressive strength than the mixtures with ground limestone filler.

29

Dust-of-fracture microfines have been used to replace either cementitious materials or aggregate. When used to replace cement, the results have generally been favorable. Ho et al. (2002) found that a dust-of-fracture granite microfine could be used for SCC. This dust-of-fracture granite microfine required higher dosages of HRWRA compared to a ground limestone filler, which was attributed to the greater fineness and to the flat and elongated shape of the granite particles. Bosiljkov (2003) utilized both dust-of-fracture limestone microfines and ground limestone filler to compensate for the lack of fine particles in poorly graded aggregates used for SCC mixtures. When used to replace cement at rates up to 50%, the dust-of-fracture limestone microfines were found to be preferable to ground limestone filler because of their greater fineness and improved particle size distribution.

When used to replace fine aggregate instead of cement, the results are generally not as favorable. Celik and Marar (1996) found that the use of dust-of-fracture microfines to replace sand in conventionally placed concrete at rates up to 30% reduced slump and air content. Compressive strengths were increased up to the 10% replacement rate, beyond which the trend was reversed. This decrease in strength at higher microfines contents was attributed to the fact that not enough cement was available. Permeability was increased at replacement rates up to 30% while drying shrinkage increased up to a replacement rate of 10%, beyond which the trend was reversed. Malhotra and Carette (1985) found that the use of dust-of-fracture limestone microfines as a replacement for sand increased the demand for water-reducing admixture and air-entraining admixture, but increased the cohesiveness of lean concrete mixtures. Compressive strength generally increased, which was attributed to improved packing and possibly to accelerated hydration, the formation of carboaluminates, and the use of superplasticizer. In addition, Malhotra and Carette found the use of dust-of-fracture limestone microfines increased flexural strength, drying shrinkage, and creep but had no effect on frost resistance. Ahmed and El-Kourd (1989) found that the use of limestone dust as a replacement for sand increased water demand for a given slump. At a constant slump—and, therefore, at a higher water content—the use of limestone dust decreased compressive and flexural strengths and increased shrinkage.

2.2.2 Empirical Approaches to Selecting Aggregates

The numerous empirical approaches to selecting aggregates may be applicable in whole or in part to proportioning SCC. Many of the approaches described in the literature in the past century are now considered outmoded. This section describes packing density, the excess paste

theory and its derivatives, the Shilstone method, water requirement equations, and the ACI 211 method. It is not intended to be comprehensive. Despite the theoretical rigor of some packing density models, packing density is considered an empirical approach because it gives an indirect indication of factors such as aggregate geometry and provides indirect predictions of concrete rheology.

2.2.2.1 Packing Density

Packing density, which is defined as the volume of solids per total bulk volume, is widely used to evaluate and combine aggregates. The geometrical characteristics of shape, angularity, texture, and particle size distribution affect packing density; therefore, packing density can be used as an indirect indicator of aggregate geometrical characteristics. Packing density also provides an indication of the voids content, which must be filled with paste. Additional paste greater than the voids content is needed to mobilize aggregates and provide a certain level of flowability. Therefore, aggregates with higher packing density will generally allow a larger volume of aggregates and lower volume of paste to be used. In general, higher packing density is preferred, although the maximum packing density may not be optimal (Johansen and Andersen 1991; Goltermann, Johansen, and Palbol 1997; Powers 1932; Powers 1968). According to Goltermann, Johansen, and Palbol (1997), concrete mixes should have more fine aggregate than what is required for the maximum packing density. It must be noted however, that a small change in sand content does not generally result in a large change in packing density. The use of a higher volume fraction of aggregate—especially coarse aggregate—can result in improvements in strength, stiffness, creep, drying shrinkage, and permeability (Johansen and Andersen 1991). The use of higher packing density with continuous grading and a narrow grading span results in reduced segregation (de Larrard 1999a). According to Hudson (2002), the difference in voids for the available aggregates in the same geographical region is about 3 to 6 percent.

In considering packing, the packing of all particles in the concrete mixture must be considered. According to de Larrard (1999b), the selection of the optimum ratio of coarse to fine aggregate may be misleading because the presence of cementitious materials provides a loosening effect. Based on a compressible packing model simulation, de Larrard (1999b) found that the ratio of coarse to fine aggregate should be increased when interaction from cementitious materials are included.

31

In addition to geometrical characteristics, packing density also depends on the method of packing (de Larrard 1999a). Packing methods range from loose packing to packing with vibration and pressure. A higher degree of packing is preferable because the variability in measured packing density is less. For the compressible packing model, de Larrard (1999a) suggests applying simultaneously a prescribed vibration regime and 10 kPa of pressure. For cementitious materials and other fine materials, several approaches are available. De Larrard (1999a) suggests determining the packing density by measuring the amount of water with or without admixture that must be added to cement to transition from a humid powder to a thick paste. Alternatively, this determination can be made by using the Vicat test for measuring the water content to reach normal consistency, which is defined in ASTM C 187, or by using the single drop test, which is described by Bigas and Gallias (2002). The single drop test is not influenced by the presence of superplasticizer. For each of these methods, the actual packing density is calculated as shown in Equation (2.10):

$$\phi = \frac{1}{1 + \rho_s \dfrac{w}{s}}$$
(2.10)

where ρ_s is the density of the solid materials, w is the mass of water, and s is the mass of solid materials. These methods also provide an indication of water demand.

Aggregates may be selected for optimal packing density by using one of several suggested ideal particle size distributions, performing empirical tests on various blends of aggregates, or using a mathematical packing model. The selection of optimal packing density is of interest in many industrial applications and has been studied extensively. Consequently, the following paragraphs are intended to provide an overview of available methods most applicable to concrete and are not intended to serve as an exhaustive overview.

Numerous ideal particle size distributions have been suggested for optimizing packing density. Based on packing model simulations, the optimal packing density of polydisperse mixtures can be achieved with continuous or gap-graded particle size distributions (de Larrard 1999a; Andersen and Johansen 1993). Based on simulations from the compressible packing model, de Larrard (1999a) found that for binary mixes, increasing the size difference between the two fractions increases packing density because interaction is reduced. The continuous grading should be chosen to minimize bleeding and segregation. Fuller and Thompson (1907) developed

32

ideal grading curves for concrete on the basis of experiments and found that these ideal curves could be approximated with a parabola, as given in Equation (2.11):

$$p_t = \left(\frac{d}{D}\right)^{\frac{1}{2}}$$ (2.11)

where p_t is the fraction of total solids (aggregate and cement) finer than size d and D is the maximum particle size. In order to avoid lean mixtures, they further stipulated that at least 7 percent of the total solids be finer than the No. 200 sieve. More generally, other parabolic particle size distributions are possible with an exponent q other than ½, as shown in Equation (2.12) (Powers 1968):

$$p_t = \left(\frac{d}{D}\right)^{q}$$ (2.12)

Andreasen and Anderson (1929) found that the voids content is reduced as the exponent q is reduced. In practice, the minimum value of q for their materials was about ½ because the smaller particles do not pack as well as larger particles. A value of 0.45 is often used for asphalt concrete mixtures (Kennedy et al. 1994) and has been suggested for concrete (Shilstone 1990; Quiroga 2003). Faury suggests the use of 0.20 as the value of the exponent (de Larrard 1999a). De Larrard (1999a) found, based on a mathematical packing model, that the particle size distribution could be expressed with an exponent of 0.20 under certain conditions. The value of the exponent for optimizing packing density was found to vary with the packing density of the individual size fractions and the degree of compaction; therefore, it was not possible to establish an optimal particle size distribution for all cases (de Larrard 1999a).

Bolomey (1947) extended the concept of a parabolic grading by adding an empirical constant, f, as shown in Equation (2.13):

$$p_t = f + (1-f)\left(\frac{d}{D}\right)^{\frac{1}{2}}$$ (2.13)

The value of f is selected based on the desired degree of workability, with higher values of f corresponding to higher degrees of workability.

Druex (de Larrard 1999a) suggested an ideal particle size distributions based on the performance of actual concretes on jobsites. The curve, when plotted on a logarithmic scale of diameter, consists of two linear regions, as shown in Figure 2.2. The value of A is selected based

on the maximum aggregate size, cement content, amount of vibration, particle shape, and sand fineness modulus.
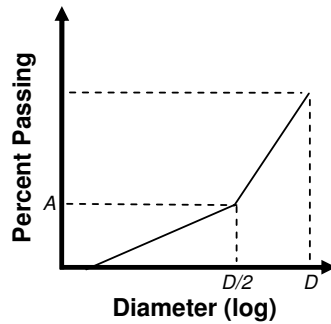
Figure 2.2: Dreux Particle Size Distribution

Weymouth developed a theory based on particle interference. The theory stated that the distance between particles in one size fraction should be at least the average diameter of the next smaller fraction (Powers 1968). This concept is expressed in Equation (2.14):

$$\left(\frac{d_0}{d_i}\right) = 1 + \frac{D_{i-1}}{D_i} \qquad (2.14)$$

where d_i is the density of the ith fraction in the concrete mixture, d_0 is the density of the ith fraction in a dry, compacted state, D_i is the diameter of the ith fraction, and D_{i-1} is the diameter of the next smaller fraction.

In 1968, Powers (p. 256) wrote that "the hypothesis that there is an ideal size grading for concrete aggregate, or for all solid material in concrete, has now become almost if not entirely abandoned."

In addition to generalized ideal grading curves, multiple mathematical models are available for computing packing density from empirical measurements on individual size fractions. These models vary from simple models of binary combinations of monosized spheres with no interaction between particles to more complex models that incorporate polydisperse blends with interaction between particles. Interaction includes loosening effect, which results from smaller particles reducing the packing density of adjacent larger particles, and wall effect, which results from larger particles reducing the packing density of adjacent smaller particles.

The Furnas model (Johansen and Andersen 1991) is for a binary model of spherical particles with the diameter of the smaller particles much less than that of the larger particles.

34

The maximum packing density is given in Equation (2.15) for the case where the fraction of the smaller particles is equal to r_1 in Equation (2.16):

$$\phi = \phi_2 + (1 - \phi_2)\phi_1 \tag{2.15}$$

$$r_1 = \frac{\phi_1(1 - \phi_2)}{\phi_2 + (1 - \phi_2)\phi_1} \tag{2.16}$$

where ϕ_1 and ϕ_2 are the eigenpacking values of the fine and coarse fractions, respectively. Other equations are available for cases where the volume of coarse or fine fraction is dominant.

The Aim and Goff model (Goltermann, Johansen, and Palbol 1997) calculates the packing density from two size fractions of monosized spheres with Equations (2.17) to (2.20):

$$y^* = \frac{p}{1+p} \tag{2.17}$$

$$p = \frac{\phi_1}{\phi_2} - \left(1 + 0.9\frac{d_1}{d_2}\right)\phi_1 \tag{2.18}$$

$$\phi = \frac{\phi_2}{(1 - y_1)} \quad \text{for } y_1 < y^* \tag{2.19}$$

$$\phi = \frac{1}{\left[\frac{y_1}{\phi_1} + (1 - y_1)\left(1 + 0.9\frac{d_1}{d_2}\right)\right]} \quad \text{for } y_1 \geq y^* \tag{2.20}$$

where y_1 and y_2 are the volume fractions of the fine and coarse fractions, respectively; ϕ_1 and ϕ_2 are the eigenpacking values of the fine and coarse fractions, respectively; and d_1 and d_2 are the characteristic diameters of the fine and coarse fractions, respectively. Goltermann, Johansen, and Palbol (1997) determined that this model did not work well for concrete aggregates.

The Toufar, Klose, and Born model (Goltermann, Johansen, and Palbol 1997) calculates packing density from two size fractions of monosized spheres with Equations (2.21) to (2.24):

$$\phi = \frac{1}{\left[\frac{y_1}{\phi_1} + \frac{y_2}{\phi_2} - y_2\left(\frac{1}{\phi_2} - 1\right)k_d k_s\right]} \tag{2.21}$$

$$k_d = \frac{d_2 - d_1}{d_1 + d_2} \tag{2.22}$$

$$k_s = 1 - \frac{1+4x}{(1+x)^4} \tag{2.23}$$

$$x = \frac{\left(\dfrac{y_1}{y_2}\right)\left(\dfrac{\phi_2}{\phi_1}\right)}{(1-\phi_2)} \tag{2.24}$$

Goltermann, Johansen, and Palbol (1997) suggest modifying the expression for k_s for cases where $x<0.4753$, as shown in Equation (2.25):

$$k_s = \frac{0.3881x}{0.4753} \text{ for } x<0.4753 \tag{2.25}$$

To combine multi-component mixtures of monosized fractions with the Toufar, Klose, and Born model, binary combinations are computed for adjacent size fractions and combined based on Equations (2.26) and (2.27) (Johansen and Andersen 1991):

$$y_{ij} = \frac{y_i y_j}{1-y_i} + \frac{y_j y_i}{1-y_j} \tag{2.26}$$

$$\phi = \frac{1}{\displaystyle\sum_{j=2}^{n}\sum_{i=1}^{j-1}\frac{y_{ij}}{\phi_{ij}}} \tag{2.27}$$

To combine multi-component mixtures of polydisperse fractions, such as coarse and fine aggregates for concrete, Goltermann, Johansen, and Palbol (1997) suggest using a characteristic diameter corresponding to the diameter with 36.8 percent retained in the fraction. For ternary blends, they suggest combining the two fractions with the highest d_1/d_2 ratio and then blending this blended fraction with the third fraction. A limitation of this approach is that the model cannot account fully for the effects of overlapping fractions. Andersen and Johansen (1993) combined the Aim and Goff model with the Toufar, Klose, and Born model to develop a series of tables to aid in combining aggregates.

The compressible packing model (de Larrard 1999a), which is based on a linear packing density model, enables the calculation of the packing density of polydisperse granular mixes with particle interaction. The model takes into account the effect of compaction technique by making a distinction between the virtual packing density, which is the maximum theoretical packing density, and the actual packing density. The packing density is defined in terms of the compaction index, K, which describes the packing process. Therefore, for a given packing with a known K, the packing density, ϕ, is defined implicitly in Equation (2.28):

$$K = \sum_{i=1}^{n} K_i = \sum_{i=1}^{n} \frac{y_i / \beta_i}{1/\phi - 1/\gamma_i} \qquad (2.28)$$

where y_i is the volume fraction of class i, β_i is the residual (virtual) packing density of class i, and γ_i is the virtual packing density when class i is dominant. The value of K can be chosen for the packing process. De Larrard (1999a) suggests a value of K of 4.1 for pouring, 4.5 for dry rodding, 9 for vibration and applied pressure of 10 kPa, and 6.7 for wet packing. The γ_i term, which takes into account particle interaction, is expressed in Equation (2.29):

$$\gamma_i = \frac{\beta_i}{1 - \sum_{j=1}^{i-1}\left[1 - \beta_i + b_{ij}\beta_i\left(1 - 1/\beta_j\right)\right]y_j - \sum_{j=i+1}^{n}\left[1 - a_{ij}\,\beta_i/\beta_j\right]y_j} \qquad (2.29)$$

where a_{ij} is the loosening effect coefficient and b_{ij} is the wall effect coefficient. These two coefficients are determined by calibration. Based on experimental data, the approximations shown in Equations (2.30) and (2.31) are suggested:

$$a_{ij} = \sqrt{1 - \left(1 - d_j/d_i\right)^{1.02}} \qquad (2.30)$$

$$b_{ij} = 1 - \left(1 - d_j/d_i\right)^{1.50} \qquad (2.31)$$

where d_i and d_j are the diameters of particles in class i and j, respectively. The virtual packing of a monodispersed fraction is calculated from the actual packing density with Equation (2.32):

$$\overline{\beta}_i = \left(1 + \frac{1}{K}\right)\phi_i \qquad (2.32)$$

The virtual packing density must be corrected for wall effect in determining the actual packing density, as represented in Equation (2.33):

$$\beta_i = \frac{\overline{\beta}_i}{1 - \left(1 - k_w\right)\left[1 - \left(1 - d/\varnothing\right)^2\left(1 - d/h\right)\right]} \qquad (2.33)$$

where $\varnothing$ is the diameter of the container, h is the height of the container, and k_w is a constant accounting for packing density and is taken as 0.88 for rounded aggregates and 0.73 for crushed aggregates.

De Larrard (1999a) uses values from the compressible packing model along with other characteristics to predict concrete properties such as slump, yield stress, plastic viscosity, and compressive strength. The compressible packing model can also be used to predict segregation by determining the filling proportion (ϕ_i/ϕ_i^*) for each size fraction, where ϕ_i^* is the maximum

37

density of size class *i* given the presence of other particles. The segregation potential of an individual size fraction is defined as shown in Equation (2.34):

$$S_i = 1 - \frac{\phi_i}{\phi_i^*} = 1 - \frac{K_i}{1 + K_i}$$

(2.34)

The segregation potential for the mix is the maximum value of S_i for a set of size fractions. The maximum segregation potential is 1.0; lower segregation potentials are preferred.

On the basis of the compressible packing model, de Larrard compared the packing densities and segregation potentials of available particle size distributions, as shown in Table 2.2.

Table 2.2: Results of Compressible Packing Model for Several Particle Size Distributions (de Larrard 1999a)

Particle Size Distribution	Packing Density	Segregation Potential
Max. Density	0.929	0.59
Fuller	0.869	0.96
Faury	0.927	0.59
Dreux	0.914	0.80
Uniform	0.891	0.85
Gap-Graded	0.928	1.00
Minimum *S*	0.926	0.53

Models for packing density have been applied to SCC. Khayat, Hu, and Laye (2002) found that SCC with near optimum aggregate packing exhibited lower viscosity, lower HRWRA demand, and similar or greater filling capacity than SCC with slightly lower aggregate packing density. The SCC with slightly lower packing density exhibited better stability due to the higher content of fines smaller than 80 µm and lower coarse aggregate volume. In the mixtures tested, the packing density was decreased by adding more sand relative to coarse aggregate as the binder content was reduced. Sedran and de Larrard (1999) described how the compressible packing model can be used to predict yield stress, plastic viscosity, and constants representing filling/passing ability and segregation resistance. Vachon, Kaplan, and Fellaki (2002) utilized the compressible packing model to select aggregates for SCC.

2.2.2.2 Excess Paste Theory

The excess paste theory advanced originally by Kennedy (1940) was based on the amount of paste in excess of that needed to fill the voids between the aggregates. The excess

paste depends on the consistency of the paste and the surface area of the aggregates. The theory is based on the workability factor, K, which is the volume of excess cement paste divided by the surface area of the aggregate and multiplied by 10,000. It is related to the mixture proportions as shown in Equation (2.35):

$$x + a = N \left[\frac{w_s - w}{w_s} + \frac{KS}{10,000} \right]$$
(2.35)

where x is cubic feet of water per sack of cement, a is absolute volume of cement in cubic feet per sack, w_s is the specific weight of aggregate in pounds per cubic foot of absolute volume, w is the unit weight of aggregate in pounds per cubic foot of dry-rodded mixed aggregate, S is the aggregate surface area in square foot per cubic foot of dry-rodded mixed aggregate (neglecting the amount passing a No. 100 sieve), and N is the cubic feet of dry-rodded mixed aggregate per sack of cement. To use the equation, the water-cement ratio is selected for a given strength and the workability factor K is selected for the desired workability at that water-cement ratio.

The theory assumes that the layer of excess paste is equivalent for all size particles. Powers (1968) found that the procedure was too complicated given its degree of accuracy and suggested that the concept of a lubricating film of defined thickness around aggregates was questionable because deformations in the paste are much more complex.

The concepts of the excess paste theory have been applied to SCC. For instance, the mixture proportioning method described by Bui and Montgomery (1999) is based, in part, on the average spacing between aggregate particles, with the assumption that particles are spherical. The effects of shape and texture are taken into account separately by considering the dry-rodded unit weight of the aggregates. Midorikawa, Pelova, and Walraven (2001) applied the excess paste theory to mortar and developed the water layer theory for mortar based on the excess paste model. Instead of calculating the excess paste, the water layer model determined the volume of excess water in mortar. The model can be used to select an optimum sand content and to compare the effects of water and HRWRA. It was further determined that the ratio of water to powder could be calculated based on the thickness of the excess paste regardless of the aggregate used. Oh, Noguchi, and Tomosawa (1999) and Hasholt, Pade, and Winnefield (2005) have also used the excess paste theory.

2.2.2.3 Specific Surface Area (Day)

In the Conad Mixtune mixture design method developed by Day (1995), workability is based mainly on the specific surface of the combined aggregate. The modified specific surface is determined based on predetermined values for each sieve size. These values are applicable for all sands, regardless of particle shape. The effect of particle shape—along with other factors such as admixtures and SCMs—is taken into account when setting the water content. The system allows the user to specify the mix suitability factor (MSF), which describes the sandiness or cohesiveness of the concrete. The mix suitability factor is computed based on Equation (2.36):

$$MSF = SS_{CA} + 0.02c - 6 + 0.25(a - 1) \qquad (2.36)$$

where SS_{CA} is the specific surface of the combined aggregate, c is the cement content, and a is the entrained air content (%). The cement content is selected based on strength requirements once the water content is known. Therefore, the aggregate characteristics and associated water and cement contents can be adjusted to reach the desired MSF. The entire system has been computerized.

2.2.2.4 Shilstone Method

Shilstone (1990) and Shilstone and Shilstone (2002) presented an empirical method for developing mixture proportions based predominately on aggregate characteristics. The main focus of the method is on aggregate grading, as Shilstone (1990) found that the source of aggregate was "immaterial" but that the combined aggregate grading curve was important. Aggregates are considered in three fractions: larger than 3/8-inch (denoted "Q" for high quality), 3/8-inch to a No. 8 sieve (denoted "I" for intermediate size), and smaller than the No. 8 sieve (denoted "W" for workability). Shilstone faults current grading limits for not considering the combined aggregate grading and identifies three important considerations for selecting concrete proportions: the relationship between the coarseness of the Q and I fractions and the W fraction, the total amount of mortar, and the aggregate particle size distribution. For the first consideration, Shilstone recommends the coarseness factor chart, which plots the workability factor, or the percentage of material passing the No. 8 sieve corrected for cement content (W with correction), versus the coarseness factor, or the amount of material retained on the 3/8-inch sieve as a percentage of the material retained on the No. 8 sieve (Q/[Q+I]). The coarseness chart has predefined zones corresponding to fresh and hardened concrete performance descriptions.

Shilstone states that more sand is needed as the coarse aggregate becomes finer, whereas less sand is needed as the sands itself becomes finer. In general, the optimum sand content must be selected to prevent mixes from being too "sticky" or "boney". In selecting intermediate aggregates, Shilstone found that particle shape has a major effect in evaluating the contribution of materials retained on the No. 4 and No. 8 sieves. The amount of mortar, defined as sand passing the No. 8 sieve and paste, is said to influence strength, drying shrinkage, durability, creep, workability, pumpability, placeability, and finishability. The amount of mortar will range from 48 to 66 percent based on the construction needs. The lack of intermediate particles will require the use of more mortar. For aggregate grading, Shilstone states that there is an optimum combination of aggregates for each cement content and set of materials and recommends using the 0.45 power chart.

2.2.2.5 Water Requirement Equations

Powers (1968) summarizes a number of equations that express the quantity of water as a function of aggregate characteristics. By using these equations, aggregate characteristics such as grading or specific surface can be altered to yield the lowest water requirement. These equations predate the widespread use of chemical admixtures and supplementary cementitious materials.

2.2.2.6 American Concrete Institute

The ACI 211 (2002) standard practice for selecting concrete proportions is a simple and widely used empirical approach that determines indirectly the relative proportions of fine and coarse aggregate. The recommended values used in the practice are generally intended for well-graded aggregates. No explicit guidance is given on blending two or more aggregates.

The total volume of coarse aggregate in a concrete mixture is solely a function of the dry-rodded unit weight of the coarse aggregate, the fineness modulus of the fine aggregate, and the maximum aggregate size. Holding all other factors constant, the volume of coarse aggregate increases as the dry-rodded unit weight of the coarse aggregate is increased, the fineness modulus of the sand is decreased, or the maximum aggregate size—which is based on member dimensions—is increased. The absolute volume of fine aggregate depends on the volumes of all other ingredients—namely fine aggregate is used to fill the remaining volume after all other constituents have been selected. Therefore, the relative amount of coarse to fine increases not just when the volume of coarse aggregate increases, but also when the amount of cement and

water increase. The amount of cement increases when the desired compressive strength increases or the amount of water increases, thereby requiring more cement for the same water-cement ratio. The amount of mixing water increases with increased aggregate angularity (defined as crushed or rounded), increased desired slump, decreased maximum aggregate size, lack of air entrainment, or use of water-reducing admixtures. Although the use of air entrainment reduces the volume of required water and cement, the increase in volume of air is generally greater than the reduction in water and cement volume. In summary, the ratio of coarse aggregate volume to fine aggregate volume increases with increased dry-rodded unit weight of coarse aggregate, decreased fineness modulus of fine aggregate, increased maximum aggregate size, increased target compressive strength, use of angular instead of rounded coarse aggregate, increased desired slump, use of air entrainment, or the lack of water-reducing admixtures.

The ACI 211 approach provides a general first approximation of mixture proportions and requires trial mixtures and further modifications. Certain aspects of the procedure are oversimplified. For instance, the use of fine aggregate fineness modulus is inadequate to differentiate between sands. In 1940, Kennedy wrote that fineness modulus was "demonstrably unsound" and no longer used.

2.2.3 Rheology-Based Approaches

Freshly mixed concrete is a concentrated suspension of aggregates and cementitious materials in water; therefore, the concepts of suspension rheology can be applied to developing mixture proportions in general and to selecting aggregates in particular. The concepts described in this subsection were primarily developed for suspensions with particles sizes smaller than 0.1 mm but can be applied to both aggregates and cementitious materials.

The rheology of concentrated suspensions can be predicted by using phenomenological models or computer simulations. The phenomenological models average the effects of adjacent particles while computer simulations are capable of discretely determining the forces acting on individual particles. It is well known from empirical evidence that the rheology of suspensions depends on the solids volume concentration, the extent of agglomeration and flocculation, particle shape characteristics, and particle size distribution (Struble et al. 1998; Tsai, Botts and Plouff 1992). In general, only the particle size distribution, and not the absolute size, influences viscosity (Struble and Sun 1995; Mooney 1952). Phenomenological models express rheology as

a function of solids volume fractions with additional parameters to account for the extent of agglomeration and flocculation, particle shape characteristics, and particle size distribution. Frequently, these additional factors are accounted for with the maximum solids fraction, which is defined as the solids volume concentration at which particle interference makes flow impossible and the viscosity approaches infinity. A material with higher maximum solids fraction—due to favorable particle shape characteristics, particle size distribution, and lack of flocculation— results in lower relative viscosity at a given solids volume fraction (Barnes, Hutton, and Walters 1999).

In general, three types of forces act on particles in a suspension: colloidal forces, which cause a net attraction or repulsion between particles due to such factors as London-van der Waals forces and electrostatic charges; Brownian forces, which cause random motion and are most significant for particles smaller than 1 μm; and viscous forces, which are proportional to the velocity difference between particles and the surrounding medium (Barnes, Hutton and Walters 1989). The formation of flocculated structures increases the complexity of the system because the flocs enclose a portion of the medium and can form irregular shapes, thereby increasing viscosity. Upon the application of shear, these flocs may break apart. At low shear rates, Brownian and colloidal forces restore the random structure of the suspension. At higher shear rates, the Brownian and colloidal forces are insufficient and the particles become oriented based on the direction of flow. For most sizes of aggregates, only viscous forces are relevant. Colloidal forces and Brownian forces, however, cannot be neglected for the very smallest of aggregate particles.

Coussot and Ancey (1999) present a conceptual framework, which is shown in Figure 2.3, for evaluating various rheological behaviors in concentrated suspensions. Suspensions with low solids volume fractions and low shear rates exhibit shear-thinning behavior and are dominated by Brownian motion. As the concentration is increased, colloidal interactions dominate at low shear rates and the suspension exhibits viscoelasticity, thixotropy, and yield stress. If the shear rate is increased from the Brownian or colloidal interaction zones, hydrodynamic effects become predominant and the suspension behaves essentially as a non-colloidal suspension. At sufficiently high shear rates, turbulence occurs. Above a certain solids volume fraction (ϕ_c), which may vary by shear rate, a network of contacting particles exists and becomes significant for describing rheological behavior. Above ϕ_c, a distinction can be made

between brief collisions at high shear rates and sustained frictional contacts at low shear rates. As the shear rate is increased from the friction zone, a thin layer of fluid exists between particles due to repulsive forces between particles. This fluid layer lubricates the contacts.
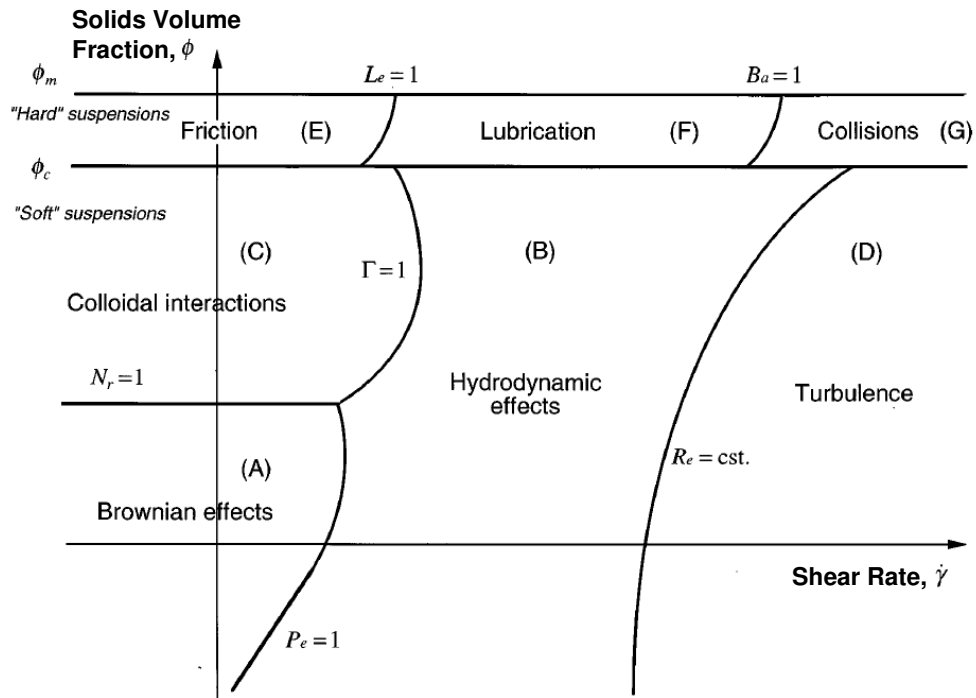
Figure 2.3: Conceptual Framework for Rheology of Concentrated Suspension (Coussot and Ancey 1999)

Multiple phenomenological equations have been developed to express the viscosity of a suspension as a function of the viscosity of the suspending medium, the solids volume fraction, and the characteristics of the particles. These equations are generally intended for dilute and semi-dilute suspensions, although attempts have been made to apply them to concentrated suspensions. As the solid volume concentration increases, particle interaction must be taken into account by averaging the effects of adjacent particles or by performing a computer simulation (Barnes, Hutton, and Walters 1989).

Einstein (1906, 1911) developed a basic equation for dilute suspensions (generally less than 10% solids volume fraction) of monosized spheres with no particle interaction, which is shown in Equation (2.37):

$$\eta = \eta_s \left(1 + 2.5\phi\right) \tag{2.37}$$

where η is the viscosity of the suspension, η_s is the viscosity of the suspending medium, and ϕ is the solids volume concentration. Numerous other equations have been developed subsequently to take into account higher solid volume concentrations, polydispersity, particle shape characteristics, and degree of flocculation (Honek, Hausnerova, Saha 2005). Particle interaction associated with higher volume fractions can be accounted for by adding higher order terms of ϕ to the Einstein equation. A generalized expression may be written as shown in Equation (2.38):

$$\eta \approx \eta_s \left(1 + [\eta]\phi + K_H \phi^2 + ...\right) \tag{2.38}$$

where $[\eta]$ is the intrinsic viscosity and K_H is the Huggins coefficient. Higher order terms than ϕ^2 are needed for concentrated suspensions. Barnes, Hutton, and Walters (1989) state that the intrinsic viscosity and Huggins coefficients are difficult to determine experimentally for shear flow.

Arrhenius (1917) developed a similar equation to Einstein's equation, as shown in Equation (2.39):

$$\eta = \eta_s \exp(2.5\phi) \tag{2.39}$$

Roscoe (1952) developed an equation for monosized spheres at higher concentrations than those covered by Einstein, as shown in Equation (2.40):

$$\eta = \eta_s (1 - 1.35\phi)^{-2.5} \tag{2.40}$$

The effects of particle interaction must be taken into account as the solids volume fraction is increased from a dilute suspension. When a particle is added to a suspension, it takes up more space than its own volume due to particle interaction. The well-known Krieger-Dougherty (1959) equation, which is an extension of the Einstein equation, takes into account the maximum solid fraction (ϕ_m), as shown in Equation (2.41):

$$\eta = \eta_s \left(1 - \frac{\phi}{\phi_m}\right)^{-[\eta]\phi_m} \tag{2.41}$$

Intrinsic viscosity is defined as the limit of the specific viscosity divided by the solids volume fraction as the solids volume fraction approaches zero, as given in Equation (2.42):

$$[\eta] = \lim_{\phi \to 0} \frac{\left(\dfrac{\eta}{\eta_s} - 1\right)}{\phi} \tag{2.42}$$

45

The intrinsic viscosity accounts for particle shape characteristics while the maximum solid fraction accounts for particle shape characteristics, degree of flocculation, and particle size distribution (Struble and Sun 1995). The intrinsic viscosity is 2.5 for spheres and increases with particle asymmetry. The maximum solid fraction and intrinsic viscosity vary with shear stress and shear rate (Barnes, Hutton, and Walters 1989; Struble and Sun 1995). Mansfield, Douglas, and Garbozci (2001) presented an approach for computing estimates of intrinsic viscosity for a variety of shapes.

The exponent in the Krieger-Dougherty equation (i.e., the negative product of the intrinsic viscosity and the maximum packing density) remains approximately constant for a wide range of materials because increasing particle asymmetry results in higher intrinsic viscosity but lower maximum solid fraction (Barnes, Hutton, and Walters 1989). Kitano, Katakoa, and Shirato (1981) utilized the Krieger-Dougherty equation with an exponent of -2. Tsai, Botts, and Plouff (1992) found the use of -2 as the exponent in the Krieger-Dougherty equation was appropriate for a range of non-colloidal suspension that varied in particle size distribution, shape characteristics, and density.

Martys (2005) suggested Equation (2.43) as an improvement on the Krieger-Dougherty equation to account for shape characteristics and polydispersity more accurately:

$$\eta = \eta_s \left(1 - \frac{\phi}{\phi_m}\right)^{-n} \left[1 + K_1 \frac{\phi}{\phi_m} + K_2 \left(\frac{\phi}{\phi_m}\right)^2 + \ldots\right] \tag{2.43}$$

where n is termed the critical exponent, $K_1 = \phi_m[\eta] - n$, and $K_2 = \phi_m^2 K_H - n\phi_m[\eta]\left(n - \frac{1}{2}\right)$.

The Krieger-Dougherty equation has been applied successfully to cement paste (Struble and Sun 1995) and concrete (Szecsy 1997). For cement paste dispersed with superplasticizer, Struble and Sun (1995) estimated the intrinsic viscosity to be approximately 5 and maximum solids volume fraction to be approximately 0.7. For concrete, Szecsy (1997) found it necessary to modify the Krieger-Dougherty equation with an empirical constant, C_t, which is a function of the percentage of sand and the water-cement ratio, as shown in Equation (2.44):

$$\eta = C_t \eta_s \left(1 - \frac{\phi}{\phi_m}\right)^{-[\eta]\phi_m} \tag{2.44}$$

Like the Krieger-Dougherty equation, the Mooney equation (1951), which is commonly expressed as shown in Equation (2.45), takes into account the intrinsic viscosity and the maximum solids volume fraction:

46

$$\eta = \eta_s \exp\left[\frac{[\eta]\phi}{\left(1 - \dfrac{\phi}{\phi_m}\right)}\right] \qquad (2.45)$$

(In the original presentation of the equation by Mooney, the intrinsic viscosity was set to 2.5 and the maximum solid fraction was replaced with $1/k$, where k was defined as the self-crowding factor.) According to Struble and Sun (1995), the Mooney equation is accurate for low volume concentrations but not for high volume concentrations. Roshavelov (1999 and 2005) applied the Mooney equation and a linear packing density model, which was utilized to compute analytically the crowding effects in a polydisperse system, to highly fluid concrete mixtures.

Farris (1968) developed an analytical method for calculating the effects of polydispersity on the viscosity of suspensions based on the known viscosity-concentration behavior of the unimodal components. The method assumed that the ratio of particle diameters in different size fractions was greater than 10, such that there is no interaction between components. The effect of adding a monosized fraction is expressed in terms of the stiffening factor, H, which reflects the increase in viscosity due to the addition of the fraction. Therefore, relative viscosity is defined based on Equation (2.46):

$$\eta_r = \prod_{i=1}^{N} H(\phi_i) \qquad (2.46)$$

The particles must be added in increasing size, such that ϕ_i is defined as the volume of the ith-fraction of particles divided by the volume of the liquid and all smaller particles. For example, the solids volume fraction of the mth-fraction is defined based on Equation (2.47):

$$\phi_m = \frac{V_m}{\displaystyle\sum_{i=0}^{m} V_i} \qquad (2.47)$$

Therefore, the total volume fraction is not the sum of the individual volume fractions. To account for particle interaction, a crowding factor, f, which varies from 0 to 1, can be applied. By optimizing Equation (2.46), Farris (1968) found that the lowest viscosity could be obtained as the number of monosized fractions becomes infinitely large. As the solids volume fraction is increased, the percentage of coarser particles relative to finer particles should be increased to obtain the optimum blend. If the concentration of coarse particles is high, the overall viscosity of the system can be increased by adding finer particles because the increase in volume fraction of

47

the finer particles is less than the decrease in volume fraction due to the reduction in volume fraction of coarser particles. As the total volume fraction is increased, the effect of particle size distribution increases, such that only optimized blends can be used at the highest volume fractions.

Barnes, Hutton, and Walters (1989) combined the Krieger-Dougherty and Farris equations for bimodal systems, as shown in Equation (2.48):

$$\eta = \eta_s \left(1 - \frac{\phi_1}{\phi_{m1}}\right)^{-[\eta_1]\phi_{m1}} \left(1 - \frac{\phi_2}{\phi_{m2}}\right)^{-[\eta_2]\phi_{m2}} \qquad (2.48)$$

Szecsy (1997) attempted to use this equation for concrete, but found it to be unacceptable.

He and Ekere (2001) accounted for particle size distribution in bimodal systems by utilizing a computer packing model to compute the maximum packing density, which was then used in a phenomenological equation for computing relative viscosity. On the basis of this approach, the authors concluded that relative viscosity decreased as the ratio of the diameter of the coarse particles to the diameter of the fine particles increased. The viscosity decreased as the ratio of coarse particles to total particles increased up to approximately 0.60 to 0.75, and then began to increase as this ratio was increased further. Struble et al. (1998) found that increasing the aggregate size increased yield stress and plastic viscosity; however, viscosity could be reduced by changing the ratio of fine to coarse aggregate to produce a higher packing density. Yield stress was minimum near the maximum packing density, but plastic viscosity was minimum at a lower sand content. Johansen and Andersen (1991), however, found that yield stress was minimum at the maximum packing density and that plastic viscosity was minimum at a higher sand content.

The alternative to applying a phenomenological equation is to utilize a computer model. Multiple computer modeling approaches are available for concentrated suspension (Barnes, Hutton, and Walters 1989; Martys 2005). Martys (2005, 402) developed computer code that utilizes dissipative particle dynamics (DPD), which he describes as a "somewhat abstract cellular-automata-based construction that, in certain regimes, recover hydrodynamics consistent with the Navier-Stokes equations" and finds it to be superior to existing fluid dynamics computational approaches.

The phenomenological equations for viscosity as a function of solids volume fraction and some computer models define viscosity as the apparent viscosity, which is shear stress divided by shear rate. The apparent viscosity is not equivalent to the plastic viscosity in the Bingham

equation. For a Bingham material, which is shown in Figure 2.4, the apparent viscosity decreases with increasing shear rate. For a shear-thinning fluid with or without a yield stress, the apparent viscosity would likewise decrease with increasing shear rate. Therefore, in applying the phenomenological equations, it is important to make comparisons with the apparent viscosity computed at well-defined shear rates. Roshavelov (2005) found that apparent viscosity and plastic viscosity were not correlated and that the apparent viscosity computed at high shear rates is the value that should be used in comparing results to phenomenological models.
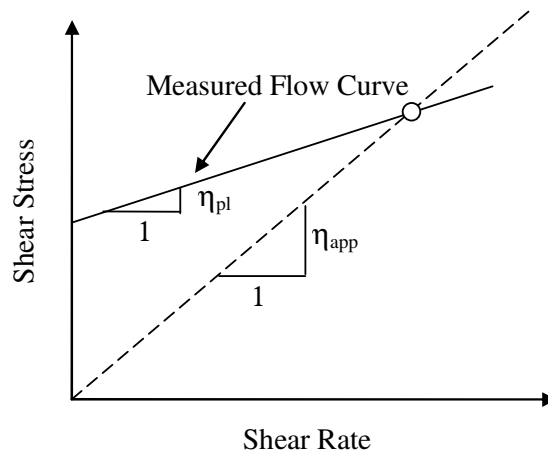
Figure 2.4: Illustration of Different Definitions of Viscosity

In applying rheology to concrete mixture proportions, several issues must be addressed. First, the presence of admixtures—or more accurately, the absence of admixtures—distorts predictions of rheology. Second, the rheology of cement paste changes with temperature and hydration. As cement particles interact with water, their effective size increases (Yahia, Tanimura, and Shimoyama 2005). Third, the lack of consensus on measurement techniques and on absolute values of rheological parameters means that rheology must be used predominantly to judge the relative effects of changes in materials and proportions. Fourth, rheology needs to be related to widely used empirical concepts of filling ability, passing ability, and segregation resistance. Although rheology can be useful in describing concrete flow, the mere knowledge of yield stress and plastic viscosity may be insufficient for predicting concrete performance. For instance, two concretes with the same rheological parameters but with different maximum aggregate sizes will exhibit different passing abilities.

49

2.3 Cement

SCC often has higher cementitious materials content than conventionally placed concrete in order to achieve adequate flowability. The potential negative consequences of high cementitious materials content include higher cost, higher heat of hydration, and increased susceptibility to shrinkage. All standard types of portland cements are generally acceptable for SCC (EFNARC 2002). Admixture performance can be strongly dependent on cement characteristics. For instance, Vikan, Justnes, and Winnefeld (2005) evaluated 6 different cements and found that the area under a rheological flow cure for cement paste was correlated to the cement characteristic given in Equation (2.49):

$$\text{cement characteristic} = a(Blaine[d(cubic C_3A) + (1-d)(C_3S)]) + b \qquad (2.49)$$

where a, b, and d are empirical factors. Cubic C_3A was included because it is considered more reactive than orthorhombic C_3A. Although C_3S is less reactive than C_3A, it was included because it is sufficiently reactive and is available in large quantity. The cubic C_3A and C_3S are multiplied by the Blaine fineness to reflect the amount of reactive material on the surface of the cement grain.

2.4 Supplementary Cementitious Materials

SCMs are often used in SCC to decrease cost, improve workability, reduce heat of hydration, and improve durability. The use of SCMs with no C_3S, C_3A, or C_4AF can make rheology easier to control (Aitcin 1998). Further, high-fineness powders decrease the size and volume of voids, which results in reductions in bleeding and segregation (Mehta and Monteiro 1993). Due to the reduction in early strength development in mixtures with fly ash or slag, the strength of such mixtures may need to be evaluated at ages beyond 28 days. In some cases, SCMs are used to reduce strength at certain ages because the amount of powder materials needed for workability would result in excessive strength if composed of only portland cement (Domone 2006). As by-products, SCMs may exhibit undesirable levels of variability.

2.4.1 Fly Ash

Fly ash has been used successfully in SCC (Domone 2006). The use of fly ash generally improves workability and delays strength development. In terms of rheology, fly ash reduces yield stress but may increase or decrease plastic viscosity. For example, Sonebi (2004) found

that the use of fly ash reduced both the yield stress and plastic viscosity of SCC. Park, Noh, and Park (2005), however, found that fly ash slightly reduced yield stress but increased the plastic viscosity of superplasticized pastes. Fly ash can also reduce bleeding and improve stability (Shadle and Somerville 2002). The influence of fly ash depends on whether cement is replaced with fly ash on a mass or volume basis. Compared to Class C fly ash, Class F fly ash reduces early strength development to a greater extent but is better for durability. Class C fly ash also delays time of set more than Class F fly ash. The reduction in early strength development for mixtures with fly ash can be offset with the use of an accelerator (Shadle and Somerville 2002).

Fly ash may contain unburned carbon. Park, Noh, and Park (2005) found that HRWRA can be adsorbed onto unburned carbon, reducing the workability.

High volume fly ash has also been used successfully in SCC (Patel et al. 2004; Christensen and Ong 2005). Additionally, ground fly ashes have been used for SCC. For instance, Xie et al. (2002) found that ultra-pulverized fly ash (UPFA) had an effect on the workability of SCC similar to that of a viscosity agent, in that it improved flowability without reducing viscosity. The optimum Blaine fineness of the UPFA was found to be 500-600 m^2/kg. The UPFA was found to increase mechanical properties and reduce drying shrinkage.

Classified fly ash, which consists of small fly ash particles separated from a parent fly ash, is another possibility for SCC. Unlike ground fly ash, classified fly ash retains a spherical shape. In fact, the particles can be more spherical and can reduce water demand to a greater degree than the parent fly ash. The small size of the classified fly ash increases the spread of the particle size distribution of the powder materials, which can also improve workability. For instance, Obla et al. (2003) reported on a classified fly ash with a mean particle size of 3 μm and 90% of material smaller than 7 μm. This smaller particle size increased the reactivity, leading to increased compressive strength and improved durability. Despite the smaller size, the use of classified fly ash reduced water demand and reduced drying and autogenous shrinkage. Even at an age of 1 day, the compressive strength could be maintained by using the classified fly ash and reducing the water-cement ratio to take advantage of the water reducing characteristics. Ferraris, Obla, and Hill (2001) found that classified fly ash reduced yield stress and plastic viscosity of pastes when used at an optimum cement replacement rate of 12%.

The ongoing implementation of various environmental regulations for coal-burning power plants continues to change the properties of fly ashes, resulting in important implications for concrete performance. The changes in fly ash quality depend on changes in federal

regulations, the implement of regulations by individual states, existing equipment in plants, the approaches used by power plant operators to comply with new regulations, and the type of coal burned.

Regulations requiring the reduction in emissions of nitrogen oxides (NO_x) from coal-burning power plants have had considerable consequences for the use of fly ash in concrete. NO_x emissions can be reduced by changing combustion systems, applying post-combustion treatments, or both (Golden 2001, US Department of Energy 2001, National Coal Council 2005). Changes to combustion systems aim to reduce the oxidation mechanisms responsible for NO_x emissions by reducing the combustion temperature or reducing the oxygen level. These changes can be accomplished by replacing older, single-stage burners with newer so-called "low-NO_x burners" or with the use of oven-fire air or reburning technologies. The use of low-NO_x burners typically increases the amount of unburned carbon, creates less spherical fly ash particles, increases the coarseness of particles, and increases the variability of the fly ash properties (Golden 2001).

Post-combustion treatments consist of applying ammonia (NH_3) or urea as apart of a selective catalytic reduction (SCR) or selective non-catalytic reduction (SNCR) processes. The ammonia and available oxygen react with NO and NO_2 to form nitrogen and water vapor. The processes are considered selective because they promote this particular reaction over other possible reactions. If a catalyst is used, it is typically solid (heterogeneous catalyst). The amount of ammonia applied to the flue gas must be optimized to reduce NO_x emissions to a sufficient degree while not leaving excessive amounts of unreacted ammonia on the fly ash, which is referred to as ammonia slip. The amount of ammonia slip depends not just on the amount of excess ammonia applied, but also on the capacity of the fly ash to adsorb ammonia. It is often economically advantageous, however, to reduce NO_x emissions to the greatest degree possible to take advantage of tradable emission credits even if it increases ammonia slip. When the fly ash is wetted during concrete mixing, ammonia gas is released. At low concentration levels, ammonia produces a noxious odor. At high levels, it can be toxic. Ammonia contents should generally be less than 50-100 ppm to avoid objectionable odors. It is generally agreed that the presence of ammonia does not detrimentally affect concrete properties; however, limited test data exist (Bittner, Gasiorowski, and Hrach 2001).

Several companies market technologies to mitigate the effects of lower fly ash quality on concrete properties (Golden 2001; Bittner, Gasiorowski, and Hrach 2001). The combustion of

coal can be optimized to reduce unburned carbon. Unburned carbon can be removed with carbon burn-out, particle size control, electrostatic precipitation, and wet separation. Several technologies are available to remove the ammonia from the fly ash, with dry processes preferable to wet processes.

2.4.2 Silica Fume

Silica fume has been used successfully in SCC (Domone 2006). Silica fume is generally known to increase cohesiveness and reduce segregation and bleeding (EFNARC 2005). It also increases compressive strength, modulus of elasticity, and flexural strength and enhances durability at all ages. This increase in strength may be particularly useful at early ages when silica fume is compared to other SCMs (Mehta and Monteiro 1993).

Silica fume may improve concrete rheology and enhance stability when used at low dosages—typically less than 4-6% by replacement of cement—but have detrimental effects on rheology at higher dosages. Any reduction in workability is generally due to silica fume's high fineness, which is offset at least partially by its spherical particle shape. According to Bache (1981 qtd. in Aitcin 1998) silica fume can improve workability because the spherical particles displace water molecules from the vicinity of cement grains so that entrapped water molecules between flocculated cement particles are freed. According to Park, Noh, and Park (2005), the high reactivity of silica fume particles can increase adsorption of HRWRA, which reduces the amount available in solution and on cement particles and, thereby, decreases workability. Detwiler and Mehta (1989) found that spherical carbon black with a similar grain size as silica fume resulted in similar workability.

For pastes designed for SCC, Vikan and Justnes (2003) found that adding silica fume at up to a 10% volume replacement increased yield stress. Plastic viscosity, however, was reduced when a polycarboxylate-based HRWRA was used and increased when a naphthalene-based HRWRA was used. The decrease in plastic viscosity was attributed to the displacement of water between cement grains and the spherical shape of the silica fume particles.

For superplasticized pastes, Park, Noh, and Park (2005) found that the use of silica fume at cement replacement rates of 5, 10, and 15% increased yield stress and plastic viscosity significantly. They suggested that silica fume be used to increase plastic viscosity to prevent segregation and that the sharp increase in yield stress be offset by the use of a ternary cementitious system with either fly ash or slag.

For conventionally placed concrete, Wallevik (1990, qtd. in Vikan and Justnes 2003) found that adding silica fume to concrete at replacement rates up to 6% significantly reduced plastic viscosity but had little effect on yield stress. Higher dosages of silica fume increased yield stress substantially but increased plastic viscosity more gradually.

2.4.3 Slag

Slag has been used successfully in SCC (Ozyildirim 2005; Billberg 2000; PCI 2003; Domone 2006). It is typically used at higher replacement rates than fly ash. It is effective in reducing heat of hydration and cost, but does not improve workability to the same extent as fly ash (Park, Noh, and Park 2005; Billberg 2000). Slag can contribute to compressive strength at ages as early as 7 days, which is faster than Class F fly ash but not fast enough for precast applications where release strengths are critical (Mehta 2001).

Chapter 3: Fresh Properties Literature Review

SCC is defined primarily in terms of its fresh properties; therefore, the characterization and control of fresh properties are critical to ensuring successful SCC performance. Fresh properties encompass all relevant characteristics of SCC prior to final setting, including flow properties, setting time, bleeding, and plastic shrinkage. Fresh properties influence not just constructability but also hardened properties like strength and durability. This chapter describes the fresh properties that are important in the production of SCC and presents available measurement techniques.

3.1   Flow Properties

Concrete flow properties are characterized in order to describe the workability of SCC. Requirements for workability can vary significantly depending on the application, even within the scope of SCC. As such, many methods are available to quantify various aspects of workability. Workability can be described in terms of specific field requirements or rheological properties.

3.1.1   Field Requirements

The workability requirements for SCC are typically defined in terms of three properties: passing ability, filling ability, and segregation resistance (EFNARC 2002). Filling ability describes the ability of concrete to flow under its own mass and completely fill formwork. Passing ability describes the ability of concrete to flow through confined conditions, such as the narrow openings between reinforcement bars. Segregation resistance describes the ability of concrete to remain uniform in terms of composition during placement and until setting. Various test methods are available to measure these properties; however, no test method exists to measure all of these properties at once. Given that these three properties are interrelated, most tests indirectly measure more than one property at a time.

Workability has also been defined in terms of static and dynamic stability (Dazcko 2002; Assaad, Khayat, and Mesbah 2003; Khayat, Assaad and Daczko 2004). Dynamic stability describes the concrete performance during the casting process. It is related to energy input—which may be from pumping, drop heights, agitation, or vibration—and passing ability—which

is affected by member dimensions and reinforcement bar spacing. Static stability describes the concrete performance immediately after energy input from casting until setting. It is related to paste rheology, aggregate shape and grading, and the density of the aggregates relative to the paste (Saak 2000; Saak, Jennings, and Shah 2001; de Larrard 1999).

Other aspects of the workability of SCC are typically improved relative to conventionally placed concrete. In general, the pumpability and finishability of SCC are improved relative to conventionally placed concrete (Bury and Christensen 2002). The formed surface finish is better due to the reduction in honeycombing and the number of bugholes (Martin 2002).

The retention of workability properties over time must be considered. Workability retention is not necessarily associated with setting time. For example, retarding admixtures can increase setting time while accelerating workability loss (Tattersall 1991).

3.1.2 Rheological Properties

Rheology, or the scientific study of the flow and deformation of matter, provides a direct approach to characterizing SCC flow properties (Koehler 2004). The goal of using rheology is to provide a consistent, repeatable, and scientific description of concrete flow properties. Fundamental rheological parameters are inherent to a material and, in theory, should be independent of the test device used. These rheological parameters can be used to compare the workability of different mixtures, to proportion new concrete mixtures, and to simulate concrete flow in computer models. It is possible to specify concrete mixtures in terms of rheological parameters. Rheological parameters, however, may not capture all relevant aspects of workability. For instance, passing ability depends primarily on aggregate characteristics and paste volume and cannot be predicted fully from rheological parameters.

The characterization of concrete rheology is based on the concept that concrete can be considered a fluid. Freshly-mixed concrete is essentially a concentrated suspension of aggregate particles in cement paste. The cement paste is a concentrated suspension of cement grains in water (Ferraris 1999). In contrast to an elastic solid—which undergoes a finite, recoverable deformation upon the application of load—a fluid deforms continuously under a constant shear stress and experiences no recovery of this deformation upon removal of the load. Therefore, in characterizing the fundamental flow properties of a material, the relationship between shear stress, τ, and shear rate, $\dot{\gamma}$, is considered. This relationship is represented graphically with a

56

flow curve. The behavior of a fluid material may be idealized with a constitutive relationship. Six such relationships equations are shown in Figure 3.1 (Hackley and Ferraris 2001).
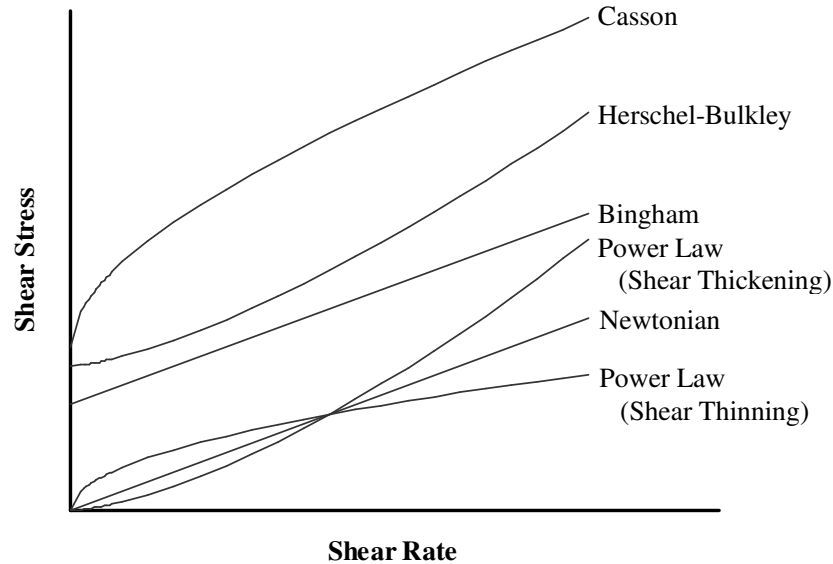
Figure 3.1: Constitutive Relationships for Fresh Concrete Plotted on a Flow Curve

The Bingham model is the most widely used constitutive relationship for concrete due to its simplicity and its ability to represent concrete flow accurately for the majority of cases (Ferraris 1999). The Bingham model requires the determination of only two parameters—yield stress, τ_0, and plastic viscosity, μ—as shown in Equation (3.1):

$$\tau = \tau_0 + \mu\dot{\gamma} \qquad (3.1)$$

In practical terms, yield stress represents the amount of stress to initiate or maintain flow while plastic viscosity describes the resistance to flow once the yield stress has been exceeded. Increased plastic viscosity results in greater resistance to flow. The apparent viscosity is equal to the shear stress divided by the shear rate at any given shear rate. Thus, for a Bingham material, the apparent viscosity decreases with increasing shear rate. Fluidity is defined as the inverse of viscosity.

For some concrete mixtures, the linear relationship between shear stress and shear rate is an oversimplification. The Herschel-Bulkley model incorporates two empirical constants, *a* and *b*, to represent non-linearity, as shown in Equation (3.2):

$$\tau = \tau_0 + a\dot{\gamma}^b \qquad (3.2)$$

If the yield stress is set to zero, the Herschel-Bulkley model describes a shear thinning or shear thickening power law fluid. Because some SCC mixtures can exhibit shear-thinning behavior (Khayat 2000), the variation in viscosity over a range of shear rates may need to be determined.

In terms of the Bingham parameters, SCC must exhibit a proper combination of yield stress and plastic viscosity in order to flow under it own mass and resist segregation. The yield stress is typically near zero to ensure that SCC will flow readily under its own mass; however, segregation can occur if the yield stress is too low. Plastic viscosity must be sufficiently high to prevent segregation, while not being too high that it restricts the speed of flow excessively.

Rheological parameters are most commonly measured with rotational rheometers. The use of rheometers is well established in many fields (Barnes, Hutton, and Walker 1989; Whorlow 1992); however, challenges exist in applying these concepts to concrete. Despite its ubiquity, concrete is a highly complex fluid with time-dependent properties and a wide range of particle sizes. Concrete rheometers are typically rate-controlled devices, such that a range of different shear rates is applied and the resulting shear stresses are measured. Typical geometrical configurations for concrete rheometers are shown in Figure 3.2. In a coaxial cylinders rheometer, one cylinder rotates relative to another, resulting in shear through the fluid between the walls of the outer and inner cylinders. The rotation of a parallel plate rheometer results in shear applied to the fluid due to a vertically and horizontally varying velocity distribution within the fluid. An impeller rheometer generates some average shear rate in the surrounding fluid that can be used in conjunction with available calibration methods to compute rheological parameters. A more complete description of available concrete rheometers is given in section 3.1.3.

Another important rheological property is thixotropy, which is defined as the reversible, time-dependent reduction in viscosity that occurs when a material is subjected to constant shear (Hackley and Ferraris 2001). Although thixotropy can be beneficial to SCC, its presence can complicate rheological measurements. Thixotropy has specific implications for lateral formwork pressures (Assaad, Khayat, and Mesbah 2003b), stability (Khayat 1999), and pumpability (Barnes 1997).

Coaxial Cylinders   *Parallel Plate*   *Impeller*
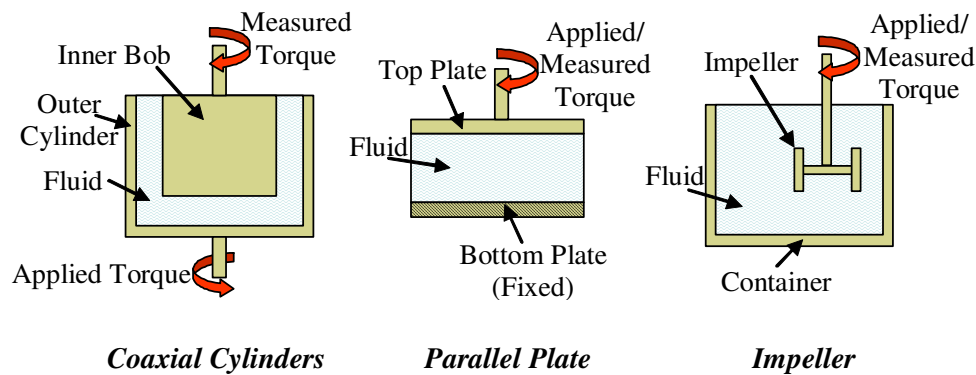
Figure 3.2: Typical Geometrical Configurations for Concrete Rheometers

Thixotropy is usually associated with flocculated suspensions, which typically exhibit a yield stress (Barnes, Hutton and Walters 1989). When a thixotropic material is at rest, a three-dimensional network structure develops over time due to factors such as bonding and colloidal forces. The application of shear causes a breakdown of this network structure and a reorientation or deformation of particles or flocs, resulting in a reduction in viscosity at a constant shear rate or shear stress. After shear is applied for sufficient time, the material reaches an equilibrium condition where the viscosity is at a minimum for the given shear rate or shear stress. When the application of shear is stopped, the three-dimensional network structure reforms and the original viscosity is eventually restored. This restoration is driven by Brownian motion, which in causing particles to move randomly also causes particles to move close enough to each other such that colloidal forces result in aggregation. Brownian motion applies mainly to particles with sizes less than 1 μm. Colloidal forces may also act on particles larger than 1 μm, resulting in aggregation even without Brownian motion. The at-rest fluid with maximum viscosity is sometimes referred to as a gel, whereas the flowing fluid with minimum viscosity is referred to as a sol. According to Barnes (1997), this concept of a gel-sol transition is more likely attributed to the presence of a yield stress or extreme shear thinning behavior, whereas the reduction in viscosity with time due to shearing is more accurately associated with thixotropy.

The transition between high viscosity and low is illustrated in Figure 3.3 for a stepwise, shear rate-controlled experiment. As the shear rate is increased instantaneously from rest to a constant value, the resulting shear stress in the fluid reaches its maximum value for the given shear rate. Over time, the shear stress decreases due to the thixotropic breakdown and eventually approaches a constant, equilibrium value. Then, when the shear rate is reduced to a lower value, the shear stress immediately decreases but then gradually increases to a new steady-state

59

equilibrium value as the three-dimensional network structure is partially rebuilt. An equilibrium shear stress is associated with each shear rate.
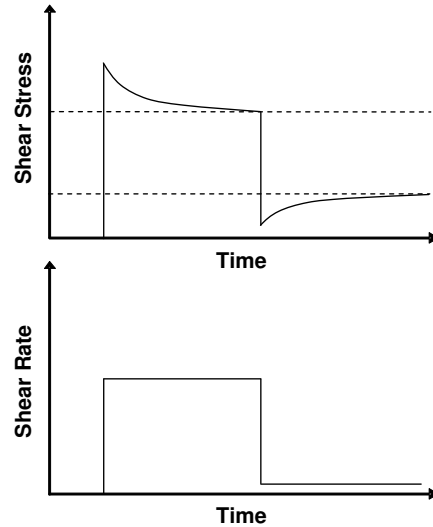
Figure 3.3: Effects of Thixotropy in Rate Controlled Time-Step Experiment

Thixotropy can manifest itself in flow curve measurements, as depicted in Figure 3.4. When the shear rate is initially increased from zero to the maximum value, the presence of thixotropy results in the measurement of shear stresses above their respective equilibrium values. Then, when the shear rate is decreased from a maximum value back to zero, the thixotropic breakdown that occurred during the up-curve measurement causes the down-curve to be below the up-curve. Although they do not explicitly mention thixotropy, Geiker et al. (2002) indicate that this flow curve hysteresis must be minimized when measuring flow curves for SCC by selecting an appropriate amount of time for each point. Doing so will avoid the effects of thixotropy while also minimizing effects due to setting and loss of workability.

The time for breakdown and recovery to occur depends on the fluid and, within the scope of concentrated suspensions, can vary from seconds to days. In general, the time required for rebuilding is much greater than the time for breakdown. Although rebuilding may take considerable time, 30-50% of the viscosity may be recovered quickly in the first few seconds or minutes (Schramm 1994). The speed of this initial recovery may be of greater consequence than the time to reach full recovery. Due to the reduced influence of Brownian motion, suspensions with larger particles typically exhibit faster breakdown times and slower rebuilding times than suspension with smaller particles (Barnes, Hutton, and Watlers 1989).

60
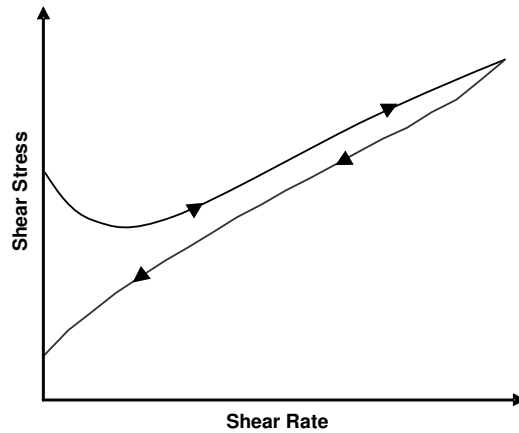
Figure 3.4: Manifestation of Thixotropy in a Flow Curve Measurement

Other fluid properties can result in similar behavior as thixotropy; however, these properties are unique and should be considered separately. First, materials can be both viscoelastic and thixotropic, as illustrated in Figure 3.5. Viscoelasticity causes a delay from the initial application of stress to the resulting final deformation (Barnes 1997). Thixotropy, however, is due to changes in the material structure while viscoelasticity is not. Second, some materials undergo an irreversible loss of viscosity, known as rheomalaxis or rheodestruction, due to such factors as sedimentation (Whorlow 1992). Third, thixotropy should not be confused with shear-thinning behavior, which describes the decrease in viscosity as a function of increasing shear rate, not shearing over time. Thixotropy typically occurs in shear-thinning fluids whereas anti-thixotropy, or the reversible, time dependent increase in viscosity during constant shearing, typically occurs in shear-thickening fluids (Barnes, Hutton, and Walters 1989).

A description of available techniques for quantifying thixotropy is provided in Section 3.1.3.3.
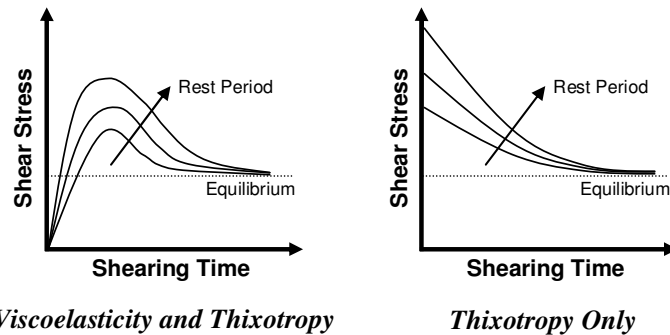
Viscoelasticity and Thixotropy   *Thixotropy Only*
Figure 3.5: Illustration of Distinction between Linear Viscoelasticity and Thixotropy (after Barnes 1997)

3.1.3 Test Methods

In selecting a test method or a series of methods for flow properties, it is important to know what each test is measuring and how this measurement can be related to field performance. Flow properties can be characterized in terms of empirical or rheological parameters. Empirical test methods typically involve the simulation of a relevant field placement condition and the measurement of a value—such as a time or distance—that serves as an index of workability. In contrast, rheological test methods measure fundamental parameters that, in theory, are not specific to the test device used. In reality, each rheometer available for cement, mortar, or concrete features various artifacts and variations in geometry and surface friction such that absolute results can vary widely (Ferraris and Brower 2001; Rahman and Nehdi 2003; Ferraris and Brower 2004). The following subsections describe available empirical and fundamental test methods.

3.1.3.1 Empirical Workability Test Methods

The available empirical workability test methods for SCC are categorized in Table 3.1 based on the property measured (filling ability, passing ability, or segregation resistance) and the type of stability considered (static of dynamic). These test methods are described in alphabetical order in the following subsections.

In addition to the distinctions made in Table 3.1 between static and dynamic tests, it is also possible to indirectly measure static stability with certain dynamic stability tests. Concrete can be placed inside a dynamic stability test apparatus, such as the v-funnel or l-box, and allowed to rest for a specified period of time. The results for tests with and without the rest period are compared to determine if segregation occurred during the rest period. In the v-funnel, for instance, the collection of coarse aggregate at the outlet of the funnel would result in an increased flow time or possibly a complete blockage. It must be cautioned that such delayed tests can also be influenced by thixotropy and loss of workability.

In evaluating empirical test methods, it must be remembered that empirical tests provide only an index of workability that may or may not be related to fundamental flow parameters. For instance, in testing conducted by Ferraris et al. (2000), the results of the v-funnel and u-box tests were not correlated to yield stress or plastic viscosity measurements as determined with the IBB rheometer and the BTRHEOM rheometer. Nielsson and Wallevik (2003) did find correlations

between plastic viscosity and T_{50}, orimet flow time, v-funnel flow time, and l-box flow time and between yield stress and slump flow; however, the scatter was described as "significant". Utsi, Emborg, and Carsward (2003) found that as long as only one rheological parameter was varied at a time, the rheological parameters measured with the BML viscometer were correlated to the results of the v-funnel and slump flow test; however, the scatter was high. Khayat, Assaad, and Daczko (2004) found that v-funnel results were a function of both yield stress and plastic viscosity.

Table 3.1: Empirical Test Methods for Flow Properties

Test Method	Properties Measured (EFNARC 2002)	Stability Type (Dazcko 2002)
Column Segregation Test	Segregation resistance	Static
Concrete Acceptance Test	Filling ability and passing ability	Dynamic
Electrical Conductivity Test	Segregation resistance	Static
Filling Vessel Test	Filling ability and passing ability	Dynamic
J-Ring	Passing ability	Dynamic
L-Box and U-Box	Filling ability and passing ability	Dynamic
Penetration Tests	Segregation resistance	Static
Segregation Test (Hardened Concrete)	Segregation resistance	Static
Settlement Column Segregation Test	Segregation resistance	Dynamic
Slump Flow (with T_{50} and VSI)	Filling ability and segregation resistance	Static/Dynamic
Surface Settlement Test	Segregation resistance	Dynamic
V-Funnel	Filling ability	Dynamic
Sieve Stability Test	Segregation resistance	Static

Many of the available empirical tests measure similar properties and, therefore, are correlated to each other to some degree. For instance, Khayat, Assaad, and Daczko (2004) found correlations between the results of the u-box, l-box, v-funnel, and j-ring tests.

Due to the lack of standardization of SCC test methods, the dimensions and details of the empirical test methods can vary within the literature. Dazcko (2003) lists dimensions of l-boxes, u-boxes, and j-rings reported by various researchers in the literature. Petersson, Gibbs, and Bartos (2003) found that variations in the amount wall friction, which is affected by test geometry and the smoothness of wall material, can have a significant influence on test results.

3.1.3.1.1   Column Segregation Test

The column segregation test (Daczko 2002; Assaad, Khayat, and Daczko 2004; ASTM C 1610), which is shown in Figure 3.6, consists of an 8-inch diameter, 26-inch tall PVC pipe split into four 6.5-inch tall sections. Each section is clamped together to form a water-tight seal. Concrete is placed into the pipe and left undisturbed for 15 minutes. Each section of the pipe is then removed and the concrete inside is collected. Each concrete sample is washed over a 5-mm (#4) sieve to retain all coarse aggregates, which are then dried. The coefficient of variation in coarse aggregate masses present in each of the four pipe sections is calculated as an indication of segregation resistance. Alternatively, the variation between just the top and bottom pipe sections can be determined. Similar tests have been presented by Rols, Ambroise, and Pera (1999); Lowke, Wiegrink, and Schiessl (2003); and El-Chabib and Nehdi (2006). Assaad, Khayat, and Daczko (2004) found that the column segregation test and the surface settlement test were affected by different factors and should be used as complementary tests.

PVC Pipe Sections:
Diameter: 8 inches
Height: 6.5 inches
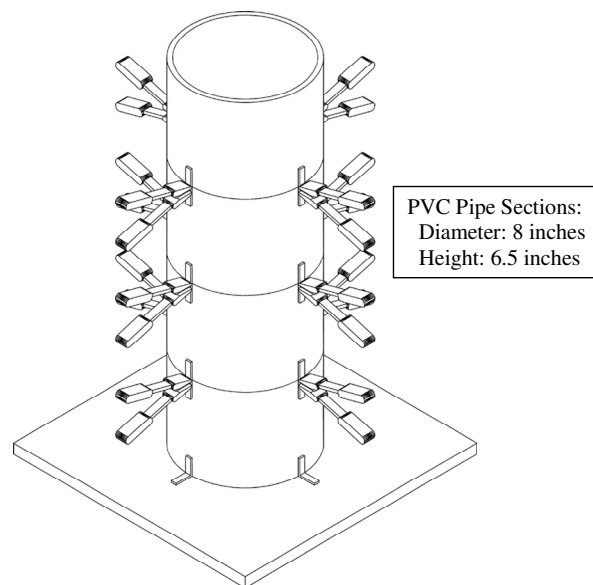
Figure 3.6: Column Segregation Test

3.1.3.1.2   Concrete Acceptance Test

The concrete acceptance test (Okamura and Ouchi 1999) is intended for use on a jobsite to verify that all concrete to be used exhibits suitable flow properties. The test consists of a 1200 mm wide, 1200 mm long, and 300 mm tall box that is positioned between the chute of a mixing truck and the hopper of a pump. Three sides of the box are enclosed while the fourth side

features a series of staggered reinforcing bars. Concrete is discharged on the side opposite of the reinforcement bars. The concrete is assessed based on whether it flows horizontally and passes through the reinforcing bars. The original device has been modified by Kubo et al. (2001) to add more obstacles for the concrete to pass and by Wantabe et al. (2003) to increase capacity.

3.1.3.1.3   Electrical Conductivity Test

The electrical conductivity test (Khayat et al. 2003; Assad, Khayat, and Daczko 2004) measures the bleeding and segregation resistance of mortar by monitoring changes in ionic conductivity throughout a column specimen. The apparatus consists of a vertical probe with 5 stainless steel electrodes spaced 60 mm apart. The probe is immersed into a 100-mm diameter, 350-mm tall cylindrical column of mortar and changes in conductivity between each of the 4 pairs of electrodes are measured for 150 minutes. Changes in conductivity reflect changes in the mortar composition due to segregation and bleeding. Stability is determined quantitatively with two segregation indexes, two bleeding indexes, and two homogeneity indexes.

3.1.3.1.4   Filling Vessel Test (Fill Box Test, Simulated Filling Test, Filling Capacity Box, Kajima Test)

The filling vessel test (EFNARC 2002; Bartos, Sonebi, and Tamimi 2002) measures the filling ability, passing ability, and segregation resistance of SCC. The apparatus consists of a clear plastic box with 35 plastic or copper 20-mm diameter bars, as shown in Figure 3.7. An early version of the test featured a wedge shaped box instead of a rectangular box and did not include a funnel. Concrete is poured at a constant rate into the funnel and allowed to flow into the box until the height of the concrete reaches the height of the top row of bars.
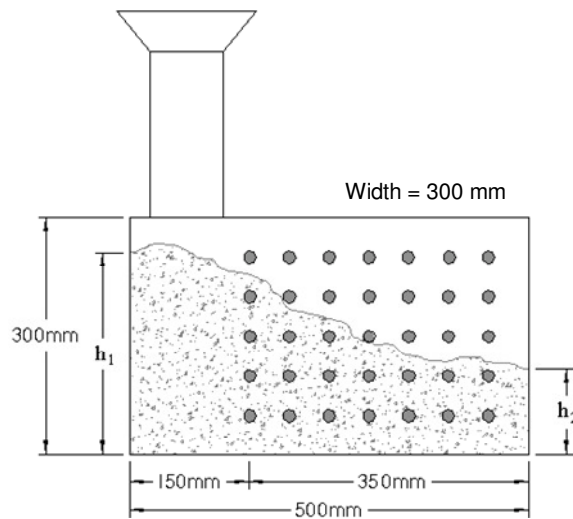
Figure 3.7: Filling Vessel

The height of the concrete at the side nearest the funnel, h_1, and the height at the opposite side, h_2, are used to calculate the average filling percentage as shown in Equation (3.3):

$$\text{Filling Percentage} = \frac{(h_1 + h_2)}{2h_1} \times 100\% \tag{3.3}$$

The closer the filling percentage is to 100%, the greater are the filling and passing abilities of the concrete. If a mixture exhibits a high slump flow but low filling percentage, this behavior could indicate that the mixture has high plastic viscosity, poor passing ability, or poor resistance to segregation. The test is a good representation of actual placement conditions; however, it is bulky and difficult to perform on site.

A similar simulated soffit test (Bartos, Sonebi, and Tamimi 2002) consists of a rectangular box with reinforcing bars placed in the box in an arrangement that simulates actual placement conditions for a given job. The reinforcing bars can be both horizontal and vertical. Concrete is placed in the box in a similar manner as with the filling vessel test. After the concrete is allowed to harden, saw-cut sections of hardened concrete are removed to judge how well the concrete filled the box and passed around reinforcing bars.

3.1.3.1.5   J-Ring Test

The j-ring test (EFNARC 2002; Bartos, Sonebi, and Tamimi 2002, ASTM C 1621) extends common filling ability test methods in order to characterize passing ability. The j-ring test device can be used with the slump flow test, orimet test, or v-funnel test. The j-ring, as

shown in Figure 3.8, is a rectangular section (30 mm by 25 mm) open steel ring with a 300-mm diameter. Vertical holes drilled in the ring allow smooth or deformed reinforcing bars to be attached to the ring. Each bar is 100 mm long. The spacing of the bars can be adjustable.

Figure 3.8: J-Ring

To conduct the j-ring test in conjunction with the slump flow test, the slump cone is placed in the center of the j-ring and filled with concrete. The slump cone is lifted and concrete is allowed to spread horizontally through the gaps between the bars. Alternatively, the orimet device or the v-funnel can be positioned above center of the j-ring. Instead of measuring just the time for concrete to exit the orimet or the v-funnel, the concrete is also allowed to spread horizontally through the j-ring.

Various interpretations of the test results have been suggested. The measurements of passing ability and filling ability are not independent. To characterize filling ability and passing ability, the horizontal spread of the concrete sample is measured after the concrete passes between the bars of the j-ring and comes to rest. The horizontal spread with the j-ring can be compared to that without the j-ring. Also, the difference in height of the concrete just inside the bars and just outside the bars is measured at four locations. In addition, Daczko (2003) has suggested assigning a visual blocking index (VBI) rating, in accordance with Table 3.2, based on the appearance of the concrete after the test. Daczko (2003) found that the j-ring was able to distinguish the ability of concrete to flow through obstacles better than the l-box or u-box and suggested using just the j-ring slump flow value for quality control purposes instead of the both the j-ring slump flow and the unrestricted slump flow.

Table 3.2: Visual Block Index Ratings (Daczko 2003)

VBI	Description
0	No evidence of blocking resulting in a pile of coarse aggregate in the middle of the patty and no evidence of bleed streaking behind the rebar obstacles.
1	A slight pile of coarse aggregate in the middle of the patty and slight evidence of bleed streaking behind the rebar obstacles.
2	A clear pile of coarse aggregate in the middle of the patty and significant bleed streaking.
3	Significant blocking of aggregate behind the rebar obstacles, will usually result in a significant decrease in flow value.

3.1.3.1.6 L-Box and U-Box Tests

The l-box and u-box tests (Kuriowa 1993; EFNARC 2002; Bartos, Sonebi, and Tamimi 2002), which are shown in Figure 3.9, measure the filling and passing ability of SCC. In the case of the l-box, concrete is initially placed in the vertical portion of the box. The gate is opened and concrete is allowed to flow through a row or reinforcement bars and into the horizontal portion of the box. The times for concrete to reach points 200 mm (T_{20}) and 400 mm (T_{40}) down the horizontal portion of the box are recorded. After the concrete comes to rest in the apparatus, the heights of the concrete at the end of the horizontal portion, H_2, and in the vertical section, H_1, are measured to compute the blocking ratio, H_2/H_1. Segregation resistance can be evaluated visually immediately after the test or the concrete can be allowed to harden and samples can be cut for further evaluation (Tanaka et al. 1993).

For the u-box, concrete is filled into one side of the box, the gate is opened, and concrete is allowed to flow through a row of reinforcement bars and into the other half of the box. Measurements are made of the time for concrete to cease flowing and of the heights on either side of the box.

Khayat, Assaad, and Daczko (2004) found correlations between the results of the u-box and l-box tests; however, there was much scatter. The l-box was found to be preferable because it gives more information about filling ability. Further, the combination of l-box and slump flow tests was found to be preferable to a combination of j-ring and slump flow tests.
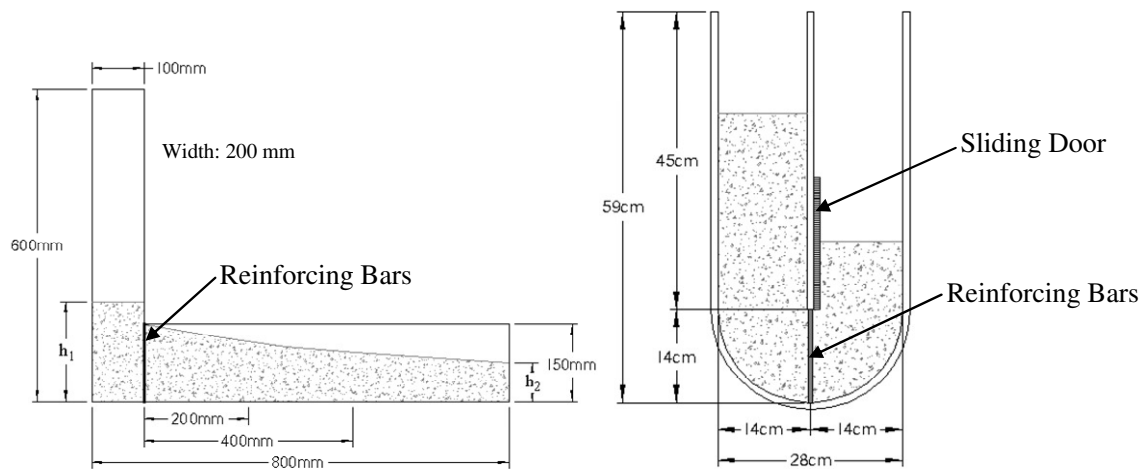
Figure 3.9: L-Box (Left) and U-Box Test Apparatus

3.1.3.1.7   Penetration Tests for Segregation Resistance

Two similar test methods, which were developed independently, measure the penetration resistance of concrete as a means of determining segregation resistance. The penetration resistance should be related to the yield stress of the concrete. The tests further make use of the fact that the settlement of coarse aggregate in SCC results in a mortar-rich region at the top of a SCC specimen, which may reduce the resistance to penetration. The test methods involve placing concrete in a column, allowing the concrete to remain at rest for a specified period of time, and measuring the condition of the material at the top of the column.

In the penetration test (Bui, Akkaya, and Shah 2002; Bui et al. 2002), SCC is placed in a container of sufficient size such that edge effects can be neglected. The top surface of the SCC is leveled and a penetration head, which is depicted in Figure 3.10, is positioned just above the surface of the concrete. In one implementation of the test, the concrete is allowed to remain undisturbed for 2 minutes before the penetration head is released into the concrete. The penetration depth after 45 seconds is recorded. A total of three such measurements are averaged. For a 54-gram penetration head, a penetration depth less than 8 mm was found to indicate acceptable resistance to segregation.

The segregation probe (Shen, Struble, and Lange 2005) consists of a 1/16-inch steel wire wrapped in a 5-inch diameter ring with a 6-inch vertical portion. Concrete is placed in a 6-inch by 12-inch cylinder and left undisturbed for two minutes. The probe, with a mass of 18 grams, is placed atop the concrete is allowed to settle under its own mass for one minute.

69
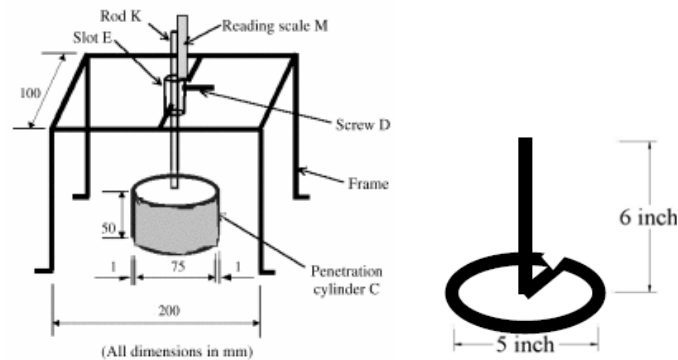
Figure 3.10: Penetration Apparatus (Left) and Segregation Probe (Bui, Akkaya, and Shah 2002; Shen, Struble, and Lange 2005)

3.1.3.1.8 Segregation Test (Hardened Concrete)

Multiple researchers have cast concrete in forms of various dimensions, allowed the concrete to harden, and then cut the concrete into sections to assess the distribution of coarse aggregates. For instance, the surface settlement test specimen can be used after it has hardened. Daczko (2002) used a rectangular column measuring 6 by 11 by 33.5 inches. Cussigh, Sonebi, and De Schutter (2003) suggest using an approach developed by Sedran where the depth to the first two coarse aggregates in a 160- by 320-mm cylinder is measured, with depths greater than 10 mm considered indicative of segregation susceptibility. Shen, Struble, and Lange (2005) cut a 6- by 12-inch cylinder in half and evaluated the distribution of coarse aggregate either with image analysis software or by assigning a visual rating on a scale of 0 to 3, with 0 indicating stability and 3 indicating severe segregation.

3.1.3.1.9 Settlement Column Segregation Test

The settlement column segregation test (Bartos, Sonebi, and Tamimi 2002) is similar to the column segregation test with the main exception that concrete in the settlement column segregation test is subjected to jolting on a drop table. The test apparatus consists of a tall, rectangular box mounted on top of a standard mortar drop table. The column, depicted in Figure 3.11, is 500 mm tall and has cross sectional dimensions of 100 by 150 mm. Three doors on opposing sides of the column allow sections of concrete to be removed at the conclusion of the test. To begin the test, concrete is placed in the column and left undisturbed for one minute. The concrete is subsequently jolted 20 times in one minute using the drop table and then left undisturbed for an additional 5 minutes. The samples from the top and the bottom of the column

70

are individually washed through a 5-mm sieve to leave only the coarse aggregate. The segregation ratio is calculated as the ratio of the mass of coarse aggregate in the top sample to the mass of coarse aggregate in the bottom sample.
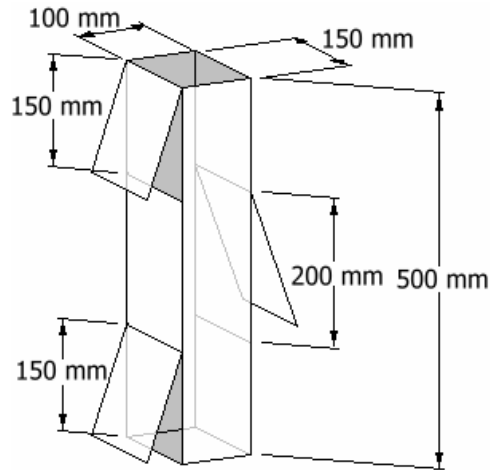
Figure 3.11: Settlement Column Segregation Test

3.1.3.1.10 Slump Flow Test (with T_{50} and Visual Stability Index)

The simplest and most widely used test method for SCC is the slump flow test (Kuroiwa et al. 1993; EFNARC 2002; Bartos, Sonebi, and Tamimi 2002; ASTM C 1611), which is pictured in Figure 3.12. To perform the test, a conventional slump cone is placed on a rigid and level non-absorbent plate and filled with concrete without tamping. The slump cone can be placed in the conventional upright orientation or inverted. The slump cone is lifted and the horizontal spread of the concrete and the time for the concrete to spread to a diameter of 500 mm (T_{50}) are measured. Emborg et al. (2003) has suggested measuring the time to flow to a diameter of 600 mm instead of 500 mm, given the available of more fluid mixtures. It is possible to assess the stability of the concrete qualitatively after performing the slump flow test. The visual stability index (VSI), the criteria for which are shown in Table 3.3, is assigned to the nearest 0.5 based on a visual evaluation of the final test specimen. According the Khayat (1999), the lack of material separation during the slump flow test is not an assurance of stability during and after placement. Khayat, Assaad, and Daczko (2004) recommend using the VSI in conjunction with other tests for stability.

Figure 3.12: Slump Flow Test

Table 3.3: Visual Stability Index Ratings (ASTM C 1611)

VSI	Criteria
0 = Highly Stable	No evidence of segregation or bleeding.
1 = Stable	No evidence of segregation and slight bleeding observed as a sheen on the concrete mass.
2 = Unstable	A slight mortar halo ≤0.5 in. (≤10 mm) and/or aggregate pile in the center of the concrete mass.
3 = Highly Unstable	Clearly segregating by evidence of a large mortar halo >0.5 in. (>10 mm) and/or a large aggregate pile in the center of the concrete mass.

3.1.3.1.11   Surface Settlement Test

The surface settlement test (Khayat and Guizani 1997; Assaad, Khayat, and Daczko 2004) measures the settlement of a plate on a column of concrete until setting. Surface settlement is related to segregation resistance. In the test, which is shown in Figure 3.13, concrete is placed in a 200-mm diameter, 800-mm tall PVC pipe and filled to a height of 700 mm. A 4-mm thick, 150-mm diameter acrylic disc is set atop the leveled SCC surface. Three 75-mm screws extend downward from the disc to anchor the disc into the concrete. A dial gage, linear variable differential transformer, or non-contact method is used to monitor the settlement of the disc over time. The first reading is taken at 60 seconds followed by subsequent readings every 15 minutes for the first three hours and every 30 minutes thereafter. The container is covered throughout the test to prevent evaporation. The total settlement—expressed as a percentage of the initial column height, should be less than 0.50% for stable SCC. Assaad, Khayat, and Daczko (2004) found that the results of the test were not correlated to yield stress or plastic viscosity. Unlike the penetration apparatus, the surface settlement test depends on the duration of the dormant period (Assaad, Khayat, and Daczko 2004).
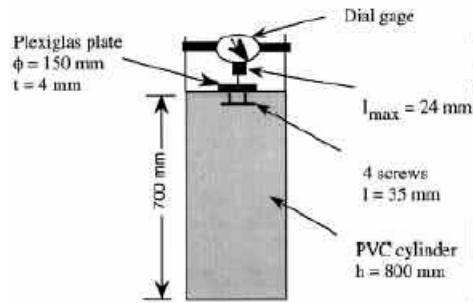
Figure 3.13: Surface Settlement Test (Khayat 1999)

3.1.3.1.12 V-Funnel Test

The v-funnel test (EFNARC 2002; Bartos, Sonebi, and Tamimi 2002), which is shown in Figure 3.14, is primarily used to measure the filling ability of SCC and can also be used to evaluate segregation resistance. To perform the test, the funnel is filled with concrete without tamping or vibration and the concrete is left undisturbed for 1 minute. Then, the gate at the bottom of the funnel is opened and the time for all concrete to exit the funnel is recoded.
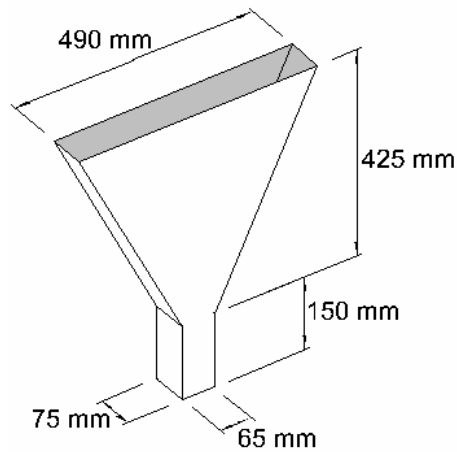
Figure 3.14: V-Funnel

In addition to reporting the flow time, the average flow through speed, V_m, can be calculated as shown in Equation (3.4):

$$V_m = \frac{0.01}{(0.065 \times 0.075) \times t_0} = \frac{2.05}{t_0}(m/s) \tag{3.4}$$

Non-uniform flow of concrete from the funnel suggests a lack of segregation resistance. According to Khayat (1999), a long flow time can be due to high paste viscosity, high

interparticle friction, or blockage of flow by coarse aggregates. Likewise, Emborg et al. (2003) found that v-funnel results were related to concrete viscosity, passing ability, and segregation resistance. Therefore, the test results may not identify the true cause of a slow flow time.

The opening size at the bottom is typically 75 x 75 mm or 75 x 65 mm. Emborg et al. (2003) has suggested using a 75 x 49 mm opening to increase the sensitivity of the measurement. In addition, a smaller version of the v-funnel is available for measurements of mortar or paste.

3.1.3.1.13 Sieve Stability Test (Vertical Mesh-Pass Tests, GTM Screen Stability Test)

The sieve stability test (EFNARC 2002; Bartos, Sonebi, and Tamimi 2002; Patel 2004), which was developed by the French contractor GTM Construction, measures the ability of SCC to remain uniform under both dynamic and static conditions. To perform the test, a 10-liter sample of concrete is placed in a sealed bucket and left undisturbed for 15 minutes to allow segregation to occur. Then, approximately 2 liters or 4.8 kg from the top of the concrete sample is poured from a height of 500 mm onto a 5-mm (#4) sieve. Mortar from the sample is allowed to flow through the sieve into a lower pan for a period of 2 minutes. The ratio of the mass of material in the pan to the total mass of concrete poured over the sieve is taken as the segregation ratio. It has been reported that the variability of test results is poor, especially when the segregation is severe (Bartos, Sonebi, and Tamimi 2002). Cussigh, Sonebi, and De Schutter (2003) found that the results of the sieve stability test were correlated with the results of the penetration apparatus test developed by Bui.

3.1.3.2 Fundamental Rheology Measurements

Multiple concrete rheometers—with various designs, advantages, and limitations—are available for measuring concrete. Most concrete rheometers are designed to measure a broader range of concrete than just SCC; however, they are particularly well suited for measurements of SCC. Highly fluid concrete mixtures, such as SCC, behave more like homogenous fluids than stiffer, less fluid concrete mixtures and, therefore, can be measured with greater accuracy and repeatability. Unlike concrete, mortar and paste do not require specially designed rheometers.

Concrete rheometers generally function by a applying a specified pre-shear regime to achieve thixotropic breakdown and then sweep the shear rate from high to low, during which time the relationship between torque and rotation speed is measured. In traditional rheological measurements, the shear rate throughout the rheometer is known analytically. In concrete

measurements, however, the yield stress and the presence of large aggregates make the determination of the distribution of shear stress and shear rate throughout the rheometer significantly more complicated (Mork 1996). The available concrete rheometers take various approaches to converting torque versus rotation speed data to yield stress and plastic viscosity. In general, the approaches can be split between those that provide relative units and fundamental units. To compute relative units, a straight line is fit to the torque (*T*) versus rotation speed (*N*) data. In the Tattersall two-point device, the intercept of this line is termed the "*g*-value" and the slope is referred to as the "*h*-value." It is assumed that the *g*-value is related to yield stress and the *h*-value to plastic viscosity. Other concrete rheometers have used this same naming convention, which is shown in Equation (3.5). This naming convention does not appear to be used in rheological measurements for anything other than cement-based materials. The *g*-value should not be confused with the shear modulus, which is denoted with a capitalized *G*.

$$T = g + hN \tag{3.5}$$

The calculation of results in fundamental units, based on the Bingham model (yield stress and plastic viscosity) or Herschel-Bulkley model (yield stress, *a*, and *b*), requires calibration or certain assumptions about distributions of shear stress and shear rate throughout the rheometer (Koehler 2004).

Several available concrete rheometers are pictured in Figure 3.15. The BML viscometer (Gjorv 1998; Ferraris and Brower 2001; Bartos, Sonebi, and Tamimi 2002; Ferraris and Brower 2004) and the ICAR rheometer (Koehler 2004) feature coaxial cylinders designs. The BML viscometer, which is intended for use in the laboratory, includes a rotating outer cylinder and fixed inner cylinder. The inner cylinder consists of vertical blades to prevent slippage. The ICAR rheometer is a portable rheometer intended for use in the field. It features a 5-inch diameter vane that is rotated in a container of concrete. The size of the container depends on the aggregate size.

The BTRHEOM rheometer (de Larrard et al. 1997; de Larrard 1999; Ferraris and Brower 2001; Bartos, Sonebi, and Tamimi 2002; Ferraris and Brower 2004) is a rate-controlled parallel plate rheometer. A simplified version of the BTRHEOM rheometer was developed to eliminate several drawbacks of the original device (Szecsy 1997).

The Tattersall two-point device (Tattersall and Bloomer 1979; Cabrera and Hopkins 1984; Tattersall 1990; Tattersall 1991; Ferraris and Brower 2001; Bartos, Sonebi, and Tamimi 2002; Ferraris and Brower 2004) and the IBB rheometer (Beaupre, Mindess, and Pigeon 1994;

Ferraris and Brower 2001; Bartos, Sonebi, and Tamimi 2002; Ferraris and Brower 2004) are impeller-type rheometers. The Tattersall device was one of the earliest attempts to measure the rheology of concrete based on the Bingham model and one of the first devices to use an impeller geometry. It features either a helical or H-shaped impeller and can be calibrated to compute results in fundamental units. The IBB rheometer is essentially an updated version of the Tattersall device. It features an H-shaped impeller and computes results in terms of g and h.

Other available rheometers include the Bertta apparatus (Leivo 1990; Ferraris 1999), the FHPCM (Yen et al. 1999; Tang et al. 2001), the CEMAGREF-IMG (Coussot and Piau 1995), and the falling-ball rheometer (Buchenau and Hillemeier 2003).

Figure 3.15: Concrete Rheometers (Clockwise from Top Left): BML, BTRHEOM, Tattersall, and IBB

3.1.3.3 Thixotropy Measurements

No single standard method is available for measuring thixotropy. Of the methods that are available, each has certain disadvantages and limitations. In fact, Barnes (1997) states that thixotropic behavior, including its experimental characterization and theoretical description, is "one of the greatest challenges facing rheologists today." Ideally, test methods should isolate thixotropy from effects due to setting or loss of workability and should differentiate between thixotropy and rheomalaxis and between thixotropy and viscoelasticity. In practice, few methods are able to achieve these goals.

Several approaches to measuring thixotropy have been applied to a wide range of different fluids. One such approach is to perform a loop test in a rheometer. In this test, the shear rate is increased from zero to a maximum value and returned to zero. This cycle can be repeated until the down flow curve measurement remains constant. The area between the maximum up and minimum down curve is calculated as an indication of thixotropy. The imposed shear rates or shear stresses can be changed in a continuous or stepwise manner. To avoid repeated flow curve measurements, Schramm (1994) suggests measuring the up curve, then maintaining the maximum shear rate until full thixotropy breakdown is achieved, and then measuring the down curve. Instead of measuring the area between the up and down curves, Whorlow (1992) suggests monitoring changes in the down curve after different shear histories, provided the down curve can be measured as quickly as possible. The loop test approach to thixotropy characterization suffers several limitations. First, the area between the up- and down-curves depends in part on the amount of time for the time for measurement of each shear rate or shear stress point on the flow curve (Whorlow 1992). Further, the initial up curve can be influenced by the initial elastic response of the fluid (Barnes 1997).

A second approach to measuring thixotropy is to perform a step-wise test, similar to that shown in Figure 3.3, where the shear rate or shear stress imposed by a rheometer is changed from one constant value to another and the break-down or build-up in shear stress or shear rate is monitored. The percentage of build-up or break-down and the time for equilibrium to be achieved can be determined (Whorlow 1992). Barnes (1997) calls this approach "simpler and more sensible" than the loop test approach. Still, it is not possible to eliminate the effects of an initial elastic response (Barnes 1997). Whorlow (1992) points out that it is important to check that the material at one shear rate is representative of the behavior at other shear rates.

A third approach is to use a start-up (or stress-growth) test where a constant strain or stress is applied to a material initially at rest (Barnes 1997). The thixotropy is indicated by the overshoot in stress for a strain-controlled test or by the increase in slope in the strain-time curve for stress-controlled tests.

In using any of these three approaches, it is important that the shear history prior to testing is well-known (Schramm 1994, Barnes 1997). Sources of this pre-testing shear could be from mixing, pumping, or filling the rheometer. The variability from shear history can be minimized by using a fixed rest period, by pre-shearing the sample for a certain time followed by a rest period, or pre-shearing the sample at a low speed followed by testing at a higher speed (Barnes 1997).

Researchers have attempted to apply these and several other approaches to concrete. In making measurements of concrete, it is often convenient to test only the mortar or paste fractions because the causes of thixotropy are primarily associated with the paste. In measuring concrete, it is important to distinguish between thixotropy and rheomalaxis, to minimize the effects of setting and workability loss, and to isolate certain viscoelastic effects. The determination of thixotropy in concrete is complicated because the definition of thixotropy is not clear for concrete. For example, non-equidimensional aggregates can reorient under shear, resulting in a reduction in viscosity. Brownian forces do not affect aggregates, so a rest period cannot alone restore the loss in viscosity caused by the reorientation of non-preferentially aligned aggregates. If the concrete is sheared in a direction other than that used in the original test, the aggregates are not in preferential alignment for the new direction of shear and, therefore, can contribute to an increase in viscosity as measured in the new direction. In this sense, it is debatable whether aggregates contribute to thixotropy according to the strict definition; however, their role is relevant when considering constructability issues such as formwork pressure and static segregation resistance. In addition, changes to the aggregates may not affect thixotropy directly; however, such changes may affect the required paste rheology needed to achieve proper concrete workability. These required changes in paste rheology can affect concrete thixotropy.

Assaad and Khayat (2003) and Assaad and Khayat (2004) used the loop test approach for measuring the thixotropy of mortar and concrete, but with some modifications. The IBB rheometer, which was fitted with a coaxial vane instead of the normal H-shaped impeller, was used to measure individual structural breakdown curves by applying separately constant rotation speeds of 0.3, 0.5, 0.7 and 0.9 rps over a period of 25 seconds and measuring the reduction in

shear stress. The specimens were re-homogenized and allowed to rest for 5 minutes between the tests at each speed. The initial and equilibrium shear stresses were taken from the structural breakdown curves and used to compute two separate flow curves. The area between these two flow curves was determined as an indication of thixotropy. This approach was time-consuming and did not distinguish thixotropy from rheomalaxis and certain viscoelastic effects.

Ghezal and Khayat (2003) used a parallel plate rheometer with mortar specimens to make stepwise measurements at alternating shear rates. Immediately after mixing, a flow curve was measured with a maximum shear rate of 70 s^{-1}. Next, three series of measurements were made with the shear rate alternated from 2 s^{-1} for 3 minutes to 0.03 s^{-1} for 5 minutes. The difference between the initial shear stress and equilibrium shear stress was taken as an indication of thixotropy. Similarly, Toussaint et al. (2001) measured thixotropy in mortars by imposing a specific shear rate regime in a rheometer. The mortar was pre-sheared at a high shear rate, allowed to rest for variable periods of between 1 and 15 minutes, and then sheared at 0.1 rpm while the gradual build-up in torque was monitored.

Billberg and Osterberg (2001) considered four techniques to measure thixotropy, all of which were said to have provided reasonable results. The first technique was referred to as the thixomethod. In this approach a specially designed apparatus was used to monitor how the amount of torque to rotate a vane from rest in an undisturbed concrete sample varied over time. Between each measurement, the vane was lowered to an undisturbed portion of the sample and allowed to remain undisturbed for 30 minutes. It was not clear whether the rotation speed was kept constant in each test. In the second technique, the BML viscometer was used to measure concrete rheology in three loops, with the first loop measured immediately after mixing and the others spaced 30 minutes apart. The first loop was varied from rest to 1 rps and back while the second two loops were varied from rest to 0.03 rps and back. The results were expressed by determining the maximum shear stress after each period of rest. The third method made use of the RAP-ACT plasticity meter, which consisted of a three-bladed impeller with a tapered bottom. The torque to rotate the impeller, as indicated on a spring-loaded gage, was determined after a period of rest. The fourth technique involved measuring the slump flow from four cones filled at the same time but removed at 30 minute intervals. These four methods did not distinguish between reversible and irreversible components of breakdown and did not take into account the effects of setting or workability loss.

Wallevik (2003) conducted oscillatory measurements of cement paste and used various equations to model the response.

3.2 Setting Time

The setting time of SCC is typically similar to that of conventionally placed concrete; however, given the use of high dosages of chemical admixtures and the possible use of supplementary cementitious materials in SCC, setting time could increase or decrease based on mixture proportions. Polycarboxylate-based HRWRAs generally result in less of a delay in setting time than sulfonate-based HRWRAs. Measurement of setting time can be accomplished with conventional methods, including the Vicat needle for cement paste (ASTM C 109) or the penetration resistance test for the sieved mortar fraction of concrete (ASTM C 403).

3.3 Bleeding

Given its low water content and high viscosity, SCC typically exhibits minimal surface bleeding (Khayat, Assaad, and Daczko 2004). In particular, the use of fine filler materials and viscosity modifying admixtures can increase the ability of the paste to retain water and result in reduced bleeding (Khayat 1999). Pressure gradients, however, can result in the movement of water through SCC, causing segregation even when surface bleeding is not present (Khayat, Assaad, and Daczko 2004).

To measure bleeding, the test method for conventionally placed concrete, described in ASTM C 232, can be used for SCC (Lachemi et al. 2004). In this method, concrete is placed in a covered container and any bleed water on the surface is removed at regular intervals. The amount of bleeding can be expressed as the volume of water per unit area of surface or as the percentage of available water that bleeds. Several other available tests are intended primarily for SCC and other highly flowable materials. In the pressure bleed test (Khayat, Assaad, and Daczko 2004), concrete is placed in a pressure vessel with a filter at the bottom. The filter permits the passage of water but blocks most solid particles greater than 1 μm. A pressure of 700 kPa is applied to the top of the concrete for 10 minutes and the amount of bleed water passing the filter is determined and expressed as a percentage of the total water in the concrete sample. In the bleeding test method (PCI 2003), which was developed in France, SCC is placed inside a volumetric air indicator. Perchlorethylene, which has a specific density of 1.59, is filled

above the concrete up to the zero mark. The amount of water that rises to the top of the perchlorethylene is measured at regular intervals up to 60 minutes. The total amount of bleed water and the rate of bleeding are determined. Lastly, the electrical conductivity test, described earlier, allows the monitoring of the movement of water within a sample and the computation of bleeding indexes.

3.4   Plastic Shrinkage

Self-consolidating concrete can be more susceptible to plastic shrinkage cracking than conventionally placed concrete because of the lack of bleed water and the high paste volume (EFNARC 2001; Khayat 1998; Hammer 2003). Turcry, Loukili, and Haidar (2002) and Turcry and Loukili (2003) found that SCC mixtures exhibited plastic shrinkage strains at least two times greater and as much as four times greater than conventionally placed concrete due mainly to the low water-powder ratio and the delayed setting time induced by the HRWRA. Due to the greater susceptibility to plastic shrinkage cracking, it was recommended that curing be started immediately after casting regardless of weather conditions. Techniques available for measuring plastic shrinkage in conventionally placed concrete are generally appropriate for SCC.

3.5   Lateral Formwork Pressure

Lateral formwork pressures can be greater in SCC than in conventionally placed concrete due to the high fluidity of SCC. The presence of thixotropy can significantly reduce formwork pressures. Assaad and Khayat (2004) found formwork pressures to be dependent on the content and type of cement and supplementary cementitious materials (SCM), type and dosage of chemical admixtures, consistency and unit weight of fresh concrete, size and shape of coarse aggregate, ambient and concrete temperatures, rate and method of casting, as well as the size and shape of the formwork.

Chapter 4: Hardened Properties Literature Review

Like conventionally placed concrete, SCC can be proportioned to have widely varying hardened properties. Differences in hardened properties between conventionally placed and self-consolidating concrete can be attributed to three main sources: modified mixture proportions, improved microstructure and homogeneity, and lack of vibration (Klug and Holschemacher 2003). Modified mixture proportions may include higher paste volumes; higher powder contents; lower water-cementitious or water-powder ratios; finer combined aggregate gradings; smaller maximum aggregate sizes; and use of SCMs, fillers, HRWRAs, and VMAs. The improved microstructure is related to the higher packing of the bulk paste and the reduced size and porosity of the interfacial transition zone. The lack of vibration eliminates defects due to vibration and ensures uniform distribution of properties. The effects of these changes in mixture characteristics can often be prognosticated based on existing data for conventionally placed concrete. Any changes in hardened properties assume that SCC is properly proportioned for workability; namely that it adequately fills formwork, passes reinforcement, and resists segregation.

Much research has been conducted to evaluate the hardened properties of SCC. In considering the results of this research, the selection of the appropriate baseline for comparing mixtures is crucial and varies by study. Mixtures are often compared at similar compressive strength; similar water-cement, water-cementitious materials, or water-powder ratio; or similar application. According to EFNARC (2005), SCC and conventionally placed concrete with similar compressive strengths should exhibit similar hardened properties. When mixtures are compared at constant water-cement ratio, the SCC mixtures often have large volumes of filler—resulting in lower water-powder ratios and possibly lower water-cementitious materials ratios. These lower water-powder or water-cementitious materials ratios are often, but not always, associated with improvements in hardened properties. For a given application, SCC can often be proportioned to have equal or better hardened properties than conventionally placed concrete by utilizing the tradeoffs associated with different mixture proportioning changes. Further complicating the comparison of conventionally placed and self-consolidating concrete is the fact that the number of mixtures and the range of mixtures chosen for comparison vary widely by study. In many cases, only a small number of mixtures are compared.

Because of the variety of approaches in comparing conventionally placed and self-consolidating concrete, conclusions vary regarding the hardened properties associated with SCC. Thus, it is necessary to evaluate separately the effects of individual changes to the concrete. As D'Ambrosia, Lange, and Brinks (2005) remark,

> …it is best not to treat SCC as a group of materials with comparable mechanical behavior. Different strategies for mixture proportioning may lead to SCC materials that have the common ability to flow into formwork without mechanical vibration, but have very different behavior when considering mechanical performance and early-age cracking risk.

This chapter describes the established relationships between mixture characteristics commonly associated with SCC and hardened concrete properties. It also presents selected data for SCC.

4.1 Microstructure

The microstructure of SCC is often superior to that of conventionally placed concrete due to the increased packing density of the bulk paste and a reduction in size and porosity of the interfacial transition zone. The low water-powder ratios necessary to achieve adequate workability are responsible for much of the improvement in microstructure. The use of HRWRA results in improved dispersion of cement. Tragardh (1999) compared conventionally placed and self-consolidating concrete mixtures with the same water-cement ratio but with a lower water-powder ratio in the SCC due to the addition of limestone filler. The SCC mixtures exhibited a denser microstructure, with the interfacial transition zone exhibiting a lower porosity and a thinner layer of calcium hydroxide. This improvement in microstructure was attributed to the addition of limestone filler and the reduction in bleeding.

4.2 Strength and Stiffness

SCC can be designed for a large range of strength and elastic modulus. Although low water-powder ratios are usually dictated by workability requirements, the water-cement ratios can be varied much more widely depending on the quantities of fillers used, including fly ash, slag, silica fume, and mineral filler. The rate of development and ultimate values of strength and elastic modulus depend on the amount and activity of these fillers.

4.2.1 Compressive Strength

Compressive strength is approximately related to the porosity of the concrete, which in turn is related to the water-cement ratio and degree of hydration. Abrams (1918) established a relationship between compressive strength (f_c') and water-cement ratio, as shown in Equation (4.1):

$$f'_c = \frac{A}{B^x} \tag{4.1}$$

where A and B are empirical constants and x is the volumetric water-cement ratio. Feret established a separate relationship, as shown in Equation (4.2):

$$f'_c = K\left(\frac{v_c}{v_c + v_w + v_a}\right)^2 \tag{4.2}$$

where K is an empirical constant and v_c, v_w, and v_a are the volumes of cement, water, and air, respectively.

Aggregate characteristics can also play an important role in compressive strength. The strength of the aggregate becomes important in moderate- to high-strength concretes. The size, shape, angularity, texture, and mineralogy can affect the quality of the interfacial transition zone and the bond between paste and aggregate. Although larger aggregates require less mixing water than smaller aggregates, the transition zone around larger aggregates is weaker, resulting in lower compressive strength. Angular and rough-textured aggregates tend to exhibit improved bond to the cement paste. The use of calcareous aggregates generally results in increased compressive strength relative to siliceous aggregates. Other main factors affecting compressive strength include the use of admixtures and SCMs, cement type, air entrainment, and curing conditions (Mehta and Monteiro 1993).

For conventionally placed and self-consolidating concrete mixtures with similar proportions but different workabilities (due to a difference in HRWRA dosage, for example), the SCC should exhibit slightly higher compressive strength due to the lack of vibration, which improves the bond between aggregate and paste (EFNARC 2005), and the improved cement dispersion resulting from the use of HRWRA. Roziere et al. (2005) found that increasing the paste volume from 29.1% to 45.7% while keeping w/cm constant reduced the 28-day compressive strength by 12%. Heirman and Vandewalle (2003) found that when a variety of fillers, including fly ash and mineral fillers, were used and the water-cement ratio (not water-cementitious materials ratio) was held constant, the compressive strength was generally higher.

84

Klug and Holschemacher (2003) found that the rate of strength development over time was generally similar for SCC and conventionally placed concrete; however, the use of limestone filler could accelerate the early development of strength whereas SCMs could increase the ultimate strength.

4.2.2   Flexural and Tensile Strengths

Flexural (f_r') and tensile (f_t') strengths are often related to compressive strength. The interfactial transition zone characteristics tend to affect tensile and flexural strength to a greater degree than compressive strength (Mehta and Monteiro 1993). Tensile and flexural strengths increase with compressive strength, but at a decreasing rate. Values of flexural strength for lightweight and normal-weight concrete have been reported to range from $7.5\sqrt{f_c'}$ to $12\sqrt{f_c'}$ (ACI 363 1992). ACI 363 (1992) recommends the use of Equation (2.1), which is based on the work of Carrasquillo et al. (1981).

$$f'_r = 11.7\sqrt{f_c'} \quad (f'_r \text{ and } f_c' \text{ in psi})$$
$$\text{for } 3,000 < f_c' < 12,000 \text{ psi}$$

(4.3)

Tensile strength may be as high as 10% and as low as 5% of compressive strength for low and high strength concrete, respectively. ACI 363 (1992) recommends the use of Equation (4.4), which is based on the work of Carrasquillo et al. (1981).

$$f'_t = 7.4\sqrt{f_c'} \quad (f'_r \text{ and } f_c' \text{ in psi})$$

(4.4)

$$\text{for } 3,000 < f_c' < 12,000 \text{ psi}$$

Separately, the CEB-FIP model code recommends the use of Equation (4.5), with the value of the constant 1.4 ranging between 0.95 and 1.85.

$$f'_t = 1.4\left(\frac{f_c'}{10}\right)^{\frac{2}{3}} \quad (f'_r \text{ and } f_c' \text{ in MPa})$$

(4.5)

The flexural and tensile strengths of SCC are typically improved relative to conventionally placed concrete due to the improved microstructure of the paste—particularly the improved interfacial transition zone and the denser bulk paste (Klug and Holschemacher 2003). Turcry, Loukili, and Haidar (2002) found that the flexural strength was slightly higher for SCC than a conventional mixture of comparable compressive strength. According to EFNARC (2005), SCC should exhibit similar tensile strength as conventionally placed concrete because

paste volume does not have a significant effect on strength. Roziere et al. (2005), however, found that increasing the paste volume of SCC reduced tensile strength slightly. Turcry, Loukili, and Haidar (2002) found that the ratio of tensile to compressive strength was between 0.087 and 0.1 for SCC and 0.075 for comparable conventionally placed concrete. Based on a database of results from around the world, Klug and Holschemacher (2003) found that for a given compressive strength, the tensile strength was comparable to or slightly higher than conventionally placed concrete.

4.2.3   Modulus of Elasticity

For concrete, which can be represented as a multi-phase material, the modulus of elasticity is a function of the volume fractions and elastic modulus of the principle constituents—that is, paste and aggregates—and the characteristics of the interfacial transition zone (Mehta and Monteiro 1993; Nilsen and Monteiro 1993; Alexander and Milne 1995; Neubauer, Jennings, and Garboczi 1996). In general, decreasing the porosity of any of the constituents increases the concrete modulus of elasticity. The paste elastic modulus, which is typically lower than that of the aggregate, is affected by factors such as the water-cement ratio, air content, SCM content, and degree of hydration. In addition, the maximum size, shape, angularity, texture, grading, and microstructure of the aggregates can affect cracking in the interfacial transition zone.

The static modulus of elasticity is frequently related to the square root of the compressive strength. Several such relationships are listed in Table 4.1. The equations shown in Table 4.1 all represent best-fit lines of data, not lower bounds, and actual values may be expected to deviate from the equations by as much as 20% (Oluokun, Burdette, and Deatherage 1991). The equations vary based on the data used for their development. For instance, the widely used equation from the ACI 318 building code was developed based on an analysis conducted by Pauw (1960) of multiple sources of compressive strength, modulus of elasticity, and unit weight data. Much of this data was for concrete with lightweight aggregates. The method of testing for elastic modulus varied between data sources in Pauw's analysis. It is frequently assumed that the unit weight of concrete is 145 lb/ft^3; however, this approximation may not always be accurate (Oloukun, Burdette, and Deatherage 1991).

The equations developed for lower strength concrete, such as the ACI 318 equation, have been shown to overestimate modulus of elasticity at higher compressive strengths. According to Carrasquillo, Nilson, and Slate (1981), the modulus of elasticity of high strength concrete is

lower than predicted by the ACI 318 equation because compressive strength depends mainly on the mortar properties while modulus of elasticity depends on both the mortar and aggregate properties. Therefore, if the mortar is weaker than the aggregate, any increase in the strength and stiffness of the mortar results in a larger increase in concrete compressive strength than in concrete modulus of elasticity.

Table 4.1: Models Relating Modulus of Elasticity (E) to Compressive Strength (f'_c) and Concrete Unit Weight (w_c) (all values in psi and lb/ft^3, unless noted otherwise)

Reference	Equation	Application Range	Comments
ACI 318 Building Code	$E = (w_c)^{1.5} 33\sqrt{f_c'}$ or $E = 57,000\sqrt{f_c'}$ For "normal-weight concrete"	$90 < w_c < 155$ lb/ft^3	Equations taken from Pauw (1960)
ACI 363R State of the Art Report on High Strength Concrete	$E = 40,000\sqrt{f_c'} + 1.0 x 10^6$	$3,000 < f_c' < 12,000$ psi	Based on data from multiple sources, equation originally suggested by Carrasquillo, Nilson, and Slate (1981)
CEB-FIP Model Code	$E = (\alpha)(21,500)\left(\dfrac{f_c'}{10}\right)^{\frac{1}{3}}$ (values in MPa) $\alpha = 1.2$ for basalt or dense limestone, 1.0 for quartzitic, 0.9 for limestone, 0.7 for sandstone	Valid up to 80 MPa (11,600 psi)	
Ahmad and Shah (1985)	$E = w_c^{2.5}\left(\sqrt{f_c'}\right)^{0.65} = w_c^{2.5}(f_c')^{0.325}$	Applicable to low and high strength concrete	
Oluokun, Burdette, and Deatherage (1991)	$E = (w_c)^{1.5} 31.770\sqrt{f_c'}$ or $E = 63,096\sqrt{f_c'}$ for concrete tested	$f_c' > 500$ psi	Valid for test ages ranging from 6 hrs to 28 days
Crouch and Pearson (1995)	$E = 41,990\sqrt{f_c'} + 2.299 x 10^6$ for neoprene capping $E = 37,440\sqrt{f_c'} + 2.531 x 10^6$ for sulfur capping	$2,000 < f_c' < 6,000$ psi	
Iravani (1996)	$E = 4,700 C_{ca}\sqrt{f_c'}$ (values in MPa) C_{ca} is selected based on the aggregate type and varies from 0.61 to 0.97	$55 < f_c' < 125$ MPa	Based on data from multiple sources

The equations relating modulus of elasticity to compressive strength and unit weight should be used with caution because modulus of elasticity is a function of more than just

compressive strength and unit weight (Mehta and Monteiro 1993; Mokhtarzadeh and French 2000; Huo, Al-Omaishi, and Tadros 2001). In particular, the modulus of elasticity has been shown to be strongly dependent on the aggregates in general and coarse aggregates in particular (Aitcin and Mehta 1990; Baalbaki et al. 1991; Mehta and Monteiro 1993; Zhou, Lydon, and Barr 1995; Iravani 1996; Cetin and Carrasquillo 1998; ACI 363). The stiffness of coarse aggregates can vary significantly from one source to another. The difference in modulus of elasticity between aggregate and paste and the physical and chemical bonds between the two influences the micro-cracking that occurs during loading and the associated modulus of elasticity and compressive strength (Carrasquillo, Nilson, and Slate 1981; Neville 1997). For instance, Baalbaki et al. (1991) found that coarse aggregate much stiffer than the mortar increased modulus of elasticity but decreased compressive strength because of the development of stress concentrations at the aggregate-mortar interface. Similar results were obtained by Cetin and Carrasquillo (1998). Aitcin and Mehta (1990) found that the bond between paste and coarse aggregate, which was affected by the aggregate properties, in turn affected concrete modulus of elasticity. Ahmad and Shah (1985) found that increasing the maximum aggregate size or the coarseness of the aggregate grading—with constant consistency and w/c—resulted in higher modulus of elasticity. Compressive strength, however, generally decreases with increasing maximum aggregate size (Neville 1997; ACI 363). Cetin and Carrasquillo (1998) found that decreasing the S/A resulted in slightly higher modulus of elasticity and lower compressive strength but found that reducing the maximum aggregate size had no effect on modulus of elasticity. As concrete strength is increased, the modulus of elasticity of the concrete depends much more on the modulus of elasticity of the aggregates and the relationship between modulus of elasticity and compressive strength is less precise (Neville 1997; Cetin and Carrasquillo 1998). As a result, it is often recommended that modulus of elasticity be measured with the particular job materials.

The test conditions are also highly influential. As concrete is dried, the modulus of elasticity decreases but the compressive strength increases (Ahmad and Shah 1985; Mokhtarzadeh and French 2000). According to Mehta and Monteiro (1993), compressive strength increases 15% and modulus of elasticity decreases 15% when the concrete is dried. The ASTM C 469 standard for modulus of elasticity specifies that cylinders be tested in a moist condition; however, some researchers have allowed specimens to dry. For instance, Carrasquillo, Nilson, and Slate (1981), whose data was used in the ACI 363 equation, allowed

their 4- by 8-inch cylinders to dry 2 hours before testing. The method of strain measurement has also been shown to affect results (Ahmad and Shah 1985).

In addition to empirical relationships relating modulus of elasticity to compressive strength, models are available to relate concrete's modulus of elasticity to the volume and elastic modulus of each of its constituents (Hansen 1960; Hashin 1962; Hirsh 1962; Counto 1964; Bache and Nepper-Christensen 1965; Popovics and Erdey 1970; Neubauer, Jennings, and Garboczi 1996). Such models typically represent concrete as a two- or three-phase material. Baalbaki et al. (1992) compared experimental data for high-strength concrete to six such two-phase models and to empirical relationships between modulus of elasticity and compressive strength. They found that both approaches provided reasonable predictions for most aggregates; however, they recommended direct testing with actual materials for better precision. Zhou et al. (1995) compared experimental data to six two-phase models and found the models gave reasonable results for 4 of 6 aggregates. The two aggregate giving poor results were steel beads and expanded clay.

In evaluating the literature on the effects of coarse aggregate on modulus of elasticity, it should be noted that the fine aggregates are typically unchanged in the experiments. The effects of fine aggregates should not be discounted because limited test data are available. Based on the representation of concrete as a three-phase material (paste, aggregate, and interfacial transition zone), the influence of fine aggregates on modulus of elasticity is significant.

The modulus of elasticity of SCC is typically equal to or slightly less than that of conventionally placed concrete due to the higher paste volume and reduced maximum aggregate size (EFNARC 2005). The modulus of elasticity of SCC may be increased, however, by the improved interfacial transition zone. Based on a database of results from around the world, Klug and Holschemacher (2003) found for a given compressive strength that the modulus of elasticity was typically lower than for conventionally placed concrete; however, the vast majority of the data points were within the expected range of the CEB-FIP model code. According to PCI (2003), the modulus of elasticity of SCC may be as low as 80% of that of comparable conventionally placed concrete. Turcry, Loukili, and Haidar (2002) found that the ratio of modulus of elasticity (GPa) to compressive strength (MPa) was approximately 0.6 for SCC and 0.7 for conventionally placed concrete. Roziere et al. (2005) found that increasing the paste volume from 29.1% to 45.7% while keeping w/cm constant reduced the 28-day modulus of elasticity by 14%. Persson (2001) found that at a constant compressive strength level, SCC and

conventionally placed concrete exhibited similar elastic modulus. Schindler et al. (2007) found that, for a given compressive strength, the SCC mixtures had similar modulus of elasticity as conventionally placed concrete mixtures at 56 days but slightly lower modulus of elasticity at 18 hours. The lower modulus at 18 hours was attributed to the use of SCMs in the SCC mixtures but not in the conventionally placed concrete mixtures. The S/A was found to have no effect on modulus of elasticity for the majority of SCC mixtures. The values of modulus of elasticity were greater than those predicted by the ACI 318 equation. Naito et al. (2005) found that the modulus of elasticity of one SCC mixture was lower than a conventionally placed concrete mixture for a given compressive strength. The SCC mixture, which was intended for prestressed concrete bridge beams, had a smaller maximum aggregate size, slightly lower w/cm, and higher S/A. Su et al. (2002) found that increasing the S/A from 0.30 to 0.55 in SCC mixtures did not significantly affect the modulus of elasticity because the total aggregate volume was constant and the stiffness of the fine and coarse aggregates were similar.

4.3   Dimensional Stability

The risk of shrinkage—including both early-age autogenous and longer term drying shrinkage—may be greater for SCC due primarily to its higher paste content. The more highly refined pore structure of SCC may also increase the risk of autogenous shrinkage. The high cementitious materials contents and low water-cementitious ratios can increase the susceptibility to thermal volume changes. To evaluate the susceptibility of SCC to cracking due to volume changes, the viscoelastic properties and tensile strength of concrete must also be evaluated. The higher volume changes sometimes associated with SCC may not necessarily result in increased cracking risk due to higher tensile strength, lower modulus of elasticity, and higher creep sometimes associated with SCC.

4.3.1   Autogenous Shrinkage

In general, changes to the mixture proportions that increase the refinement of the pore structure increase autogenous shrinkage. These changes include reducing the water-cementitious materials ratio below 0.40 (Tazawa and Miyazawa 1995b, Aitcin 1999, Li, Wee, and Wong 2002; Zhang et al. 2003), using slag (Tazawa and Miyazawa 1995a; Li, Wee, and Wong 2002), using silica fume (Tazawa and Miyazawa 1995a, Zhang, Tam, and Leow 2003; Jensen and Hansen 2001; Li, Wee, and Wong 2002), and increasing the fineness of cement (Tazawa and

90

Miyazawa 1995a). The use of fly ash has minimal effect on autogenous shrinkage because its particle size is similar to that of cement (Bentz et al. 2001).

Turcry, Loukili, and Haidar (2002) and Suksawang, Nassif, and Najim (2005) found that autogenous shrinkage was higher for SCC than for comparable, conventionally placed concrete mixtures. D'Ambrosia, Lange, and Brinks (2005) found that the autogenous shrinkage of SCC mixtures increased significantly as the paste volume was increased and as the water-cementitious materials ratio was reduced below 0.40. Roziere et al. (2005), however, found the autogenous shrinkage of SCC mixtures to be very low due to the relatively high water-cement ratio of the tested SCC mixtures and because limestone filler and fly ash were found to reduce autogenous shrinkage.

4.3.2 Drying Shrinkage

The main factors affecting drying shrinkage—aside from exposure conditions and element geometry—are the total contents of water and paste and the aggregate characteristics. Because drying shrinkage is mainly the result of the loss of adsorbed water from the paste, higher paste volumes and total water contents are associated with increased shrinkage (Kosmatka, Kerkhoff, and Panarese 2000). Increasing the water-cement ratio at a constant cement content or increasing the cement content at a constant water-cement ratio will increase drying shrinkage, although this increase is predominately due to the higher paste volume. Bissonnette, Pascale, and Pigeon (1999) found that water-cement ratio had little effect on shrinkage when the paste volume was held constant; however, increasing the paste volume at constant water-cement ratio resulted in increased shrinkage. The fineness and composition of cement generally has negligible effect on drying shrinkage (Mehta and Monteiro 1993; Koskatka, Kerkhoff, and Panarese 2000). Additionally, SCMs usually have little effect on drying shrinkage. Accelerators and some water reducers can increase drying shrinkage. The use of aggregates with high stiffness and low shrinkage decreases drying shrinkage (Mehta and Monteiro 1993; Koskatka, Kerkhoff, and Panarese 2000; EFNARC 2005). Other aggregate characteristics primarily affect shrinkage indirectly by controlling the amount of the paste and water needed in the mixture (Mehta and Monteiro 1993; ACI Committee 209 1997).

The drying shrinkage of SCC may be higher than in conventionally placed concrete primarily due to the higher paste volumes (Hammer 2003; EFNARC 2005). The drying shrinkage of SCC may be reduced, however, due to the denser microstructure (Klug and

Holschemacher 2003). The total water content of SCC mixtures may be no greater than in comparable conventionally placed concrete. Based on a database of results from around the world, Klug and Holschemacher (2003) found that the drying shrinkage of SCC was typically 10-50% higher than that predicted by the CEB-FIP model code. Turcry, Loukili, and Haidar (2002) found that the drying shrinkage strains of two different SCC mixtures were similar to comparable, conventional mixtures due to the offsetting effects of increased paste volume and reduced water-powder ratio. Suksawang, Nassif, and Najim (2005) measured increased drying shrinkage in SCC compared to a comparable conventional mixture. Roziere et al. (2005) found that total shrinkage of SCC—including autogenous and drying—increased linearly with paste volume and that limestone filler and, to a lesser extent, fly ash reduced drying shrinkage. Attiogbe, See, and Daczko (2002) found that reducing the sand-aggregate ratio reduced drying shrinkage of SCC. Persson (2001) found that at a constant compressive strength, drying shrinkage was similar in SCC and conventionally placed concrete. Bui and Montgomery (1999a) found that reducing the water-binder ratio and paste volume and the use of limestone filler could reduce the drying shrinkage of SCC; however, the fresh properties had to be appropriate for good compaction and no segregation. Heirman and Vandewalle (2003) found that when a variety of fillers were added to SCC without changing the cement content and water-cement ratio, the shrinkage increased relative to conventionally placed concrete. In comparing a SCC mixture and conventional mixture with similar water-cement ratios but with higher powder content in the SCC, Vieira and Bettencourt (2003) found the shrinkage to be nearly identical. In evaluating SCC for prestressed concrete applications, Schindler et al. (2007) found that the drying shrinkage strains of 21 SCC mixtures were equal to or less than in two conventionally placed concrete mixtures and that changing the S/A had no effect on shrinkage. Naito et al. (2005) found that the drying shrinkage of one SCC mixture was approximately 40% higher than a conventionally placed concrete mixture of comparable compressive strength. The SCC mixture, which was intended for prestressed concrete bridge beams, had a smaller maximum aggregate size, slightly lower w/cm, and higher S/A.

4.4   Durability and Transport Properties

The potential for improved durability was one of the main original motivations for the development of SCC. The improved microstructure and better consolidation associated with SCC relative to conventionally placed concrete often results in improved durability. The

transport properties of concrete depend primarily on the paste volume, pore structure of the paste, and interfacial transition zone (Zhu, Quinn, and Bartos 2001). Although SCC has higher paste volume, the pore structure of the bulk paste and the interfacial transition zone characteristics are often improved due to the low water-cementitious materials ratios and the use of SCMs. The improved stability, reduction in bleeding, and elimination of vibration can lead to a denser interfacial transition zone and improved durability.

4.4.1   Permeability and Diffusivity

Permeability and diffusivity are related to the total porosity and the size and continuity of the voids in the concrete. In addition, diffusivity is related to the binding capacity of the cement paste. Permeability and diffusivity are reduced by improving the pore structure—including reducing the volume of pores, the sizes of pores, and connectivity of pores in both the paste and aggregates—and improving the transition zone. The pore structure of the paste can be improved by reducing the water-cementitious materials ratio, reducing the water content, providing proper curing, and using SCMs. While SCMs may not reduce porosity, they refine the pore structure, resulting in less connectivity of the pores. This refinement is due to the fact that the calcium silicate hydrate occupies a greater volume than the calcium hydroxide and pozzolan from which it forms. Very fine particles—such as silica fume—can enhance the physical packing and improve the pore structure. Permeability and diffusivity are reduced with increased hydration. Although higher curing temperatures may accelerate hydration earlier, they create a coarser structure, resulting in higher long-term permeability and diffusivity than the same mixture cured at a lower temperature. According to Mehta and Monteiro (1993) the paste is not the principle contributor to permeability in well-cured concrete unless the water-cement ratio is excessive (for example, greater than 0.7). Therefore, the properties of the transition zone and any micro-cracking that occurs in the transition zone are of more importance. The capacity of the cement paste to bind ions is enhanced with the use of SCMs and cements with higher C_3A contents. In particular, the hydration products of slag are known to bind chloride ions effectively.

The permeability and diffusivity of SCC may be higher or lower than conventionally placed concrete depending on the mixture proportions. The low water-cementitious materials ratio and frequent use of SCMs are favorable for improving permeability and diffusivity; however, not all SCMs have the same effect. For instance, Suksawang, Nassif, and Najim (2005) found that the rapid chloride permeability test results increased or decreased relative to a

comparable conventional mixture depending on the type of SCM used. Similarly, Zhu, Quinn, and Bartos (2001) found that the chloride diffusion of SCC depended strongly on the type of filler used. When the same filler was used in conventionally placed and self-consolidating mixtures, the chloride diffusion was similar. In contrast, the capillary water absorption and oxygen permeability coefficients were found to be significantly lower for SCC regardless of the type of filler used. Audenaert, Boel, and De Schutter (2002) found that decreasing the water-cement and water-powder ratios in SCC mixtures and using fillers with finer gradings reduced the chloride penetration. Tragardh (1999) found that a SCC mixture with similar water-cement ratio as a conventional mixture—but with lower water-powder ratio due to the addition of limestone filler—exhibited lower chloride diffusion.

4.4.2   Freeze-Thaw Durability

Freeze-thaw damage may be caused by internal frost damage or salt-scaling. Resistance to internal frost damage is enhanced by providing an adequate air void system—including proper total air void volume as well as proper air void size and spacing. It can also be enhanced by using low water-cementitious materials ratios and SCMs to reduce both permeability and, in particular, the number of large pores. Increasing the concrete strength also enhances resistance to internal frost damage. Salt-scaling can be prevented by providing an adequate entrained air void system, reducing the water-cementitious materials ratio, and providing proper finishing and curing practices. There is some evidence that the use of fly ash or slag may reduce salt-scaling resistance.

The freeze-thaw durability of SCC is frequently comparable to or better than that of conventionally placed concrete. The low water-cementitious materials ratios and ability to adequately entrain air can enhance the freeze-thaw resistance. The use of fly ash and slag, however, may reduce salt-scaling resistance. Persson (2003) found the internal frost resistance of SCC to be better than comparable conventionally placed concrete and the salt-scaling resistance to be similar. Heirman and Vandewalle (2003) found that when a variety of fillers were used and the water-cement ratio was held constant, the freeze-thaw durability was similar but the salt-scaling resistance decreased relative to conventionally placed concrete. Audenaert, Boel, and De Schutter (2002) found that reducing the water-cement and water-powder ratios in SCC mixtures improved internal frost resistance.

The use of some HRWRAs under certain conditions may detrimentally affect the air content and characteristics of the air void system. Khayat and Assaad (2002), however, found that the air void characteristics of SCC were similar to those of conventionally placed concrete and that air void stability could be improved by increasing the cementitious materials content and reducing the water-cementitious materials ratio or by including a VMA in mixtures with low cementitious materials contents and high water-cementitious materials ratios.

4.4.3 Abrasion Resistance

Abrasion resistance is related primarily to compressive strength, type of aggregate, and surface finish (Lane 1978; Liu 1981). Compressive strength is generally considered to be the most important parameter, with higher compressive strengths associated with higher abrasion resistance. Abrasion resistance is also improved by using hard, dense aggregates and aggregates that bond well to the cement. The paste itself does not have a high resistance to abrasion (Mehta and Monteiro 1993). Lane (1978) recommends limiting the amount of aggregate passing the No. 50 and No. 100 sieves to enhance abrasion resistance. Separately, ASTM C 33 limits the amount of dust-of-fracture material finer than the No. 200 sieve in manufactured sands to 5% of the fine aggregate mass in structures subjected to abrasion and 7% in all other structures. Proper finishing and curing techniques, along with the use of a hard-steel trowel finish as opposed to a wood or magnesium float finish result in higher abrasion resistance. Little data exist specifically for the abrasion resistance of SCC.

Chapter 5: Mixture Proportioning Literature Review

Numerous mixture proportioning methods have been proposed for SCC. This chapter summarizes 13 mixture proportioning methods described in the literature. The methods vary widely in overall approach, in the range of materials and performance characteristics considered, and in the level of complexity.

SCC mixture proportions depend, in large part, on the application. Requirements for hardened properties, filling ability, segregation resistance, and especially passing ability may vary widely by application. These factors must be considered prior to starting the mixture proportioning process. All mixture proportioning methods must ensure adequate yield stress and plastic viscosity of the concrete. According to Yahia et al. (1999), a low yield stress is important for filling ability while high mortar plastic viscosity is needed for placement in highly congested sections and for mixtures with high coarse aggregate contents. High deformability can be achieved by limiting the coarse aggregate volume while segregation resistance can be achieved by controlling the mortar rheology through reducing the w/cm, increasing the powder content, or adding VMA.

Mixture proportioning can be broadly split between three approaches based on the method of achieving sufficient viscosity and segregation resistance: powder-type, VMA-type, and combination-type. In powder-type SCC, the powder content is high and w/p low. In VMA-type SCC, the powder content is reduced and the w/p is increased relative to powder-type SCC and a VMA is added to ensure segregation resistance. The paste volume, however, may not change significantly between the two types. Combination-type SCC combines both moderately high powder content and the use of a VMA. According to the Japanese Society of Civil Engineers (1999), the powder content in powder-type SCC should be approximately 16%-19% of the concrete volume (500-600 kg/m^3 or 850-1000 lb/yd^3 based on only cement) and can comprise a wide variety of powders, such as portland cement, fly ash, slag, and limestone filler. The water-powder ratio of powder-type SCC typically ranges from 0.28 to 0.37. In contrast, the powder content of VMA-type SCC is typically 300-500 kg/m^3 (500-850 lb/yd^3 or 9.5 to 16% of the concrete volume based on only cement) and composed entirely of portland cement. The water content of VMA-type SCC may be greater than 18% of concrete volume (300 lb/yd^3). For combination-type SCC, the powder content is typically greater than 13% of the total concrete

volume and the w/cm is restricted to a narrow range. These powder contents are summarized in Table 5.1.

Table 5.1: Typical Powder Contents of Based on JSCE Recommendations (1999)

Parameter	Powder Content	Mass* (kg/m^3)	Mass* (lb/yd^3)
Powder-Type	16-19%	500-600	850-1000
VMA-Type	9.5-16%	300-500	500-850
Combination-Type	>13%	>410	>690

*Based on portland cement only

According to an analysis of 68 SCC case studies conducted by Domone (2006), mixture proportions for SCC vary widely such that there is not a unique solution for any given application. The analysis found that coarse aggregate contents varied from 28 to 38% of concrete volume, paste content varied from 30 to 42% of concrete volume, powder content ranged from 445 to 605 kg/m^3, water-powder ratio ranged from 0.26 to 0.48, and fine aggregate content varied from 38 to 54% of mortar volume. The majority of case studies used maximum coarse aggregate sizes of 16 to 20 mm. Nearly all mixtures used some type of non-portland cement powder, with limestone powder the most common addition. In general, the SCC mixture proportions—when compared to conventional, vibrated concrete—were characterized by lower coarse aggregate contents, increased paste contents, higher powder contents, low water-powder ratios, high HRWRA dosages, and the use of VMA is some cases.

Separately, EFNARC (2001) has provided typical values for SCC mixture proportions, as given in Table 5.2.

Table 5.2: Typical Mixture Proportioning Values Suggested by EFNARC (2001)

Parameter	Typical Values
Water/powder (volume)	0.80-1.10
Total powder content	160-240 l/m^3
Coarse aggregate volume	28-35%
Water content	<200 l/m^3

The following sections describe the individual mixture proportioning methods. These descriptions are based on the information available in the cited references and, therefore, may not fully represent all aspects of the methods and may not reflect the latest versions of the methods.

5.1   Proportioning Methods

5.1.1   ACBM Paste Rheology Model/Minimum Paste Volume Method

The ACBM Paste Rheology Model is the result of the input of several researchers. Saak, Jennings, and Shah (2001) originally introduced the concept of a self-flow zone, defined in terms of a range of paste yield stress and apparent viscosity values necessary to achieve both self-flow and segregation resistance. The model was later modified by Bui, Akkaya, and Shah (2002) to include the effects of aggregates by expanding on the Minimum Paste Volume Method, which was developed earlier by Bui and Montgomery (1999) and Bui (2002).

To ensure segregation resistance and self-flow simultaneously, Saak, Jennings, and Shah (2001) developed an analytical model of a single aggregate in cement paste. Based on this model, which was verified experimentally, they defined a self-flow zone in terms of paste yield stress and paste apparent viscosity. The zone was defined by a minimum yield stress and apparent viscosity for segregation resistance and a maximum yield stress and apparent viscosity for self-flow. The paste composition of the SCC mixture was adjusted to be in the self-flow zone.

To incorporate the effects of aggregates, criteria for the solid phase (aggregates) and liquid phase (paste) are considered separately. The solid phase criteria are established to prevent blocking of aggregates while the liquid phase criteria are considered to ensure adequate segregation resistance, flowability, and form-surface finishability. To proportion mixtures, the minimum paste volumes required for the solid phase and liquid phase criteria are computed separately and the limiting case for paste volume is selected. Then, the paste rheology is established to complete the mixture proportions.

The minimum paste volume to satisfy the solid phase criteria is based on the aggregate grading and reinforcement size. The maximum aggregate volume (V_{abmax}) is computed in Equation (2.1):

$$V_{ab\,max} = \frac{\rho_g + (\rho_s - \rho_g)N_{ga}}{\sum \dfrac{P_{vgm}N_{ga}\rho_s}{V_{abm}} + \sum \dfrac{P_{vsn}(1-N_{ga})\rho_g}{V_{abn}}} \tag{5.1}$$

where ρ_g and ρ_s are the specific gravities of the coarse and fine aggregates, respectively; N_{ga} is the ratio of coarse aggregate to total aggregate; P_{vgm} is the volume ratio of coarse aggregate in aggregate group m (i.e. between two sieves) to the total coarse aggregate content; P_{vsn} is the

98

volume ratio of fine aggregate group n to total fine aggregate content; V_{abm} and V_{abn} are the blocking volumes of m and n groups of coarse and fine aggregates, respectively. The blocking volumes are computed with a series of equations based on the aggregate size and the reinforcement size and clear spacing, as described in Bui and Montgomery (1999). The solid phase criteria indicate that increasing the amount of larger particles reduces the volume of total aggregate permitted for a given reinforcement bar clear spacing.

The minimum paste volume to satisfy the liquid phase criteria is based on the average spacing between aggregates, which is computed with Equation (5.2):

$$D_{SS} = D_{AV}\left(\sqrt[3]{1 + \frac{V_p - V_{Void}}{V_C - V_P}} - 1 \right) \tag{5.2}$$

where V_P is the paste volume, V_c is total concrete volume (nominally 1 cubic meter or 1 cubic yard), and V_{void} is the volume of voids between densely compacted aggregates (dry-rodded unit weight of combined aggregates, determined in accordance with ASTM C 29), and D_{av} is the average aggregate diameter, computed based on Equation (5.3):

$$D_{AV} = \frac{\sum d_i m_i}{\sum m_i} \tag{5.3}$$

where d_i is the average size of fraction i and m_i is percentage of mass between the upper and lower sieve size for size fraction i. The values of D_{SS} and D_{AV} are assumed to represent the majority of aggregate characteristics. The minimum paste volume (V_{pdmin}) is computed based on the minimum average aggregate spacing (D_{ssmin}), as shown in Equation (5.4):

$$V_{pd\,min} = V_t \frac{V_t - V_{void}}{\left[\dfrac{D_{ss\,min}}{D_{av}} + 1 \right]^3} \tag{5.4}$$

The minimum average aggregate spacing must be selected before computing the minimum paste volume for the liquid phase criteria. It is not a standard value, but depends on factors such as the water-binder ratio and the aggregate size. It can be determined experimentally.

For proportioning, the minimum paste volume is computed for various N_{ga} values for both the liquid and solid phase criteria. An example of the results of such calculations is illustrated in Figure 5.1.

99
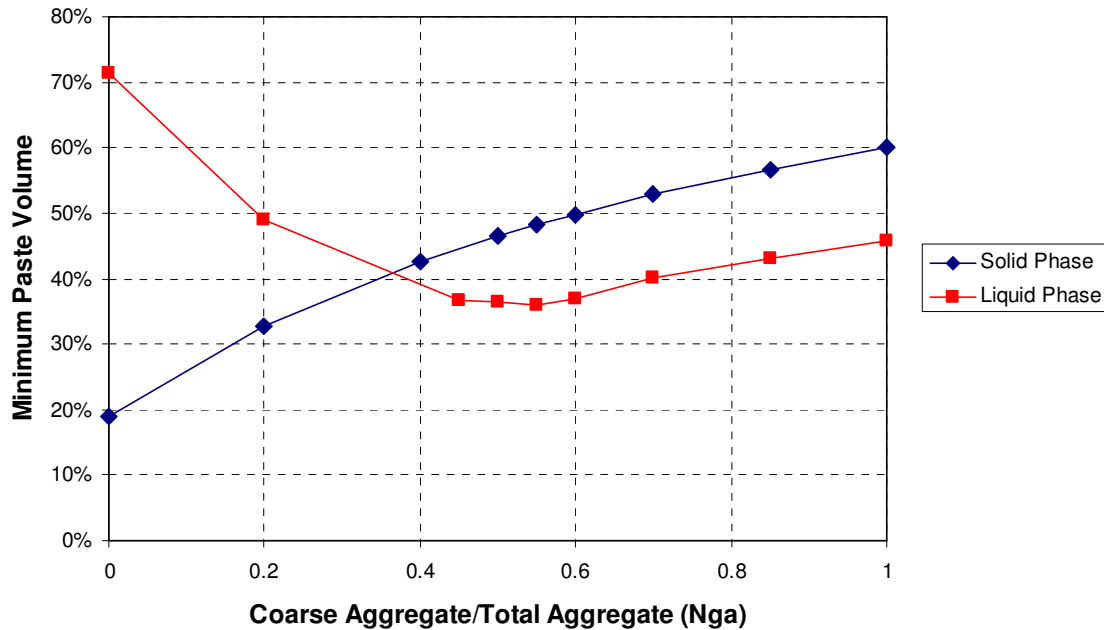
Figure 5.1: Example of Liquid and Solid Phase Criteria

With the minimum paste volume selected, the paste rheology must be optimized. Bui, Akkaya, and Shah (2002) extended the model further by evaluating over 70 concrete mixtures with varying workability. The data was used to develop a rheology model that illustrates trends between paste rheology, average aggregate size, and average aggregate spacing. For example, it was found that as the average aggregate spacing was increased, the optimum ratio of paste mini-slump-flow to viscosity decreased. Thus, as the paste volume is increased for a given aggregate, the paste mini-slump-flow should be reduced and the paste viscosity should be increased. It was also shown that below a certain average aggregate spacing, SCC could not be produced regardless of the paste rheology. For a constant aggregate spacing, decreasing the average aggregate size reduced the optimum ratio of paste mini-slump-flow to viscosity. This rheological model can be used for mixture proportioning to reduce the amount of laboratory work. Bui (2002) adds that the optimum water-binder ratio and ratio of coarse to total aggregate can be selected on the basis of empirical tests to achieve low binder content and low HRWRA dosage.

5.1.2 Compressible Packing Model

The compressible packing model developed by de Larrard (1999a) has been applied to SCC (Sedran et al. 1996; Sedran and de Larrard 1999). The intent of the model is to reduce the

high paste volumes sometimes associated with SCC. The method includes a detailed packing model to optimize aggregate packing. The model includes equations to compute concrete yield stress, plastic viscosity, and segregation resistance. In addition, a parameter has been developed to predict filling/passing ability.

For proportioning SCC mixtures, the required inputs are the size distributions, specific gravities, and packing densities of the constituents and the saturation dosage of the HRWRA. Because several constants in the compressible packing model depend on the HRWRA, approximately 10 trial batches with different HRWRA and water contents must be tested for rheology and segregation resistance in order to determine these constants. The model equations are used to compute yield stress, plastic viscosity, and parameters describing filling/passing ability and segregation resistance. Limits are established for each of these four parameters. Gap-graded mixtures must be avoided to ensure segregation resistance even though they may result in high packing density. Requirements for hardened properties must also be included. The initial trial proportions are optimized numerically by the model and must then be verified with laboratory trial batches.

5.1.3 Concrete Manager Software

The "Concrete Manager" software program utilizes a theoretical model to predict concrete rheology and to optimize the proportions of concrete mixtures (Roshavelov 1999, Roshavelov 2002, Roshavelov 2005). The model used in the software includes both a packing model and Mooney's equation for the relative viscosity of concentrated suspensions. The packing density is first computed from the packing model and then used in Mooney's equation to predict the relative viscosity, which can be related to empirical measures of concrete workability.

The development of trial mixture proportions is completed by the Concrete Manager software. First, the desired relative viscosity is selected based on factors such as placement methods, formwork configuration, and reinforcement confinement. Second, the software is used to design an initial trial mixture that both achieves the required viscosity and optimizes proportions. In the third step, a trial batch is mixed and rheological parameters of yield stress, plastic viscosity, and apparent viscosity are measured with a unique capillary rheometer. For the fourth step, the results from the trial batch are compared to the computer calculations and adjustments to the mixture proportions are made as necessary. According to Roshavelov (2005), the predicted apparent viscosities match measured apparent viscosities well.

5.1.4 Densified Mixture Design Algorithm Method

The Densified Mixture Design Algorithm (DMDA) for proportioning high-performance concrete (Chang 2004) has been applied to SCC (Hwang and Chen 2002; Li and Hwang 2003; Chen, Tsai, and Hwang 2003; Hwang and Tsai 2005). The DMDA was developed in Taiwan. It aims to maximize the volume of solid materials and minimize the contents of water and cement.

In the first step, the densities of various blends of aggregates are considered in order to select the blend with the maximum density. Fly ash is considered to be part of the aggregate. The blends are evaluated in a multi-step process. First, the blend of fly ash and fine aggregate resulting in the maximum density is determined. Then, this optimum blend of fly ash and fine aggregate is blended with various amounts of coarse aggregate to select the maximum packing density of all three components. In the second step, the volume of paste (V_p) is calculated by increasing the volume of voids between the aggregate (V_v) by a factor (N), which is given in Equation (5.5):

$$N = \frac{V_p}{V_v} = 1 + \frac{St}{V_v} \qquad (5.5)$$

where S is the surface area of aggregates and t is the thickness of paste around aggregates. Next, the water-cementitious materials ratio is established based on strength and durability requirements. Finally, the water content, cement amount and HRWRA are determined, subject to a minimum water-cement ratio of 0.42 (to prevent autogenous shrinkage) and a maximum water content of 160 kg/m^3.

5.1.5 Excess Paste Theory

Oh, Noguchi, and Tomosawa (1999) applied the concept of the excess paste theory, which was originally developed by Kennedy (1940), to SCC. The excess paste theory requires the determination of the excess paste volume, which is the paste in excess of that needed to fill the voids between the aggregates. This excess paste is divided by the surface area of the aggregates to determine the thickness of the excess paste. Multiple methods are available for determining the surface area of the aggregates, including a novel approach suggested by Oh, Noguchi, and Tomosawa (1999). Other methods—including the Minimum Paste Volume Method and Densified Mixture Design Algorithm—incorporate concepts of the excess paste theory.

Oh, Noguchi, and Tomosawa (1999) found that increasing the thickness of the excess paste resulted in decreases in yield stress and plastic viscosity. There was not a unique relationship between the thickness of excess paste and the Bingham parameters for different paste compositions. A unique relationship was found, however, between the relative thickness of excess paste and the relative Bingham parameters. The relative thickness of excess paste (Γ) was defined as the thickness of the excess paste divided by the projected diameter of the aggregate. The relative thickness of excess paste can be computed for an entire aggregate grading by summation of each individual size fraction, as shown in Equation (5.6):

$$\Gamma = \frac{P_e}{\sum_{i}^{n} n_i s_i D_{p_i}} \tag{5.6}$$

where P_e is the volume of excess paste, n_i is the number of particles in size class i, s_i is the surface area of particles in size class i, and D_{p_i} is the projected diameter of the particles in size class i. Alternatively, Hasholt, Pade, and Winnefield (2005) defined the relative thickness of excess paste as shown in Equation (5.7):

$$\Gamma = \frac{1 - \dfrac{\varphi}{\varphi^*}}{\dfrac{f}{k}\varphi} \tag{5.7}$$

where φ is the actual packing density of the aggregates, φ^* is the maximum packing density of the aggregates, and f/k is a factor describing the shape of the aggregates. The value of f/k is 6 for spheres and increases as the shape deviates from that of a sphere.

The relative Bingham parameters are calculated by dividing the Bingham parameters of the concrete by those of the paste. The relationships between relative thickness of excess paste and the relative plastic viscosity (η_r), and relative yield stress (τ_{y_r}) are given in Equations (5.8) and (5.9):

$$\eta_r = 0.0705\Gamma^{-1.69} + 1 \tag{5.8}$$

$$\tau_{y_r} = 0.0525\Gamma^{-2.22} + 1 \tag{5.9}$$

Therefore, by determining the specific surface area of the aggregates and the rheology of the paste, the rheology of the concrete can be computed for any paste volume.

Hasholt, Pade, and Winnefield (2005) evaluated the work of Oh, Noguchi, and Tomosawa (1999) for a range of concrete mixtures and found that it was not possible to link concrete rheology to paste or mortar rheology using the excess paste theory when the concrete, paste, and mortar were measured with different rheometers. The model did perform satisfactorily, however, when inverse calculations were used to compute paste rheology from concrete rheology measurements.

5.1.6   Gomes et al. (2001) High Strength SCC Method

Gomes et al. (2001) presented an empirical method for developing high strength SCC mixture proportions. The method considers SCC as a two-phase material consisting of paste and aggregate. Each phase is optimized separately.

In the first step, the paste composition is optimized by determining the optimum ratios of water/cement, silica fume/cement, HRWRA/cement, and filler/cement. The value of water/cement is set at 0.40 and decreased progressively to obtain the desired compressive strength. The value of silica fume/cement is fixed at 0.1. The ratio of HRWRA/cement is selected by determining the saturation dosage of HRWRA with the Marsh funnel test. The saturation dosage is defined as the dosage beyond which the flow time does not change substantially. The optimum value of filler/cement is determined with the mini-slump flow test by measuring pastes with various filler/cement values at the saturation dosage of HRWRA. The optimum value of filler/cement is selected as the value resulting in a certain mini-slump spread diameter and spread time when tested with the saturation dosage of HRWRA.

In the second step, the aggregates are selected by determining the blend of fine and coarse aggregates that results in the lowest voids content. The voids content is determined based on the shoveling procedure in ASTM C 29.

With the optimum paste composition and aggregate blend selected, the third step involves selecting the appropriate paste volume. Concrete mixtures with various paste volumes are measured for filling ability, passing ability, and compressive strength. The minimum acceptable paste volume is selected.

5.1.7   Particle-Matrix Model

The Particle-Matrix Model was originally developed by Ernst Mortsell for conventionally placed concrete (Mortsell, Maage, and Smeplass 1996) and has since been extended to SCC with

mixed success (Smeplass and Mortsell 2001; Pedersen and Mortsell 2001; Reknes 2001). The model splits concrete between the matrix phase—which consists of water, admixtures, and all particles smaller than 0.125 mm—and the particle phase—which consists of all particles larger than 0.125 mm. Workability is assumed to depend on the matrix rheology, the characteristics of the particles, and the volume of matrix. The matrix rheology is described with the flow resistance ratio (λ_Q) and the particle characteristics are described with the air voids modulus (Hm).

The matrix flow resistance ratio is measured with the FlowCyl, which is a modification of the Marsh funnel test. An electronic ruler with data logger is added to measure the flow rate as a function of the height of the matrix in the FlowCyl. The flow rate versus height of matrix in the FlowCyl is plotted for an ideal fluid and for the tested material. The difference between these two curves is computed as the loss-curve. The flow resistance ratio is defined as the ratio of the area under the loss-curve to the area under the ideal fluid curve. The value of the flow resistance ratio varies from 0.0 for an ideal fluid with no loss to 1.0 for a fluid that does not flow. The flow resistance ratio is typically 0.1 for water and between 0.6 and 0.8 for SCC (Pedersen and Mortsell 2001). The flow resistance ratio has been said to be correlated to plastic viscosity (Pedersen and Mortsell 2001); however, Mortsell, Maage, and Smeplass (1996) asserted that it is a better measurement of paste properties than viscosity. The flow resistance ratio does not capture the effect of yield stress, which may be a major limitation in applying the measurement to SCC (Pedersen and Mortsell 2001).

The air void modulus (Hm) is computed based on the characteristics and volume fractions of the fine and coarse aggregates, based on Equation (5.10):

$$Hm = v_1 \left[\frac{Hs}{Fm_s^{0.5}} + Ts \right] + v_2 \left[\frac{Hp}{Fm_p^{0.5}} + Tp \right] \qquad (5.10)$$

where v_1 and v_2 are the volume fractions of sand and coarse aggregate, respectively; Hs and Hp are the void contents in the compacted sand and coarse aggregate, respectively; Ts and Tp are the aggregate parameters for sand and coarse aggregate, respectively; and Fm_s and Fm_p are the fineness moduli of the sand and coarse aggregate, respectively. The air void modulus is intended to equal the paste volume when the mixture changes from no-slump to a small slump. The fineness modulus is included to adjust for the fact that the sand has a greater effect on workability than coarse aggregates do. The value of Ts and Tp can be found by regression

analysis of multiple mixtures where the water content is adjusted to change from a zero slump to a non-zero slump.

With the matrix composition and aggregate blend characterized, workability is measured for various matrix volumes. An equation is fitted to the plot of a workability parameter—such as slump flow, yield stress, or plastic viscosity—versus matrix volume. Such equations are developed for multiple matrix flow resistance ratios and aggregate air void moduli. Equations can also be developed to relate the matrix composition to the flow resistance ratio. The use of these equations enables the prediction of the effects of changes in mixture proportions and the selection of optimum mixture proportions.

5.1.8   Rational Mix Design Method

The Rational Mix Design Method was developed in Japan and has been presented in various forms by multiple authors—including but not limited to Okamura and Ozawa (1995); Ouchi, Hibino, and Okamura (1997); Edamatsu, Nishida, and Ouchi (1999); Okamura, and Ouchi (2003). The use of this method has been suggested in Europe by EFNARC (2001) and in the US by the Precast/Prestressed Concrete Institute (PCI 2003).

The method generally consists of six steps. First, the desired air content is established. Typically, the air content is set at 2% unless air entrainment is required. Second, the coarse aggregate volume is set at 50 to 60% of the coarse aggregate bulk density. Thus, a coarse aggregate with a dry-rodded unit weight of 100 lb/ft^3 would be used at 50 to 60 lb/ft^3 in concrete, or 1350 to 1620 lb/yd^3. The exact amount depends on the aggregate's maximum size and shape, with smaller aggregates and rounded aggregates used in higher volumes. Third, the sand volume is set at 40-50% of the mortar volume. Alternatively, Okamura and Ozawa (1995) suggested that equal volumes of sand and coarse aggregate be used. Elsewhere, Edamatsu, Nishida, and Ouchi (1999) suggested a method for determining the optimum sand content. This method involves the use of the mini-v-funnel test and mini-slump flow test for mortars (Figure 5.2). Glass beads are added to these mortars to represent the interaction between sand and coarse aggregate. The ratio of mini-v-funnel flow time with and without the glass beads is evaluated to select the proper sand content. For the purposes of this method, material in the sand below a certain size is considered powder. Okamura and Ozawa (1995) recommend material finer 90 μm be considered powder while EFNARC (2001) recommends 125 μm.

Fourth, the water-powder ratio for zero flow in paste is determined by measuring the mini-slump flow in pastes at various w/p (1.1, 1.2, 1.3, and 1.4 by volume) and extrapolating the w/p for zero flow (β_p). The value of β_p typically ranges from 0.7 to 1.0 depending on the characteristics of the powder, which includes cement and any additions (Okamura and Ozawa 1995). The mini-slump cone typically used has a top diameter of 70 mm, a bottom diameter of 100 mm and a height of 60 mm (Figure 5.2). Fifth, the optimum water-powder ratio and HRWRA dosage are determined in the paste, based on measurements with the mini-slump cone and mini-v-funnel (Figure 5.2). Various water-powder ratios in the range of 0.8 to 0.9 β_p are used to reach a target mini-slump flow and mini-v-funnel flow time. Generally, the water-powder ratio is changed in order to modify mini-v-funnel flow time, which is related to viscosity. EFNARC (2001) suggested a target mini-slump flow of 240 to 260 mm and a mini-v-funnel time of 7-11 seconds. Ouchi, Hibino, and Okamura (1997) suggested a target value for mini-slump flow of 245 mm and a target mini-v-funnel flow time of 10 seconds. Sixth, tests are performed on trial batches of concrete to finalize the mixture proportions.
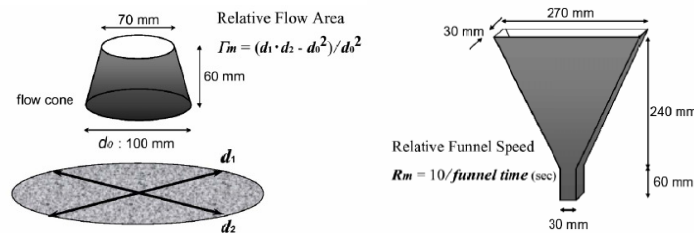
Figure 5.2: Mini-Slump Flow Cone and Mini-V-Funnel Used to Evaluate Paste Properties in the Rational Mixture Design Method (Okamura 2003)

5.1.9   Statistical Design of Experiments Approach

Multiple researchers have used statistical design of experiments (DOE) techniques to evaluate the effects of mixture proportions, select trial proportions, and optimize proportions. DOE techniques provide a way to evaluate the effects of different factors in a statistically sound manner and with a minimum number of mixtures. Regression models are fitted to the results of each measured response. A summary of four such approaches is presented in Table 5.3.

A central composite response surface is the most commonly used approach. Some prior knowledge of both the materials to be used and SCC proportioning is required to select the values of factors used in the experiment design such that all or most mixtures exhibit SCC or near-SCC flow characteristics. Although the absolute values of the modeled responses may

change when different materials are used, the general relative trends illustrated for a certain set of materials and proportions may remain consistent when a different set of materials is used (Ghezal and Khayat 2002).

Table 5.3: Summary of Statistical Design of Experiments Approaches

Reference	Experiment Design	Factors	Other Parameters	Responses
Khayat, Ghezal, and Hadriche (1999)	Central composite response surface with 5 factors and 32 points (16 fractional factorial points, 10 star points, 6 center points)	Water-cement ratio (0.37-0.50), cementitious materials content (360-600 kg/m^3), viscosity enhancing agent dosage (0.05-0.20% by mass of water), HRWRA dosage (0.30-1.10% by mass of binder), volume of coarse aggregate (240-400 l/m^3)	Fine aggregate content varied to achieve volume	Slump flow, rheological parameters (IBB rheometer), filling capacity, v-funnel flow time, surface settlement, compressive strength at 7 and 28 days
Ghezal and Khayat (2001); Ghezal and Khayat (2002)	Central composite response surface with 4 factors and 21 points (8 fractional factorial points, 8 star points, 5 central points)	HRWRA content (0.12 to 0.65% by mass of powder), cement content (250-400 kg/m^3), limestone filler content (0-120 kg/m^3), water-powder ratio (0.38-0.72)	Coarse aggregate content held constant, fine aggregate content varied to achieve volume; constant dosage of VMA in all mixtures	Initial slump flow, slump flow after 45 minutes, rheological parameters (IBB), v-funnel flow time, surface settlement, compressive strength at 1 and 28 days
Sonebi, Bahadori-Jahromi, and Bartos (2003); Sonebi (2004a); Sonebi (2004b)	Central composite response surface with 4 factors and 21 points (8 fractional factorial points, 8 star points, 5 central points)	Cement content (183-317 kg/m^3), fly ash content (59-261 kg/m^3), HRWRA dosage (0-1% by mass of powder), water-powder ratio (0.38-0.72)	Coarse aggregate content held constant, fine aggregate content varied to achieve volume	Slump flow, loss of fluidity, orimet flow time, v-funnel flow time, l-box H_1, l-box ratio, j-ring with Orimet, j-ring with slump cone, rheological parameters (IBB rheometer), compressive strength at 7, 28, and 90 days
Patel et al. (2004)	Central composite response surface with 4 factors and 21 points (8 fractional factorial points, 8 star points, 5 central points)	Total binder content (350-450 kg/m^3), fly ash content (30-60% mass replacement of cement), HRWRA content (0.1 to 0.6% by mass of cementing materials), water-binder ratio (0.33-0.45)	Coarse aggregate content held constant, fine aggregate content varied to achieve volume	Slump flow, compressive strength at 1 and 28 days, rapid chloride permeability (other properties were measured but not modeled statistically)

Similarly, Nehdi, Chabib, and Naggar (2001), developed artificial neural networks to predict SCC performance based on mixture proportions. The values of slump flow, filling

capacity, segregation resistance, and 28-day compressive strength were modeled. The success of the model was limited by the amount of data used to train the model. It was suggested that the model could be used in mixture proportioning to limit the number of laboratory trial batches. Mixture proportions could be created and tested in the artificial neural network model to select mixtures to achieve the required properties.

5.1.10 Su, Hsu, and Chai (2001) Method

The mixture proportioning method developed by Su, Hsu, and Chai (2001) consists of selecting the aggregate volume and then filling the voids between aggregates with paste of the appropriate composition.

In the first step, the coarse and fine aggregates are proportioned based on their loosely packed densities, which are determined in accordance with ASTM C 29 but with the aggregates dropped from a height of 300 mm. The masses of coarse and fine aggregates in concrete are increased by a packing factor (*PF*), which reflects the increase in packing density of the aggregates in actual concrete mixtures. The packing factor is defined as the ratio of the mass of tightly packed aggregate in concrete to the mass of loosely packed aggregate. It is chosen by the designer, with higher packing factors associated with higher aggregate contents. In an example, Su, Hsu and Chai showed that increasing the packing factor resulted in a lower paste volume with a higher w/cm and a lower concrete strength. The masses of coarse (W_{coarse}) and fine (W_{fine}) aggregates are calculated based on Equations (5.11) and (5.12):

$$W_{coarse} = PF \times UW_{coarse-loose} \times \left(1 - \frac{S}{A}\right) \tag{5.11}$$

$$W_{fine} = PF \times UW_{fine-loose} \times \frac{S}{A} \tag{5.12}$$

where $UW_{coarse-loose}$ and $UW_{fine-loose}$ are the loosely packed densities of coarse and fine aggregates, respectively, and S/A is the sand-aggregate ratio. In the second step, the cement content is selected based on strength requirements, as shown in Equation (5.13):

$$C = \frac{f'_c}{20} \tag{5.13}$$

where *C* is the cement content in kg/m^3 and f'_c is the compressive strength in psi. This relationship is based on empirical data from Taiwan and may vary for other regions. In the third step, the water content required by the cement is calculated from the water-cement ratio needed

for strength. Thus, the water content for cement is the required water-cement ratio multiplied by the cement content. In the fourth step, the total volume of fly ash paste and slag paste to fill the remaining volume of the concrete is determined. The flow table test is used to determine separately the water-fly ash and water-slag ratios to achieve the same flow as the cement paste already selected. In step 5, the total mixing water is calculated as the sum of the water contents required for the fly ash, slag, and cement pastes. Lastly, trial batches are evaluated and the proportions are adjusted.

5.1.11 Swedish Cement and Concrete Research Institute (CBI) Model

The Swedish Cement and Concrete Research Institute (CBI) Model is based on the assumption that SCC is a suspension of aggregates in paste (Billberg 2002). The model incorporates aspects of the Minimum Paste Volume Method developed by Van Bui (Bui and Montgomery 1999). The CBI model splits concrete between the solid fraction, which consists of all particles greater than 0.125 mm, and the "micro-mortar" fraction, which consists of water, admixtures, air, and particles smaller than 0.125 mm. The model can be used to fulfill requirements for rheology and passing ability.

First, design and detailing criteria and contractor requirements are considered. Design criteria may include requirements for strength and durability, which may impose limits on parameters such as water-cement ratio, sand-aggregate ratio, and air content. Detailing requirements involve geometrical limitations due to formwork geometry and reinforcement spacing. Contractor requirements may include the rate of strength development and rate of slump flow loss.

With these criteria evaluated, the first step in selecting mixture proportions is to set the ratio of coarse-to-total aggregate and the minimum micro-mortar volume. These two parameters are based on the blocking criteria and the void content of the aggregate. The minimum paste volume for blocking is selected based on the criteria presented by Bui and Montgomery (1999) and subsequently modified by CBI. Petersson and Billberg (1999) found that adding a viscosity modifying admixture enabled only a small reduction in paste volume. The minimum volume of micro-mortar for blocking criteria increases with increasing coarse aggregate-to-total aggregate ratio, decreasing clear spacing between reinforcement, or increasing aggregate angularity. The dry-rodded void content is measured at various ratios of coarse-to-total aggregate in order to evaluate the ratio with the minimum void content. The actual minimum micro-mortar content is

greater than the dry-rodded void content in the aggregate. Second, the micro-mortar rheology is established based on rheometer measurements. Third, the performance of trial concrete mixtures is evaluated. The slump flow with T_{50} and VSI and the l-box are used to evaluate fresh concrete properties.

5.1.12 Technical Center of Italcementi Group (CTG) Method

The CTG Mixture Proportioning Method was developed at the Technical Center of Italcementi Group (CTG) in 1997 and has been used worldwide by Italcementi Group (Vachon, Kaplan, and Fellaki 2002).

The method involves four steps. First, the paste composition is designed for strength requirements. Second, the paste volume is selected to achieve necessary fluidity and resist segregation. This paste volume—which constitutes water, air, and all particles smaller than 80 μm—is set at 37% in most cases as a starting point. Third, the aggregate is selected to prevent segregation and blocking. Fourth, the HRWRA dosage and, if necessary, the VMA dosage are selected. Values for the paste content and aggregate grading are established empirically based on testing or previous experience.

5.1.13 University of Rostock (Germany) Method

The mixture proportioning method developed at the University of Rostock in Germany aims to determine the optimum water content for SCC based on the water demand of the individual solid components (Marquardt, Diederichs, and Vala 2001; Marquardt, Diederichs, and Vala 2002). Additionally, the paste volume is selected based on the voids content of the aggregates and the HRWRA dosage is adjusted to achieve sufficient fluidity.

In the first step, the aggregate grading is selected. The aggregate grading should have sufficient sand volume and high packing density. In the second step, the volumes of paste and aggregate in the concrete are determined. The concrete is assumed to comprise three volumes: the volume of aggregate (V_g), the volume of the paste required to fill the voids between the aggregates (V_{LHP}), and the volume of surplus paste (V_{LU}). The total paste volume ($V_L = V_{LHP} + V_{LU}$) is related to V_{LHP} by a factor κ:

$$\kappa = \frac{V_L}{V_{LHP}} \qquad (5.14)$$

The value of κ depends on the shape and size of the aggregates and is normally set between 1.9 and 2.1 for SCC. To determine the total paste volume needed, the compacted volume of aggregate (V_{G0}) and volume of voids between the compacted aggregates (V_{HP0}) are measured for the selected grading. The values of V_{LHP}, V_G, and V_L are calculated based on Equations (5.15) to (5.17):

$$V_{LHP} = \frac{1000}{\kappa + \dfrac{V_{G0}}{V_{HP0}}} \tag{5.15}$$

$$V_G = \frac{V_{LHP} V_{G0}}{V_{HP0}} \tag{5.16}$$

$$V_L = \kappa V_{LHP} \tag{5.17}$$

In the third step, the cement type and quantity is selected based on hardened property requirements. For the fourth step, the types of additives, such as fly ash or limestone powder; the type of HRWRA; the type of VMA; and the air void content are selected. In the fifth step, the water demand of all solid components is determined. For the aggregates, the water demand is calculated as the water needed to cover all particle surfaces with a thin layer of water and to partially fill the space between particles. It can be determined either by centrifugation of water-saturated aggregates or based on the specific surface area of the aggregates. The water demand of powder constituents is determined by measuring the power consumption of a mixer as water is gradually added to the powder. As water is added, the power consumption increases from a minimum value when only powder is in the mixer to a maximum value before beginning to decrease. The water content corresponding to the maximum power consumption is considered the water demand. The water demand is determined separately for each powder constituent.

The sixth step involves calculating the mixture proportions. The total water content is the sum of the water demand from the aggregate and each individual powder constituent. The volumes of additives such as fly ash are adjusted to achieve proper total concrete volume. In the final step, trial mixtures are evaluated. The flowability of the mixture is adjusted by changing the dosage of HRWRA.

5.2   Summary

The mixture proportioning methods described in this chapter are summarized in Table 5.4. Although each mixture proportioning method takes a different approach, the methods do share some similarities. Most methods—with the exception of the Rational Mix Design Method and the referenced statistical design of experiments test plans—assume that SCC is a suspension of aggregates in paste. These methods must establish three things: the paste volume, paste composition, and aggregate blend. The paste volume is set to be greater than the volume of the voids between the compacted aggregates. The methods of compacting the aggregates and of selecting the paste volume vary with each method. The paste composition is usually designed independently of the rest of the mixture based on measurements of flow properties, hardened properties, or both. Each method uses a different series of tests and has different target values for selecting the paste composition. Some methods are very specific about the target paste properties while others are much more open-ended. The aggregate blends are often, but not always, selected to achieve the minimum voids between the aggregates. In the final step, the paste volume, paste composition, and aggregate blend are combined for the preliminary, trial concrete batch or batches.

The approach of assuming that SCC is a suspension is not without limitations due to the ways this approach has been implemented. When the optimized paste volume and paste composition, which are typically determined separately, are combined in the concrete mixture proportions, the concrete rheology may not be optimum. Furthermore, when the aggregate blend is selected on the basis of minimizing the voids content, the resulting concrete flow properties may not be ideal. Some of the mixture proportioning methods are not flexible or provide limited guidance in allowing the paste volume, paste composition, and aggregate blends to be modified when tested together in the combined concrete mixture proportions.

In some methods, the aggregate void content is assumed to account for all aggregate properties—including packing, size, grading, shape, angularity, and texture. Other methods assign an additional factor or measure additional properties (such as surface area) to account for some of these other aggregate properties. It is not clear whether these approaches are sufficient for capturing the aggregate properties. For instance, a crushed aggregate and rounded aggregate, each with the same voids content, would likely result in much different workability.

Given the wide range of materials that are used in producing SCC, the ability to modify concrete mixture proportions efficiently once the initial trial batch is computed is crucial to

ensuring successful mixture proportions. In fact, it is unreasonable to expect a mixture proportioning method to result in the optimized proportions initially without subsequent modifications based on measurements of concrete mixtures. Most methods, however, provide little if any guidance on modifying the initial trial proportions.

The methods also vary widely in their level of completeness. Some of the methods provide limited guidance for selecting and varying the values of some key parameters, which increases the number of concrete tests required to establish the effects of these parameters. Other methods focus on specific applications, such as high strength concrete, and do not provide guidance for other applications.

Table 5.4: Summary of SCC Mixture Proportioning Techniques

Method	Basic Concepts	Development	Unique Features	Limitations
ACBM Paste Rheology Model/Minimum Paste Volume Method	The minimum paste volume is selected based on either the solid phase (blocking) or liquid phase (segregation, flowability, form surface finishability) criteria. The paste rheology is then determined on the basis of laboratory testing. The concept of a self-flow zone, defined in terms of paste yield stress and apparent viscosity, is introduced to ensure segregation resistance and flowability.	The method was developed by multiple researchers working at different times. Bui pioneered Minimum Paste Volume Method and combined it with other work done at ACBM, including that of Saak.	The method provides detailed equations to compute the paste volume required for blocking resistance. Equations are also available for liquid phase criteria; however, assumptions must be made regarding average spacing between aggregates.	Limited guidance is available for selecting the average spacing between aggregates and for optimizing paste rheology.
Compressible Packing Model	Proportioning is based on a packing model. Equations are available for computing yield stress, plastic viscosity, a parameter representing filling/passing ability, and a parameter representing segregation resistance.	The method is based on the compressible packing model published by de Larrard. It has been expanded for SCC with the inclusion of a parameter describing filling/passing ability.	The method uses a detailed packing model to optimize aggregates and includes the ability to compute yield stress, plastic viscosity, and parameters for filling/passing ability and segregation resistance.	The use of the model requires proprietary software. The calculation of yield stress and plastic viscosity is based on empirical measurements with the BTRHEOM, which typically gives higher values than other rheometers.

Table 5.4: Summary of SCC Mixture Proportioning Techniques (Continued)

Method	Basic Concepts	Development	Unique Features	Limitations
Concrete Manager Software	The method combines a packing model and the Mooney equation for relative viscosity to predict workability. The software program optimizes the trial mixtures.	The method was developed by Roshavelov and incorporated into a software package. It is similar to the solid suspension model/compressible packing model proposed by de Larrard.	The method includes the ability to predict apparent viscosity. A unique capillary rheometer is used to evaluate trial concrete batches.	The selection of proportions must be completed in the software. The necessary calculations are complex.
Densified Mixture Design Algorithm	The optimum blend of aggregate and fly ash resulting in the lowest voids content is selected. The paste volume is set as the volume of voids between the aggregates and fly ash, increased by a factor *N*. The composition of the paste is selected for hardened properties.	The method was developed in Taiwan for high-performance concrete and has been extended to SCC.	Fly ash is considered as part of the aggregate and not the paste.	The method is primarily intended for high-strength concrete. The aggregate/fly ash combination giving the minimum voids content may not be optimal for workability.
Excess Paste Theory	The relative thickness of excess paste is computed and used to predict the yield stress and plastic viscosity of the concrete relative to the paste.	The method is based on the excess paste theory originally proposed by Kennedy in 1940. This theory has been used by other researchers since then for both conventionally placed concrete and SCC.	The model has been shown to predict both yield stress and plastic viscosity of SCC accurately, based on the aggregate properties, paste volume, and paste rheology.	Various approaches are available for determining aggregate surface area. The approach suggested by the authors is computationally intensive, especially when fine aggregate is considered. The yield stress and plastic viscosity must be determined in a consistent manner on both the paste and concrete so that they can be related.

Table 5.4: Summary of SCC Mixture Proportioning Techniques (Continued)

Method	Basic Concepts	Development	Unique Features	Limitations
Gomes et al. (2001) High-Strength SCC Method	The optimum paste composition is determined with the Marsh funnel and mini-slump cone, subject to limits on strength. The blend of aggregates resulting in the lowest voids content is selected. Various paste volumes are tested to achieve the optimum workability and compressive strength.	The method was developed based on previous concepts for proportioning high-strength and high-performance concrete.	The application of procedures to optimize the paste composition to achieve high strength is unique for SCC.	The method is mainly intended for high-strength SCC. The aggregate combination giving the minimum voids content may not be optimal for workability. The approach for selecting the optimum paste composition may not result in the lowest paste volume. Accordingly, in selecting the paste volume, it may be appropriate to alter the paste composition to achieve lower paste volume.
Particle-Matrix Model	The model is based on paste volume, paste rheology, and aggregate properties. The paste rheology is characterized with the flow resistance ratio, which is measured with the FlowCyl device. The aggregates are characterized with the air voids modulus, which depends on the aggregate volumes, fineness moduli, and empirically determined aggregate parameters. Workability is measured at various paste volumes for each flow resistance ratio and air void modulus. The resulting equations are used to predict the effects of changes in mixture proportions.	The model was originally developed by Ernst Mortsell for conventionally placed concrete and has been extended to SCC with mixed success.	The flow resistance ratio and air voids modulus are unique parameters describing the paste rheology and aggregate characteristics, respectively.	The model has been applied with mixed success. The developer of the model has stated that more work is needed in optimizing the paste rheology. The air void modulus is complicated to compute, particularly in determining the aggregate parameters. The flow resistance ratio may not be the best parameter to characterize paste rheology. The flow resistance ratio and air voids modulus have limited physical meanings.

Table 5.4: Summary of SCC Mixture Proportioning Techniques (Continued)

Method	Basic Concepts	Development	Unique Features	Limitations
Rational Mix Design Method	The coarse aggregate content in the concrete is set to 50 to 60% of the coarse aggregate bulk density. The fine aggregate content in the mortar is set to 40-50% of the mortar volume. The water-powder ratio and HRWRA dosage are determined with mini-slump flow and mini-v-funnel measurements of paste in order to reach prescribed target values.	The method was originally developed in Japan and has been presented by various researchers. The method has evolved; however, the basic principles remain the same. The use of the method has been suggested by organizations around the world, including EFNARC and PCI.	The fine and coarse aggregate contents are selected based on specific multiples of bulk density. A unique method of selecting optimum paste rheology with the mini-slump flow test and mini-v-funnel is provided.	The method is rather restrictive in the way it sets the coarse and fine aggregate contents and establishes the target paste flow properties. The resulting proportions may not be optimal in concrete.
Statistical Design of Experiments Approach	Statistical design of experiments techniques are used to evaluate the effects of 4-5 parameters in a statistically efficient way. Regression models are used to evaluate data and optimize proportions.	The statistical concepts are well-known and widely used in many industries. They have been implemented for SCC by multiple researchers.		The resulting regression models are specific to only the materials and range of proportions considered. In some cases, many of the mixtures in the reported test plans do not exhibit SCC flow characteristics. Some prior knowledge of the materials and SCC proportioning is required to establish the test plan.
Su, Hsu, and Chai Method	The fine and coarse aggregates are set as the loosely packed densities, increased by a packing factor. The cement content and water-cement ratio are selected based on strength requirements. Fly ash and slag pastes are added to fill the remaining volume. The water demand of fly ash and slag are determined separately with the flow table test.	The method was originally developed in Taiwan.	The method uses a packing factor to select the contents of sand and coarse aggregate.	Not all of the values needed for selecting initial proportions are well defined. Several factors such as the packing factor, sand-aggregate ratio, and relative amounts of slag and fly ash must be chosen *a priori* by the designer; however, little or no guidance is given. The water is selected in three separate processes and does not take into consideration the combined effect of the total water content on strength or workability until trial concrete proportions are evaluated.

117

Table 5.4: Summary of SCC Mixture Proportioning Techniques (Continued)

Method	Basic Concepts	Development	Unique Features	Limitations
Swedish Cement and Concrete Research Institute (CBI) Model	The blend of fine and coarse aggregate is selected to achieve the minimum void content. The paste volume is selected based on the voids between the aggregate or the blocking criteria. The paste composition is selected based on rheology measurements. The mixture is finalized based on trial concrete batches.	The method was developed at the Swedish Cement and Concrete Research Institute. It is based in part on work done previously by Van Bui in the Minimum Paste Volume Method.	The method has detailed criteria for ensuring passing ability.	Criteria for the selection of micro-mortar rheology and the amount of micro-mortar are not well-established.
Technical Center of Italcementi (CTG) Method	The paste composition is designed for strength and the paste volume is set for workability. The aggregates are selected to achieve segregation and blocking resistance.	The method was developed by Italcementi in France and used by the company throughout the world.		The method is simple and typically relies on previous empirical experience.
University of Rostock (Germany) Method	The aggregate blend is selected and the paste volume is selected based on a factor κ, which depends on the size and shape of the aggregates. The water demand of each solid component is determined separately. These water contents are added to select the total water content and establish the final mixture proportions.	The method was developed at the University of Rostock in Germany.	The method evaluates the voids between the aggregate, but does not suggest that the aggregate blend with minimum voids be selected. The methods uses unique approaches for the selection of the paste volume and the determination of the water demand of the solid components	The method computes a single water content, which may produce an inappropriate viscosity. Further, the water demand of the concrete mixture may vary as the paste volume is varied. Limited guidance is given on selecting an aggregate blend. The determination of water demand for aggregates by centrifugation may not be feasible for all labs.

Chapter 6: Materials

This chapter describes the properties of all materials and the material characterization techniques used in this project.

6.1   Aggregates

A total of 7 coarse aggregates (predominantly retained on a #4 sieve), 4 intermediate aggregates (predominantly between the 0.5-inch and #8 sieve), and 12 fine aggregates (predominantly passing a #4 sieve) were used. The properties of the coarse, intermediate, and fine aggregates are listed in Tables 6.1 to 6.3. The coarse aggregates were obtained with either 1-inch or ¾-inch maximum aggregate sizes and typically met the grading requirements for the #57 or #67 sizes specified in ASTM C 33. The fine aggregates were obtained as either concrete sand meeting the grading requirements of ASTM C 33, concrete sand not meeting the grading requirements of ASTM C 33, or screenings. According to the aggregate producers, three of the fine aggregates received as screenings or as not meeting the grading requirements of ASTM C 33 are used in concrete in some cases (DL-01-F, LS-04-F, LS-06-F).   Therefore, these three aggregates were evaluated in their as-received condition.   The other three fine aggregates received as screenings or as not meeting the grading requirements of ASTM C 33 (LS-05-F, GR-01-F, TR-01F) were sieved and re-blended to the grading shown in Table 6.4 because these aggregates are not commonly used in concrete in their as-received gradings.

For each aggregate, specific gravity and absorption were determined in accordance with ASTM C 127 for coarse and intermediate aggregates and ASTM C 128 for fine aggregates; packing density and voids content were determined using the rodding and shoveling procedures described in ASTM C 29; and grading was determined in accordance with ASTM C 136 and ASTM C 117. Specific surface area was calculated based on grading data, assuming spherical particles. Therefore, specific surface area does not reflect aggregate shape, angularity, or texture. Further, specific surface area is not intended to reflect absolute size because aggregate packing and concrete rheology are typically considered a function of particle size distribution, not absolute particle size. Increasing the maximum aggregate size is often beneficial for packing and rheology because of the improved particle size distribution and increased spread of sizes, not because of the larger absolute maximum size. The methylene blue value was determined in

accordance with AASHTO TP57 on material passing the No. 200 sieve, which was obtained from dry sieving. Methylene blue test results were expressed in milligrams of methylene blue per grams of microfines.

Shape characteristics of the coarse, intermediate, and fine aggregates were measured with a HAVER Computer Particle Analyzer (CPA). The device captures a two-dimensional silhouette image of particles as they fall from a vibrating chute. The feed rate of particles from the chute is adjusted to ensure physical separation of particles in the image. Two resolutions are available: 60 μm to 26 mm (nominal 0.1 to 12 mm) and 90 μm to 68 mm (nominal 0.2 to 26 mm). The smaller resolution range is used for the fine aggregates and the larger resolution range is used for the intermediate and coarse aggregates. The two dimensional images are used to conduct size and shape analyses. For shape analysis, the following parameters are computed: Martin diameter (dimension of line that splits the particle into two equal areas), Feret diameter (maximum distance between two parallel lines drawn tangent to particle), maximum cut (longest length in projected area), sphericity (actual circumference of projected area divided by circumference of circle with the same area as the projection), L/W (Feret diameter/maximum cut), and the mean square deviation from unity of L/W. In addition, the size of each particle is determined as the diameter of a circle having an area equivalent to the projected area of the particle. The volume of each particle is computed assuming a spherical shape. The shape parameters are computed for each individual particle and as average values for various size classes, which are preset in the HAVER CPA software. For the evaluation of aggregate sources in this project, single values of L/W and sphericity were computed for the entire particle size distribution based on the total surface area of each fraction, as shown in Equation (6.1):

$$P = \sum_{i}^{i=n} \left[\frac{A_i N_i}{\sum_{i}^{i=n} A_i N_i} P_i \right] \tag{6.1}$$

where P = parameter (i.e., L/W or sphericity), A_i = average spherical 3-D surface area for the ith size class, N_i = number of particles for the ith size class, and P_i = parameter for the ith size class. The number of particles in each size class was computed based on Equation (6.2):

$$N_i = (\% \text{ retained})_i \, V_i \tag{6.2}$$

120

where V_i is the volume of a sphere with a diameter equal to the average upper and lower limits of the size class. This approach gives greater weight to smaller particles than computing a simple average of all size classes.

The shape characteristics of the fine aggregates were further evaluated with the uncompacted void content test, which is described ASTM C 1252. The uncompacted void content test was performed with Test Method A (standard graded sample) so that the results would be influenced predominantly by shape characteristics and not grading.

Table 6.1: Coarse Aggregate Properties

			DO-01-C		LS-01-C		LS-02-C		LS-03-C		NA-02-C		LS-04-C		LS-05-C	
Location			Burnet, TX		Perch Hill, TX		Garden Ridge, TX		Stringtown, OK		Victoria, TX		Ft. Myers, FL		Maryville, TN	
Minearology			Dolomite		Limestone		Limestone		Limestone		River Gravel		Limestone		Limestone	
Specific Gravity (SSD)			2.78		2.67		2.59		2.54		2.59		2.39		2.82	
Specific Gravity (OD)			2.76		2.65		2.55		2.51		2.57		2.29		2.81	
Absorption Capacity (%)			0.68		0.83		1.43		1.24		0.78		4.15		0.41	
Unit Weight, Dry Rodded (lb/ft^3)			101.0		98.8		93.4		90.1		105.4		81.1		102.2	
Unit Weight, Loose (lb/ft^3)			90.4		90.8		87.2		80.8		99.6		72.7		94.2	
Pkg. Density, Dry Rodded (%)			58.7		59.9		58.6		57.5		65.8		56.6		58.4	
Pkg. Density, Loose (%)			52.6		55.0		54.7		51.5		62.2		50.7		53.7	
CPA Sphericity			1.122		1.126		1.112		1.156		1.108		1.143			
CPA Length/Width			1.469		1.517		1.432		1.570		1.440		1.417			
US Sieve	Opening Size		Sieve Analysis													
	(in)	(mm)	%Ret	%Pass	%Ret	%Pass	%Ret	%Pass	%Ret	%Pass	%Ret	%Pass	%Ret	%Pass	%Ret	%Pass
1"	1.000	25.4	0.0	100.0	0.0	100.0	0.0	100.0	0.0	100.0	0.0	100.0	0.0	100.0	0.0	100.0
3/4"	0.750	19.1	6.8	93.2	5.3	94.7	4.9	95.1	19.3	80.7	5.2	94.8	26.2	73.8	8.2	91.8
1/2"	0.500	12.7	48.5	44.6	17.7	76.9	24.5	70.5	28.5	52.2	30.5	64.3	28.6	45.2	46.6	45.1
3/8"	0.375	9.53	29.0	15.6	14.7	62.2	32.3	38.2	19.2	33.0	23.9	40.4	30.5	14.7	31.1	14.0
#4	0.187	4.8	13.8	1.8	44.2	18.0	38.0	0.2	26.4	6.6	32.6	7.8	9.0	5.6	13.2	0.9
#8	0.093	2.36	0.0	0.0	15.9	2.1	0.0	0.0	4.4	2.2	5.7	2.2	0.0	0.0	0.0	0.8
#16	0.046	1.18	0.0	0.0	1.2	0.9	0.0	0.0	1.0	1.2	0.7	1.5	0.0	0.0	0.0	0.8
#30	0.024	0.6	0.0	0.0	0.3	0.6	0.0	0.0	0.1	1.1	0.2	1.2	0.0	0.0	0.0	0.8

Notes:
1. All data are for as-received materials.
2. Data obtained with following tests: specific gravity and absorption (ASTM C 127); unit weight, packing density, and voids content (ASTM C 29); sieve analysis (ASTM C 136)

Table 6.2: Intermediate Aggregate Properties

			DO-01-I		LS-01-I		LS-O2-I		LS-05-I	
Location			Burnet, TX		Perch Hill, TX		Garden Ridge, TX		Maryville, TN	
Minearology			Dolomite		Limestone		Limestone		Limestone	
Specific Gravity (SSD)			2.77		2.68		2.77		2.82	
Specific Gravity (OD)			2.74		2.66		2.74		2.81	
Absorption Capacity (%)			0.01		0.01		0.01		0.00	
Unit Weight, Dry Rodded (lb/ft^3)			97.1		95.3		96.2		101.8	
Unit Weight, Loose (lb/ft^3)			88.3		85.4		89.0		94.7	
Pkg. Density, Dry Rodded (%)			56.7		57.5		59.0		58.0	
Pkg. Density, Loose (%)			51.6		51.6		54.7		54.0	
CPA Sphericity			1.149		1.130		1.125			
CPA Length/Width			1.522		1.518		1.485			
US Sieve	Opening Size		Sieve Analysis							
	(in)	(mm)	%Ret	%Pass	%Ret	%Pass	%Ret	%Pass	%Ret	%Pass
1/2"	0.500	12.7	0.0	100.0	0.3	99.7	0.0	100.0	5.3	94.7
3/8"	0.375	9.5	1.8	98.2	23.6	76.2	0.7	99.3	27.3	67.4
#4	0.046	1.18	63.6	34.5	74.8	1.3	72.4	26.9	63.1	4.3
#8	0.093	2.36	29.9	4.6	0.9	0.4	20.4	6.5	1.7	2.5
#16	0.046	1.18	3.2	1.4	0.2	0.3	5.6	0.9	0.0	2.5

Notes:
1. All data are for as-received materials.
2. Data obtained with following tests: specific gravity and absorption (ASTM C 127); unit weight, packing density, and voids content (ASTM C 29); sieve analysis (ASTM C 136)

Table 6.3: Fine Aggregate Properties

	DO-01-F	DL-01-F	GR-01-F	TR-01-F	LS-01-F	LS-02-F
Location	Burnet, TX	Manteno, IL	Liberty, SC	Texas	Perch Hill, TX	Garden Ridge, TX
Minearology	Dolomite	Dolomitic Limestone	Granite	Traprock	Limestone	Limestone
Gradation Received	Concrete Sand	Concrete Sand	Screenings	Screenings	Concrete Sand	Concrete Sand
Fineness Modulus	3.32	2.59	2.11	3.95	3.47	2.76
Specific Gravity (SSD)	2.92	2.75	2.69	3.00	2.67	2.61
Specific Gravity (OD)	2.91	2.72	2.68	2.96	2.65	2.57
Absorption Capacity (%)	0.32	1.27	0.56	1.39	0.58	1.62
Unit Weight, Dry Rodded (lb/ft^3)	108.4	104.2	104.9	120.5	106.2	106.7
Unit Weight, Loose (lb/ft^3)	99.5	94.8	94.3	109.0	92.3	96.8
Pkg. Density, Dry Rodded (%)	59.6	61.4	62.9	65.2	64.2	66.6
Pkg. Density, Loose (%)	54.7	55.9	56.5	59.0	55.8	60.4
Methylene Blue Value (mg/g)	1.25	3.375	0.625	7.875	7.5	0.875
Uncompacted Voids (%)	49.7	48.6	48.3	46.4	43.8	44.1
CPA Sphericity	1.111		1.196	1.122	1.144	1.126
CPA Length/Width	1.520		1.501	1.508	1.502	1.492

US Sieve	Opening Size		Sieve Analysis										
	(in)	(mm)	%Ret	%Pass	%Ret	%Pass	%Ret	%Pass	%Ret	%Pass	%Ret	%Pass	%Ret	%Pass
#4	0.187	4.75	0.4	99.6	1.0	99.0	0.1	99.9	23.0	77.0	4.1	95.9	0.0	100.0
#8	0.093	2.36	21.6	77.9	17.7	81.4	11.1	88.8	29.0	48.0	29.0	67.0	4.5	95.4
#16	0.046	1.18	30.8	47.2	21.9	59.5	15.0	73.9	17.3	30.7	26.8	40.2	33.7	61.7
#30	0.024	0.6	19.7	27.5	15.5	43.9	14.1	59.8	9.1	21.6	14.9	25.3	24.2	37.5
#50	0.012	0.3	14.5	12.9	11.5	32.4	17.7	42.1	5.9	15.8	10.1	15.2	17.4	20.1
#100	0.006	0.15	9.5	3.4	7.9	24.5	17.6	24.5	3.9	11.9	6.2	9.1	11.1	9.0
#200	0.003	0.075	2.6	0.8	6.4	18.0	11.0	13.5	2.2	9.7	2.8	6.3	3.7	5.3
Pan			0.8		18.0		13.5		9.7		6.3		5.3	

Notes:

1. All gradation data and fineness modulus values are for as-received materials.
2. Values other than gradation and fineness modulus for TR-01-F, GR-01-F, and LS-05-F are based on reblended gradation used in concrete and mortar testing not as-received gradation. Data for all other aggregates from as-received gradations.
3. Data obtained with following tests: specific gravity and absorption (ASTM C 128); unit weight, packing density, and voids content (ASTM C 29); methylene blue value (AASHTO TP 57); uncompacted voids (ASTM C 1252); sieve analysis (ASTM C 136), % passing # 200 sieve (ASTM C 117)

Table 6.3: Fine Aggregate Properties (Continued)

	LS-03-F	LS-04-F	LS-05-F	LS-06-F	NA-01-F	NA-02-F
Location	Stringtown, OK	Ft. Myers, FL	Maryville, TN	Calica, MX	Austin, TX	Victoria, TX
Minearology	Limestone	Limestone	Limestone	Limestone	River Sand	River Sand
Gradation Received	Concrete Sand	Concrete Sand	Screenings	Screenings	Concrete Sand	Concrete Sand
Fineness Modulus	3.81	2.49	3.04	2.86	2.58	2.72
Specific Gravity (SSD)	2.57	2.56	2.79	2.46	2.60	2.58
Specific Gravity (OD)	2.56	2.46	2.77	2.33	2.59	2.56
Absorption Capacity (%)	0.43	4.16	0.61	5.41	0.56	0.54
Unit Weight, Dry Rodded (lb/ft^3)	90.4	93.6	116.4	98.7	108.9	106.3
Unit Weight, Loose (lb/ft^3)	84.6	84.3	105.4	87.6	99.0	98.3
Pkg. Density, Dry Rodded (%)	55.6	61.1	67.3	67.8	67.6	66.4
Pkg. Density, Loose (%)	52.0	55.0	61.0	60.2	61.4	61.4
Methylene Blue Value (mg/g)	6.125	2.75	1	2.25	7.125	18
Uncompacted Voids (%)	48.3	47.4	45.5	45.6	41.0	40.3
CPA Sphericity	1.134	1.087			1.085	1.075
CPA Length/Width	1.576	1.484			1.452	1.453

US Sieve	Opening Size		Sieve Analysis										
	(in)	(mm)	%Ret	%Pass	%Ret	%Pass	%Ret	%Pass	%Ret	%Pass	%Ret	%Pass	%Ret	%Pass
#4	0.187	4.75	5.6	94.4	0.1	99.9	2.3	97.7	6.9	93.1	1.5	98.5	1.0	99.0
#8	0.093	2.36	34.7	59.7	8.6	91.2	25.8	71.9	21.1	72.0	11.6	86.9	12.5	86.5
#16	0.046	1.18	27.1	32.6	22.1	69.1	22.5	49.4	18.8	53.2	11.8	75.1	12.7	73.8
#30	0.024	0.6	14.5	18.1	18.7	50.4	14.6	34.8	12.4	40.8	21.7	53.4	24.5	49.3
#50	0.012	0.3	8.7	9.4	18.9	31.6	10.1	24.7	10.0	30.8	32.5	20.9	33.3	16.0
#100	0.006	0.15	4.9	4.5	23.2	8.4	7.1	17.6	6.7	24.1	14.2	6.8	12.2	3.8
#200	0.003	0.075	1.6	2.9	4.7	3.7	6.5	11.1	4.4	19.7	5.0	1.8	2.6	1.2
Pan			2.9		3.7		11.1		19.7		1.8		1.2	

Notes:

1. All gradation data and fineness modulus values are for as-received materials.
2. Values other than gradation and fineness modulus for TR-01-F, GR-01-F, and LS-05-F are based on reblended gradation used in concrete and mortar testing not as-received gradation. Data for all other aggregates from as-received gradations.
3. Data obtained with following tests: specific gravity and absorption (ASTM C 128); unit weight, packing density, and voids content (ASTM C 29); methylene blue value (AASHTO TP 57); uncompacted voids (ASTM C 1252); sieve analysis (ASTM C 136), % passing # 200 sieve (ASTM C 117)

Table 6.4: Grading for GR-01-F, TR-01-F, and LS-05-F Used in Place of As-Received Grading

Sieve	% Retained	% Passing
#4	0.0	100.0
#8	7.7	92.3
#16	23.1	69.2
#30	30.8	38.5
#50	20.5	17.9
#100	12.8	5.1
#200	1.5	3.6
Pan	3.6	

For the five fine aggregates with high microfines contents (DL-01-F, LS-05-F, LS-06-F, GR-01-F, and TR-01F), the microfines were removed by sieving and then evaluated separately. In addition, settling pond fines were obtained for LS-02-F. The properties of these microfines are shown in Table 6.5. The methylene blue test was performed in accordance with AASHTO TP 57. The single drop test was performed based on the description of Bigas and Gallias (2002) and Bigas and Gallias (2003). In the single drop test, a bed of loosely packed microfines is placed in an open dish. A 0.2 ml drop of water is added to the microfines. After approximately 20 seconds, the resulting agglomeration of water and microfines is carefully removed with a needle. The results of the test are expressed as the water-fines volume ratio of the agglomeration (w/f). In addition, the packing density of the fines in the agglomeration is computed. The test is repeated 15 times on each material. Laser diffraction measurements for particle size distribution were performed at the National Institute for Standard and Technology (NIST) using the wet method with isopropyl alcohol. Laser diffraction measurements are based on the assumption of spherical particles. Specific surface area and span were determined from the laser diffraction data. Span is calculated with Equation (6.3):

$$\text{span} = \frac{d(0.9) - d(0.1)}{d(0.5)} \tag{6.3}$$

where d(0.9) is the diameter with 90 percent passing, d(0.5) is the diameter with 50 percent passing, and d(0.1) is the diameter with 10 percent passing. The complete laser diffraction measurements are provided in Appendix A.

Table 6.5: Summary of Microfines Properties

Fine Aggregate ID	Mineralogy	Source	Methylene Blue Value (mg/g)	Single Drop Test		Laser Diffraction	
				w/f	Pkg. Density	Span	SSA (1/μm)
DL-01-F	Dolomitic Limestone	Manteno, IL	3.38	0.370	0.730	2.638	0.965
LS-02-F	Limestone	Garden Ridge, TX	1.63	0.401	0.714	6.673	1.394
LS-05-F	Limestone	Maryville, TN	1.00	0.374	0.728	3.042	1.214
LS-06-F	Limestone	Calica, MX	2.25	0.415	0.707	4.688	1.806
GR-01-F	Granite	Liberty, SC	0.63	0.559	0.642	2.192	0.467
TR-01-F	Traprock	TX	7.88	0.471	0.680	3.302	1.243

The correlations between aggregate properties were evaluated, as shown in Tables 6.6 to 6.8. High absolute values of correlation coefficients only indicate that properties are associated with each other—not that one property causes another. High correlations between properties increase the difficultly of associating certain concrete performance characteristics to aggregate properties because it is not clear how much of an effect to attribute to each aggregate property. For coarse and intermediate aggregates, a high degree of correlation exists between specific gravity and absorption capacity (-0.861), between voids in dry-rodded aggregate and loose aggregate (0.972), between CPA sphericity and voids in dry-rodded aggregate (0.705) and loose aggregate (0.741), and between CPA length/width and CPA sphericity (0.603). For fine aggregates, a high degree of correlation exists between CPA length/width and fineness modulus (0.813), between voids in dry-rodded aggregate and loose aggregate (0.952), between uncompacted voids content and voids in the dry-rodded aggregate (0.713) and loose aggregate (0.746), between CPA length/width and the voids in the dry-rodded aggregate (0.851) and loose aggregate (0.828), and between CPA length/width and uncompacted voids content. For microfines, a high degree of correlation exists between specific surface area and absorption capacity (0.787), between single drop test packing density and methylene blue value (-0.656), and between specific surface area and span (0.677).

Table 6.6: Correlations between Coarse and Intermediate Aggregate Properties

	Sp. Gravity (SSD)	Abs. Capacity	Voids, Dry Rodded	Voids, Loose	CPA Sphericity	CPA Length/ Width
Sp. Gravity (SSD)	1	-0.861	0.043	-0.033	-0.198	0.354
Abs. Capacity		1	0.162	0.212	0.204	-0.530
Voids, Dry Rodded			1	0.972	0.705	0.313
Voids, Loose				1	0.741	0.357
CPA Sphericity					1	0.603
CPA Length/Width						1

Table 6.7: Correlations between Fine Aggregate Properties

	Fineness Modulus	Sp. Gravity (SSD)	Abs. Capacity	Voids, Dry Rodded	Voids, Loose	Methylene Blue	Uncpctd. Voids	CPA Sphericity	CPA Length/ Width
Fineness Modulus	1	0.038	-0.337	0.588	0.613	0.030	0.273	0.328	0.813
Sp. Gravity (SSD)		1	-0.469	0.114	0.098	-0.124	0.385	0.178	0.215
Abs. Capacity			1	-0.207	-0.099	-0.259	0.086	-0.305	-0.182
Voids, Dry Rodded				1	0.952	-0.151	0.713	0.238	0.851
Voids, Loose					1	-0.251	0.746	0.378	0.828
Methylene Blue						1	-0.657	-0.507	-0.365
Uncpctd. Voids							1	0.496	0.749
CPA Sphericity								1	0.474
CPA Length/Width									1

Table 6.8: Correlations between Microfines Properties

	Sp. Gravity (SSD)*	Abs. Capacity *	Methylene Blue	Pkg. Density (Sgl. Drop)	Span	Specific Surface Area
Sp. Gravity (SSD)*	1	-0.708	0.653	-0.264	-0.553	-0.421
Abs. Capacity*		1	0.004	-0.084	0.471	0.787
Methylene Blue			1	-0.656	-0.099	0.182
Pkg. Density (Sgl. Drop)				1	0.148	0.125
Span					1	0.677
Specific Surface Area						1
*Measured on fine aggregate						

6.2   Cementitious Materials

A total of four cements and three fly ashes were used. The four cements, which are described in Table 6.9, include a Type I, a Type I/II and two Type III cements as defined in ASTM C 150. The Blaine fineness, equivalent alkalis, SO_3 content, and Bogue composition values were supplied by the manufacturers.

Table 6.9: Summary of Portland Cement Properties

ID	Type	Source	Blaine (m²/kg)	Na₂Oeq (%)	SO₃ (%)	Bogue Composition (%)			
						C₃S	C₂S	C₃A	C₄AF
PC-01-I/II	I/II	Hunter, TX	379	0.42	2.8	63.7	10.7	6.5	9.7
PC-02-III	III	San Antonio, TX	539	0.50	3.5	56.6	16.3	7.2	10.3
PC-03-I	I	San Antonio, TX	358	0.56	3.3	59.5	14.5	11.5	3.7
PC-03-III	III	San Antonio, TX	552	0.54	4.3	57.8	14.0	9.7	5.7

The three fly ashes, which are shown in Table 6.10, include two Type F and one Type C fly ashes as defined in ASTM C 618. The loss on ignition, specific gravity, CaO content, and $SiO_2+AL_2O_3+Fe_2O_3$ content were supplied by the manufacturers. FA-01-F is from a coal power plant utilizing 'low-NOx burner' technology.

Table 6.10: Summary of Fly Ash Properties

ID	Class	Source	LOI	SG	CaO	SiO₂+ AL₂O₃ +Fe₂O₃
FA-01-F	F	Rockdale, TX	1.05	2.33	13.92	79.21
FA-02-F	F	Jewett, TX	0.11	2.39	9.90	83.71
FA-03-C	C	Thompson, TX	0.28	2.80	27.77	56.49

The single drop test and laser diffraction measurements for particle size distribution were performed on the cementitious materials. The results are shown in Table 6.11.

Table 6.11: Single Drop and Laser Diffraction Measurements of Cementitious Materials

ID	Single Drop Test		Laser Diffraction	
	w/f	Pkg. Density	Span	SSA (1/μm)
PC-01-I/II	0.584	0.631	2.990	1.729
PC-02-III			3.122	2.179
PC-03-I			3.047	1.523
PC-03-III			2.856	2.046
FA-01-F	0.231	0.812	4.934	1.347
FA-02-F	0.178	0.849	6.113	1.706
FA-03-C	0.387	0.721		

Further details of the cementitious materials are available in Appendix A.

6.3 Chemical Admixtures

The chemical admixtures, all of which were obtained directly from the manufacturers, are summarized in Table 6.12. The admixture manufactures were BASF Admixtures Inc.,

Cleveland, OH; Sika Corp., Lyndhurst, NJ; and W.R. Grace & Co.-Conn., Cambridge, MA. In this dissertation, the dosage of HRWRA is typically expressed in percentage terms as the mass of admixture solids divided by the mass of cementitious materials (denoted % cm mass). The specific gravity and solids content of each admixture were determined in accordance with ASTM C 494.

Table 6.12: Summary of Chemical Admixtures

ID	Manufacturer	Trade Name	ASTM C 494 Type	Description
High-Range Water-Reducing Admixtures				
HRWRA-01	BASF	Glenium 3400 NV	A, F	Polycarboxylate ether-based
HRWRA-02	Sika	ViscoCrete 2100	A, F	Polycarboxylate ether-based
HRWRA-03	W.R. Grace	ADVA Cast 530	F	Polycarboxylate ether-based
HRWRA-04	W.R. Grace	ADVA 380		Polycarboxylate ether-based
HRWRA-05	BASF	Rheobuild 1000	A, F	Naphthalene
HRWRA-06	BASF	PS-1466	A, F	Polycarboxylate ether-based
Mid-Range Water Reducing Admixtures				
MRWRA-01	BASF	Polyheed 997	A, F	5-15% water reduction
Viscosity-Modifying Admixtures				
VMA-01	BASF	Rheomac VMA 362		
VMA-02	BASF	Rheomac VMA 450		
Retarder				
RET-01	BASF	Delvo Stabilizer	B, D	

Chapter 7: Target SCC Properties

This chapter summarizes the criteria used to evaluate the test results presented in this dissertation. Although the precise definition of what constitutes SCC can vary depending on the application, the goal of the research was to define SCC broadly. Experiments were designed so that the effect of one factor or a single set of factors could be evaluated while holding all other factors constant and while still achieving SCC workability properties. To achieve this goal, it was typically necessary to proportion mixtures to accommodate a wide range of constituent properties—mainly by increasing the paste volume—and to use a broad definition of SCC. For some materials in some mixtures, the resulting mixtures were not ideal SCC mixtures for a variety of reasons. For instance, the viscosity was too high or too low or the passing ability was poor. Such mixtures would need to be modified for use in the field. It is still possible, however, to evaluate the relative effects of changes in different factors even without all mixtures exhibiting ideal SCC properties. Based on such test results, mixtures can be optimized for certain applications. For instance, the effects of changes to aggregate characteristics can be compared to changes in mixture proportions or non-aggregate materials to produce economical and robust mixtures. The mixtures used were selected primarily for ready mixed concrete applications; however, most of the findings are applicable to precast concrete applications.

The mixtures used in this research were evaluated in terms of empirical workability properties, rheological properties, and hardened properties. The required flow properties are summarized in Table 7.1. The empirical workability properties considered were filling ability, passing ability, and segregation resistance. Filling ability was measured mainly with the slump flow test and was also observed qualitatively by noting how well paste filled the spaces between aggregates and how well concrete flowed into the forms for flexure and shrinkage specimens. The HRWRA dosage was varied to achieve a constant slump flow of 25 +/- 1 inch for concrete and 9 inches for mortar. By keeping the slump flow constant but adjusting the HRWRA dosage, all mixtures exhibited SCC or near-SCC performance. Passing ability can vary significantly depending on the application—from sections with no reinforcement to highly congested reinforcement. Therefore, passing ability was measured with the j-ring but no specific target value was used. In generally, however, j-ring test results of $\Delta h < 0.5$ inches should result in acceptable passing ability for most applications. All mixtures must exhibit segregation

resistance regardless of the application. Segregation resistance was evaluated with the visual stability index of the slump flow test.

In terms of rheology, SCC must exhibit proper yield stress, plastic viscosity, thixotropy, and workability retention. The yield stress must be near zero in order to ensure self-flow; however, a small yield stress is needed to prevent segregation. Therefore, a target yield stress of 10-80 Pa was used. The plastic viscosity should not be too low or too high. If the plastic viscosity is too low, dynamic stability can be reduced and static segregation can be exacerbated. If the plastic viscosity is too high, the concrete can be sticky and difficult to move or pump. Therefore, a target plastic viscosity of 20-40 Pa.s was used. Thixotropy is essential to ensuring segregation resistance and reducing formwork pressure. The build-up of an at-rest structure due to thixotropy results in an increase in static, at-rest yield stress. The low dynamic yield stress needed for self-flow is typically insufficient to resist segregation and can cause high formwork pressures. Therefore, it is important that concrete be thixotropic, resulting in a sufficiently fast build-up in the static yield stress. If the thixotropy is too great, however, the mixture can be impractical to place and result in cold joints.   The exact amount of thixotropy needed depends on the application. Because thixotropy is related mainly to the paste characteristics, it was only evaluated for a few concrete mixtures with microfines or VMA. Workability retention depends on the application. The workability retention must be sufficient to accommodate transportation and placement; however, any additional workability retention is unnecessary. If high fluidity is maintained after the concrete is placed in formwork, the potential for segregation may be greater and formwork pressure may decrease more slowly. Because workability retention can vary significantly between applications, it was only measured on concrete mixtures comparing different HRWRAs and no specific target value was established.

Table 7.1: Requirements for Flow Properties for SCC

Property	Application Dependency	Measurement	Target
Filling Ability	Low	Slump Flow	24-26 inches
Passing Ability	High	J-Ring	n/a
Segregation Resistance	Low	Slump Flow VSI	VSI < 1.0
Yield Stress	Minimal	ICAR Rheometer	10-80 Pa
Plastic Viscosity	Moderate	ICAR Rheometer	20-40 Pa.s
Thixotropy	Moderate	ICAR Rheometer	n/a
Workability Retention	High	ICAR Rheometer, Slump Flow	n/a

The following hardened properties were evaluated: compressive strength, flexural strength, modulus of elasticity, drying shrinkage, chloride permeability, and abrasion resistance. These properties were measured to evaluate the effects of changes in constituents and mixture proportions and to evaluate the suitability of existing established models such as relationships between modulus of elasticity and compressive strength. The hardened properties of the SCC mixtures were also compared to two conventionally placed concrete mixtures. The potential for the thaumasite form of sulfate attack—which is associated with the use of limestone powder in cold, sulfate-rich environments and possibly other conditions (Section 2.2.1.3)—was not evaluated.

The test results presented in this dissertation are applicable only to the ranges of materials and mixture proportions tested and are not necessarily applicable to all SCC mixtures. Efforts were made to use a wide range of materials and mixture proportions; however, the term SCC describes a broad class of concrete mixtures and it was not possible to test the full range of possible materials and mixture proportions. Specific SCC mixtures should be evaluated in reference to the materials and mixture proportions used rather than associating specific concrete performance to all SCC mixtures.

Chapter 8: Paste Rheology Measurements

Paste rheology measurements were conducted at the National Institute of Standards and Technology (NIST) to evaluate various HRWRAs, VMAs, cements, fly ashes, and aggregate microfines. This chapter summarizes the materials, measurement techniques, and results from these tests. All test data are provided in Appendix C.

8.1   Materials and Testing Procedures

The effects of 4 cements, 3 fly ashes, 2 aggregate microfines, 5 HRWRAs, and 2 VMAs on paste rheology were tested. The cements consisted of one Type I cement (PC-03-I), one Type I/II cement (PC-01-I/II), and 2 Type III cements (PC-02-III, PC-03-III). The fly ashes consisted of 2 class F fly ashes (FA-01-F, FA-02-F). Two sources of FA-01-F were used—one from before the conversion to "low-NOx" burner technology in the coal power plant and one from after the conversion. The 2 microfines were GR-01-F and LS-02-F. The HRWRAs were HRWRA-01, HRWRA-02, HRWRA-03, HRWRA-04, and HRWRA-05. The VMAs were VMA-01 and VMA-02.

All cement paste rheology measurements were made with a parallel plate rheometer (Haake Rheostress RS75), which is shown in Figure 8.1. The material was sheared between two 35-mm-diameter serrated parallel plates, which were maintained at a vertical gap distance of 0.400 mm. The test procedure consisted of increasing the shear rate from 1 s^{-1} to 70 s^{-1} over a period of 160 s. Next, upward and downward flow curves were measured by changing the shear rate in a step-wise manner from 1 s^{-1} to 50 s^{-1} and then back to 1 s^{-1}. Ten points were measured for each of the upward and downward curves. The duration of measurement for each point was long enough to achieve equilibrium conditions, with a maximum limit of 20 seconds. The Bingham constitutive model was fit to the downward curve. In cases where rebuilding of the paste structure due to thixotropy increased the measured torque at a shear rate of 1 s^{-1}, this point was removed for the calculation of Bingham parameters. A water bath was used to maintain the temperature of the specimen at approximately 23°C during the rheology tests. The pastes were mixed in a temperature-controlled mixer using the following procedure:

- Add water and admixture to the mixer.
- Mix at 4,050 rpm while gradually adding the cement and other powders for 30 seconds.

- Increase the mixer speed to 10,040 rpm for 30 seconds.
- Stop the mixer for 2.5 minutes; scrape down the sides of the mixer.
- Mix for 30 seconds at 10,040 rpm.

The water bath used to cool the paste during mixing was maintained at 15°C. Immediately after mixing, 1 ml of cement paste was transferred by syringe to the rheometer. The plates were then moved to the correct gap size and measurements were started.

**Figure 8.1: Parallel Plate Rheometer for Paste Measurements**

8.2   Test Results and Discussion

8.2.1   HRWRA

To compare the 4 polycarboxylate-based HRWRAs, each admixture was tested at five different dosages in a paste consisting of PC-01-I/II cement at a w/c of 0.30. In general, all HRWRAs except HRWRA-04 reduced the yield stress (Figure 8.2) and plastic viscosity (Figure 8.3) to near-zero values, after which increasing dosages of HRWRA had negligible effect. HRWRA-04 reduced the yield stress to near-zero values but did not reduce the plastic viscosity

132

below 0.2 Pa.s in the range of dosages considered. The saturation dosage was less for yield stress than for plastic viscosity. With sufficiently high dosages of HRWRA, the rheology of the paste begins to approach that of water, which is unsuitable for concrete. Although the yield stress should be near zero to ensure self-flow, a small yield stress and sufficiently high plastic viscosity are necessary to ensure the suspension of aggregates. The polycarboxylate-based admixtures were able to provide this property because the saturation dosage for plastic viscosity was higher than that for yield stress.

In contrast to the polycarboxylate-based HRWRAs, the naphthalene-based HRWRA (HRWRA-05) reduced the plastic viscosity so low that it could not be measured reliably by the rheometer with the given shear rate regime, as indicated in the flow curves plotted in Figure 8.4. This near-zero plastic viscosity was obtained at much higher yield stresses than with the polycarboxylate-based HRWRAs. These higher yield stresses were magnified due to the increases in shear stress that occurred over time and at low shear rates, resulting in the up curves being below the down curves.
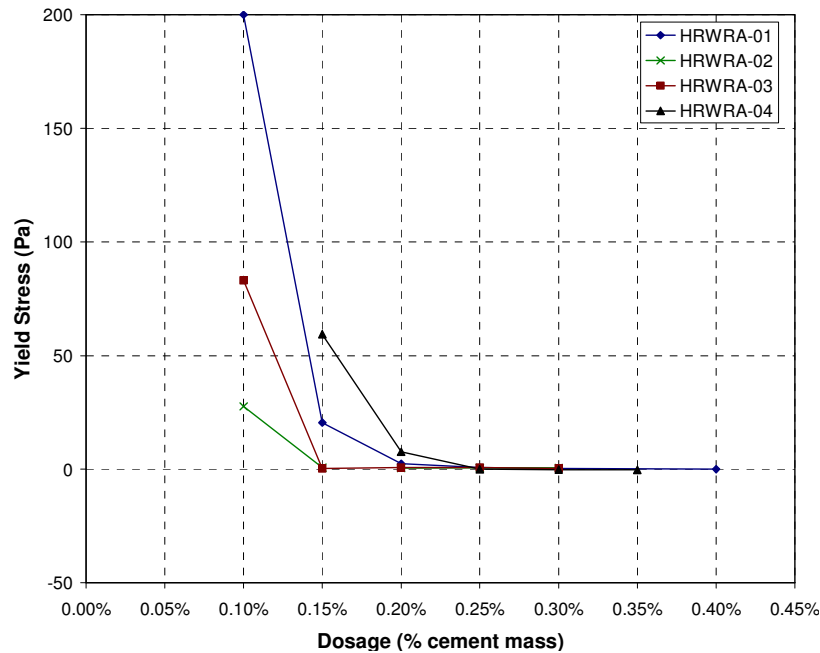
Figure 8.2: Effect of HRWRA Dosage on Yield Stress (PC-01-I/II, w/c = 0.30)

133
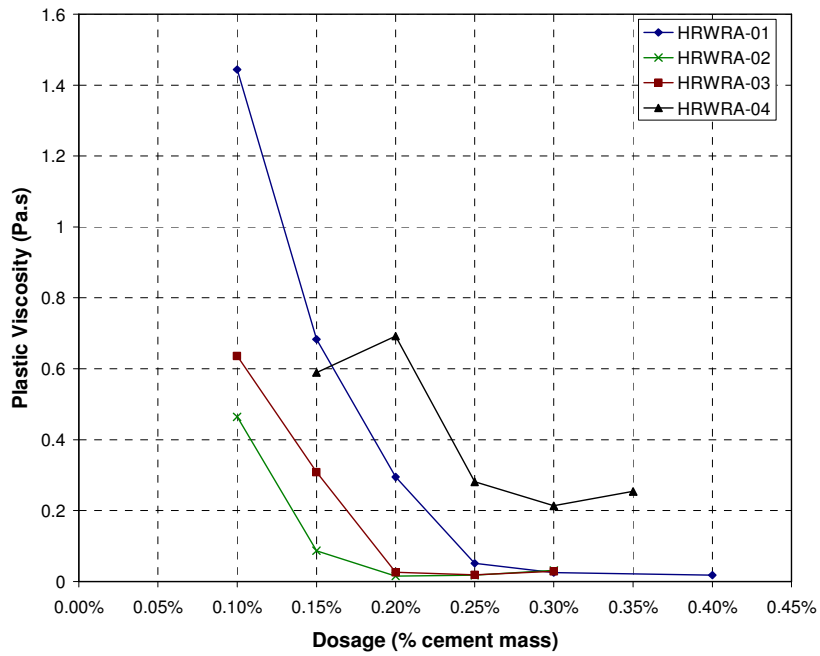
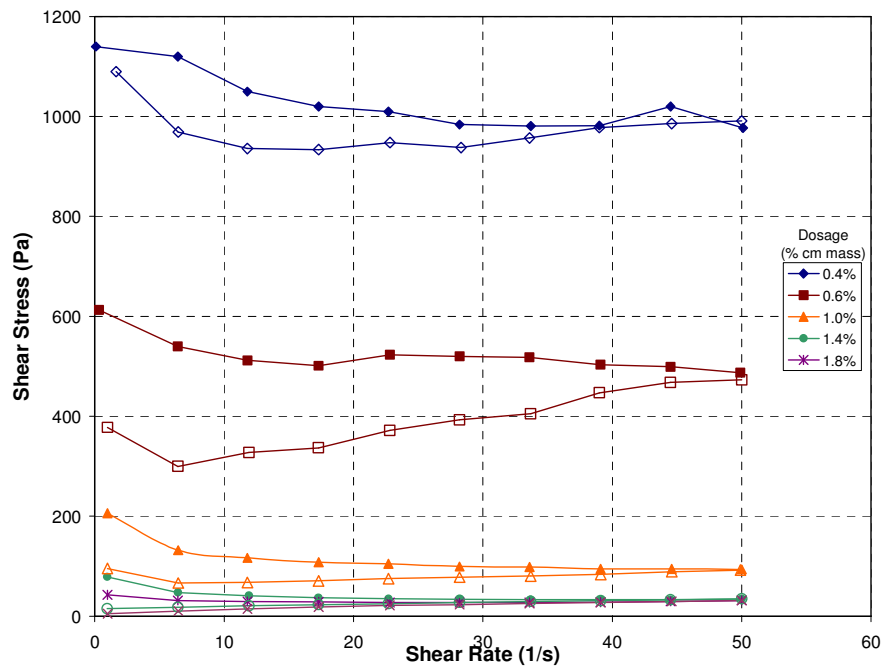**Figure 8.3: Effect of HRWRA Dosage on Plastic Viscosity (PC-01-I/II, w/c = 0.30)**

Figure 8.4: Flow Curves for HRWRA-05 with Up-Curve (Open Points) and Down-Curve (Solid Points), (PC-01-I/II, w/c = 0.30)

134

### 8.2.2 Cement-HRWRA Interaction

To evaluate the interaction of polycarboxylate-based HRWRAs with different cements, each of the 4 cements was tested with and without HRWRA. When tested at a w/c of 0.40 with no admixture, the 2 Type III cements exhibited significantly higher yield stresses and plastic viscosities than the other two cements (Figure 8.5). Such a result was expected due to the higher fineness of the Type III cements. When a constant dosage of HRWRA-02 was used at a w/c of 0.30, the Type I/II cement exhibited the lowest yield stress and plastic viscosity (Figure 8.6). Even though the PC-03-I cement exhibited the lowest yield stress and plastic viscosity in the pastes with no admixture, it exhibited higher yield stress and plastic viscosity than the PC-01-I/II cement when tested with HRWRA-02. This discrepancy is likely due partially to the lower C_3A content of the Type I/II cement. The PC-02-III cement exhibited higher yield stress and plastic viscosity than the PC-03-III cement, which was partially reflected in the pastes with no admixture. Compared to the PC-03-III cement, the PC-02-III cement has lower C_3A and SO_3 contents and lower fineness, which would predict lower HRWRA demand.

The different cements were also compared with HRWRA-01, as shown in Figure 8.7. The 2 Type III cements exhibited significantly higher yield stresses than the Type I/II and Type I cements; however, the plastic viscosity of the PC-02-III paste was between those of the Type I/II and Type I cements and significantly lower than the PC-03-III cement. Although the yield stress and plastic viscosity of the PC-03-III paste was lower than the PC-02-III paste when tested with HRWRA-02, the yield stress and plastic viscosity were higher in the PC-03-III paste when tested with HRWRA-01.

The responses of paste to HRWRA-01 and HRWRA-02 were compared for the PC-01-I/II and PC-02-III cements (Figure 8.8 and Figure 8.9). For both HRWRAs, the saturation dosage for yield stress was twice as high for the PC-02-III cement as for the PC-01-I/II cement. For plastic viscosity, neither admixture reduced the plastic viscosity for the PC-02-III cement as significantly as for the PC-01-I/II cement. By producing a near-zero yield stress but a plastic viscosity between 0.2 and 0.4 Pa.s, the pastes with PC-02-III cement and either HRWRA-01 or HRWRA-02 performed similarly to the pastes with PC-01-I/II cement and HRWRA-04.
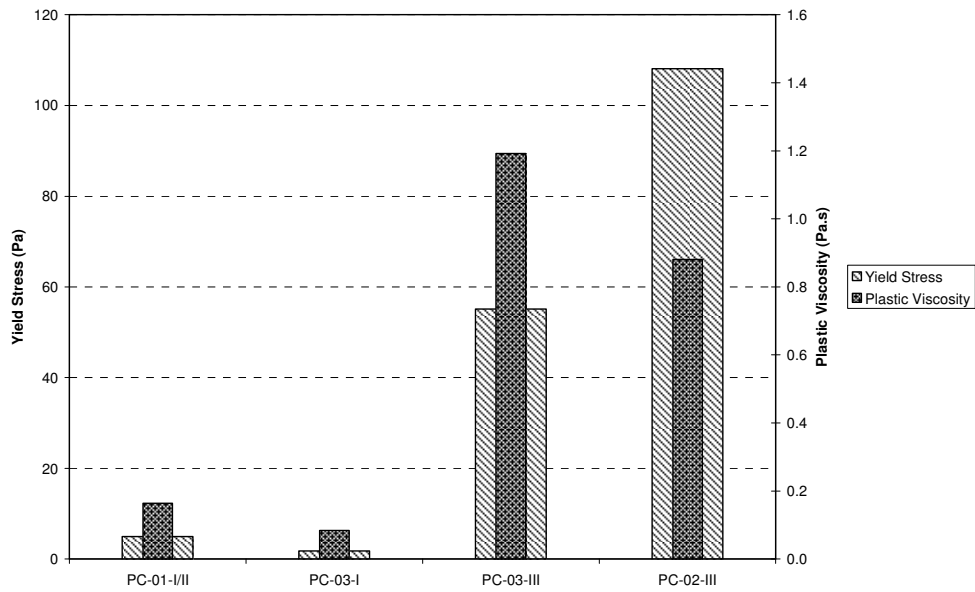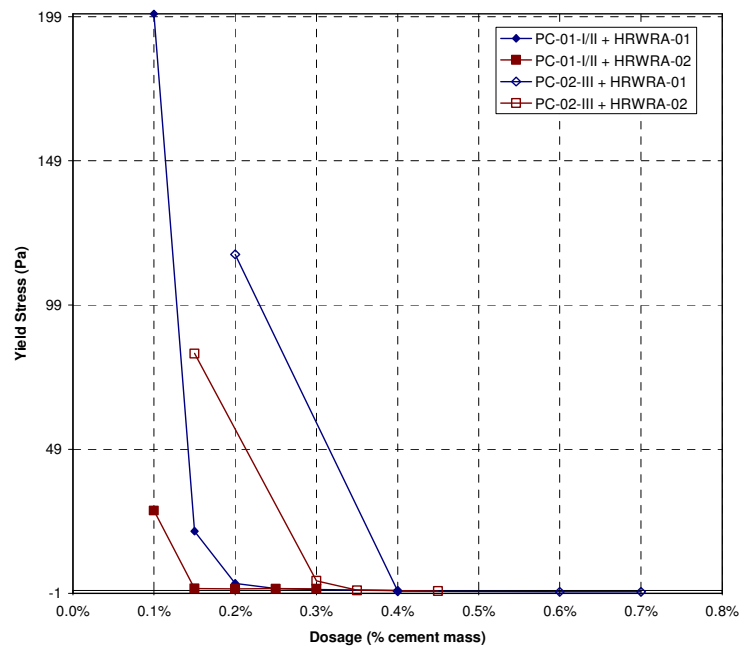
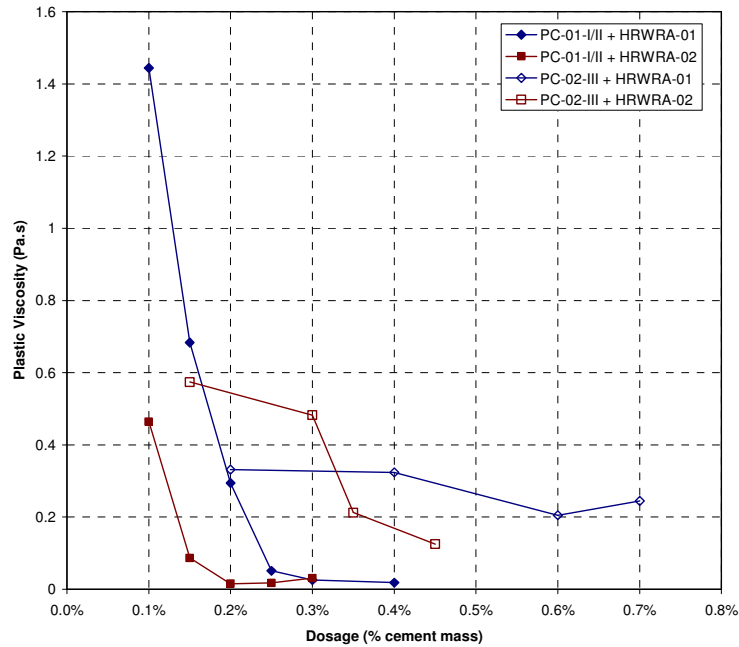**Figure 8.5: Comparison of Cements at w/c = 0.40 with No Admixture**
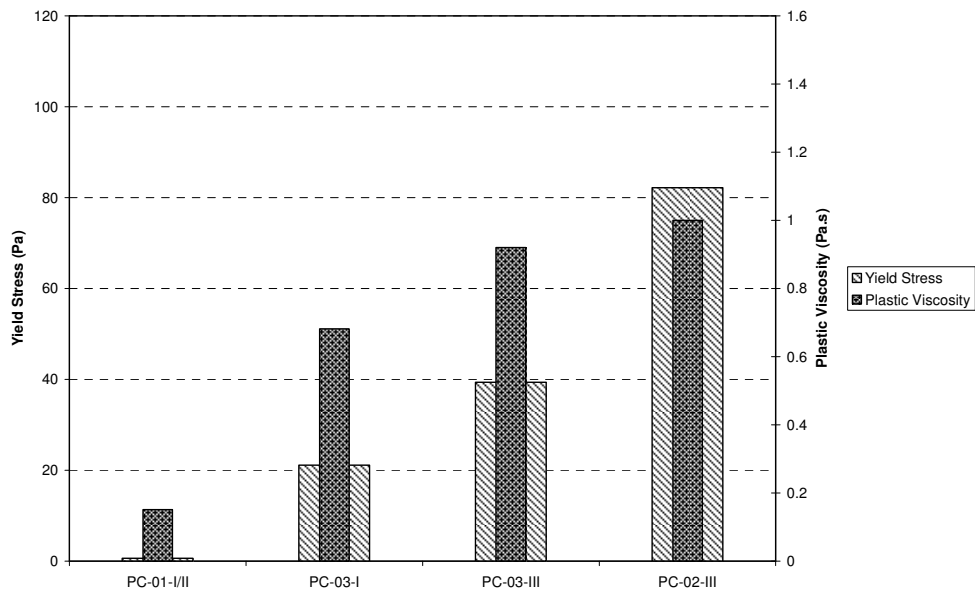
Figure 8.6: Comparison of Cements at w/c = 0.30 with HRWRA-02 at 0.15% of cement mass

136
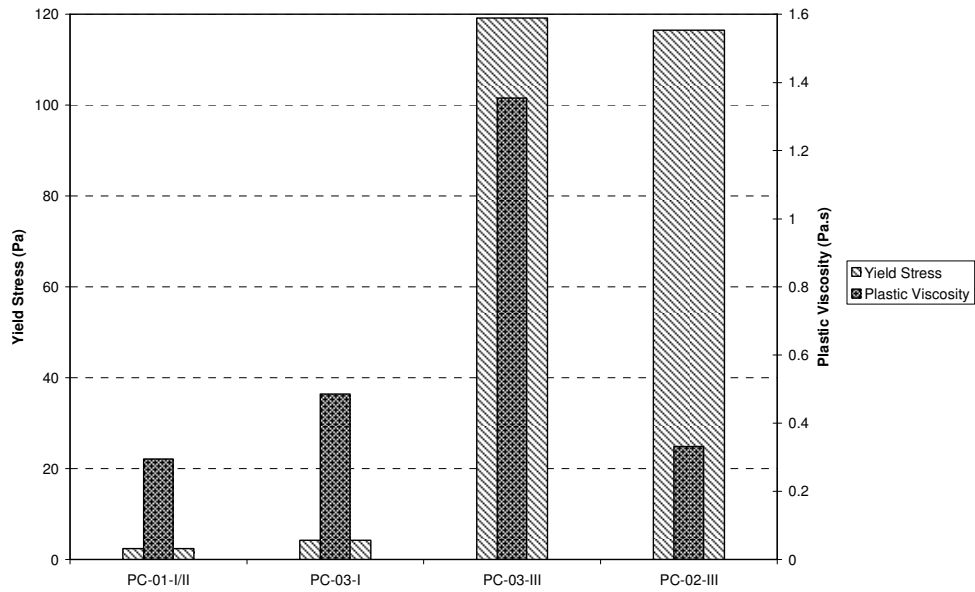
Figure 8.7: Comparison of Cements at w/c = 0.30 with HRWRA-01 at 0.20% of cement mass

Figure 8.8: Effects of HRWRA Dosage on Yield Stress for PC-01-I/II and PC-02-III Cements (w/c = 0.30)

Figure 8.9: Effects of HRWRA Dosage on Plastic Viscosity for PC-01-I/II and PC-02-III Cements (w/c = 0.30)

8.2.3 VMA

The rheological properties of the two different VMAs were compared by first measuring the flow curves of the as-received aqueous solutions. As shown in Figure 8.10, both exhibited shear-thinning behavior; however, VMA-02 was much more potent. Indeed, the recommended dosage of VMA-02 (0.5-4.0 oz/cwt) is less than that of VMA-01 (2-14 oz/cwt).

The two VMAs were next tested at the manufacturer's recommended dosage ranges. As indicated in Figure 8.11, both VMAs increased the plastic viscosity at their minimum dosages while having essentially no effect on yield stress. Near the maximum dosages; however, the increases in yield stress were greater than the increases in the plastic viscosity for both VMAs. Although the percentage increases in yield stress were large for both VMAs, the yield stresses were all relatively low in absolute terms. For a given increase in yield stress, VMA-02 resulted in a greater increase in plastic viscosity than VMA-01. Further, VMA-02 resulted in a significantly greater increase in apparent viscosity than VMA-01, as indicated in Figure 8.12. Therefore, if the objective of using a VMA is to increase only plastic viscosity, the admixtures should be used at low dosages. If the resulting increase in plastic viscosity is insufficient, VMA-02 is preferred over VMA-01 because it will result in a smaller increase in yield stress for a

given increase in plastic viscosity. Both VMAs also resulted in shear thinning behavior, as indicated in Figure 8.13 and Figure 8.14. Although VMA-02 resulted in a greater increase in apparent viscosity at its maximum dosage, VMA-01 resulted in a greater degree of shear thinning, as indicated in the exponent terms in the Herschel-Bulkley models.

The ability of the VMAs to minimize the effects of variations in water content was evaluated by testing pastes with varying water contents but constant HRWRA and VMA dosages. As indicated in Figure 8.15, the variation in yield stress due to changes in water content was mitigated by VMA-01 but not by VMA-02. Similarly, Figure 8.16 indicates that VMA-01 mitigated variations in plastic viscosity to a much greater degree than VMA-02. Therefore, if the objective is to minimize variations in yield stress and plastic viscosity due to changes in water content, VMA-01 is preferred over VMA-02 assuming that the effects of each admixture are similar at other dosages.
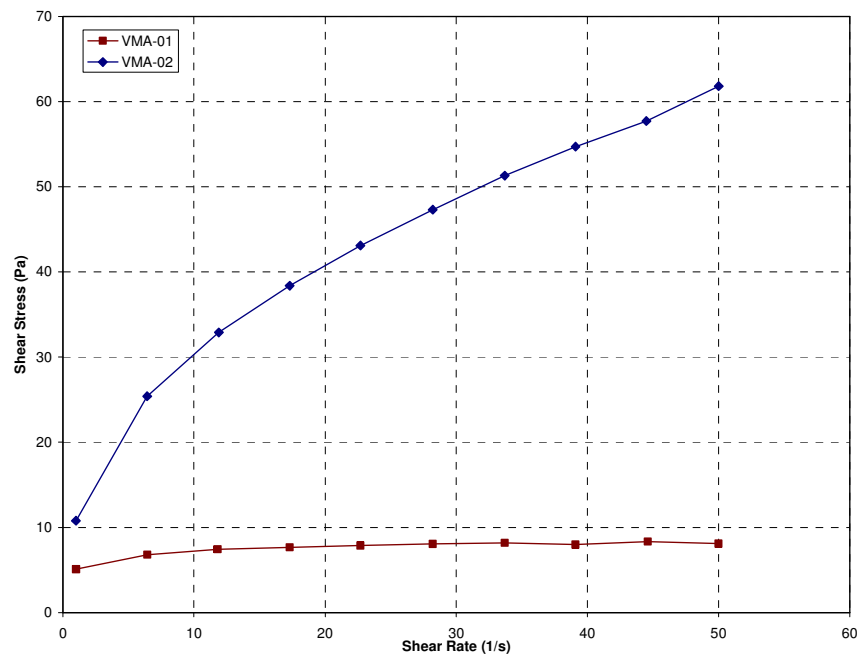
Figure 8.10: Measured Flow Curves for As-Received Aqueous Solutions of VMAs
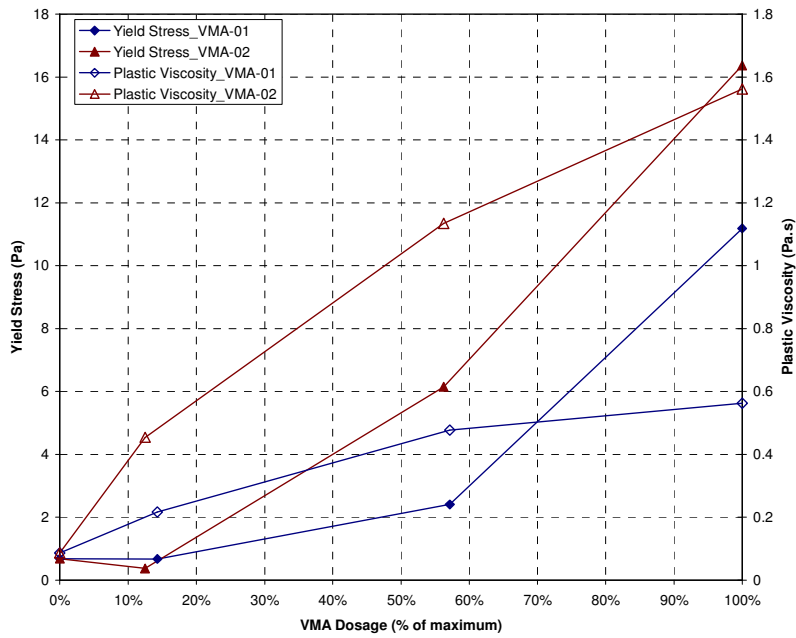
Figure 8.11: Effects of VMAs on Rheological Properties (PC-01-I/II cement, w/c=0.30, HRWRA-02 at 0.15% of cement mass)
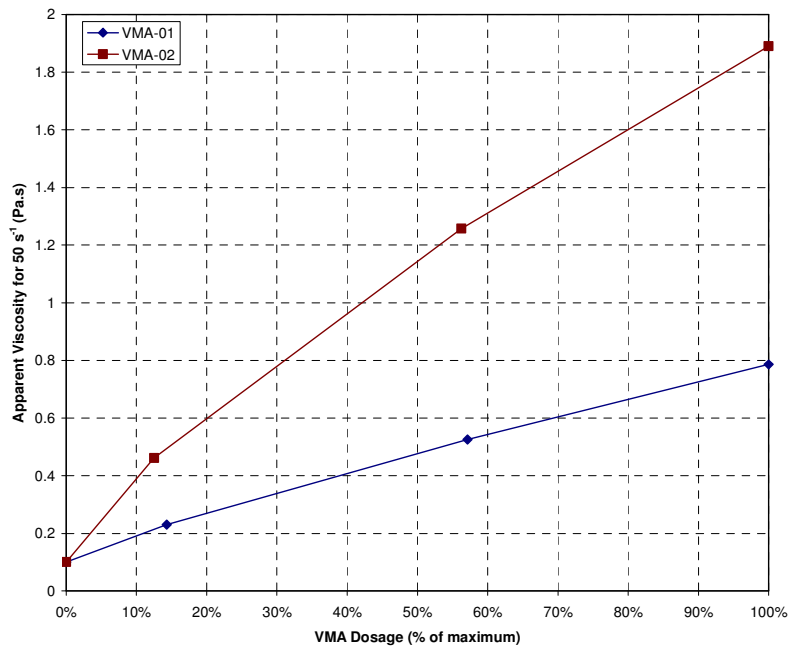
Figure 8.12: Effects of VMAs on Apparent Viscosities at 50 s^{-1} (PC-01-I/II cement, w/c=0.30, HRWRA-02 at 0.15% of cement mass)
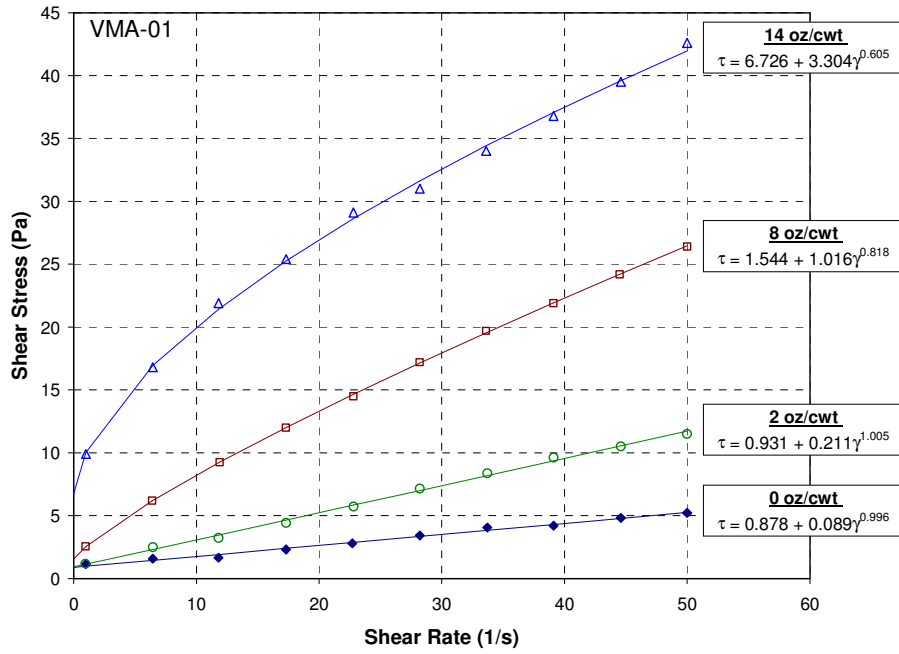
Figure 8.13: Effects of VMA-01 on Flow Curves (PC-01-I/II cement, w/c=0.30, HRWRA-02 at 0.15% of cement mass)
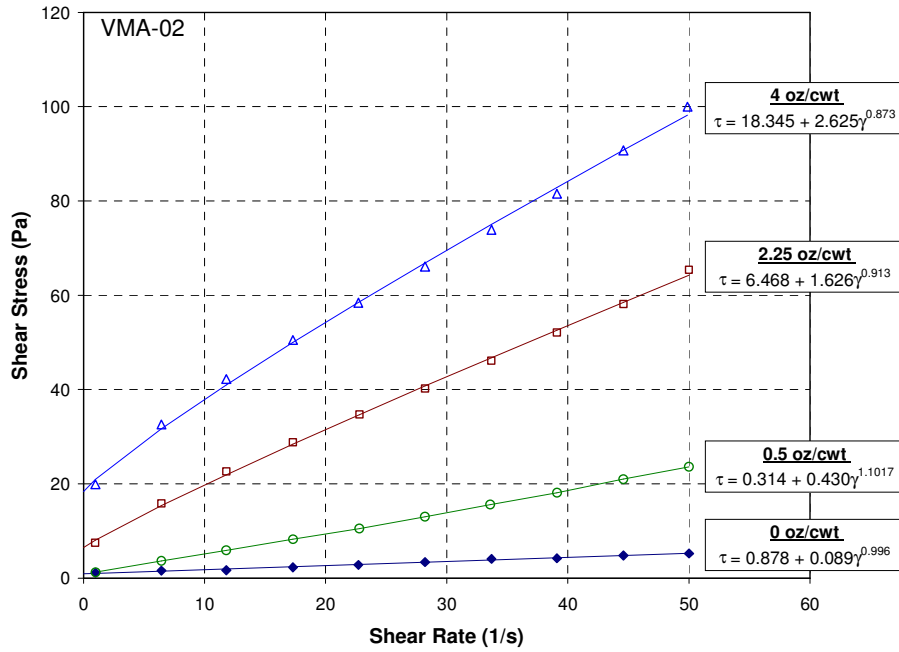

Figure 8.14: Effects of VMA-02 on Flow Curves (PC-01-I/II cement, w/c=0.30, HRWRA-02 at 0.15% of cement mass)
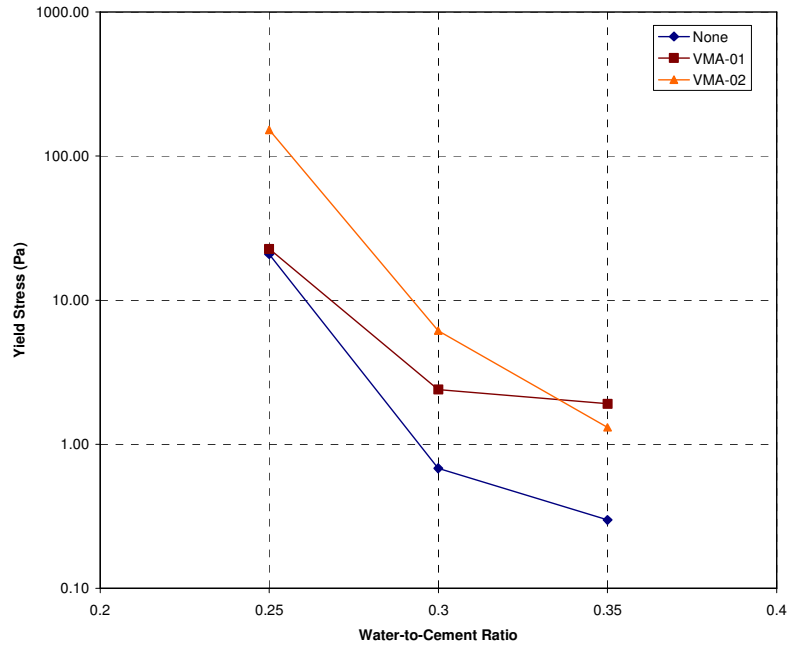
Figure 8.15: Sensitivity of Yield Stress to Changes in Water Content (PC-01-I/II cement, HRWRA-02 at 0.15% of cement mass, VMA-01 at 8 oz/cwt, VMA-02 at 2.25 oz/cwt)
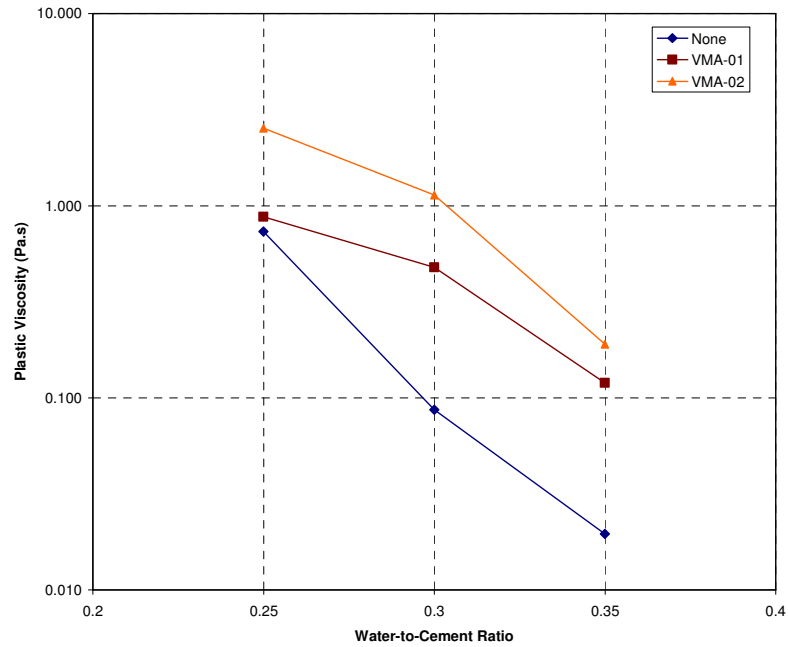
Figure 8.16: Sensitivity of Plastic Viscosity to Changes in Water Content (PC-01-I/II cement, HRWRA-02 at 0.15% cement, VMA-01 at 8 oz/cwt, VMA-02 at 2.25 oz/cwt)

8.2.4 Fly Ash

The effects of fly ash were evaluated by replacing cement with fly ash at a rate of 15% by volume and maintaining a constant solids volume concentration. The volume of HRWRA was held constant. The reductions in yield stress and plastic viscosity were similar for each of the three fly ashes tested, as shown in Figure 8.17. Although both yield stress and plastic viscosity were reduced, the reduction in yield stress was greater in percentage terms. In the paste rheology measurements presented here, the differences in performance were due to difference in particle size distribution as well as shape and texture because the solids volume concentration was held constant. In typical industry practice, the fly ash would be replaced by mass—not volume—and the water-cementitious materials ratio—not the solids volume concentration—would be held constant. The use of mass replacement instead of volume replacement results in the use of more fly ash because of the lower density of fly ash. The use of a constant water-cementitious materials ratio instead of a constant solids volume concentration results in the use of less water and, thus, a higher solids volume concentration. Therefore, the tests reported here may not match the effects for tests when the pastes are proportioned in accordance with typical industry practice. Based on typical industry practice for proportioning, the use of fly ash with lower specific gravity will result in higher solids volume concentration and reduced improvement in rheological properties assuming all other characteristics are constant. In addition, the lower yield stress associated with the mixtures with fly ash would allow a reduction in HRWRA dosage to reach a given slump flow. This reduction in HRWRA dosage would result in increased yield stress and plastic viscosity. The use of fly ash from before and after the conversion to low NO_x burner technology resulted in approximately the same reduction in yield stress and plastic viscosity for the case considered.
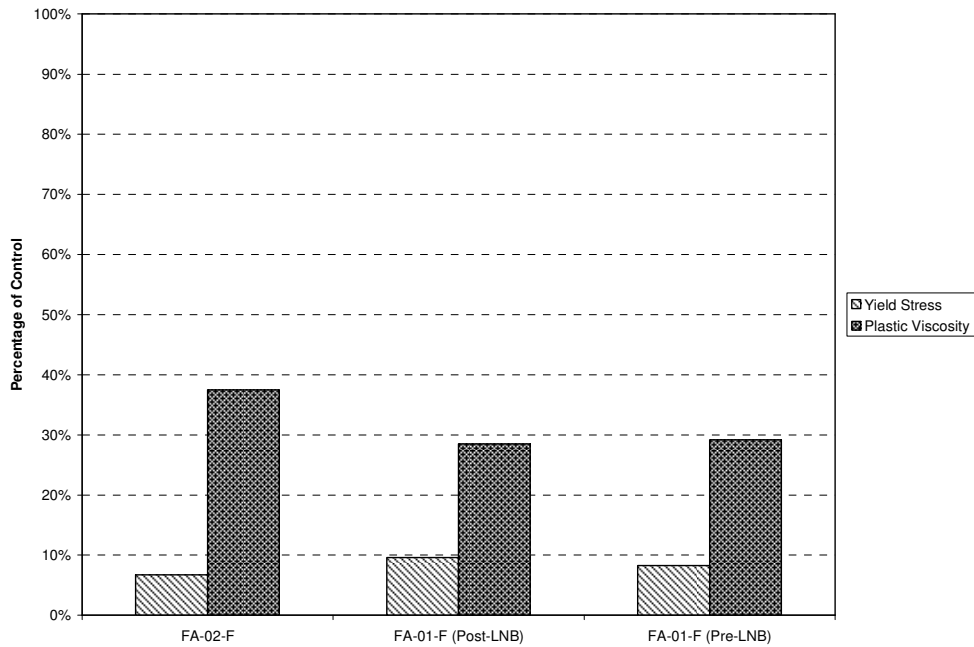
Figure 8.17: Comparison of Fly Ash Performance (φ=0.514, 15% volume replacement, constant HRWRA-02 volume based on 0.15% of cement mass in control mixture)

8.2.5 Microfines

Microfines were tested at a volume replacement rate of 15% of cement. As indicated in Figure 8.18, when the water-to-cement ratio was held constant, the microfines significantly increased the Bingham parameters. This increase was mainly due to the increased solid volume concentration of the pastes. When the solids volume concentration was held constant, the effects of the microfines on rheological properties were substantially less. The granite microfines performed better than the limestone microfines at both a constant w/c and constant solids volume concentration.
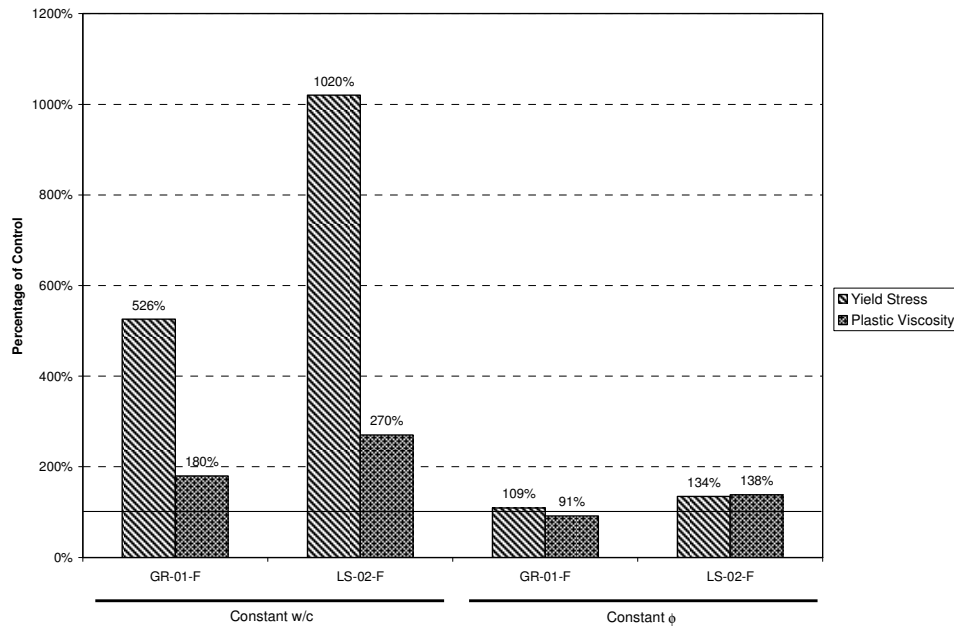
Figure 8.18: Comparison of Microfines at Constant w/c and Solids Volume Fraction (PC-01-I/II cement, w/c =0.40)

8.3   Conclusions

The following conclusions can be drawn based on the test results presented in this chapter:

- The polycarboxylate-based HRWRAs generally decreased both yield stress and plastic viscosity to near-zero values at saturation dosages; however, the saturation dosage was lower for yield stress than for plastic viscosity.

- The naphthalene-based HRWRA required significantly higher dosages than polycarboxylate-based HRWRAs to achieve a comparable reduction in yield stress. At a given reduction in yield stress, the naphthalene-based HRWRA decreased the plastic viscosity to a much greater degree than did the polycarboxylate-based HRWRAs.

- The Type III cements exhibited higher yield stress and plastic viscosity than comparable mixtures with Type I and Type I/II cements when tested with and without HRWRA.

- The relative performances of different cements in pastes without HRWRA were not directly reflected in pastes with HRWRA, which was due to differences in the interaction of the HRWRAs with cement.

- The yield stress saturation dosage for PC-02-III cement was twice as high as that for PC-01-I/II cement for both HRWRA-01 and HRWRA-02.

- The as-received aqueous solutions of the two tested VMAs exhibited shear-thinning behavior.

- The two VMAs increased only the plastic viscosity at low dosages but increased both yield stress and plastic viscosity at higher dosages. For a given increase in yield stress, VMA-02 resulted in a greater increase in plastic viscosity while VMA-01 resulted in a greater degree of shear thinning.

- VMA-01 mitigated changes in yield stress and plastic viscosity due to changes in water content to a greater degree than VMA-02.

- The three fly ashes, when tested at a constant solids volume concentration and constant HRWRA volume, resulted in similar reductions in Bingham parameters. For each fly ash, the decreases were greater for yield stress than plastic viscosity.

- The two aggregate microfines, when tested at a constant solids volume concentration, resulted in much smaller changes in yield stress and plastic viscosity than when a constant water-cement ratio was used. In both cases, the effects on rheological properties were less for the granite microfines than the limestone microfines.

Chapter 9: Effects of Aggregates in Mortar

The effects of aggregates in mortar were evaluated by considering separately the effects of fine aggregate shape characteristics, fine aggregate grading, microfines content, and mixture proportions. These effects were evaluated in three sets of tests. In the first set of tests, the effects of shape characteristics and grading were determined by varying the grading for a given aggregate source (fixed shape characteristics, variable grading) and by changing the aggregate source for a given grading (variable shape characteristics, fixed grading). In the second set of tests, the effects of microfines were evaluated by using various amounts of microfines in a mortar mixture as part of either the aggregate volume (constant w/cm, variable w/p) or powder volume (variable w/cm, constant w/p). In the third set of tests, the effects of mortar mixture proportions—namely paste volume, water-powder ratio, and fly ash dosage—were evaluated for three different fine aggregates. All test data are provided in Appendix C.

9.1 Materials, Mixture Proportions, and Test Procedures

The standard mortar mixture used to evaluate the effects of fine aggregate shape characteristics, fine aggregate grading, and microfines content was based on a successful concrete mixture. Both the concrete and mortar mixtures are shown in Table 9.1. The concrete mixture incorporated NA-02-C and NA-02-F aggregates and had a total cementitious materials content of 700 lb/yd^3, a paste volume of 30.9%, a w/cm of 0.35, and a fly ash replacement rate of 25% by mass. The mortar mixture was obtained by removing the coarse aggregate volume and leaving unchanged the relative volumes of the remaining constituents. The mixture utilizes PC-01-I/II cement, FA-02-F fly ash, and HRWRA-02 admixture.

Table 9.1. Mortar Mixture Proportions for Evaluation of Fine Aggregate Shape Characteristics and Grading and Microfines Content

| Material | ID | Concrete | | Mortar |
		Volume (%)	Mass (lb/yd^3)	Volume (%)
Fine Aggregate	variable	34.6	variable	52.8
Coarse Aggregate	variable	34.6	variable	--
Cement	PC-01-I/II	9.9	525	15.1
Fly Ash	FA-02-F	4.5	175	6.8
Water		14.5	245	22.2
Air		2.0	0	3.1

The fresh properties were evaluated with the mini-slump flow test and mini-v-funnel test, which are depicted in Figure 9.1. The mini-slump flow test consisted of the mini-slump cone (ASTM C 230) centered on a level, plastic plate. The mini-slump cone was filled with mortar and immediately lifted. The time for the mortar to spread to a diameter of 8 inches (T_8) and the final flow diameter were recorded. For all tests, the HRWRA was adjusted to achieve a mini-slump flow of 9 inches. The mini-v-funnel test was performed by filling the mini-v-funnel in one lift, pausing for one minute, opening the bottom gate, and measuring the time for the mortar to flow out of the funnel.
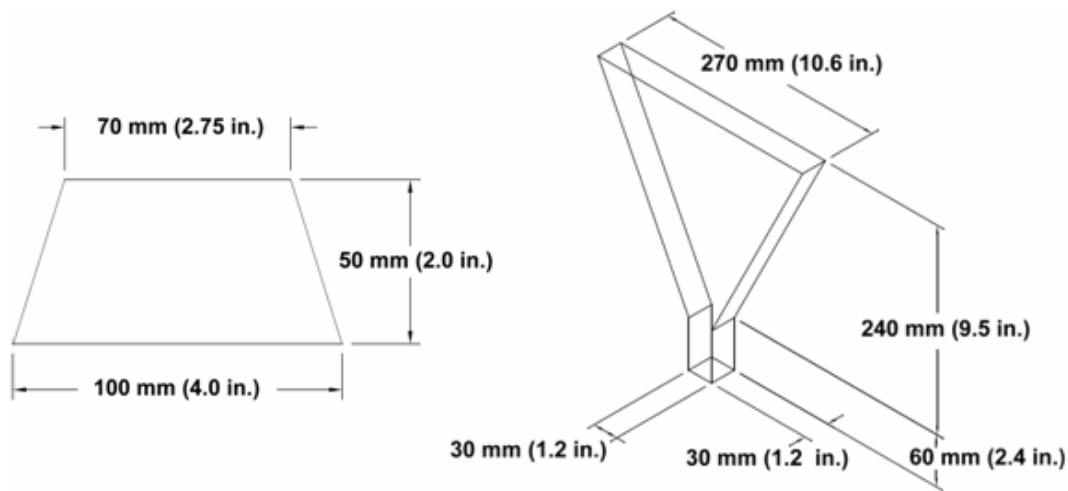
Figure 9.1: Mini-Slump Flow Cone (Left) and Mini-V-Funnel

The mini-slump flow test and mini-v-funnel test were selected because their results should be related to yield stress and plastic viscosity, respectively. Indeed, it has been shown previously that slump flow is related mainly to yield stress (Roussel, Stefani, and Leroy 2005; Testing-SCC 2005), that the slump flow time is related mainly to plastic viscosity (Testing-SCC 2005) or to both yield stress and plastic viscosity (Khayat, Assaad, and Daczko 2004), and that the v-funnel time is related mainly to plastic viscosity (Testing-SCC 2005) or to both yield stress and plastic viscosity (Khayat, Assaad, and Daczko 2004; Roussel and Leroy 2005). By maintaining a constant target mini-slump flow for all mixtures, the yield stress should remain relatively constant. With the yield stress constant, the mini-v-funnel time and T_8 should be a function primarily of plastic viscosity. Figure 9.2 shows a strong correlation between mini-v-funnel time and plastic viscosity measured on a set of mortar mixtures that had varying mini-slump flows. These two simple and inexpensive test methods can be used in industry

laboratories to evaluate rheological properties efficiently. The mini-slump flow cone is commercially available in the United States and the mini-v-funnel can be constructed at a relatively low cost.
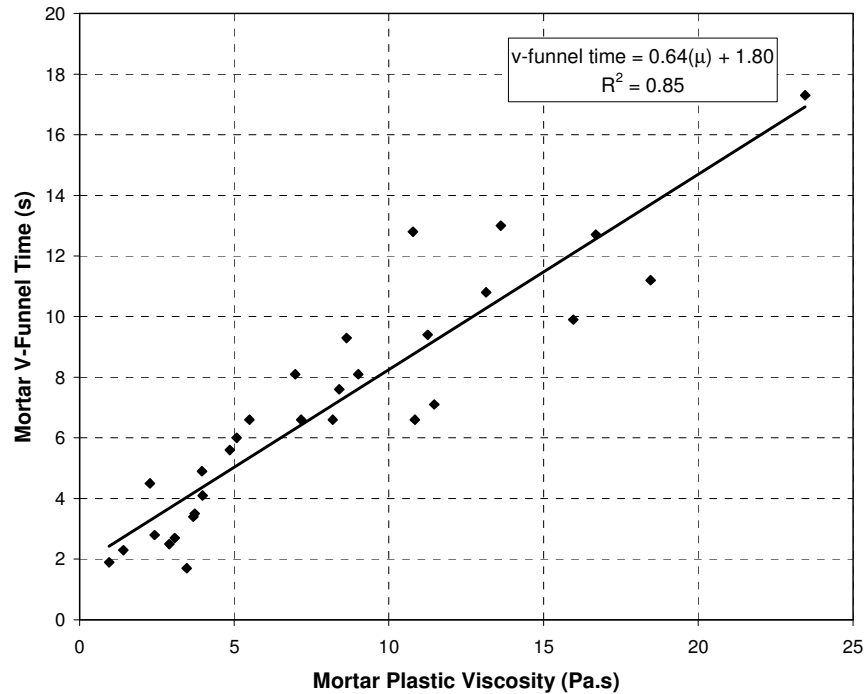
Figure 9.2: Relationship between Plastic Viscosity and V-Funnel Time (Koehler et al. 2007)

Figure 9.3, which shows all test data described in this chapter, indicates a correlation between mini-v-funnel time and T_8. The correlation is expected because, when used at a constant slump flow, the two tests each measure a value related to plastic viscosity. The correlation, however, is poor for high values of mini-v-funnel time and T_8 because such viscous mortar mixtures in some cases had insufficient paste volume or water content, resulting in higher variability and several obvious outliers. The mini-v-funnel test is believed to be a more reliable test because the longer measurement times can be determined more precisely. Therefore, the mini-v-funnel time is used for the remainder of this chapter. Figure 9.4 indicates a poor correlation between the HRWRA demand for a 9-inch mini-slump flow and the corresponding mini-v-funnel time, even when potential outliers are removed.
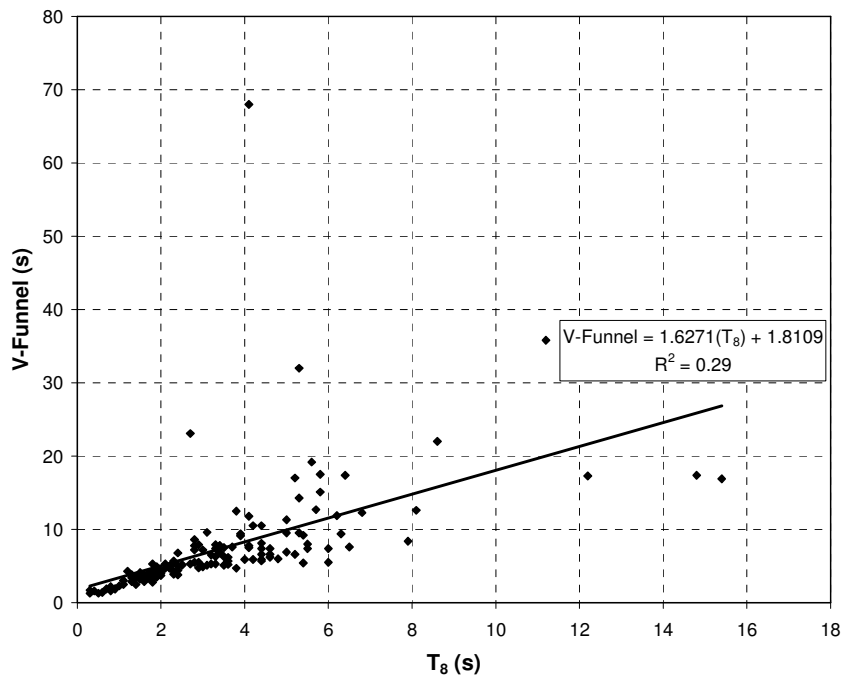
Figure 9.3: Relationship between T_8 and V-Funnel Time for All Test Data (Mini-Slump Flow of 9 Inches)
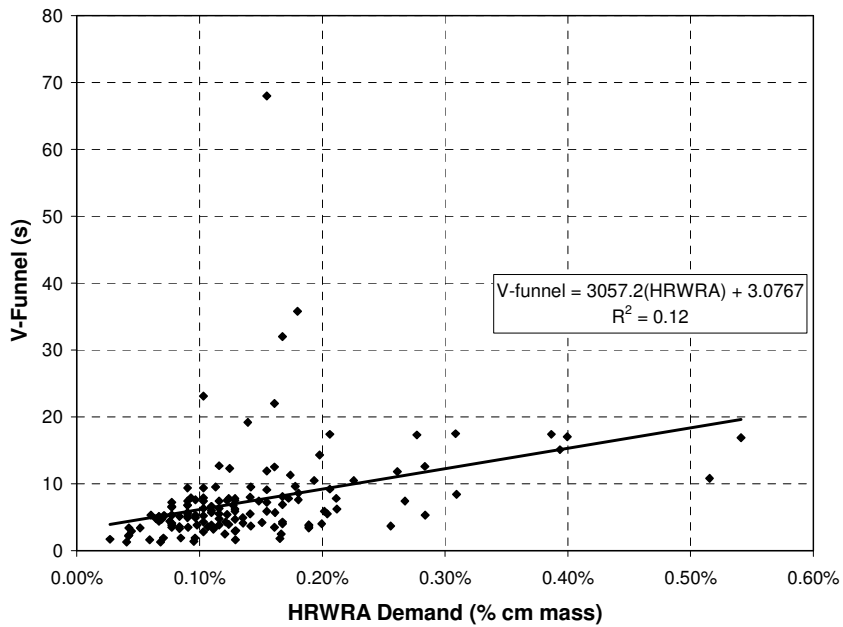
Figure 9.4: Relationship between HRWRA Demand and V-Funnel Time

In general, low HRWRA demand and low mini-v-funnel times are preferred. A lower HRWRA demand reduces cost. The mortar viscosity for use in concrete should not be too low in

order to prevent problems such as segregation and should not be too high in order for the mixture to be adequately flowable. Materials that reduce mortar viscosity are favorable because their use can offset other factors that increase viscosity. The concrete HRWRA demand and viscosity depend on not only the mortar properties but also the volume of mortar and properties of the coarse aggregate.

The mixing procedure used for all mortar mixtures described in this chapter is described in Table 9.2. The mortar mixer met the requirements of ASTM C 305.

Table 9.2. Mortar Mixing Procedure

1. Add oven-dry sand and water; mix on slow speed (145 rpm) for **30 seconds**.
2. Let water soak into aggregates for **4 minutes, 30 seconds**.
3. Add cement gradually, while running mixer at slow speed for **30 seconds**.
4. Mix at medium speed (285 rpm) for **30 seconds**.
5. Pause for **1 minute**. Scrape sides of mixer bowl and add admixture.
6. Mix at medium speed for **120 seconds**.
7. Test. (verify 9-inch mini-slump flow first, then conduct other tests)
8. If needed to achieve target mini-slump flow, add more admixture and mix for **60 seconds**. Retest.

9.2 Effects of Fine Aggregates

9.2.1 Test Plan

The effects of fine aggregate shape characteristics (shape, angularity, and texture) and grading were evaluated by measuring 12 different fine aggregates in 5 different gradings. This test plan allowed the effects of shape characteristics and the effects of grading to be evaluated independently. By varying the grading for a given aggregate source, the shape characteristics remained approximately unchanged. Similarly, when varying the aggregate source for a given grading, the main differences between each mixture were the shape characteristics.

The five gradings for each fine aggregate were the as-received grading, the as-received grading with microfines removed, the 0.45 power curve grading, a coarse sand grading, and a fine sand grading. The later three gradings are shown in Figure 9.5. The microfines were removed from these three gradings to isolate any effects of microfines on flow properties. The microfines were considered separately.
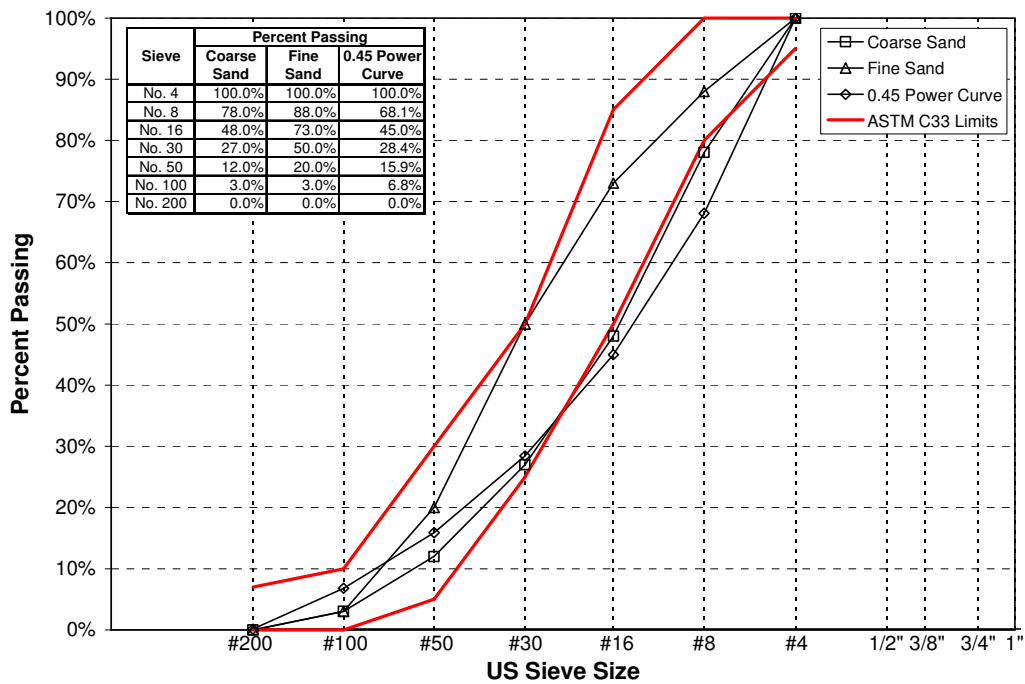
151

	Percent Passing		
Sieve	Coarse Sand	Fine Sand	0.45 Power Curve
No. 4	100.0%	100.0%	100.0%
No. 8	78.0%	88.0%	68.1%
No. 16	48.0%	73.0%	45.0%
No. 30	27.0%	50.0%	28.4%
No. 50	12.0%	20.0%	15.9%
No. 100	3.0%	3.0%	6.8%
No. 200	0.0%	0.0%	0.0%

Figure 9.5: Standard Gradings

9.2.2 Test Results

Both the shape characteristics and grading significantly affected the HRWRA demand and mini-v-funnel time, as indicated in Figure 9.6 and Figure 9.7. For each given standard grading, the HRWRA demand and mini-v-funnel time varied significantly as the aggregate source changed, indicating the effect of shape characteristics. For a given aggregate source, the effects of grading varied from minor in some cases—such as for LS-05-F, LS-06-F, TR-01-F, and NA-01-F—to substantial in other cases—such as for DO-01-F, DL-01-F, or GR-01-F. In general, the well-shaped aggregates, which resulted in low HRWRA demand and mini-v-funnel time, exhibited the smallest differences in performance as grading was changed. Mixtures with poorly shaped aggregates require greater paste volumes than those with well-shaped aggregates. Increasing the paste volume increases robustness with respect to aggregate properties. Therefore, mixtures with well-shaped aggregates were much more robust and were less sensitive to changes in grading. If the paste volume in the mixtures with well-shaped aggregates were reduced, the differences in performance between each grading would be greater. Similarly, the differences between well-shaped aggregates for a given grading would be magnified.

In addition to the HRWRA demand and mini-v-funnel times, it is also important to consider the harshness of the mixtures. If the amount of fine particles is insufficient—due either

to the lack of powder in the paste or to the lack of sufficient fine particles from the sand—the mixture can be harsh. In certain cases, the yield stress and plastic viscosity of the paste can be reduced to such a degree that the paste does not mobilize the aggregate particles but instead flows out of the aggregate matrix, leaving behind a pile of aggregate in the center of the slump flow specimen. Harsh mixes were observed for DO-01-F, LS-03-F, and GR-01-F.

The two natural sands (NA-01-F and NA-02-F) both resulted in low HRWRA demand and low mini-v-funnel time. Such a result was expected due to the favorable shape characteristics of these fine aggregates. Several of the manufactured sands exhibited performance that was similar to or better than the two natural sands. In particular, LS-02-F and LS-06-F performed well when compared to the natural sands, regardless of the grading.

Several of the poorly performing fine aggregates could be improved by changing the grading. For instance DO-01-F, LS-03-F and GR-01-F resulted in mixtures that were extremely viscous and required impractically high HRWRA dosages for certain gradings. These mixtures could be improved substantially by changing the grading. For example, the as-received grading for DO-01-F exhibited an excessively high mini-v-funnel time. By changing to the 0.45 power curve grading, the HRWRA demand and mini-v-funnel time were decreased dramatically.

The elimination of microfines from the as-received grading increased or decreased the HRWRA dosage and mini-v-funnel time depending on the aggregate source. It should be noted that the amount of microfines depended on the as-received grading and varied widely. For instance, the natural sands had much lower contents than most of the manufactured sands. In many cases, the as-received grading was not ideal for achieving SCC properties. Therefore, it may be possible to rectify a poorly performing aggregate by changing the grading, which could be a more viable option than changing fine aggregates or altering mixture proportions.
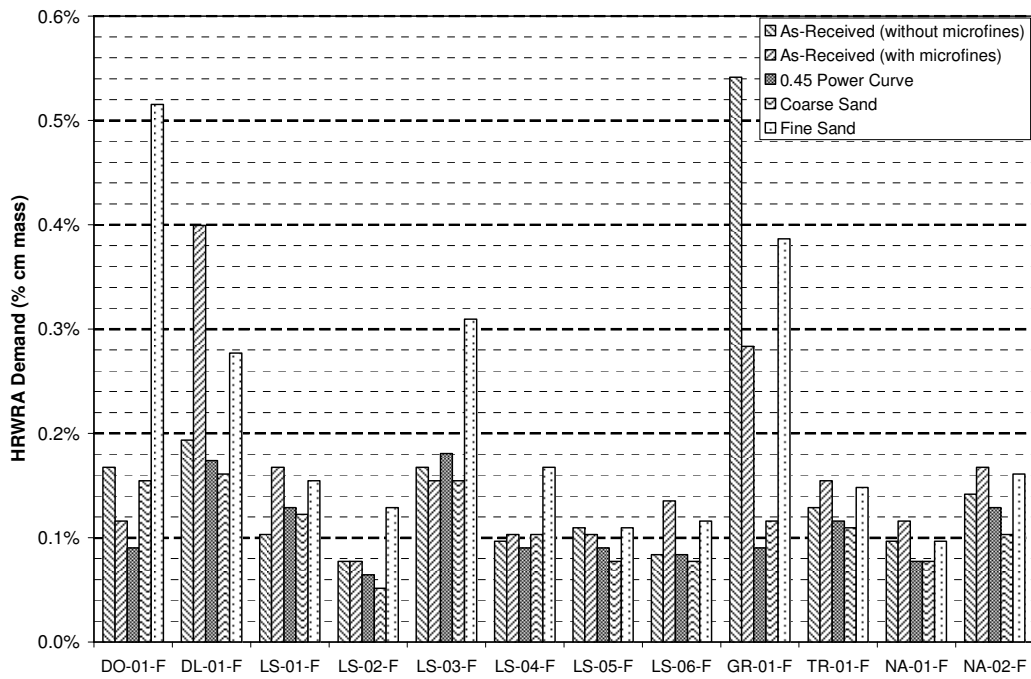
Figure 9.6: Effect of Sand Characteristics on HRWRA Demand
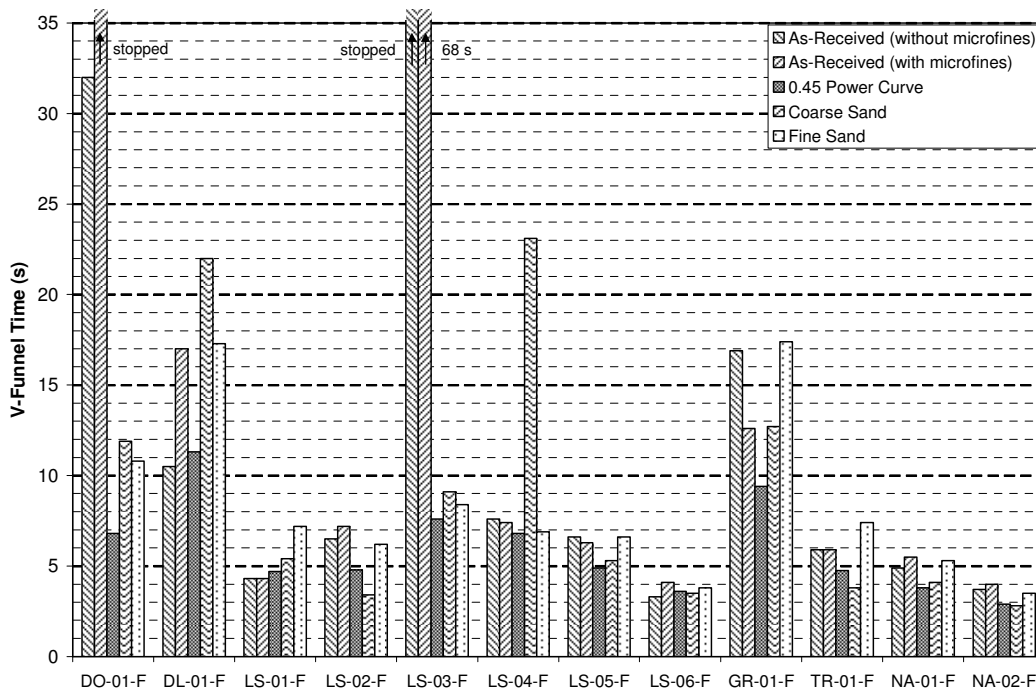
Figure 9.7: Effect of Fine Aggregate Characteristics on V-Funnel Time

The results for each grading are summarized in the box plots in Figure 9.8, which indicate the minimum, lower quartile, median, upper quartile, and maximum values for each

parameter. The range of results was highest in the two as-received gradings because the results were influenced by both shape characteristics and grading. The median HRWRA demand and mini-v-funnel time and the range of results were lowest for the 0.45 power curve grading. The median HRWRA demand and mini-v-funnel time for the coarse sand grading, however, were only slightly higher than for the 0.45 power curve grading. The fine sand exhibited a large range of results for HRWRA demand but not for mini-v-funnel time. As noted earlier, the minimum HRWRA demand and v-funnel time may not be optimal because in some cases the coarse sands can be harsh due to the lack of fine particles. The following conclusions can be reached regarding grading: (1) the 0.45 power curve grading results in consistently low HRWRA and plastic viscosity because of the high packing density, (2) a coarser grading also results in low HRWRA demand and plastic viscosity but may be harsh due to the lack of fine materials, and (3) a finer grading typically results in higher HRWRA demand and plastic viscosity but may have better overall workability because of the increased fine material and lack of harshness.
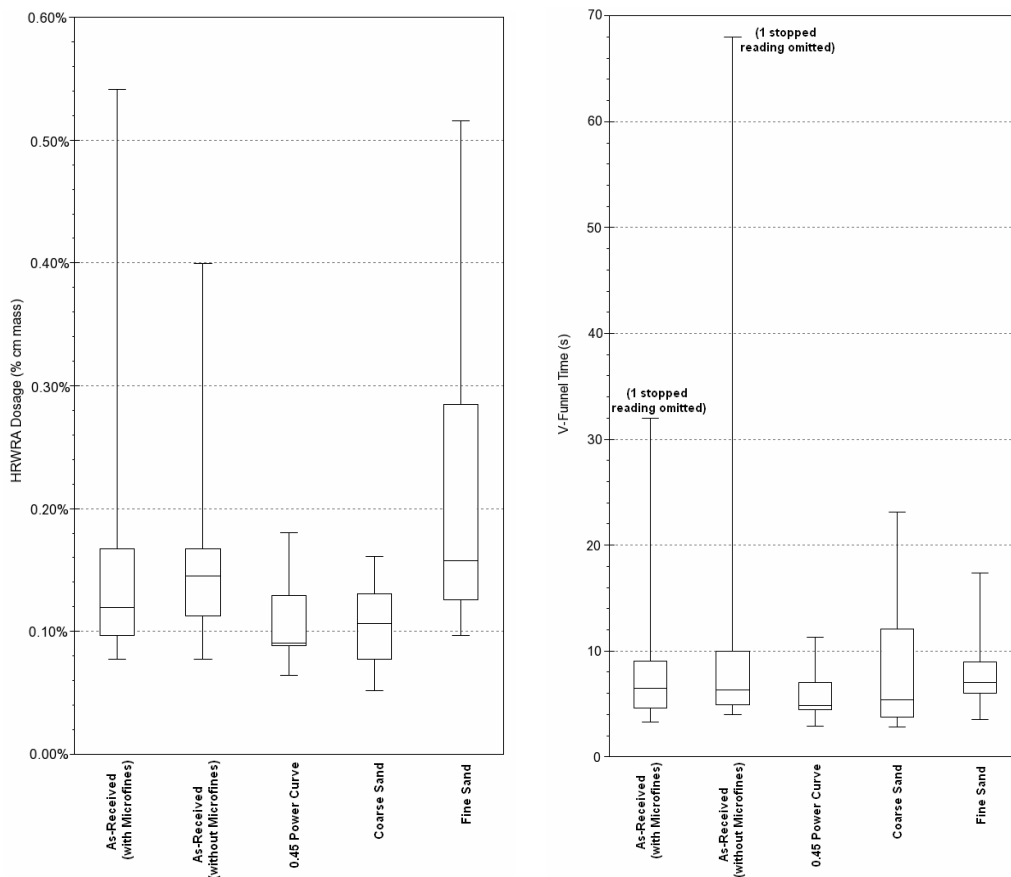
Figure 9.8: Box Plots for HRWRA Dosage and V-Funnel Time

155

In order to examine further the effects of shape characteristics and grading, the test results were compared to the sphericity indices, length-width ratios (L/W), uncompacted voids contents, and packing densities of the sands. As shown in Figure 9.9 and Figure 9.10, the L/W and sphericity index are not independently correlated to either HRWRA demand or mini-v-funnel time for any of the three standard gradings. Figure 9.11 indicates that increasing uncompacted voids content is associated with higher HRWRA demand and mini-v-funnel time; however, the scatter is large. The relationships between dry-rodded packing density and HRWRA demand and mini-v-funnel time for the as-received grading are shown in Figure 9.12. Packing density is often used to represent the combined effects of shape, angularity, texture, and grading. Although no correlation existed between packing density and HRWRA demand, a better correlation existed for mini-v-funnel time. Still, packing density can only provide an approximate prediction of mini-v-funnel time.
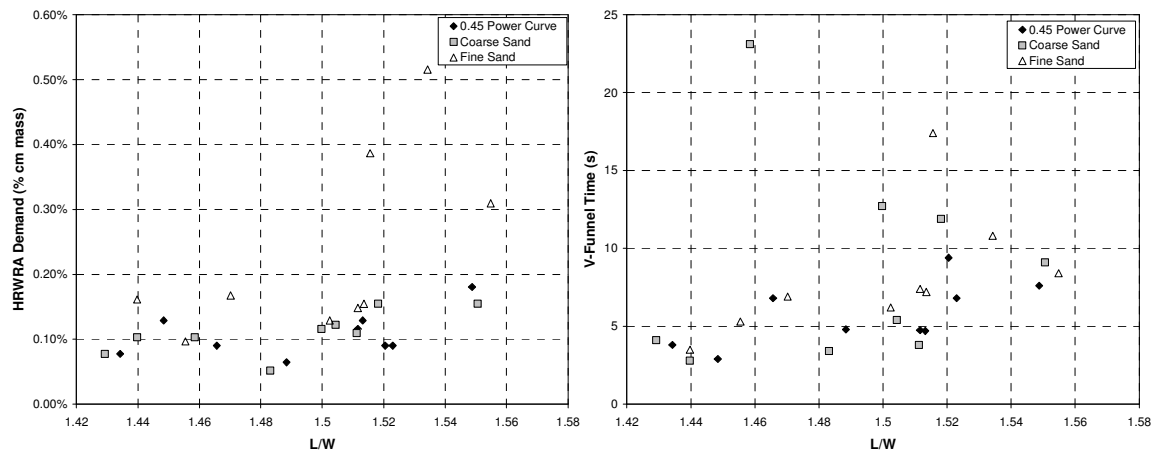
Figure 9.9: Effect of L/W Index on HRWRA Demand and V-Funnel Time
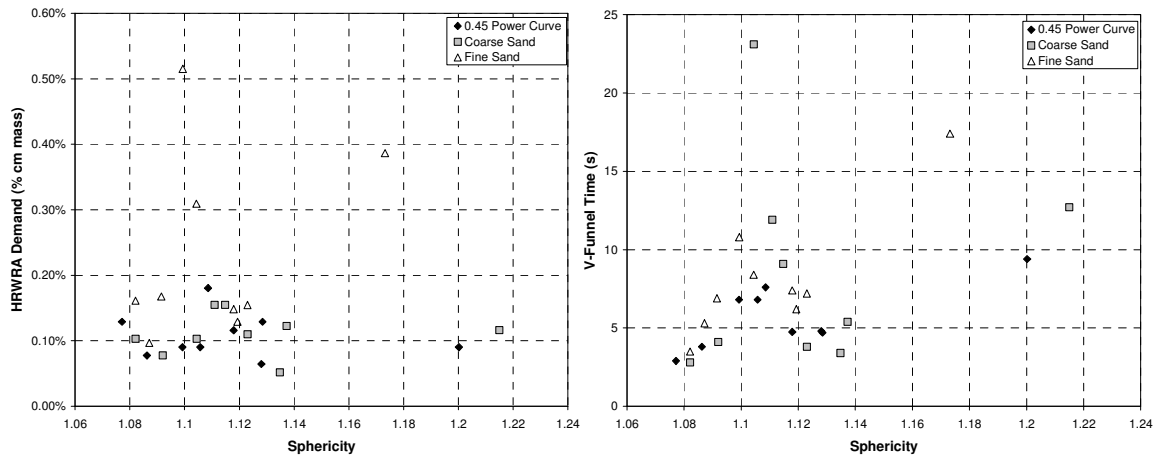
Figure 9.10: Effect of Sphericity Index on HRWRA Demand and V-Funnel Time
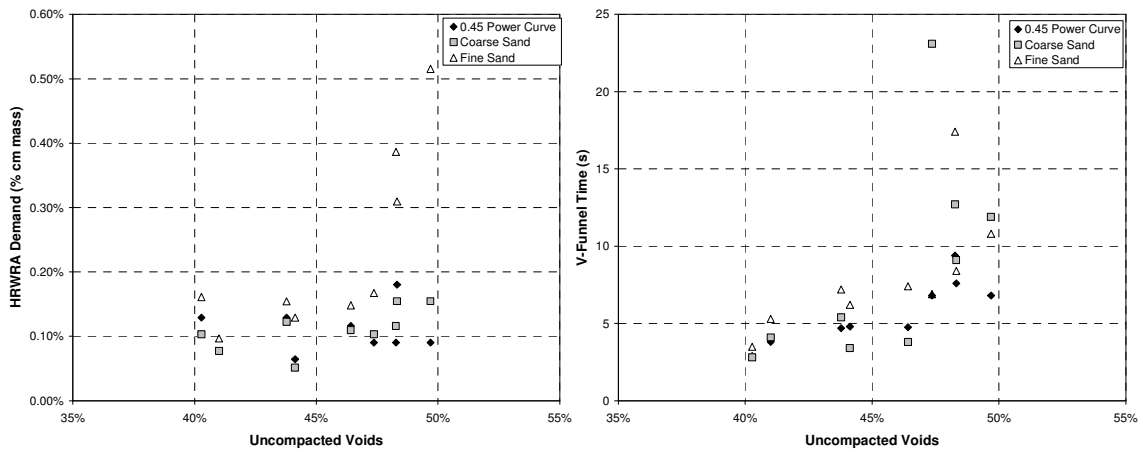
Figure 9.11: Effect of Uncompacted Voids Content on HRWRA Demand and V-Funnel Time

157
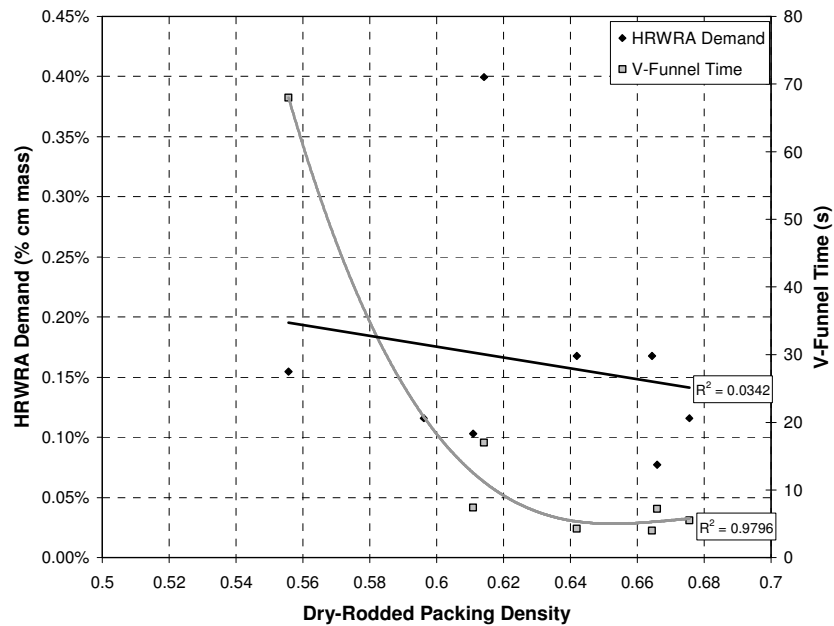
Figure 9.12: Effect of Dry-Rodded Packing Density on HRWRA Dosage and V-Funnel Time (As-Received Gradings with Microfines)

To examine the effects of multiple aggregate parameters at once on flow properties, multiple regression models were developed. Models were developed for each of the three standard gradings with sphericity, L/W, specific gravity, and absorption capacity used as variables (Table 9.3). Each model reflects only shape, angularity, and texture because grading is held constant. The degree of fit was generally poor for the models of HRWRA demand but better for models of mini-v-funnel time. The models, which are plotted in Figure 9.13, indicate that the mini-v-funnel time increased as the sphericity index (less sphericity) and L/W ratio increased. For a given increase in sphericity index or L/W ratio, the magnitude of the increase in mini-v-funnel time was much greater for the fine sand grading than the other gradings. The inability of the sphericity index and L/W ratio to provide better predictions of the flow properties indicates that these parameters do not capture adequately all aspects of shape, angularity, and texture. In particular, these parameters do not measure texture at all and do not measure angularity as well as they measure shape. Further, the measurements are based on 2-dimensional instead of 3-dimensional images and may not have sufficient resolution for sand.

158

Table 9.3: Multiple Regressions for Standard Gradings

	0.45 Power Curve		Coarse Sand		Fine Sand	
	HRWRA	**V-Funnel**	**HRWRA**	**V-Funnel**	**HRWRA**	**V-Funnel**
	(% cm mass)	**(s)**	**(% cm mass)**	**(s)**	**(% cm mass)**	**(s)**
Transformation	ln(y)	Sqrt(y)	y	y	1/sqrt(y)	1/sqrt(y)
$R^2_{adjusted}$	0.838	0.801	0.398	0.932	0.362	0.846
Intercept	365.77	-5.063	-0.00320	-41.86	102.53	2.293
SPHR	-673.31					
L/W						
SG						
ABS		-58.89		-1223.3		
$(SPHR)^2$						
$(L/W)^2$	-82.60		0.00194		-35.25	
$(SG)^2$						
$(ABS)^2$		1572.2		36585.6		-242.87
(SPRH)(L/W)	336.91	4.597		32.66		-0.983
(SPRH)(SG)	58.56					-0.108
(SPRH)(ABS)						
(L/W)(SG)	-43.41					
(L/W)(ABS)						6.317
(SG)(ABS)						
Regression Details: quadratic model, stepwise regression; p-value = 0.25; transformation with highest $R^2_{adjusted}$ selected; transformations considered: y, 1/y, ln(y), sqrt(y), 1/sqrt(y)						
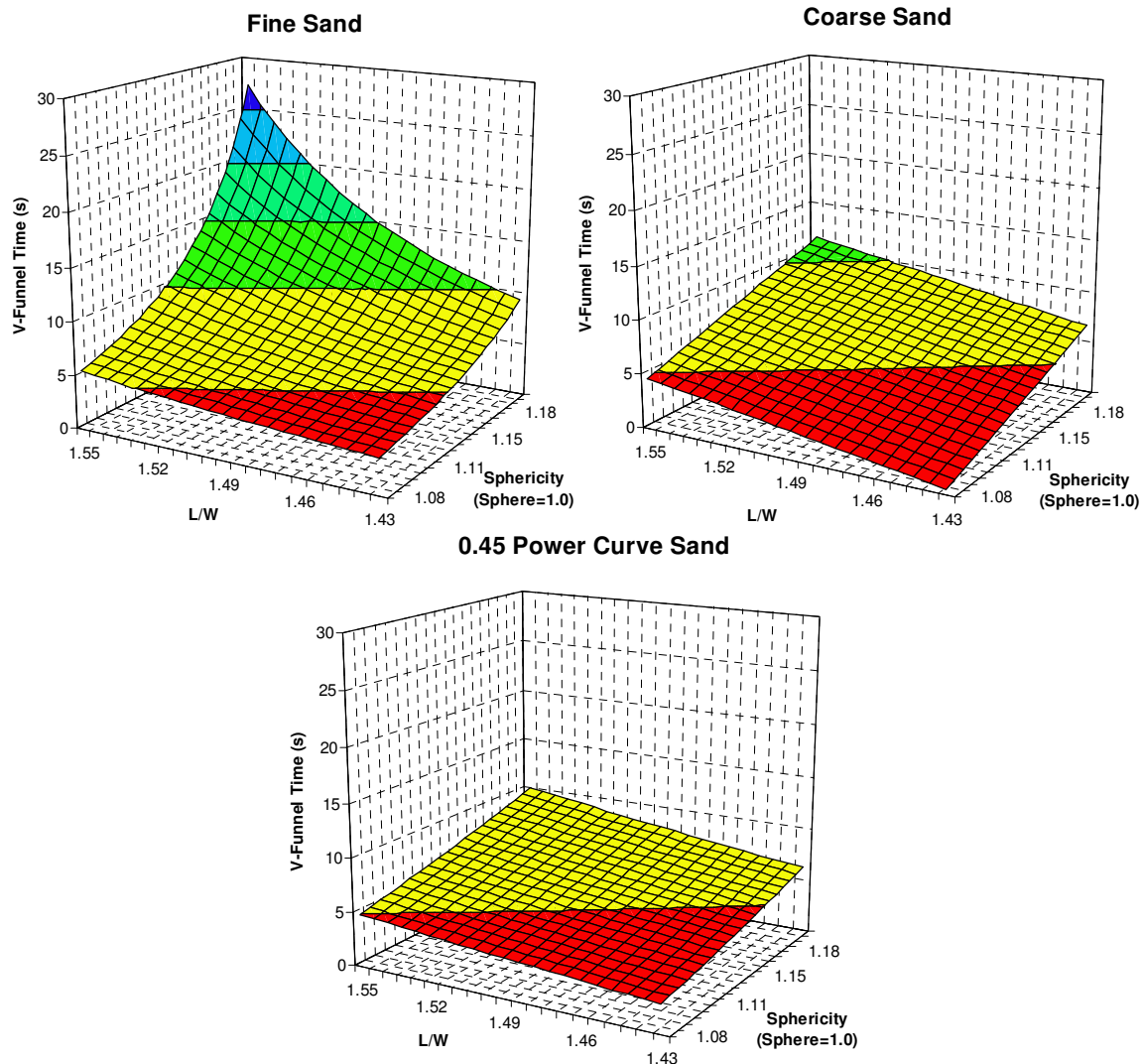
Figure 9.13: Effect of Sphericity and L/W on Mini-V-Funnel Time (Absorption Capacity=0.9%, Specific Gravity=2.50)

To evaluate the combined effects of shape characteristics and grading, multiple regression models were developed for the as-received grading as shown in Table 9.4. The parameters considered included sphericity (SPHR), length-width ratio (L/W), packing density (PKG), specific surface area (SSA), specific gravity (SG), and absorption capacity (ABS). The specific surface area was calculated assuming spherical particles and, therefore, reflects only grading and not shape, texture, or angularity. Based on these models, HRWRA demand was found to increase with increasing packing density, increasing specific surface area, and decreasing absorption capacity (Figure 9.14). Mini-v-funnel time increased with increasing specific surface area, increasing L/W, increasing sphericity index, and increasing specific gravity

160

(Figure 9.15). An optimum packing density was associated with a minimum mini-v-funnel time. Due to partial correlation between the different shape parameters, between the shape parameters and packing density, and between the specific surface area and packing density, the multiple regression models may overstate or understate the relative importance of each parameter. Additionally, the specific gravity and absorption likely affect the shape and angularity of particles—with softer, less dense particle resulted in improved shape and angularity.

Table 9.4: Multiple Regression Models for Sand Shape Characteristics and Grading (As-Received Sand with Microfines)

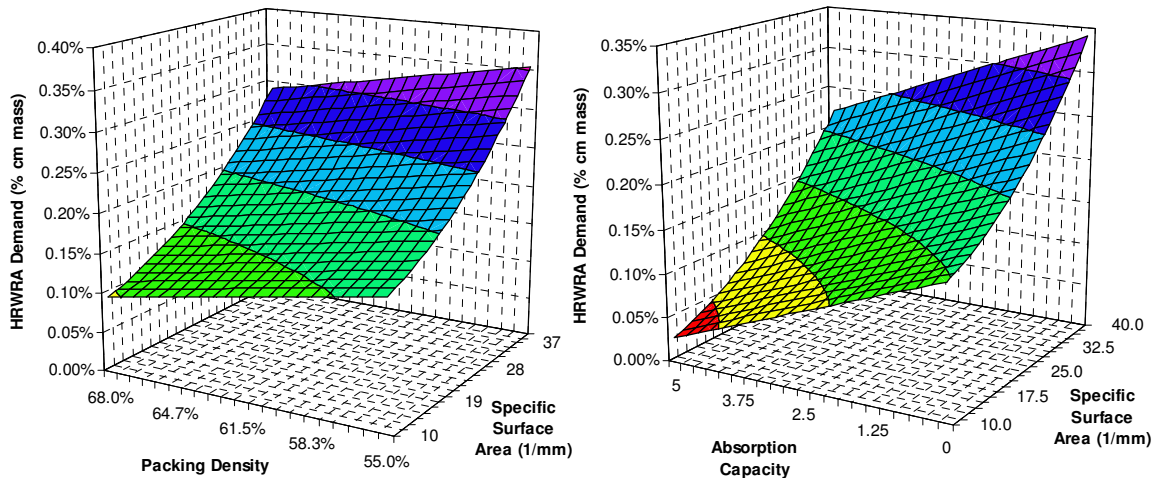| Model	$R^2_{adjusted}$
HRWRA = 0.135 +.000128(SSA)^2 – 0.548(PKG)(ABS) + 0.316(ABS)	0.784
(V-Funnel)$^{0.5}$ = 339.59 – 1070.2(PKG) + 832.36(PKG)^2 + 0.01770(SG)(SSA) + 3.387(SPHR)(L/W)	0.993
Regression Details: quadratic model, stepwise regression; p-value = 0.25; transformation with highest $R^2_{adjusted}$ selected; transformations considered: y, 1/y, ln(y), sqrt(y), 1/sqrt(y)	

Figure 9.14: Effects of Shape Characteristics and Grading on HRWRA Demand (As-Received Sand with Microfines)
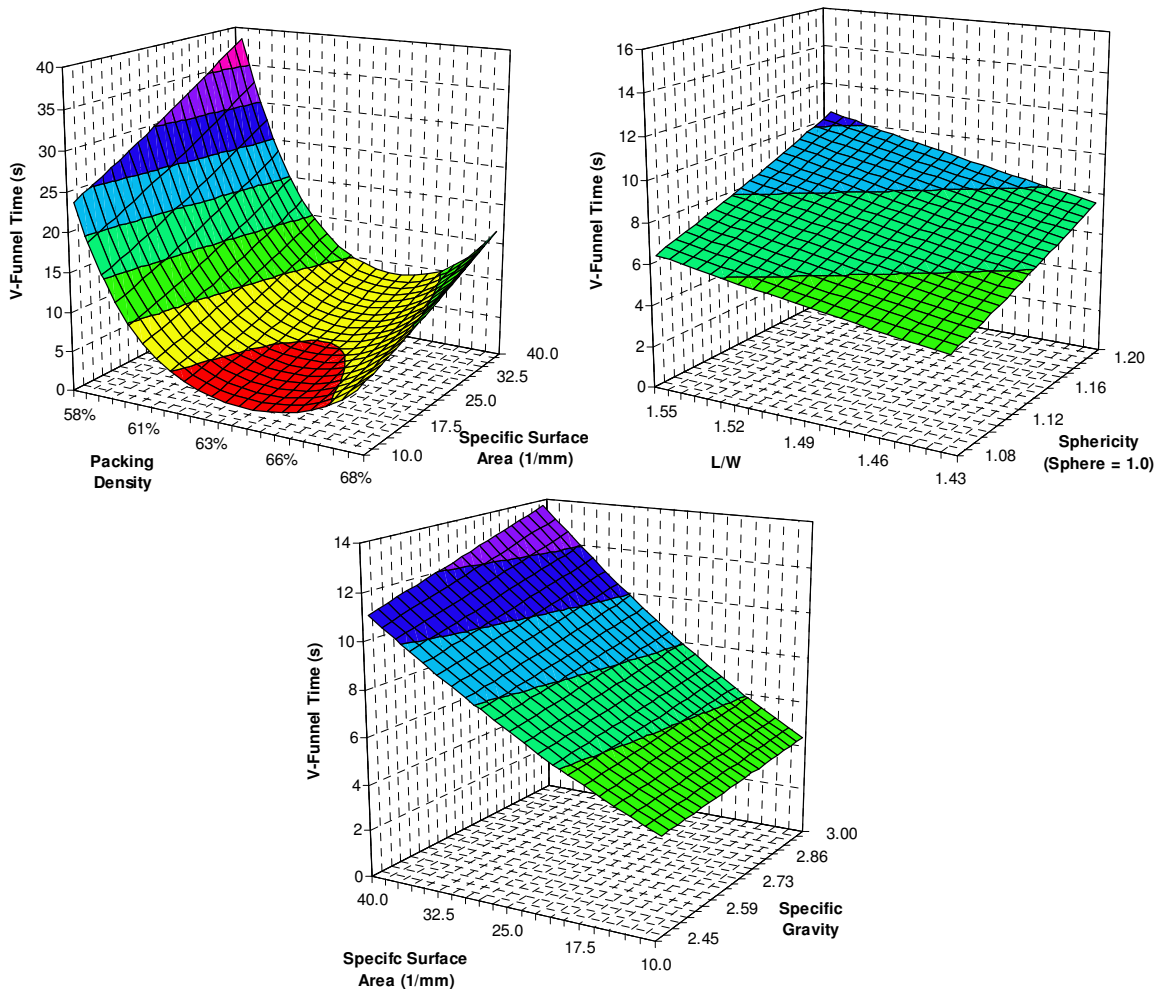
Figure 9.15: Effects of Shape Characteristics and Grading on V-Funnel Time (As-Received Sand with Microfines)

9.3 Effects of Microfines

9.3.1 Test Plan

The effects of microfines were evaluated by measuring mortar mixtures with variable microfines contents, used as part of either the fine aggregate volume or powder volume. Figure 9.16 illustrates the distinction between using microfines as part of the aggregate volume or power volume. Microfines are of similar size as cement and fly ash and essentially act as powder. When microfines are accounted for as fine aggregate volume, the paste volume increases, the water-powder ratio decreases, and the water-cementitious materials ratio remains unchanged. When microfines are accounted for as part of the powder, the paste volume and

162

water-power ratio are unchanged but the water-cementitious materials ratio increases. The mixture proportions are summarized in Table 9.5. Microfines were used to replace fine aggregate volume at rates of 0, 5, 10, 15, and 20% of fine aggregate volume. In the second set of mixtures, microfines were used as part of the powder volume at a rate of 15% of fine aggregate volume. Two control mixtures were used—the first reflecting the w/cm for the mixture with microfines used as sand volume and the second reflecting the w/cm for the mixtures with microfines used as powder volume.
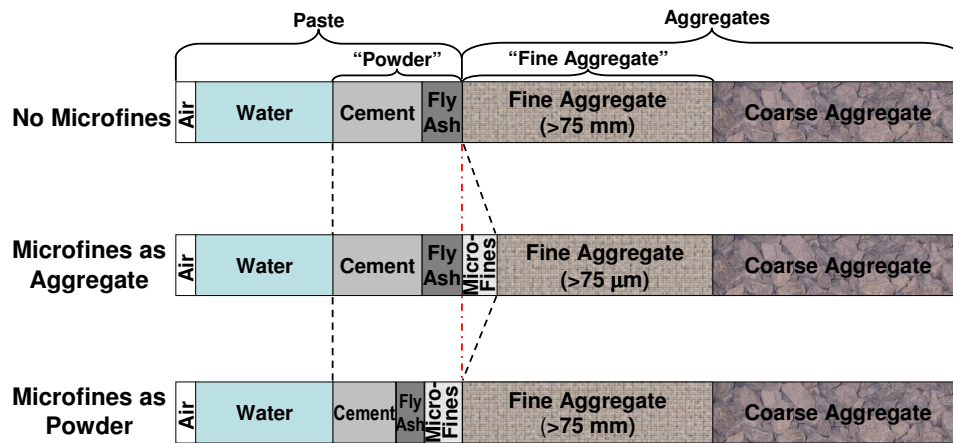
Figure 9.16: Illustration of Distinction in Replacing Aggregate or Powder Volume

The fine aggregate used in all mixtures was LS-02-F, which was washed and sieved to remove all microfines, then re-blended to its as-received grading without microfines. For each mixture, the HRWRA demand for a 9-inch mini-slump flow and the corresponding mini-v-funnel time were determined. Compressive strength and drying shrinkage were determined for the control mixtures with no microfines and for the mixtures with 15% microfines used as aggregate and as powder. Compressive strength was measured at 28 days on 2-inch cubes in accordance with ASTM C 109. Drying shrinkage was measured with 1-inch by 1-inch by 11-inch prisms (10-inch gage length) in accordance with ASTM C 157. The prisms were stored in limewater for the first 28 days and then transferred to an environmental chamber at 23°C and 50% relative humidity for the remainder of the test.

Table 9.5: Mortar Mixture Proportions for Evaluation of Microfines (Proportions by Percent Volume)

	Microfines as Fine Aggregate Volume[1]					Microfines as Powder Volume[1]	
	0%	**5%**	**10%**	**15%**	**20%**	**0%**	**15%**
Sand[2]	54.5	51.7	49.0	46.3	43.6	54.5	54.5
Microfines	0	2.7	5.4	8.2	10.9	0	8.2
Cement	15.6	15.6	15.6	15.6	15.6	12.1	10.0
Fly Ash	7.0	7.0	7.0	7.0	7.0	5.5	4.5
Water	22.9	22.9	22.9	22.9	22.9	27.9	22.9
w/cm^{3}	0.35	0.35	0.35	0.35	0.35	0.547	0.547
w/p[4]	1.013	0.904	0.817	0.744	0.684	1.586	1.013

[1]Percentage of microfines expressed as volume of sand
[2]The fine aggregate, excluding microfines, was LS-02-F for all mixtures
[3]Expressed by mass
[4]Expressedy by volume

9.3.2   Test Results

The use of microfines as part of the fine aggregate volume increased the HRWRA demand in all but one case, as indicated in Figure 9.17. Only the addition of 5% of LS-06-F microfines decreased the HRWRA demand. The magnitude of change varied significantly, with LS-06-F and LS-02-F resulting in the smallest changes in HRWRA demand and TR-01-F and DL-01-F resulting in the largest changes in HRWRA demand. In contrast, the mini-v-funnel time at a 5% rate decreased for all but the GR-01-F microfines, as indicated in Figure 9.18. At the maximum 20% rate, the mini-v-funnel time increased relative to the control for all but the LS-06-F microfines.
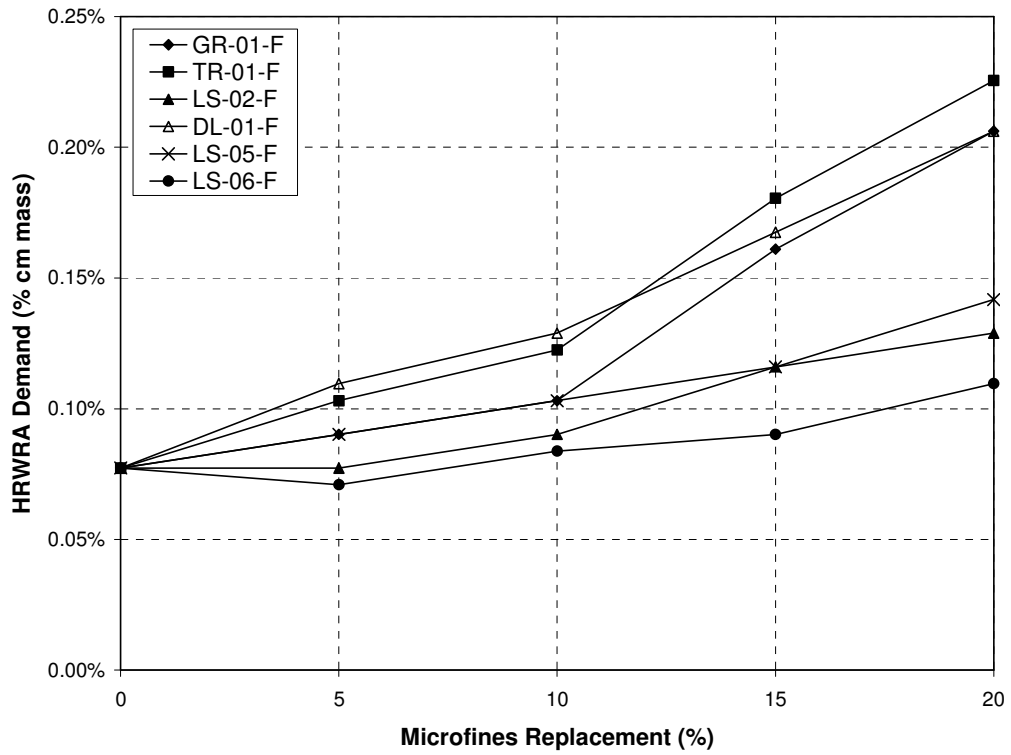
Figure 9.17: Effect of Microfines Replacement Rate (of Sand) on HRWRA Demand
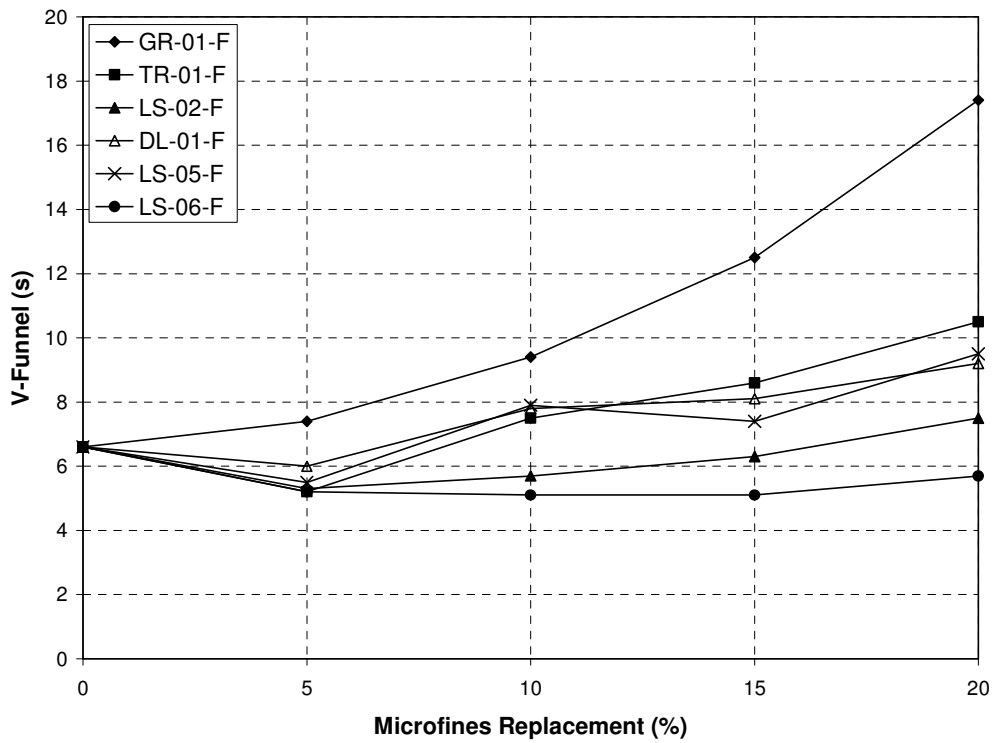
Figure 9.18: Effect of Microfines Replacement (of Sand) on V-Funnel Time

165

The increase in HRWRA demand due to the use of microfines as a part of the sand volume was expected because of the reduction in water-powder ratio, which was partially offset by the increase in paste volume. When the microfines were used as part of the powder volume, however, the water-powder ratio remained constant. In this case, the HRWRA demand and mini-v-funnel times were less than when the same volume of microfines was used as part of the sand volume, as indicated in Figure 9.19 and Figure 9.20. For a constant water-powder ratio, the use of microfines generally resulted in a small increase in HRWRA demand and a reduction in mini-v-funnel flow time. When microfines were used as part of the powder, the total cementitious materials content was reduced. The cost savings of reducing the cementitious materials content may offset any increase in HRWRA demand. Due to the potentially wide range of cementitious materials that could be used and the wide range of material costs, any cost savings should be evaluated on a case-by-case basis.
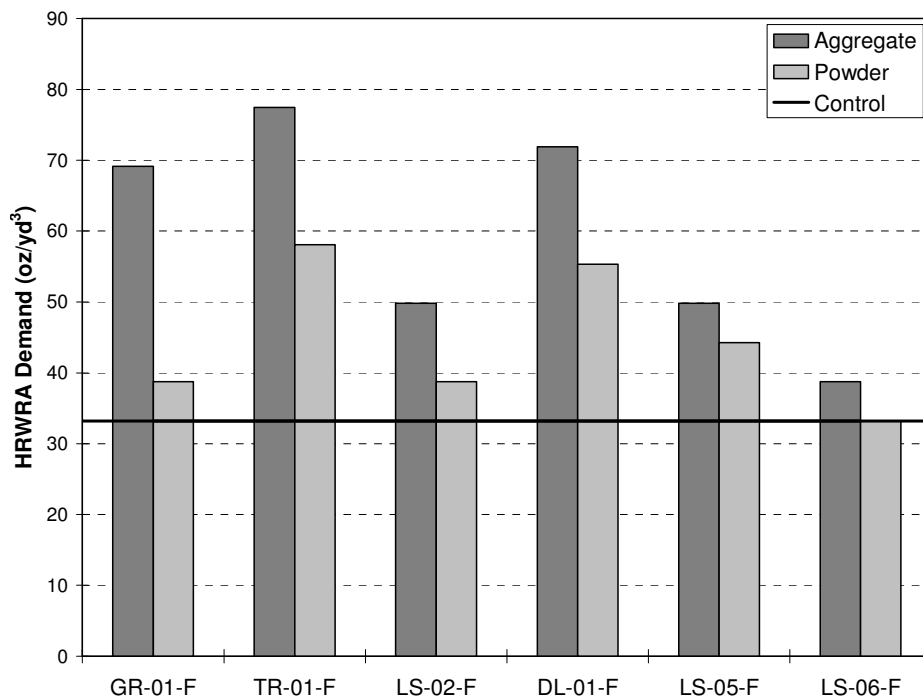
Figure 9.19: Effect of Microfines on HRWRA Demand (15% of Aggregate Volume, Used as Aggregate or Powder)
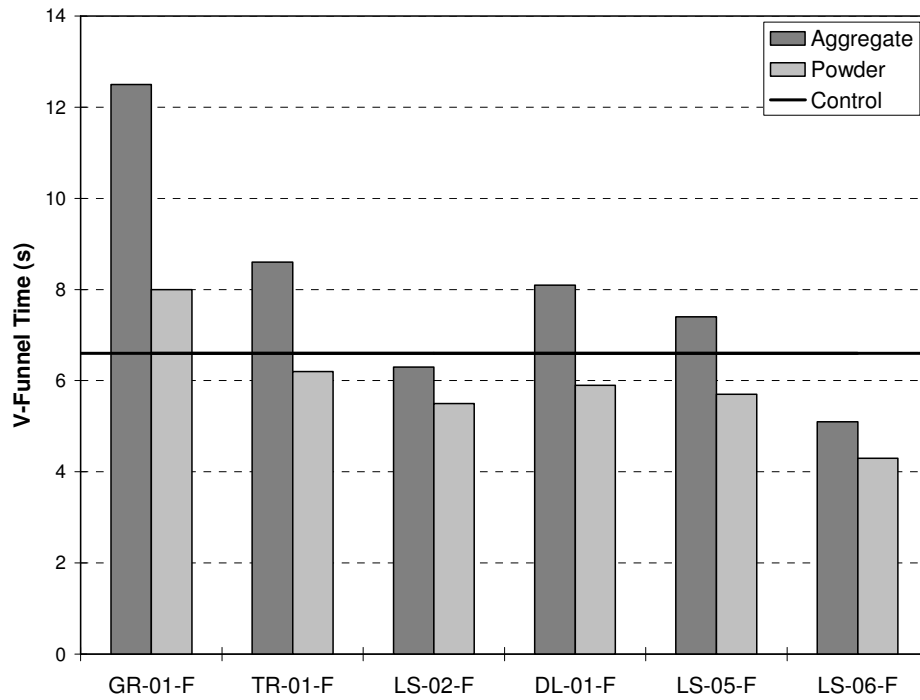
Figure 9.20: Effect of Microfines on Mini-V-Funnel Time (15% of Aggregate Volume, Used as Aggregate or Powder)

The use of 15% microfines as part of the sand increased the 28-day compressive strength by an average of 9.7%. When microfines were used as part of the powder, the water-power ratio remained unchanged but the water-cementitious materials ratio was increased from 0.35 to 0.547, resulting in a decrease in compressive strength. Compared to a control mixture with a w/cm of 0.547, the 28-day compressive strength increased by as much as 13.8% in the case of TR-01-F microfines and decreased by as much as 17.8% in the case of LS-02-F microfines.
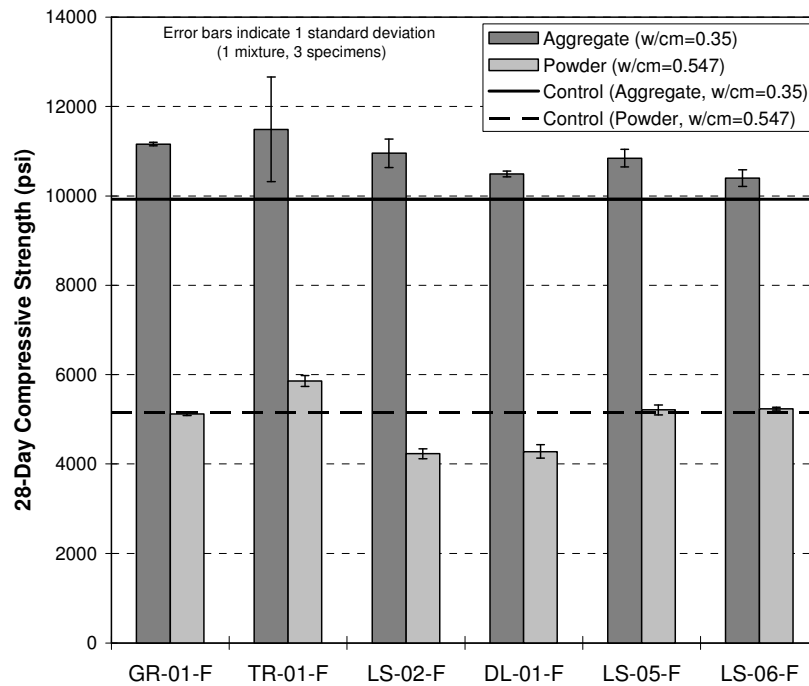
Figure 9.21: Effect of Microfines on 28-Day Compressive Strength (15% of Aggregate Volume, Used as Aggregate or Powder)

The use of microfines as part of the aggregate volume increased drying shrinkage, as shown in Figure 9.22. In this case, the powder content and the paste volume increased, which would be expected to increase drying shrinkage. When microfines were used as part of the powder, the paste volume remained unchanged. In this case, drying shrinkage increased relative to the control mixture with a constant water-powder ratio but decreased relative to the control mixture with constant water-cementitious materials ratio. Compared to the control mixture with constant water-powder ratio, the amount of total water and powder are the same; therefore, the increase in shrinkage when microfines were used as part of the powder volume was typically less than when microfines are used as part of the fine aggregate volume. For the same paste volume and total water content, microfines used as part of the powder volume increased the drying shrinkage. Compared to the control mixture with constant water-cementitious materials ratio, the mixtures with microfines as part of the powder volume had lower water content, which would be expected to decrease shrinkage.

168
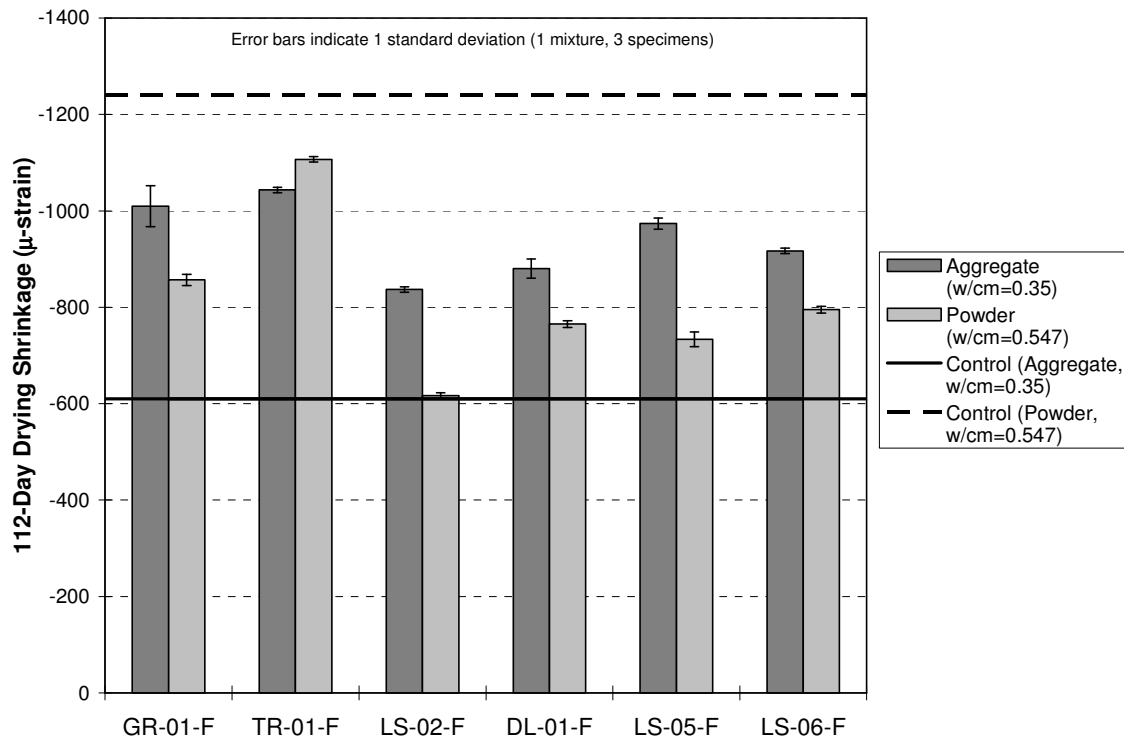
Figure 9.22: Effect of Microfines on 112-Day Drying Shrinkage (15% of Aggregate Volume, Used As Aggregate or Powder)

Because the HRWRA dosage was changed in each mixture, it was necessary to evaluate the independent effect of HRWRA dosage on compressive strength and shrinkage. As shown in Figure 9.23, increasing the HRWRA dosage did increase compressive strength by approximately 35% at a dosage of 0.18% of cementitious materials mass but had negligible effect on drying shrinkage. Therefore, part of the change in compressive strength associated with the use of microfines may be due to the increase in HRWRA dosage. A similar increase in compressive strength with increasing HRWRA dosage was reported by Koehler et al. (2007).

169
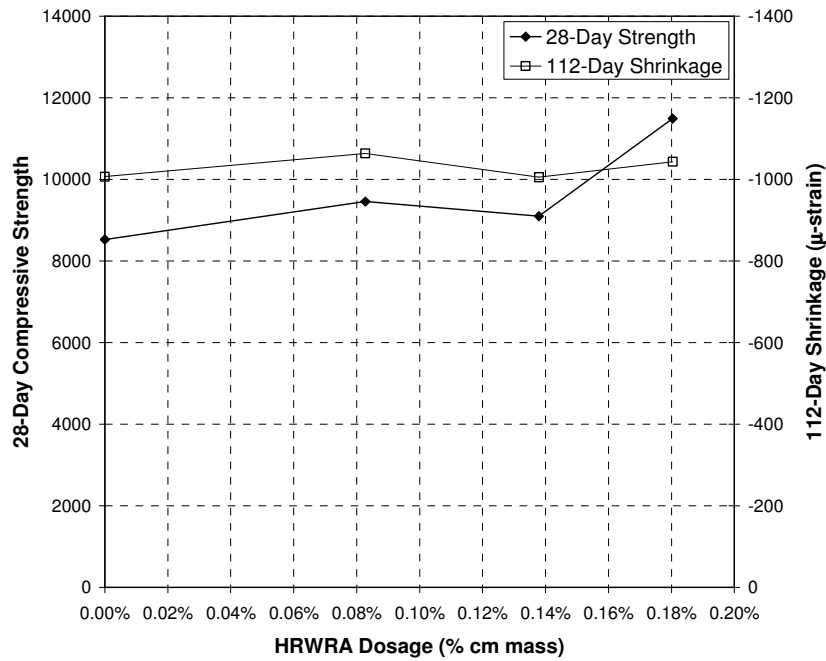
Figure 9.23: Effect of HRWRA Dosage on 28-Day Compressive Strength and 112-Day Drying Shrinkage (TR-01-F Microfines, 15% Replacement of Sand Volume)

In order to evaluate the effects of specific microfines characteristics on mortar performance, the test results were compared to the packing densities (single drop test), spans, specific surface areas, and methylene blue values of the microfines. Figure 9.24 indicates that no single characteristic is sufficient to explain the HRWRA demand or mini-v-funnel time of the mortar mixtures. The best correlations were found for specific surface area and span, while very poor correlations were found for packing density and methylene blue value. Increasing the span and specific surface area led to a reduction in HRWRA demand and mini-v-funnel time.
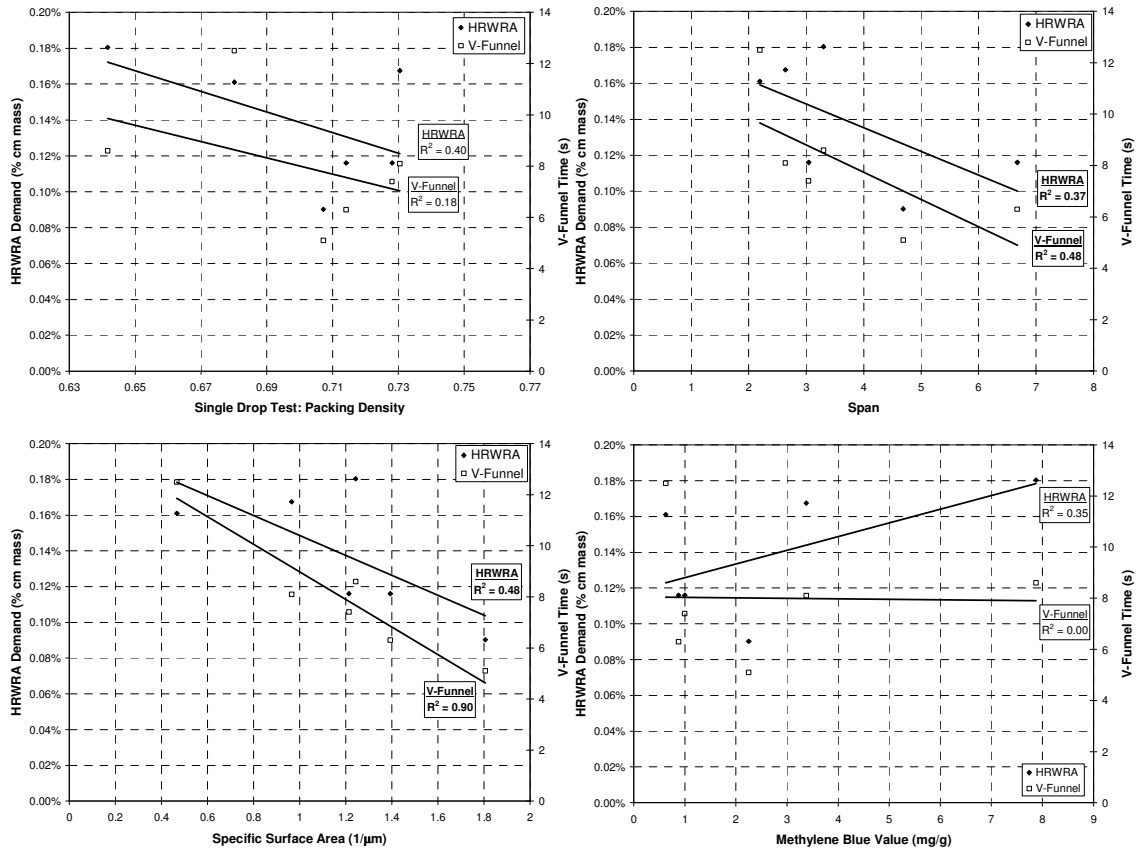
Figure 9.24: Effects of Microfines Characteristics on HRWRA Demand and V-Funnel Demand (Replacement of Sand, 15% Rate)

Similarly, no single characteristic of the microfines was sufficient to explain the compressive strength or drying shrinkage of the mortars with microfines, as indicated in Figure 9.25 and Figure 9.26, respectively. For compressive strength, the highest correlation was for packing density. The decrease in strength with increasing packing density could be due partially to the lower HRWRA dosages associated with higher packing densities. For drying shrinkage, the highest correlation was for methylene blue value, with higher methylene blue value associated with higher drying shrinkage.
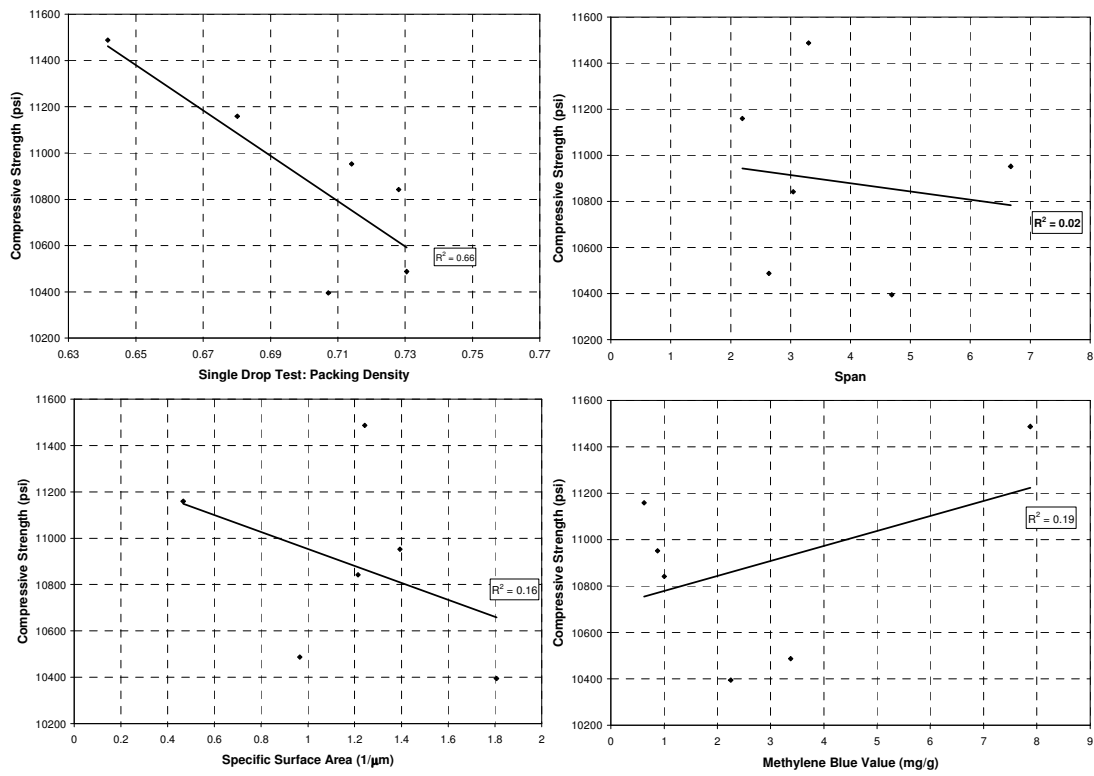
Figure 9.25: Effects of Microfines Characteristics on Compressive Strength (Replacement of Sand, 15% Rate)
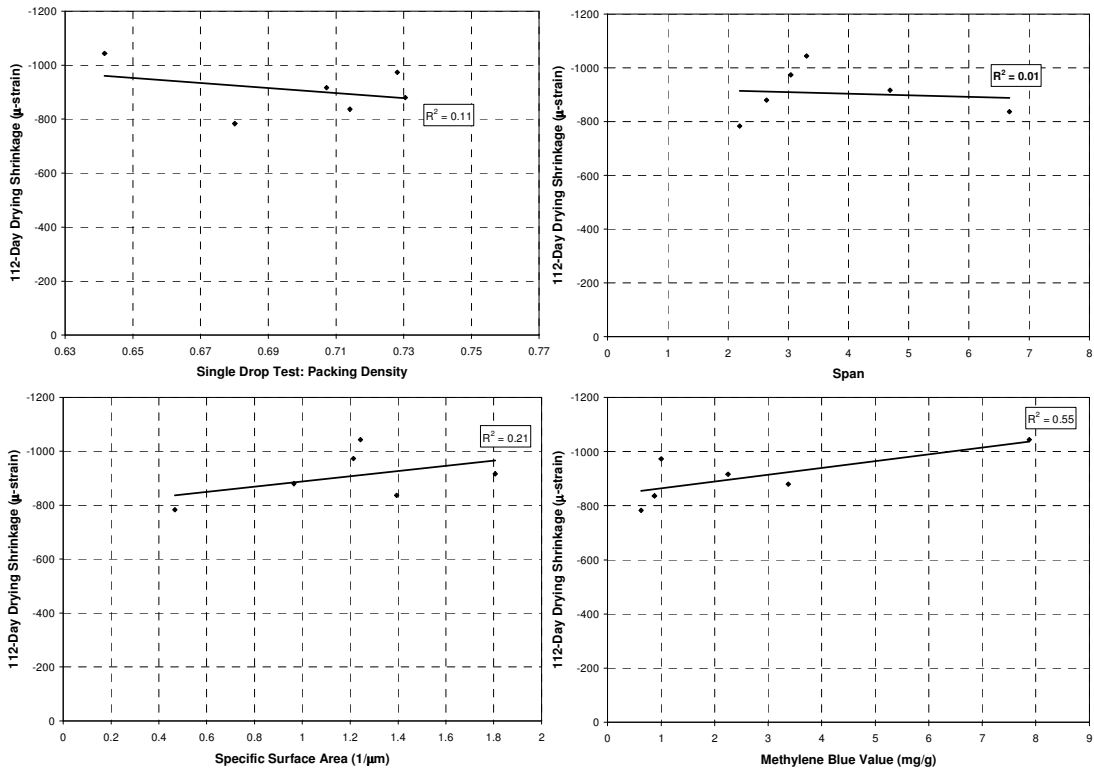
Figure 9.26: Effects of Microfines Characteristics on Drying Shrinkage (Replacement of Sand, 15% Rate)

Because no single factor explained the performance of microfines, multiple regression models were developed for the microfines used as part of the aggregate volume. The independent variables were percentage microfines (PCT), single drop test packing density (PKG), span (SPAN), specific surface area (SSA), and methylene blue value (MBV). The resulting multiple regression models, which are applicable to the specific materials and mixture proportions tested, are given in Table 9.6 and plotted in Figure 9.27 and Figure 9.28.

Table 9.6: Multiple Regression Models for Microfines as Fine Aggregate

Equation	$R^2_{adjusted}$
HRWRA Demand (oz/yd^3) = 16.861 + 0.0672$(PCT)^2$ + 33.320$(PKG)^2$ + 2.959(PCT)(PKG) – 1.897(PCT)(SSA) + 0.310(PCT)(MBV)	0.977
Mini-V-Funnel Time (s) = 6.420 + 2.147(PCT) + 0.0140$(PCT)^2$ – 2.533(PCT)(PKG) - 0.0248(PCT)(SPAN - 0.0271(PCT)(SSA) – 0.00228(PCT)(MBV)	0.948
Regression Details: quadratic model, stepwise regression; p-value = 0.10; transformation with highest $R^2_{adjusted}$ selected; transformations considered: y, 1/y, ln(y), sqrt(y), 1/sqrt(y)	

173

The span and specific surface area represent the particle size distribution while the packing density reflects both the particle size distribution and shape characteristics. The span had no effect on HRWRA demand; however, increasing the span resulted in a slight reduction in mini-v-funnel time. The reduction in mini-v-funnel time was expected because higher span is associated with greater polydispersity. Higher specific surface area resulted in significant decreases in both HRWRA demand and mini-v-funnel time. The span and specific surface area of the microfines; however, do not take into consideration the combined grading of the powder materials. Increasing the packing density resulted in a very small increase in HRWRA demand and a relatively larger decrease in mini-v-funnel time. An improvement in workability was expected with increasing packing density. Higher methylene blue values resulted in significant increases in HRWRA demand, which was expected if it can be assumed that the methylene blue value is related to the presence of clay. The HRWRA was likely consumed by the clay particles prior to providing dispersion of the powder materials. Once sufficient HRWRA dosage was provided to offset the effects of the clay, the mini-v-funnel time was reduced slightly. Therefore, mortars composed of microfines with high methylene blue values can provide acceptable workability if sufficient HRWRA is provided to be consumed by the clay particles and provide dispersion of the powder materials. The high dosages of HRWRA may render the use of such aggregate uneconomical.
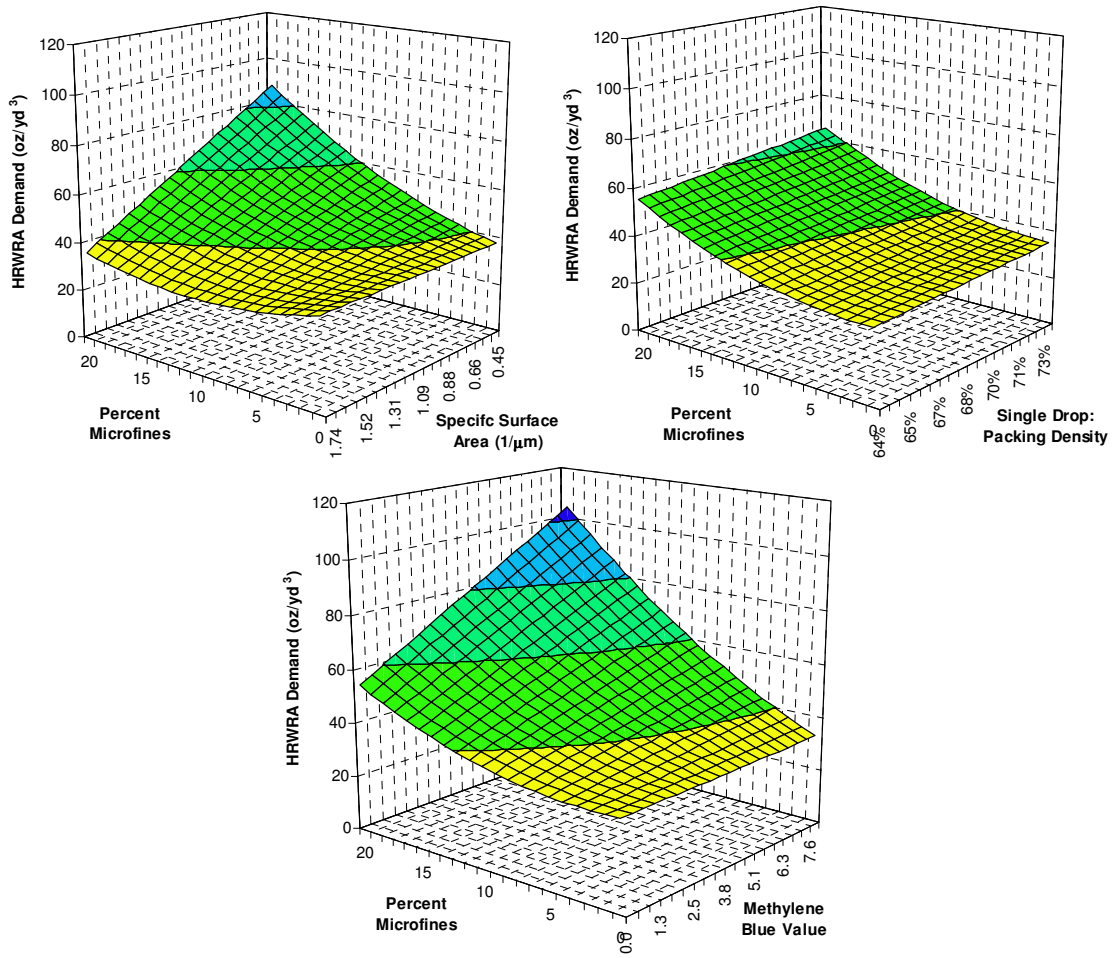
Figure 9.27: Effect of Microfines Characteristics on HRWRA Demand
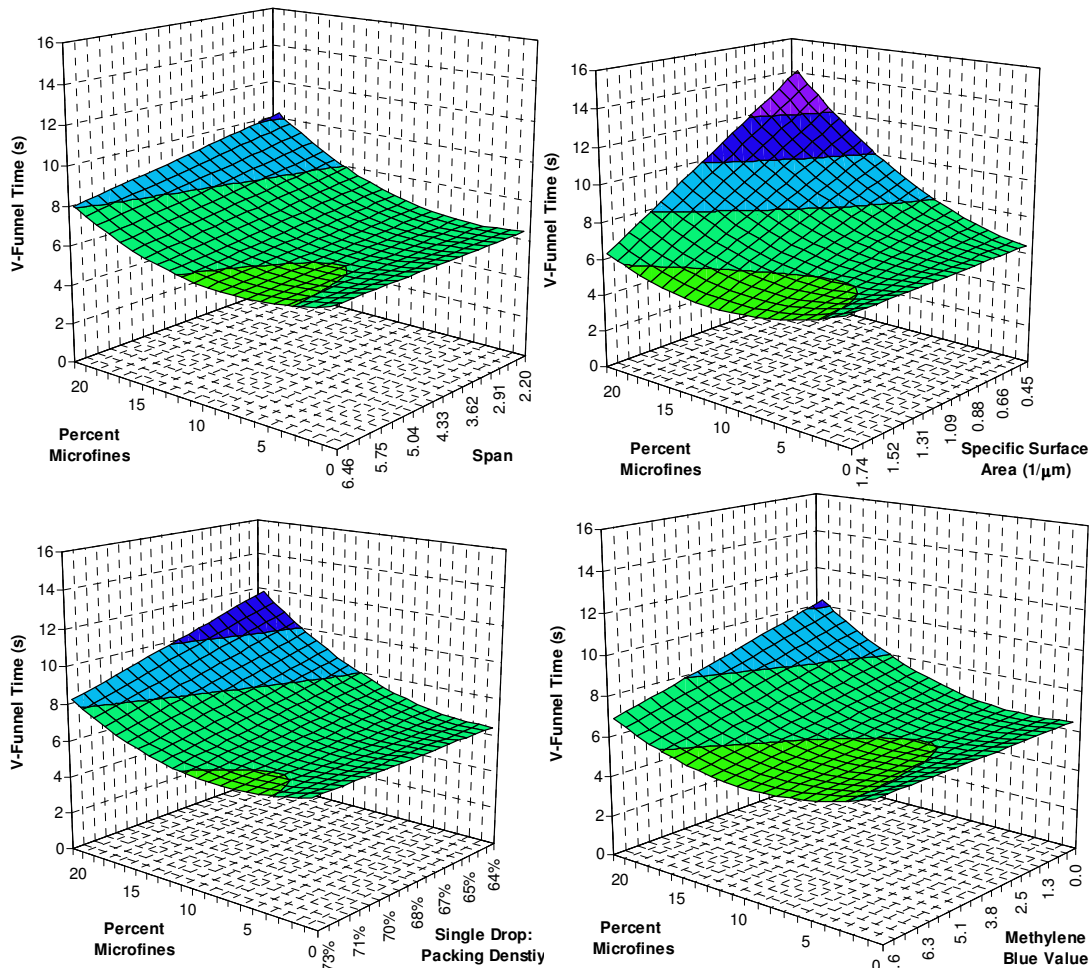
Figure 9.28: Effect of Microfines Characteristics on V-Funnel Time

To investigate the properties of the microfines further, the combined gradings of the microfines and cementitious materials were considered. Because microfines comprise only 26.4% of the powder volume, the particle size distributions of the combined materials do not vary significantly from that of the cementitious materials only, as shown in Figure 9.29. The span, specific surface area, and packing densities of the individual and combined gradings are listed in Table 9.7. There is a high degree of correlation between the individual and combined gradings for span and specific surface area; however, there is poor correlation for packing density (Figure 9.30). There is no correlation between the span or specific surface area of the microfines and the packing density of the microfines; however, there are correlations between each the span and specific surface area of the microfines and the packing density of the combined aggregates, as indicated in Figure 9.31. These results suggest that increasing the span

176

or the specific surface area of the microfines results in increased packing density of the combined powder materials.
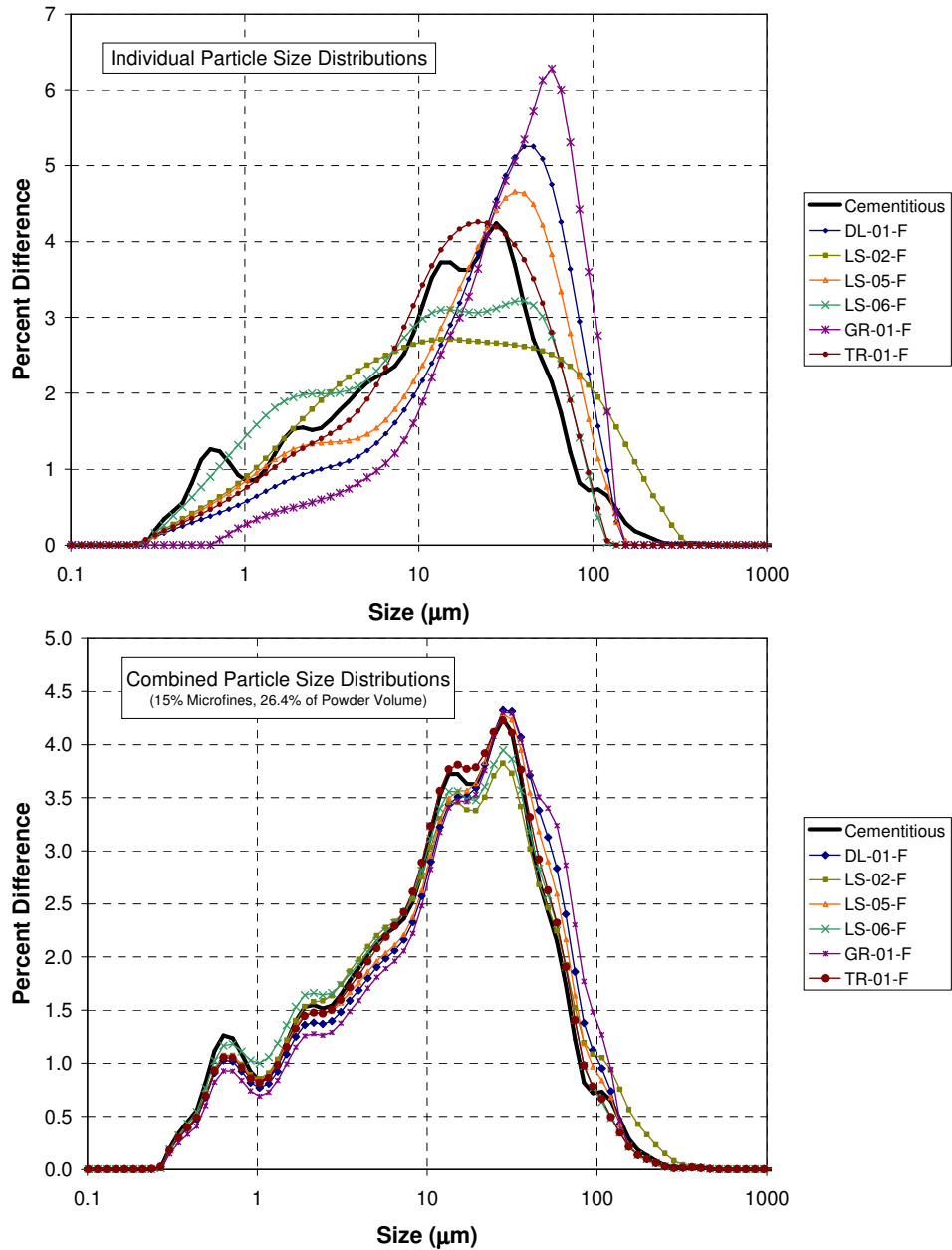
Figure 9.29: Individual and Combined Gradings of Microfines and Cementitious Materials

Table 9.7: Gradings and Packing Parameters for Combined Gradings

Microfines	Microfines Only			Combined Microfines and Cementitious Materials[1]		
	Span	Specific Surface Area (1/μm)	Single Drop Packing Density	Span	Specific Surface Area (1/μm)	Single Drop Packing Density
DL-01-F	2.638	0.965	0.730	3.616	1.522	0.679
LS-02-F	6.673	1.394	0.714	4.451	1.635	0.702
LS-05-F	3.042	1.214	0.728	3.683	1.588	0.695
LS-06-F	4.688	1.806	0.707	3.985	1.744	0.686
GR-01-F	2.192	0.467	0.680	3.602	1.390	0.667
TR-01-F	3.302	1.243	0.642	3.656	1.595	0.675
Cement	2.990	1.729	0.631			
Fly Ash	6.113	1.706	0.849			
Cementitious materials	3.786	1.722	0.674			

[1]Combination consists of 50.7% cement, 22.9% fly ash, 26.4% microfines, by volume (corresponds to use of 15% microfines, as percentage of sand, used as sand)
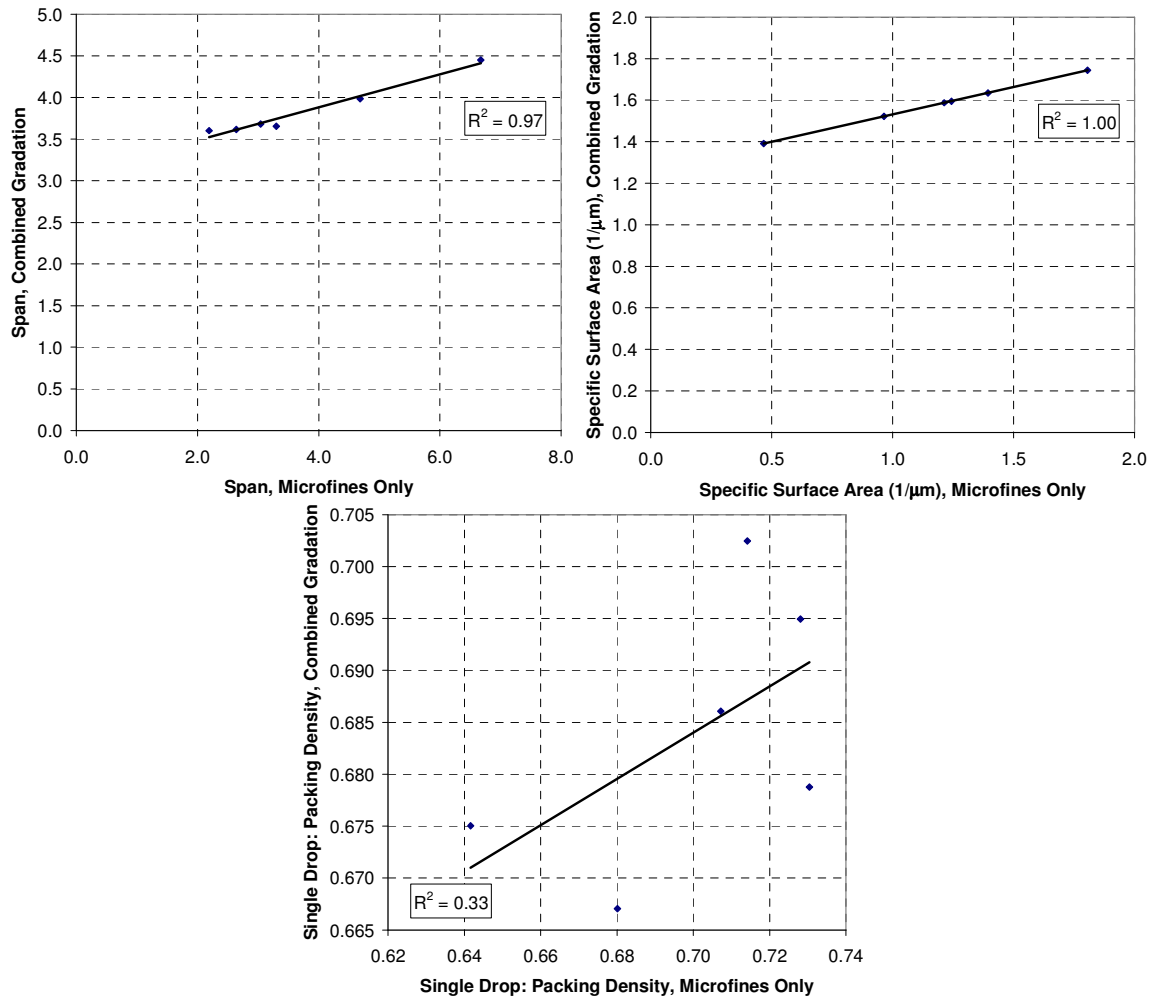
Figure 9.30: Span, Specific Surface Area, and Packing Density in Individual and Combined Gradings

179
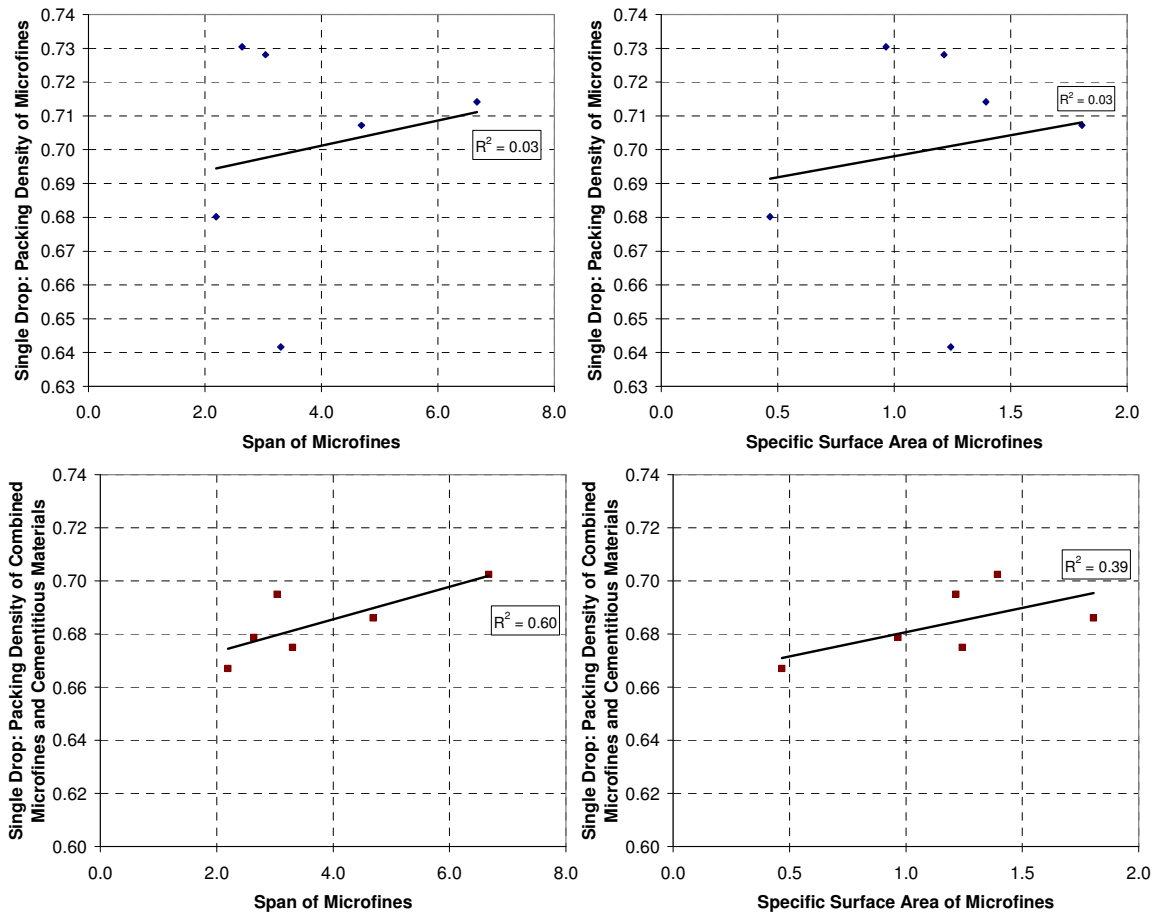
Figure 9.31: Effect of Span and Specific Surface Area of Microfines on Packing Densities of Microfines and Combined Materials

Multiple regression models were developed based on combined gradings for the use of 15% microfines as either fine aggregate or powder, as shown in Table 9.8. The results were similar for HRWRA whether the individual or combined gradings were considered. Specifically, HRWRA demand decreased with decreasing methylene blue value or increasing specific surface area and decreased slightly with decreasing packing density (Figure 9.32). The mini-v-funnel time decreased with increasing specific surface area and decreasing methylene blue value. The packing density of the combined grading did not have an effect on mini-v-funnel time; however, it should be noted that the range of packing densities was narrower for combined grading than just the microfines. In general, increasing the span and specific surface area of the microfines increased the packing density of the combined powder and improved the workability. Therefore, it is important to consider not just the fineness of the microfines, but how they fit into the

combined powder grading. Finer microfines with a wider span can increase the polydispersity of the combined grading. These findings are consistent with the results of Yahia, Tanimura, and Shimoyama (2005), who showed that limestone filler improves workability to the extent that it improves the combined particle size distribution. It should be noted that the shape characteristics of the microfines were not quantified independently and may not be fully represented in the multiple regression models.

Figure 9.33 indicates that increasing the specific surface area of the powder increases shrinkage while increasing the span slightly reduces shrinkage. Increasing the specific gravity of the microfines also increased shrinkage.

Table 9.8: Multiple Regression Models for Microfines (15% Rate as Sand or Powder)

Equation	Factors	$R^2_{adjusted}$
Microfines as Sand, Individual Grading		
$\ln(HRWRA) = 4.238 - 0.223(SSA)^2 + 0.0916(PKG)(MBV)$	PKG, SSA, SPAN, MBV	0.967
$1/\sqrt{v\text{-funnel}} = 0.236 + 0.137(PKG)(SSA) - 0.00180(MBV)^2 + 0.00412(SPAN)(MBV)$	PKG, SSA, SPAN, MBV	0.995
$f'_c(28d) = 17463.5 - 9232.9(PKG) - 18.40(ABS)^2$	PKG, SSA, SPAN, MBV, SG, ABS	0.862
Shrinkage not statistically significant	PKG, SSA, SPAN, MBV, SG, ABS	--
Microfines as Sand, Combined Grading		
$\sqrt{HRWRA} = 16.29 - 8.536(PKG)(SSA) + 0.325(PKG)(MBV)$	PKG, SSA, SPAN, MBV	0.880
$1/(v\text{-funnel}) = -0.120 + 0.104(SSA)^2 - 0.000442(MBV)^2$	PKG, SSA, SPAN, MBV	0.977
Compressive strength not statistically significant	PKG, SSA, SPAN, MBV, SG, ABS	--
$\sqrt{shrinkage} = 15.88 + 5.173(SSA)(SG) - 0.768(SPAN)(SG)$	PKG, SSA, SPAN, MBV, SG, ABS	0.963
Microfines as Powder, Individual Grading		
$HRWRA = 35.43 + 17.73(PKG)(MBV) - 6.925(SSA)(MBV)$	PKG, SSA, SPAN, MBV	0.893
$\sqrt{v\text{-funnel}} = 3.047 - 0.796(PKG)(SSA)$	PKG, SSA, SPAN, MBV	0.948
Compressive strength not statistically significant	PKG, SSA, SPAN, MBV, SG, ABS	--
$shrinkage = 2647.9 - 2611.8(PKG) - 4.149(SPAN)^2 + 18.56(SSA)(MBV)$	PKG, SSA, SPAN, MBV, SG, ABS	0.997
Regression Details: quadratic model, stepwise regression; p-value = 0.20; transformation with highest $R^2_{adjusted}$ selected; transformations considered: y, 1/y, ln(y), sqrt(y), 1/sqrt(y)		
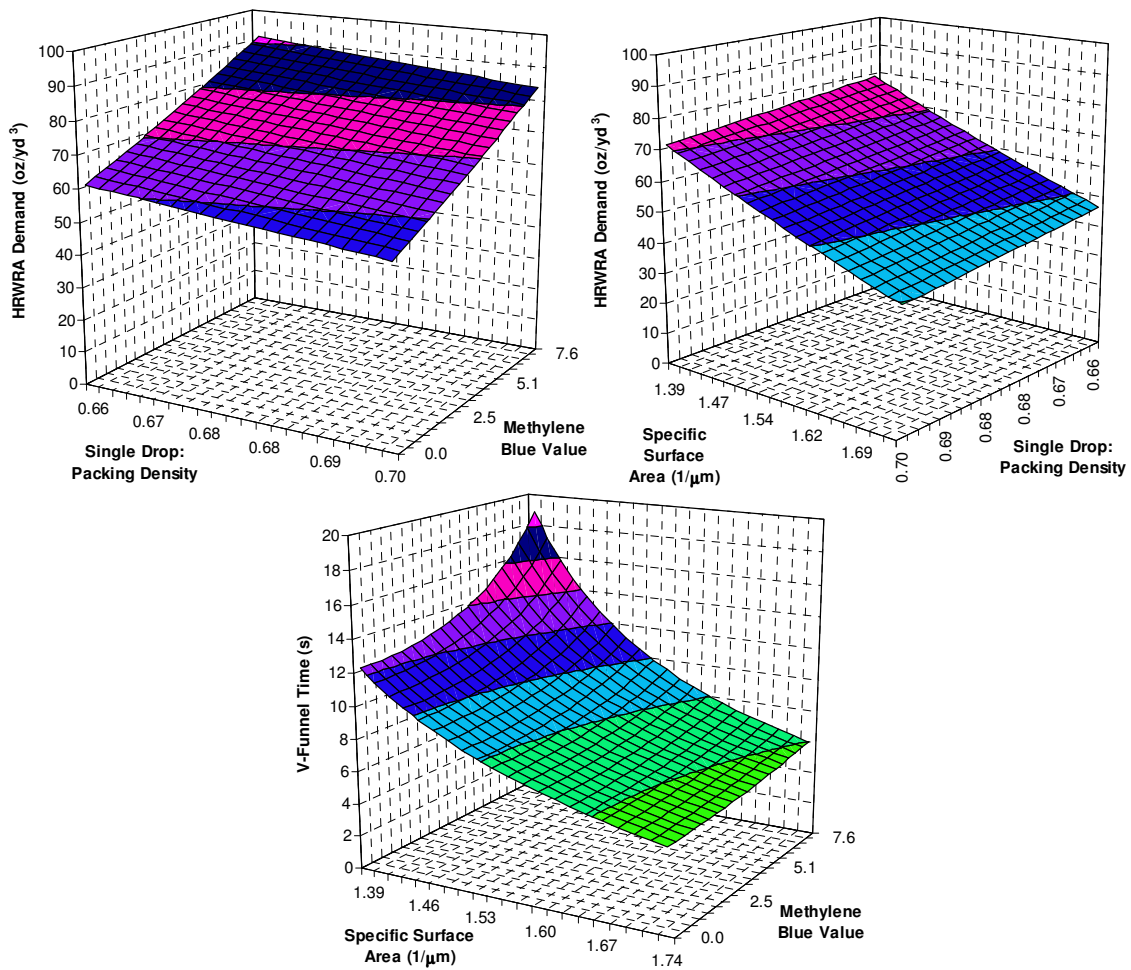
Figure 9.32: Effects of Microfines Characteristics (Combined Powder Grading) on HRWRA Demand and V-Funnel Time (15% Microfines, Used as Aggregate)

182
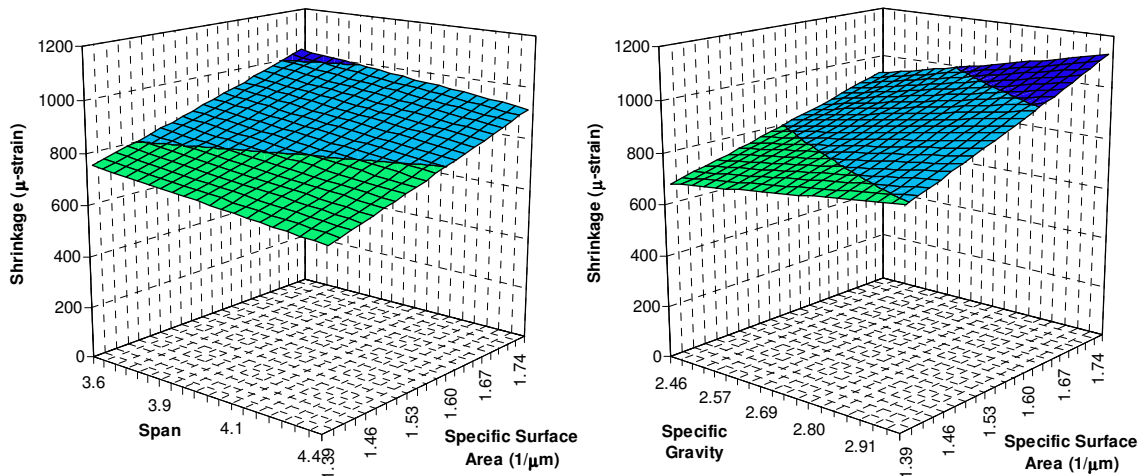
Figure 9.33: Effects of Microfines Characteristics (Combined Powder Grading) on Drying Shrinkage (15% Microfines, Used as Aggregate)

9.4 Effects of Mixture Proportions

9.4.1 Test Plan

The effects of mortar mixture proportions—namely paste volume and paste composition—were evaluated. The goal was to determine how mortar mixtures can be adjusted to account for changes in aggregate properties. Separate response surface experiment designs were used for three aggregates; namely a natural sand (NA-02-F), a manufactured sand with low microfines content (LS-02-F), and a manufactured sand with high microfines content (DL-01-F). Each response surface was an inscribed central composite design with eight factorial points (-1, 1), six star points (-1.68, 1.68), and six center points (0). The factors were paste volume, fly ash replacement rate (mass), and paste solids volume fraction ratio. The values of the factors used for each aggregate are shown in Table 9.9. The responses were HRWRA demand for 9-inch mini-slump flow, mini-v-funnel time, and compressive strength at 24 hours and 28 days.

Table 9.9: Response Surface Designs (All Factors by Volume)

	Coded Factors				
	-1.68	-1	0	1	1.68
LS-02-F					
Paste Volume (PV), %	43.0	46.9	52.5	58.2	62.0
Fly Ash Dosage (FA), %	0.0	6.2	15.7	25.8	33.0
Paste Solid Vol. Fraction	0.448	0.477	0.519	0.562	0.590
NA-02-F					
Paste Volume (PV), %	40.6	44.6	50.5	56.4	60.4
Fly Ash Dosage (FA), %	0.0	6.2	15.7	25.8	33.0
Paste Solid Vol. Fraction	0.426	0.456	0.500	0.544	0.574
DL-01-F					
Paste Volume (PV), %	50.8	54.1	59.0	63.8	67.2
Fly Ash Dosage (FA), %	0.0	6.2	15.7	25.8	33.0
Paste Solid Vol. Fraction	0.459	0.479	0.509	0.539	0.560
Note: paste volume includes water, cement, fly ash, microfines					

9.4.2 Test Results

Multiple regression models were developed for each aggregate. The regression models were developed with microfines included in the paste volume and w/p expressed by volume, which allows a direct comparison between each of the three aggregates. The w/c, w/cm, and the fly ash replacement rate are expressed by mass, which is typical of industry practice and also allows a direct comparison between each of the three aggregates. The multiple regression models are shown in Table 9.10 and Table 9.11.

Table 9.10: Multiple Regression Model for HRWRA Demand and Mini-V-Funnel Time

	LS-02-F		NA-02-F		DL-02-F	
	HRWRA	V-Funnel	HRWRA	V-Funnel	HRWRA	V-Funnel
	(%cm mass)	(s)	(%cm mass)	(s)	(%cm mass)	(s)
Transformation	1/sqrt(y)	1/sqrt(y)	ln(y)	1/sqrt(y)	sqrt(y)	1/sqrt(y)
$R^2_{adjusted}$	0.948	0.960	0.946	0.978	0.988	0.983
Intercept	-0.240	-0.408	3.018	-0.453	6.687	-0.519
PV					-0.112	
FA				0.00686		0.00468
w/p						
$(PV)^2$					0.000834	
$(FA)^2$			-.000468			
$(w/p)^2$						
(PV)(FA)		0.000106			-.000161	
(PV)(w/p)	0.0187	0.0155	-0.0423	0.0176	-0.0188	0.0169
(FA)(w/p)	0.0136					
w/p by volume, fly ash by mass						
Regression Details: quadratic model, stepwise regression; p-value = 0.10; transformation with highest $R^2_{adjusted}$ selected; transformations considered: y, 1/y, ln(y), sqrt(y), 1/sqrt(y)						

Table 9.11: Multiple Regression Models for Compressive Strength

	24-Hour f'_c				28-Day f'_c		
	LS-02-F	**NA-02-F**	**DL-01-F**		**LS-02-F**	**NA-02-F**	**DL-01-F**
Transformation	$1/y$	sqrt(y)	sqrt(y)	Transformation	$1/\sqrt{y}$	$1/y$	$1/\sqrt{y}$
$R^2_{adjusted}$	0.988	0.988	0.990	$R^2_{adjusted}$	0.771	0.918	0.985
Intercept	1.36×10^{-5}	167.0	159.3	Intercept	0.00632	6.15×10^{-5}	0.00681
PV				PV			
FA		0.173		FA			
w/c		-365.3	-228.8	w/cm	0.0106		
$(PV)^2$				$(PV)^2$			
$(FA)^2$				$(FA)^2$	1.37×10^{-6}		
$(w/c)^2$	0.00138	257.5	137.2	$(w/cm)^2$		0.000288	0.0149
(PV)(FA)			0.00320	(PV)(FA)		3.30×10^{-8}	
(PV)(w/c)			-0.719	(PV)(w/cm)			
(FA)(w/c)				(FA)(w/cm)		7.09×10^{-6}	0.000144
w/c, w/cm, fly ash by mass							
Regression Details: quadratic model, stepwise regression; p-value = 0.10; transformation with highest $R^2_{adjusted}$ selected; transformations considered: y, 1/y, ln(y), sqrt(y), 1/sqrt(y)							

The trends were generally consistent between each aggregate. As expected, increasing the paste volume, w/p, or fly ash dosage resulted in lower HRWRA for all aggregates (Figure 9.34). For a given paste volume, w/p, and fly ash dosage, the LS-02-F sand resulted in the lowest HRWRA demand and the DL-01-F sand the highest. Similarly, Figure 9.35 indicates that increasing the paste volume, w/p, or fly ash dosage resulted in lower mini-v-funnel time. For a given paste volume, w/p, and fly ash dosage, the NA-02-F sand resulted in the lowest mini-v-funnel time and the DL-01-F sand the highest. Increasing either the paste volume or w/p resulted in a reduced sensitivity of the mini-v-funnel time to changes in the other parameters. For instance, relative percentage changes in the mini-v-funnel time for a given change in fly ash content or w/p were less at higher paste volumes, suggesting that mixtures are more robust at higher w/cm and paste volume. In addition, the difference in mini-v-funnel time between aggregates was less at higher paste volumes and water-powder ratios, as shown in Figure 9.36. In contrast, Figure 9.36 also shows that increasing the fly ash dosage did not enhance the robustness to nearly the same degree.

The changes in HRWRA demand and mini-v-funnel time can be compared to the effects of aggregate characteristics. For instance, increasing the methylene blue value from zero to 8 mg/g at 20% microfines content resulted in an approximate doubling of the HRWRA demand. In comparison, the use of 30% fly ash with LS-02-F resulted in an approximate 50% reduction in HRWRA demand regardless of the paste volume. Similarly, for the DL-01-F aggregate,

increasing the paste volume from 50 to 60% and using 30% fly ash resulted in an approximate 50% reduction in HRWRA demand. Many similar comparisons can be made. Therefore, the multiple regression models for mixture proportions can show how challenging aggregates can be accommodated in SCC. Each mixture must be optimized based on locally available materials and local economics.
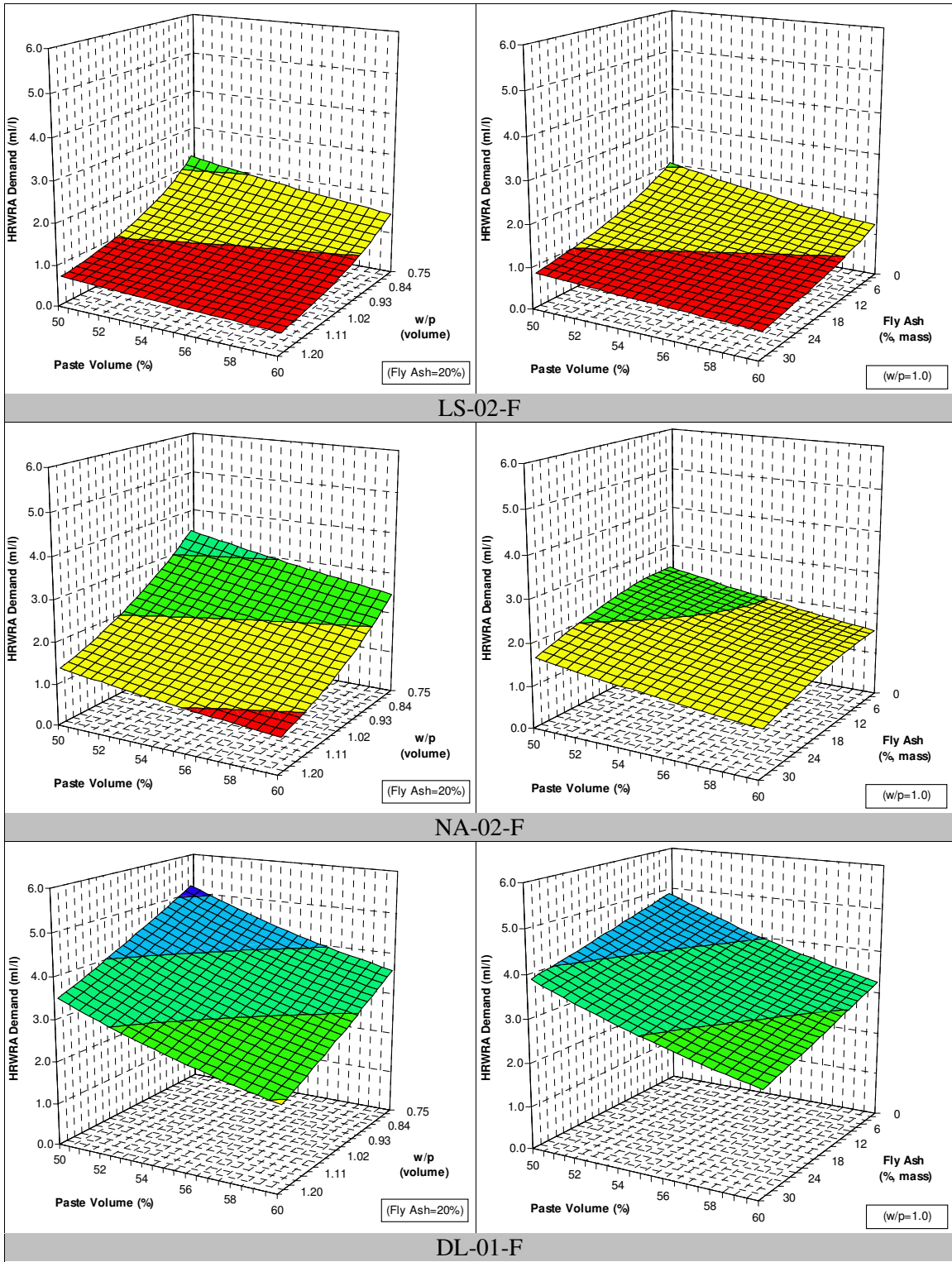
Figure 9.34: Multiple Regression Models for HRWRA Demand

187
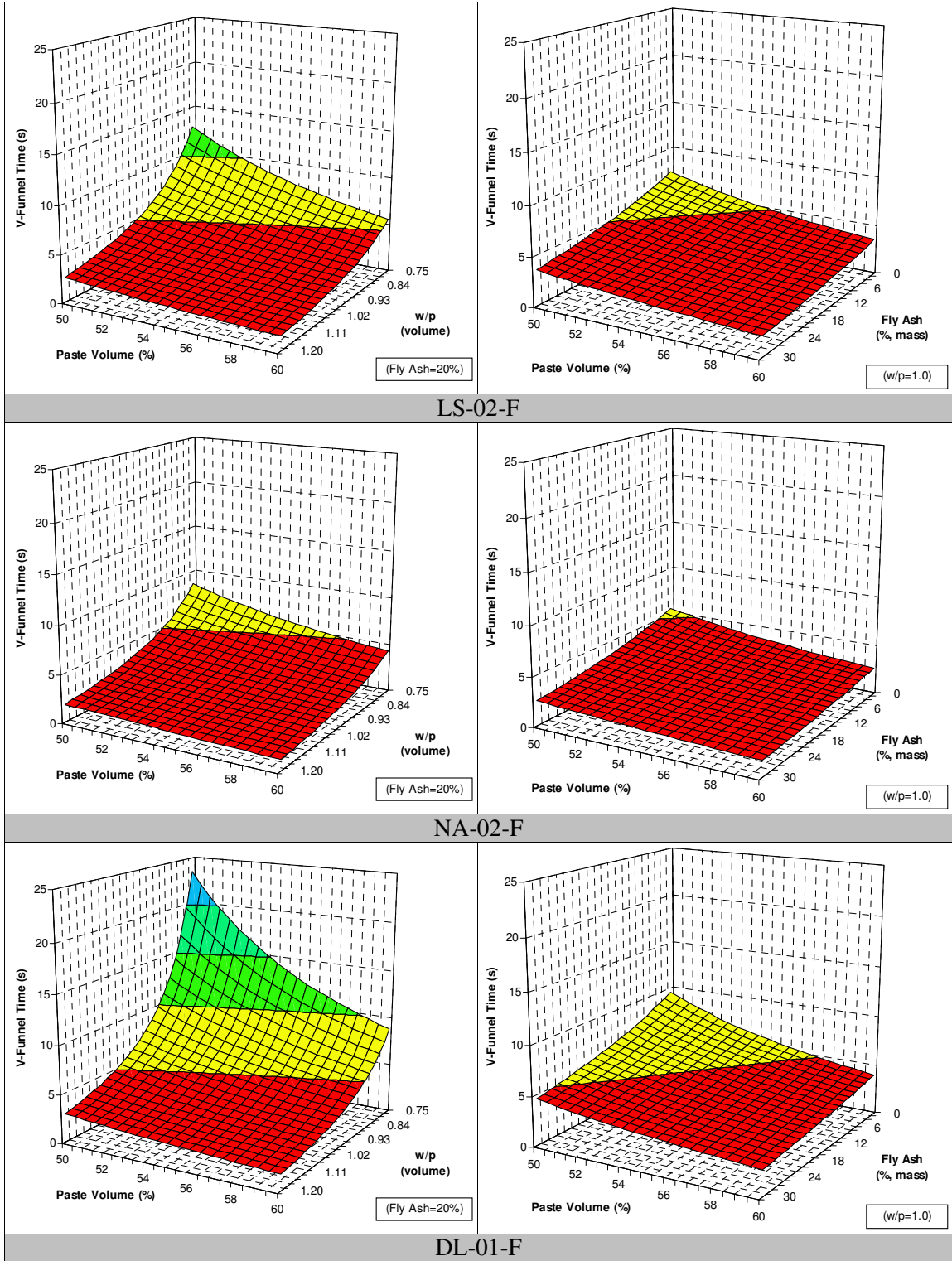
Figure 9.35: Multiple Regression Models for Mini-V-Funnel Time
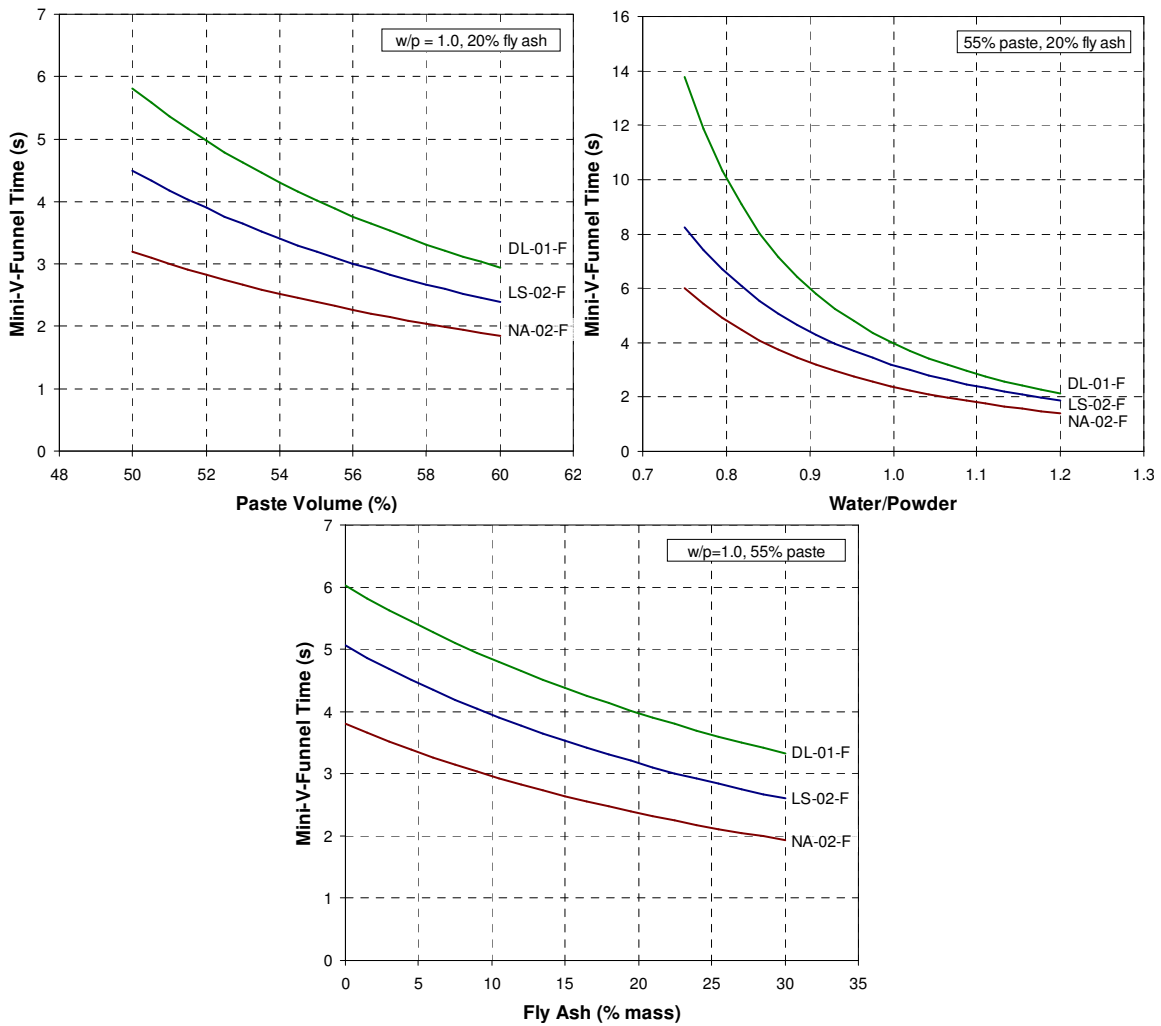
Figure 9.36: Evaluation of Mini-V-Funnel Time at Various Paste Volume, Water/Powder, and Fly Ash Dosages

The 24-hour compressive strength was affected primarily by the water-cement ratio (Figure 9.37). The use of fly ash slightly increased the 24-hour compressive strength for NA-02-F and DL-01-F while increasing the paste volume slightly decreased the 24-hour compressive strength for DL-01-F. This result was expected because class F fly ash typically exhibits little pozzolanic activity by 24 hours. Further, the compressive strength is primarily affected by the strength of the paste and the quality of the transition zone, which are determined primarily by the w/c for a given aggregate. For a given paste volume, w/c, and fly ash dosage, the DL-01-F sand exhibited the highest 24-hour compressive strength, which was likely due to the high content of microfines and the greater angularity and rougher surface texture of the DL-01-F sand.

189
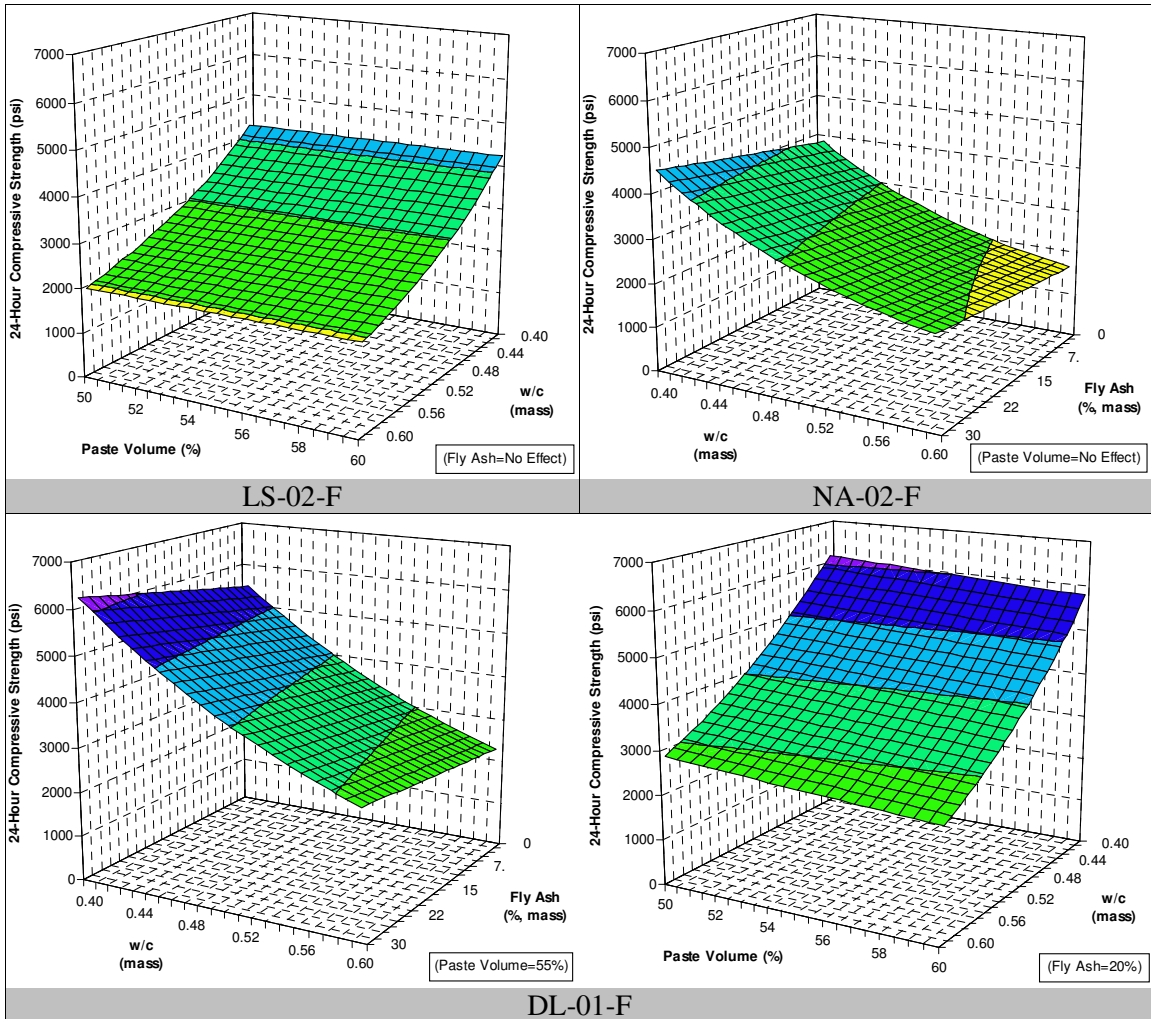
Figure 9.37:Multiple Regression Models for 24-Hour Compressive Strength

At 28 days, the compressive strength was mainly affected by the w/cm and the fly ash dosage, as indicated in Figure 9.38. As expected, increasing the w/cm reduced the 28-day compressive strength. Increasing the fly ash dosage resulted in a reduction in compressive strength, indicating that the pozzolanic effect of the fly ash was incomplete at 28 days and that compressive strength should be evaluated at later ages in order to capture more accurately the ultimate strength. For a given paste volume, w/cm, and fly ash dosage, the DL-01-F sand resulted in the highest 28-day compressive strength, which was consistent with the results at 24 hours.
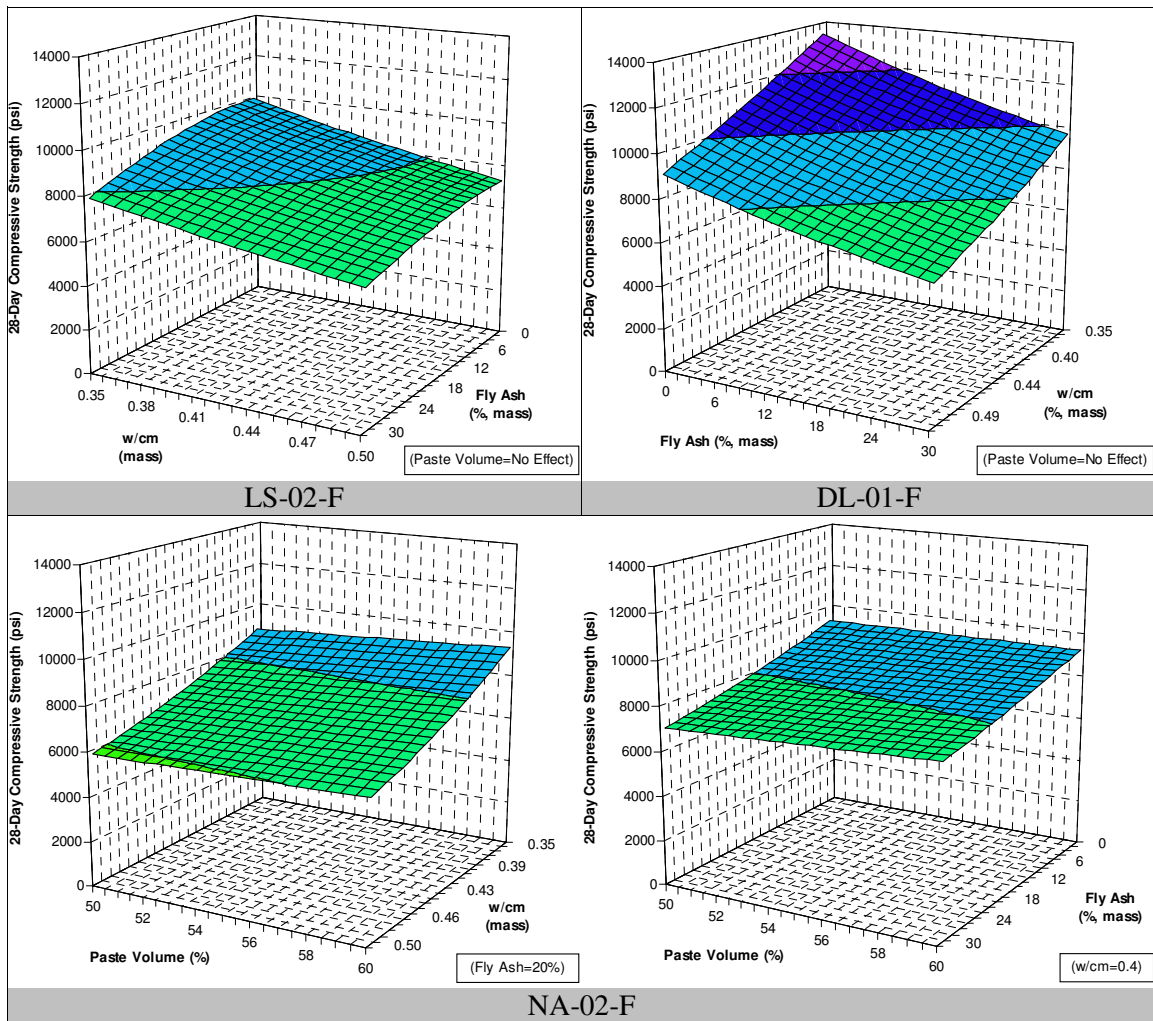
Figure 9.38: Multiple Regression Models for 28-Day Compressive Strength

9.5 Conclusions

Based on the data presented in this chapter, the following conclusions can be reached:

- The use of the mini-slump flow and mini-v-funnel tests provided a simple and effective means for evaluating the effects of changes in material properties and mixture proportions. By maintaining the constant slump flow in all mixtures, the yield stress remained approximately constant and the mini-v-funnel time was closely related to plastic viscosity.

- The effects of aggregate shape characteristics and grading were both significant in determining fresh flow properties of self-consolidating mortar mixtures.

- The 0.45 power curve grading resulted in consistently low HRWRA and plastic viscosity because of the high packing density. A coarser grading also resulted in low HRWRA demand and plastic viscosity but was harsh in some cases due to the lack of fine materials. A finer grading typically resulted in higher HRWRA demand and plastic viscosity but usually had better overall workability because of the increased amount of fine material and lack of harshness. In most cases, the as-received grading was not optimal for achieving the lowest HRWRA demand and mini-v-funnel time.

- No single parameter describing shape or grading was sufficient for predicting mortar flow properties. Instead, it was necessary to evaluate the simultaneous effects of multiple parameters. In general, the flow properties were improved by reducing the sphericity index (more spherical), reducing the length-width ratio, increasing the packing density, reducing the uncompacted voids content, and reducing the specific surface area. The specific surface area should not be reduced too far in order to avoid harsh mixtures.

- When microfines were used as part of the fine aggregate volume—resulting in higher paste volume, constant w/cm, and lower w/p—the HRWRA demand increased, the v-funnel time increased or decreased, the compressive strength increased, and the drying shrinkage increased.

- When microfines were used as part of the powder volume—resulting in constant paste volume and w/p and lower w/cm—the HRWRA demand increased in 5 of 6 cases and the v-funnel time decreased in 5 of 6 cases. The compressive strength decreased relative to the control mixture with constant w/p and increased or decreased relative to the control mixture with constant w/cm. The drying shrinkage increased relative to the control mixture with constant w/p and decreased relative to the control mixture with constant w/cm.

- For proportioning, microfines should be accounted for as part of the paste volume, not the aggregate volume. The water-powder ratio should be used to evaluate workability and the water-cement or water-cementitious materials ratio should be used to evaluate compressive strength.

- Workability was improved for microfines with increased specific surface area, span, and packing density. Increasing methylene blue value resulted in higher HRWRA demand; however, the workability was otherwise acceptable.

- Microfines with higher span and specific surface area resulted in greater packing density and improved workability due to the improved particle size distribution of the combined powder.

- Increasing the paste volume, water-powder ratio, and fly ash dosage were shown to reduce the HRWRA demand and mini-v-funnel time. These results illustrate how mixture proportions can be changed to accommodate changes in aggregate characteristics.

Chapter 10: Effects of Aggregates in Concrete

The effects of aggregates in concrete were evaluated by considering separately the effects of fine aggregates, coarse aggregates, and microfines. First, fine aggregates were evaluated by using the 12 fine aggregates in their as-received gradings and in a standard grading. Second, coarse aggregates were evaluated by using the 7 coarse aggregates in their as-received gradings and in 3 standard gradings. Third, fine and coarse aggregates were evaluated at various paste volumes. Fourth, microfines were evaluated by using the 6 microfines as either part of the aggregate volume or powder volume. All test data are provided in Appendix C.

10.1   Materials, Mixture Proportions, and Test Procedures

The standard concrete mixture used to evaluate the effects of fine aggregates, coarse aggregates, and microfines is shown in Table 10.1. The mixture, which features a 35.9% paste volume and a w/cm of 0.37, was selected to achieve SCC flow properties with nearly all aggregates considered in this study. Therefore, it is not the optimal mixture for all aggregates but does allow a direct comparison of aggregate properties. For many of the aggregates, the water content and paste volume could be reduced for greater economy. The HRWRA dosage (HRWRA-02) was varied in each mixture to reach a slump flow of 24-26 inches. The coarse aggregates, fine aggregates, and microfines were each varied one at a time. The control fine and coarse aggregates were LS-02-F and NA-02-C.

Workability was measured with the slump flow test, j-ring test, v-funnel test, ICAR rheometer, and visual rankings. The slump flow test—including measurements of T_{50} and VSI—was performed in accordance with ASTM C 1611. The j-ring test was performed in accordance with ASTM C 1621, with the clear spacing between bars set at 1.5 inches. For the j-ring test, the average difference in the height of concrete between the outside and inside of the j-ring, measured at four locations around the ring, was taken as an indication of passing ability. For both the slump flow and j-ring tests, the slump mold was used in the inverted position. The v-funnel test, which is depicted in Figure 10.1, was conducted by filling the v-funnel in one lift, pausing for 1 minute, opening the bottom gate, and measuring the time for all concrete to be discharged. The ICAR rheometer, which is shown in Figure 10.2, was used to perform a flow curve test. The four-bladed vane of the rheometer was 5 inches in diameter and height. The

container was 11 in diameter and filled with concrete to a height of 11 inches. The test protocol consisted of a 20-second pre-shear period at a constant speed of 0.60 rps followed by 7 flow curve points in descending order from 0.60 to 0.05 rps. The Bingham model parameters were computed based on the Reiner-Riwlin equation for the 7 descending flow curve points. Only the plastic viscosity was evaluated for this research instead of both yield stress and plastic viscosity because at a constant slump flow, the yield stress should be approximately constant. Visual rankings for filling ability, passing ability, and segregation resistance were made for each mixture on a scale of 0 to 3, with 0 being the best. Additionally, a visual determination was made as to whether each mixture contained sufficient paste volume.

Table 10.1: Mixture Proportions for Evaluation of the Effects of Aggregate in Concrete

Material	Proportions	
	Volume (%)	Mass (lb/yd^3)
Fine Aggregate[1]	32.0	variable
Coarse Aggregate[2]	32.0	variable
Cement (PC-01-I/II)	11.3	600
Fly Ash (FA-02-F)	5.1	200
Water	17.6	296
Air	2.0	--
HRWRA-02	Variable (24-26-in. slump flow)	
w/cm	0.37	
S/A	0.50	
Fly Ash Dosage (mass)	25%	
Paste Volume	35.9%	
[1] Control Fine Aggregate: LS-02-F [2] Control Coarse Aggregate: NA-02-C		
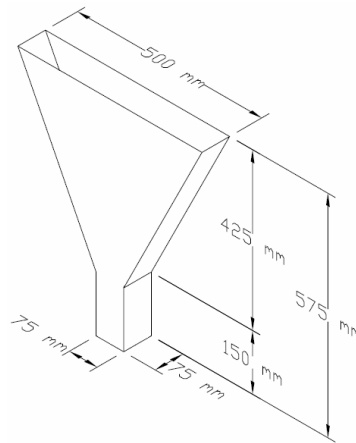
Figure 10.1: V-Funnel Test
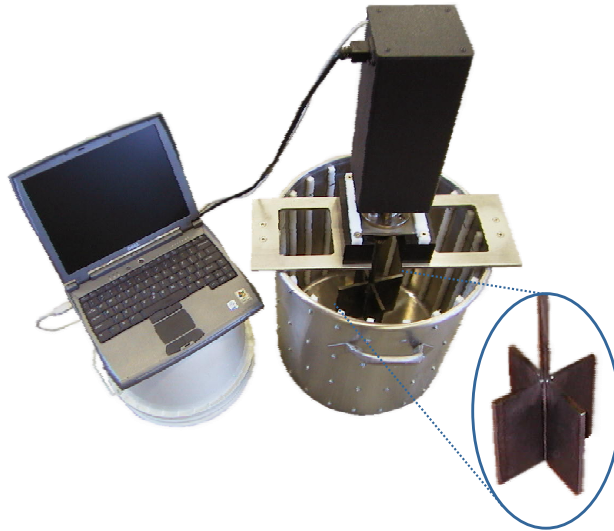
Figure 10.2: ICAR Rheometer

The following hardened properties were measured for all mixtures: compressive strength, modulus of elasticity, flexural strength, drying shrinkage, and chloride permeability. Compressive strength was evaluated at 24 hours and 28 days on 4 by 8-inch cylinders in accordance with ASTM C 39. Static modulus of elasticity was evaluated on 4 by 8-inch cylinders at 28 days in accordance with ASTM C 469. Flexure strength was evaluated at 28 days on 4.5 by 4.5 by 15.5-inch simply supported beams (13.5-inch span length) with third point loading in accordance with ASTM C 78. Drying shrinkage was measured on 3 by 3 by 11.25-inch specimens (10-inch gage length) in accordance with ASTM C 157. The shrinkage specimens were demolded at 23 ½ +/- ½ hours, stored in lime-saturated water at 23°C to an age of 3 days, and then stored on racks at 23°C and 50% relative humidity for the remainder of the test (to 112 days). Chloride permeability was measured after 91 days in accordance with ASTM C 1202. Two, two-inch thick permeability specimens were cut from one 4 by 8-inch cylinder for each mixture. In addition to these tests, abrasion resistance was measured on the mixtures used to evaluate microfines. The abrasion tests were conducted on three formed-surface specimens for each mixture at 91 days with the rotating cutter method in accordance with ASTM C 944. A double load of 44 lb was applied for 8 minutes for each abrasion specimen.

The mixing procedure used for all SCC mixtures is shown in Table 10.2 The aggregates were batched in a moist condition, with appropriate moisture corrections. All mixtures were mixed in 2.5-cubic foot batches in a rotating drum mixer. Materials were stored at approximately 23°C at least 12 hours prior to mixing. Concrete was mixed and cast into

specimens at this same ambient temperature. Specimens for compressive strength, modulus of elasticity, flexural strength, chloride permeability, and abrasion resistance were demolded the following day and stored at 23°C and 100% relative humidity after demolding until the time of testing. Abrasion specimens were allowed to dry for 7 days prior to testing.

Table 10.2: Concrete Mixing Procedure

1. Add aggregate and approximately 2/3 of mixing water to mixer. Run mixer to blend ingredients.
2. Add cementitious materials.
3. Start mixer and add remaining mixing water. Include any admixtures other than HWRA in this mixing water.
4. Mix for **3 minutes**.
5. Stop mixing for **3 minutes**. Scrape sides of mixer. Add HRWRA at end of rest period.
6. Mix for **6 minutes**. Adjust HRWRA dosage to reach desired workability.
7. Measure slump flow. If additional admixture is needed, adjust dosage and mix for at least **1 minute**.
8. Discharge concrete from mixer upon reaching the desired slump flow. Test.

Two conventionally placed concrete control mixtures, listed in Table 10.3, were evaluated for comparison to the SCC mixtures. These conventional mixtures were proportioned based on the ACI 211 procedure and were intended for general ready mixed concrete applications. The two mixtures include the same amount of water; however, mixture CC1 includes 4.5 sacks of cementitious materials and a w/cm of 0.60 whereas mixture CC2 includes 6 sacks of cementitious materials and a w/cm of 0.45. Both mixtures have a S/A of 0.40 and a 20% fly ash replacement rate.

Multiple regression models were developed to relate specific aggregate characteristics to SCC performance. Although these models are generally useful in explaining such relationships, they should be interpreted with caution. The multiple regression models may not identify the correct relationships and may not properly assign relative weights to each factor due to the limited number of data points for each test series, the limited capabilities of the factors to capture the aggregate characteristics fully and accurately, the limited ranges of the factors, and correlations between factors.

Table 10.3: Conventionally Placed Concrete Control Mixtures

	CC1	CC2
Fine Aggregate, LS-02-F (lb/yd^3)	1309	1254
Coarse Aggregate, NA-02-C (lb/yd^3)	1948	1874
Cement, PC-01-I/II (lb/yd^3)	338.4	451.2
Fly Ash, FA-02-F (lb/yd^3)	84.6	112.8
Water	253.8	253.8
Water-Reducer, MRWRA-01 (oz/cwt)	10	8
w/cm	0.60	0.45
S/A	0.40	0.40
Fly Ash Dosage, Mass (%)	20	20
Paste Volume (%)	25.6	28.4
Total Cementitious Materials (lb/yd^3)	423	564
Slump (inches)	6	5.5
Yield Stress, Stress Growth, 0.025 rps (Pa)	1366	2333
Yield Stress, Flow Curve (Pa)	150	374
Plastic Viscosity (Pa.s)	30.6	38.5
Compressive Strength, 24-hr (psi)	593	1131
Compressive Strength, 28-day (psi)	5300	7273
Modulus of Elasticity, 28-day (ksi)	5284	6511
Flexural Strength, 28-day (psi)	692	881
Drying Shrinkage, 112-day (μ-strain)	510	560
Chloride Permeability, 91-day (coulombs)	1725	1345
Abrasion Mass Loss, 91-day (grams)	7.7	4.9

10.2 Effects of Fine Aggregates

10.2.1 Test Plan

The 12 fine aggregates were tested in two gradings: standard and as-received. The standard grading was the 0.45 power curve sand grading used in the mortar mixtures (Chapter 9). This 0.45 power curve sand grading did not include microfines, which were considered separately. The as-received gradings did include microfines.

10.2.2 Test Results

The fine aggregates significantly affected the HRWRA demand, plastic viscosity, and j-ring blocking. As shown in Figure 10.3, DL-01-F and LS-03-F exhibited the highest HRWRA demand for both the as-received and standard gradings. These two aggregates were highly angular manufactured sands. LS-02-F, a well-shaped manufactured sand, resulted in the lowest HRWRA demand. The two natural sands did not exhibit the lowest HRWRA demand even

when tested in the standard grading. The standard grading consistently exhibited lower HRWRA demand than the as-received grading, which was likely partially a result of the lack of microfines and typical reduction in other fine sizes in the standard grading.

The HRWRA demand was found to be insufficient for describing flow properties fully because some aggregates exhibited low HRWRA demand but resulted in viscous or harsh mixtures. Indeed, the trends in HRWRA demand did not match the trends in plastic viscosity shown in Figure 10.4. For the as-received sands, the plastic viscosity varied significantly from nearly 40 Pa.s for the DL-01-F sand to less than 5 Pa.s for the NA-02-F sand. The two natural sands exhibited the lowest viscosity, while LS-02-F, the well-shaped manufactured sand, also performed well. As with HRWRA demand, the standard grading consistently resulted in lower plastic viscosity than the as-received grading.

In general, the aggregates with high plastic viscosity were also associated with high j-ring blocking because the morphological characteristics that increase viscosity also increase j-ring blocking (Figure 10.5). Although it would be expected that coarse aggregates, due to their size, should have the biggest effect on passing ability, fine aggregate characteristics played a significant role. In general, the test results indicate that any increase in fine aggregate angularity and reduction in equi-dimensionality resulted in increased compacted voids content and increased interparticle friction, which were manifested in increased HRWRA demand, plastic viscosity, and j-ring blocking.
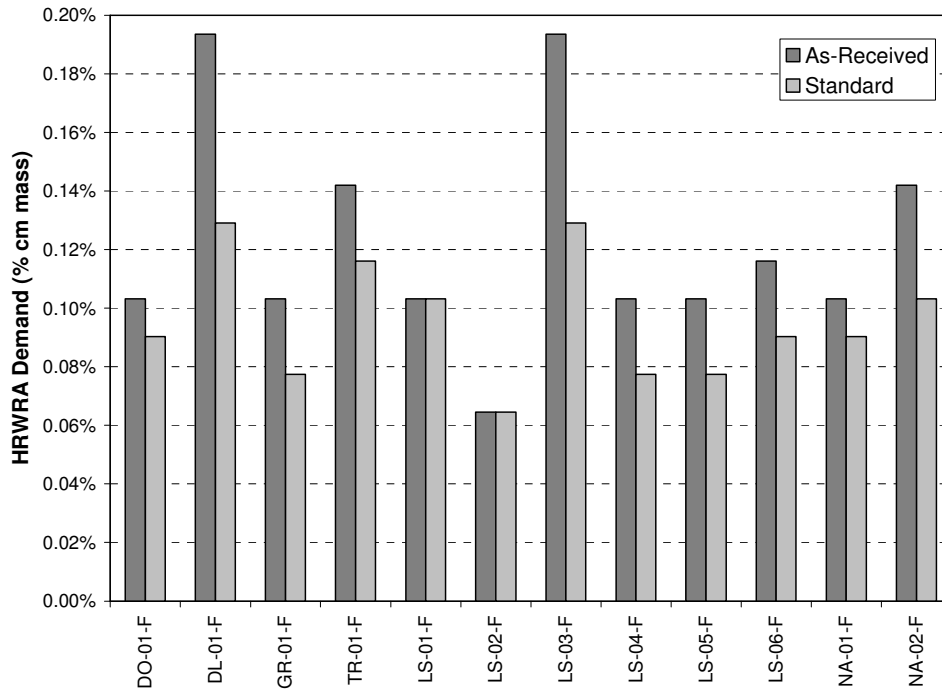
Figure 10.3: Effects of Fine Aggregates on HRWRA Demand
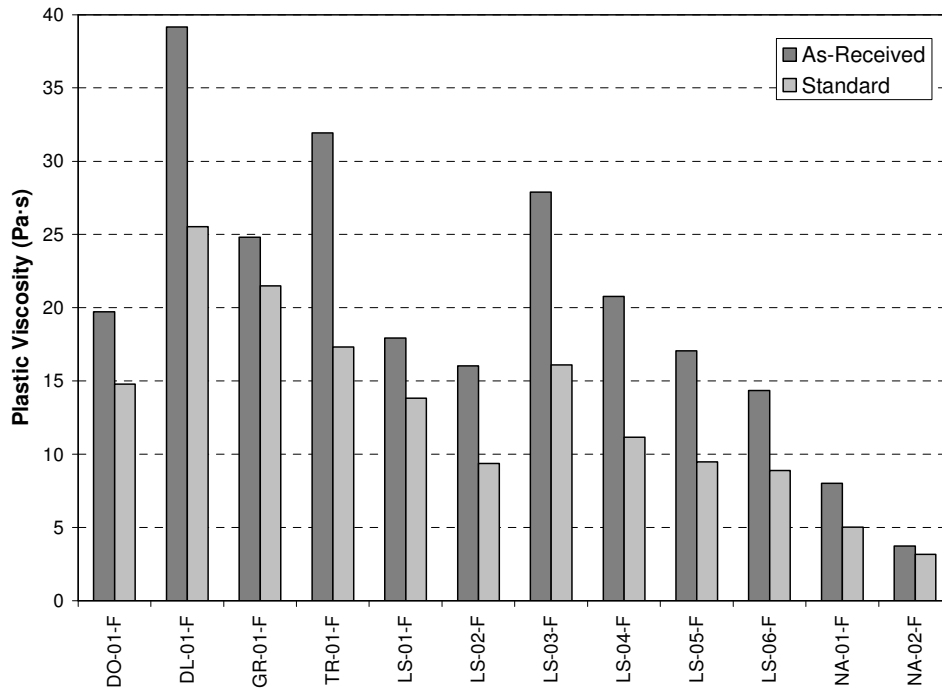
Figure 10.4: Effects of Fine Aggregates on Plastic Viscosity

200
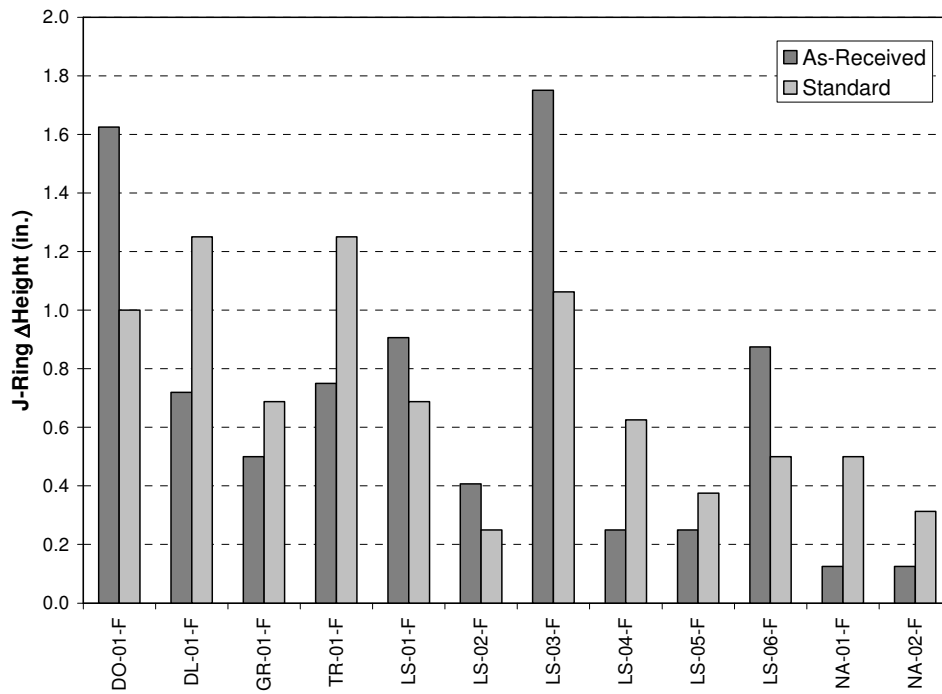
Figure 10.5: Effects of Fine Aggregates on J-Ring Blocking

The hardened properties varied with aggregate source and grading, although not to the extent that the workability varied. The compressive strength varied from approximately 7,000 to 9,000 psi for most mixtures depending on the fine aggregate source and grading, as shown in Figure 10.6. The sands DO-01-F and GR-01-F resulted in significantly lower compressive strengths; however, the paste volume was determined to be insufficient in these mixtures. The resulting lack of consolidation, bleeding, and excessive HRWRA dosage likely was the main cause of the reduction in compressive strength. The modulus of elasticity, which is shown in Figure 10.7, varied from approximately 5,000 to 6,500 ksi, depending on the aggregate and grading. The aggregate source had a larger effect than grading on modulus of elasticity. The LS-04-F and LS-06-F fine aggregates—which are porous and have high absorption capacities—resulted in mixtures with the lowest elastic modulus measurements. The low elastic moduli recorded for GR-01-F and LS-03-F were likely due, at least partially, to the insufficient paste volume in these mixtures. The modulus of rupture, which is shown in Figure 10.8, did not vary significantly with aggregate source or grading. The rapid chloride permeability was considered very low or low for all aggregates, due mainly to the low w/cm, the use of fly ash, and the 91 days of moist curing prior to testing (Figure 10.9). In fact, the rapid chloride permeabilities for the SCC mixtures were all lower than the conventional control mixtures. The highest chloride

201

permeabilities were recorded for the two porous, high absorption capacity aggregates, LS-04-F and LS-05-F. The drying shrinkage varied between approximately 400 and 500 micro-strain at 28 days, as indicated in Figure 10.10. This shrinkage was less than that recorded for the two conventional control mixtures.
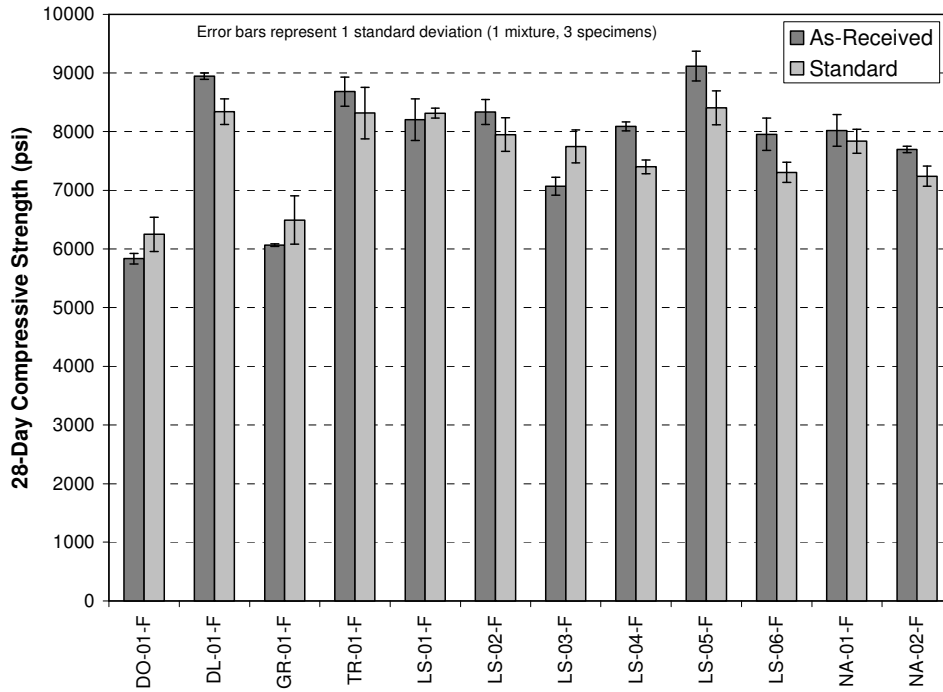
Figure 10.6: Effects of Fine Aggregates on Compressive Strength
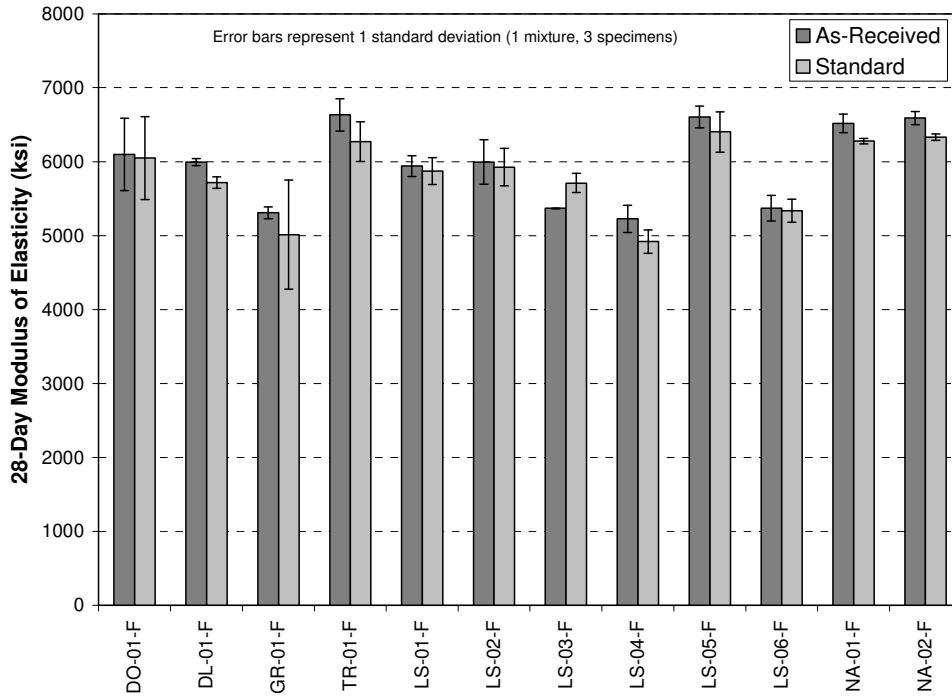
Figure 10.7: Effects of Fine Aggregates on Modulus of Elasticity
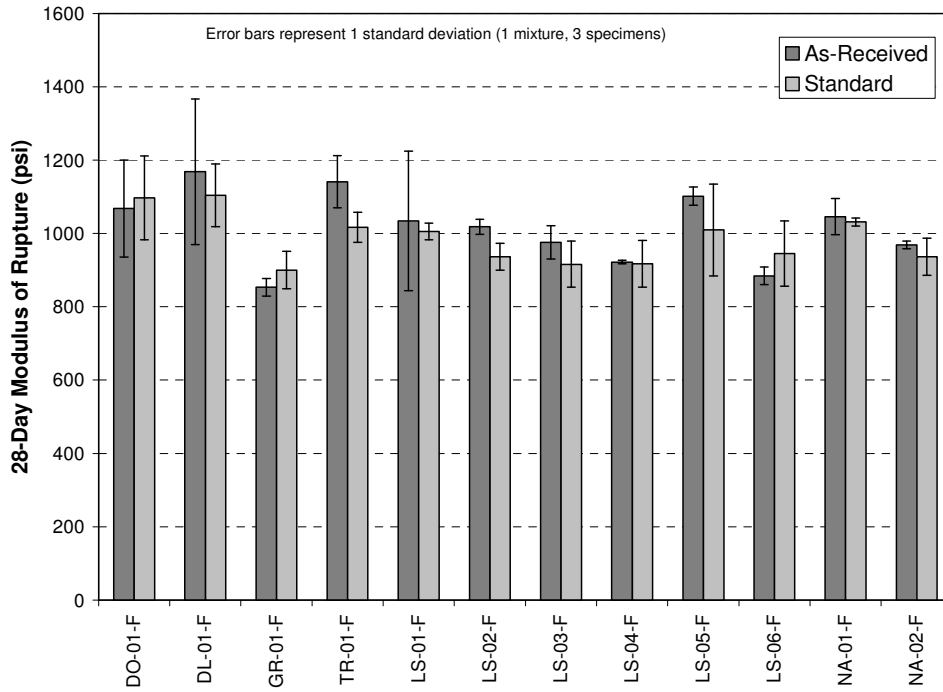
Figure 10.8: Effects of Fine Aggregates on Flexural Strength

203
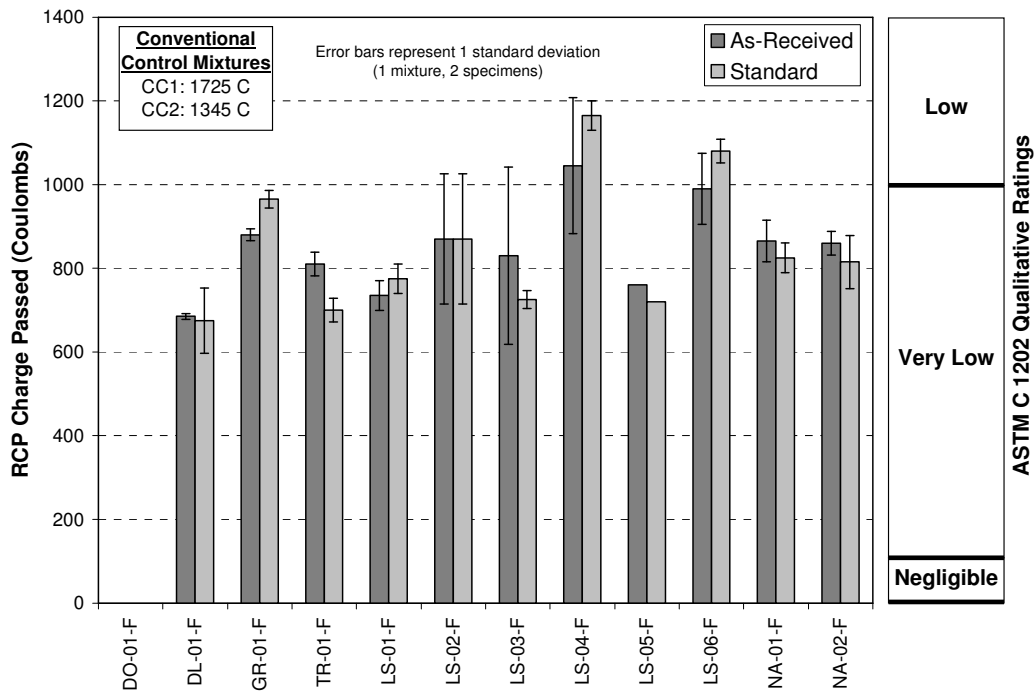
Figure 10.9: Effects of Fine Aggregates on Rapid Chloride Permeability
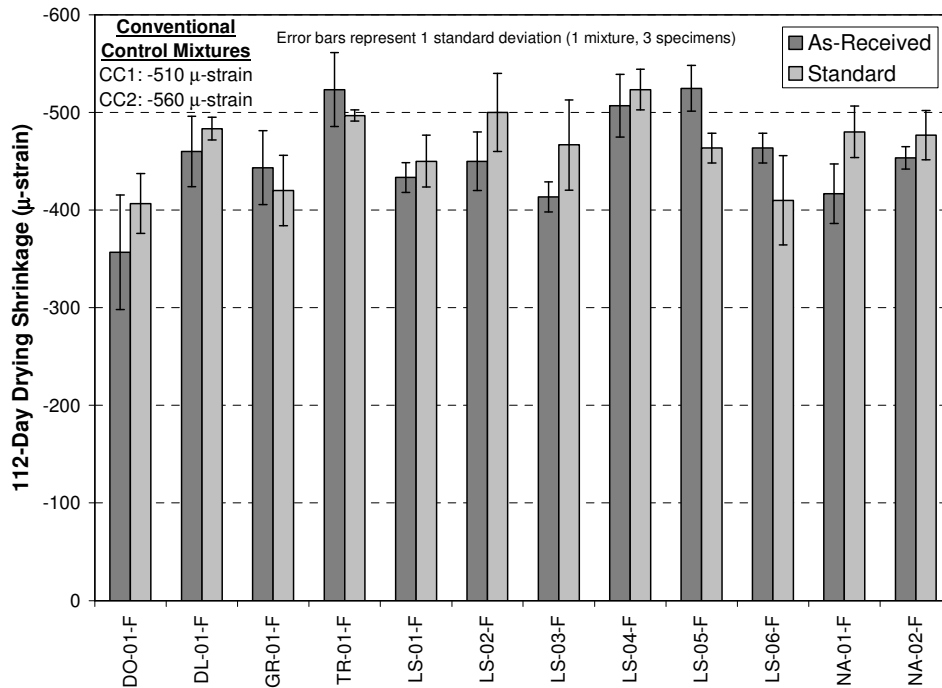
Figure 10.10: Effects of Fine Aggregates on Drying Shrinkage

The comparable results from the mortar and concrete testing for fine aggregate shape characteristics and grading were correlated, as shown in Figure 10.11; however, the scatter was

high. The lack of sufficient paste volume and interaction between coarse and fine aggregates were likely the main contributors to the scatter.
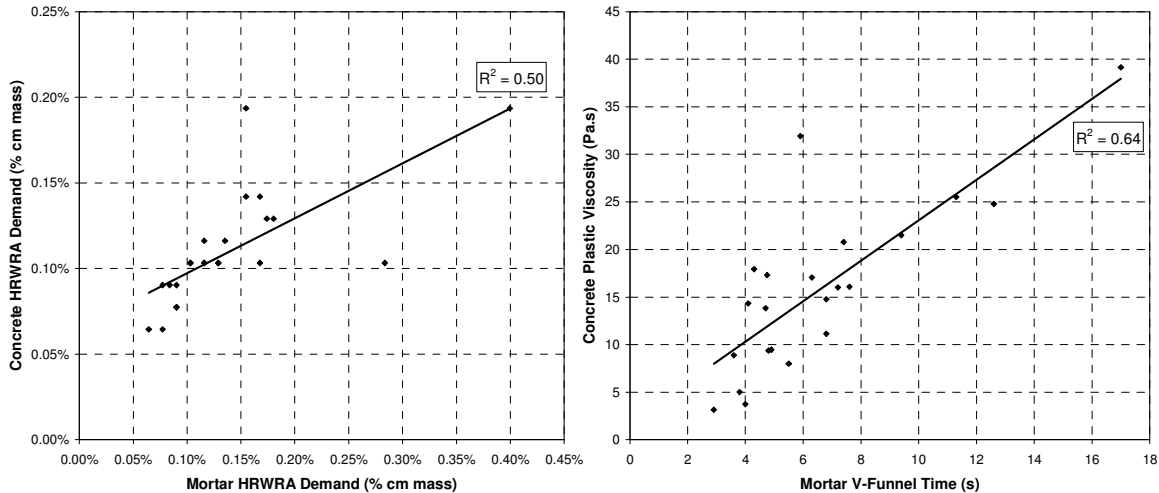
Figure 10.11: Comparison of Mortar and Concrete Properties for Fine Aggregate Mixtures

To evaluate the combined effects of fine aggregate shape characteristics and grading, multiple regression models were developed for fresh and hardened properties for the mixtures with as-received gradings. The factors used for the model were sphericity index, L/W, specific surface area, packing density, specific gravity, and absorption capacity. The specific surface area was calculated assuming spherical particles and, therefore, reflects only grading and not shape, texture, or angularity. Models with high $R^2_{adjusted}$ (>0.60) were obtained for T_{50}, plastic viscosity, j-ring, 24-hour and 28-day compressive strength, modulus of elasticity, flexural strength, rapid chloride permeability, and drying shrinkage (Table 10.4).

For plastic viscosity, the results were consistent with the mortar tests for mini-v-funnel time. As indicated in Figure 10.12, the plastic viscosity increased with increasing specific surface area, specific gravity, sphericity index, and L/W and with decreasing packing density. These results indicate that finer, more poorly shaped aggregates with low packing densities are associated with higher plastic viscosity. J-ring blocking was affected primarily by the length-width ratio as shown in Figure 10.13, with increased length/width resulting in increased j-ring blocking. This reduction in shape caused increased interparticle friction and increased compacted voids content, which reduced the capacity of the concrete to flow between reinforcing bars. Figure 10.14 indicates that compressive strength was primarily influenced by specific surface area and specific gravity, with increases in specific surface area and specific gravity

associated with increases in compressive strength. These results were expected because finer, denser aggregates are known to result in increased compressive strength. Increasing the packing density also resulted in higher compressive strength. The effect of aggregate shape as measured by the HAVER CPA was minimal, with increased sphericity index and reduced L/W resulting in a slight increase in compressive strength. Modulus of elasticity increased with increasing packing density and L/W and decreasing specific surface area (Figure 10.15). The decrease in modulus of elasticity and increase in compressive strength associated with increasing specific surface area was consistent with expectations. For instance, Shah and Ahmad (1985) found that increasing the coarseness of the aggregate grading resulted in increased modulus of elasticity, whereas compressive strength generally decreases with increasing coarseness. As indicated in Figure 10.16, increased modulus of rupture was associated with increased specific gravity and packing density, which was consistent with expectations. Rapid chloride permeability was found to increase with increased absorption capacity and packing density, as indicated in Figure 10.17. The effects of specific gravity and specific surface area on rapid chloride permeability were negligible. The increase in rapid chloride permeability with absorption capacity was expected because more porous aggregates should result in more permeable concrete. Figure 10.18 indicates that drying shrinkage increased with increased absorption capacity and specific gravity. An aggregate with higher absorption capacity is likely to be less stiff and provide less restraint to shrinkage. Although shrinkage does increase with increased specific gravity, the increase in shrinkage with increased absorption capacity was much greater. Increasing the specific surface area slightly decreased the drying shrinkage.

Table 10.4: Multiple Regression Models for Sand Characteristics (As-Received Grading)

Model	$R^2_{adjusted}$
$T_{50} = -25.84 + 12.83(L/W) + 6.092(SPHR)(SG) - 5.053(PKG)(SG) + 0.04286(ABS)^2$	0.991
Plastic Viscosity $= 9968.1 - 13531.8(L/W) + 3.114(SSA)(SG) - 9.396(PKG)(SSA) + 4566.1(L/W)^2 + 29.14(SPHR)^2$	0.940
$1/(J\text{-ring}) = 2720.6 - 3548.0(L/W) + 1156.9(L/W)^2 + 0.04548(ABS)^2$	0.990
$(f'_c\{24\text{-hr}\})^{0.5} = 24.19 + 7.091(SPHR)(SG) + 0.07829(SSA)(SG)$	0.908
$1/(f'_c\{28\text{-d}\}) = 1.80\text{x}10^{-4} - 2.611\text{x}10^{-5}(SPHR)(SG) - 2.531\text{x}10^{-6}(PKG)(SSA) + 2.883\text{x}10\text{-}5(SPHR)(L/W)$	0.999
$(E\{28\text{-d}\})^{-0.5} = 0.2075 + 5.378\text{x}10^{-6}(SSA)^2 - 0.00979(L/W)(PKG)$	0.964
$f'_r\{28\text{-d}\} = 37.56 + 565.5(PKG)(SG)$	0.895
Shrinkage $= 397.49 + 73.73(SG)(ABS) - 8.465(SSA)(ABS)$	0.919
$RCP\{91\text{-d}\} = -173.5 + 25.11(ABS)^2 + 2622.3(PKG)^2 - 3.939(SSA)(SG)$	0.995
Regression Details: quadratic model, stepwise regression; p-value = 0.25; transformation with highest $R^2_{adjusted}$ selected; transformations considered: y, 1/y, ln(y), sqrt(y), 1/sqrt(y); mixtures with insufficient paste volume (DO-01-F, GR-01-F, LS-03-F) removed for hardened property models	
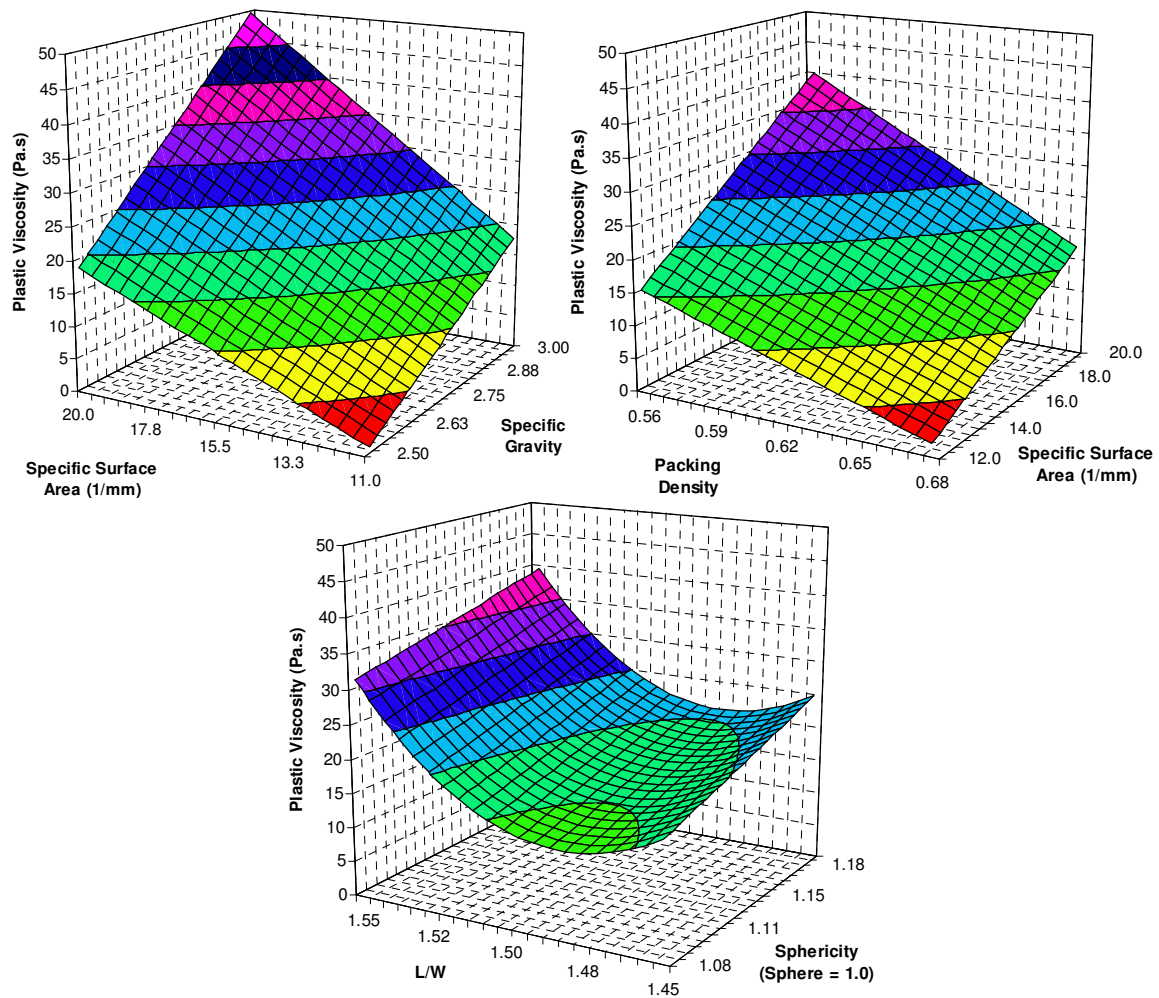
Figure 10.12: Effects of Fine Aggregate Characteristics on Plastic Viscosity (As-Received Gradings)
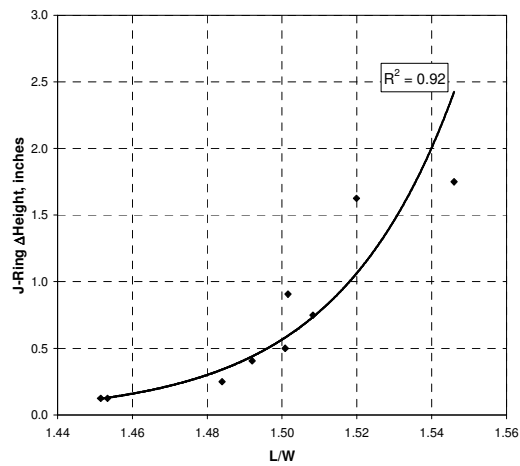
Figure 10.13: Effect of Fine Aggregate Length/Width on J-Ring Blocking (As-Received Gradings)

207
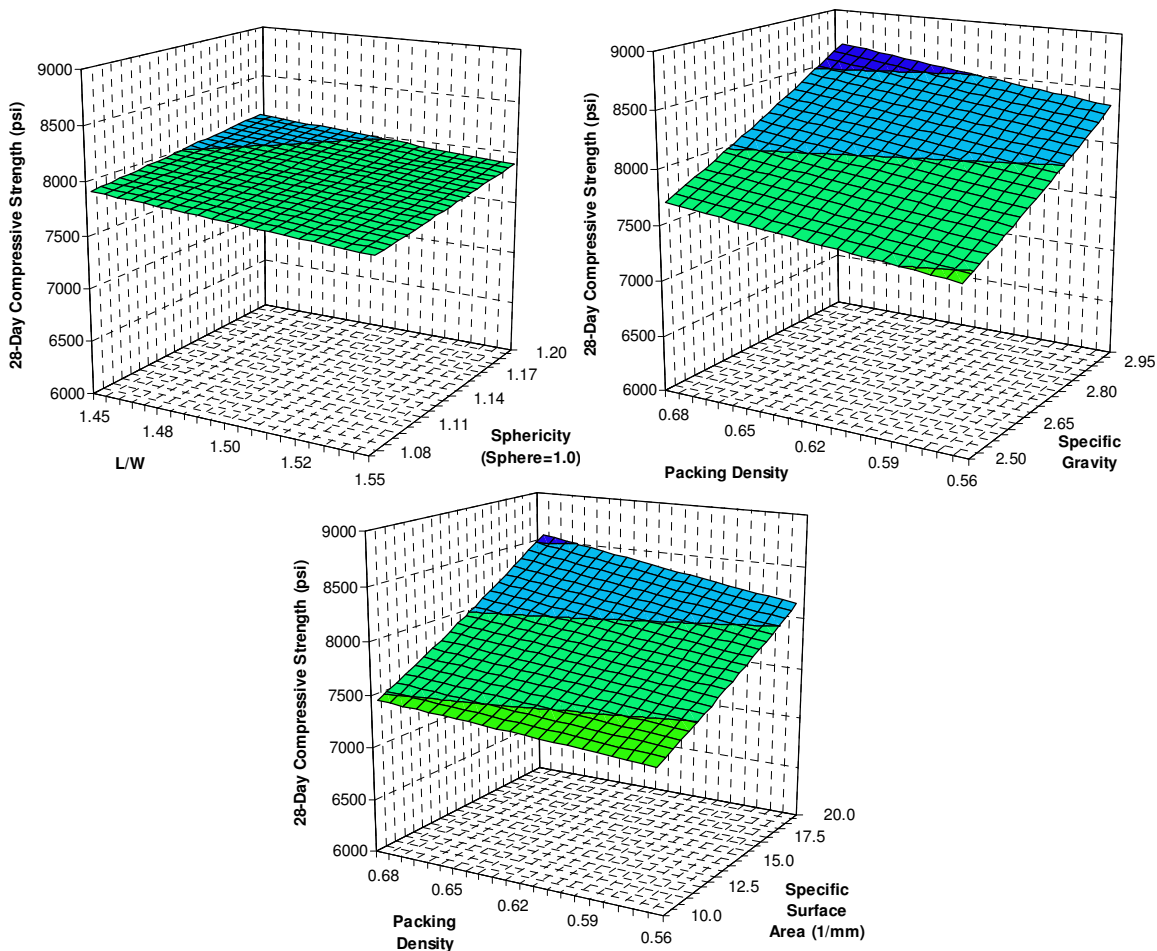
Figure 10.14: Effects of Fine Aggregate Characteristics on 28-Day Compressive Strength (As-Received Gradings)
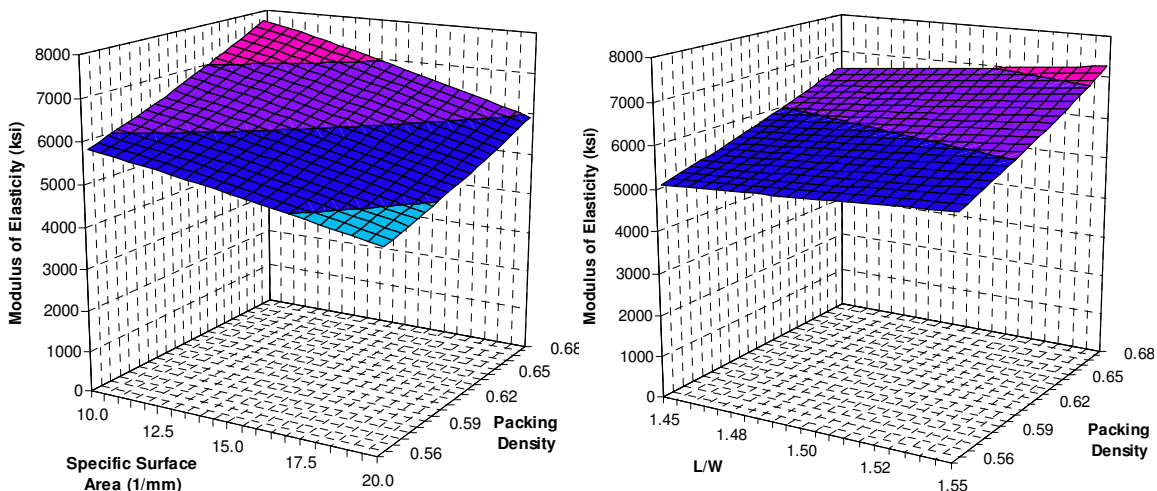
Figure 10.15: Effects of Fine Aggregate Characteristics on 28-Day Modulus of Elasticity (As-Received Gradings)

208
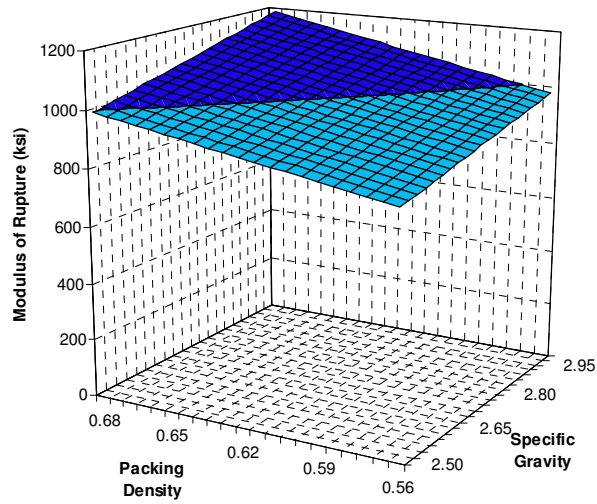
Figure 10.16: Effects of Fine Aggregate Characteristics on 28-Day Flexural Strength (As-Received Gradings)
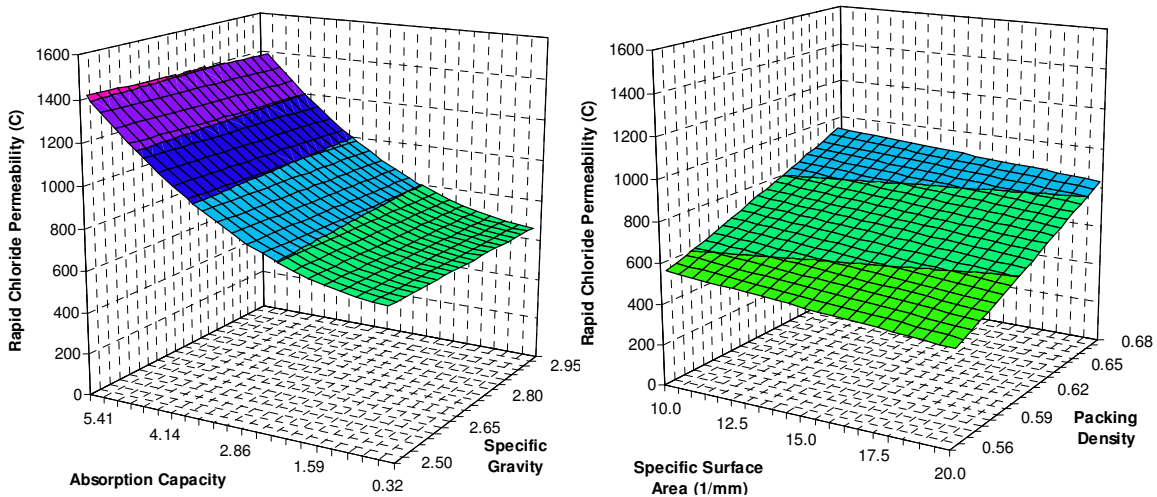
Figure 10.17: Effects of Fine Aggregate Characteristics on 91-Day Rapid Chloride Permeability (As-Received Gradings)

209
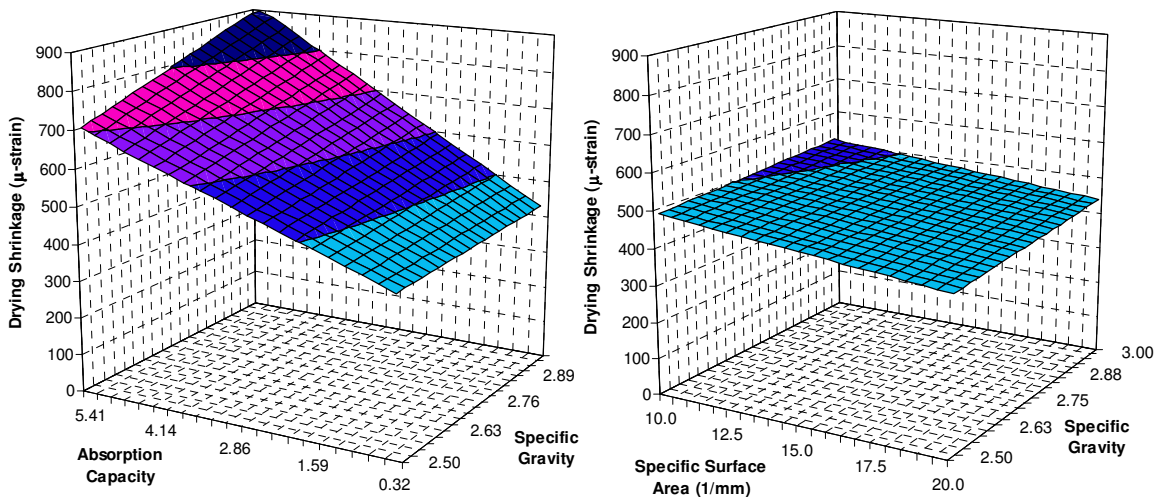
Figure 10.18: Effects of Fine Aggregate Characteristics on 112-Day Drying Shrinkage (As-Received Gradings)

10.3 Effects of Coarse Aggregates

10.3.1 Test Plan

The 7 coarse aggregates were tested in 4 gradings: as-received and 3 standard gradings. The 3 standard gradings, which are shown in Figure 10.19, were a gap grading, a 0.45 power curve grading (with ¾-inch maximum aggregate size and microfines included), and an intermediate grading between the gap and 0.45 power curve grading. The control fine aggregate, LS-02-F, was used in its as-received grading except for the 0.45 power curve grading.

Sieve	Percent Passing		
	Gap	Inter-mediate	0.45 Power Curve
1"	100.0%	100.0%	100.0%
3/4"	96.0%	97.5%	100.0%
5/8"	86.0%	90.5%	92.1%
1/2"	73.5%	82.0%	83.3%
3/8"	58.0%	69.0%	73.2%
1/4"	52.5%	57.5%	61.0%
#4	50.0%	52.0%	53.8%
#8	47.7%	47.7%	39.4%
#16	30.8%	30.8%	28.8%
#30	18.7%	18.7%	21.1%
#50	10.0%	10.0%	15.4%
#100	4.5%	4.5%	11.3%
#200	2.6%	2.6%	8.3%
Pan			
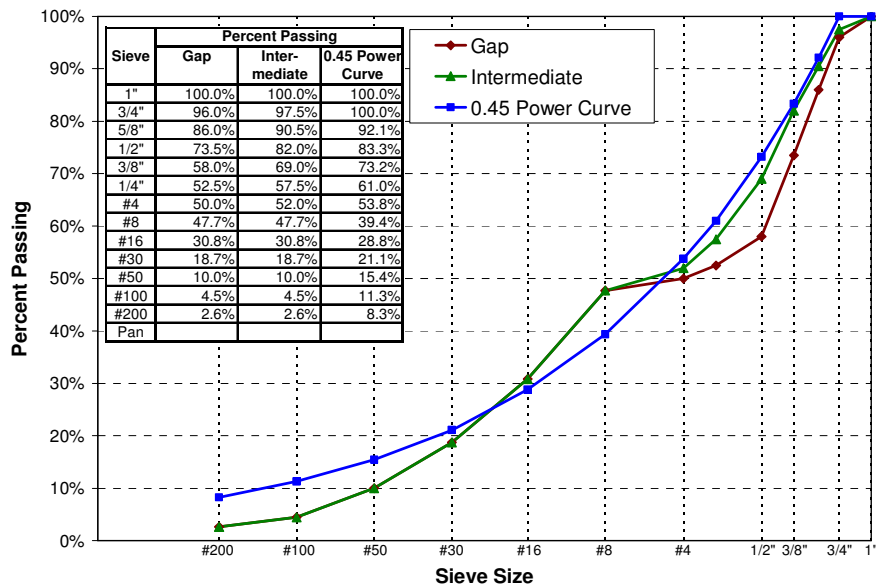
Figure 10.19: Coarse Aggregate Gradings

10.3.2 Test Results

The effects of coarse aggregates on HRWRA demand, plastic viscosity, and j-ring blocking were not as substantial as the effects of fine aggregate. Such a result was expected because the smaller the size of a particle, the greater the effects of its morphological characteristics on workability should be. As shown in Figure 10.20, the HRWRA demand was nearly unchanged regardless of the aggregate source or grading. The plastic viscosity, however, did vary with both aggregate source and grading as indicated in Figure 10.21. The natural river gravel exhibited the lowest viscosity, which was expected due to its favorable morphological characteristics. No clear trend in plastic viscosity was evident in comparing the three standard gradings, suggesting that a single ideal grading does not exist and that the best grading depends in part on the aggregate shape characteristics. Additionally it should be noted that the high microfines content for the 0.45 power curve grading resulted in lower water-powder ratio than the other mixtures, likely reducing workability. The j-ring results varied significantly depending on the aggregate source and grading, with the natural river gravel exhibiting the lowest j-ring blocking (Figure 10.22). The gap grading could be expected to exhibit the highest j-ring blocking of the three standard gradings because it contained the highest fraction of large particles; however, no clear trend was evident. This lack of trend, as well as the large difference in j-ring result between different aggregates in the same grading, suggests that the shape and angularity characteristics are highly influential for passing ability.
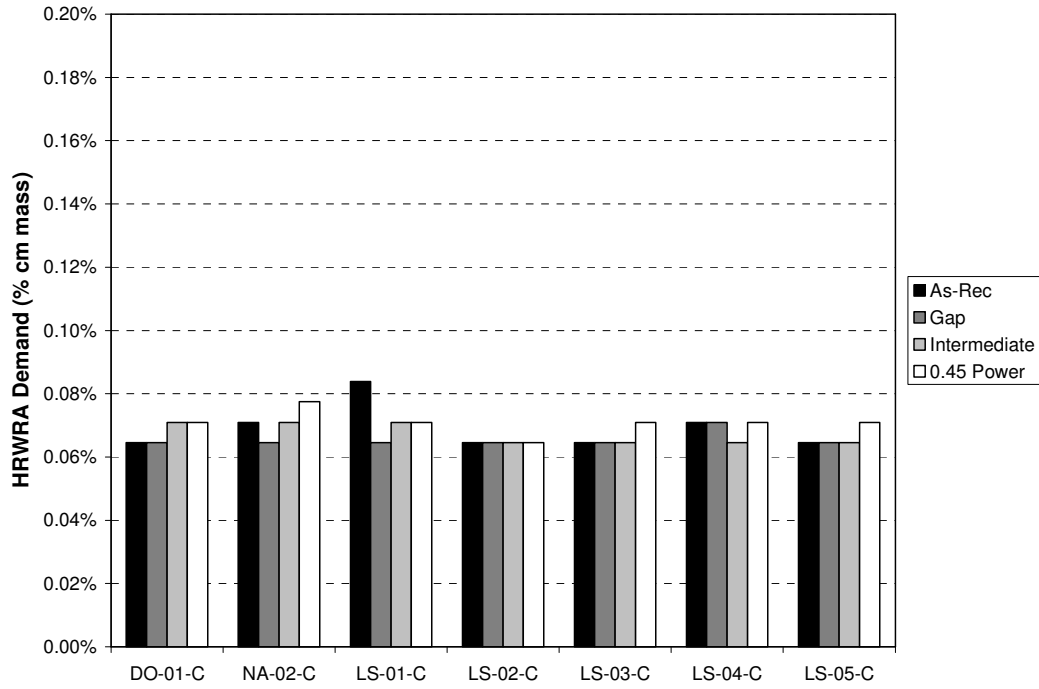
Figure 10.20: Effects of Coarse Aggregates on HRWRA Demand
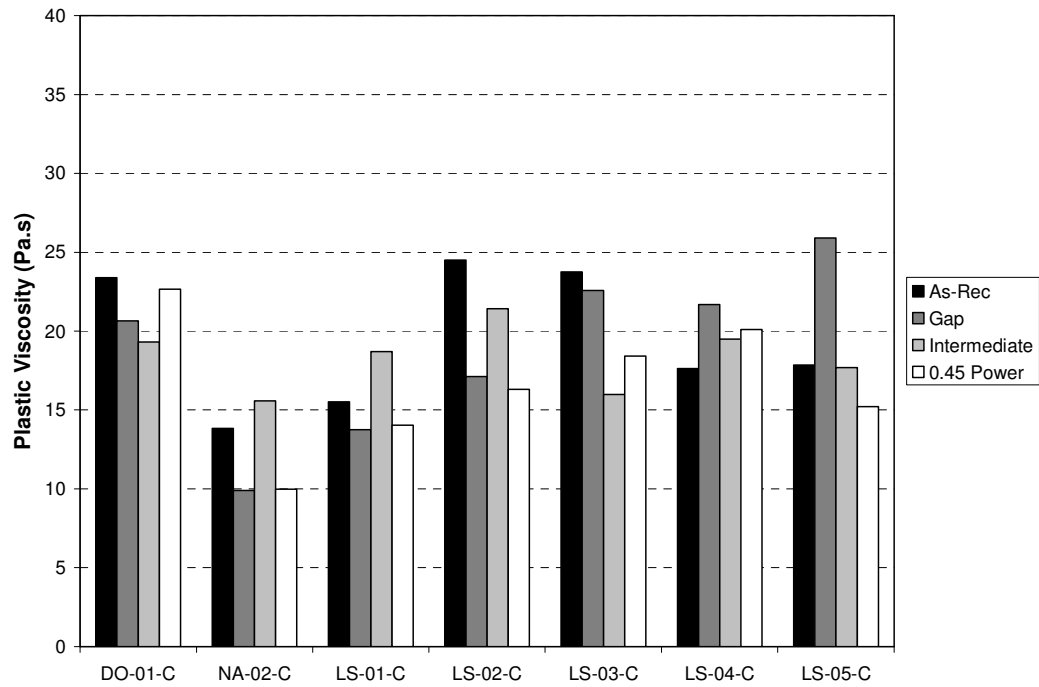
Figure 10.21: Effects of Coarse Aggregates on Plastic Viscosity

212
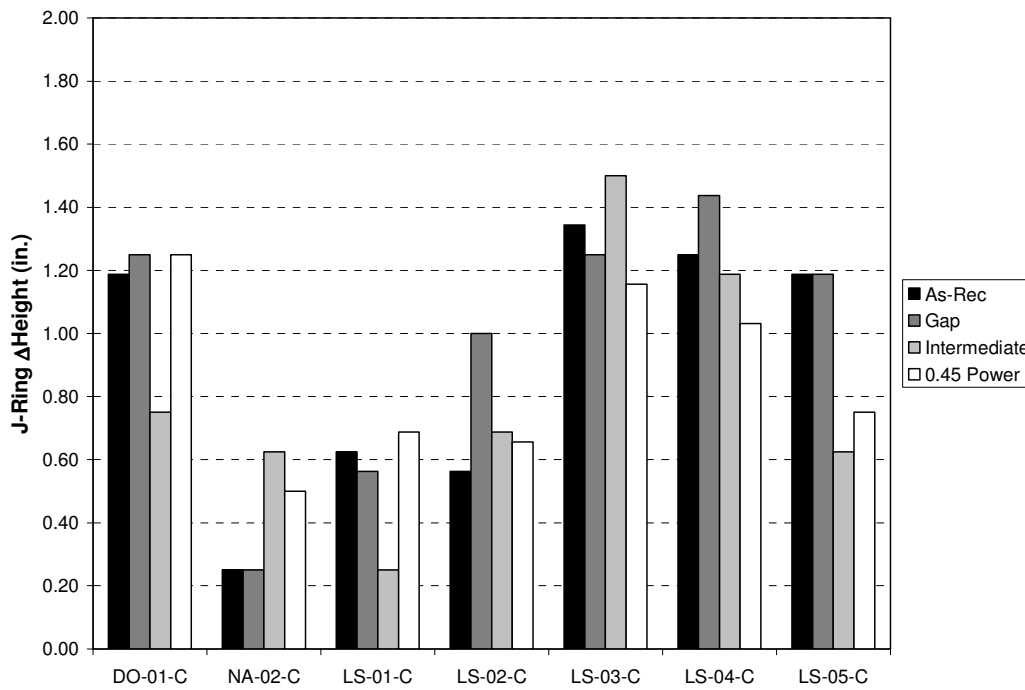
Figure 10.22: Effects of Coarse Aggregates on J-Ring Blocking

In general, the greatest effect of the coarse aggregates on hardened properties was the coarse aggregate source whereas grading had little or no effect. The compressive strength at 28 days varied from approximately 7,000 to 9,000 psi depending on the aggregate source and grading, as indicated in Figure 10.23. There was no clear trend for one grading relative to another—the largest effect was the aggregate source. The modulus of elasticity varied from approximately 4,500 psi to 6,000 psi, as shown in Figure 10.24. Like compressive strength, the aggregate type and not grading had the largest effect on modulus of elasticity. The lowest modulus of elasticity occurred for LS-04-C, which is a porous, high absorption capacity aggregate. The highest elastic modulus measurements were for LS-05-C and DO-01-C, which are dense, low absorption capacity aggregates. The flexural strength did not vary significantly when either the aggregate or grading was changed, as indicated in Figure 10.25. The rapid chloride permeability results, shown in Figure 10.26, were very low and did not vary substantially between aggregates except for the LS-04-C aggregate, which is porous and has a high absorption capacity. Figure 10.27 indicates that the greatest effect on shrinkage was the aggregate source, not the grading. The LS-03-C aggregate produced the highest shrinkage whereas LS-01-C produced the lowest shrinkage of the limestone aggregates.

The workability properties of plastic viscosity and passing ability varied to a greater extent than the hardened properties for both fine and coarse aggregates. Accordingly, the changes in mixture proportions required to achieve adequate workability for different aggregates, such as changing the paste volume or water content, would be expected to have a greater effect on hardened properties than changing the aggregate type or grading in most cases. Therefore, the biggest changes in hardened properties due to the aggregates are likely to be indirect.
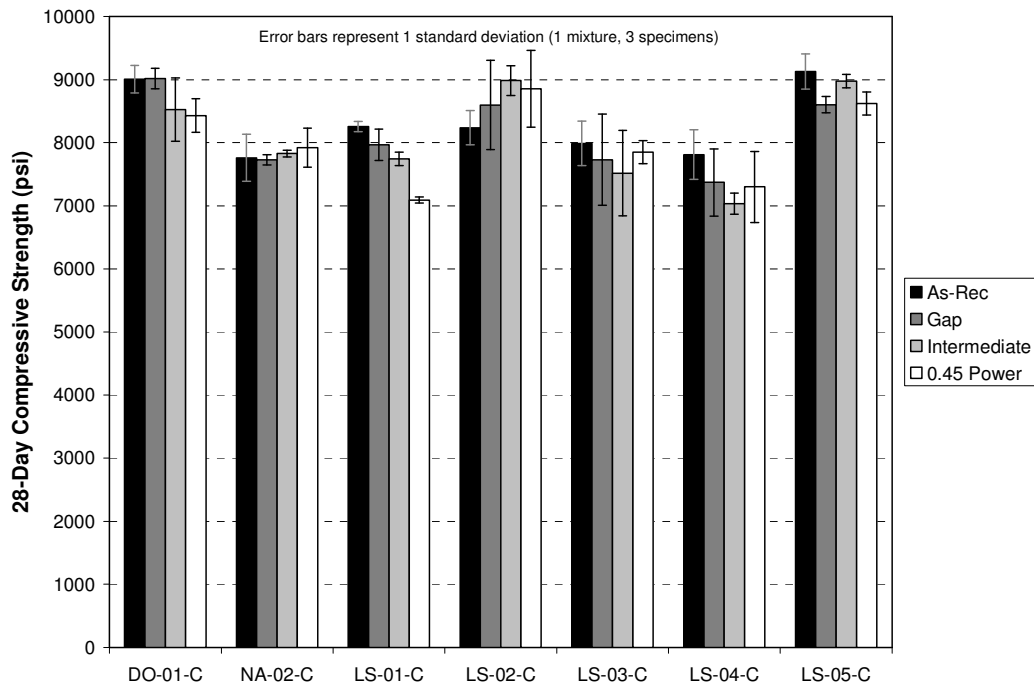
Figure 10.23: Effects of Coarse Aggregates on 28-Day Compressive Strength
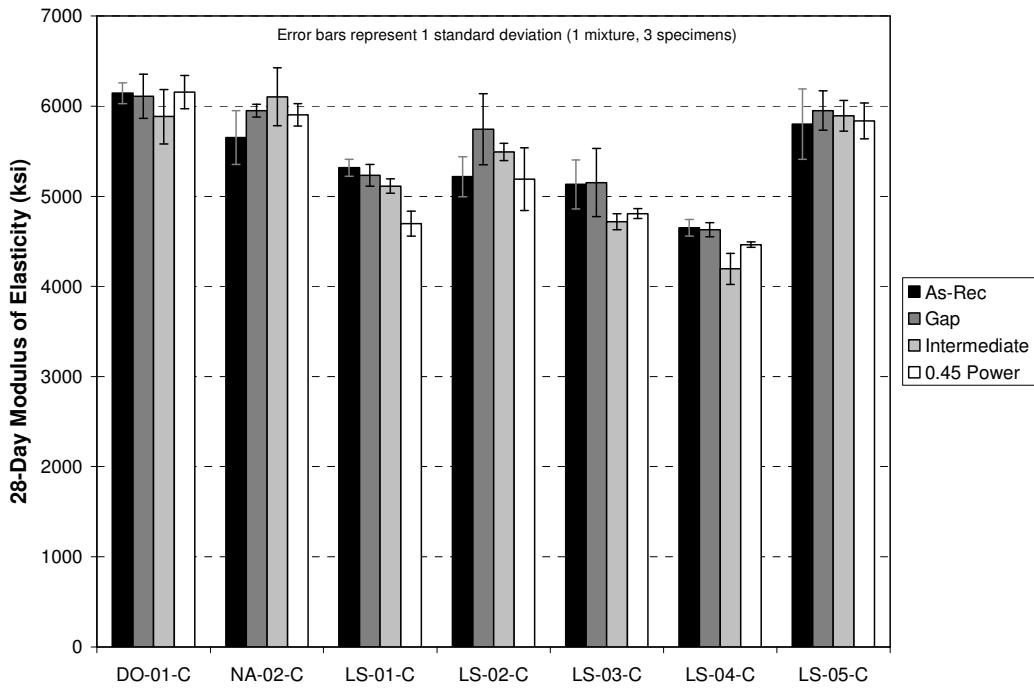
Figure 10.24: Effects of Coarse Aggregates on 28-Day Modulus of Elasticity
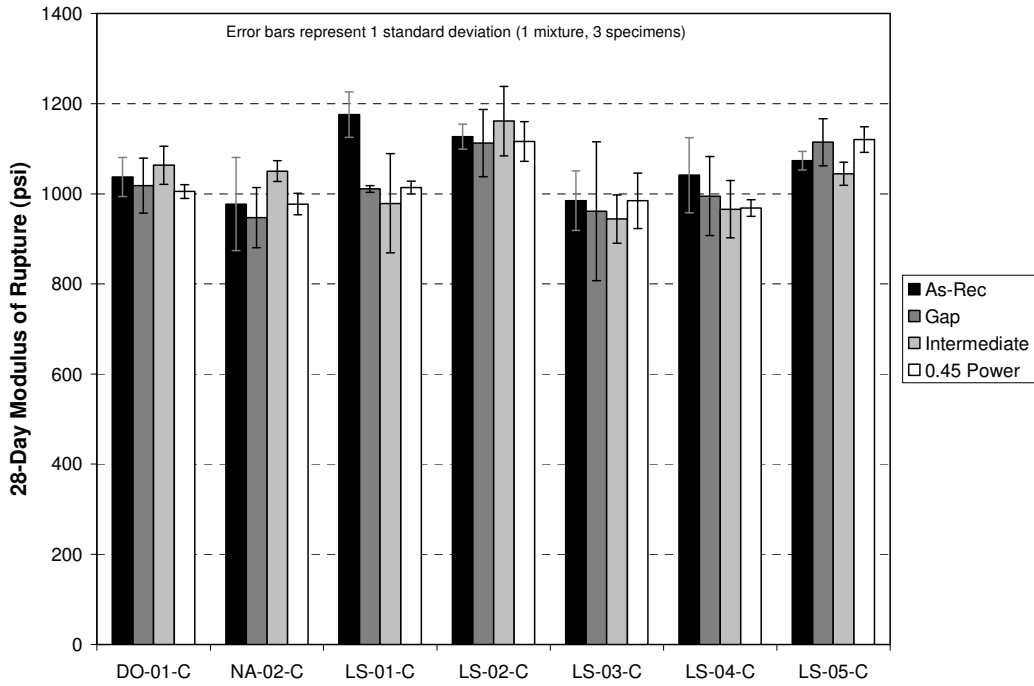
Figure 10.25: Effects of Coarse Aggregates on 28-Day Flexural Strength

215
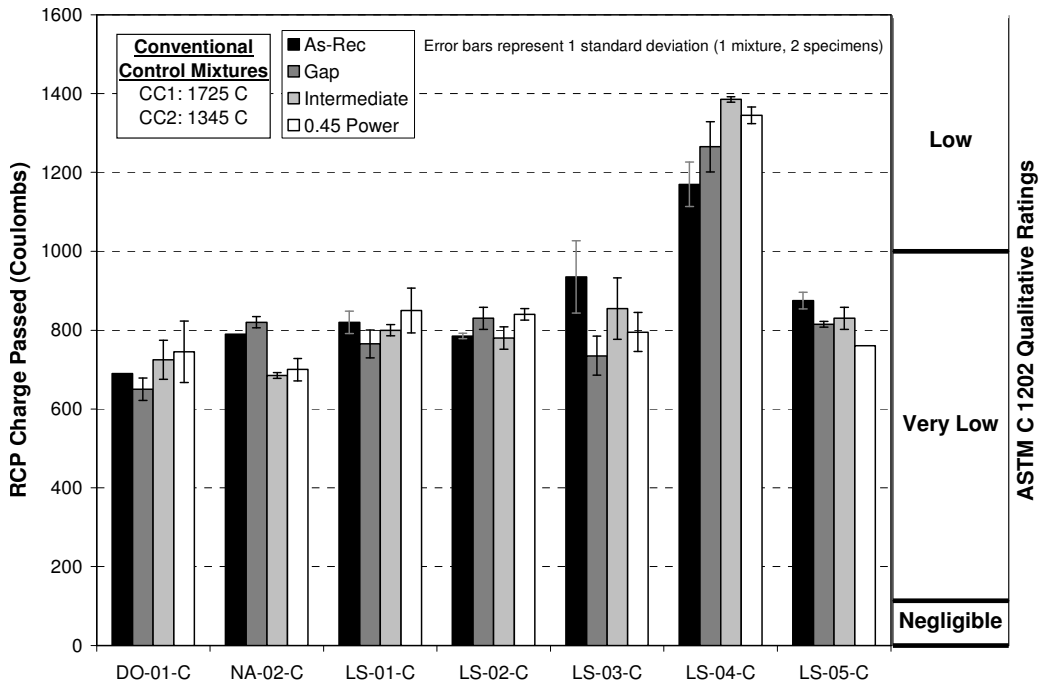
Figure 10.26: Effects of Coarse Aggregates on 91-Day Rapid Chloride Permeability
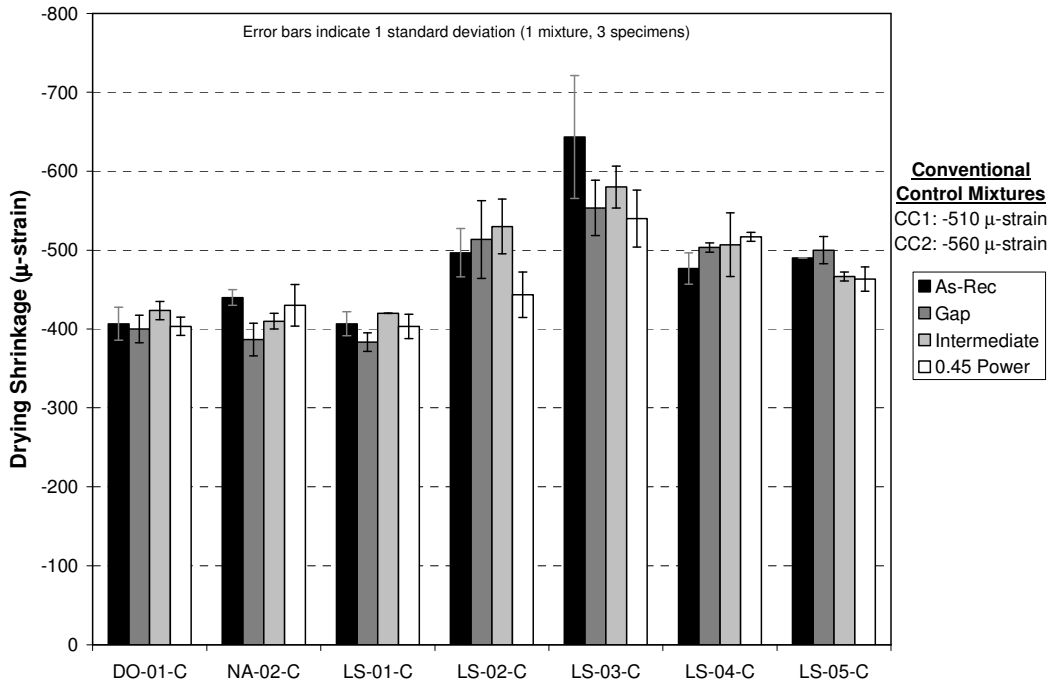
Figure 10.27: Effects of Coarse Aggregates on 112- Day Drying Shrinkage

Multiple regression models were developed for fresh and hardened properties based on the sphericity index, length/width, packing density, specific surface area, specific gravity, and

216

absorption capacity. The specific surface area was calculated assuming spherical particles and, therefore, reflects only grading and not shape, angularity, or texture. The results, which are shown in Table 10.5, were generally consistent with expectations. The models were not statistically significant for HRWRA demand, flexural strength, and shrinkage ($R^2_{adjusted}$ < 0.60). The results indicated that plastic viscosity decreased with increasing packing density, absorption capacity, specific surface area, and sphericity index, as shown in Figure 10.28. Packing density had the largest effect. The decrease in viscosity with increased absorption capacity could be related to the improved shape of softer manufactured aggregates with higher absorption capacities. The decrease in plastic viscosity with increasing sphericity index was unexpected; however, this result may be due to the limited number of data points, the narrow range of sphericity values, or collinearity of sphericity index with other parameters. The magnitude of j-ring blocking decreased with increasing specific surface area and reduced sphericity index, as plotted in Figure 10.29. Increasing the packing density slightly reduced the j-ring blocking. These results indicate that gradings with fewer coarser particles and aggregates with better shape characteristics result in greater passing ability. The 28-day compressive strength was primarily affected by coarse aggregate specific gravity, with increased specific gravity resulting in higher compressive strength (Figure 10.30). This result was expected because denser aggregates should result in higher compressive strength. The effects of packing density, sphericity, and L/W on compressive strength were small. The decrease in strength with increased packing density could be due to the angular shape and coarse texture of low packing density aggregates, which would be expected to increase strength. Figure 10.31 indicates that modulus of elasticity increased with decreasing specific surface area and absorption capacity. The effect of the L/W ratio was small. These results were consistent with expectations and with fine aggregate results because denser aggregates should be stiffer, resulting in higher concrete modulus of elasticity, and coarser gradings should be associated with higher modulus of elasticity. Finally, rapid chloride permeability was affected mainly by specific gravity, with denser aggregates associated with reduced rapid chloride permeability (Figure 10.32).

Table 10.5: Multiple Regression Models for Coarse Aggregate Shape Characteristics and Grading (As-Received Gradings)

Model	$R^2_{adjusted}$
$1/(T_{50}) = 0.685 + 0.312(PKG)(L/W) - 0.0850(SG)^2 - 0.103(ABS)(SSA)$	0.963
$1/(Plastic\ Viscosity) = -0.276 + 0.470(PKG)(SPHR) + 0.01624(SSA)(ABS)$	0.671
$J\text{-}ring = -18.18 + 17.44(SPHR) - 1.853(PKG)(SSA)$	0.959
$f'_c\{24\text{-}hr\} = 3072.7 + 0.0205(ABS)^2 - 15.89(ABS)(PKG)$	0.794
$f'_c\{28\text{-}d\} = -4181.2 + 2542.1(SG)(SPHR) - 6504.5(PKG)(L/W) + 1347.1(SG)(PKG)$	0.998
$1/(E\{28\text{-}d\}) = 1.01 \times 10^{-4} + 5.95 \times 10^{-5}(ABS)(SSA) - 1.917 \times 10^{-6}(ABS)^2 + 2.234 \times 10^{-5}$	0.980
$(RCP\{91\text{-}d\})^{0.5} = -2626.2 - 20.06(SG) + 4747.9(SPHR) - 2080.9(SPHR)^2$	0.985
Regression Details: quadratic model, stepwise regression; p-value = 0.25; transformation with highest $R^2_{adjusted}$ selected; transformations considered: y, 1/y, ln(y), sqrt(y), 1/sqrt(y)	
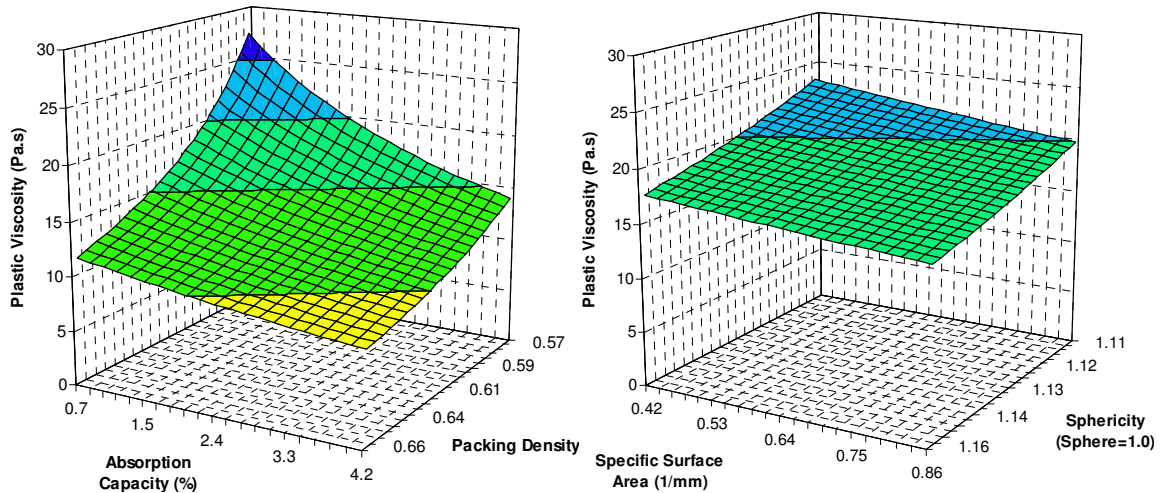
Figure 10.28: Effects of Coarse Aggregate Characteristics on Plastic Viscosity (As-Received Gradings)
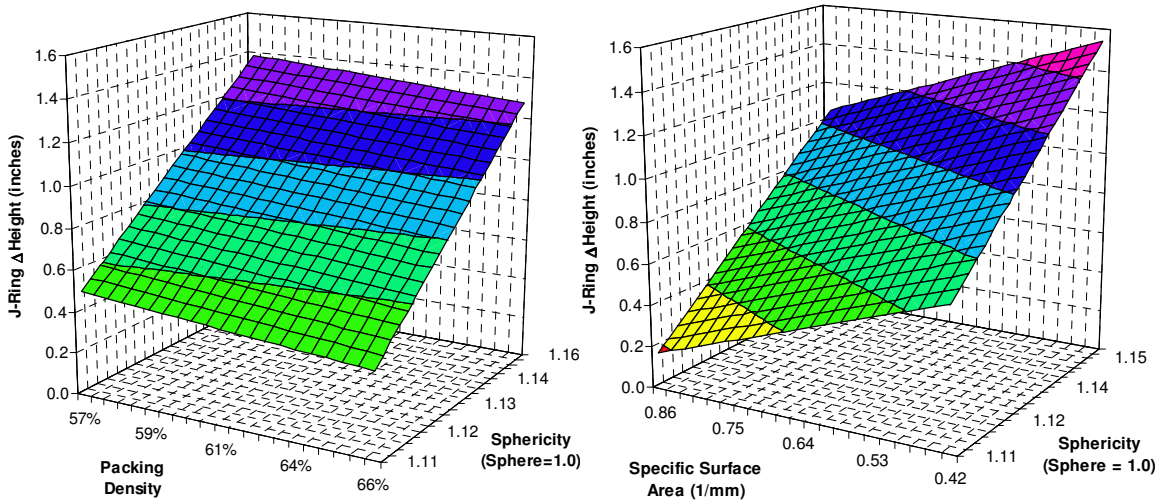
Figure 10.29: Effects of Coarse Aggregate Characteristics on J-Ring Blocking (As-Received Gradings)

218
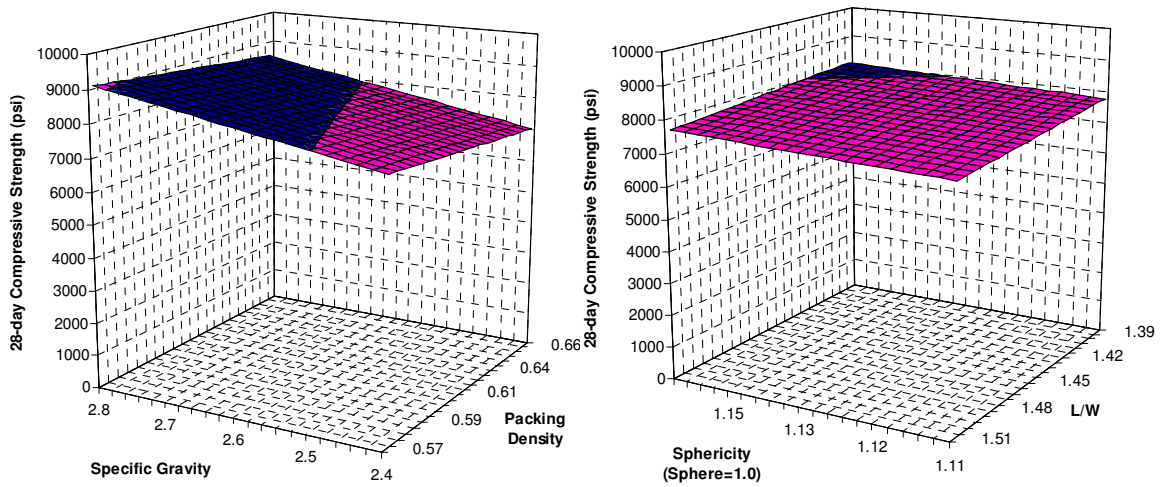
Figure 10.30: Effects of Coarse Aggregate Characteristics on 28-Day Compressive Strength (As-Received Gradings)
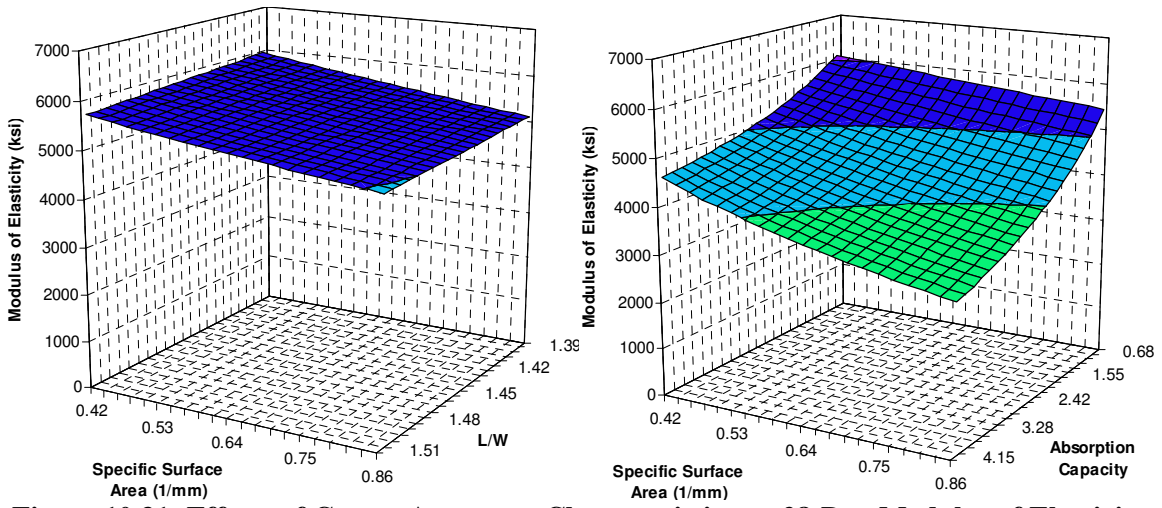
Figure 10.31: Effects of Coarse Aggregate Characteristics on 28-Day Modulus of Elasticity (As-Received Gradings)
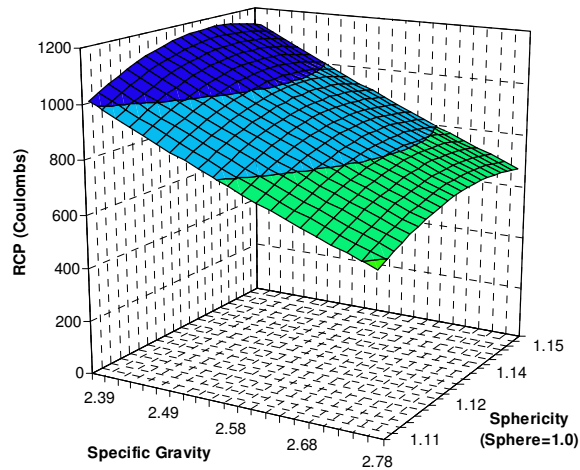
Figure 10.32: Effects of Coarse Aggregate Characteristics on 91-Day Rapid Chloride Permeability (As-Received Gradings)

10.4 Effects of Aggregates at Various Paste Volumes

10.4.1 Test Plan

For the concrete mixtures described in Sections 10.2 and 10.3, the paste volume and paste composition were held constant. While this allowed a direct comparison between aggregates, it was not the optimal mixture in all cases. Depending on the aggregate characteristics, the paste volume could have been increased or decreased to achieve the optimal mixture. In mixtures where the paste volume was higher than optimal, the variations in performance characteristics between aggregates were reduced because paste volume increases robustness with respect to aggregate properties. When the paste volume was lower than optimal, SCC workability properties were poor. Therefore, to compare aggregate characteristics more fully, four different aggregate combinations were evaluated at varying paste volumes. The control case with LS-02-F sand and NA-02-C coarse aggregate was used as the baseline. The test data for this control mixture are presented in Section 11.1 (w/p=1.0, w/c= 0.415, w/cm=0.35, S/A=0.45). The DO-01-C coarse aggregate, which is angular and has a high paste volume demand, was used in both a gap and continuous grading as shown in Table 10.6. The two gradings are plotted in Figure 10.33. The DO-01-F sand, which is harsh and angular, was used with NA-02-C coarse aggregate as shown in Table 10.7. As the paste volume was increased for each aggregate, the fly ash dosage and w/cm were held constant to allow a comparison of hardened properties.

Table 10.6: Mixture Proportions for Evaluation of DO-01-C Coarse Aggregate at Various Paste Volumes

Mix[1]	Paste Volume (%)[2]	w/p	Mixture Proportions (lb/yd^3)[3]					
			Cement	Fly Ash	Coarse Agg.	Inter-mediate Agg.	Fine Agg.	Water
P1 (cont.)	34.1	0.944	633.8	117.7	1043.3	693.0	1335.7	263.0
P2 (cont.)	36.6	0.954	684.9	127.2	1004.7	667.4	1286.2	284.2
P3 (cont.)	39.0	0.963	736.7	136.8	966.0	641.7	1236.7	305.7
P4 (cont.)	41.4	0.971	788.6	146.5	927.4	616.0	1187.3	327.3
P5 (gap)	34.1	0.944	633.8	117.7	1738.8		1335.7	263.0
P6 (gap)	36.6	0.954	684.9	127.2	1674.4		1286.2	284.2
P7 (gap)	39.0	0.963	736.7	136.8	1610.0		1236.7	305.7
P8 (gap)	41.4	0.971	788.6	146.5	1545.6		1187.3	327.3

[1]All mixes have w/cm = 0.35, S/A = 0.45, 15.7% fly ash by mass
[2]Paste volume includes cement, fly ash, water, and microfines
[3]Cement: PC-01-I/II; Fly Ash: FA-02-F; Coarse Aggregate: DO-01-C; Intermediate Aggregate: DO-01-I; Fine Aggregate: LS-02-F
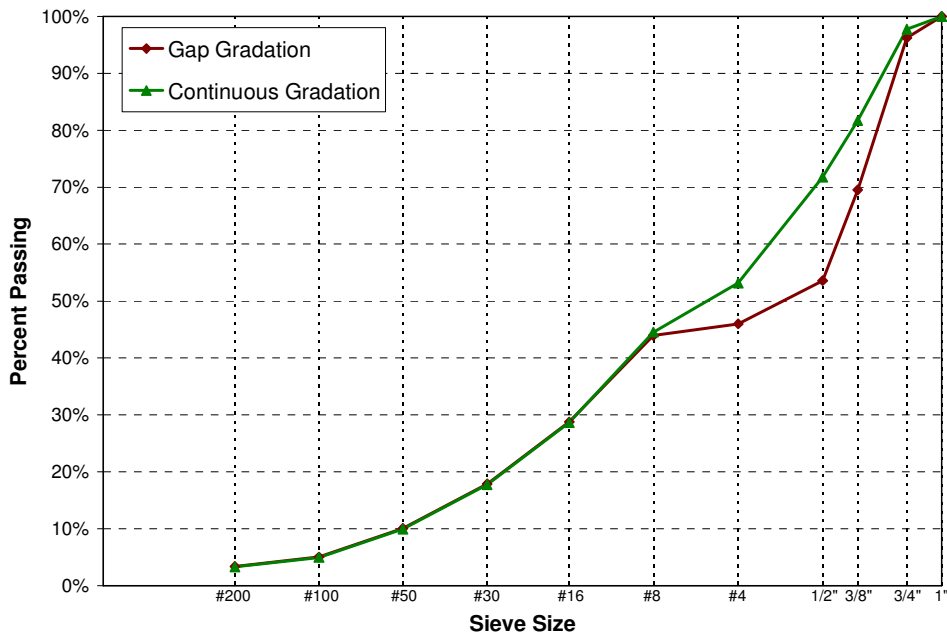
Figure 10.33: Gap and Continuous Gradings for Evaluation of DO-01-C at Various Paste Volumes

Table 10.7: Mixture Proportions for Evaluation of DO-01-F Fine Aggregate at Various Paste Volumes

Mix[1]	Paste Volume (%)[2]	w/p	Mixture Proportions (lb/yd^3)[3]				
			Cement	Fly Ash	Coarse Agg.	Fine Agg.	Water
P9	32.7	1.031	633.0	117.6	1613.7	1494.3	262.7
P10	35.2	1.032	684.9	127.2	1554.0	1439.0	284.2
P11	37.7	1.034	736.7	136.8	1494.2	1383.6	305.7
P12	40.2	1.035	788.6	146.5	1434.4	1328.3	327.3
P13	42.7	1.036	840.5	156.1	1374.7	1273.0	348.8

[1]All mixes have w/cm = 0.35, S/A = 0.45, 15.7% fly ash by mass
[2]Paste volume includes cement, fly ash, water, and microfines
[3]Cement: PC-01-I/II; Fly Ash: FA-02-F; Coarse Aggregate: DO-01-C; Fine Aggregate: LS-02-F

10.4.2 Test Results

Increasing the paste volume resulted in improved workability, reflected in reduced HRWRA demand (Figure 10.34), plastic viscosity (Figure 10.35), and j-ring blocking (Figure 10.36). The difference in performance between the aggregates decreased as the paste volume increased. For instance, HRWRA demand was similar above a paste volume of approximately 37%. At 32% paste volume, the plastic viscosity varied from 28 to 45 Pa·s while the difference was 9 to 13 Pa·s at 41% paste volume. Therefore, increasing the paste volume increases mixture robustness with respect to aggregate properties and allows the accommodation of poorly graded or poorly shaped aggregates.

For the DO-01-C coarse aggregate, the gap grading resulted in lower HRWRA demand and plastic viscosity but greater j-ring blocking than the continuous grading. For the gap grading, the decrease in HRWRA demand and plastic viscosity relative to the continuous grading was likely due to the reduced interaction between the intermediate-sized aggregates while the higher j-ring blocking was due to the higher fraction of larger sized particles. The gap grading exhibited a packing density of 72.5% while the continuous grading exhibited a packing density of 70.8%. The use of the harsh, angular sand (DO-01-F) resulted in increased HRWRA demand, plastic viscosity, and j-ring blocking relative to the base case at all paste volumes except the high paste volumes where the differences in workability parameters were minimal. Several of the mixtures did not have adequate paste volume for achieving SCC workability. To achieve sufficient filling ability, the paste volume needed to be approximately 37% for the DO-01-C gap graded mixture, 38% for the DO-01-C continuously graded mixture, 38% for the DO-01-F mixture, and 32% for the baseline mixture.

For mixtures that did not contain sufficient paste volume, the compressive strength was reduced due to the resulting severe bleeding and segregation, as indicated in Figure 10.37 and Figure 10.38. For mixtures where the amount of paste volume was borderline, the compressive strength was not reduced because the mixtures only exhibited harshness and poor filling ability, not severe bleeding and segregation. Above the minimum paste volume, the paste volume had no effect on compressive strength. The gap grading had consistently higher compressive strength at 24 hours than the continuously graded mixture, which was likely related to the higher packing density. At 28 days, the compressive strengths of the two gradings were similar. The DO-02-F sand had similar compressive strength as the baseline case, despite the fact that the DO-02-F sand was more angular and would, therefore, be expected to have better bond to the paste. Figure 10.39 indicates that paste volume had essentially no effect on modulus of elasticity, even when the paste volume was insufficient. The gap grading exhibited slightly higher modulus of elasticity than the continuous grading, while the baseline case exhibited the highest modulus of elasticity, likely due to the high stiffness of the NA-02-C coarse aggregate. Figure 10.40 indicates that the flexural strengths did not vary with paste volume when sufficient paste volume was provided. Although rapid chloride permeability was found to increase with paste volume for the baseline mixture, paste volume was found to have little effect on rapid chloride permeability for the other three aggregate sets, as shown in Figure 10.41. Figure 10.42 indicates that drying shrinkage increased significantly with increased paste volume. For a given paste volume, the shrinkage was similar regardless of the aggregate, suggesting that paste volume is the dominant factor affecting shrinkage.
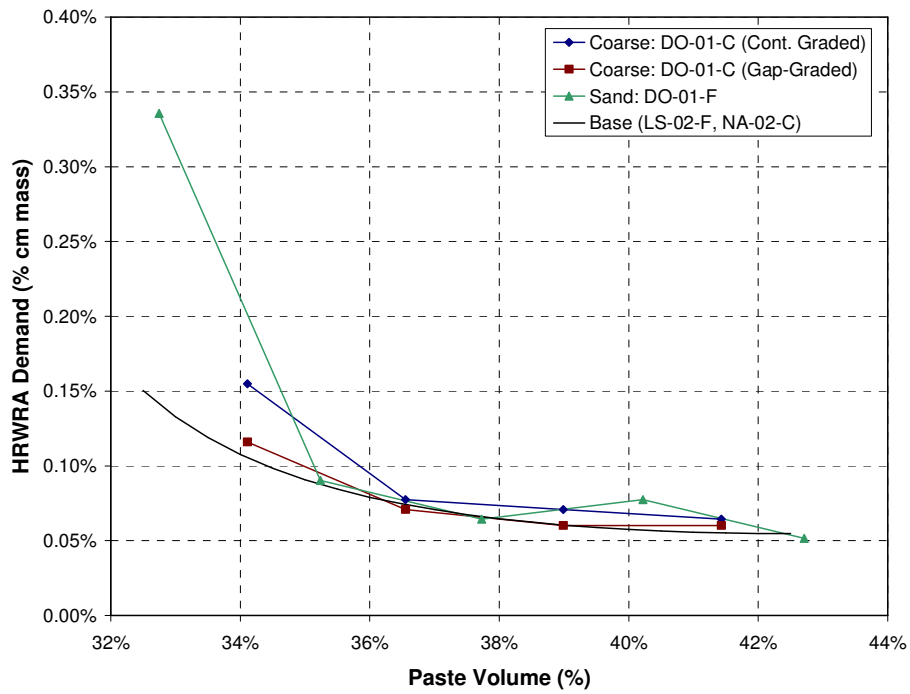
Figure 10.34: Effects of Aggregate Characteristics on HRWRA Demand at Various Paste Volumes
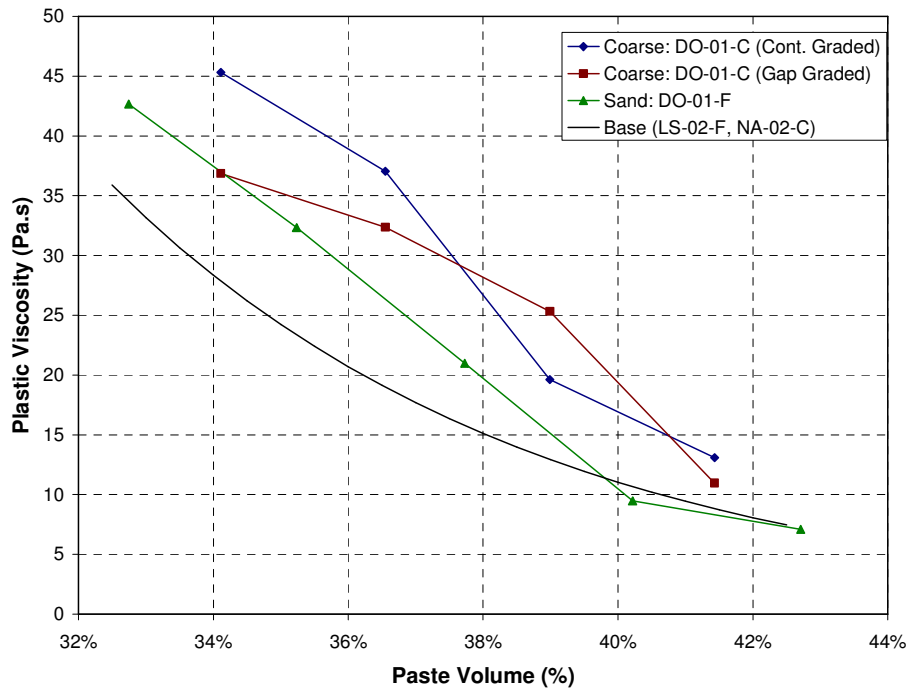
Figure 10.35: Effects of Aggregate Characteristics on Plastic Viscosity at Various Paste Volumes
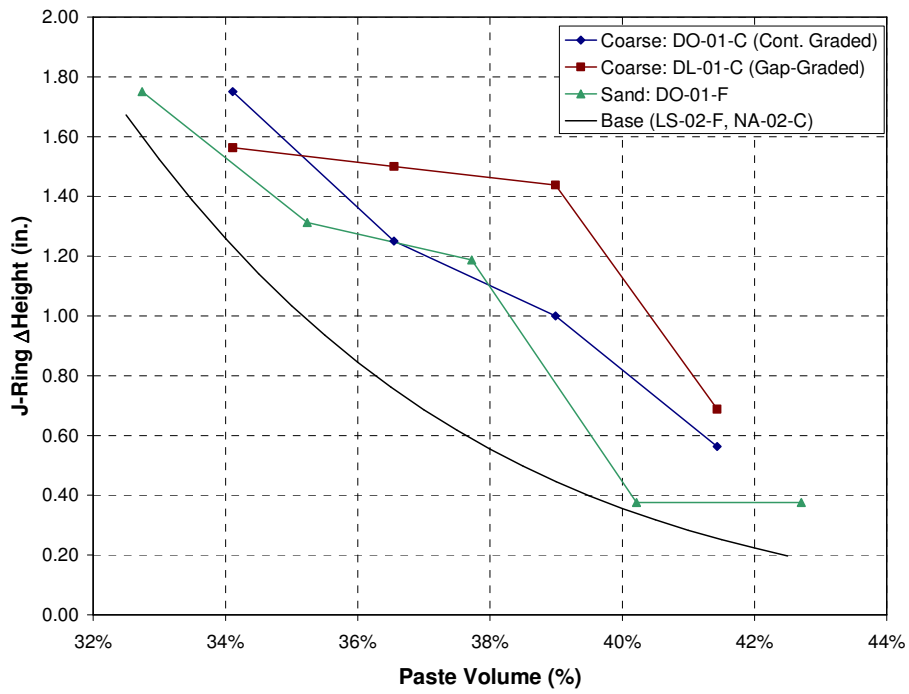
Figure 10.36: Effects of Aggregate Characteristics on J-Ring Blocking at Various Paste Volumes
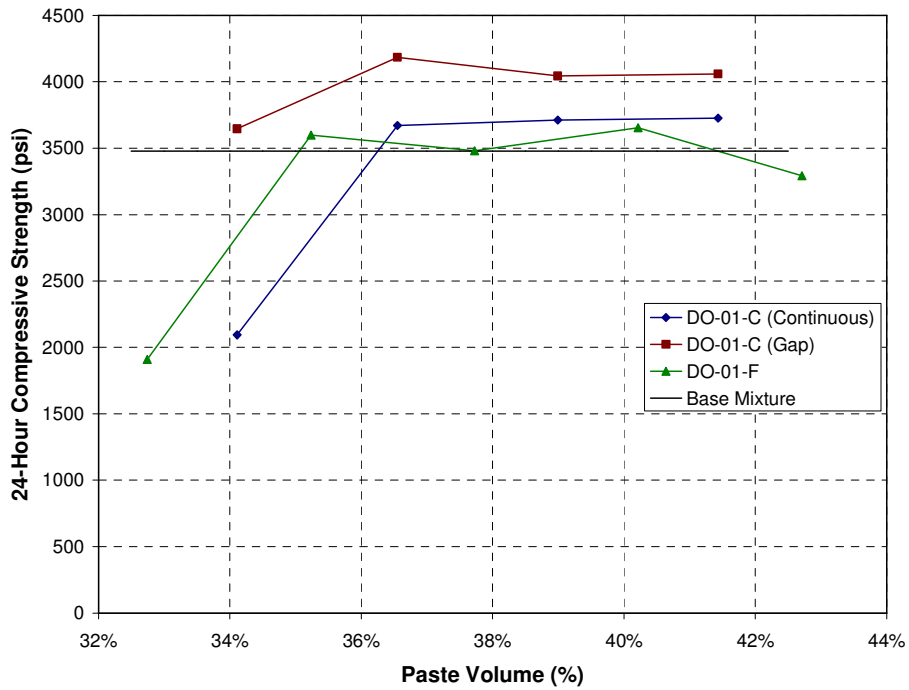
Figure 10.37: Effects of Aggregate Characteristics on 24-Hour Compressive Strength at Various Paste Volumes

225
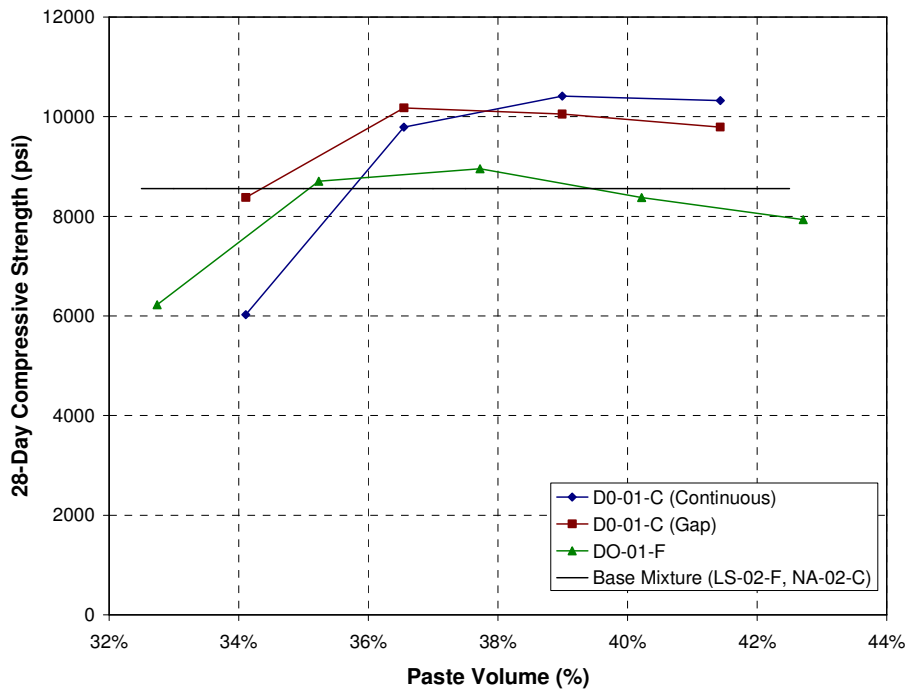
Figure 10.38: Effects of Aggregate Characteristics on 28-Day Compressive Strength at Various Paste Volumes
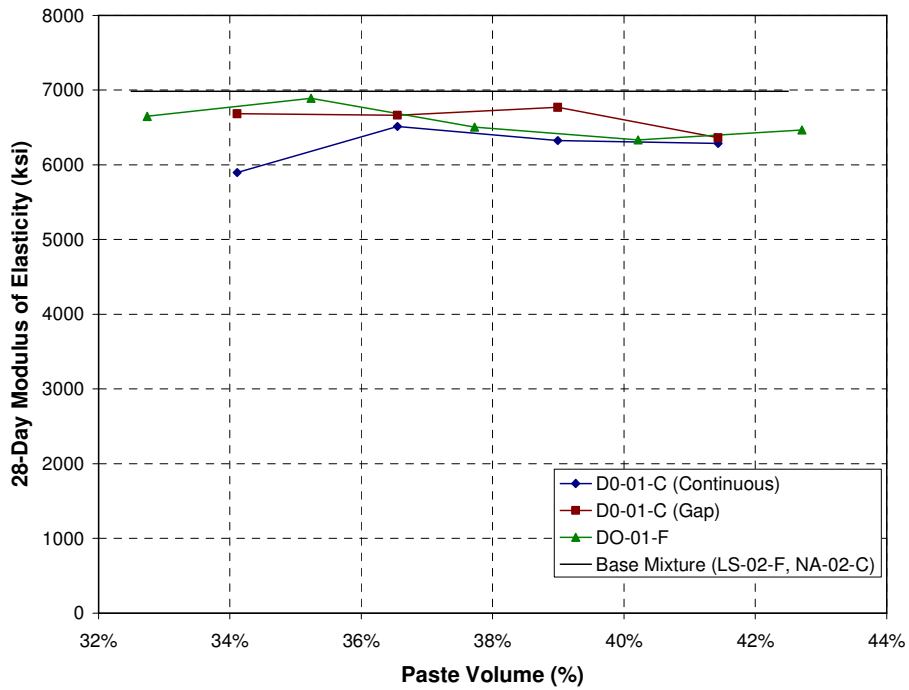
Figure 10.39: Effects of Aggregate Characteristics on 28-Day Modulus of Elasticity at Various Paste Volumes
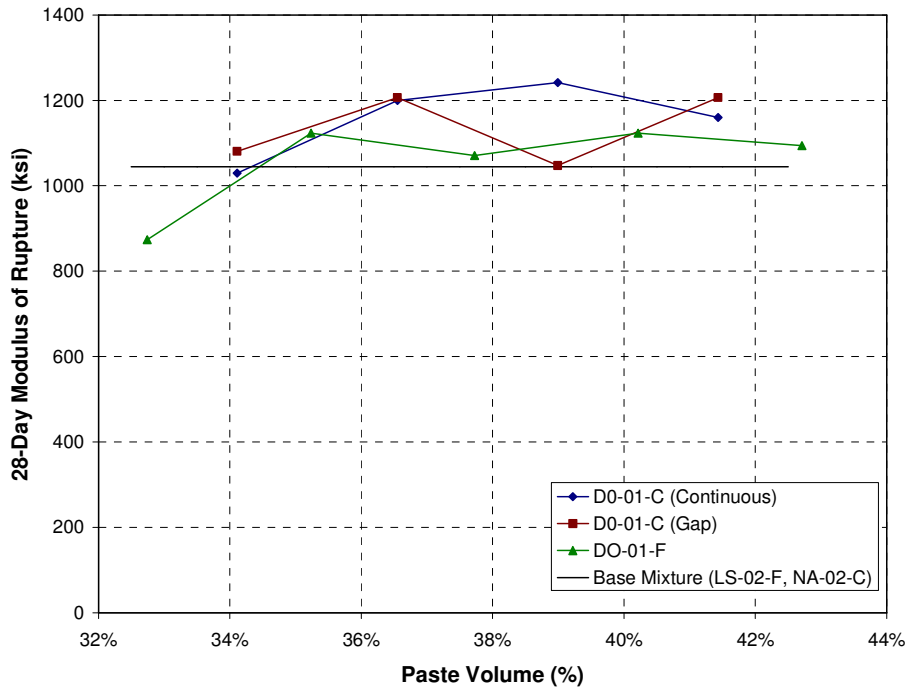
Figure 10.40: Effects of Aggregate Characteristics on 28-Day Flexural Strength at Various Paste Volumes
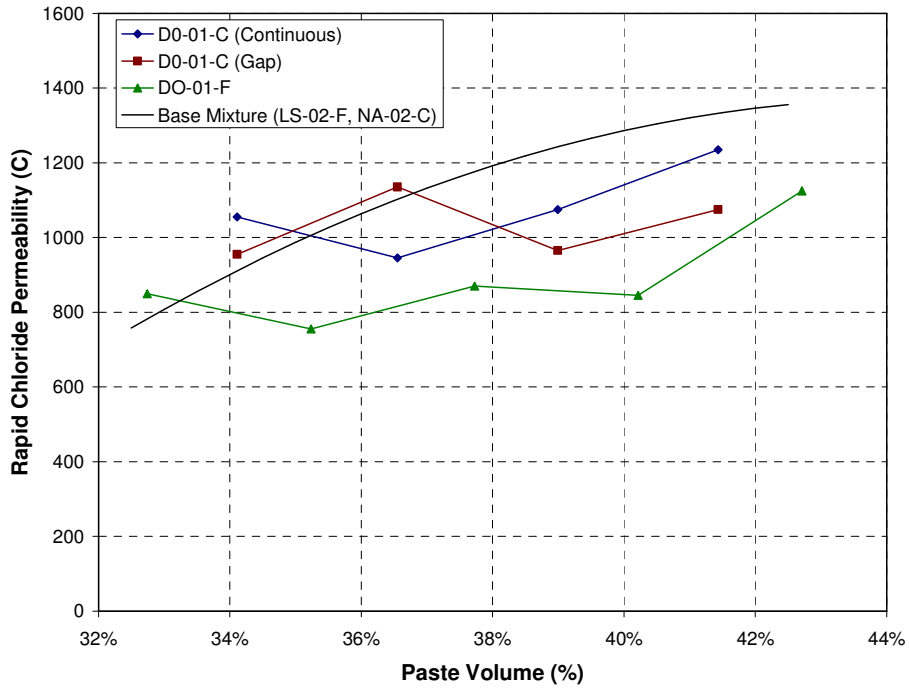
Figure 10.41: Effects of Aggregate Characteristics on 91-Day Rapid Chloride Permeability at Various Paste Volumes
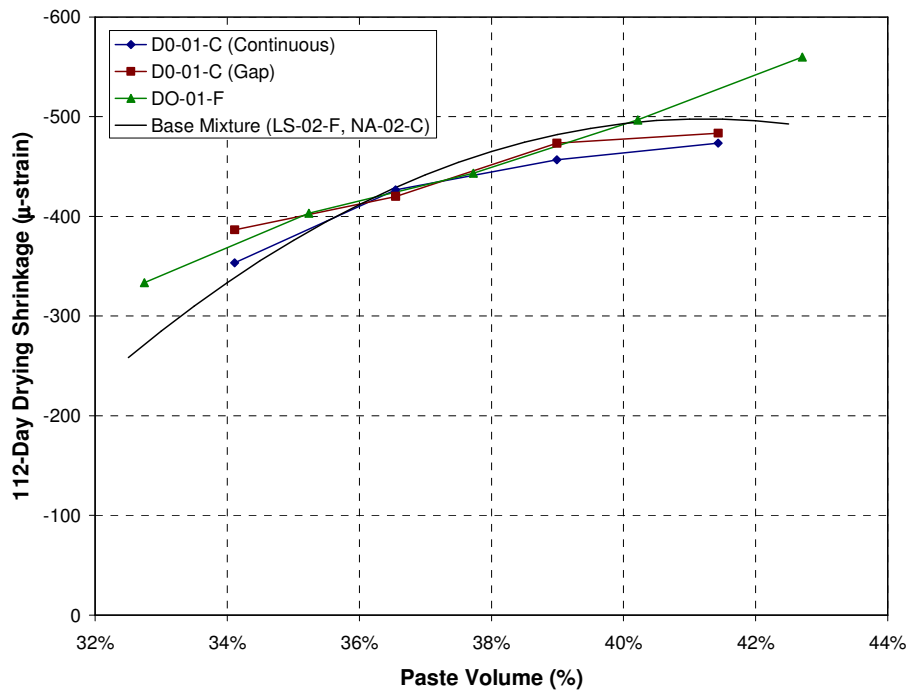
Figure 10.42: Effects of Aggregate Characteristics on 112-Day Drying Shrinkage at Various Paste Volumes

10.5 Effects of Microfines

10.5.1 Test Plan

The 6 microfines were used at a rate of 15% of the fine aggregate volume and were accounted for as either part of the aggregate volume (constant w/cm, decreased w/p, increased paste volume) or the powder volume (increased w/cm, constant w/p, constant paste volume). The mixture proportions are listed in Table 10.8. Microfines were used as part of the aggregate volume or powder volume. Two control mixtures were used. Control 1, which corresponds to the mixture shown in Table 10.1, was used for comparisions of workability. When microfines were used as part of the powder volume, the w/p decreased and the paste volume increased relative to Control 1. When microfines were used as part of the powder volume, and w/p and paste volume were held constant relative to Control 1. Because the use of microfines as part of the powder volume resulted in a reduction in cementitious materials content and increase in w/cm, the Control 2 mixture was tested to maintain a constant w/cm of 0.524. The fine aggregate for all mixtures, LS-02-F, was used in its as-received grading after being washed over

a #200 sieve to remove all microfines. The coarse aggregate for all mixtures, NA-02-C, was used in its as-received grading.

Table 10.8: Mixture Proportions for Microfines (Percent Volume)

	Microfines as Aggregate[1]		Microfines as Powder[1]	
	0% (Control 1)[2]	15%	0% (Control 2)[3]	15%
Coarse Aggregate[4]	32.0	32.0	32.0	32.0
Fine Aggregate[5]	32.0	27.2	32.0	32.0
Microfines	0	4.8	0.0	4.8
Cement	11.3	11.3	9.3	8.0
Fly Ash	5.1	5.1	4.2	3.6
Water	17.6	17.6	20.5	17.6
Air	2.0	2.0	2.0	2.0
w/cm[6]	0.37	0.37	0.524	0.524
w/p[7]	1.073	0.829	1.518	1.073
Paste Volume[8]	35.9	40.8	35.9	35.9

[1]Percentage of microfines expressed as volume of fine aggregate
[2]Control 1 mix used for comparison of workability (corresponds to mixture in Table 10.1)
[3]No HRWRA added, did not achieve SCC properties
[4]The coarse aggregate was NA-02-C for all mixtures
[5]The fine aggregate, washed to remove microfines, was LS-02-F for all mixtures
[6]Expressed by mass
[7]Expressedy by volume
[8]Includes cement, fly ash, air, water, and microfines

10.5.2 Test Results

The use of microfines as either part of the aggregate volume or powder volume generally resulted in increased HRWRA demand (expressed in oz/yd^3) and plastic viscosity, as indicated in Figure 10.43 and Figure 10.44. The increase in these two parameters was consistently greater when microfines were used as part of the aggregate volume instead of the powder volume. This trend was expected because of the reduction in water-powder ratio, which was partially offset by the increase in total paste volume, when microfines were used as part of the aggregate. When aggregates were used as part of the powder, the water-powder ratio and paste volume remained unchanged; therefore, any change in HRWRA demand was attributable to the characteristics of the microfines, such as shape characteristics, grading, and methylene blue value. When aggregates were used as part of the powder, the volume of cementitious materials was reduced to maintain a constant total powder volume. The reduction in cost associated with this reduction in cementitious materials may more than offset the cost of any additional HRWRA. J-ring blocking

did not change significantly regardless of whether microfines were used as part of the aggregate or powder volume, as indicated in Figure 10.45. In all cases, the degree of j-ring blocking was very low.
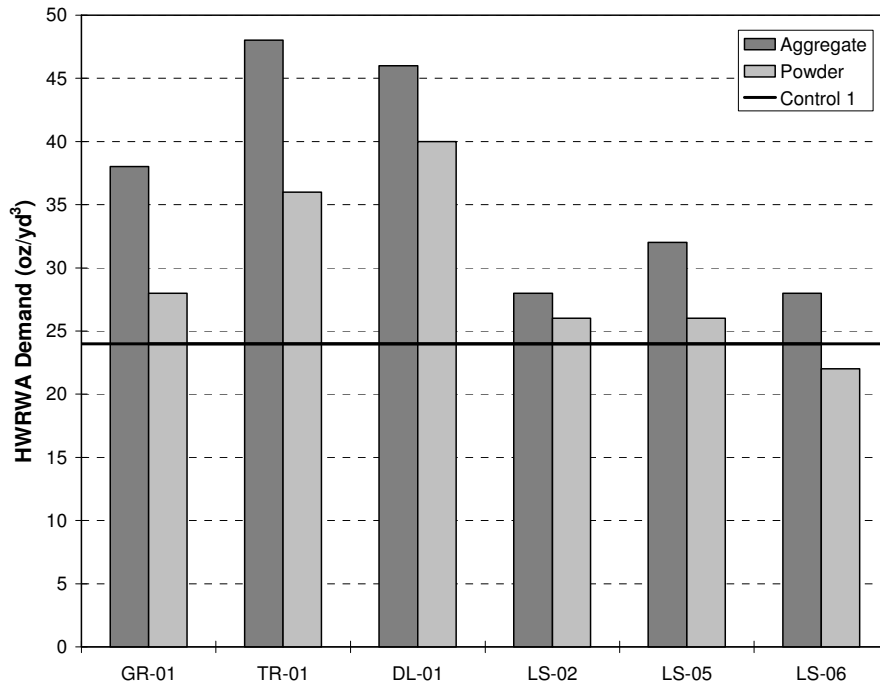
Figure 10.43: Effects of Microfines on HRWRA Demand
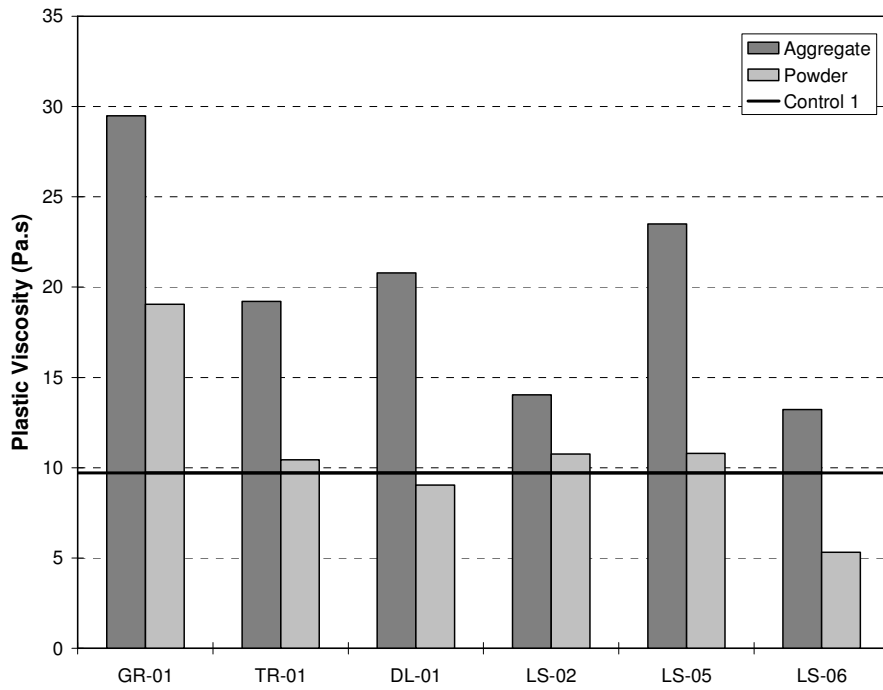
Figure 10.44: Effects of Microfines on Plastic Viscosity
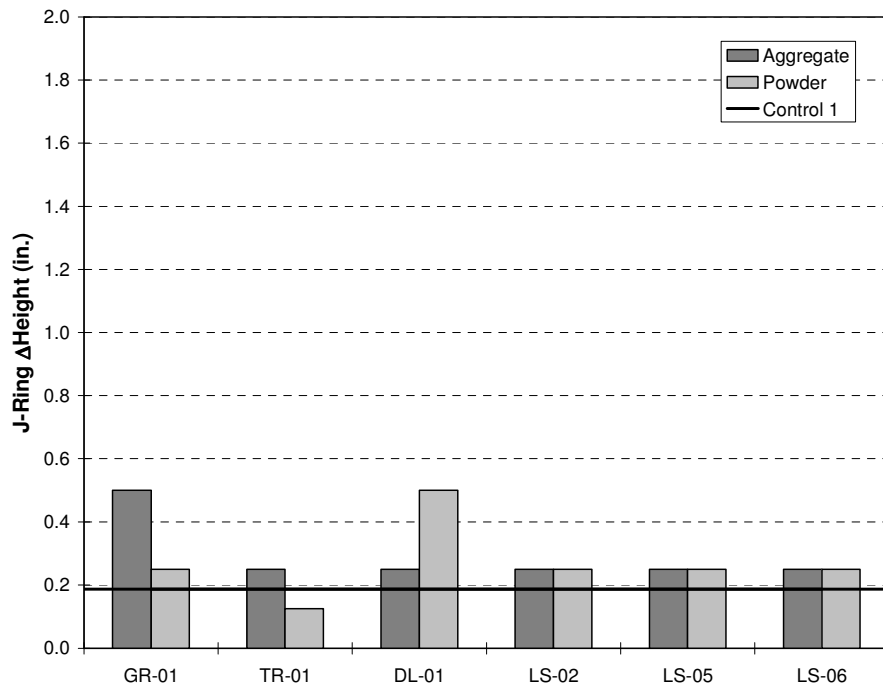
Figure 10.45: Effects of Microfines on J-Ring Blocking

In general, microfines had little to no effect on hardened properties when compared at constant w/cm. The effects of microfines on hardened properties were especially minimal when

231

compared to the potential effects of changing other mixture parameters, such as the w/cm, paste volume, and content of SCMs. In all cases, the hardened properties were of general high quality due to the low w/cms and use of fly ash. For a constant w/cm, the use of microfines typically resulted in an increase in compressive strength at both 24 hours and 28 days as shown in Figure 10.46 and Figure 10.47. When microfines were used as part of the powder instead of part of the aggregates, the resulting reduction in cementitious materials content and increase in w/cm resulted in a reduction in strength. However, at a constant w/cm, the compressive strength increased in all but one case when microfines were used. As indicated in Figure 10.48, the use of microfines resulted in essentially no change in modulus of elasticity at a constant w/cm, which was expected because modulus of elasticity is primarily affected by the stiffness and volume of the fine aggregates, coarse aggregates, and paste and the quality of the transition zone. The use of microfines had minimal effect on flexural strength for a constant w/cm, as indicated in Figure 10.49. The greater scatter in flexural strength results was expected due to the greater inherent variability of the test method. When microfines were used as part of the aggregate volume, the rapid chloride permeability was essentially unchanged (Figure 10.50). In this case it is likely the benefit of the reduction in water-powder ratio was offset by the increase in paste volume. When microfines were used as part of the powder, the rapid chloride permeability decreased by an average of 14% for a constant w/cm—likely reflecting the reduction in w/p—and increased by an average of 65% for a constant w/p—likely reflecting the increase in w/cm. In all cases, the rapid chloride permeability was low or very low based on ASTM C 1202 qualitative ratings—due to the low water-cementitious materials ratio, use of fly ash, and 91 days of moist curing prior to testing. Drying shrinkage increased only slightly with the use of microfines at a constant w/cm, as indicated in Figure 10.51. When microfines were used as part of the aggregate volume, the slight increase in drying shrinkage was likely due to the increase in paste volume. The drying shrinkage was less in 5 of 6 cases when microfines were used as part of the powder volume rather than the aggregate volume, likely reflecting the decrease in paste volume. The drying shrinkage was generally less in the SCC mixtures than in the two conventional control mixtures. Lastly, the use of microfines as part of either the aggregate or powder volume resulted in a reduction in abrasion loss at constant w/cm in all but one case, as shown in Figure 10.52. The improvement in abrasion resistance was likely due in part to the slight increase in compressive strength at a constant w/cm and the fact that the fine and coarse aggregate type remained constant.
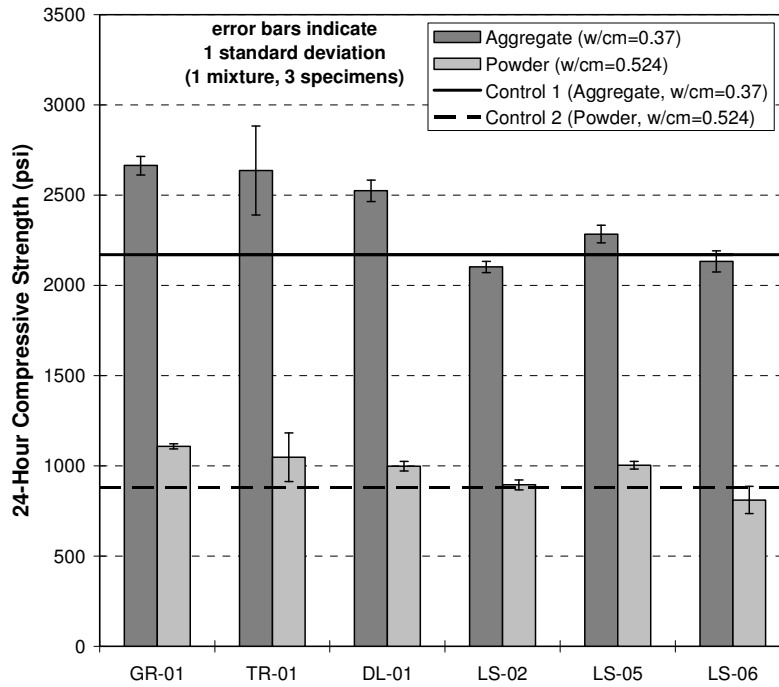
Figure 10.46: Effects of Microfines on 24-Hour Compressive Strength
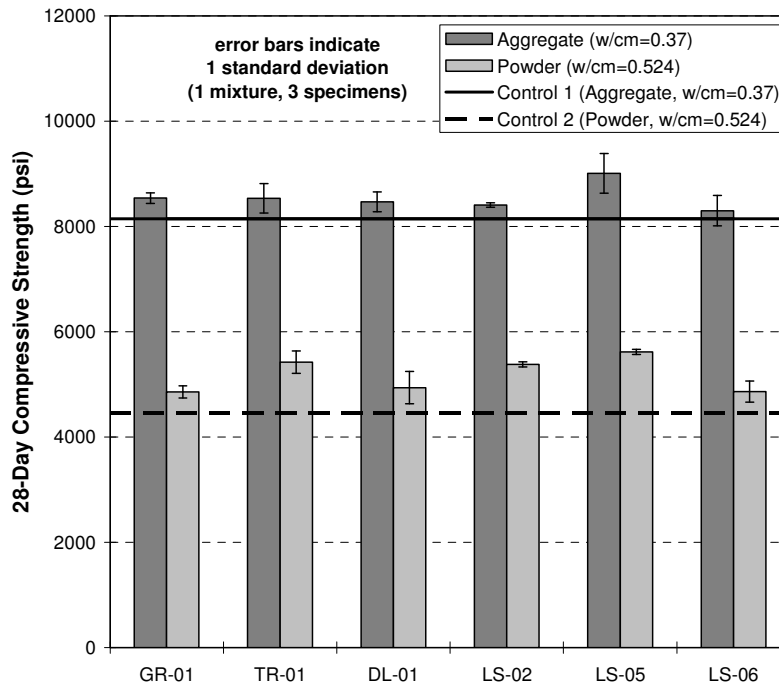
Figure 10.47: Effects of Microfines on 28-Day Compressive Strength

233
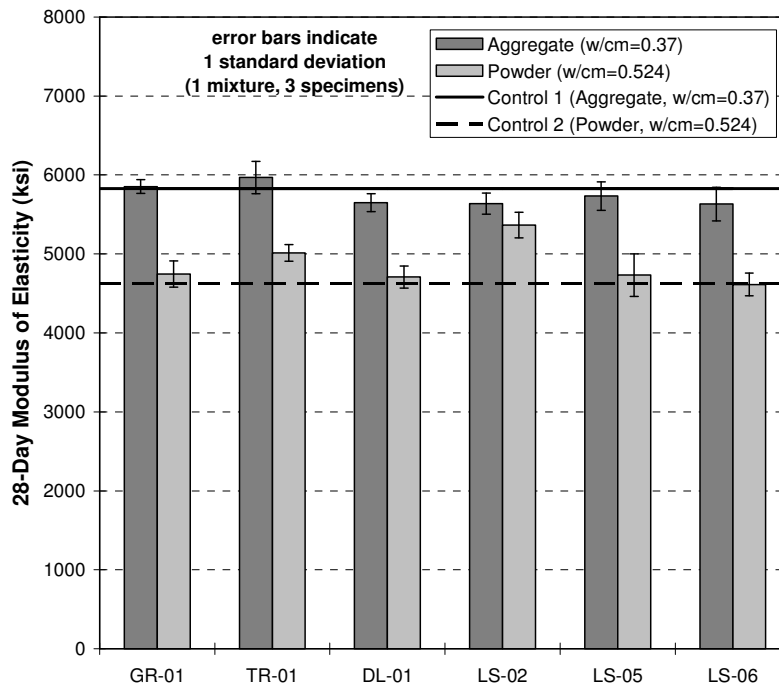
Figure 10.48: Effects of Microfines on 28-Day Modulus of Elasticity
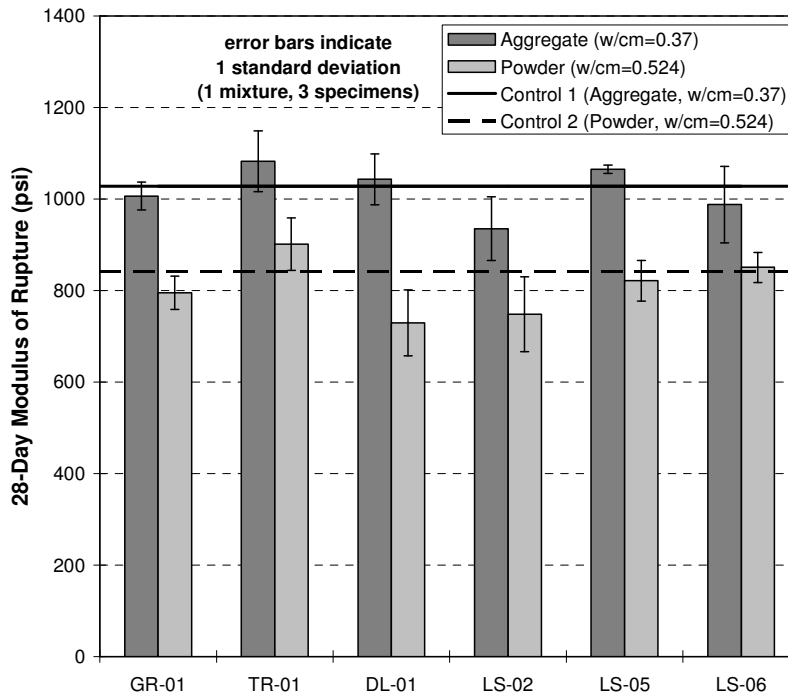
Figure 10.49: Effects of Microfines on 28-Day Flexural Strength
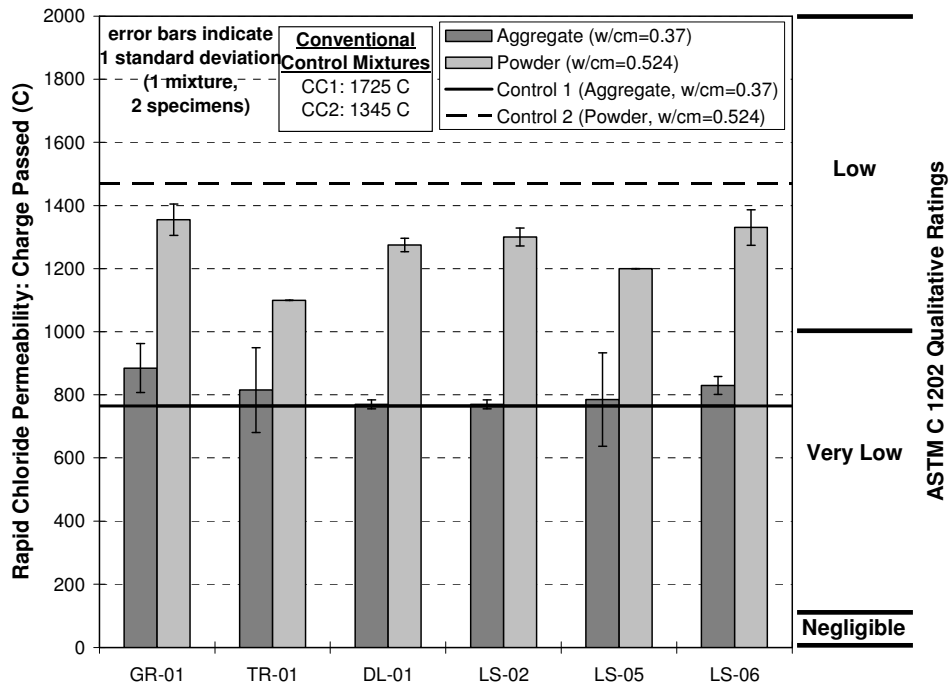
Figure 10.50: Effects of Microfines on 91-Day Rapid Chloride Permeability
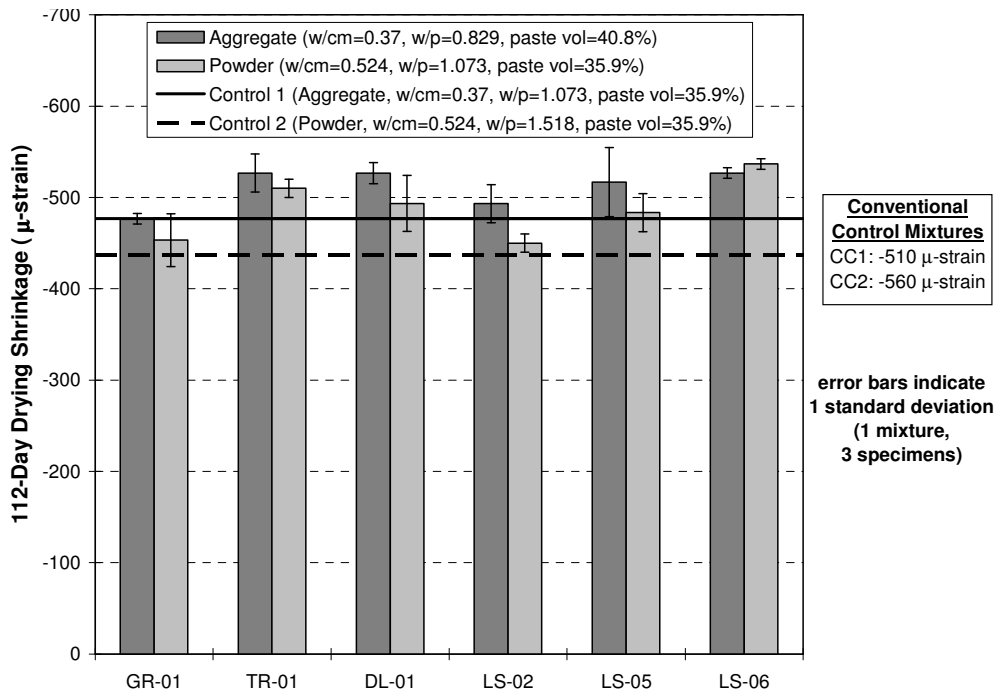
Figure 10.51: Effects of Microfines on 112-Day Drying Shrinkage

235
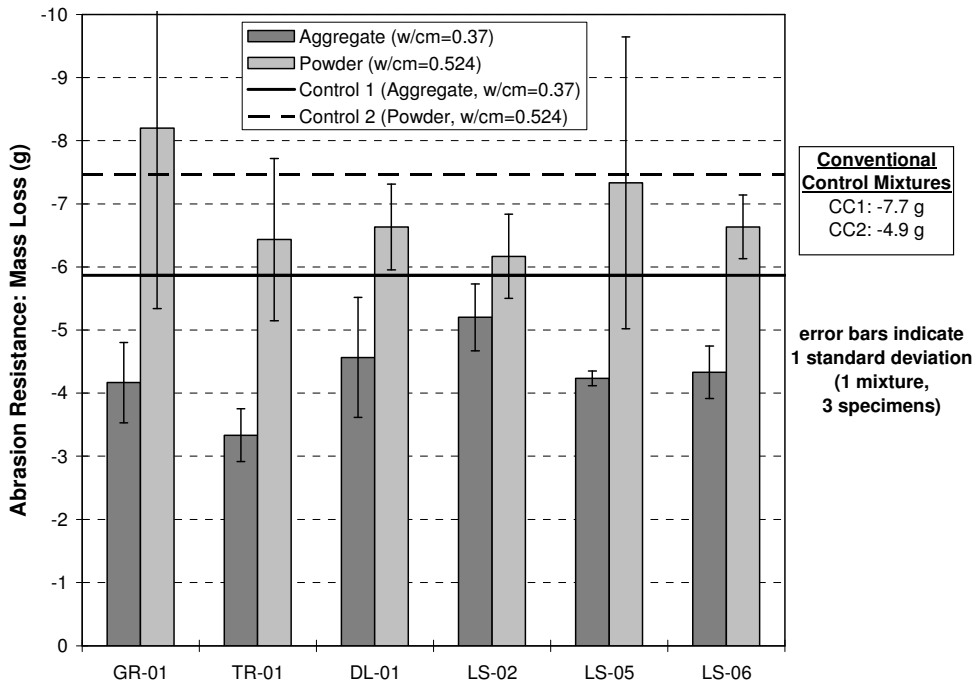
Figure 10.52: Effects of Microfines on 91-Day Abrasion Resistance

The comparable results from the mortar and concrete testing for microfines were well correlated for HRWRA demand and plastic viscosity (Figure 10.53), but not for compressive strength and shrinkage (Figure 10.54). The range of results was smaller for hardened properties than fresh properties, particularly when compared to the expected variability in the test results.
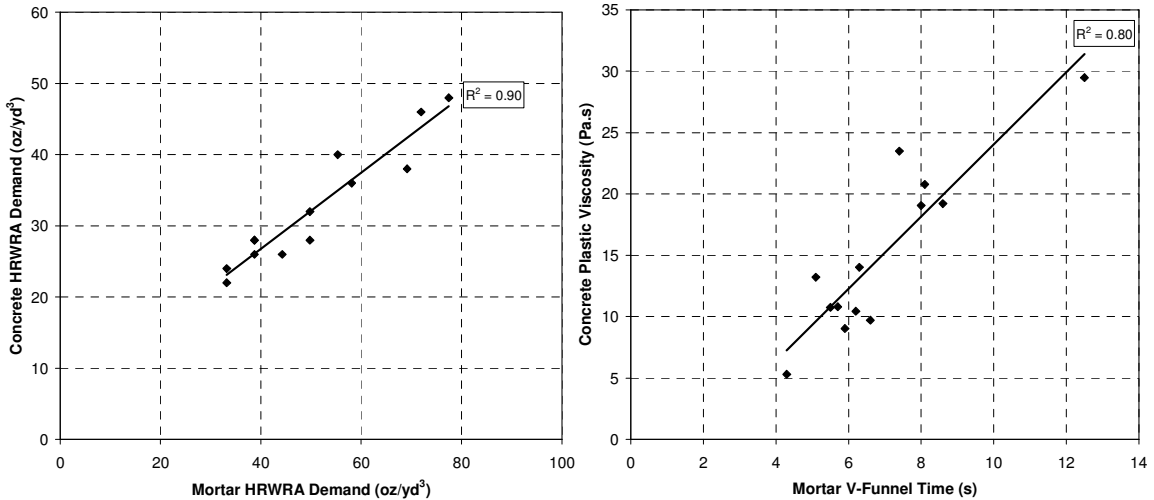
Figure 10.53: Comparison of Mortar and Concrete Workability for Microfines Mixtures

236
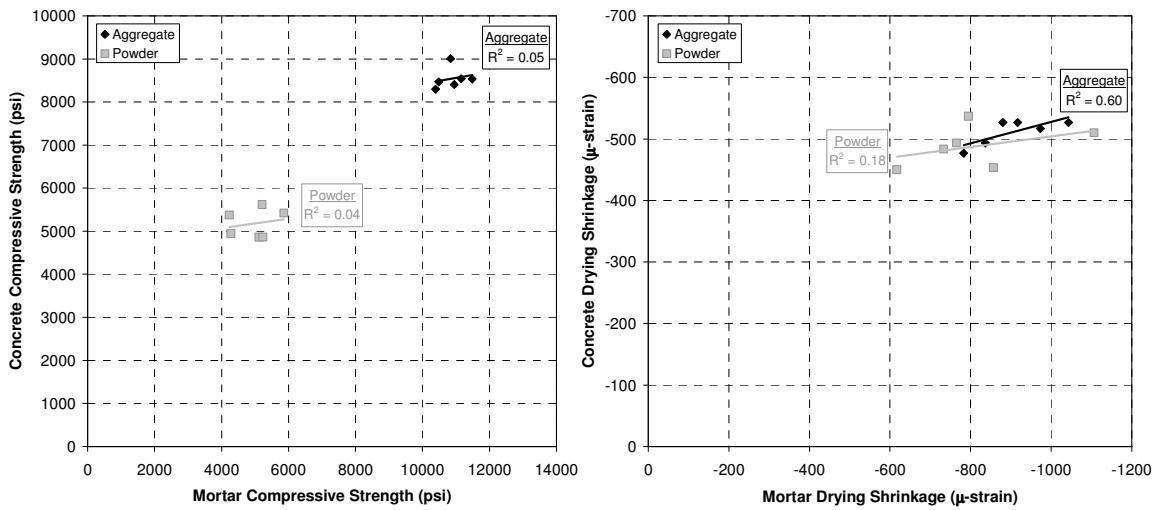
Figure 10.54: Comparison of Mortar and Concrete Hardened Properties for Microfines Mixtures

Multiple regression models were developed for the effects of microfines characteristics on workability and hardened properties. The models, which are listed in Table 10.9, were developed for microfines used as aggregate or powder. The results were generally consistent with those of the mortar mixtures. As indicated in Figure 10.55, the HRWRA demand decreased with increasing specific surface area and with decreasing methylene blue value. The effect of packing density on HRWRA demand was minimal. The plastic viscosity decreased with increasing specific surface area and span.

Table 10.9: Multiple Regression Models for Microfines (15% Rate as Sand or Powder)

Equation	Factors	$R^2_{adjusted}$
Microfines as Aggregate		
$HRWRA = 35.36 + 8.034(PKG)(MBV) - 5.875(SSA)^2 - 0.304(MBV)^2$	PKG, SSA, SPAN, MBV	0.990
$Plastic\ Viscosity = 32.08 - 1.787(SPAN)(SSA) - 14.64(PKG)(MBV) + 8.690(MBV)$	PKG, SSA, SPAN, MBV	1.000
$1/(f'_c\{24\text{-}hr\}) = 3.378\times10^{-6} + 1.110\times10^{-5}(SPAN)(SSA) + 5.210\times10^{-4}(PKG)$	PKG, SSA, SPAN, MBV, SG, ABS	0.912
28-day compressive strength not statistically significant	PKG, SSA, SPAN, MBV, SG, ABS	--
$E\{28\text{-}d\} = 7627.8 - 2762.1(PKG) - 6.941(SPAN)(ABS)$	PKG, SSA, SPAN, MBV, SG, ABS	0.917
$1/(f'_r\{28\text{-}d\}) = 0.00127 + 1.227\times10^{-5}(SPAN)^2 - 3.515\times10^{-5}(SPAN)(SG) - 7.284\times10^{-5}(PKG)(SG)$	PKG, SSA, SPAN, MBV, SG, ABS	0.999
$RCP\{91\text{-}d\} = 1643.3 - 404.57(PKG)(SG) - 11.68(SPAN)(SSA)$	PKG, SSA, SPAN, MBV, SG, ABS	0.866
$(Shrinkage\ \{112\text{-}d\})^{0.5} = 13.83 + 0.0555(MBV)(ABS) + 4.306(PKG)(SG) + 0.247(PKG)(ABS)$	PKG, SSA, SPAN, MBV, SG, ABS	0.999
$1/(Abrasion\ \{91\text{-}d\}) = 0.236 + 0.00113(MBV)^2 - 9.26\times10^{-4}(SPAN)^2$	PKG, SSA, SPAN, MBV, SG, ABS	0.792
Microfines as Powder		
$(HRWRA)^{0.5} = 4.901 + 1.328(PKG)(MBV) - 0.573(SSA)(MBV)$	PKG, SSA, SPAN, MBV	0.991
$(Plastic\ Viscosity)^{-0.5} = 0.181 + 0.01015(SPAN)(SSA)$	PKG, SSA, SPAN, MBV	0.894
$Ln(f'_c\{24\text{-}hr\}) = 7.313 - 0.0743(SPAN)(ABS) - 0.641(PKG)^2 + 0.0125(SPAN)(SSA)$	PKG, SSA, SPAN, MBV, SG, ABS	0.982
28-day compressive strength not statistically significant	PKG, SSA, SPAN, MBV, SG, ABS	--
$E\{28\text{-}d\} = 4892.4 + 147.7(SPAN)(SG) - 125.96(SPAN)(SSA) - 1293.9(PKG)$	PKG, SSA, SPAN, MBV, SG, ABS	0.999
28-day modulus of rupture not statistically significant	PKG, SSA, SPAN, MBV, SG, ABS	--
$RCP\{91\text{-}d\} = 2167.0 - 104.73(SG)^2 - 158.24(PKG)(SSA)$	PKG, SSA, SPAN, MBV, SG, ABS	0.989
$(Shrinkage\{112\text{-}d\})^{-0.5} = 0.06206 - 1.03\times10^{-4}(ABS)(MBV) - 0.00875(PKG)(SG) - 3.70\times10^{-4}(ABS)$	PKG, SSA, SPAN, MBV, SG, ABS	1.000
$1/(Abrasion\{91\text{-}d\}) = 0.101 + 0.00316(SPAN)(SG) + 0.05632(PKG)(MBV) - 0.03317(MBV)$	PKG, SSA, SPAN, MBV, SG, ABS	0.992
Regression Details: quadratic model, stepwise regression; p-value = 0.25; transformation with highest $R^2_{adjusted}$ selected; transformations considered: y, 1/y, ln(y), sqrt(y), 1/sqrt(y)		
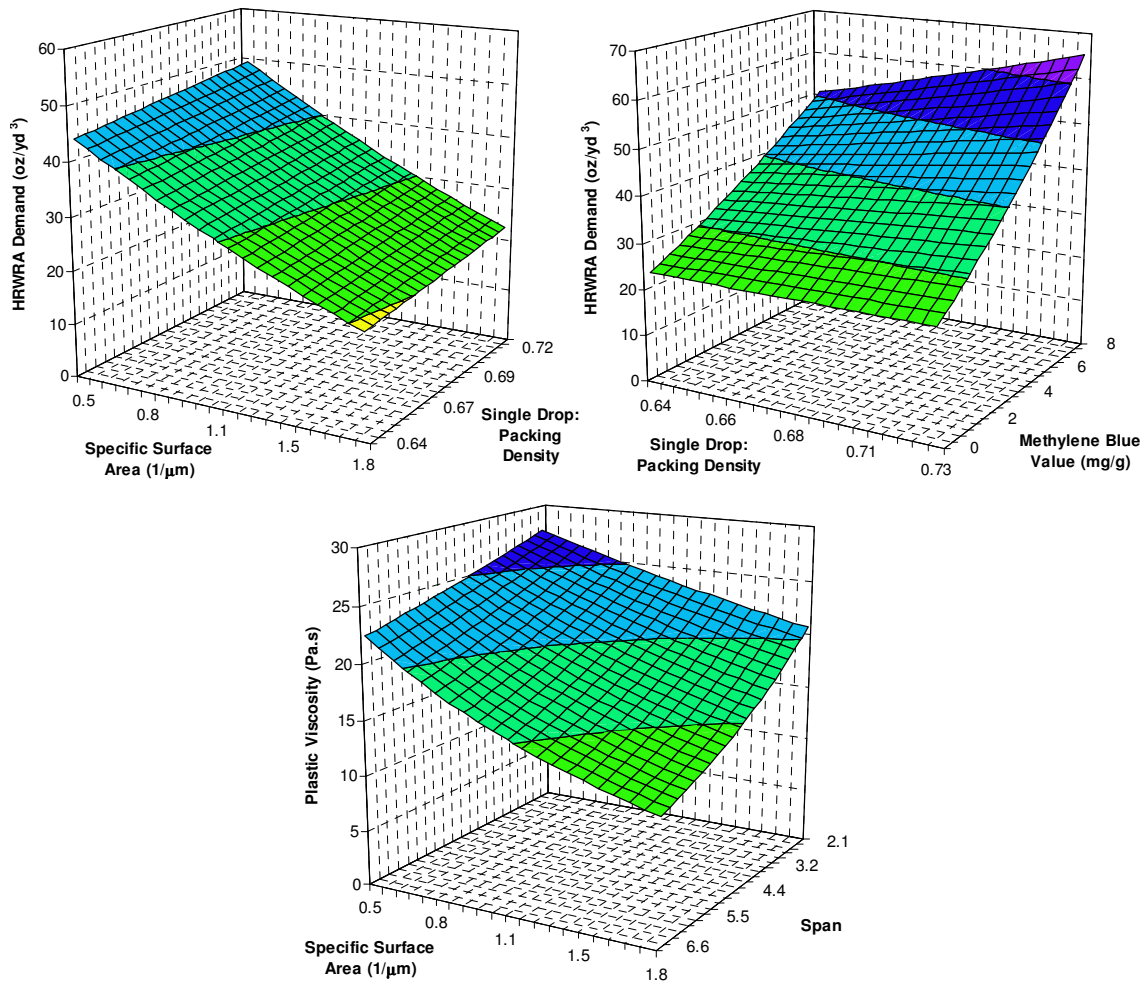
Figure 10.55: Effects of Microfines Characteristics on Fresh Properties (Microfines as Powder)

10.6   Conclusions

The following conclusions can be drawn based on the test results presented in this chapter:

- The findings for the concrete mixtures regarding fine aggregates and microfines were generally consistent with the finding for the mortar mixtures.

- Both fine and coarse aggregates were shown to have significant influence on SCC flow properties; however, the fine aggregates considered in this study had a larger effect than the coarse aggregates.

- In general, the natural aggregates, well-shaped manufactured sands, and well-shaped crushed coarse aggregates exhibited low compacted voids content and low interparticle

friction, which resulted in low HRWRA demand, low plastic viscosity, and low j-ring blocking.

- The relative effects of aggregate characteristics were much more significant for workability than for hardened properties. Therefore, in most cases, the effects of aggregate characteristics on hardened properties will be indirect. That is, changes in mixture proportions required to achieve adequate workability for a certain aggregate are likely to have greater effects on hardened properties than the characteristics of the aggregates themselves.

- Increasing the paste volume increases mixture robustness by decreasing the difference in workability between different aggregates. Challenging aggregates can be accommodated by increasing the paste volume.

- When evaluated at various paste volumes for a single aggregate, the gap-graded mixture was found to exhibit lower HRWRA demand and plastic viscosity but higher j-ring blocking than the continuously graded mixture.

- The use of microfines as either part of the aggregate or powder typically increased the HRWRA demand (volume of HRWRA per volume of concrete) and plastic viscosity. The increase in these parameters was less when microfines were used as part of the powder instead of aggregate volume.

- The use of microfines had little impact on hardened properties when the w/cm was held constant. For a constant w/cm, the use of microfines resulted in an increase in compressive strength at 24 hours and 28 days, no change in modulus of elasticity or flexural strength, no change or a slight reduction in rapid chloride permeability, a minimal increase in drying shrinkage, and an increase in abrasion resistance.

- When proportioning SCC mixtures, microfines should be considered a powder material and be accounted for as part of the paste volume. The water-powder ratio should be used for workability properties, the water-cement ratio for early-age hardened properties, and the water-cementitious materials ratio for long-term hardened properties.

Chapter 11: Effects of Constituents Other Than Aggregates in Concrete

The effects of constituents other than aggregates on the workability and hardened properties of concrete were tested to evaluate SCC mixture proportioning, to determine effective means of accommodating varying aggregate characteristics, and to confirm the applicability of trends established in previous chapters to a wider range of materials. First, the effects of mixture proportions—namely paste volume, water content, fly ash dosage, and sand-aggregate ratio—were evaluated. Next, the effects of 3 fly ashes, 4 HRWRAs, and one VMA were evaluated. The mixing and testing procedures used in these tests were identical to those used in Chapter 10. All test data are provided in Appendix C.

11.1 Effects of Mixture Proportions

The effects of mixture proportions were evaluated with two sets of materials. For the first set of materials, mixtures were tested based on a response surface experiment design and multiple regression models were fit to the results. For the second set of materials, multiple regression models were fit to data from Koehler et al. (2007), which covered a range of mixture proportions but were not based on a specific experimental design.

11.1.1 Material Set 1

Material set 1 included NA-02-C coarse aggregate, LS-02-F fine aggregate, PC-01-I/II cement, FA-02-F fly ash, and HRWRA-02. The effects of mixture proportions were evaluated by varying the paste volume, water-cementitious materials ratio, fly ash dosage, and sand-aggregate ratio. The slump flow was held constant at 24-26 inches by adjusting the HRWRA dosage. An inscribed central composite response surface experiment design was used. The response surface consisted of 8 fractional factorial points (-1, 1), 8 star points (-1.68, 1.68) and 5 center points (0), for a total of 21 mixtures. The levels of each factor are shown in Table 11.1. The responses were HRWRA demand for a 24-26-inch slump flow, T_{50}, v-funnel time, j-ring blocking, rheology, 24-hour and 28-day compressive strength, 28-day elastic modulus, 28-day flexural strength, 91-day rapid chloride permeability, and 112-day drying shrinkage.

Table 11.1: Response Surface Factors for Evaluation of Effects of Mixture Proportions (Material Set 1)

	Coded Factors				
	-1.68	**-1**	**0**	**1**	**1.68**
Paste Volume[1] (PV), %	29.7	32.5	36.6	40.6	43.4
w/cm^{2}	0.30	0.32	0.35	0.38	0.40
Fly Ash Dosage[2] (FA), %	0.0	8.1	20.0	31.9	40.0
S/A[2]	0.40	0.42	0.45	0.48	0.50
[1]Paste volume includes water, cement, fly ash, air, microfines					
[2]w/cm and fly ash dosage expressed by mass, S/A by volume					

Multiple regression models were developed for the response surface test results and are listed in Table 11.2. Water content was represented with w/p for workability and shrinkage, w/c for 24-hour compressive strength, and w/cm for all other hardened properties. Four of the mixtures were determined to have insufficient paste volume for achieving SCC flow properties and were not included in the models.

Table 11.2: Multiple Regression Models for Evaluation of Mixture Proportions

Equation	Factors	$R^2_{adjusted}$
$(HRWRA)^{-0.5} = -26.69 + 1.434(PV) - 0.01685(PV)^2 + 0.128(FA)(W/P) - 0.217(FA)(S/A)$	PV, FA, W/P, S/A	0.888
$sqrt(T_{50}) = 6.000 - 0.110(PV)(W/P) - 0.108(FA)(S/A) + 0.03258(FA)(W/P)$	PV, FA, W/P, S/A	0.952
$Ln(Plastic Viscosity) = 9.314 - 0.157(PV)(W/P) - 0.08861(FA)(S/A)$	PV, FA, W/P, S/A	0.936
$Ln(J\text{-}Ring) = 6.260 - 0.00285(PV)^2 - 0.02942(FA)(W/P) - 5.061(S/A)(W/P)$	PV, FA, W/P, S/A	0.819
$f'_c\{24\text{-}hr\} = 15481.6 - 43175.1(W/C) + 34338.8(W/C)^2$	PV, FA, W/C, S/A	0.798
$f'_c\{28\text{-}d\} = 13527 - 126.89(FA)(W/CM) - 27142(S/A)(W/CM)$	PV, FA, W/CM, S/A	0.387
$E\{28\text{-}d\} = 8865.9 - 10737.5(S/A)(W/CM) - 97.44(PV)(W/CM) - 0.751(FA)^2 + 0.712(PV)(FA)$	PV, FA, W/CM, S/A	0.738
$1/(f'_r\{28\text{-}d\}) = 4.29 \times 10^{-4} + 3.18 \times 10^{-3}(S/A)(W/CM) + 1.130 \times 10^{-7}(FA)^2$	PV, FA, W/CM, S/A	0.804
$RCP\{91\text{-}d\} = 6873.4 + 1.110(FA)^2 + 1206.1(PV)(W/CM) - 2.801(PV)(FA) - 41515.6(W/CM) - 4.246(PV)^2 + 47.26(FA)(S/A)$	PV, FA, W/CM, S/A	0.964
$Shrinkage\{112\text{-}d\} = -3244.3 + 178.31(PV) - 14.26(FA)(W/P) + 25.87(FA)(S/A) - 2.107(PV)^2$	PV, FA, W/P, S/A	0.700
Regression Details: quadratic model, stepwise regression; p-value = 0.10 for fresh properties, 0.20 for hardened properties; transformation with highest $R^2_{adjusted}$ selected; transformations considered: y, 1/y, ln(y), sqrt(y), 1/sqrt(y)		

Figure 11.1 indicates that paste volume and w/p had the largest effects on HRWRA demand for a constant slump flow, with increasing paste volume and w/p reducing HRWRA demand. Increasing the paste volume increases the spacing between aggregates and reduces interparticle friction, which results in lower concrete yield stress. Lower concrete yield stress, in

turn, results in lower HRWRA dosage needed to reduce the yield stress to that required for SCC self-flow. Higher water-powder ratios reduce the yield stress of the paste, which results in a lower amount of HRWRA required to deflocculate powdered materials. Increasing the fly ash dosage and reducing the S/A also resulted in a reduction in HRWRA demand. The spherical nature of fly ash reduces interparticle friction. The decrease in HRWRA demand with increasing S/A matched the mortar results where coarser gradings resulted in lower HRWRA demand. Increasing the fineness of the aggregate grading results in greater potential contact area between aggregates, which can cause increased interparticle friction.

Increasing the paste volume, w/p, and fly ash dosage all significantly decreased the plastic viscosity, as indicated in Figure 11.2. The S/A had essentially no effect on plastic viscosity for a constant slump flow. For a constant HRWRA dosage, however, increasing the S/A would be expected to result in a reduced plastic viscosity. As with HRWRA demand, increasing the paste volume reduces the interparticle friction between aggregates while increasing the w/p and fly ash dosage decrease the interparticle friction between powder constituents, all of which result in reduced plastic viscosity.

J-ring blocking was primarily reduced by increasing the paste volume, as indicated in Figure 11.3. Increasing the paste volume reduces the amount of coarse aggregate that must pass through the reinforcing bars and reduces interparticle friction between aggregates. In addition, increasing the w/p and the fly ash dosage also resulted in reduced j-ring blocking. Both of these factors reduce interparticle friction within the paste fraction. Increasing the S/A also reduced blocking because of the reduction in coarse aggregates that must pass through the j-ring.

The water-cement ratio was the only factor affecting 24-hour compressive strength, as indicated in Figure 11.4. At this early age, the fly ash did not react to an extent necessary to contribute to strength. The 28-day compressive strength increased with decreasing w/cm and fly ash dosage, as indicated in Figure 11.5. At 28-days, the fly ash contributed to the strength development of the mixture, but likely not to its full extent. Therefore, compressive strength should generally be evaluated at ages beyond 28 days for mixtures containing SCMs such as class F fly ash. Decreasing the S/A resulted in an increase in 28-day compressive strength. It is generally expected that increasing the coarseness of an aggregate grading (decreasing the S/A) should result in a reduction in compressive strength. In this case; however, other factors such as the strength and bond characteristics of the coarse aggregate relative to that of the fine aggregate

may have contributed to the increase in strength with increased coarse aggregate volume. The paste volume had no effect on 28-day compressive strength.

Figure 11.6 indicates that modulus of elasticity was found to increase primarily with decreasing w/cm, which was expected because of the increase in modulus of elasticity with compressive strength. The modulus of elasticity increased with decreasing paste volume, which was expected because the stiffness of the paste is less than that of the aggregate. The change in elastic modulus with paste volume, however, was small. A slightly larger decrease in elastic modulus occurred with increasing S/A ratio. This decrease in elastic modulus was expected because modulus is known to generally increase with increased coarseness of the aggregate grading. Further, if the coarse aggregate is stiffer than the fine aggregate, an increase in modulus would also be expected with decreasing S/A. Indeed, the NA-02 aggregate was found in Chapter 10 to result in higher elastic modulus than LS-02 aggregate. Increasing the fly ash dosage increased the modulus of elasticity at low dosages and decreased the modulus of elasticity at high dosages. It was expected that increasing the fly ash dosage would have decreased the modulus of elasticity at all dosages because of the reduction in compressive strength. Any improvement in the transition zone due to the presence of fly ash could have contributed to the increase in modulus of elasticity; however, further investigation would be required.

The flexural strength increased with decreasing w/cm, fly ash dosage, and S/A (Figure 11.7). Paste volume had no effect on flexural strength. The results for flexural strength generally matched those for compressive strength; however, the effect of fly ash was not as significant for flexural strength as for compressive strength. As with modulus of elasticity, the fly ash could have improved the transition zone, which is important for flexural strength.

Figure 11.8 indicates that the use of fly ash significantly reduced rapid chloride permeability, which was expected due to the pozzolanic activity of the fly ash. Increasing the w/cm resulted in an increase in rapid chloride permeability at paste volumes greater than approximately 35%. Likewise, increasing the paste volume resulted in an increase in rapid chloride permeability at w/cm greater than approximately 0.32. The increased w/cm increased the permeability of the paste, resulting in increased concrete rapid chloride permeability. Increasing the amount of more permeable paste also resulted in increased rapid chloride permeability. The S/A had essentially no effect on rapid chloride permeability, which was expected provided the fine and coarse aggregates are of similar permeability.

244

Figure 11.9 indicates that shrinkage increased significantly with increased paste volume. This result was expected due to the reduction in volume of aggregates, which provide restraint against shrinkage, and the increase in total water content. For a given paste volume, increasing the w/p resulted in decreased drying shrinkage despite the greater total water content. Increasing the fly ash dosage and decreasing the S/A ratio resulted in decreased drying shrinkage.
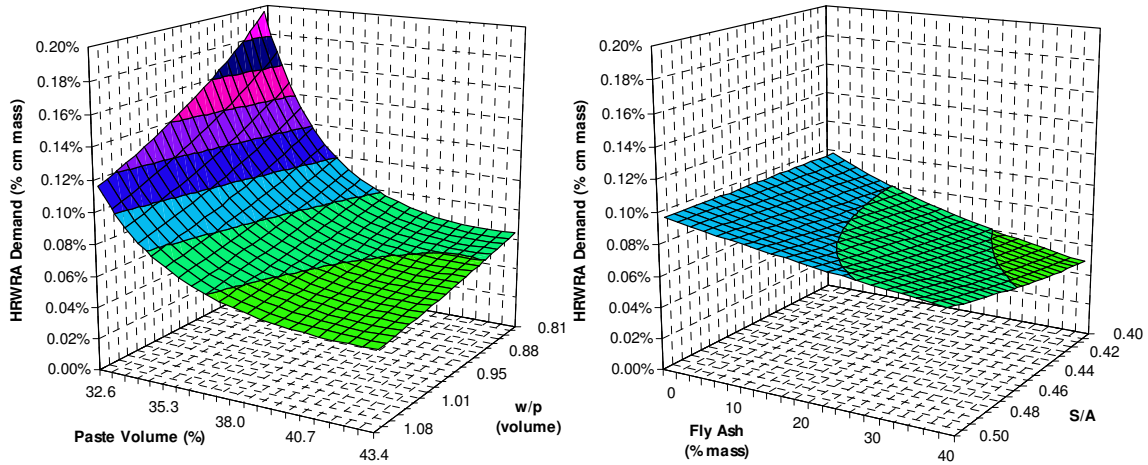
Figure 11.1: Effects of Mixture Proportions on HRWRA Demand
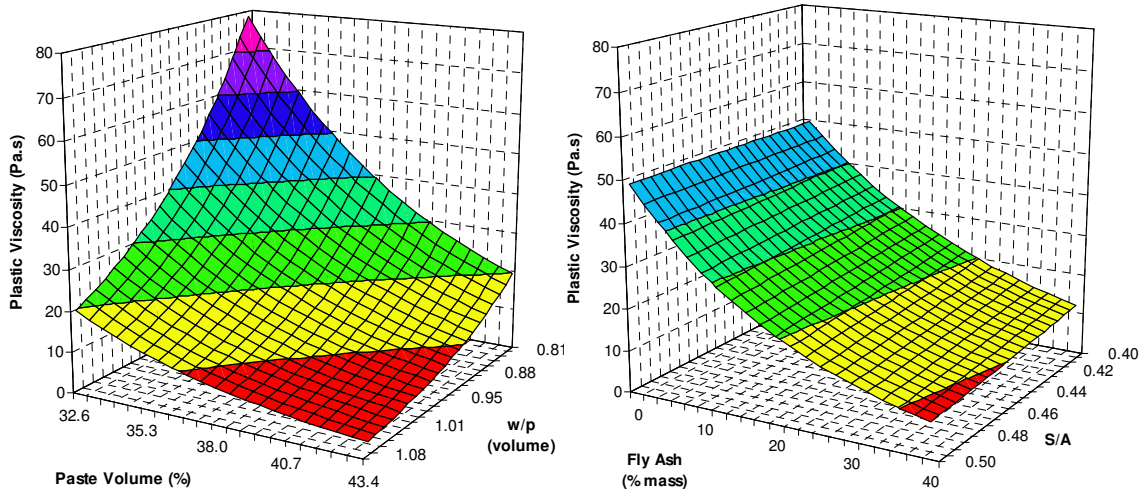
Figure 11.2: Effects of Mixture Proportions on Plastic Viscosity
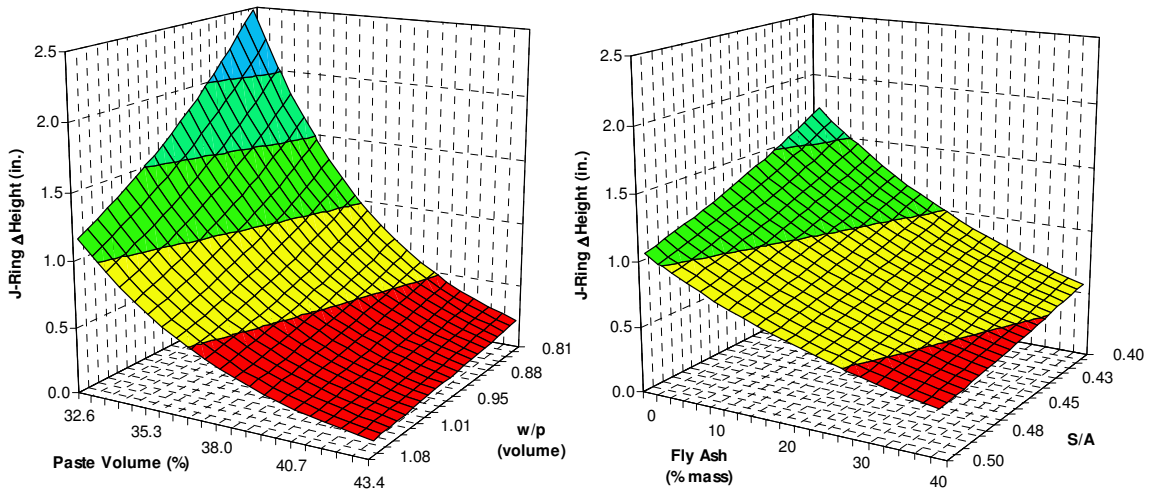
Figure 11.3: Effects of Mixture Proportions on J-Ring Blocking
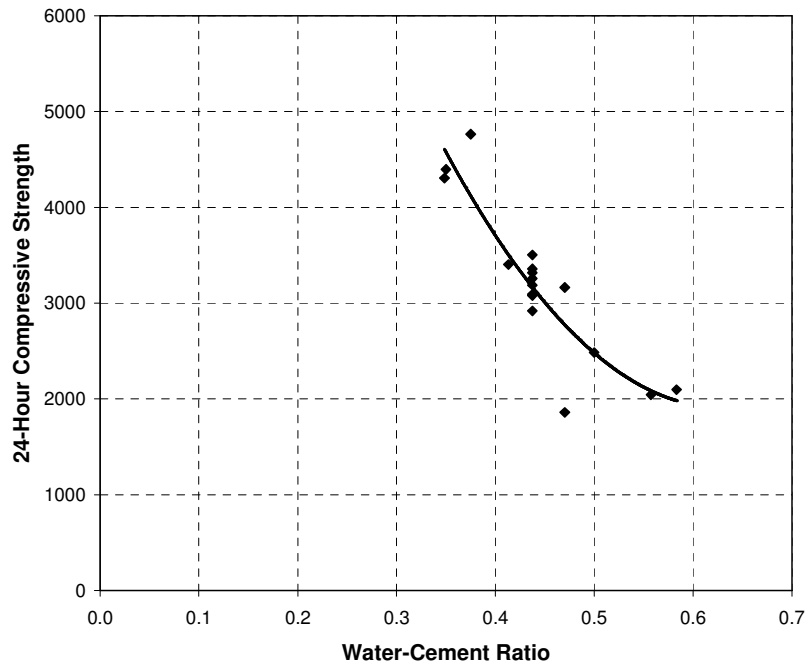
Figure 11.4: Effects of Mixture Proportions on 24-Hour Compressive Strength
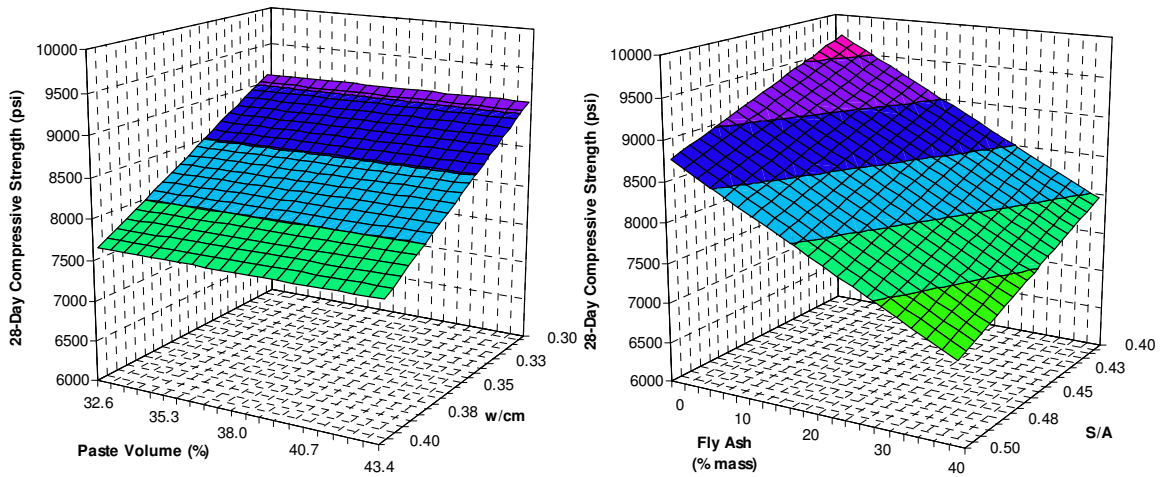
Figure 11.5: Effects of Mixture Proportions on 28-Day Compressive Strength
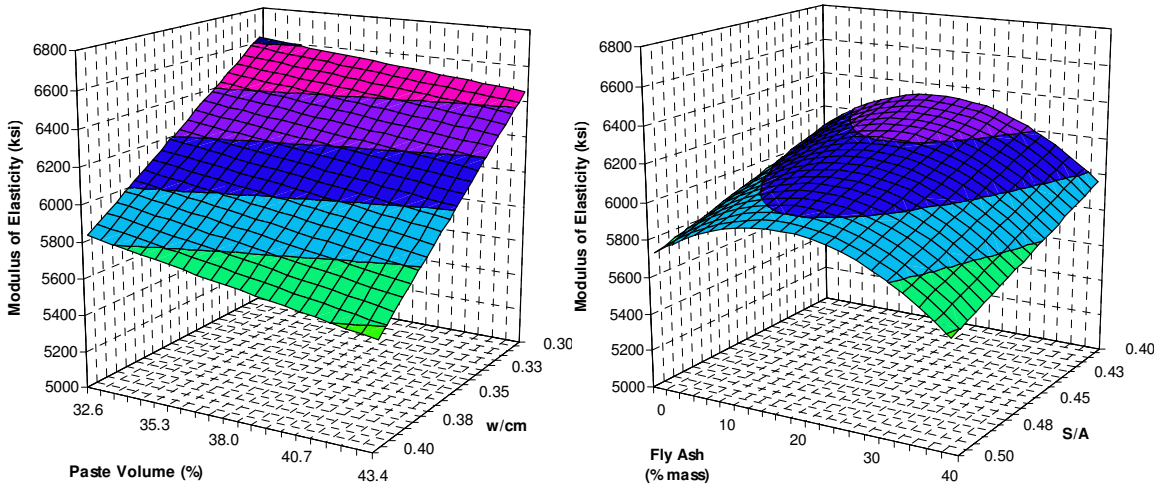
Figure 11.6: Effects of Mixture Proportions on 28-Day Modulus of Elasticity
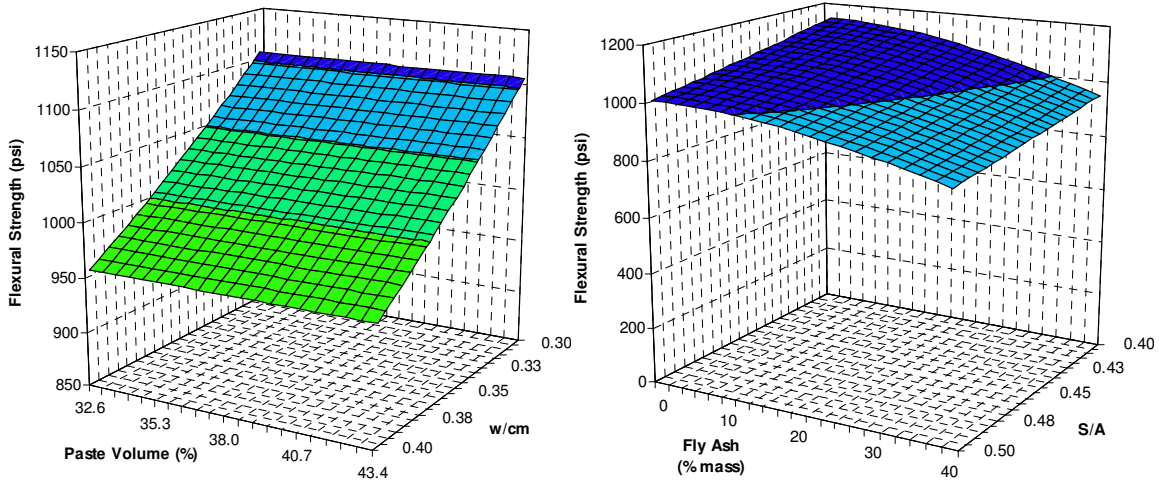
Figure 11.7: Effects of Mixture Proportions on 28-Day Flexural Strength

247
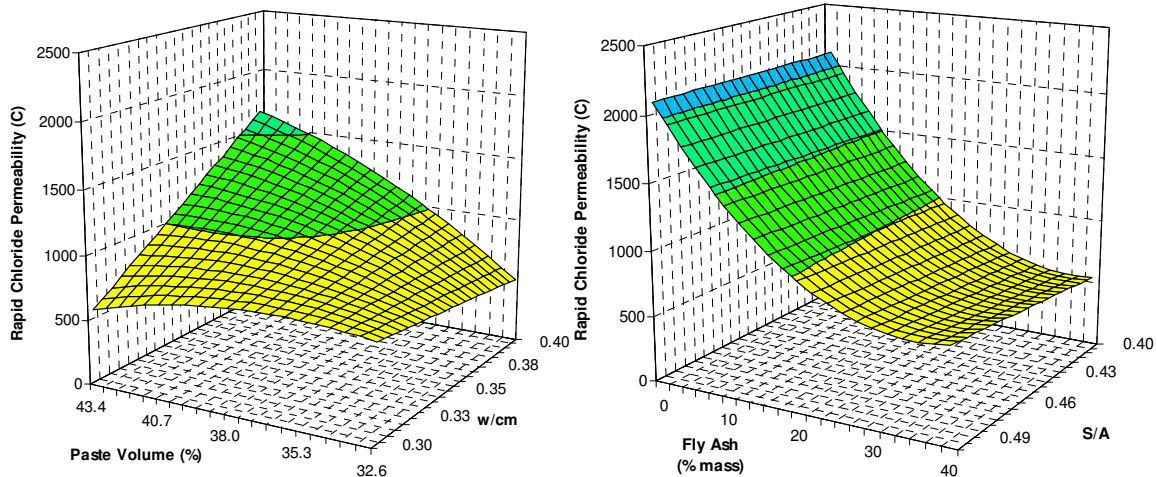
Figure 11.8: Effects of Mixture Proportions on 91-Day Rapid Chloride Permeability
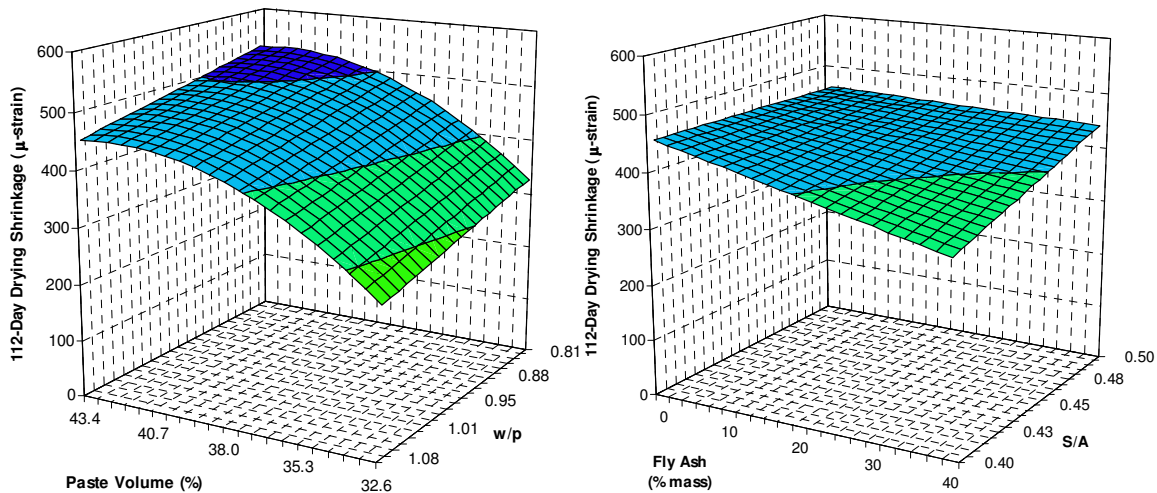
Figure 11.9: Effects of Mixture Proportions on 112-Day Drying Shrinkage

Providing sufficient paste volume for filling ability, passing ability, and robustness is essential to achieving proper SCC workability. Paste volume can be increased by adding some combination of air, water, or powder materials. The choice of materials added to increase paste volume can have a significant influence on concrete rheology. Figure 11.10 illustrates that increasing the paste volume by adding water decreases HRWRA demand most dramatically while increasing paste volume by adding cement keeps the HRWRA demand approximately constant. Increasing paste volume with constant paste composition also results in reduced HRWRA demand. Similarly, Figure 11.11 indicates that adding paste of constant composition or increasing the paste volume by adding water both reduce plastic viscosity while increasing the

248

paste volume by adding cement results in increased plastic viscosity. Adding fly ash to increase paste volume results in constant plastic viscosity. Therefore, to maintain an approximately constant concrete plastic viscosity as the paste volume is increased, the powder volume should be increased at a faster rate than the water volume. The relative amounts of powder and water to maintain constant plastic viscosity depend on the characteristics of the materials used. In contrast, the ACI 211 mixture proportioning procedure for conventionally placed concrete fixes the total water content based solely on the aggregate characteristics and amount of air entrainment. For the ACI 211 approach, holding the water content constant while increasing the cementitious materials constant would result in increased viscosity. However, the sand content would also be reduced under the ACI 211 approach, which would likely offset part of this increase in viscosity.
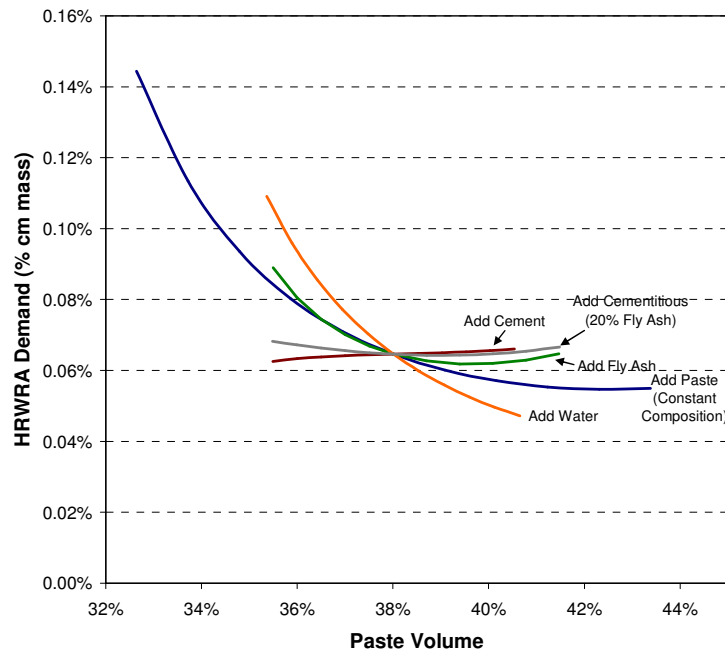
Figure 11.10: Effects of Various Methods of Changing the Paste Volume on HRWRA Demand (Constant Slump Flow, Material Set 1)
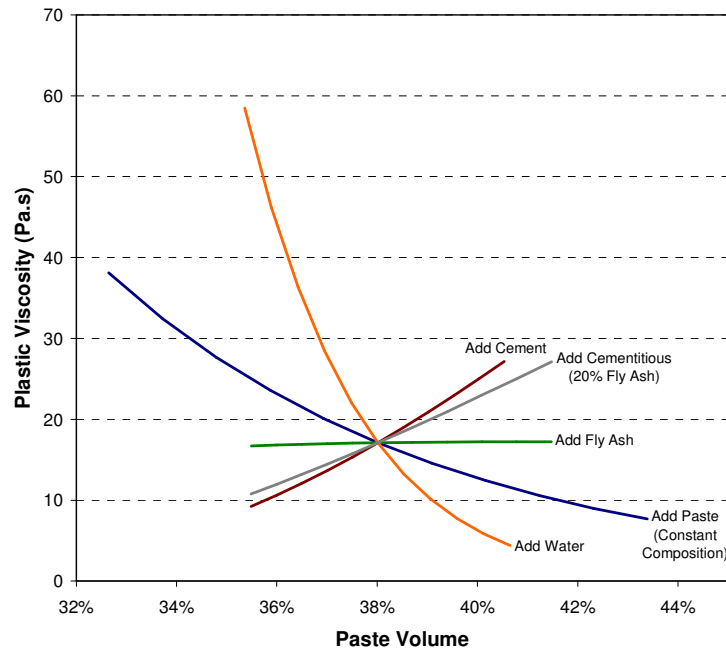
Figure 11.11: Effects of Various Methods of Changing the Paste Volume on Plastic Viscosity (Constant Slump Flow, Material Set 1)

11.1.2 Material Set 2

Material set 2 included NA-02-C coarse aggregate, NA-02-F fine aggregate, PC-03-III cement, FA-01-F fly ash, and HRWRA-01. The factors varied were paste volume, water-powder ratio, fly ash dosage, sand-aggregate ratio, and slump flow. The ranges of these factors are listed in Table 11.3. The responses were HRWRA demand for various slump flows, T_{50}, and j-ring blocking.

Table 11.3: Range of Factors for Evaluation of Effects of Mixture Proportions (Material Set 2)

	Minimum	Maximum
Paste Volume[1] (PV), %	28.9	40.4
w/p[2]	0.78	1.26
Fly Ash Dosage[2] (FA), %	0	32
S/A[2]	0.35	0.50
Slump Flow (SF)	23.5	31.0
[1]Paste volume includes water, cement, fly ash, and air [2]Fly ash dosage expressed by mass; w/p and S/A by volume		

Multiple regression models were developed for the test results and are listed in Table 11.4. The results from material set 2 were consistent with the results from material set 1.

250

Although the directions of trends were consistent between the two material sets, the magnitudes of the relative effects varied due to differences in material characteristics.

Table 11.4: Multiple Regression Models for Evaluation of Mixture Proportions

Equation	$R^2_{adjusted}$
$(HRWRA)^{-1} = 0.01842 + 0.207(PV)(W/P) - 0.154(S/A)(SF) + 0.00286(PV)(FA) - 0.00255(FA)(SF) - 1.727(W/P)^2$	0.895
$\ln(T_{50}) = 3.280 - 0.9296(PV)(W/P) - 0.00342(FA)(SF) + 0.00242(PV)(FA) + 2.460(SA)^2$	0.783
$\text{sqrt}(J\text{-Ring}) = 3.087 - 0.120(PV)(S/A) + 0.888(S/A)(W/P) - 0.03179(SF)$	0.466
Regression Details: quadratic model, stepwise regression; p-value = 0.10 for fresh properties; transformation with highest $R^2_{adjusted}$ selected; transformations considered: y, 1/y, ln(y), sqrt(y), 1/sqrt(y)	

As with material set 1, increases in paste volume and w/p resulted in decreased HRWRA demand for a given slump flow (Figure 11.12). The relative effects of fly ash and S/A were much smaller than for material set 1. HRWRA demand decreased when the fly ash dosage increased and S/A decreased.

Figure 11.13 indicates that the water-powder ratio had the largest effect on T_{50}, which is assumed to be correlated to plastic viscosity. This trend is consistent with the effect on plastic viscosity for material set 1. Unlike material set 1, the effects of paste volume and fly ash on T_{50} were much less although the directions of the effects were consistent. Increases in S/A resulted in larger relative increases in T_{50} than for plastic viscosity in material set 1. Increasing the slump flow resulted in a decrease in T_{50}, which was expected because of the increased dispersion of the powder associated with the higher HRWRA dosages needed for higher slump flows.

As with material set 1, the results of material set 2 indicate that increasing the paste volume and S/A reduced j-ring blocking (Figure 11.14). Additionally, increasing the w/p and slump flow reduced j-ring blocking because concrete with greater flowability should more readily flow through narrow spaces. Fly ash had no effect on j-ring blocking.
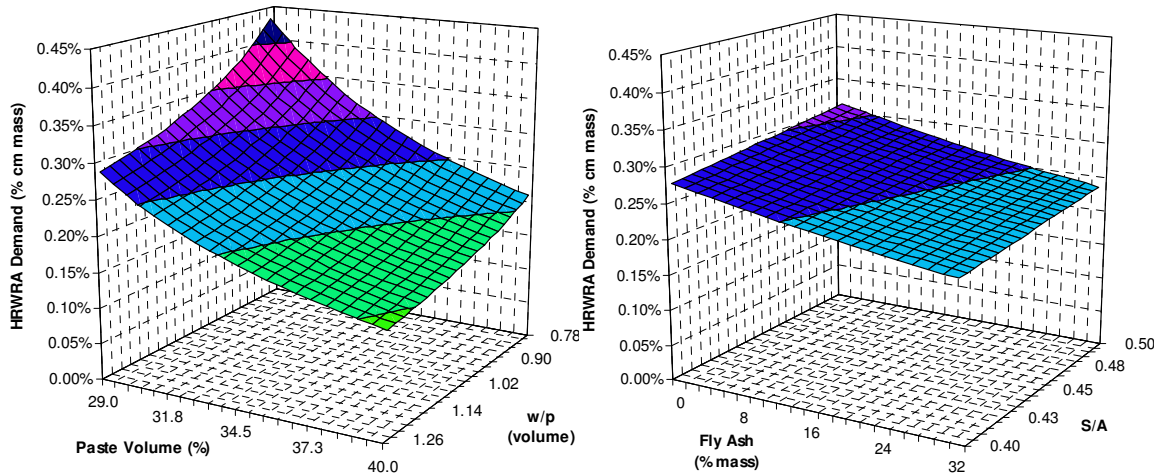
Figure 11.12: Effects of Mixture Proportions on HRWRA Demand (25-Inch Slump Flow)
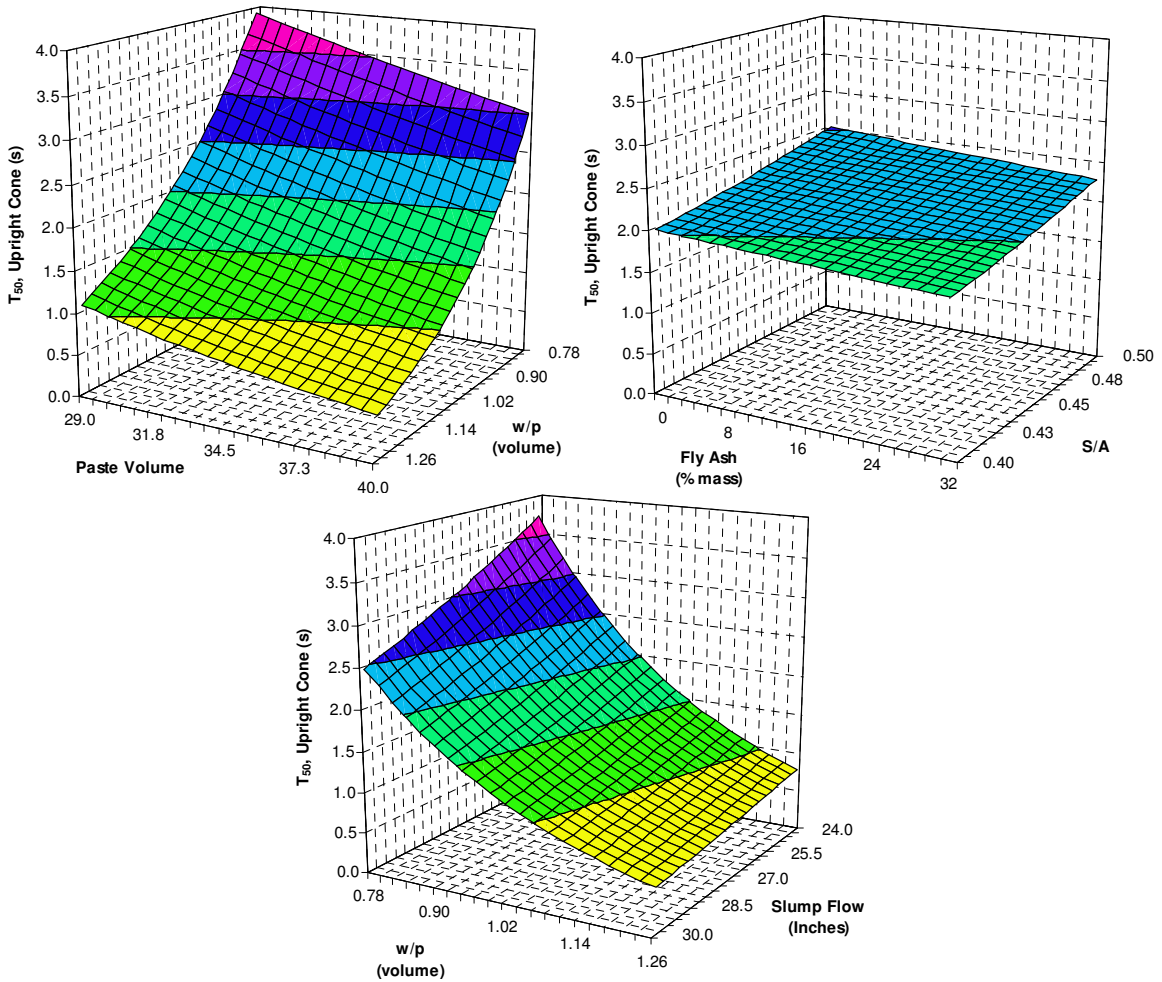
Figure 11.13: Effects of Mixture Proportions on T$_{50}$ (25-Inch Slump Flow Unless Indicated Otherwise)
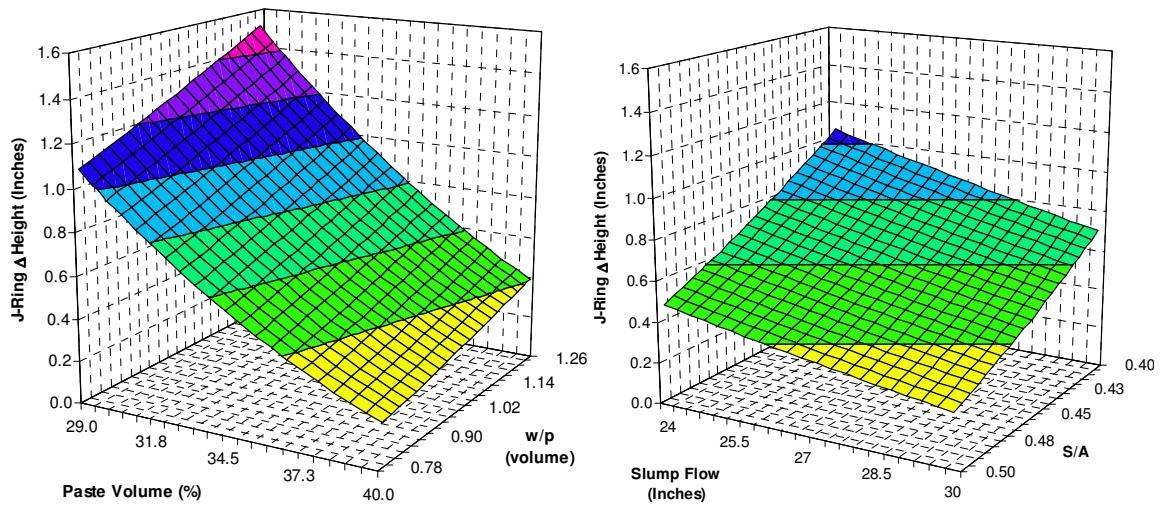
Figure 11.14: Effects of Mixture Proportions on J-Ring Blocking

Figure 11.17 and Figure 11.16 compare the effects of various approaches to increasing paste volume. The results generally match those for material set 1; however, added fly ash to increase paste volume resulted in an increase in plastic viscosity, as measured indirectly with slump flow T_{50}. This difference reflected that the fly ash used for material set 1 exhibited better characteristics for workability. As with material set 1, increasing the cementitious materials content while keeping the water content constant did not result in a constant workability.
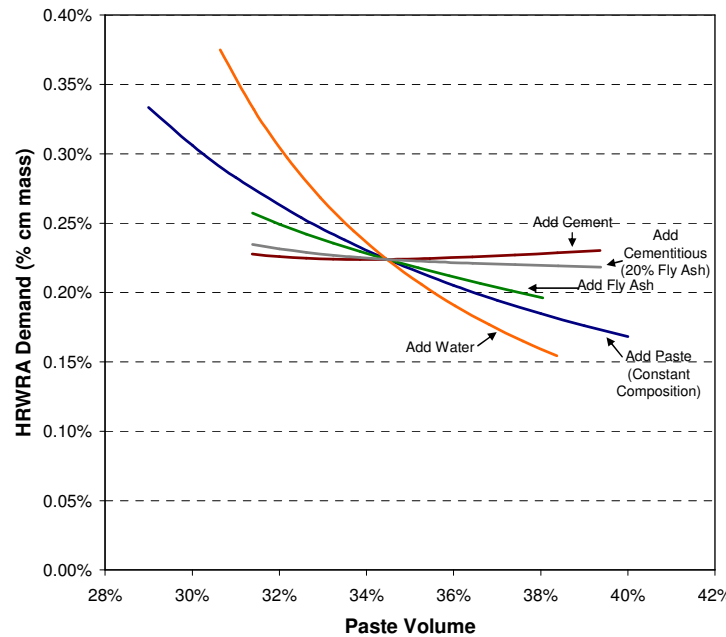
Figure 11.15: Effects of Various Methods of Changing the Paste Volume on HRWRA Demand (Constant Slump Flow, Material Set 2)
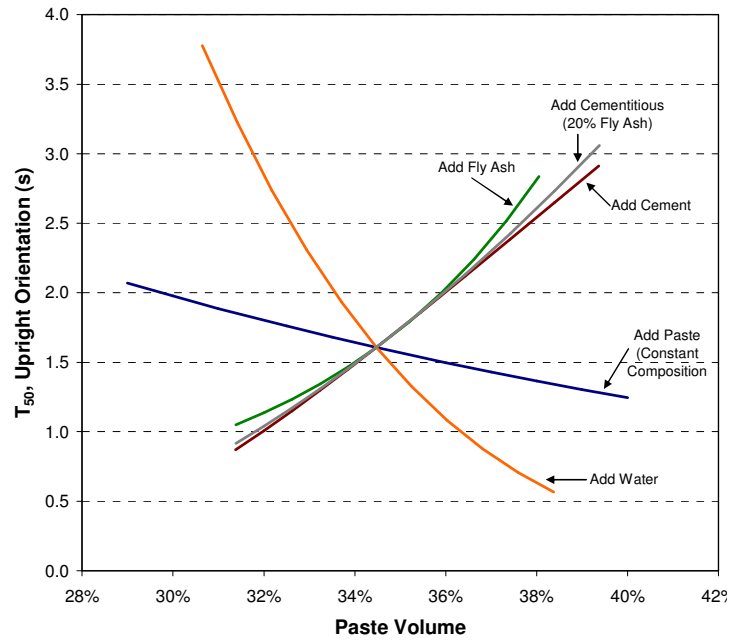
Figure 11.16: Effects of Various Methods of Changing the Paste Volume on Plastic Viscosity (Constant Slump Flow, Material Set 2)

11.2 Effects of High-Range Water-Reducing Admixture

The effects of 4 HRWRAs on slump flow, rheological parameters, workability retention, and compressive strength development were compared. The HRWRAs evaluated were HRWRA-01, HRWRA-02, HRWRA-04, and HRWRA-06. The mixture proportions are listed in Table 11.5. Each admixture was tested in two batches. In the first batch, the HRWRA dosage was varied and the slump flow and rheology were measured. In the second batch, the HRWRA dosage was set to reach an initial slump flow of 26-28 inches and the workability retention was monitored over time. Between tests, the concrete was returned to the mixer and agitated continuously. Cylinders were obtained from the second batch and tested for compressive strength at 1, 3, 7, and 28 days.

Table 11.5: Mixture Proportions for Comparison of HRWRAs

	Mass (lb/yd³)
Fine Aggregate, LS-02-F	1207.1
Coarse Aggregate, NA-02-C	1464.0
Cement, PC-01-I/II	945.3
Fly Ash	--
Water	323.3
w/c	0.342
S/A	0.45
Paste Volume (%)	39.0

When compared at the same HRWRA dosage, expressed in mass of admixture solids per cement mass, the slump flows were similar, as indicated in Figure 11.17. The HRWRAs essentially resulted in a linear increase in slump flow up to a slump flow of approximately 30 inches. In terms of rheology, Figure 11.18 indicates that increasing the HRWRA dosage decreased yield stress sharply up to a certain dosage, beyond which the change in yield stress was more gradual. This change from sharp to gradual decrease in yield stress corresponds to a slump flow of approximately 15-20 inches. The plastic viscosity continued to decrease beyond this transition in the rate of change in yield stress. Relative to the range of possible plastic viscosities for SCC, the plastic viscosities were all low and did not vary significantly over the range of HRWRA dosages considered. These results reflect that the greatest difference between non-SCC and SCC is the yield stress.
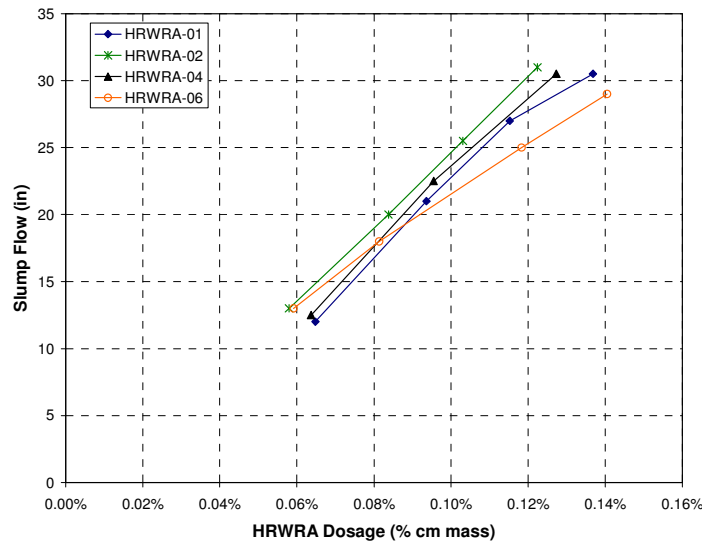
Figure 11.17: Effects of HRWRA Dosage on Slump Flow

255
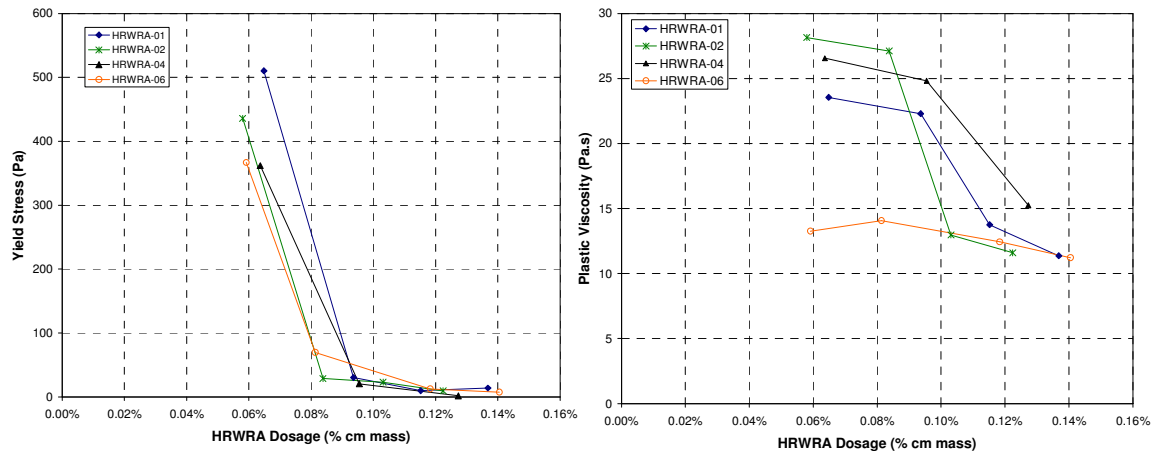
Figure 11.18: Effects of HRWRA Dosage on Yield Stress and Plastic Viscosity

The workability retention varied widely between the HRWRAs, as indicated for slump flow in Figure 11.19. HRWRA-04 and HRWRA-06, which are primarily intended for ready mixed concrete applications, had the longest workability retentions. The relative changes in slump flow were matched in the yield stress measurements, as indicated in Figure 11.20. In contrast, Figure 11.21 indicates that the plastic viscosity remained essentially constant with time. Although the plastic viscosity remained constant, the apparent viscosity did increase with time due to the higher yield stress. The changes in yield stress and plastic viscosity with time reflect that the main fundamental difference between SCC and conventionally placed concrete is the yield stress. Ensuring a near-zero yield stress is essential for all SCC. Once the yield stress is near zero, the most salient difference in workability is the plastic viscosity.

The plots in workability retention reflect just one specific mixture and one specific case. Workability retention depends not just on the characteristics of the specific HRWRA. Other factors affecting workability retention may include the dosage of HRWRA, the type and dosage of retarder, the mixture proportions, the weather conditions, the concrete temperature, and the degree of agitation of the sample.
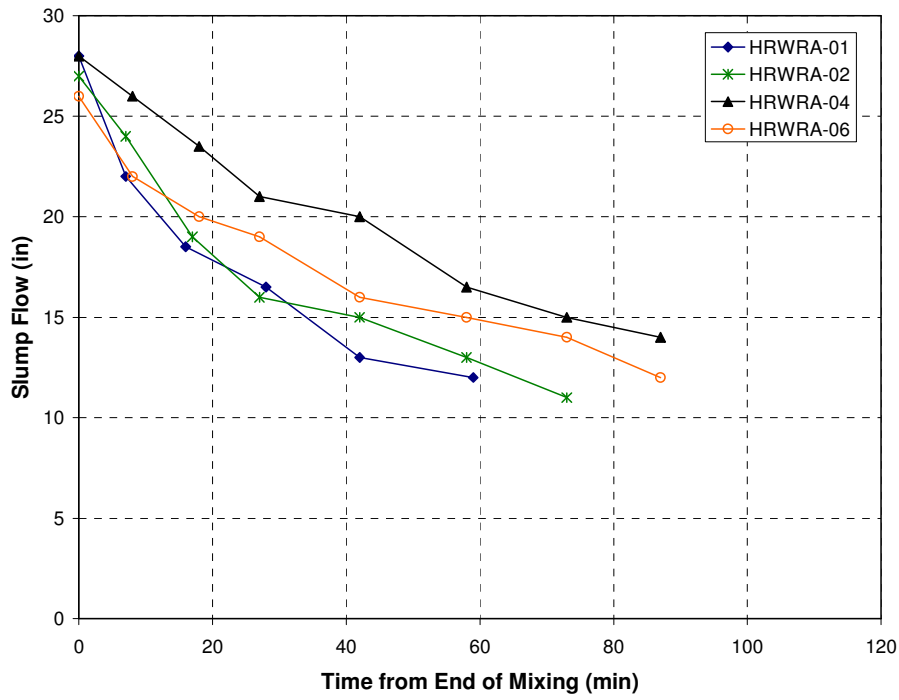
Figure 11.19: Effect of HRWRA on Slump Flow Retention
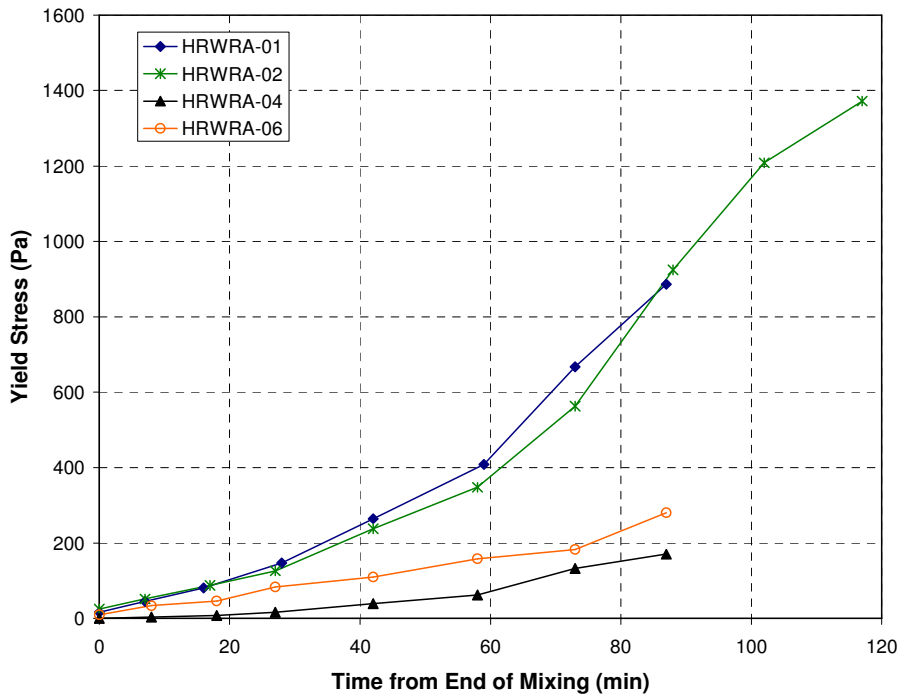
Figure 11.20: Effect of HRWRA on Yield Stress Retention

257
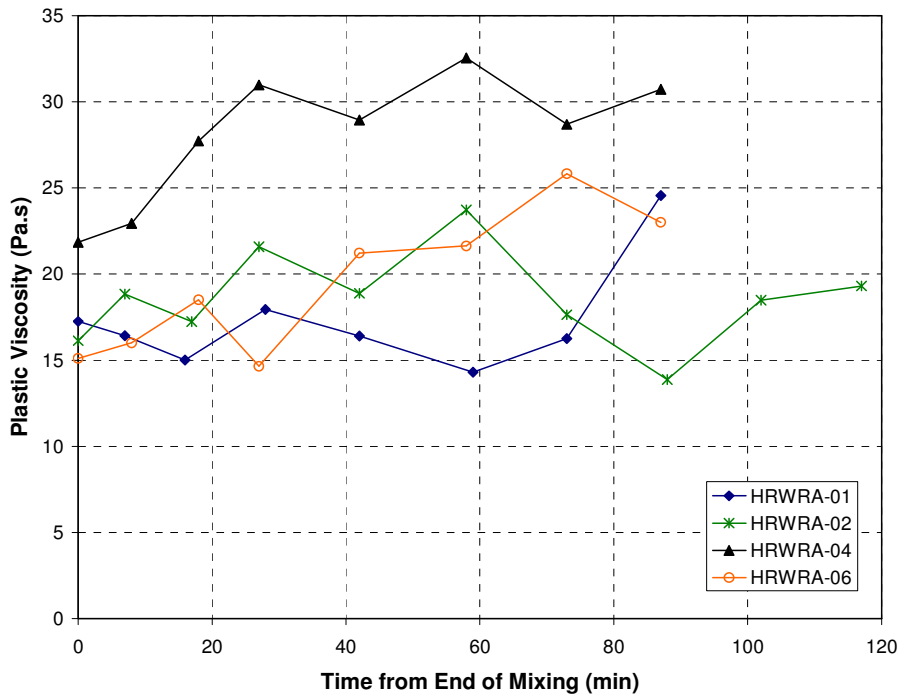
Figure 11.21: Effect of HRWRA on Plastic Viscosity Retention

The development of compressive strength was similar for the 4 mixtures (Figure 11.22). The compressive strength varied from 4,500 to 4,900 psi at one day and from 8,800 to 9,700 psi at 28 days.
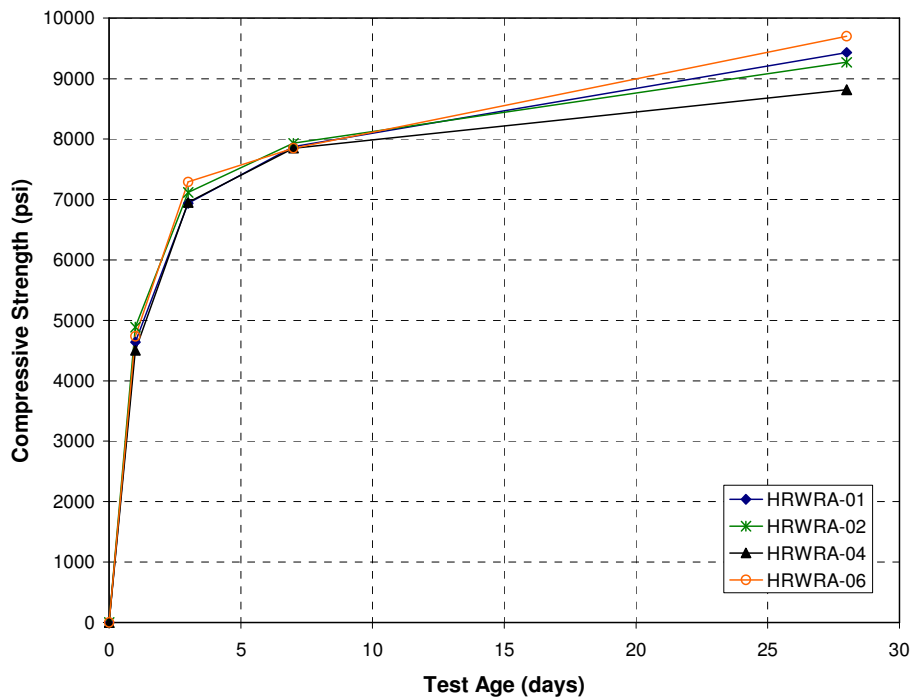
Figure 11.22: Effect of HRWRA on Compressive Strength Development

11.3 Effects of Fly Ash

The performance of the standard fly ash used throughout the research, FA-02-F, was compared to alternate Class F (FA-01-F) and Class C (FA-03-C) fly ashes. The alternate fly ashes were tested at replacement rates of 20, 30, and 40% of the cement mass. The concrete mixture, which is shown in Table 11.6, had a constant paste volume of 36.6%, w/cm of 0.35, and S/A of 0.45. The dosage of HRWRA-02 was adjusted to reach a constant slump flow of 24-26 inches.

The fly ashes all resulted in improvements in workability; however, the degree of improvement varied between fly ashes. The reduction in HRWRA demand for a 24-26-inch slump flow at 40% fly ash replacement rate varied from none for FA-01-F to 30% for FA-02-F, as indicated in Figure 11.23. In contrast, all fly ashes resulted in a reduction in plastic viscosity, with the Class C fly ash resulting in the largest decrease (Figure 11.24). The use of fly ash also consistently reduced the j-ring blocking, as indicated in Figure 11.25, with FA-01-F providing the greatest reduction.

Table 11.6: Mixture Proportions for Comparison of Fly Ashes

Fly Ash	Fly Ash Dosage (%)	Mixture Proportions (lb/yd^3)				
		Cement	Fly Ash	Coarse Aggregate	Fine Aggregate	Water
Control	0	833.0	0.0	1560.0	1286.1	291.5
FA-01-F	20	644.8	161.2	1554.0	1286.1	282.1
	30	555.2	237.9	1554.0	1286.1	277.6
	40	468.4	312.3	1554.0	1286.1	273.2
FA-02-F	20	645.1	161.3	1560.0	1286.1	282.3
	40	470.2	313.4	1560.0	1286.1	274.3
FA-03-C	20	658.6	164.6	1554.0	1286.1	288.1
	30	572.9	245.5	1554.0	1286.1	286.4
	40	488.2	325.5	1554.0	1286.1	284.8
All mixtures have paste volume (including cement, fly ash, microfines, water, air) of 36.6%, w/cm of 0.35, and S/A of 0.45.						

The three fly ashes resulted in similar reductions in 24-hour compressive strengths, suggesting that the pozzolanic activity of each fly ash was insufficient to provide a meaningful contribution to strength in the first 24 hours (Figure 11.26). By 28 days, however, the Class C fly ash contributed greater pozzolanic activity for the development of compressive strength than the two Class F fly ashes, as reflected in the in the slight increase in compressive strength at this age (Figure 11.27). Likewise, the Class C fly ash resulted in greater modulus of elasticity and modulus of rupture, as indicated in Figure 11.28 and Figure 11.29, respectively. The Class F fly ashes; however, resulted in greater reductions in rapid chloride permeability (Figure 11.30). Whereas the Class C fly ash resulted in an increase in drying shrinkage, the Class F fly ashes resulted in no change or slight reductions (Figure 11.31). Therefore, as expected from conventionally placed concrete, the Class C fly ash contributed more to strength while the Class F fly ashes contributed more to durability.
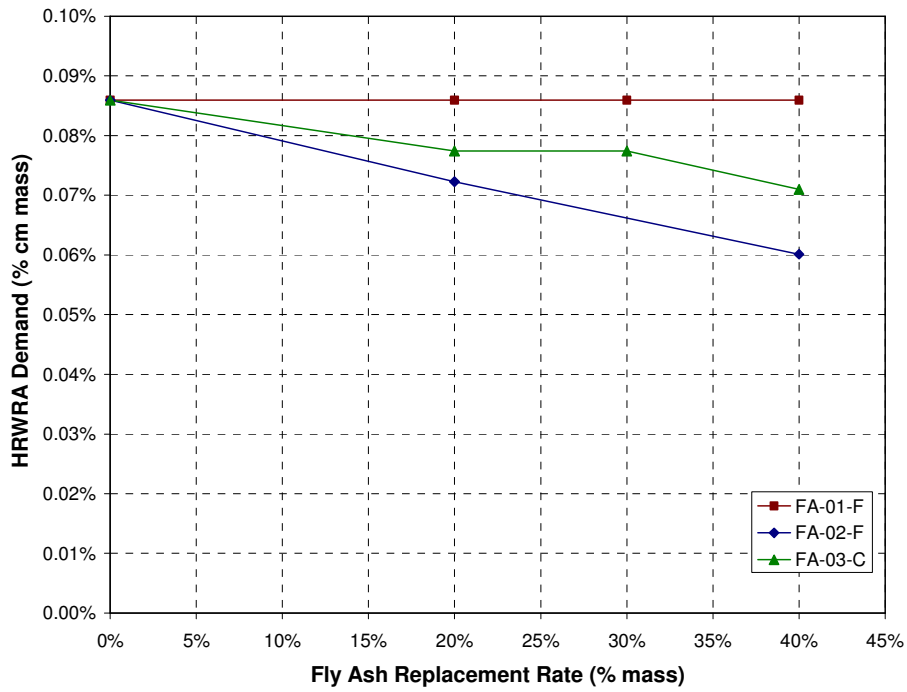
Figure 11.23: Effect of Fly Ash on HRWRA Demand
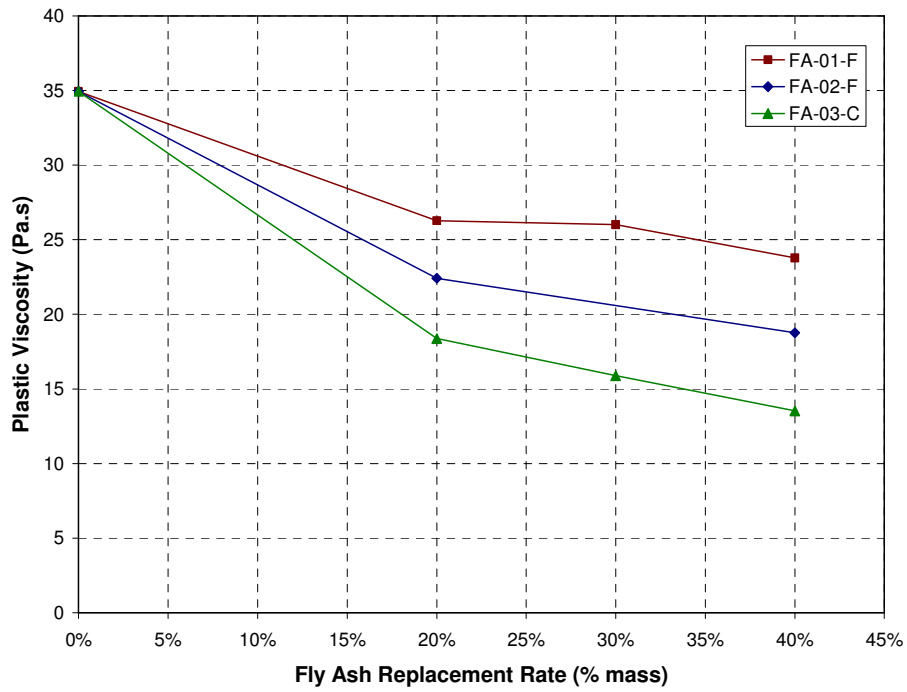
Figure 11.24: Effect of Fly Ash on Plastic Viscosity

261
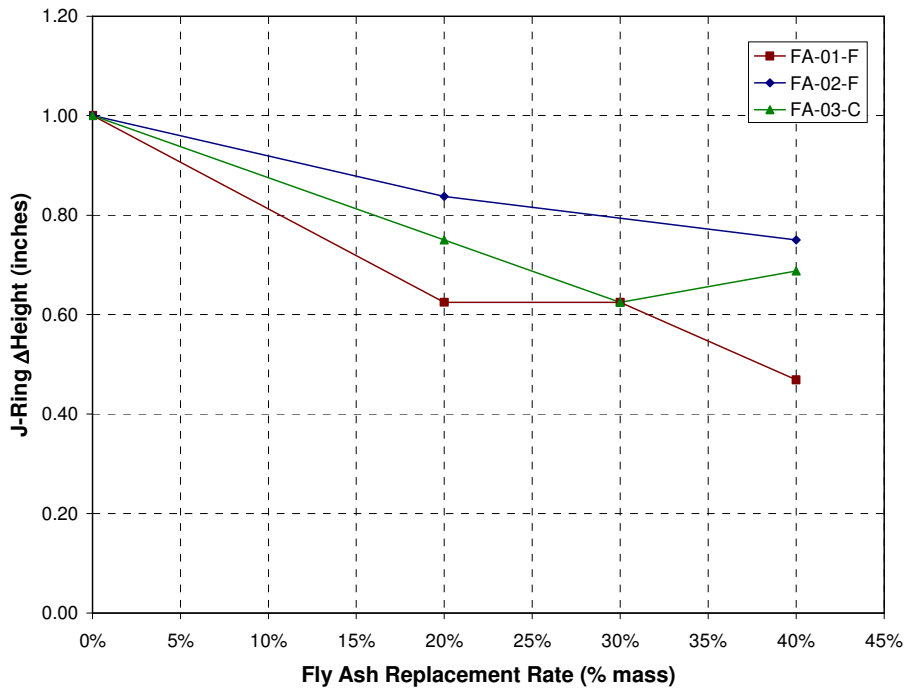
Figure 11.25: Effect of Fly Ash on J-Ring Blocking
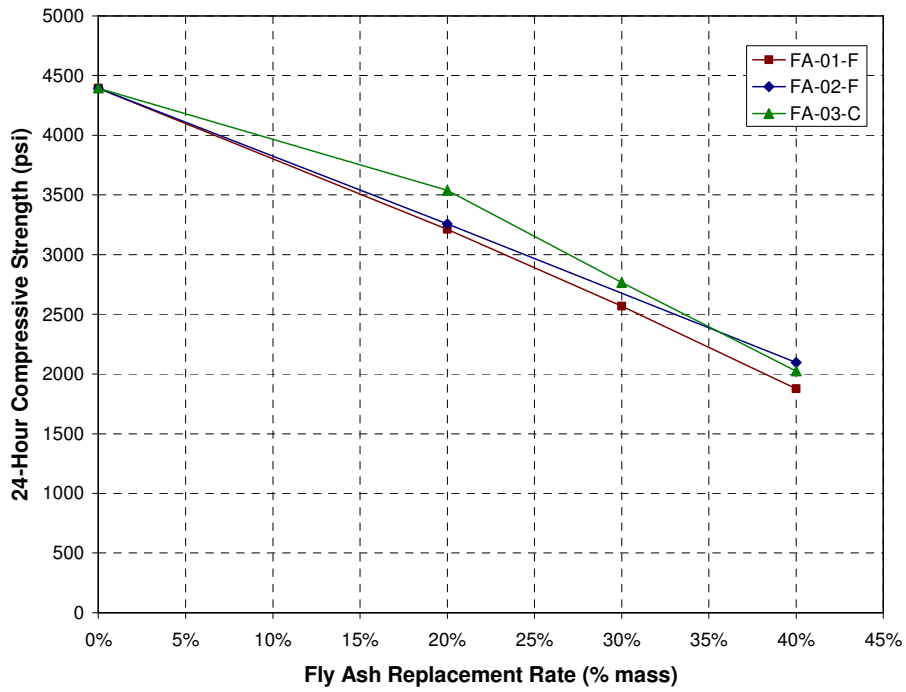
Figure 11.26: Effect of Fly Ash on 24-Hour Compressive Strength
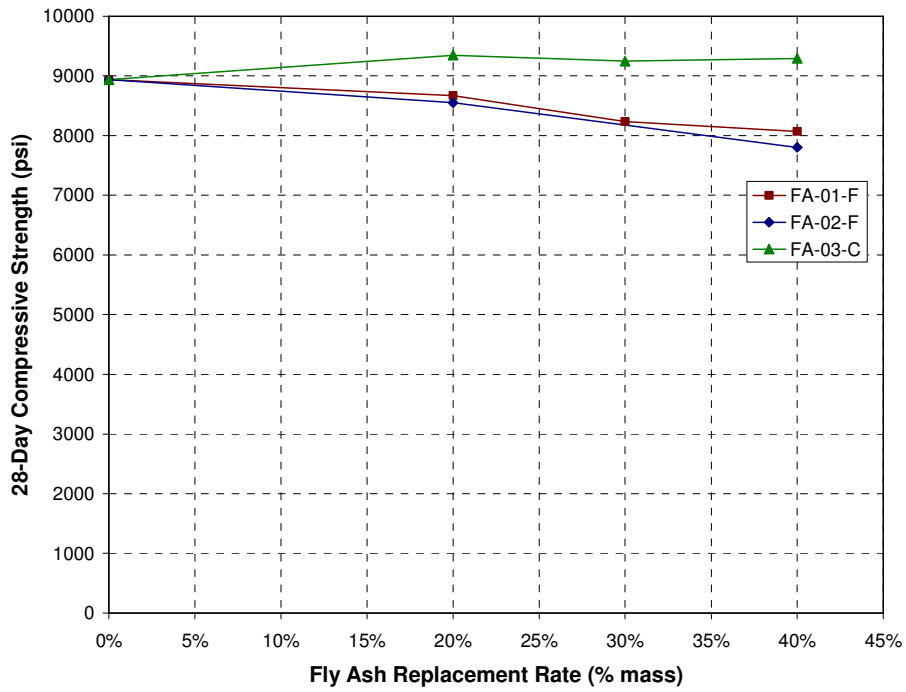
Figure 11.27: Effect of Fly Ash on 28-Day Compressive Strength
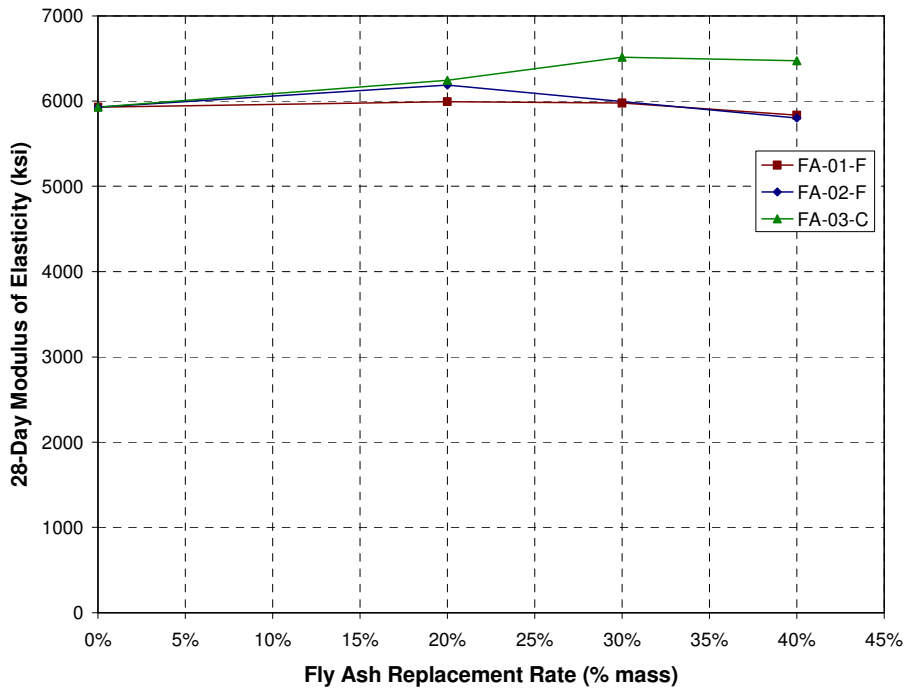
Figure 11.28: Effect of Fly Ash on 28-Day Modulus of Elasticity

263
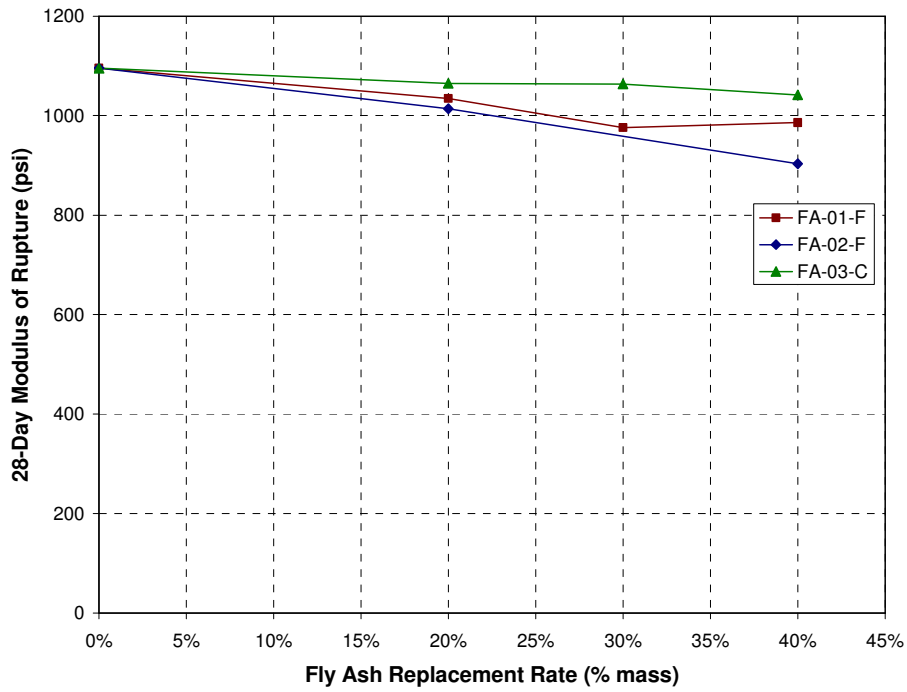
Figure 11.29: Effect of Fly Ash on 28-Day Flexural Strength
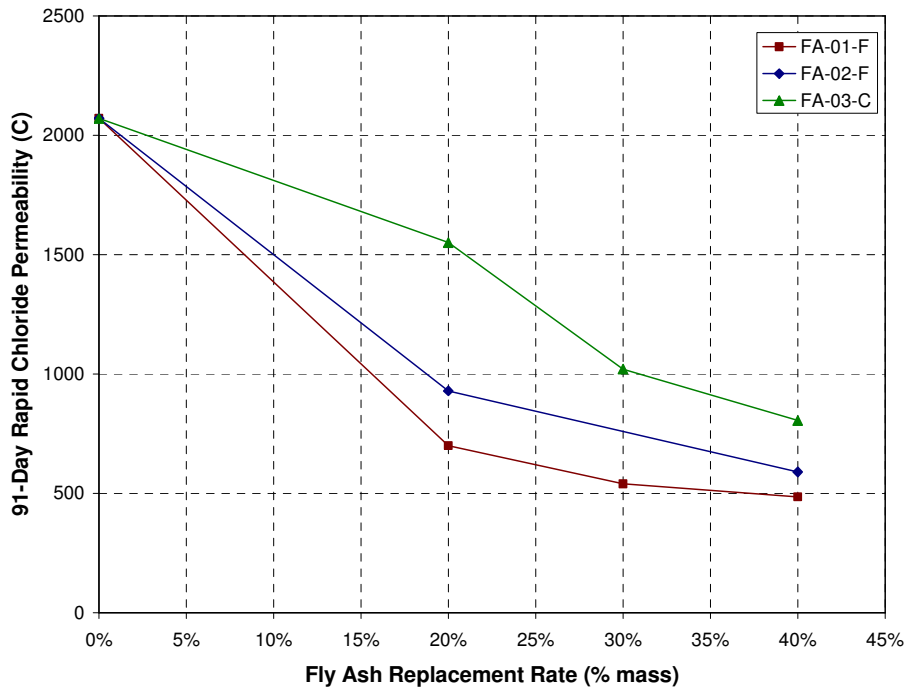
Figure 11.30: Effect of Fly Ash on 91-Day Rapid Chloride Permeability
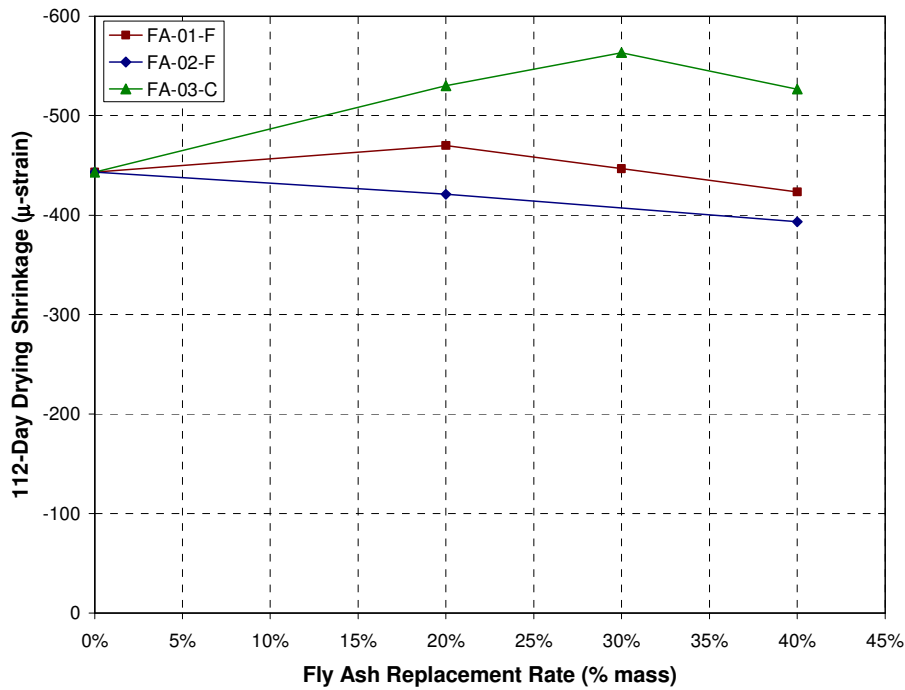
Figure 11.31: Effect of Fly Ash on 112-Day Drying Shrinkage

11.4 Effects of Viscosity-Modifying Admixture

One viscosity modifying admixture, VMA-01, was evaluated in concrete for its effects on workability and hardened properties and its effect on the required minimum paste volume for workability. In the first series of tests, the effect of VMA dosage was evaluated by varying the dosage over the range of the manufacturer's recommended dosages. In the second series of tests, the effect of VMA on the required minimum paste volume for workability was evaluated by varying the paste volume in mixtures with and without VMA.

To compare the effects of VMA dosage on SCC performance, the VMA dosage was varied in the mixture shown in Table 11.7. The dosage was varied from 2 to 14 oz/cwt, which was the manufacturer's range of recommended dosages. A control mixture with no VMA was also tested. A separate batch was tested for each dosage.

To evaluate the effects of VMA on rheology, rheometer measurements were conducted to characterize the magnitude of thixotropy and the degree of shear thinning. To characterize thixotropy, upward and downward flow curves were measured initially and after the concrete was allowed to remain undisturbed in the rheometer container for 5 minutes. The upward curve consisted of 10 speeds measured in ascending order from 0.05 rps to 0.6 rps while the subsequent downward curve consisted of the same 10 speeds measured in descending order. The maximum

speed of 0.6 rps was maintained for 20 seconds between the upward and downward flow curves to ensure full breakdown of any thixotropic structure. The area between the upward and downward rheograms was calculated as one measure of thixotropy. In addition, the torque versus time data for the initial point on the upward curve was evaluated as a stress growth test. The change in yield stress between zero and 5 minutes computed from the stress growth test was used as a second measure of thixotropy.

Table 11.7: Mixture Proportions for Comparison of VMA Dosage

	Mass (lb/yd^3)
Fine Aggregate, LS-02-F	1408.2
Coarse Aggregate, NA-02-C	1397.5
Cement, PC-01-I/II	600
Fly Ash, FA-02-F	200
Water	296
w/cm	0.37
S/A	0.50
Fly Ash Dosage (% mass)	25
Paste Volume (%)	35.9

The main effect of the VMA was to increase the shear-thinning character of the mixtures, as indicated in Figure 11.32. To capture this shear-thinning character, the Herschel-Bulkley model was used instead of the Bingham model. The use of 2 oz/cwt decreased the exponent in the Herschel-Bulkley model from 0.90 to 0.44. An exponent of 1.0 indicates no shear thinning while exponents less than 1.0 indicate increasing degrees of shear thinning. Further dosages of VMA beyond 2 oz/cwt did not substantially change the degree of shear thinning; however, they did result in an upward parallel shift in the rheograms. The shear thinning character has been shown to be advantageous for SCC because the higher apparent viscosity at low shear rates ensures segregation resistance while the lower apparent viscosity at high shear rates is favorable for mixing and placing. The upward parallel shift in the rheograms would likely further enhance the stability of the mixtures.

The VMA also resulted in increased thixotropy as manifested in the upward and downward rheograms plotted in Figure 11.33. Figure 11.34 indicates that the largest increase in thixotropy, as determined both from the increase in breakdown area between the curves and the difference in stress growth yield stresses, was largest at the low dosage of 2 oz/cwt. Just as with

the shear thinning character of the mixtures, the magnitude of thixotropy did not increase with further addition of VMA.

The use of VMA resulted in negligible changes in HRWRA dosage required to achieve a 24-26-inch slump flow, as shown in Figure 11.35. The decrease in HRWRA dosage recorded was small and could have been due to the reduced slump flows at VMA dosages of 8 and 14 oz/cwt. In addition, the stress growth yield stress increased with increasing VMA dosage. Therefore, the HRWRA dosage would need to be increased to maintain a constant stress growth yield stress with increasing VMA dosage. The use of VMA resulted in negligible changes in 24-hour and 28-day compressive strength (Figure 11.36), a slight reduction in 28-day modulus of elasticity (Figure 11.37), negligible change in 28-day flexural strength (Figure 11.38), a slight increase in 91-day rapid chloride permeability (Figure 11.39), and negligible change in 112-day drying shrinkage (Figure 11.40).
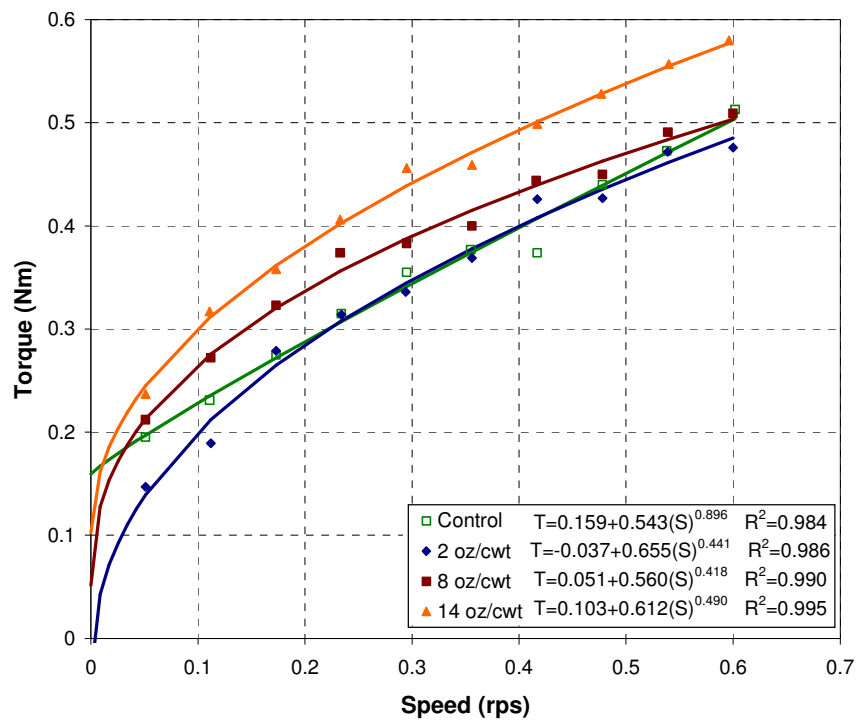
Figure 11.32: Effect of VMA Dosage on Rheograms (Initial Measurements Immediately after Mixing)

267
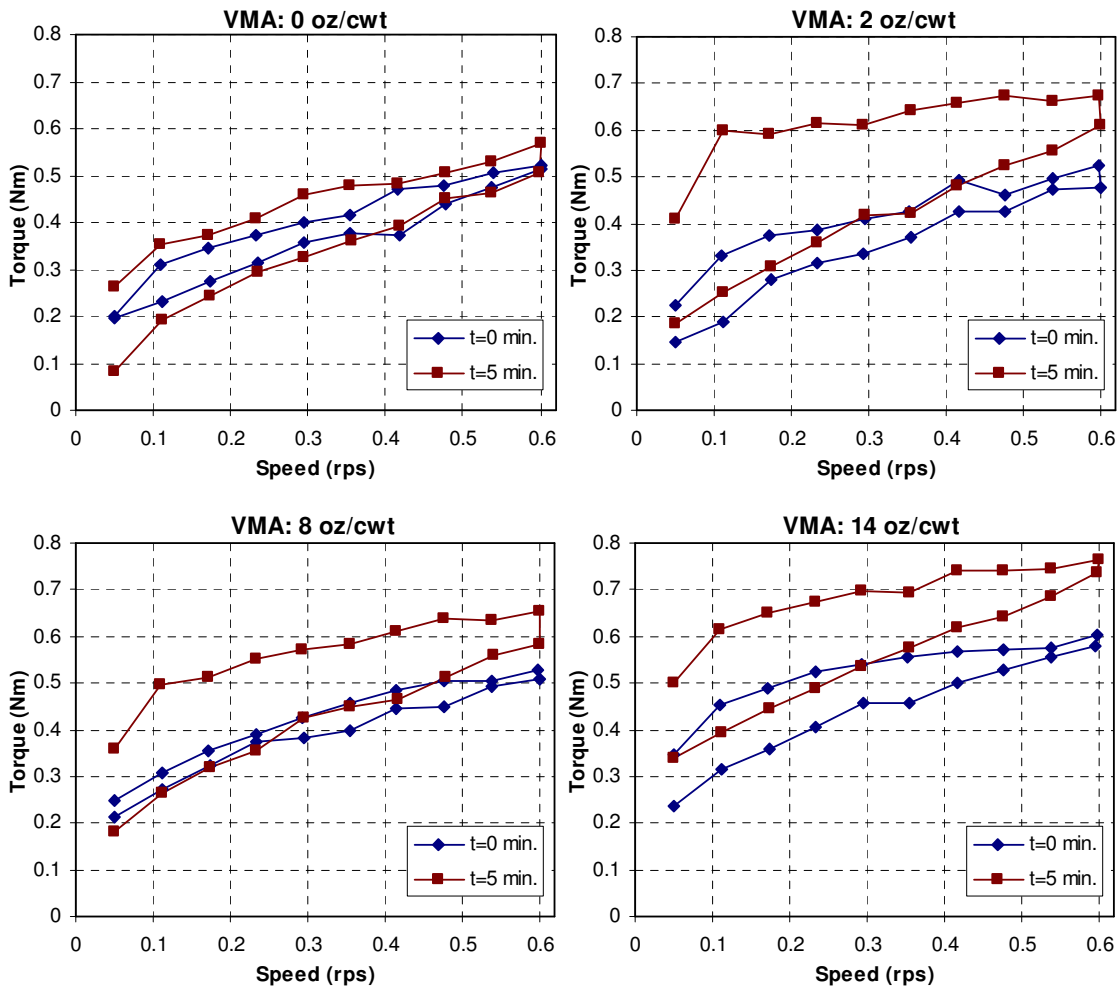
Figure 11.33: Effect of VMA Dosage on Thixotropy
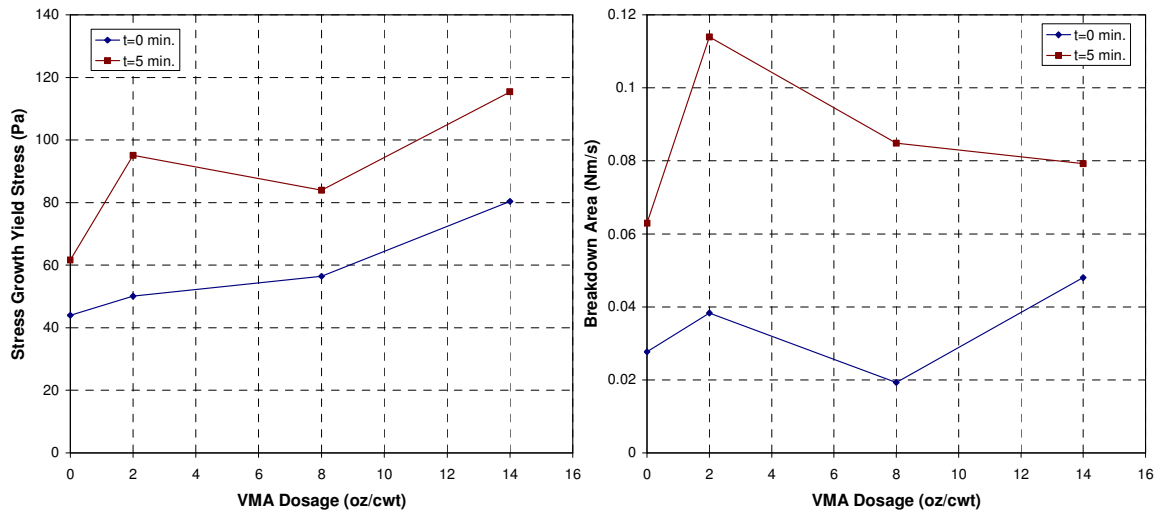
Figure 11.34: Effect of VMA Dosage on Thixotropy Parameters
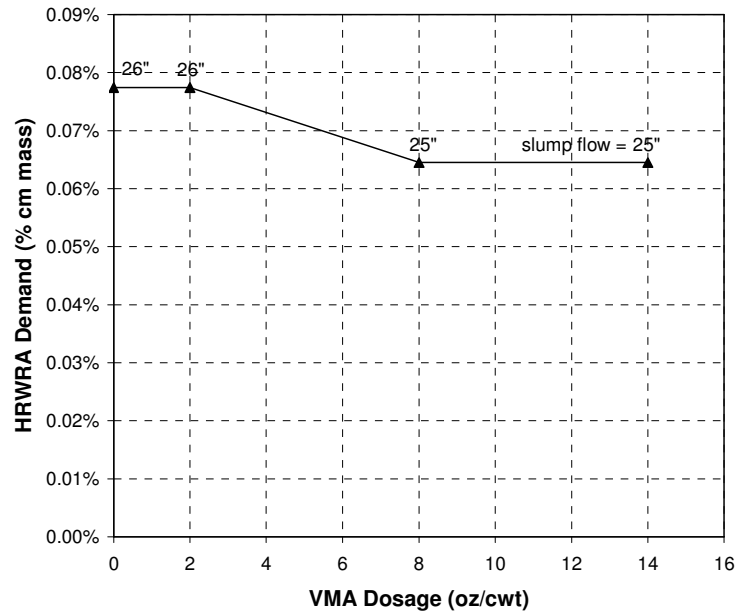
Figure 11.35: Effect of VMA Dosage on HRWRA Demand
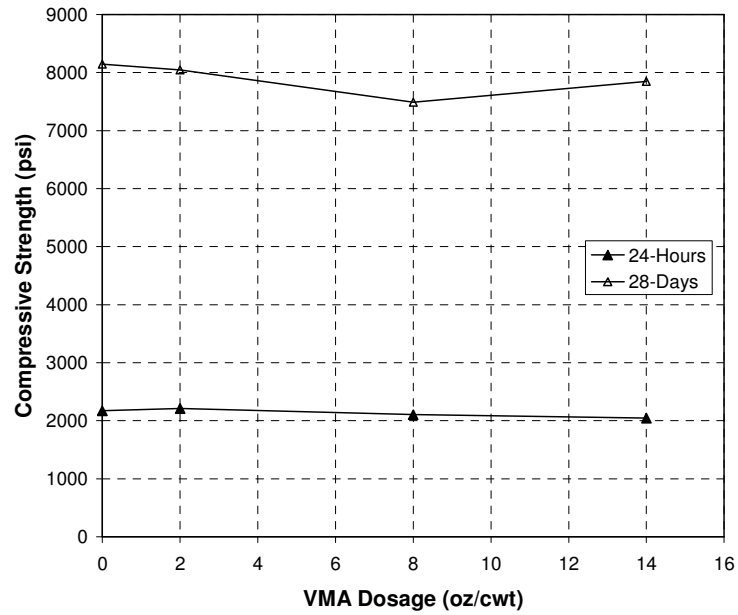
Figure 11.36: Effect of VMA Dosage on Compressive Strength
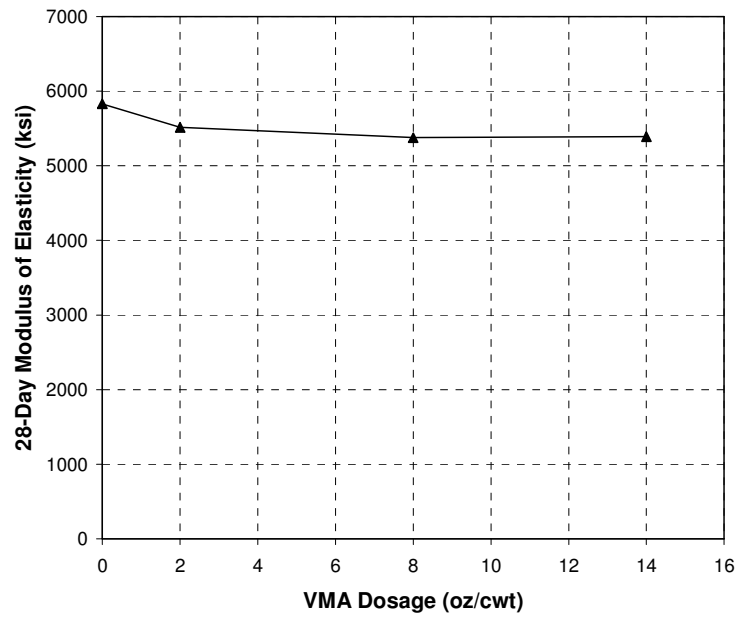
Figure 11.37: Effect of VMA Dosage on 28-Day Modulus of Elasticity
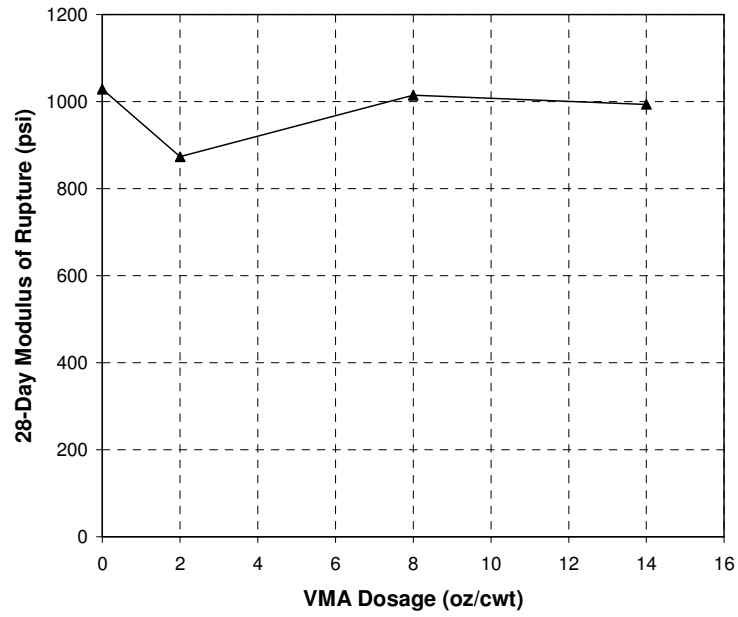
Figure 11.38: Effect of VMA Dosage on 28-Day Flexural Strength
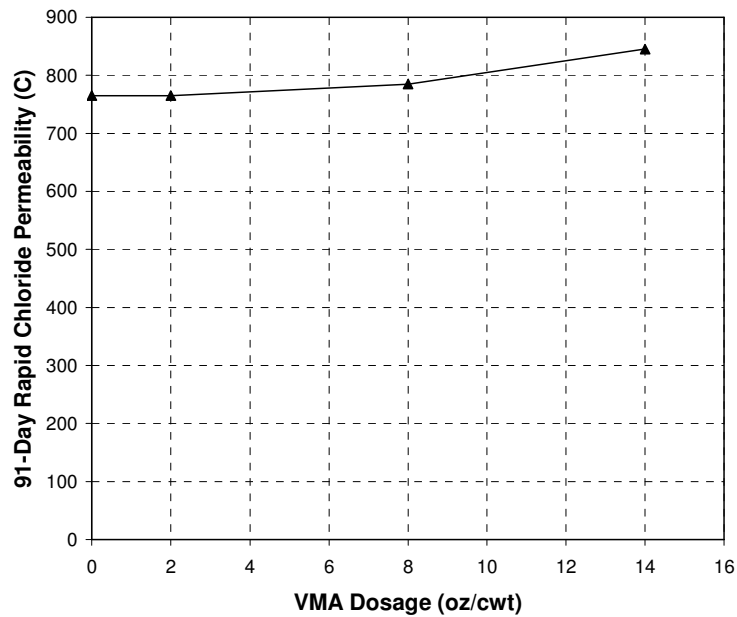
Figure 11.39: Effect of VMA Dosage on 91-Day Rapid Chloride Permeability
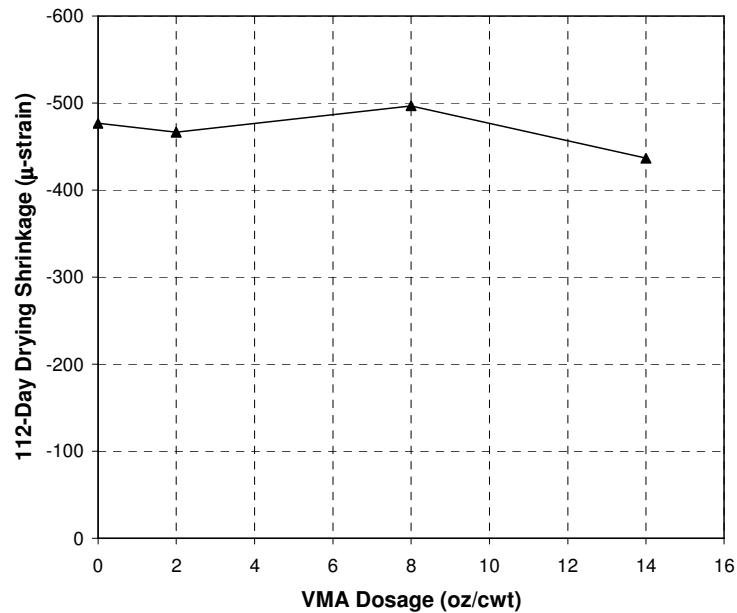
Figure 11.40: Effect of VMA Dosage on 112-Day Drying Shrinkage

In the second series of tests, the effect of VMA on the required paste volume for filling ability was evaluated by measuring mixtures of various paste volumes with and without VMA, as listed in Table 11.8. The mixtures evaluated were used earlier to evaluate the effect of DO-01-F fine aggregate at various paste volumes (Section 10.4). The VMA was used at the manufacturer's maximum recommended dosage of 14 oz/cwt.

271

Table 11.8: Mixture Proportions for Evaluation of VMA at Various Paste Volumes

Mix[1]	Paste Volume (%)[2]	w/p	Mixture Proportions (lb/yd³)[3]					
			Cement	Fly Ash	Coarse Agg.	Fine Agg.	Water	VMA[4]
VPV1	32.7	1.031	633.0	117.6	1613.7	1494.3	262.7	14
VPV2	35.2	1.032	684.9	127.2	1554.0	1439.0	284.2	14
VPV3	37.7	1.034	736.7	136.8	1494.2	1383.6	305.7	14
P9	32.7	1.031	633.0	117.6	1613.7	1494.3	262.7	
P10	35.2	1.032	684.9	127.2	1554.0	1439.0	284.2	
P11	37.7	1.034	736.7	136.8	1494.2	1383.6	305.7	
P12	40.2	1.035	788.6	146.5	1434.4	1328.3	327.3	
P13	42.7	1.036	840.5	156.1	1374.7	1273.0	348.8	

[1]All mixes have w/cm = 0.35, S/A = 0.45, 15.7% fly ash by mass, mixtures denoted with 'P' tested without VMA, mixtures denoted with 'VPV' tested with VMA
[2]Paste volume includes air, cement, fly ash, water, and microfines
[3]Cement: PC-01-I/II; fly ash: FA-02-F; coarse aggregate: DO-01-C; fine aggregate: LS-02-F
[4]Expressed in oz/cwt

The use of VMA did not reduce the amount of paste volume required to achieve SCC workability. The series of mixtures tested without VMA required a minimum paste volume of approximately 38%, while all mixtures below 38% paste volume tested with VMA were determined to have insufficient paste volume. When tested at various paste volumes, the use of VMA was found to increase HRWRA demand (Figure 11.41), reduce plastic viscosity (Figure 11.42), not affect j-ring blocking (Figure 11.43), reduce compressive strength at 24 hours (Figure 11.44) and 28 days (Figure 11.45), not affect 28-day modulus of elasticity (Figure 11.46), not affect 28-day modulus of rupture (Figure 11.47), increase rapid chloride permeability (Figure 11.48), and not affect 112-day drying shrinkage (Figure 11.49). The results should be interpreted with caution because the mixtures below 38% paste volume were determined to have insufficient paste volume. The resulting bleeding, segregation, poor consolidation, and harshness could have affected the reported results. At the lowest paste volume, the VMA did not result in a shear thinning character in the measured rheogram, as shown in Figure 11.50. At higher paste volumes, the shear thinning character was evident. It is likely that the characteristics of the paste did not have a consequential effect on the concrete properties at the lowest paste volume. As the paste volume increased, the characteristics of the paste should have had greater impact on the concrete characteristics.
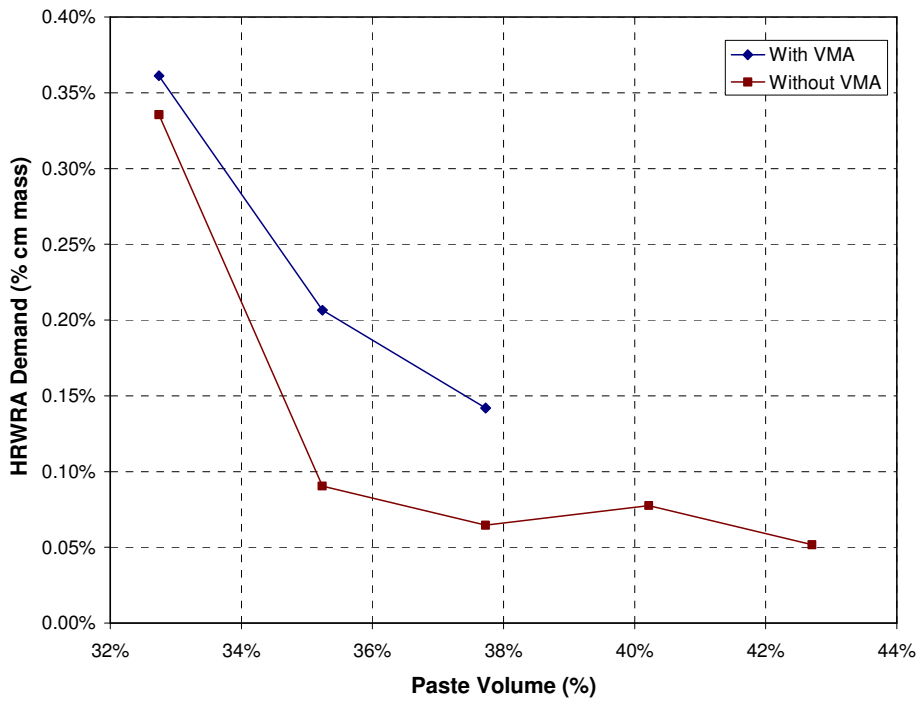
Figure 11.41: Effect of VMA on HRWRA Demand at Various Paste Volumes
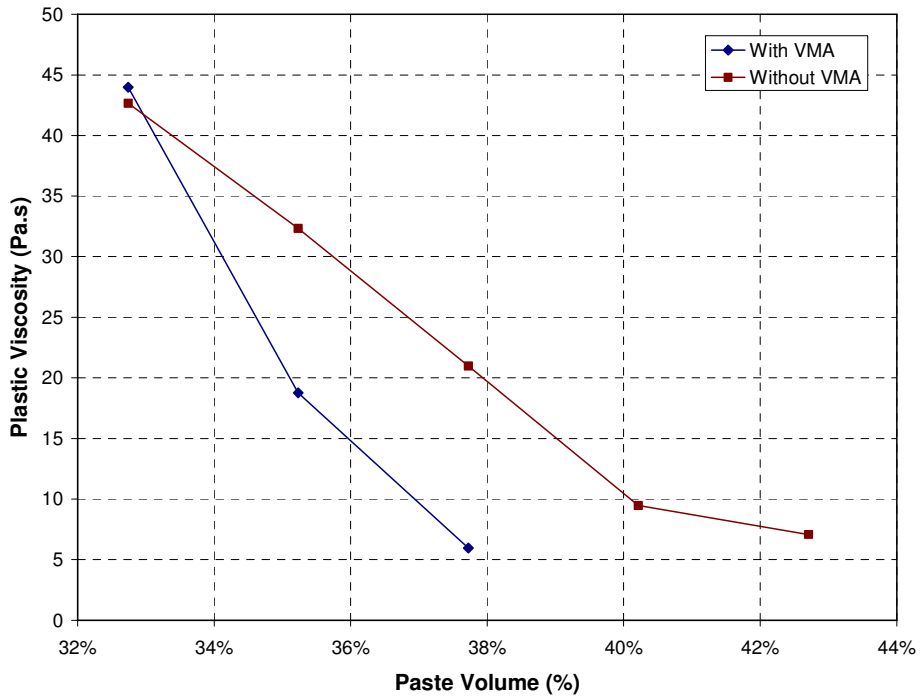
Figure 11.42: Effect of VMA on Plastic Viscosity at Various Paste Volumes

273
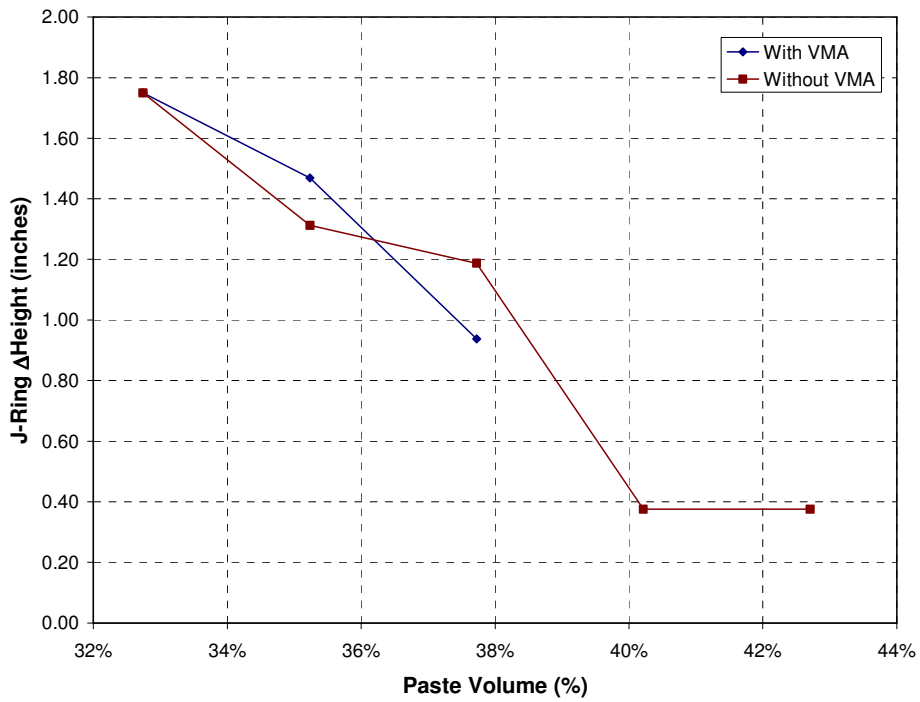
Figure 11.43: Effect of VMA on J-Ring Blocking at Various Paste Volumes
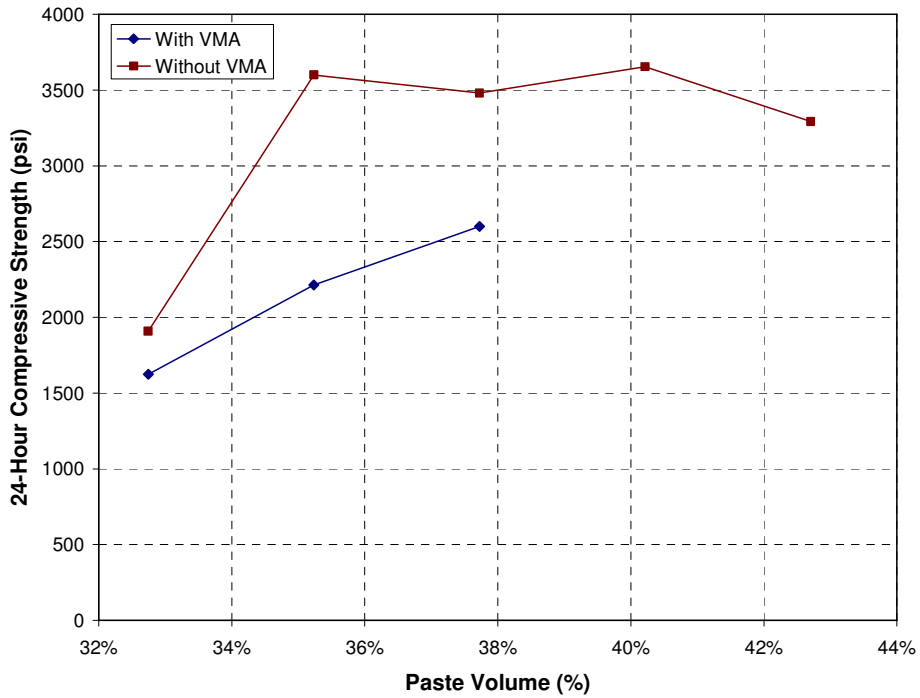
Figure 11.44: Effect of VMA on 24-Hour Compressive Strength at Various Paste Volumes

274
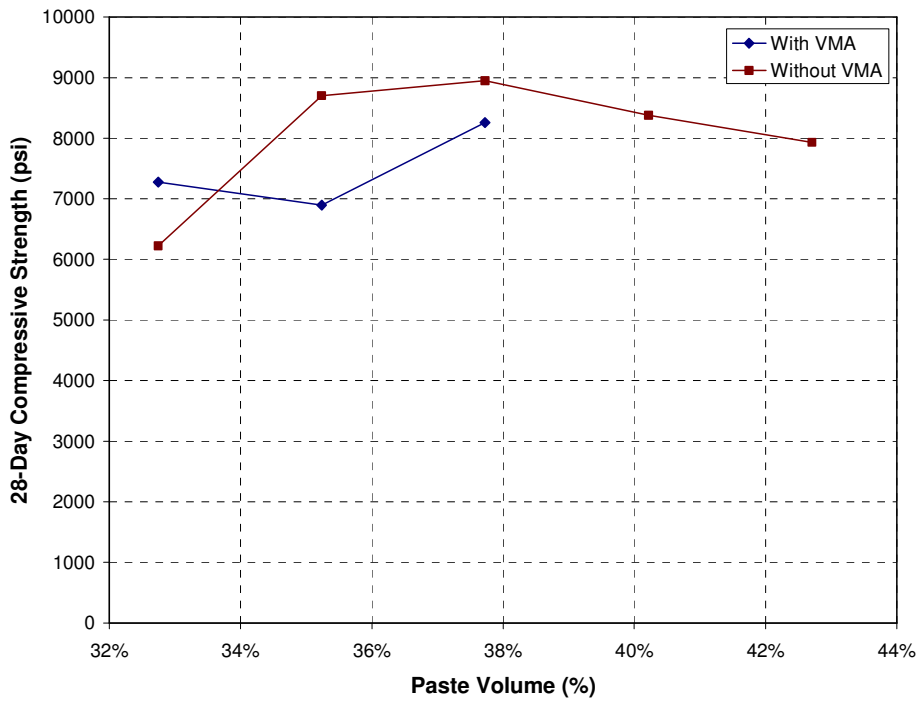
Figure 11.45: Effect of VMA on 28-Day Compressive Strength at Various Paste Volumes
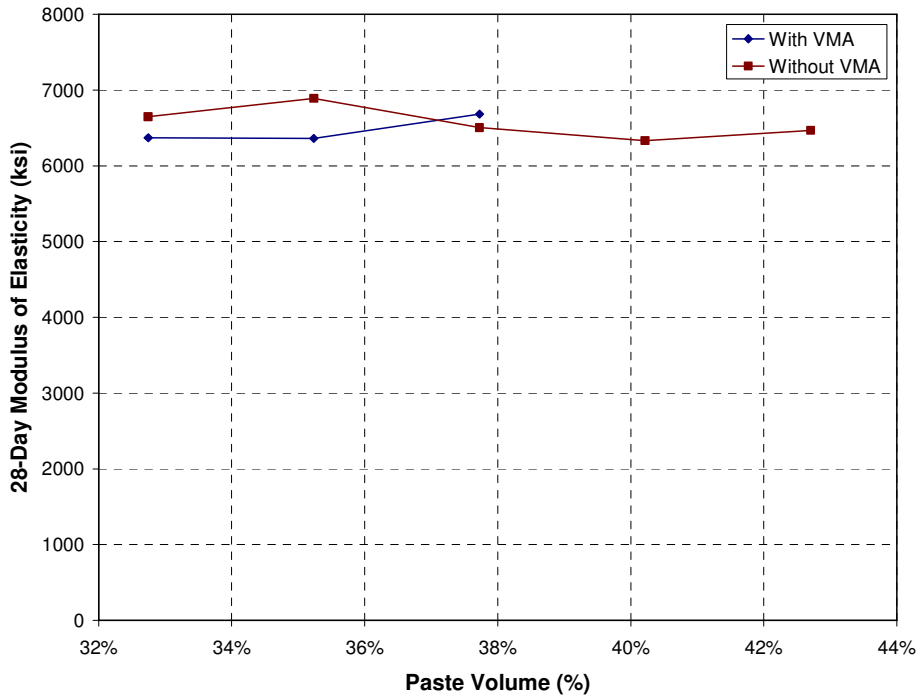
Figure 11.46: Effect of VMA on 28-Day Modulus of Elasticity at Various Paste Volumes

275
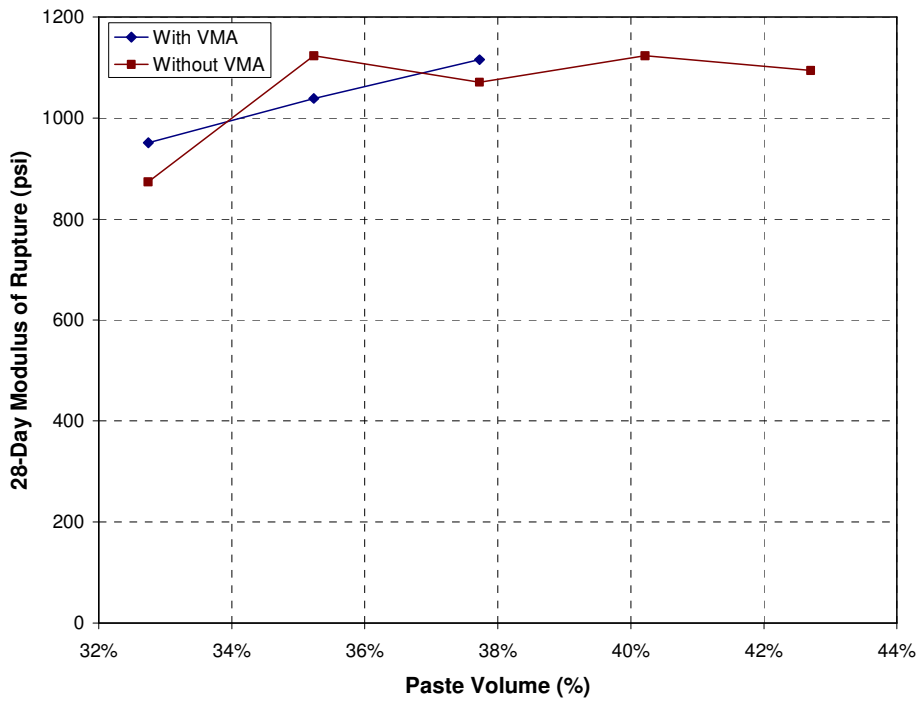
Figure 11.47: Effect of VMA on 28-Day Flexural Strength at Various Paste Volumes
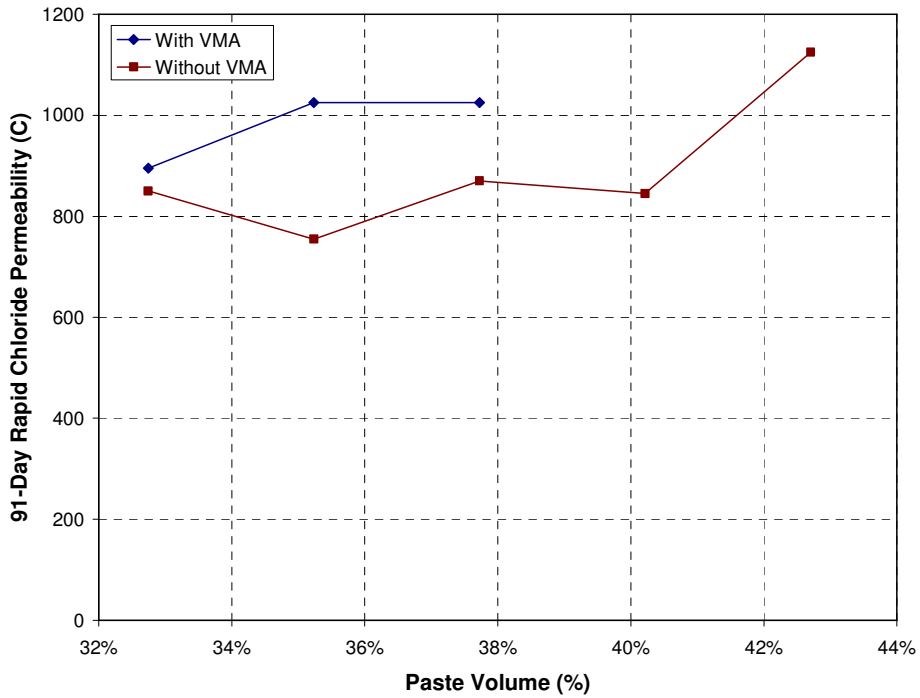
Figure 11.48: Effect of VMA on 91-Day Rapid Chloride Permeability at Various Paste Volumes
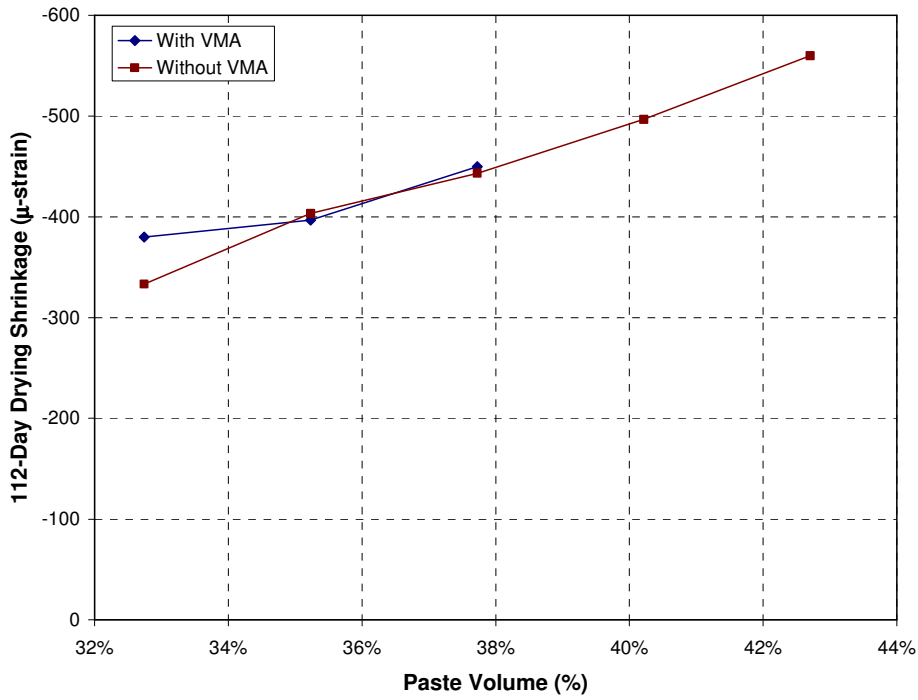
Figure 11.49: Effect of VMA on 112-Day Drying Shrinkage at Various Paste Volumes
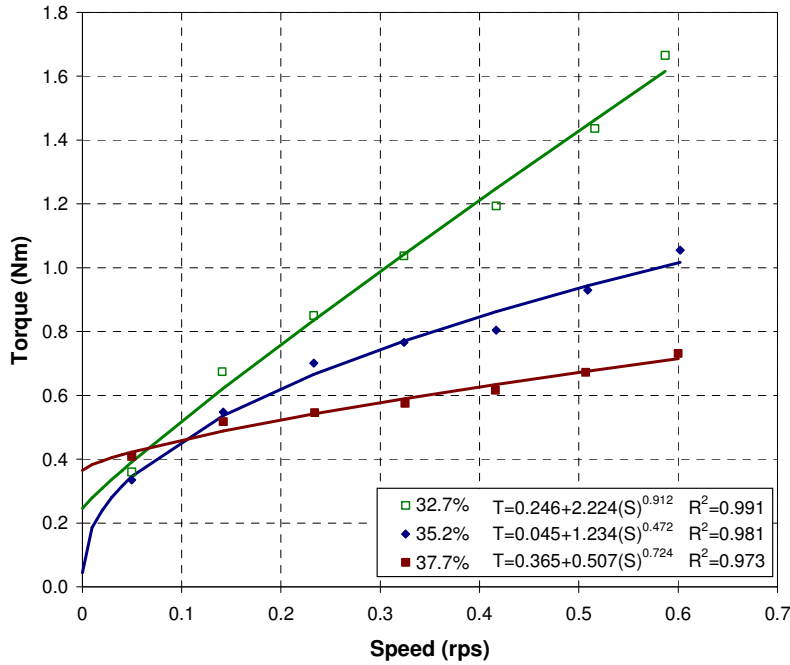
Figure 11.50: Effect of VMA on Shear Thinning Character at Various Paste Volumes

11.5   Conclusions

The following conclusions can be drawn based on the test results presented in this chapter:

- The effects of paste volume, water content, fly ash dosage, and sand-aggregate ratio on workability and hardened properties were consistent for the two material sets tested. Increasing the paste volume, water-powder ratio, and fly ash dosage improved SCC workability as measured in terms of HRWRA demand, plastic viscosity, and j-ring blocking, while increasing the S/A ratio mainly resulted in reduced j-ring blocking and slightly increased HRWRA demand and plastic viscosity. Compressive and flexural strengths were most significantly affected by the w/c at 24 hours and the w/cm and fly ash dosage at 28 days. The modulus of elasticity decreased slightly with increased paste volume and S/A but was mainly affected by the w/cm. Rapid chloride permeability increased with increasing paste volume and w/cm and decreasing fly ash dosage, while drying shrinkage mainly increased with increasing paste volume.

- The four HRWRAs that were compared in concrete resulted in similar workability and compressive strength development when compared at equivalent admixture solids volumes. The workability retention was better for the two HRWRAs intended for ready mixed concrete applications.

- The results from the HRWRA testing highlighted that the fundamental difference between the workability of SCC and conventionally placed concrete is the near-zero yield stress required for SCC. The main effect of HRWRA was significantly decreased yield stress while plastic viscosity was decreased by a much smaller relative amount.

- The use of fly ash resulted in improved workability, although the extent of the improvement depended on the particular fly ash used. Compared to the two Class F fly ashes, the Class C fly ash resulted in higher compressive and flexural strengths at 28 days but also higher 91-day rapid chloride permeability and 112-day drying shrinkage.

- The VMA tested in concrete resulted in a shear-thinning character and an increase in thixotropy. The use of this VMA did not reduce the minimum paste volume required to achieve SCC workability properties. Further, the particular VMA tested had minimal effects on hardened properties.

Chapter 12: Comparison of Paste, Mortar, and Concrete Measurements

The test results for paste, mortar, and concrete were compared to establish relationships between each of these phases. These relationships can be used to establish target properties for paste and mortar and to simplify the testing required for selecting materials and proportions. Understanding how paste and mortar rheology affect concrete workability aids in selecting mixture proportions and evaluating concrete workability. For instance, because HRWRA acts on paste, understanding how paste rheology affects concrete workability is important for selecting the correct HRWRA dosage for concrete. In addition, this chapter explores the relationships between modulus of elasticity and compressive strength and between modulus of rupture and compressive strength.

12.1 Workability

12.1.2 Relationship between Paste and Concrete

To achieve SCC workability, the concrete must exhibit near-zero yield stress and moderate plastic viscosity. The main fundamental difference between SCC and conventionally placed concrete is the yield stress. Compared to conventionally placed concrete, the yield stress is often one to two orders of magnitude lower for SCC (less than 100 Pa for SCC). The relative reduction in plastic viscosity is much less. In fact, the plastic viscosity of SCC may be similar to that of conventionally placed concrete. For instance, a 6-inch slump concrete may have a yield stress of 600 Pa and a plastic viscosity of 40 Pa.s whereas a SCC mixture may have a yield stress of 20 Pa and a plastic viscosity of 40 Pa.s. The change in concrete yield stress is directly related to the paste rheology because the HRWRA, which is mainly responsible for the decrease in yield stress, acts on the paste. Whereas it is possible to reduce the yield stress and plastic viscosity of paste to near zero, it is only possible to decrease the yield stress of concrete to near zero. The plastic viscosity of concrete is not reduced to near zero because of the contribution of aggregates to plastic viscosity and the need for a sufficiently high paste plastic viscosity to prevent instability.

Although the addition of HRWRA is the main cause of the drastic reduction in concrete yield stress associated with SCC, the paste volume and paste composition must be appropriate so that the concrete is stable and placeable when the yield stress is reduced to near zero. Figure 12.1 indicates that the yield stress is reduced to near zero in both concrete and paste as the HRWRA dosage is increased. The paste and concrete mixtures compared in this figure have the same cement. The solids volume fraction of the paste fraction of the concrete (0.514) matches that of the paste only mixtures. (The paste solid fraction is considered to consist of all power finer than 75 μm, including microfines. The powder consists of cement and aggregate microfines for the concrete mixtures but only cement for the paste only mixtures.) As HRWRA dosage is increased, the yield stress is first reduced drastically and then reduced gradually after reaching an inflection point. The inflection point for concrete occurred at a lower dosage than for paste, which was likely due to the high paste volume of the concrete, the use of different rheometers for paste and concrete, and the inclusion of aggregate microfines instead of only cement as part of the paste solids volume fraction. A lower paste volume in the concrete—with the same paste composition—would have resulted in inflection points at higher HRWRA dosages. The behavior of concrete beyond the inflection point is important even though the relative difference in yield stress is minimal. Figure 12.2 indicates that the change in slump flow with changes in yield stress increases with reduced yield stress, such that a very small change in yield stress results in a large change in slump flow at low yield stresses. In this case, the inflection point occurred at a yield stress of approximately 30 Pa, which corresponded to a slump flow of approximately 20-22 inches. This slump flow range represents the approximate transition between conventionally placed concrete and SCC.

Figure 12.3 indicates that it is possible to reduce the plastic viscosity of paste to near zero at sufficiently high HRWRA dosages. Indeed, the rheology of the paste can approach that of water. This paste rheology is clearly unsuitable because a paste with rheology near that of water would have insufficient viscosity and would quickly flow out of the aggregate matrix without mobilizing aggregate particles. This paste would also have little thixotropy due to the high degree of dispersion. The paste reached zero plastic viscosity at higher dosages than the yield stress, resulting in a range of dosages with near zero yield stress but non-zero plastic viscosity. In the case shown in Figure 12.3, the near zero paste plastic viscosity occurred after the concrete slump flow reached 32 inches, which is approximately the maximum possible slump flow for SCC. If the paste volume were lower, the plastic viscosity may have been reduced to near zero

prior to reaching a 32-inch slump flow. Such a condition would explain the observed severe bleeding and instability in mixtures lacking sufficient paste volume. Therefore, the concrete paste volume must be sufficient such that the paste plastic viscosity is not reduced to near zero prior to achieving the desired slump flow. For a certain paste composition, the main factor affecting this needed paste volume is the aggregate.

The recorded yield stresses were of the same approximate order of magnitude for paste and concrete while the concrete plastic viscosities were more than an order of magnitude greater than the paste plastic viscosities. Therefore, the inclusion of aggregates contributes mainly to concrete plastic viscosity. If adequate paste volume is provided to achieve SCC workability properties for a given aggregate and the paste composition is within a certain appropriate range for the given aggregate and paste volume, the concrete yield stress can be reduced to near zero. Therefore, the main difference in rheology from one SCC to another is the plastic viscosity. Improving the aggregate shape and paste composition and increasing the paste volume can result in reduced plastic viscosity. In addition, improving the aggregate and changing the paste volume can reduce the HRWRA demand needed to reach the range of yield stresses and slump flows associated with SCC.

The higher plastic viscosities associated with polycarboxylate-based HRWRAs relative to naphthalene-based HRWRAs are generally beneficial in securing the desired paste and concrete rheological properties. In some cases, however, the plastic viscosities associated with a polycarboxylate-based HRWRA may be too high, especially in cases with low water-powder ratios. The variation in plastic viscosities produced by different polycarboxylate-based HRWRA also mean that a polycarboxylate-based HRWRA appropriate for one application may not be the best for another application.

Comparing paste and concrete rheology at a constant w/cm or w/p is indirect because paste measured separately from concrete does not exhibit the same behavior as the paste in concrete for three main reasons. First, there is interaction between powder materials in the paste and larger aggregate particles in concrete. Blending two particle distributions together changes the overall particle size distribution, resulting in greater polydispersity among other things. As such, removing all powder particles smaller a certain size for separate testing does not fully reflect the behavior of that material in the concrete mixture. Furthermore, the powder from the aggregates changes the water-powder ratio of the paste in concrete. There is not a discrete division between aggregate particles that should be accounted for as part of the paste or

aggregate; however, some aggregate particles are typically the same size as cement, slag, and fly ash particles. Second, the shear rates during testing are different for paste tested separately from concrete and paste in concrete. For a given bulk shear rate, the aggregates affect the shear rate experienced by the paste in concrete. The shear rate experienced by paste in concrete can be much more variable than paste measured separately. Third, the mixing history is different for paste mixed separately from the concrete and for paste in concrete. The paste in the concrete and paste mixed separately from the concrete are mixed for different time periods under different shear rates.

Further complicating the comparison of paste and concrete rheology is the fact that changes to aggregate characteristics or paste volume can change the paste rheology needed to achieve SCC workability. For instance, a concrete mixture with a more angular aggregate but the same paste volume would require different paste rheology. The required paste rheology changes as the paste volume in a given mixture is changed. Nonetheless, paste measurements can be used to evaluate the relative effects of changes in materials and proportions for chemical admixtures and powder materials.
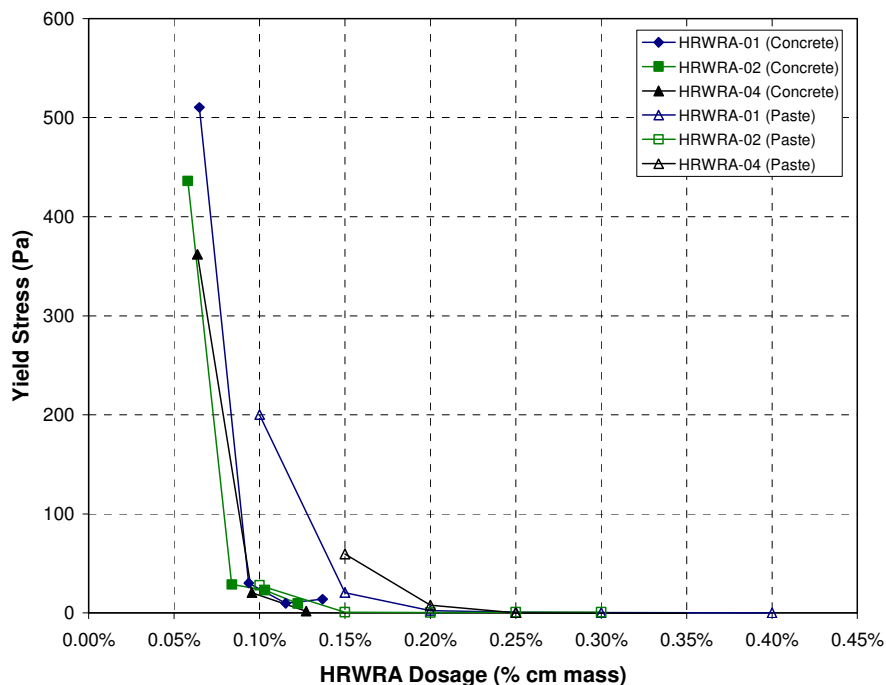
Figure 12.1: Comparison of Effects of HRWRA Dosage on Yield Stress for Concrete and Paste
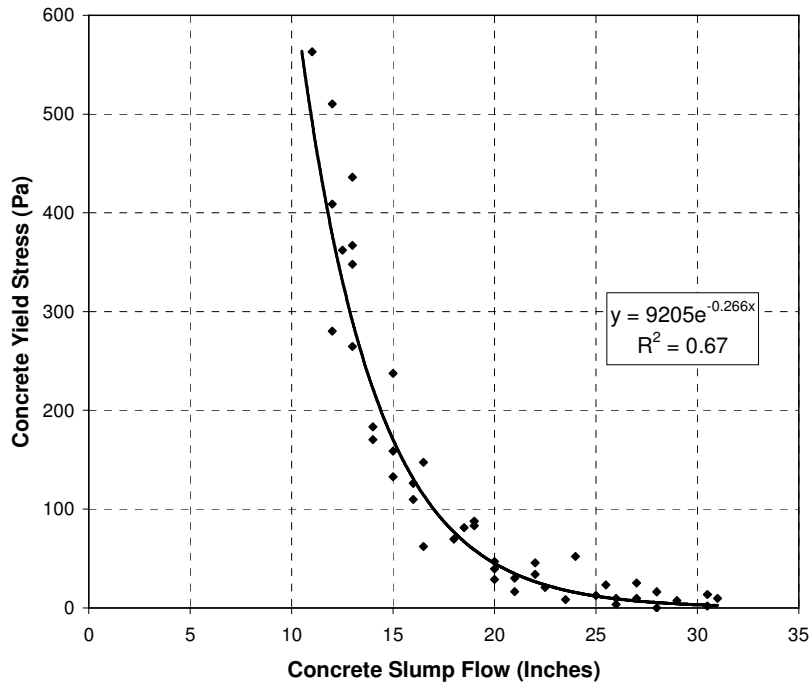
Figure 12.2: Relationship between Concrete Yield Stress and Slump Flow (Constant Mixture Proportions, Variable HRWRA Type and Dosage)

The equation shown on Figure 12.2 is:

$$y = 9205e^{-0.266x}$$
$$R^2 = 0.67$$
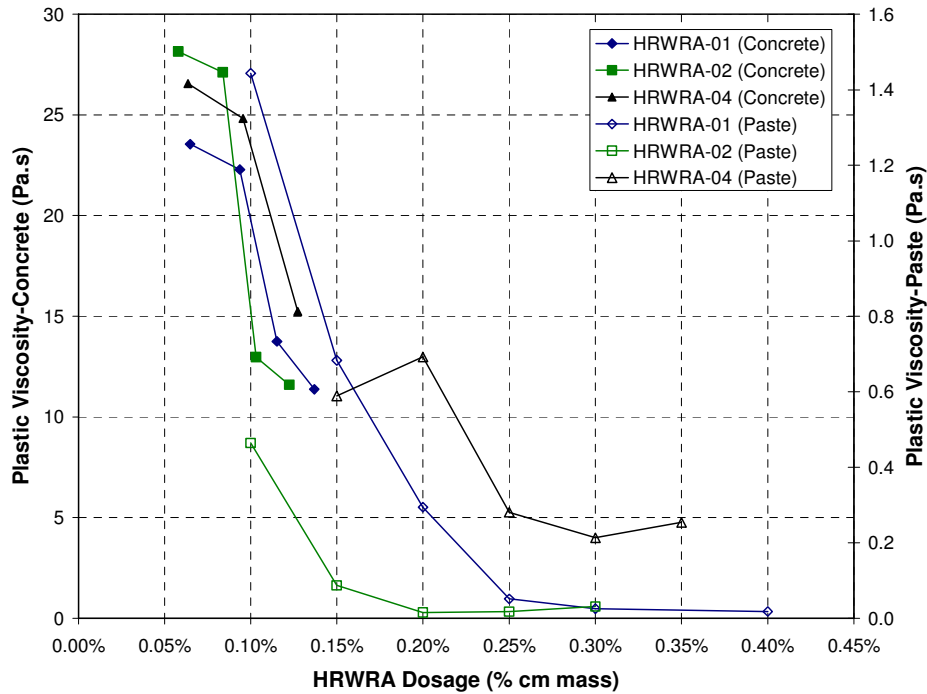
Figure 12.3: Comparison of Effects of HRWRA Dosage on Plastic Viscosity for Concrete and Paste

283

12.1.2 Relationship between Mortar and Concrete

The fresh properties for comparable mortar and concrete mixtures were well correlated. Figure 12.4 indicates that the mortar and concrete HRWRA demand was generally well correlated. The water-powder ratio was higher for the mortar mixtures than for the concrete mixtures, which was partially responsible for the higher HRWRA dosages in mortar than in concrete. Further, varying the paste volume of the concrete or mortar would be expected to affect the HRWRA demand. In this case, the mortar mixtures had higher paste volume while the concrete mixtures had greater polydispersity. As with paste, a discrete size separating mortar from concrete does not exist—the use of the No. 4 sieve is for convenience and is based on industry practice. Still, mortar measurements can be used to evaluate the relative effects of materials and mixture proportions in mortar.

Figure 12.5 shows that the mortar mini-v-funnel time, which should be directly related to mortar plastic viscosity, was well correlated to concrete plastic viscosity. The overall correlation was poor, however, between the mortar and concrete v-funnel times, as indicated in Figure 12.6. This poor correlation was due to some of the concrete mixtures having insufficient paste volume, which resulted in blockage at the v-funnel outlet and a sharp increase in v-funnel time. The correlation between mortar and concrete v-funnel time was better for mixtures with adequate paste volume. Therefore, in order to use v-funnel as an approximate indication of plastic viscosity, the mortar or concrete must have adequate paste volume, segregation resistance, and passing ability for use in the v-funnel. In other words, the mortar or concrete must be considered homogenous for the purpose of v-funnel measurements. The correlation between mortar T_8 and concrete T_{50} was poor, as indicated in Figure 12.7. This poor correlation was likely due to the poor precision of the test method.

The correlation between mortar and concrete fresh properties indicates that mortar tests can be used to evaluate materials and proportions. Changes in mortar materials and proportions that reduce HRWRA demand and viscosity are generally favorable because they can offset other factors that increase paste volume.
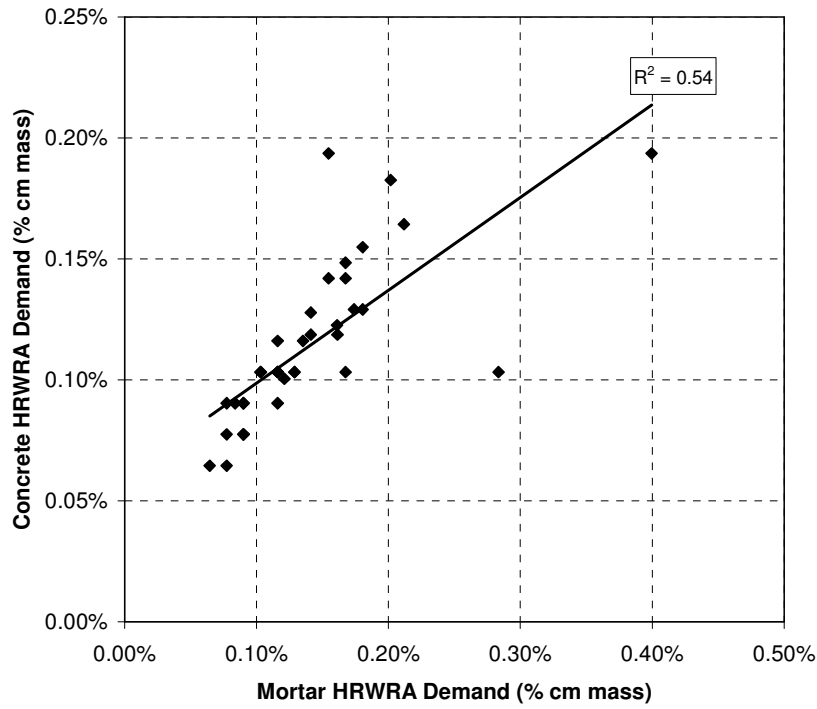
Figure 12.4: Relationship between Mortar and Concrete HRWRA Demand for Comparable Mixtures
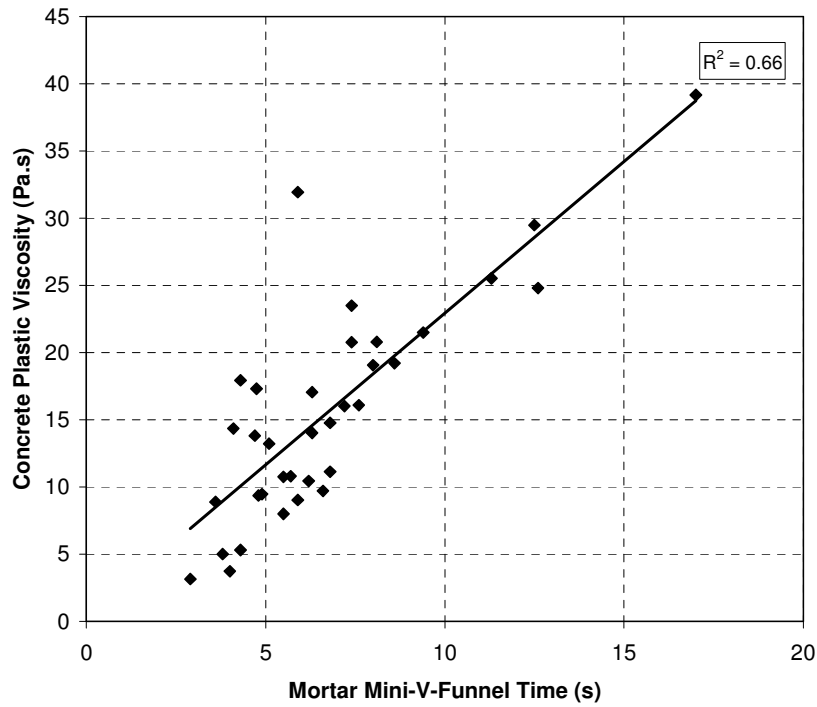
Figure 12.5: Relationship between Mortar Mini-V-Funnel and Concrete Plastic Viscosity for Comparable Mixtures

285
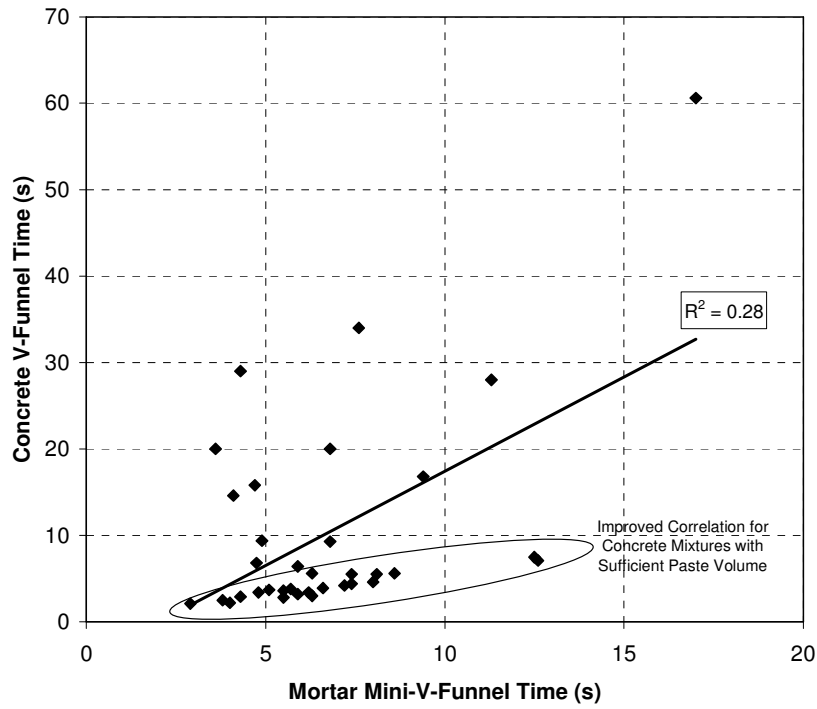
Figure 12.6: Relationship between Mortar Mini-V-Funnel and Concrete V-Funnel for Comparable Mixtures
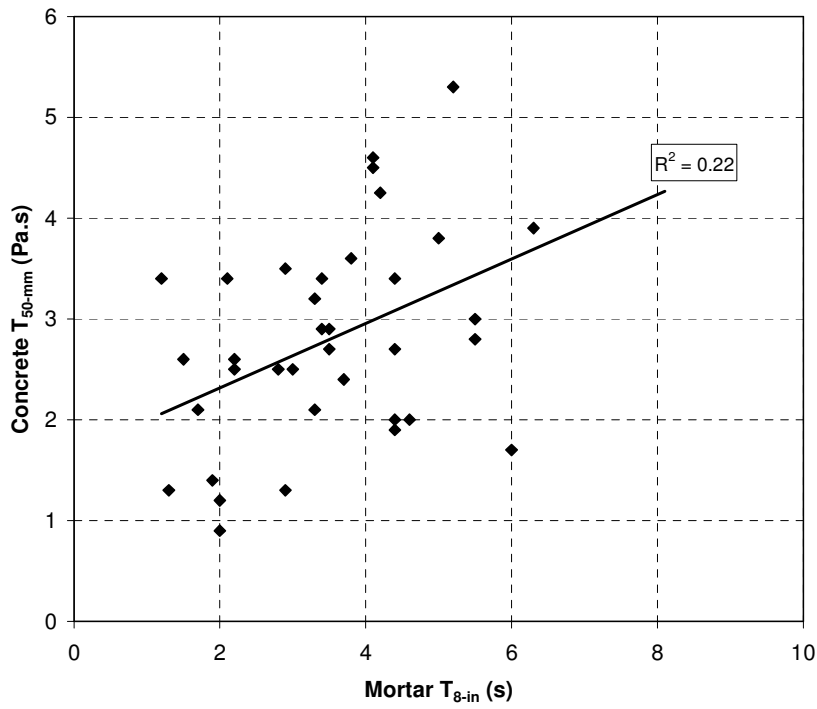
Figure 12.7: Relationship between Mortar T_8 and Concrete T_{50} for Comparable Mixtures

12.1.3 Minimum Paste Volume for Workability

A minimum paste volume must be provided in all mixtures to achieve SCC workability. The minimum paste volume needed for filling ability is independent from that needed for passing ability—each should be evaluated separately. Mixtures with insufficient paste volume for filling ability may not achieve the desired slump flow regardless of the HRWRA dosage, may be highly viscous, may exhibit severe bleeding and segregation, and may appear harsh. Mixtures with insufficient paste volume for passing ability exhibit too much blocking for the application.

SCC can be considered a suspension of aggregates in paste, as depicted schematically in Figure 12.8. Sufficient paste must be provided to fill the voids between compacted aggregates. If only this amount of paste were provided, the interparticle friction between aggregates would prevent flow. Therefore, to achieve filling ability, additional paste volume is needed to separate aggregates, resulting in reduced interparticle friction between aggregates. This paste to separate aggregates essentially lubricates the aggregates. The provision of minimum paste volume for filling ability is analogous to the maximum solids volume fraction in phenomenological models for concentrated suspensions, such as the Krieger-Daugherty equation. The maximum solids volume fraction is assumed to represent grading and shape characteristics and be independent of the rheology of the suspending medium. For passing ability, increasing the paste volume for a given aggregate increases passing ability by reducing the volume of aggregate that must pass through narrow spaces and by reducing the interparticle friction between aggregates. For a given aggregate, paste volume must be increased until adequate passing ability is achieved for the application. In addition, decreasing the yield stress and plastic viscosity of the paste may increase passing ability.
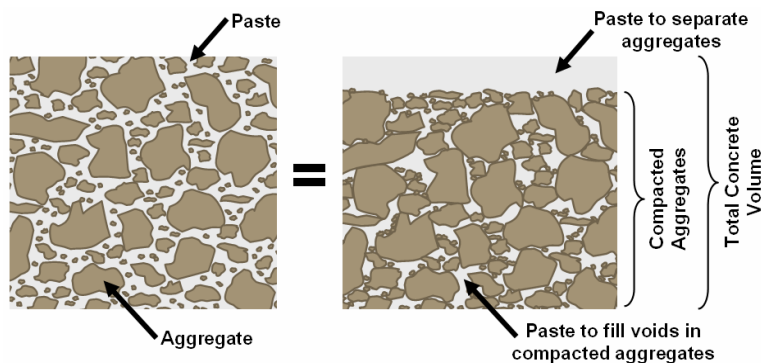
Figure 12.8: Schematic Representation of Aggregate in Cement Paste

For filling ability, the total paste volume ($V_{paste\text{-}filling\_abiltiy}$) is computed as the sum of the paste to fill voids ($V_{paste\text{-}voids}$) and to provide spacing between aggregates ($V_{paste\text{-}spacing}$), as shown in Equation (12.1):

$$V_{paste-filling\_ability} = V_{paste-voids} + V_{paste-spacing} \tag{12.1}$$

The volume of paste to fill the voids between aggregates can be computed as a function of the volume of aggregates (V_{agg}, expressed as percentage of total concrete volume) and the void content in the compacted aggregates ($\%voids_{compacted\_agg}$, expressed as a percentage of the bulk compacted aggregate volume), as shown in Equation (12.2):

$$V_{paste-voids} = V_{agg} \frac{\%voids_{compacted\_agg}}{100 - \%voids_{compacted\_agg}} \tag{12.2}$$

At least three approaches are available to determine the paste needed to separate aggregates. First, Marquardt, Diederichs, and Vala (2002) express the volume of paste beyond that needed to fill voids between the aggregates as a function of the volume of paste required to fill the voids between aggregates. For this approach, the volume of paste can be computed by multiplying the volume of paste to fill voids between aggregates by a factor f, as shown in Equation (12.3):

$$V_{agg} + \left(\left(V_{paste-voids}\right) + \left(V_{paste-voids}\right)(f)\right) = 100\% \tag{12.3}$$

The total paste volume required can then be computed as shown in Equation (12.4):

$$V_{paste} = 100 - \frac{100}{1 + \left(\dfrac{\%voids_{compacted\_agg}}{100 - \%voids_{compacted\_agg}}\right)(1 + f)} \tag{12.4}$$

Marquardt, Diederichs, and Vala (2002) recommend that the value of f be between 0.9 to 1.1 depending on the aggregate shape and angularity. (The original equations from Marquardt, Diederichs, and Vala (2002) were re-written in Equations (12.3) and (12.4) for greater clarity and consistency.)

Second, the volume of paste to separate aggregates can be computed as a function of the specific surface area of the aggregate. This approach was first used in the excess paste theory (Kennedy 1940) and has been applied in various formats to SCC by Bui and Montgomery (1999); Oh, Noguchi, and Tomosawa (1999); Midorikawa, Pelova, and Walraven (2001); and Hasholt, Pade, and Winnefield (2005). In this case, an average thickness of paste surrounding

288

aggregates (*t*) is selected and the specific surface area (*SSA*) is estimated or measured. The total paste volume can then be computed as shown in Equation (12.5):

$$V_{paste} = 100 - \frac{100(1 - (t)(SSA))}{1 + \left(\dfrac{\%voids_{compacted\_agg}}{100 - \%voids_{compacted\_agg}}\right)}$$

(12.5)

Third, the volume of paste to separate aggregates can be selected as a constant value. In this case, the total paste volume can be computed as shown in Equation (12.6):

$$V_{paste} = 100 - \frac{100 - V_{paste-spacing}}{1 + \left(\dfrac{\%voids_{compacted\_agg}}{100 - \%voids_{compacted\_agg}}\right)}$$

(12.6)

$$= 100 - \frac{(100 - V_{paste-spacing})(100 - \%voids_{compacted\_agg})}{100}$$

This third approach is analagous to the b/b$_0$ appraoch in ACI 211; however, it is applied to all aggregates in a mixture instead of just the coarse aggregate. The value of the spacing paste volume, which is directly correlated to b/b$_0$, is set as a function of the aggregate shape and angularity (as discussed below) rather than the fine aggregate fineness modulus. Further, the b/b$_0$ appraoch is used to determine the coarse aggregate volume while the approach shown here determines the paste volume, which is just 100 minus the aggregate volume.

To quantify the paste volume needed for filling ability, the data presented in this dissertation were analyzed. First, mortar and concrete mixtures with constant paste volume and variable aggregates were analyzed. At the time of testing, a determination was made as to whether the volume of paste in each mixture was sufficient for filling ability. Table 12.1 shows the values of *f* and $V_{paste-spacing}$ for combinations of various aggregates. For mixtures with sufficient paste volume, the value of *f* ranged from 0.50 to 1.08 and the spacing paste volume varied from 12.8 to 19.6%. For mixture with borderline paste volume, the value of *f* ranged from 0.31 to 0.72 and the spacing paste volume varied from 10.8 to 19.1%. For mixtures with insufficient paste volume, the value of *f* ranged from 0.04 to 0.62 and the spacing paste volume varied from 1.9 to 13.7%.

Table 12.1: Evaluation of Minimum Required Paste Volume—Variable Aggregate Source

Mixture	Coarse	Fine	% Voids in Compacted Aggregate	Sufficient Paste Volume?	*f*	Spacing Paste Volume	Filling Paste Volume
Mortar		**DO-01-F**	**40.4**	**No**	**0.23**	**8.6**	**36.9**
Mortar		**DL-01-F**	**38.6**	**No**	**0.33**	**11.3**	**34.2**
Mortar		LS-01-F	35.8	Yes	0.50	15.1	30.4
Mortar		LS-02-F	33.4	Yes	0.66	18.2	27.3
Mortar		**LS-03-F**	**44.4**	**No**	**0.04**	**1.9**	**43.6**
Mortar		*LS-04-F*	*38.9*	*Borderline*	*0.31*	*10.8*	*34.7*
Mortar		*LS-05-F*	*32.7*	*Borderline*	*0.72*	*19.1*	*26.4*
Mortar		LS-06-F	32.2	Yes	0.76	19.6	25.9
Mortar		**GR-01-F**	**37.1**	**No**	**0.41**	**13.3**	**32.2**
Mortar		TR-01-F	34.8	Yes	0.57	16.5	29.0
Mortar		NA-01-F	32.4	Yes	0.74	19.3	26.2
Mortar		NA-02-F	33.6	Yes	0.65	18.0	27.5
F1	**NA-02-C**	**DO-01-F**	**31.5**	**No**	**0.22**	**6.5**	**29.4**
F3	*NA-02-C*	*DL-01-F*	*27.9*	*Borderline*	*0.45*	*11.2*	*24.7*
F5	**NA-02-C**	**GR-01-F**	**28.5**	**No**	**0.41**	**10.4**	**25.5**
F7	NA-02-C	TR-01-F	21.2	Yes	1.08	18.6	23.5
F9	*NA-02-C*	*LS-01-F*	*27.9*	*Borderline*	*0.44*	*11.1*	*24.8*
F11	NA-02-C	LS-02-F	24.2	Yes	0.76	15.5	20.4
F13	**NA-02-C**	**LS-03-F**	**31.6**	**No**	**0.21**	**6.3**	**29.6**
F15	NA-02-C	LS-04-F	25.7	Yes	0.62	13.8	22.1
F17	NA-02-C	LS-05-F	23.2	Yes	0.85	16.5	19.4
F19	*NA-02-C*	*LS-06-F*	*27.6*	*Borderline*	*0.47*	*11.4*	*24.5*
F21	NA-02-C	NA-01-F	22.8	Yes	0.89	16.9	19.0
F23	NA-02-C	NA-02-F	23.0	Yes	0.88	16.8	19.1
C1	**DO-01-C**	**LS-02-F**	**25.7**	**No**	**0.62**	**13.7**	**22.2**
C5	NA-02	LS-02-F	24.2	Yes	0.76	15.5	20.4
C9	**LS-01-C**	**LS-02-F**	**27.6**	**No**	**0.47**	**11.5**	**24.4**
C13	LS-02-C	LS-02-F	25.2	Yes	0.66	14.3	21.6
C17	LS-03-C	LS-02-F	26.5	Yes	0.55	12.8	23.1
C21	LS-04-C	LS-02-F	25.2	Yes	0.67	14.3	21.6
C25	LS-05-C	LS-02-F	24.1	Yes	0.76	15.5	20.4
All concrete mixtures: 35.9% paste volume with 50% fine, 50% coarse aggregate							

In addition, mortar and concrete mixtures with variable paste volumes and variable aggregates were analyzed. The minimum paste volume for filling ability for each mixture was estimated and the corresponding values of *f* and spacing paste volume calculated as shown in Table 12.2. The value of *f* varied from 0.27 to 0.55 and the spacing paste volume varied from 7.8 to 15.7%.

Table 12.2: Evaluation of Minimum Required Paste Volume—Variable Paste Volume

Mixtures	Coarse	Inter-mediate	Fine	% Voids in Compacted Aggregate	Estimated Minimum Paste Volume[3]	f	Spacing Paste Volume	Filling Paste Volume
Mortar			LS-02-F	33.4	42.0	0.44	12.9	29.1
Mortar			NA-02-F	33.6	39.0	0.27	8.2	30.8
Mortar			DO-01-F	40.4	49.0	0.42	14.5	34.5
Mortar			GR-01-F	45.5	47.0	0.50	15.7	31.3
P9-P13[1]	NA-02-C		DO-01-F	31.5	39.0	0.39	11.0	28.0
P1-P4[1]	DO-01-C	DO-01-I	LS-02-F	29.2	38.0	0.49	12.5	25.5
P5-P8[1]	DO-01-C		LS-02-F	27.5	37.0	0.55	13.1	23.9
O1-O21[2]	NA-02-C		LS-02-F	26.1	32.3	0.35	8.4	23.9
O1-O21[2]	NA-02-C		LS-02-F	26.0	32.0	0.34	8.2	23.8
O1-O21[2]	NA-02-C		LS-02-F	25.4	31.5	0.35	8.2	23.3
O1-O21[2]	NA-02-C		LS-02-F	25.2	31.0	0.34	7.8	23.2
O1-O21[2]	NA-02-C		LS-02-F	24.2	30.7	0.39	8.6	22.1

1. Based on mixtures with variable paste volume, constant fly ash and w/cm
2. Based on mixtures with variable paste volume, fly ash, w/cm
3. For filling ability

Based on Table 12.1 and Table 12.2, the minimum values of f can be expected to range from approximately 0.25 to 0.75 while the minimum values of $V_{paste-spacing}$ can be expected to range from approximately 8% to 16%. These paste volumes are the minimum required—additional paste can be provided to increase robustness with respect to aggregate properties. It should be noted that the values of f determined in Table 12.1 and Table 12.2 are significantly below the values of 0.9 to 1.1 recommended by Marquardt, Diederichs, and Vala (2002).

If it is assumed that the purpose of the spacing paste volume is to reduce interparticle friction between aggregates, the minimum required volume of spacing paste should depend on the aggregate shape and angularity. Additionally, a finer grading would have more potential contact area between aggregates, resulting in greater interparticle friction. Based on the data in Table 12.1 and Table 12.2, however, the predominant effect on the required spacing paste volume is aggregate shape and angularity. Increasing the maximum aggregate size generally improves rheology and increases packing. This benefit is not due to the absolute size of the aggregates, but rather to the improved grading and greater spread of sizes (polydispersity). It has been well established in suspension rheology that the particle size distribution and not the absolute particle size influences suspension rheology. Likewise, adding an appropriate amount of particles finer than cement can improve the grading and increase the spread of sizes within the paste. Much of the improvement in increasing the maximum aggregate size is reflected in reduced voids between compacted aggregates (increased packing density). Therefore, the

volume of spacing paste volume generally does not need to be modified as the maximum aggregate size is increased or the grading is changed. Thus, the volume of spacing paste can be assumed to be a function of aggregate shape and angularity.

To evaluate the effects of paste rheology on the minimum required spacing paste volume, the minimum paste volume was determined for mortar mixtures with constant aggregate and varying paste rheology. The aggregate for all mixtures was DO-01-F and the paste rheology was varied by changing the water-cementitious materials ratio from 0.30 to 0.50 and by using a VMA. The results, which are shown in Table 12.3, indicate that the paste rheology had minimal effect on the minimum paste volume for filling ability. Increasing the w/cm from 0.30 to 0.50 resulted in a decrease in the estimated minimum paste volume from 50 to 49%. For practical purposes, this difference in paste volume is negligible. The use of VMA had no effect. In addition, the concrete mixtures O1-O21 shown in Table 12.2 varied in paste rheology and paste volume. For these mixtures, the effect of paste rheology appeared to be negligible. Therefore, in proportioning, it is reasonable to assume that the minimum paste volume for filling ability depends solely on the aggregate characteristics. The only exception would be in mixtures with paste rheology significantly different from that typically used for SCC, such as in mixtures with extremely high or low water-powder ratios. This finding is consistent with the concept of a maximum solids volume fraction in models for suspensions such as the Krieger-Daugherty model. Providing a minimum paste volume is necessary to achieve SCC workability; however, merely providing the minimum paste volume does not assure SCC workability unless the paste rheology is also correct.

For proportioning purposes, it is recommended that Equation (12.6) be used to compute the minimum paste volume for filling ability. The paste volume to separate aggregates should be selected based on the aggregate shape and angularity and should vary from 8% for equidimensional, well-rounded aggregates to 16% for poorly shaped, angular aggregates. In some cases, spacing paste volumes greater than 16% may be required.

Table 12.3: Effects of Paste Rheology on Minimum Paste Volume for Filing Ability

w/cm	Estimated Minimum Paste Volume	Paste Volume	HRWRA Demand	Mini-V-Funnel	Sufficient Paste Volume?	Comments
	%	%	% cm mass	s		
0.30	50	45	0.467	270	no	Severe segregation, bubbles, bleeding
		47	0.203	15.2	no	Severe segregation, bubbles, bleeding
		49	0.104	10.4	borderline	Minimal bleeding, bubbles
		51	0.075	9.7	yes	Good
0.35	50	45	0.336	39	no	Severe segregation, bubbles, bleeding
		47	0.117	13.2	no	Severe segregation, bubbles, bleeding
		49	0.070	6.6	borderline	Minimal bleeding, bubbles
		51	0.061	4.8	yes	Good
0.40	49	45	0.294	24	no	Severe segregation, bubbles, bleeding
		47	0.094	12	no	Moderate segregation, bleeding
		49	0.060	3.8	yes	Good
		51	0.051	3.2	yes	Good
0.50	49	45	0.111	500	no	Severe segregation, bubbles, bleeding
		47	0.062	3.6	no	Moderate segregation, bleeding
		49	0.043	1.8	yes	Good
		51	0.041	1.8	yes	Good
0.50 and VMA	49	45	0.111	5.8	no	Severe segregation, bubbles, bleeding
		47	0.062	3.6	no	Moderate segregation, bleeding
		49	0.051	1.3	yes	Good

Notes:
1. Powder consisted of 75% cement, 25% fly ash by mass.
2. Aggregate: DO-01-F
3. HRWRA dosage adjusted to reach 9-inch mini-slump flow. Mini-v-funnel time corresponds to this mini-slump flow.
4. VMA used at 8 oz/cwt

12.2 Hardened Properties

The hardened properties of concrete are generally a function of the volumes and properties of the paste, aggregates, and transition zone. The volumes and properties of all three of these phases must be taken into consideration when evaluating SCC hardened properties. SCC typically utilizes higher paste volume than conventionally placed concrete; however, the transition zone is often improved. For modulus of elasticity, the higher paste volume may result in reduced concrete modulus of elasticity due to the lower modulus of elasticity of the paste relative to the aggregates. The improved properties of the paste and transition zone—due in large part to the increased dispersion caused by the HRWRA, the reduced w/p and w/cm, and use of SCMs—may increase the modulus of elasticity and modulus of rupture. For simplicity, however, it is often convenient to relate modulus of elasticity and modulus of rupture to compressive strength. The following subsections evaluate the applicability of such published relationships to the data presented in this dissertation.

12.2.1 Modulus of Elasticity

The relationship between compressive strength and modulus of elasticity is plotted in Figure 12.9 for all SCC mixtures evaluated. The scatter in the data is mainly due to the range of aggregates and mixture proportions evaluated. The majority of elastic modulus measurements are greater than predicted by the ACI 318 equation for normal-strength concrete and all but one is greater than predicted by the ACI 363 equation for high-strength concrete. The elastic modulus measurements are, however, mostly lower than predicited by the CEB-FIP equation with a value of α of 1.2, which is considered appropriate for basalt and dense limestones. The control coarse aggregate (NA-02-C), which was used for all but the comparison of coarse aggregate characteristics, was a relatively dense and stiff siliceous river gravel, resulting in relatively high concrete elastic modulus measurements. Had a less stiff aggregate been used as the control, all results would likely be systematically lower. In addition, all concrete specimens for compressive strength and modulus of elasticity were tested in a moist condition. Testing specimens in a moist condition is known to increase modulus of elasticity and reduce compressive strength, which could also be partially responsible for most of the elastic modulus measurements being greater than predicted by the two ACI equations.
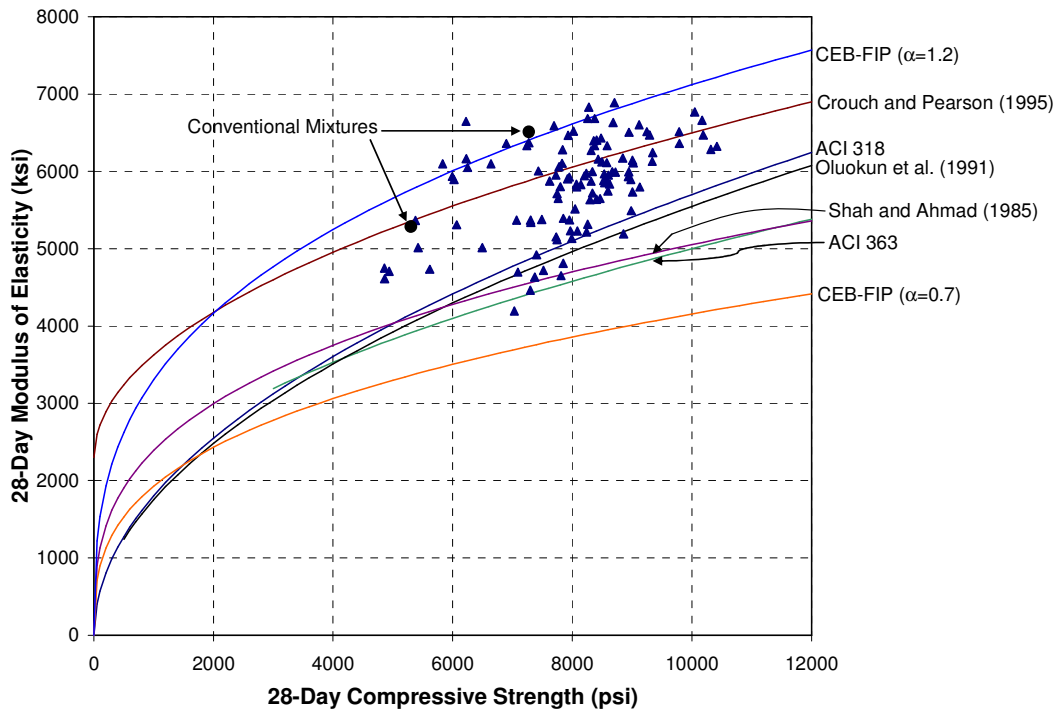
Figure 12.9: Relationship between Compressive Strength and Modulus of Elasticity at 28 Days for All SCC Test Data

294

To identify the effects of aggregates and mixture proportions on the strength versus modulus of elasticity relationship, the data were plotted in Figure 12.10 based on the mixture parameter varied. The largest variations in modulus of elasticity occurred when the fine and coarse aggregates were varied. Varying the coarse aggregate mostly reduced the modulus of elasticity for a given compressive strength, suggesting the control coarse aggregate was stiffer than most of the other coarse aggregates tested. In contrast, the control fine aggregate produced a modulus of elasticity near the median when the fine aggregate was varied. Changing the microfines content resulted in the smallest variation in elastic modulus for a given compressive strength. Varying the mixture proportions produced smaller variations in elastic modulus for a given compressive strength than changing the aggregates. If the mixture proportions had been varied to a greater extent, the variation in elastic modulus may have been more than for changing the aggregates.
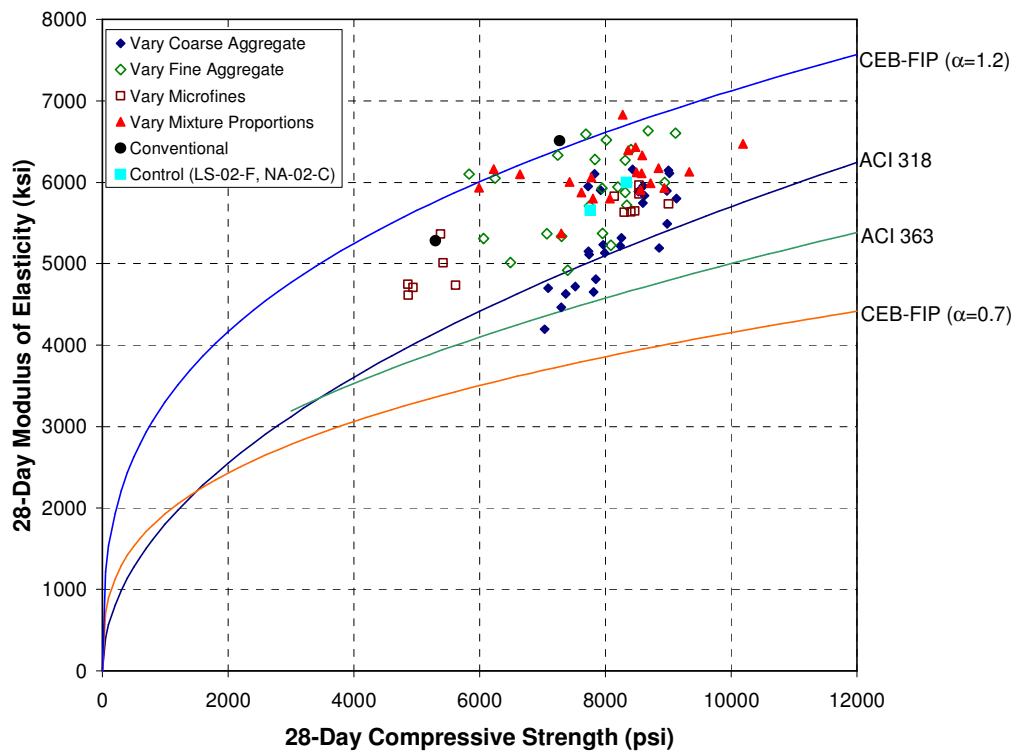
Figure 12.10: Relationship between Compressive Strength and Modulus of Elasticity at 28 Days for Various Categories of Test Data

In Chapter 11, it was shown that increasing the paste volume or S/A resulted in lower modulus of elasticity and that the use of fly ash did not reduce the modulus of elasticity to the

same extent as compressive strength. Indeed, the conventionally placed concrete mixtures, which feature lower paste volume than all SCC mixtures and lower S/A than the majority of SCC mixtures generally exhibited higher modulus of elasticity for a given compressive strength. When compared to mixtures with the same fine and coarse aggregates, Table 12.4 indicates that relative to the conventionally placed concrete mixture with w/cm of 0.45, the ratio of modulus of elasticity to the square root of compressive strength was 15% lower for the control SCC mixture and an average of 11% lower when the mixture proportions were varied.

When evaluating the modulus of elasticity of SCC mixtures, the coarse and fine aggregate sources as well as the mixture proportions should be taken into consideration. Although the modulus of elasticity at a given compressive strength was generally slightly reduced relative to conventionally placed concrete mixtures, changing the aggregate often had a larger effect than increasing the paste volume or S/A.

In using equations relating compressive strength and modulus of elasticity, structural designers should recognize that the modulus of elasticity at a certain compressive strength can vary widely. The equations relating modulus of elasticity and compressive strength represent average values and not lower bounds, such as a certain fractile. In addition, each equation was developed on a limited set of data tested under conditions that may not be directly representative of field members. As such, an appropriate level of caution should be exercised when using these equations.

Table 12.4: Comparison of Strength versus Elastic Modulus Relationship for Mixtures with LS-02-F and NA-02-C

Mixture	f'_c	E	$\dfrac{E}{\sqrt{f'_c}}$
	psi	ksi	
SCC Control (Average)	8,049	5,824	64.9
Vary Mixture Proportions (Average)	8,106	6,092	67.9
Conventional (w/cm = 0.45)	5,300	5,284	72.6
Conventional (w/cm = 0.60)	7,273	6,511	76.3
ACI 318			57.0

12.2.2 Modulus of Rupture

The relationship between compressive strength and modulus of rupture is plotted in Figure 12.11 for all SCC mixtures evaluated. For a given compressive strength, the modulus of rupture values were generally greater than the two conventional mixtures and were in the upper

296

half of the range of $7.5\sqrt{f'_c}$ to $12\sqrt{f'_c}$ that has been reported for normal-weight concrete. For high-strength concrete, ACI 363 recommends the modulus of rupture be taken as $11.7\sqrt{f'_c}$, which would slightly overestimate the modulus of rupture. When compared to mixtures with the same fine and coarse aggregates, Table 12.5 indicates that relative to the conventionally placed concrete mixture with a w/cm of 0.45, the ratio of modulus of rupture to the square root of compressive strength was 8% higher for both the control SCC mixture and for the average of the series where mixture proportions were varied. It was shown in Chapter 11 that the paste volume had no effect on modulus of rupture and that increasing the S/A slightly reduced modulus of rupture. Therefore, the difference between SCC and conventionally placed concrete is likely not due to these factors. Figure 12.12 indicates that varying any one factor—including coarse aggregate source, fine aggregate source, microfines source, or mixture proportions—did not result in a relatively larger variation in modulus of rupture than the other factors. It is likely that the improved transition zone and strong bond associated with SCC resulted in the higher modulus of rupture.

Just as with case of the relationship between modulus of elasticity and compressive strength, structural designers should recognize that the modulus of rupture at a certain compressive strength can vary widely. The equations relating modulus of rupture and compressive strength represent average values and not lower bounds. As such, an appropriate level of caution should be exercised when using these equations.
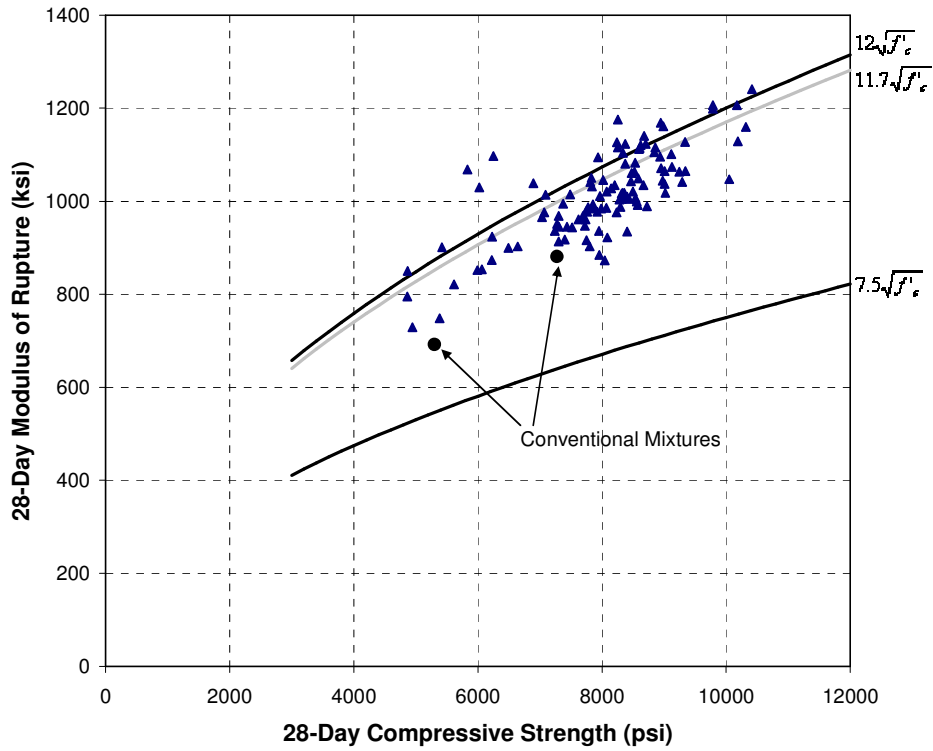
Figure 12.11: Relationship between Compressive Strength and Modulus of Rupture at 28 Days for All SCC Test Data

Table 12.5: Comparison of Strength versus Modulus of Rupture Relationship for Mixtures with LS-02-F and NA-02-C

Mixture	f'_c	f'_r	$\dfrac{f'_r}{\sqrt{f'_c}}$
	psi	**ksi**	
SCC Control (Average)	8,049	998	11.1
Vary Mixture Proportions (Average)	8,106	1,000	11.1
Conventional (w/cm = 0.45)	5,300	692	9.5
Conventional (w/cm = 0.60)	7,273	881	10.3

298
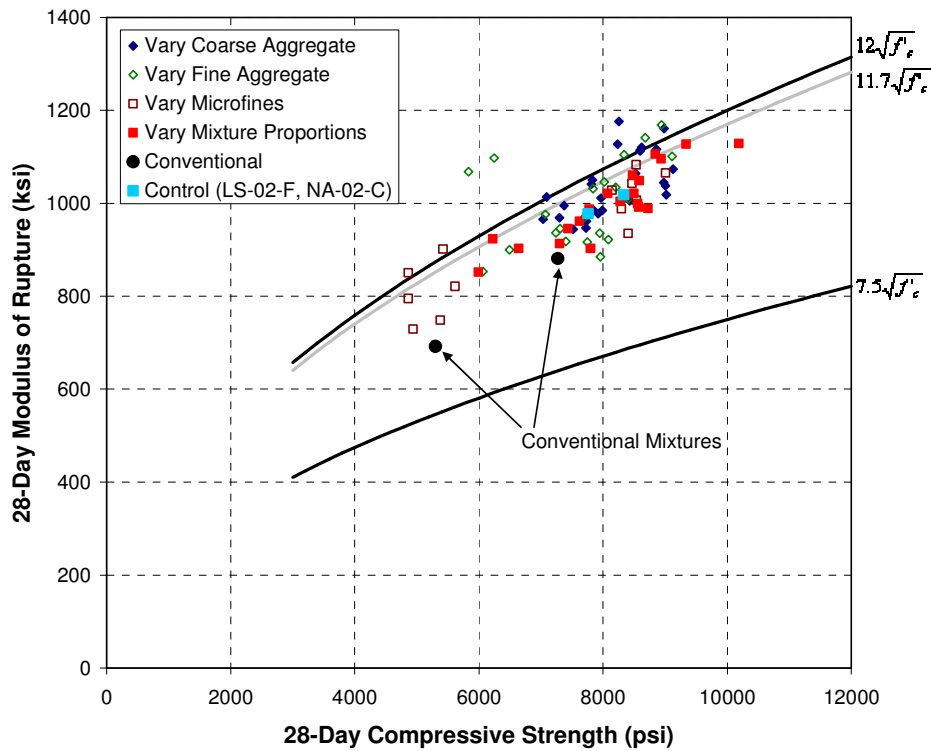
Figure 12.12: Relationship between Compressive Strength and Modulus of Elasticity at 28 Days for Various Categories of Test Data

12.3 Conclusions

The following conclusions can be drawn based on the information presented in this chapter:

- The yield stress is the main fundamental difference between the workability of SCC and conventionally placed concrete. For a given concrete mixture, the slump flow and yield stress are correlated. Small changes in yield stress result in large differences in slump flow over the range of workability considered to be SCC.

- The addition of HRWRA is the main cause of the drastic reduction in concrete yield stress associated with SCC. In addition, the paste volume and paste composition must be appropriate so that the concrete is stable and placeable when the yield stress is reduced to near zero. Although it is possible to reduce the yield stress and plastic viscosity of the paste to near zero, such paste would be inappropriate for concrete.

- Paste flow properties can be used to evaluate materials and proportions for use in concrete. In relating the properties of paste to concrete, it is important to recognize that paste measured separately from the concrete does not exhibit the same properties as the

same paste in the concrete for three reasons. First, there is interaction between powder materials in the paste and larger aggregate particles in the concrete. Second, the shear rates during testing are different for paste tested separately from concrete and paste in concrete. Third, the mixing history is different for paste mixed separately from concrete and paste in concrete.

- Mortar workability can be used to evaluate materials and proportions for use in concrete. The mortar mini-slump flow (HRWRA demand) and mini-v-funnel tests were well correlated to concrete results provided the paste volumes were sufficient to consider the mortar and concrete as homogenous fluids for the purpose of rheology characterization. As with paste measurements, mortar measured separately from the concrete does not exhibit the same properties as the same mortar in the concrete.

- A minimum paste volume must be provided to achieve SCC workability. The minimum paste volumes for filling ability and passing ability are independent and should be determined separately. For filling ability, a minimum paste volume must be provided to fill voids between aggregates and reduce interparticle friction between aggregates. The minimum filling ability can be computed as a function of the voids content in compacted aggregates and the shape and angularity of the aggregate. For passing ability, a minimum paste volume must be provided to reduce the volume of aggregate that must pass through narrow spaces and to reduce interparticle friction.

- For a given compressive strength, the modulus of elasticity of the SCC mixtures varied considerably as the fine and coarse aggregates and mixture proportions were changed. For a given compressive strength, fine aggregate source, and coarse aggregate source, the elastic modulus measurements of the SCC mixtures were lower than for the conventionally placed concrete mixtures. Changing the coarse or fine aggregate may have a greater influence on modulus of elasticity than varying the paste volume or S/A. Therefore, in evaluating the modulus of elasticity of SCC, the volumes and properties of the paste, aggregates, and transition zone should be considered.

- For a given compressive strength, the modulus of rupture measurements of the SCC mixtures were typically slightly higher than for the conventionally placed concrete mixtures.

Chapter 13: ICAR Mixture Proportioning Procedure for SCC

The research results described in this dissertation were used along with well-established principles from concrete and suspension rheology literature to develop a new, comprehensive mixture proportioning procedure for SCC, which will be called the "ICAR mixture proportioning procedure." The ICAR mixture proportioning procedure is based on a fundamental, rheology-based framework for concrete workability and is designed and written to be accessible and comprehensible. The procedure provides specific guidelines for each aspect of the mixture proportioning process but intentionally avoids long calculations or restrictive, discrete inputs. Instead, deliberate laboratory testing is conducted with actual job materials to establish final mixture proportions efficiently. All required testing is conducted with methods standardized by ASTM International.

13.1 Definitions

Aggregate Compacted Voids Content: The volume of voids between fully compacted aggregates (100% - packing density). For purposes of this mixture proportioning procedure, the compacted voids content is determined in accordance with ASTM C 29 (dry-rodded compaction) on the combined aggregate grading. The compacted voids content is calculated as shown in (13.1):

$$\%voids_{compacted\_agg} = \left(1 - \frac{DRUW}{\left(62.4\,{}^{lb}\!/_{ft^3}\right)\sum_{i=1}^{n}\left(p_i\left(SG_{OD}\right)_i\right)}\right)*100\% \tag{13.1}$$

where DRUW is the dry-rodded unit weight of the combined aggregate (lb/ft^3), p_i is the volume of aggregate fraction i divided by the total aggregate volume, and $(SG_{OD})_i$ is the oven-dry specific gravity of aggregate fraction i.

Angularity: The sharpness of the corners and edges of a particle. (Shape describes a particle on the coarsest scale, angularity an intermediate scale, and texture the finest scale.) For SCC, the angularity characteristics of the aggregates and powder are relevant.

Filling Ability: The ability of concrete to flow under its own mass and completely fill formwork.

Passing Ability: The ability of concrete to flow through confined conditions, such as the narrow openings between reinforcing bars.

301

Paste Volume: The volume of water, air, and powder.

Plastic Viscosity: The resistance to flow once the yield stress is exceeded. Mixtures with high plastic viscosity are often described as "sticky" or "cohesive". Concrete with higher plastic viscosity takes longer to flow. It is closely related to T_{50} and v-funnel time (higher plastic viscosity → higher T_{50} and v-funnel time). It is computed as the slope of the shear stress versus shear rate plot from rheometer flow curve measurements.

Powder: Solid materials finer than approximately 75 μm (No. 200 sieve) including cement, supplementary cementitious materials (SCMs), and mineral fillers (e.g. finely ground limestone or other minerals and dust-of-fracture aggregate microfines). (There is not a discrete size for distinguishing solid materials that should be included in the paste; however, 75 μm is a reasonable and practical value.)

Rheology: The scientific study of flow. In the context of SCC, rheology refers to the evaluation and manipulation of yield stress, plastic viscosity, and thixotropy to achieve desired levels of filling ability, passing ability, and segregation resistance.

Robustness: The ability of concrete to maintain acceptable performance when variations occur in materials, mixture proportions, and other production variables.

Segregation Resistance: The ability of concrete to remain uniform in terms of composition during placement and until setting. Segregation resistance encompasses both dynamic and static stability.

Shape: The relative dimensions of a particle. Common descriptors of shape include flatness, elongation, and sphericity. (Shape describes a particle on the coarsest scale, texture the finest scale, and angularity an intermediate scale.) For SCC, the shape characteristics of the aggregates and powder are relevant.

Shear Thinning Fluid: A fluid with higher viscosity at low shear rates than at high shear rates.

Stability, Dynamic: The resistance to segregation when external energy is applied to concrete—namely during placement.

Stability, Static: The resistance to segregation when no external energy is applied to concrete—namely from immediately after placement and until setting.

Texture: The roughness of a particle on a scale smaller than that used for shape and angularity. (Shape describes a particle on the coarsest scale, texture the finest scale, and angularity an intermediate scale.) For SCC, the texture characteristics of the aggregates and powder are relevant.

Thixotropy: The reversible, time-dependent decrease in viscosity in a fluid subjected to shearing. For SCC, thixotropy is important for formwork pressure and segregation resistance.

Workability: The empirical description of concrete flow performance. For SCC, workability encompasses filling ability, passing ability, and segregation resistance. Workability is affected by rheology.

Yield Stress: The amount of stress to initiate (static yield stress) or maintain (dynamic yield stress) flow. It is closely related to slump flow (lower yield stress → higher slump flow). It is calculated as the intercept of the shear stress versus shear rate plot from rheometer flow curve measurements.

13.2 Framework

The ICAR mixture proportioning procedure is based on the representation of SCC as a suspension of aggregates in paste, as depicted schematically in Figure 13.1. This representation provides a consistent, fundamental framework for evaluating mixture proportions. To proportion SCC, three factors are altered: the aggregates, the paste volume, and the paste composition. The aggregates are first selected based on grading, maximum size, and shape, angularity, and texture. Instead of considering the properties of the fine, intermediate, and coarse aggregates separately, the properties of the combined aggregates are evaluated simultaneously. Next, the paste volume is established for the given aggregates. Paste is defined to consist of water, air, and all solid materials finer than approximately 75 μm including cement, cementitious materials, and mineral fillers. A minimum amount of paste must be provided to achieve SCC properties. The required minimum paste volume depends mainly on the aggregates and is largely independent of the composition of the paste. Lastly, the paste composition—namely the relative amounts of water, powder, and air and the blend of powder—is optimized to achieve the desired concrete rheology and hardened properties. Increasing the paste volume is not necessarily associated with increasing the cement or cementitious materials content.
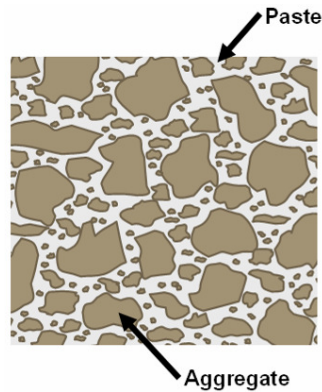
Figure 13.1: Schematic Representation of Aggregate in Cement Paste

13.3 Criteria for Evaluating SCC

The required workability and hardened properties of SCC mixtures can vary widely depending on the application. Workability should be evaluated in terms of filling ability, passing ability, and segregation resistance. Each of these three workability characteristics should be evaluated independently. The extent to which SCC must exhibit filling ability, passing ability, and segregation resistance should be established based on the application (Table 13.1). Hardened properties should be evaluated in the same manner as for conventionally placed concrete. The relationships between hardened properties and materials and mixture proportions for conventionally placed concrete generally apply to SCC. Certain modifications to mixture proportions needed to ensure workability may affect hardened properties. These modifications may include higher paste volume, increased sand-aggregate ratio, and reduced maximum aggregate size. Conversely, requirements for hardened properties may result in limits on certain parameters important to achieving workability, such as cement content, paste volume, and water-cementitious materials ratio. In many applications, the low water-cementitious materials ratios and use of SCMs required to achieve workability result in hardened properties that significantly exceed design requirements. When possible, care should be taken to not unnecessarily over-design for hardened properties.

Table 13.1: Workability Criteria

Property	Discussion
Filling Ability	<u>Requirements vary moderately.</u> Members with tight spaces—such as with narrow widths or congested reinforcement—and applications where concrete must flow long horizontal distances may require greater filling ability. High placement energy—such as that generated by pumping or by gravity acting on a large mass of concrete—may reduce filling ability requirements.
Passing Ability	<u>Requirements vary widely.</u> Applications may range from unreinforced or lightly reinforced sections (no passing ability requirements) to narrow sections containing highly congested reinforcement (strict passing ability requirements).
Segregation Resistance	<u>Requirements vary little, if at all.</u> All mixtures must exhibit segregation resistance. Requirements for dynamic stability may be higher for sections with highly congested reinforcement or applications were concrete is dropped from vertical heights or required to flow long horizontal distances.

The methods to test and achieve workability are described in Table 13.2. To achieve filling ability, concrete must have adequate paste volume and paste rheology for the given combined aggregate. Sufficient paste volume ensures that voids between aggregates are filled and that sufficient spacing is provided between aggregates. If the concrete contains insufficient paste volume, the paste will not convey the aggregates regardless of the rheology of the paste. In this case, increasing the HRWRA dosage may result in very low paste viscosity and severe bleeding. Paste with very low viscosity will quickly flow out of the aggregates without mobilizing the aggregates. In the slump flow test, the concrete will not achieve the desired slump flow with adequate stability, if it at all. Even with the proper paste volume, concrete must also have proper rheology, which is directly affected by the paste rheology. Proper paste rheology ensures that the paste can convey aggregates uniformly as the concrete flows and that the concrete can fill all corners of the formwork. Concrete that is too viscous may be difficult to pump and place. Low concrete viscosities may result in poor dynamic stability. Harsh concrete mixtures can occur when the paste volume or paste viscosity is too low. In such a case, the concrete does not flow smoothly and may not completely fill all corners of the formwork and produce a smooth top-surface finish. Filling ability should be tested with the slump flow test, including measurements of the time to spread 50 mm (T_{50}) and visual stability index (VSI). The slump flow spread ensures that the yield stress is sufficiently low for the concrete to flow under its own mass. The final adjustment of slump flow should be made by varying the HRWRA dosage. Minimum and maximum limits should be imposed on T_{50}—minimum limits ensure the concrete exhibits adequate stability while maximum limits ensure the concrete is not too difficult to place. The VSI is a quick but approximate indication of the stability of the mixture; however, an acceptable VSI does not ensure adequate stability. In addition, a visual assessment of harshness should be made. When testing concrete in the laboratory or producing it in the field, a

constant slump flow should be maintained for all mixtures because slump flow is the main characteristic distinguishing SCC from conventionally placed concrete. The value of the required slump flow depends on the application. With the slump flow constant, the effects of changing proportions on filling ability, passing ability, and segregation resistance can be evaluated. Typically, the range of HRWRA dosages corresponding to the range of slump flows associated with SCC is small.

Table 13.2: Methods to Test and Achieve SCC Fresh Properties

Property	How to Test		How To Achieve
	Method	Criteria	
Filling Ability	Slump Flow (ASTM C 1611) *Inverted cone orientation recommended.*	• <u>Minimum slump flow</u>. Values can range from 22 to 30 inches depending on the degree of filling ability. Values of 24-27 inches appropriate for most applications. The ability to achieve higher slump flows than needed without segregation is a demonstration of robustness. • <u>Minimum and maximum T_{50}</u>. Minimum values ensure stability; maximum values ensure placeability. For inverted cone orientation, values of 2-7 s appropriate for most applications. • <u>Maximum VSI</u>. Can be used for severe cases of segregation. Values of 1.0 or less acceptable for most applications.	• <u>Aggregate</u>: improve shape and angularity to reduce interparticle friction, use finer grading to reduce harshness or coarser grading to reduce viscosity • <u>Paste Volume</u>: ensure sufficient minimum paste volume to fill voids between aggregates and reduce interparticle friction between aggregates • <u>Paste Composition</u>: ensure viscosity is not too high (sticky) or too low (instability); increase HRWRA dosage to increase slump flow
Passing Ability	J-Ring (ASTM C 1621)	• <u>Maximum change in height from inside to outside of ring</u>. Can be as low as no difference. Values of 0.5-1.0 inches acceptable for most moderately reinforced sections. No need to measure for unreinforced or lightly reinforced elements *(Alternate criterion: maximum difference in slump flow with and without j-ring.)* • Size and spacing of bars should be constant, vary acceptable change in height or in slump flow based on application.	• <u>Aggregate</u>: reduce amount of larger particles by reducing coarseness of grading or maximum aggregate size, improve shape and angularity to reduce interparticle friction • <u>Paste Volume</u>: increase paste volume to reduce aggregate volume and interparticle friction between aggregates • <u>Paste Composition</u>: reduce paste viscosity or increase HRWRA dosage to increase slump flow
Segregation Resistance	Column Segregation (ASTM C 1610)	• <u>Maximum segregation index</u>. A value of 15% is appropriate for most applications but may need to be reduced in some applications. • For prequalification of mixtures, tests should be performed the over range of water contents and HRWRA dosages possible during production. • Proper sampling is crucial.	• <u>Aggregate</u>: Use continuous grading (avoid gap gradings), reduce coarseness of aggregate grading or maximum aggregate size • <u>Paste Volume</u>: increase paste volume • <u>Paste Composition</u>: ensure paste viscosity not too high or too low, reduce slump flow (lower HRWRA dosage), optimize workability retention (accelerate loss of slump flow in formwork), use VMA

Passing ability is primarily affected by the aggregate characteristics and the paste volume. Reducing the maximum aggregate size and coarseness of an aggregate grading and improving the aggregate shape and angularity result in increased passing ability. Increasing the paste volume reduces the volume of aggregates and reduces the interparticle friction between aggregates. In addition, reducing the paste yield stress or viscosity improves passing ability. Passing ability should be measured with the j-ring because it provides an independent measurement of passing ability. The j-ring test can be evaluated by measuring either the difference in height between the inside and outside of the ring or the difference in slump flow measured with and without the ring. It is strongly recommended that the difference in height be measured because (1) the difference in slump flow with and without the j-ring is often within the precision of the slump flow test and (2) the difference in slump flow may not reflect the extent of blocking (such as when the thickness of the concrete flowing out of the j-ring is thinner than for the concrete tested without the j-ring—due to differences in blocking—but the spread is approximately the same). The size and spacing of reinforcement bars should remain constant while the maximum value for the change in height should be established for the application.

Segregation resistance encompasses both static and dynamic stability. Static stability is affected by the relative densities of the aggregate and paste, the rheology of the paste with time, the aggregate shape and grading, and the characteristics of the element (such as width and spacing of reinforcement). Changing the paste rheology is generally the most productive means of improving static stability. The paste should have sufficiently high yield stress and plastic viscosity and should exhibit sufficient thixotropy. Improving the aggregate grading is also effective for reducing segregation resistance. Dynamic stability is mainly affected by the cohesiveness and passing ability of the concrete. Static stability should be measured with the column segregation test while dynamic stability is usually measured indirectly with measurements of filling and passing ability.

Testing requirements vary between the laboratory and field. To qualify mixtures in the laboratory, the slump flow, j-ring, and column segregation tests should be used to evaluate filling ability, passing ability, and segregation resistance, respectively. Additionally, the robustness of each of these characteristics should be evaluated by varying the water content and HRWRA dosage over the ranges expected to be encountered in production. In the field, it is often only necessary to perform the slump flow test. The slump flow spread should be used in the field to verify that the HRWRA dosage is correct while T_{50} should be used to evaluate unexpected

307

variations in mixture proportions (most likely water content). The j-ring test does not normally need to be used in the field because passing ability primarily depends on the aggregates and paste volume and to a much lesser extent on paste rheology. As long as the aggregates and paste volume remain reasonably consistent in the field and the slump flow test is used to ensure proper concrete rheology, it is not necessary to measure passing ability in the field. The column segregation test is too time-consuming for use in the field. In performing the column segregation test in the laboratory, representative sampling is crucial. When using the column segregation test to qualify mixtures, it is especially important to test at a range of water contents and HRWRA dosages because (1) segregation resistance is highly dependent on paste rheology and (2) it is possible for the paste rheology to vary substantially due to small variations in HRWRA dosage and water content (such as from variations in aggregate moisture conditions). If tests are conducted in the laboratory with the range of paste rheology expected to be encountered during production—by varying the water content and HRWRA dosage—no further segregation testing is required in the field provided the slump flow test is used to monitor concrete rheology indirectly (with slump flow and T_{50}).

Rheology can be used to characterize concrete flow characteristics and to optimize mixtures for filling ability, passing ability, and segregation resistance. Rheology involves measuring yield stress, plastic viscosity, and thixotropy. Yield stress describes the stress to initiate (static yield stress) or maintain (dynamic yield stress) flow. The yield stress should be near zero to ensure concrete flows under it own mass. Plastic viscosity describes the resistance to flow once the yield stress is exceeded. Mixtures with high plastic viscosity appear sticky and cohesive. Plastic viscosity should not be too low, which would result in instability, or too high, which would result in mixtures that are difficult to pump and place. Thixotropy describes the reversible, time-dependent reduction in viscosity in a concrete subjected to deformation (shearing). Thixotropy is caused by the build-up of a structure in fresh concrete at rest. This structure, which provides an initial resistance to deformation, is destroyed upon application of sufficient deformation to the concrete. Thixotropy, which is manifested in the difference between static and dynamic yield stress or the breakdown area between upward and downward rheometer flow curves, contributes to increased segregation resistance and reduced formwork pressures. Too much thixotropy; however, reduces placeability.

Concrete rheology is a function of the aggregates, paste volume, and paste rheology. Angular and poorly shaped aggregates increase yield stress and plastic viscosity. Increasing the

308

paste volume reduces yield stress and plastic viscosity. If the aggregates and paste volume are held constant, changes in paste rheology are generally matched in concrete rheology (e.g. increasing paste yield stress and viscosity increases concrete yield stress and viscosity). To increase filling ability and passing ability, the yield stress and plastic viscosity should be reduced. If the yield stress and plastic viscosity are too low; however, the concrete may become unstable, resulting in reduced filling and passing abilities. To increase segregation resistance, the yield stress and plastic viscosity should generally be increased.

Rheology is normally measured with a rheometer; however, certain empirical tests are correlated with rheological parameters. Specifically, reductions in yield stress generally result in higher slump flows while increases in plastic viscosity generally result in higher T_{50} and v-funnel flow times. Even if rheology parameters are not measured with a rheometer, considering workability in terms of rheology is often useful.

13.4 Methodology

The ICAR SCC mixture proportioning procedure consists of three steps: select aggregates, select paste volume, and select paste composition. The procedure is conducted in this order because paste volume depends primarily on the aggregate characteristics and paste composition depends on the aggregate characteristics and paste volume. The role of each factor is summarized in Table 13.3 and the specific tasks for each step are listed in Table 13.4. Table 13.5 indicates how changes in mixture proportions affect specific aspects of SCC workability.

Table 13.3: Role of Factors to Control in Mixture Proportioning

Factor	Objective	Sub-Factors	Target	Typical Values
Aggregates	Minimize voids content (increase packing density) and reduce interparticle friction; limit grading as needed for passing ability and segregation resistance	Maximum Size	Reduce for passing ability or segregation resistance	¾ or 1 inch for most applications; reduce to as low as 3/8 inch for challenging passing ability
		Grading	None universally optimal, best depends on aggregate and application	Continuous gradings with high packing density preferred, 0.45 power curve or finer, S/A=0.40-0.50
		Shape, Angularity, Texture	Reduce interparticle friction	Equidimensional, rounded aggregates preferred but any can be accommodated
Paste Volume	Ensure filling and passing ability by filling voids in compacted aggregates and separating aggregates (lubrication), provide additional paste for robustness with respect to aggregate properties	Filling Ability	Fill voids and lubricate aggregates	Total paste volume = 28-40%
		Passing Ability	Reduce aggregate volume and interparticle friction	
		Robustness	Minimize effects of changes in materials and proportions	
Paste Composition	Ensure adequate concrete rheology (yield stress, plastic viscosity, thixotropy) and hardened properties (strength, stiffness, durability), optimize economy	Water	w/p for rheology, w/c for early-age hardened properties (for SCMs with low initial reactivity), w/cm for long-term hardened properties	w/p = 0.30-0.45, may be higher with VMA
		Powder	Relative amounts of cement, SCMs, and mineral fillers for economy, strength, durability, and to fill paste volume	Fly ash, slag, silica fume, ground limestone filler, dust-of-fracture aggregate microfines
		Air	As needed for durability	Same requirements as for conventionally placed concrete
Adjust HRWRA dosage to reach desired slump flow (yield stress for self-flow)				

Table 13.4: Summary of ICAR SCC Mixture Proportioning Procedure

STEP 1: **Aggregates**	1. Select individual aggregate sources (fine, intermediate, coarse sizes)
	2. Evaluate various aggregate blends.
	  a. Maximum aggregate size
	  b. Grading (0.45 power curve, percent retained on each sieve)
	  c. Shape and angularity (visually rate on scale of 1 to 5)
	3. Determine compacted voids content of each blend.

STEP 2: **Paste Volume**	1. Determine minimum paste volume for filling and passing ability. Select the larger.
	  a. Paste volume for filling ability (Calculate from compacted voids content and visual rating of shape and angularity. Confirm with tests with various paste volumes and constant paste composition. Concrete should be able to achieve target slump flow without bleeding or segregation.)
	  b. Paste volume for passing ability (Establish with tests with various paste volumes and constant paste composition.)
	2. Add paste volume for robustness with respect to aggregate properties.

STEP 3: **Paste Composition**	1. Select cement, SCMs, and mineral fillers. 2. Select maximum w/c and w/cm and maximum and minimum SCM rates for early-age and long-term hardened properties. If mineral fillers affect hardened properties, specify maximum and minimum rates. 3. Select air content for durability (assume 2% if not air entrained). 4. Select w/p (typically 0.30-0.45, may be higher with VMA) and powder blend (subject to limits on hardend properties) for workability. 5. Calculate paste composition. 6. Evaluate trial mixtures and adjust paste composition based on Table 13.5.

Table 13.5: Effects of Mixture Proportions on SCC Workability

		Slump Flow	Viscosity	Filling Ability	Passing Ability	Segregation Resistance
Aggregates	↑ Maximum Size	↑	↓	↑↓	↓	↓
	Grading	Higher pkg. density; coarser or gap grading: ↑	Higher pkg. density or gap grading: ↓	↑↓	Finer grading: ↑	Continuous or finer grading: ↑
	Improved Shape	↑	↓	↑	↑	↓
	Increased Angularity	↓	↑	↓	↓	↑
	↑ Paste Volume	↑	↓	↑	↑	↑
Paste Composition	↑ Water/Powder	↑	↓	↑	↑	Not too high or too low: ↑
	Fly Ash	↑	↓	↑	↑	↑↓
	Slag	↑↓	↑↓	↑↓	↑↓	↑↓
	Silica Fume (Low %)	↑↓	↓	↑	↑	↑↓
	Silica Fume (High %)	↓	↑	↑↓	↓	↑↓
	VMA	↓	↑	↑	↑↓	↑
	HRWRA	↑	↓	↑	↑	↓
	Air	↑↓	↓	↑	↑	↑↓

Notes:
1. There are exceptions for every case.
2. Slump flow is inversely proportional to yield stress. Viscosity is proportional to T_{50} or v-funnel time.
3. This table reflects trends over the range of values typical for SCC and may not apply for extreme values. For instance, increasing water/powder to extremely high values will not improve filling or passing abilities. Stated effects assume mixtures are adjusted to achieve SCC slump flow before and after change.

13.4.1 Selection of Aggregates

Aggregates should be selected to maximize aggregate content for the given application because aggregates are the lowest-cost component aside from water and higher aggregate contents are often associated with improved hardened properties. The three sub-factors for selecting aggregate characteristics are maximum size, grading, and shape, angularity, and texture. Additionally, certain clays present in aggregates may increase HRWRA demand for a given slump flow. Both grading and shape, angularity, and texture are important: consideration of one at the exclusion of the other is inappropriate. The properties of the combined aggregates should be considered.

Maximum Size. The maximum aggregate size should usually be selected as large as possible provided the workability requirements can be achieved. Larger maximum aggregate sizes are beneficial for workability to the extent that they increase the range of aggregate sizes and result in improved grading. The maximum aggregate size can be reduced to increase passing ability and segregation resistance. A maximum aggregate size of ¾ or 1 inch is acceptable for most applications. The maximum aggregate size may be reduced to as low as 3/8 inch to ensure passing ability.

Grading. There is not a universally optimal grading for SCC. The best grading depends on the application and the aggregate. For example, a grading with a large fraction of coarse particles may reduce HRWRA demand and plastic viscosity but result in poor passing ability. Further, the net effect of adding a poorly shaped aggregate to improve grading may be adverse. In general, continuously graded aggregate—namely without a deficiency or excessive amount of material on any two consecutive sieves (Figure 13.2)—and gradings with high packing densities are favorable. Gap gradings often result in lower concrete HRWRA demand and plastic viscosity; however, they should normally be avoided because they result in increased segregation. In many cases, the 0.45 power curve is a favorable grading because it provides high packing density and is associated with low concrete HRWRA demand and plastic viscosity. The 0.45 power curve is developed on a plot of percent passing versus size, where the sizes are raised to the 0.45 power. A straight line is normally drawn from the origin to the maximum aggregate size, as shown in Figure 13.2. This approach; however, results in a large volume of material passing the No. 200 sieve, which should more appropriately be considered powder and accounted for as part of the paste. Therefore, in constructing the 0.45 power curve, the straight line should be drawn between the No. 200 sieve and the maximum aggregate size. Gradings

finer than the 0.45 power curve are also usually preferred to coarser gradings because they reduce harshness. As a first approach when combining two aggregates, the sand-aggregate ratio should be set between 0.40 and 0.50. It is often favorable to blend three or more aggregates in cases where combining fewer aggregates would result in a gap grading. Because smaller aggregate sizes are commonly used for SCC (e.g. ¾ or 1 inch), problems with gap gradings may not be as severe as if larger maximum aggregate sizes were used (e.g. 1.5 inches).
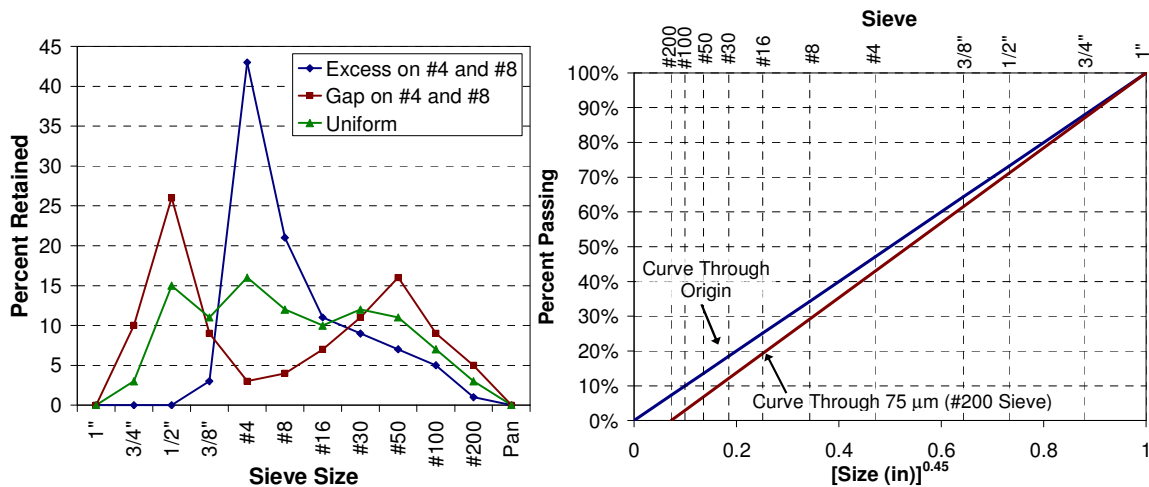
Figure 13.2: Example Percent Retained Plots and 0.45 Power Curve Plot

Shape, Angularity, and Texture.   The shape and angularity of aggregates can significantly affect workability by influencing the aggregate compacted voids content and the interparticle friction between aggregates. Equidimensional, well-rounded aggregates are best for workability; however, aggregates of all shape and angularity can be accommodated in SCC by increasing the paste volume. Once the paste volume is sufficient for a given aggregate, concrete workability can be further enhanced by adjusting the paste composition. Texture has minimal effect on workability. A visual examination is typically sufficient for characterizing aggregate shape and angularity. Table 13.6 should be used to assign a single visual rating, on a scale of 1 to 5, representing both shape and angularity. A single rating should be assigned to each combined grading. For instance, a crushed coarse aggregate with a rating of 5 blended with a well-shaped natural sand with a rating of 1 would receive a rating of 3 for the combined grading. When possible, historic data on the performance of a particular aggregate in SCC is the best guide for assigning the visual shape and angularity rating.

313

To select aggregates, various aggregate sources should be considered (fine, intermediate, and coarse sizes). Various blends of the aggregates should be evaluated in terms of maximum aggregate size, grading, and shape and angularity. The compacted voids content and visual shape and angularity rating should be determined on all aggregate blends. Measuring the compacted voids content on a series of aggregate blends—such as for a range of S/A values—can be used to identify the minimum voids content. The minimum voids content (maximum packing density) may not be optimal in all cases because other considerations—such as passing ability, segregation resistance, or harshness—may be more important.

Table 13.6: Guidelines for Assigning Visual Shape and Angularity Rating

	Visual Shape and Angularity Rating (R_{S-A})				
	Well-Shaped, Well Rounded			Poorly Shaped, Highly Angular	
	1	2	3	4	5
Shape	most particles near equidimensional	modest deviation from equidimensional	most particles not equidimensional but also not flat or elongated	some flat and/or elongated particles	few particles equidimensional; abundance of flat and/or elongated particles
Angularity	well-rounded	rounded	sub-angular or sub-rounded	angular	highly angular
Examples	most river/glacial gravels and sands	partially crushed river/glacial gravels or some very well-shaped manufactured sands	well-shaped crushed coarse aggregate or manufactured sand with most corners > 90°	crushed coarse aggregate or manufactured sand with some corners ≤90°	crushed coarse aggregate or manufactured sand with many corners ≤90° and large convex areas

13.4.2 Selection of Paste Volume

A minimum paste volume must be provided to ensure filling ability and passing ability. Without the minimum paste volume, SCC workability properties cannot be achieved, regardless of the composition of the paste (e.g. power content, w/p, use of VMA, etc.). The minimum required paste volume should be determined separately for filling ability and passing ability. Additional paste volume in excess of the minimum required for filling or passing ability increases robustness with respect to aggregate properties.

The minimum paste volume for filling ability is depicted conceptually in Figure 13.3. Concrete without the minimum paste volume for filling ability may not achieve the desired slump flow regardless of the HRWRA dosage, may be highly viscous, may exhibit severe bleeding and segregation, and may appear harsh. A certain amount of paste must be provided to fill the voids between compacted aggregates. If only this amount of paste were provided, the concrete would not flow due to the significant interparticle friction between aggregates. Therefore, additional paste must be provided to separate aggregates. This paste used to separate the aggregates provides lubrication by reducing interparticle friction between aggregates.
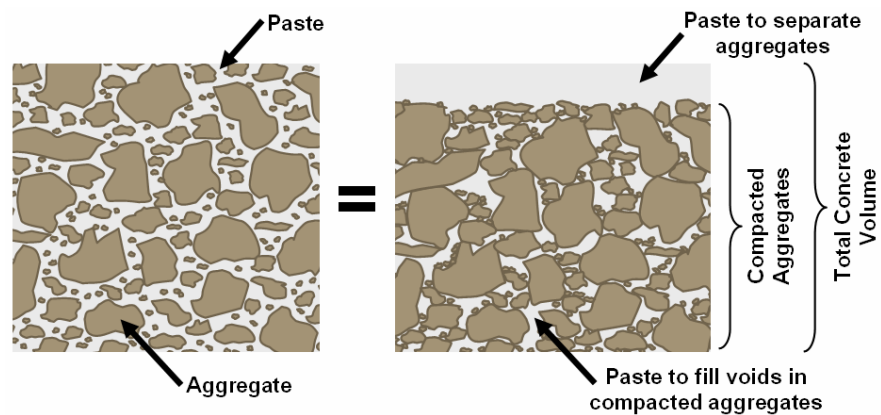
Figure 13.3: Schematic Representation of Aggregate in Cement Paste

The total amount of paste for filling ability ($V_{paste\text{-}filling\_ability}$) is the sum of the paste to fill the voids ($V_{paste\text{-}voids}$) and to provide spacing between aggregates ($V_{paste\text{-}spacing}$), as expressed in Equation (13.2):

$$V_{paste-filling\_ability} = V_{paste-voids} + V_{paste-spacing} \tag{13.2}$$

The minimum amount of paste needed to provide spacing between aggregates depends primarily on the shape and angularity of the combined aggregate and ranges from 8% for equidimensional, well-rounded aggregates (visual shape and angularity rating of 1) to 16% for poorly shaped, angular aggregates (visual shape and angularity rating of 5). (Aggregates with extremely poor shape and angularity characteristics may require even more than 16%.) The minimum paste volume for filling ability is largely independent of the paste composition—provided the paste composition is within the range of typical SCC mixtures. The total paste volume for filling ability (expressed as a percentage of concrete volume) can be calculated as a function of the paste volume for spacing (expressed as a percentage of concrete volume) and the

315

percentage of voids in the compacted aggregate ($\%voids_{compacted\_agg}$, expressed as a percentage of the bulk aggregate volume), as shown in Equation (13.3):

$$V_{paste-filling\_ability} = 100 - \frac{(100 - V_{paste-spacing})(100 - \%voids_{compacted\_agg})}{100}$$ (13.3)

The amount of spacing paste can be calculated from the visual shape and angularity rating (R_{S-A}), as indicated in Equation (13.4):

$$V_{paste-spacing} = 8 + \left(\frac{16-8}{4}\right)(R_{S-A} - 1)$$ (13.4)

Equation (13.3) indicates that the paste volume for filling ability can be reduced by reducing the compacted aggregate voids content (by increasing the maximum aggregate size, improving the grading, improving the shape and angularity) or by improving the shape and angularity to reduce the volume of spacing paste. It is recommended that tests with various paste volume be conducted to confirm the calculated minimum paste volume. For instance, if a minimum paste volume of 32% is calculated with Equation (13.3), trial batches should be measured at 30, 32, and 34% to determine the minimum sufficient paste volume (not necessarily the optimal workability because proper paste composition must be established also). Because the minimum paste volume for filling ability is largely independent of the paste composition, the paste composition should be near that expected in the final mixture and should be held constant as the paste volume is varied.

For passing ability, sufficient paste volume is needed to reduce the volume of coarse aggregates and to reduce interparticle friction between aggregate particles. The amount of paste depends mainly on the aggregates (higher maximum sizes and coarser gradings increase the amount of large particles that must pass, reducing passing ability; angular and poorly shaped aggregates increase interparticle friction between aggregates, reducing passing ability) and the paste volume (higher paste volumes decrease the volume of aggregate that must pass and reduce interparticle friction between aggregates, increasing passing ability). The amount of paste needed depends to a lesser extent on the rheology of the paste (lower paste viscosity and higher slump flow result in increased passing ability). To determine the amount of paste needed for passing ability, it is recommended that testing be conducted with the j-ring at various paste volumes with constant paste composition (the paste composition should be near that expected in the final mixture). The determination of minimum paste volume for passing ability for unreinforced or lightly reinforced sections is unnecessary.

If the minimum paste volume for passing ability is higher than that for filling ability, it may be beneficial to modify the aggregate grading by decreasing the maximum aggregate size or decreasing the coarseness of the grading (e.g. higher S/A). This change would reduce the overall minimum paste volume needed by decreasing the minimum paste volume for passing ability, even though the minimum paste volume for filling ability would likely be increased.

The larger of the paste volumes required for filling or passing ability should be selected. Additional paste can be used to increase robustness with respect to aggregate properties. The amount of paste needed for robustness depends on the level of quality control and expected variations in materials.

13.4.3 Selection of Paste Composition

With the paste volume determined, the composition of the paste is selected to achieve the required workability and hardened properties. Selecting the paste composition involves selecting the relative amounts of water, powder, and air and the blend of powder (Table 13.7). Admixtures are also added at this stage. In selecting admixtures and powder materials, the compatibility of these materials with each other should be considered. Incompatibilities between materials may result in inadequate concrete performance or prohibitive material costs.

The paste composition selection is the stage where the distinction between powder-type and VMA-type SCC is made (Table 13.8). Powder-type SCC consists of high powder contents—with a large portion of the powder content comprised of SCMs and fillers—and a low water-powder ratio. VMA-type SCC utilizes lower powder contents and higher water-powder ratios and, therefore, must incorporate a VMA to ensure stability. The minimum paste volume for filling ability is the same for powder-type and VMA-type SCC.

Table 13.7: Selection of Paste Composition

	Parameter	Purpose
Water	Water/Cement	Early-age hardened properties
	Water/Cementitious Materials	Long-term hardened properties
	Water/Powder	Workability
Powder	Cement	Strength and durability
	SCMs	Improve workability and durability, reduce heat, reduce cost
	Mineral Fillers	Improve workability, reduce cost
Air	Air Content	Durability

Water Content. The water content is established by selecting limits on water/cement (early-age hardened properties), water/cementitious materials (long-term hardened properties),

and water/powder (workability). The high degree of powder dispersion achieved with high dosages of HRWRA may increase the w/c or w/cm needed for a given strength level compared to conventionally placed concrete with no or low dosages of HRWRA. If the powder consists only of cement and SCMs, the w/p is equal to the w/cm. The total water content per unit volume of concrete (e.g. lb/yd^3) is usually similar to that in conventionally placed concrete. The w/p typically varies from 0.30 to 0.45. Higher values of w/p can be used; however, a VMA is typically required. Increasing the w/p decreases the HRWRA demand for a constant slump flow and reduces plastic viscosity. As the paste volume is increased for a given aggregate, the paste viscosity should be reduced. As a first approximation, the total water content per unit volume of concrete should be held constant as the paste volume is increased.

Powder Blend. Given the high powder contents required to achieve SCC workability, it is often necessary to include SCMs or mineral fillers as part of the powder. The powder content must contain a minimum amount of cement for strength and durability. SCMs can be used to improve workability and durability, reduce heat of hydration, and reduce cost. Mineral fillers significantly finer than cement typically enhance workability and may contribute to accelerated strength gain. Mineral fillers approximately the same size of cement typically have minimal effects on workability and do not contribute to strength.

Air Content. Air content requirements for SCC—namely total air content, bubble size, and bubble spacing—are similar to those for conventionally placed concrete.

To select the paste composition, limits on some of the factors listed in Table 13.7 can be used to compute the relative amounts of water, powder, and air. Typical ranges of values for powder content and water-powder ratio are given in Table 13.8. This table should be used as a general guideline only; trial batches of concrete should be used to establish final proportions. Table 13.5 describes how to adjust paste composition to achieve desired workability properties. In achieving the correct workability, the paste composition should be adjusted to reach the proper slump flow and viscosity. Slump flow is adjusted by varying the HRWRA dosage. The HRWRA demand for a given slump flow can be reduced by varying the paste composition, paste volume, and aggregates. The viscosity determines the ease with which the concrete can be placed and should not be too low (poor stability) or too high (sticky and cohesive). Tests can be conducted on paste or mortar to evaluate the relative effects of various constituents; however, the final paste composition should be verified in concrete. Examples of paste composition calculations are shown in Table 13.9. Tests for filling ability, passing ability, and segregation

resistance should be performed prior to selecting final mixture proportions, if not on every trial batch.

Table 13.8: Typical Paste Compositions

	Powder-Type	VMA-Type
Powder Content	650-900 lb/yd^3	<650
Water/Powder	0.30-0.45	>0.45
Admixture	HRWRA only	HRWRA and VMA
Note: These values are given as a general guideline as there is not a discrete distinction between powder- and VMA-type SCC. Mixtures near the transition between powder and VMA-type may incorporate aspects of each type (e.g. combination type)		

Table 13.9: Sample Calculations for Paste Composition

Case	Specified Parameters	Parameters							Proportions (lb/yd^3)					
		Paste Volume	w/p	w/cm	w/c	Fly Ash	Mineral Filler	Air	Water	Cement	Mineral Filler	Fly Ash	Coarse	Fine
1	w/cm≤0.60	32%	0.40	0.40	0.40	0%	0%	2%	281.8	704.5	--	0.0	1489.4	1489.4
2	w/cm≤0.60	32%	0.37	0.37	0.529	30%	0%	2%	260.7	493.1	--	211.6	1489.4	1489.4
3	w/cm≤0.60	32%	0.40	0.60	0.60	0%	33.3%	2%	269.4	449.0	224.5	--	1489.4	1489.4
4	w/cm≤0.40, w/c≤0.50	32%	0.40	0.40	0.50	20%	0%	2%	274.2	548.4	--	137.1	1489.4	1489.4
5	w/cm≤0.40, w/c≤0.50	36%	0.325	0325	0.50	35%	0%	2%	274.9	549.8	--	296.1	1401.8	1401.8
6	w/cm≤0.40, w/c≤0.50 6% air	32%	0.40	0.40	0.50	20%	0%	6%	237.6	475.3	--	118.8	1489.4	1489.4

Case 1: Hardened properties do not control. The maximum w/cm is set for 0.60; however, the w/p must be lower to ensure workability. Since cement is the only powder, w/p=w/c=w/cm.
Case 2: The same requirement as case 1, but 30% fly ash is used for economy. The w/p ratio is reduced to offset the reduction in viscosity due to fly ash. Since all powders are cementitious, w/p=w/cm
Case 3: The same requirements as case 1, but mineral filler (microfines) is used, resulting in the specified w/cm.
Case 4: The maximum w/cm is set for long-term properties and w/c is limited to ensure sufficient early-age strength. The fly ash content is maximized while maintaining the specified w/cm and w/c.
Case 5: The same requirements as case 4, but passing ability requirements dictate a higher minimum paste volume. The paste volume is increased by adding fly ash, resulting in a lower w/p and w/cm. The viscosity is approximately unchanged because the increased paste volume and fly ash content reduce viscosity, while the lower w/p increases viscosity.
Case 6: The same requirements as case 4 but with 6% air.

Workability retention should be considered in establishing the paste composition. Factors affecting workability retention are shown in Table 13.10.

Table 13.10: Factors Affecting Workability Retention

Factor	Role in Workability Retention
HRWRA type and dosage	Polycarboxylate-based HRWRA admixtures can be designed for various amounts of workability retention. Increasing the dosage increases workability retention.
Retarder type and dosage	Retarders may increase, decrease, or have no effect on workability retention, depending on the chemical composition of the retarder. Increasing the dosage generally increases the effect of the retarder.
Cement, filler, and SCM types and amounts	The physical and chemical properties of the powder constituents affect workability retention.
Concrete rheology	Mixtures that are more viscous tend to have longer workability retention.
Other (weather, agitation)	Hot and dry conditions accelerate the loss of workability. Agitation may increase or decrease workability retention.

13.5 Optimization of Mixtures

Mixtures should be optimized to achieve desired filling ability, passing ability, segregation resistance, hardened properties, economy, and robustness. The optimization of mixtures is often an iterative process, as indicated in Table 13.11. For instance, if the paste volume is too high, resulting in poor economy and reduced hardened properties, the aggregates can be improved. When the paste volume and aggregates are changed, it may be necessary to adjust the paste composition to achieve proper workability. Table 13.5 provides specific guidelines for adjusting mixture proportions to achieve SCC workability.

Table 13.11: Optimization of Mixtures

Step	Tasks	Adjustments
STEP 1 Aggregates	Evaluate various aggregates and gradings, determine voids between compacted aggregates	Paste volume too high? Adjust aggregates.
STEP 2 Paste Volume	Evaluate passing ability and filling ability for range of paste volumes, maintain constant paste composition	Aggregates Changed? Adjust pate volume. Poor robustness? Increase paste volume.
STEP 3 Paste Composition	With paste volume and aggregates set, vary paste composition for workability and hardened properties	Paste volume or aggregates changed? Adjust paste composition.

13.6 Examples

The following examples illustrate the ICAR SCC mixture proportioning procedure.

13.6.1 Example 1: Precast, Prestressed Concrete

Requirements

A SCC mixture is needed for precast, prestressed girders. The 16-hour release strength must be 5,000 psi based on a specified temperature history; the 28-day strength is specified as

9,000 psi. For filling ability, the specified slump flow is 26-28 inches with a T_{50} between 3 and 7 seconds and a VSI of less than 1.0. For filling ability, the j-ring change in height from inside to outside of the ring is specified as less than 0.50 inches due to the highly congested strands and bars. For segregation resistance, the segregation index from the column segregation test is specified as less than 15%. No air entrainment is required.

Step 1: Aggregates

Two coarse aggregates (3/4" maximum aggregate size) are to be considered: a well-shaped river gravel (specific gravity = 2.59) and crushed limestone coarse aggregate (specific gravity = 2.59). A well-shaped natural sand is used with both aggregates (specific gravity = 2.58). The aggregates are considered at S/A values of 0.40 to 0.50. The visual shape and angularity index is determined to be 1.0 for the river gravel-natural sand blend and 3.0 for the crushed limestone-natural sand blend. The aggregate gradings, shown in Figure 13.4, are considered acceptable for SCC.

Step 2: Paste Volume

The paste volume is computed for filling ability based on Equation (13.3) for each aggregate, as indicate in Table 13.12. Passing ability is evaluated by varying the paste volume with constant paste composition and evaluating j-ring results. As indicated in Figure 13.5, the paste volume for passing ability is reduced with reduced coarse aggregate volume (higher S/A) and improved shape and angularity (river gravel versus crushed limestone). Due to the highly congested reinforcement, passing ability requirements control the selection of minimum paste volume. Additional paste volume of 1% is added to each blend for robustness with respect to aggregate properties.

Step 3: Paste Composition

A Type III cement (specific gravity = 3.15) and Class F fly ash (specific gravity = 2.33) are selected to comprise the powder. To achieve the required 16-hour compressive strength, the w/c must be 0.41 for the river gravel and 0.45 for the crushed limestone. Fly ash is used to improve workability, reduce heat of hydration, improve durability, and improve economy. The final mixture proportions for each blend are shown in Table 13.13, based on the results of trial concrete batches. The w/p is set for workability. Increasing the paste volume or fly ash dosage

for a given aggregate requires a lower w/p for the same approximate workability. Because all powder is cementitious, the w/cm is equal to the w/p. In this example, the microfines content is low and can be neglected in computing the w/p and paste volume. The w/cm is more than adequate to achieve the 28-day compressive strength requirement of 9,000 psi.
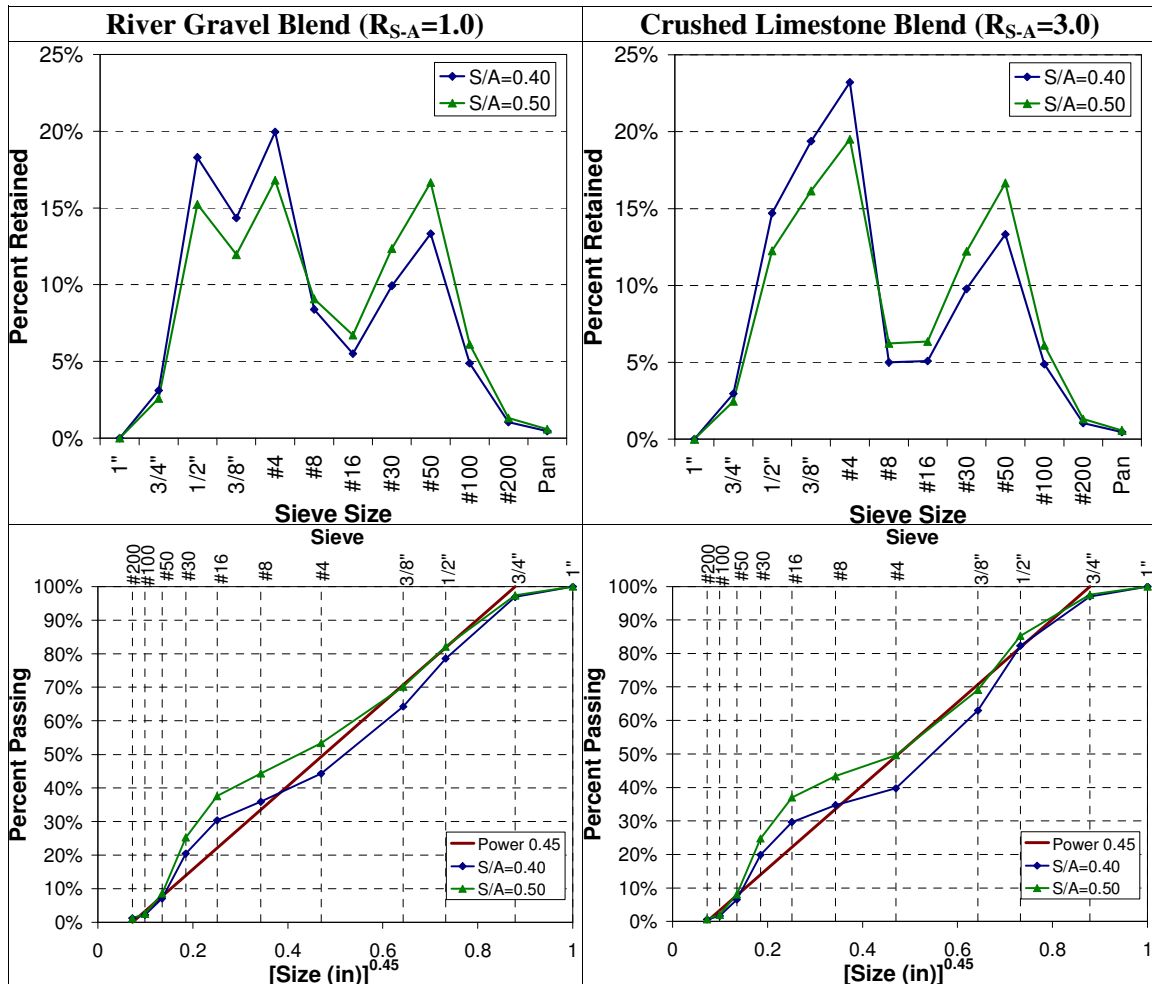
Figure 13.4: Example 1 Gradings

Table 13.12: Example 1 Required Paste Volumes

| S/A | River Gravel | | | Crushed Limestone | | |
| | Voids Content | Req'd Paste Volume | | Voids Content | Req'd Paste Volume | |
		Filling	Passing		Filling	Passing
0.40	23.9	30	36	23.9	33	41
0.50	23.2	29	32	22.7	32	36
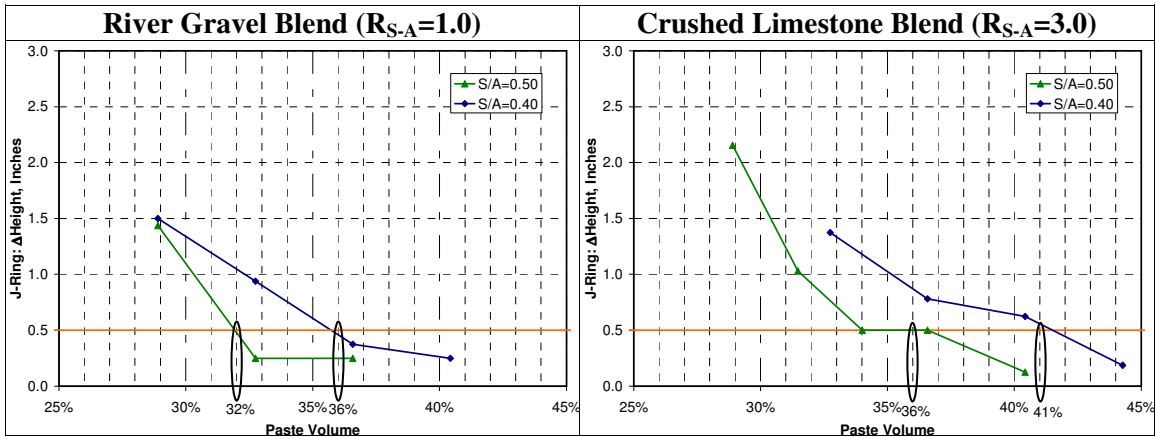
Figure 13.5: Example 1 Minimum Paste Volume for Passing Ability

Table 13.13: Example 1 Paste Composition

Mixture	Parameters						Proportions (lb/yd³)				
	Paste Volume	w/p	w/cm	w/c	Fly Ash	Air	Water	Cement	Fly Ash	Coarse	Fine
River Gravel, S/A=0.40	37%	0.28	0.28	0.412	32%	2%	260.8	633.3	298.0	1649.5	1095.4
River Gravel, S/A=0.50	33%	0.33	0.33	0.413	20%	2%	257.3	623.8	156.0	1461.8	1456.2
Limestone, S/A=0.40	42%	0.27	0.27	0.45	40%	2%	287.8	639.6	426.4	1518.5	1008.5
Limestone, S/A=0.50	36%	0.30	0.30	0.448	33%	2%	270.4	603.8	297.4	1374.5	1369.2

13.6.2 Example 2: Ready Mixed Concrete

Requirements

A SCC mixture is required for use in a lightly reinforced slab on grade. The specifications require a maximum w/cm of 0.50 and 5% entrained air content. Because the concrete may need to flow long horizontal distances, the slump flow is set to 26-28 inches with a T_{50} of 3-6 s and a VSI ≤ 1.0. A maximum segregation index for the column segregation test is specified as 15%.

Step 1: Aggregates

A rounded, well-shaped fine aggregate (specific gravity = 2.60) and a crushed limestone coarse aggregate with a ¾" maximum aggregate size (specific gravity = 2.60) are selected. The visual shape and angularity index is determined to be 3.0. After considering blends of these two aggregates at S/A values of 0.40 to 0.50, the blend with an S/A of 0.50 is selected because it results in the minimum compacted voids content of 23.9%. The higher S/A results in more of the well-shaped sand and less of the angular, poorly shaped coarse aggregate, which allows lower paste volume and improved workability. The resulting grading, shown in Figure 13.6, is

323

reasonably continuous (no excess or deficiency on consecutive sieves) and is finer than the 0.45 power curve.
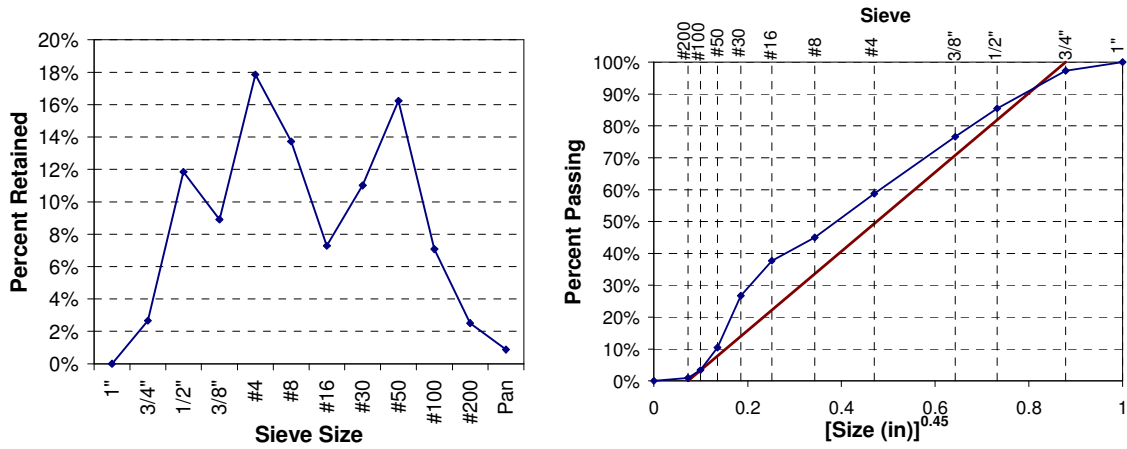
Figure 13.6: Example 2 Aggregate Grading

Step 2: Paste Volume

The volume of spacing paste and total paste are computed in Equations (13.5) and (13.6).

$$V_{paste-spacing} = 8 + \left(\frac{16-8}{4}\right)(R_{S-A} - 1) = 8 + \left(\frac{16-8}{4}\right)(3-1) = 12 \tag{13.5}$$

$$V_{paste-filling\_ability} = 100 - \frac{(100 - V_{paste-spacing})(100 - \%voids_{compacted\_agg})}{100}$$

$$= 100 - \frac{(100-12)(100-23.9)}{100} = 33.0 \tag{13.6}$$

Because the concrete is to be used in a lightly reinforced slab, it is unnecessary to check passing ability requirements. Concrete mixtures are evaluated at paste volumes of 31, 33, and 35% to confirm the minimum required paste volume. The mixture with 31% paste volume is viscous and exhibits severe bleeding, suggesting inadequate paste volume for filling ability. The mixture with 33%, however, has adequate paste volume. The 33% paste volume required for filling ability is increased by 2% to 35% to assure robustness with respect to aggregate properties.

Step 3: Paste Composition

A Type I cement (specific gravity = 3.15) and Class F fly ash (specific gravity = 2.40) are selected to comprise the powder. Trial mixtures are evaluated by varying the fly ash dosage and

w/p, as shown in Table 13.14. The fly ash is used at a rate of 35% of the powder mass to improve economy and workability while the w/p is set at 0.36 to establish the target workability. In this example, the microfines content is low and can be neglected in computing the w/p and paste volume.

Table 13.14: Example 2 Paste Composition

Trial	Parameters						Proportions (lb/yd^3)					Comments
	Paste Volume	w/p	w/cm	w/c	Fly Ash	Air	Water	Cement	Fly Ash	Coarse	Fine	
1	35%	0.40	0.40	0.40	0	5%	281.8	704.5	0.0	1423.7	1423.7	Uneconomical (cement too high)
2	35%	0.40	0.40	0.615	35%	5%	268.8	436.9	235.1	1423.7	1423.7	Viscosity too low ($T_{50}=$ 1.2s), should reduce w/p
3	35%	0.38	0.38	0.584	35%	5%	262.3	448.8	241.5	1423.7	1423.7	Viscosity too low $T_{50}=$ 2.4s), should reduce w/p
4	35%	0.36	0.36	0.554	35%	5%	255.5	461.4	248.3	1423.7	1423.7	Good, FINAL MIXTURE

Chapter 14: Evaluation of Workability Test Methods

When the research described in this dissertation began, no workability test methods for SCC had been standardized in the United States. Although many test methods had been proposed, limited information was available on exactly what each test measured and on why certain tests should be used. Many of the details of each test, such as dimensions and procedures, varied throughout the world. As a result, seven test methods were selected for extensive evaluation to identify the best test methods for routine use based on sound, engineering justifications. The seven test methods evaluated were the column segregation test, j-ring test, l-box test, penetration apparatus test, sieve stability test, slump flow test, and v-funnel test. These test methods were evaluated as part of the research described in this dissertation and a concurrent project at the University of Texas on the use of SCC for precast, prestressed bridge beams (Koehler et al. 2007). The data presented in this chapter are from both research projects and, therefore, cover a wide range of materials and mixture proportions. The specific test procedures are included in Appendix B.

14.1 Criteria for Evaluation of Test Methods

Each test method was evaluated based on its suitability for routine use in the laboratory for evaluating materials and developing mixture proportions and in the field for quality control. The following criteria were established to evaluate the test methods.

Well-Defined Results. The test results should clearly indicate filling ability, passing ability, segregation resistance (static or dynamic stability), a fundamental rheological parameter, or some other relevant property. The test results should be suitable for use in specifications.

Independent Measurements. Tests should measure filling ability, passing ability, and segregation resistance independently. By measuring only one of these properties at a time, the results can be used to identify specific problems with a mixture and implement solutions. In contrast, pass/fail-type tests that measure some combination of filling ability, passing ability, or segregation resistance indicate when a mixture is inadequate but provide little information for correcting problems. For instance, a test that measures both filling ability and passing ability

simultaneously would be unsuitable because if the test results indicate inadequate workability, it would be impossible to determine whether the concrete lacks filling ability, passing ability, or both. To some extent, filling ability, passing ability, and segregation resistance are interrelated; therefore, some overlap is inevitable. Tests can, however, measure one aspect of workability predominantly.

Simplicity. The equipment, test procedures, and interpretation of test results should be simple. The test should be standardized and the number of variations and options minimized. Minimal training should be required.

Use of Results. It should be possible to implement test results directly with minimal analysis. If concrete is unsuitable, the test should provide information on exactly why the concrete is unsuitable so action can be taken to rectify the problem or reject the mixture.

Use in Field. Test methods intended for use in the field must be lightweight, rugged, easy to perform in a variety of locations and circumstances, easy to clean, and low in cost. These same aspects are also desirable in tests intended for use primarily in the laboratory. When possible, the same tests should be performed in the laboratory and field.

Repeatability and Reproducibility. The test results must be robust and reliable, particularly given the potentially severe consequence of inadequate SCC workability.

14.2 Evaluation of Test Methods

14.2.1 Column Segregation Test

14.2.1.1   Discussion of Test

The column segregation test provides an independent measurement of segregation resistance by replicating static conditions in formwork and quantifying the segregation of coarse aggregate after a fixed time. Although increasing the slump flow generally increases the risk of segregation, the column segregation test does not provide an indication of filling ability. Figure 14.1 indicates that the results of the column segregation test are well correlated to those of the

sieve stability test. A 15% static segregation in the column segregation test corresponds to a 15% reading form the sieve stability test; which was found to be appropriate by the European Testing SCC project (de Schutter 2005, Testing-SCC 2005).
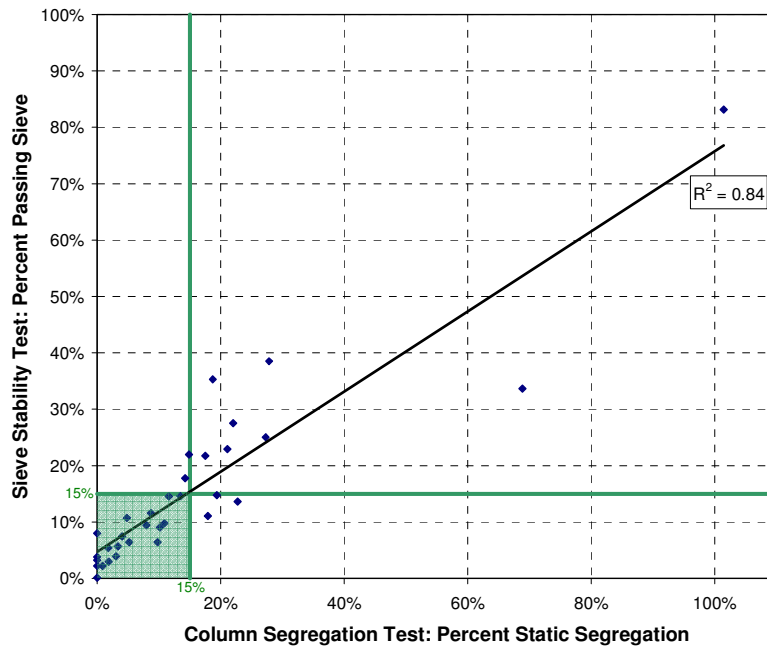
Figure 14.1: Relationship between Column Segregation Test and Sieve Stability Test (Koehler et al. 2007)

There are variations in the test apparatus, test procedure, and measurement of results that are important to interpreting results consistently. The test apparatus typically consists of four 6.5-inch long, 8-inch diameter pipe sections. The 8-inch diameter is representative of most field applications—reducing the diameter would likely reduce the amount of segregation recorded. The total height of 26 inches is adequate for measuring a significant difference in coarse aggregate mass between the top and bottom of the column. Other sizes of cylinders—varying from 4 by 8-inch cylinders to much larger columns—have been used to measure static segregation, though usually not by removing coarse aggregate in the same fashion as in the column segregation test. The version of the test evaluated by the European Testing SCC project featured a rectangular cross section and was attached to a drop table to accelerate segregation.

The test procedure mainly differs in when the coarse aggregate variation is measured. ASTM C 1621 requires the concrete to be left undisturbed for 15 minutes, which should be adequate for most cases. In other cases, concrete is allowed to harden and is then cut open to

quantify the distribution of coarse aggregate. The ASTM C 1621 procedure allows aggregate mass to be determined when the aggregates are in saturated-surface dry condition, which enables the test to be completed sooner but may increase the variability of test results.

Several different ways of calculating test results have been reported. Results have been computed as a function of the relative amount of aggregate in just the top and bottom sections or in all four sections. The use of only the top and bottom sections is the preferred approach because it requires less work and the relative difference in aggregate mass in the middle two sections is likely to be low in most cases. A variety of ratios of aggregate mass in the top and bottom sections have been used; however, one is not clearly better than the others.

In performing the column segregation test, proper sampling is crucial. Concrete should not be segregated when it is first put into the column. Therefore, the source of the concrete—such as a wheelbarrow—should not be segregated and the act of filling the column should not cause segregation. Because paste rheology strongly influences the degree of static segregation, the rheology of the concrete at the anticipated time of placement in the field should be considered. For instance, a laboratory-mixed concrete that is tested immediately after mixing may not be similar to the same mixture that is mixed in a truck, transported for 30 minutes, and then pumped to its final location. Mixtures with workability retention beyond the time of placement are more likely to segregate over time because the yield stress and plastic viscosity remain low for a longer time.

The column segregation test is difficult and time-consuming to perform. The most difficult aspect of the test procedure is the removal of concrete from the pipe sections. Various collector plates have been developed; however, all require at least two people and do not adequately minimize the potential for spilling concrete. The test takes at least 30 minutes to perform—including filling the column, allowing the concrete to remain undisturbed for 15 minutes, collecting the concrete from the column, washing and sieving the aggregate, and drying the aggregate to its saturated surface-dry condition. If the aggregate is oven-dried, results are not available for at least several more hours. The need for a balance to determine aggregate mass makes the test further impractical for use in the field.

14.2.1.2　　　Advantages and Disadvantages

The advantages of the column segregation test include:

- The test provides an independent measurement of static stability.

- The test conditions generally reflect field conditions.

The disadvantages of the column segregation test include:
- The test does not measure dynamic stability.
- The test is difficult and time-consuming to perform and requires the use of a balance. Therefore, it is unsuitable for field use.
- Errors in sampling can influence test results significantly.

14.2.1.3　　　Recommendations

Either the column segregation test or the sieve stability test should be used to measure static segregation resistance. The results of the two tests are well-correlated; however, the sieve stability test is easier to perform. In performing the column segregation test, the procedure described in ASTM C 1621 is suitable. The test is not appropriate as a rapid field acceptance test. When using the test in the laboratory to qualify mixture proportions, mixtures should be prepared with the range of water contents and HRWRA dosages expected during production. If these mixtures exhibit adequate segregation resistance and the slump flow test is used in the field to control concrete rheology indirectly, it is not necessary to use the column segregation test in the field.

14.2.2 J-Ring Test

14.2.2.1　　　Discussion of Test

The j-ring test provides an independent measurement of passing ability. Increasing the slump flow (filling ability) typically results in less j-ring blocking; however, it is likely that this trend is also present in field conditions. It is not affected by slump flow nearly to the extent as the l-box test. The European Testing-SCC project selected the j-ring, along with the l-box, as reference test methods for passing ability; however, they favored the l-box because of the availability of more field experience with the l-box.

There are variations in the test apparatus, test procedure, and measurement of results that are important to interpreting results consistently. The test apparatus can vary in the size and spacing of bars. Either smooth or deformed reinforcing bars can be used in the test. The use of deformed bars is more representative of US construction practices. In other parts of the world,

330

smooth bars can be used in construction. Due to the role of friction in affecting passing ability, the use of deformed bars is preferred. In any case, deformed or smooth bars should be used consistently. The bar size is typically ½ or $^5/_8$ inches. The spacing of bars, however, can vary widely. It is possible to vary either the reinforcing bars or the acceptance criteria—namely the change in height, change in slump flow, or test value—based on the application. While both approaches are acceptable, the use of constant bar spacing is more practical because it allows the same j-ring apparatus to be used in all cases without adjustment. The limitation of using the same bar spacing is that the standard bar spacing may not adequately represent field conditions for concrete with very large aggregate sizes or for applications with very narrow clear spacing. In the ASTM C 1621 standard, the clear spacing is approximately 1.75 inches, which appears to be an appropriate compromise. If the bar spacing is varied, it should be based on the actual bar spacing in the field and not the maximum aggregate size. The diameter of the ring is mostly consistent. The diameter of 12 inches is appropriate because it is small enough to evaluate mixtures with a wide range of slump flows and is large enough to contain a sufficient number of bars.

The main variation in the test procedure is the orientation of the slump cone. The use of the inverted slump cone orientation is recommended for the same reasons as for the slump test. In addition, if the cone is used in the inverted orientation, the foot pieces on the cone do not need to be removed so that the cone will fit within the j-ring.

The test results can be reported as the difference in height between the inside and outside of the j-ring, the change in slump flow spread with and without the j-ring, or the "test value" which is a function of the height of concrete inside and outside and at the center of the j-ring. In some cases, T_{50} flow time is also measured. The change in height between the inside to outside of the ring is the best approach because of its simplicity, precision, and ability to best reflect the extent of passing ability. The j-ring test value (PCI 2003) is computed as shown in Equation (14.1) based on four measurements of the height of concrete inside (h_{inside}) and outside ($h_{outside}$) of the ring and one measurement at the center of the ring (h_{center}):

$$\mathrm{J-Ring\ Test\ Value} = 2\big[median(h_{inside} - h_{outside})\big] - median(h_{center} - h_{inside}) \qquad (14.1)$$

This calculation of the test value is unnecessarily complex. The difference in height between the inside and outside of the ring is much easier to determine. Figure 14.2 indicates a high correlation between the j-ring test value and change in height, suggesting the added calculation for the j-ring test value is of no benefit. The difference in height is typically measured at four

331

locations equally spaced around the ring. The use of multiple measurements is important because some variation in blocking around the ring is possible. To simplify the determination of a single value, the median of three measurements can be used. The inside measurement can be made at the center of the ring or just inside the ring. Either approach is acceptable; however, the exact approach used must be indicated when reporting results. The measurement of the difference in slump flow with and without the j-ring is unsuitable. First, the difference in slump flow with and without the j-ring is often within the precision of the slump flow test. According to ASTM C 1611, two slump flow tests conducted by the same operator on the same batch of concrete should not differ by more than 3 inches. ASTM C 1621 specifies that differences in slump flow measurements over 2 inches reflect "noticeable to extreme blocking". This characterization of "extreme" blocking is not supported because it is within the expected precision of the slump flow test. Indeed, Figure 14.2 indicates a high degree of scatter between the change in slump flow and the change in height j-ring measurements. All plotted data were determined in the laboratory, where the potential for variation is likely to be less than in the field. Second, the difference in slump flow may not reflect the extent of blocking, notwithstanding the lack of precision. In some cases, the thickness of the concrete flowing out of the j-ring is thinner than for the concrete tested without the j-ring—due to differences in blocking—but the spread is approximately the same. This scenario is illustrated in Figure 14.3. The measurement of T_{50} (or similar distance) with the j-ring is unnecessary because this same measurement made with the unobstructed slump flow test provides a better measurement of viscosity and the change in height between the inside and outside of the j-ring provides an adequate indication of passing ability.
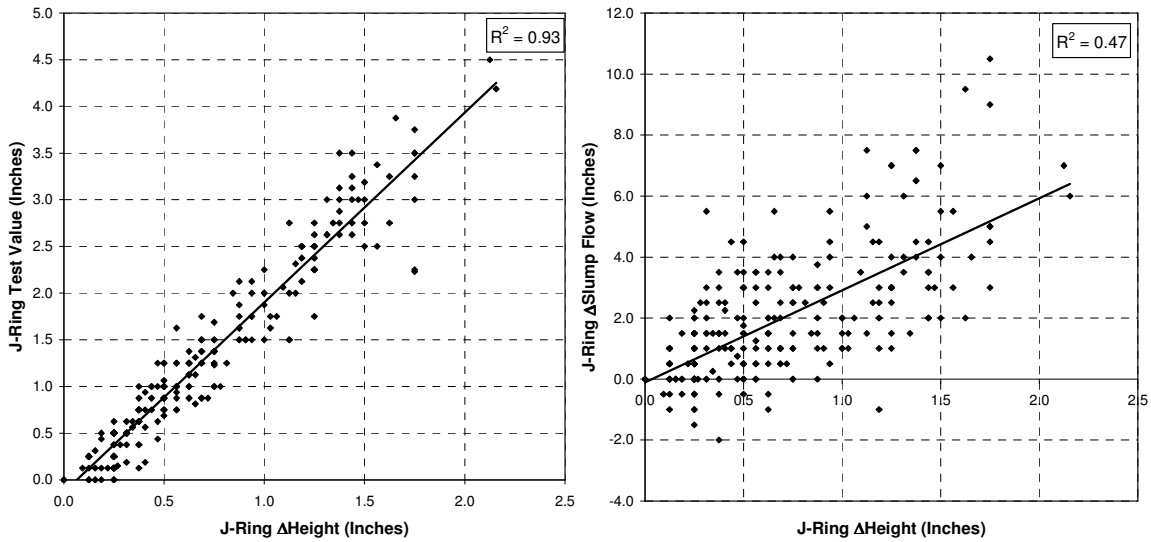
Figure 14.2: Relationship between J-Ring Test Value and ΔHeight and ΔSlump Flow
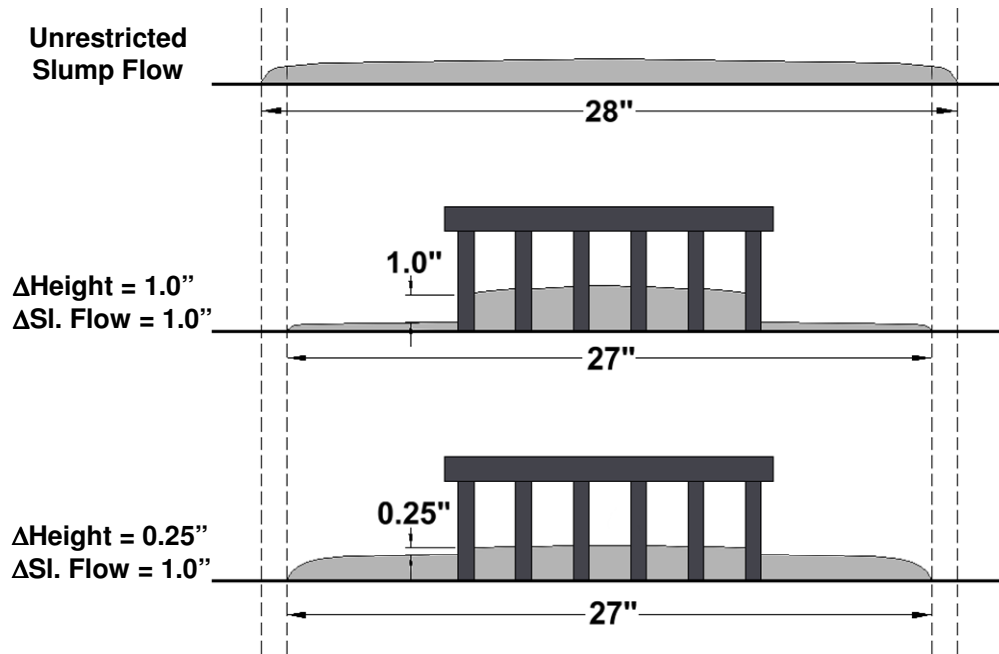
Figure 14.3: Representation of J-Ring Results with Same Restricted Slump Flows

The relationship between j-ring results and concrete field performance is not well established. In the field, the energy from a large mass of concrete moving through formwork can push concrete through the openings between reinforcing bars. The mass of concrete pushing concrete through the j-ring is much smaller by comparison. The effects of this lack of mass may be exacerbated for highly viscous or highly thixotropic mixtures. In general, however, the test

does reflect actual field conditions reasonably well and does effectively distinguish mixtures with varying degrees of passing ability due to changes in mixture proportions.

14.2.2.2 Advantages and Disadvantages

The advantages of the j-ring test include:

- The test independently measures passing ability.
- The test represents field conditions well and accurately distinguishes between mixtures with varying degrees of passing ability.
- The equipment is low in cost and portable. Although it is mainly needed in the laboratory, it can be easily used in the field (especially when compared to the l-box).

The disadvantages of the j-ring test include:

- Relationships between j-ring results and field performance are not well-established.
- The limited mass of concrete available to push concrete through the openings in the j-ring may not be representative of field conditions. (This limitation, however, is conservative.)
- The use of a single spacing of reinforcing bars for all tests may overestimate passing ability for highly congested sections.

14.2.2.3 Recommendations

The j-ring test is a simple and effective test for independently measuring passing ability and is appropriate for use in specifications. The test should be performed with the slump cone in the inverted position. Test results should be reported as the difference in height of concrete between the inside and outside of the j-ring (median of three equally spaced measurements). The measurement of the difference in slump flow with and without the j-ring is inappropriate and not advised. The reinforcing bar spacing should be constant—the spacing in ASTM C 1621 is reasonable—and the maximum acceptable change in height varied based on the application.

The test should be used in the laboratory when developing and qualifying mixture proportions. Because passing ability primarily depends on aggregate characteristics and paste volume and to a much lesser extent on paste rheology, the test does not need to be performed in the field if the slump flow test is used to control concrete rheology indirectly and the paste volume and aggregate characteristics remain reasonably constant.

14.2.3 L-Box Test

14.2.3.1   Discussion of Test

The l-box test provides a measurement of passing and filling ability. It has been used widely throughout the world and was selected by the European Testing SCC project as a reference test for passing ability. The l-box is similar to the u-box test. The l-box test was chosen for evaluation in this research because it is easier to visualize the flow of the concrete in the test—especially any blocking behind the bars—and the apparatus is easier to clean.

The l-box test results are a function of both passing ability and filling ability because the extent to which concrete flows down the horizontal portion of the box depends on the yield stress (filling ability) of the concrete and the extent of blocking caused by the row of bars. Indeed, the degree of correlation between the l-box and j-ring is poor, as shown in Figure 14.4. Similarly, the European Testing SCC project found the correlation was "not very good" between l-box and j-ring. Therefore, the test is essentially a pass/fail test because it is not clear whether concrete with a low blocking ratio exhibits inadequate filling ability, passing ability, or both. Nguyen, Roussel, and Coussot (2006) found that for a homogenous yield stress fluid (no blocking), the blocking ratio is a function only of yield stress and density. While measuring the difference in blocking ratio with and without the bars would isolate the effects of filling ability and passing ability, such an approach would be much more time-consuming. It would not be feasible to measure passing ability independently by determining the difference in concrete height on either side of the bars because concrete may not completely flow out of the vertical portion of the box in all cases, including when the filling ability is inadequate.
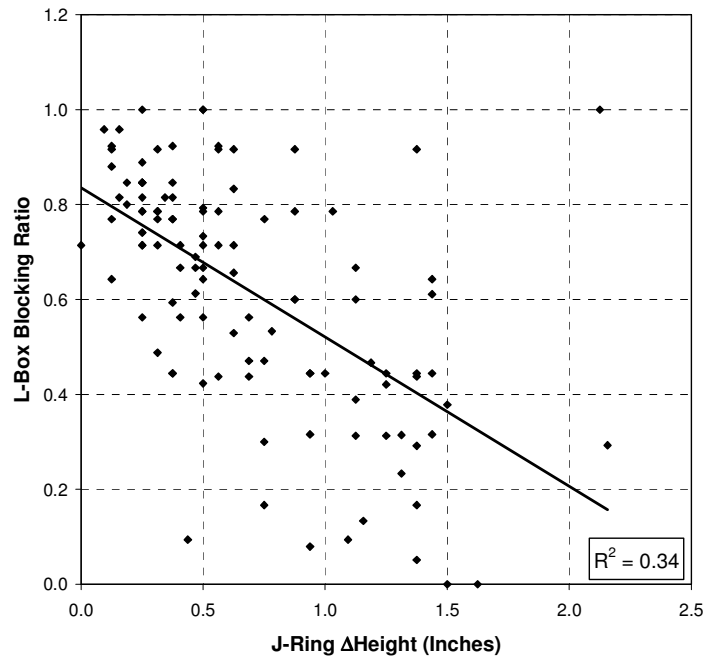
Figure 14.4: Relationship between L-Box and J-Ring Test Results

There are variations in the test apparatus, test procedure, and measurement of results that are important to interpreting results consistently. The test apparatus varies in dimensions, materials, and reinforcing bar spacing. The main differences in dimensions are in the cross section of the vertical portion and the total length of the horizontal portion of the box. These differences render it impossible to compare one box to another. The l-box is frequently constructed of plastic or plywood. Due to the large surface area in contact with concrete, the surface finish is likely more important than in the slump flow test. Petersson, Gibbs, and Bartos (2003) found differences in wall surface finish to affect results significantly. The European Testing SCC project, however, found that differences in surface finish were negligible. The options for bar spacing are limited because no more than three bars can realistically be fit in the opening.

The main difference in the test procedure is the length of time the concrete is allowed to remain in the box before the gate is opened. Any delays in opening the box would likely reduce the blocking ratio because of any thixotropy or segregation.

In nearly all cases, the test results are computed in terms of the blocking ratio, defined as the ratio of concrete height in the horizontal portion to the vertical portion of the box. The term "blocking ratio" is a misnomer because higher blocking ratios correspond to less blocking,

greater filling ability, or both. A term such as "passing ratio" or the use of the inverse of the blocking ratio as defined above would be more appropriate. In some cases, the time for concrete to flow a certain distance down the horizontal leg of the box is measured. This distance should be as long as possible to increase measurement precision. Figure 14.5 indicates that the correlation between slump flow T_{50} and l-box T_{40} is poor. The slump flow T_{50} is primarily related to plastic viscosity while the l-box T_{40} is related to both plastic viscosity and degree of blocking. The measurement of l-box T_{40} is unnecessary because plastic viscosity and degree of blocking are best measured independently with other tests.
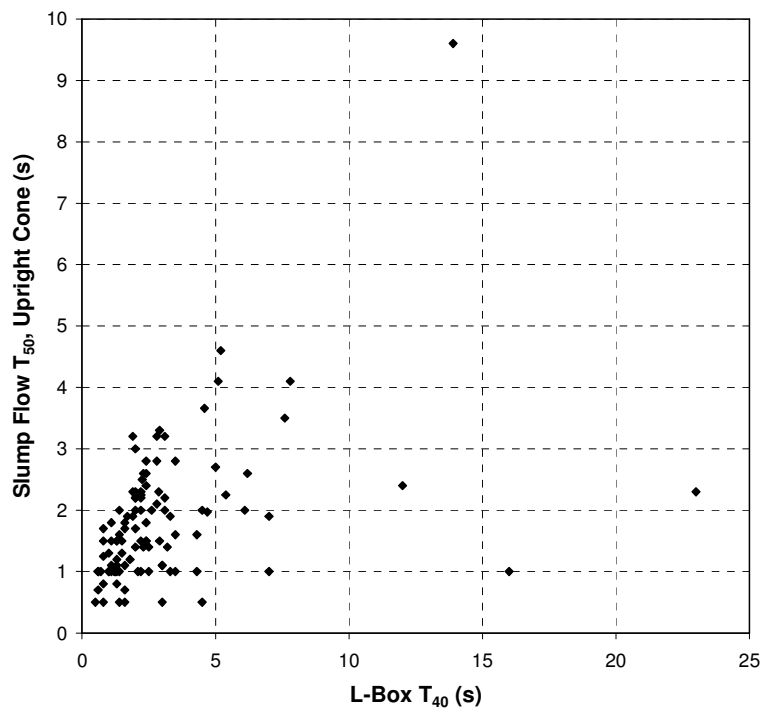
Figure 14.5: Comparison of L-Box T_{40} and Slump Flow T_{50} (Upright)

The calculation of blocking ratio requires three calculations: the heights of concrete in each end (from the distance from the top of the box to the concrete) and then the blocking ratio from the two heights. As such, results are not available immediately. It would be preferable to measure one value and perform no calculations. Accordingly, the possibility of measuring just the distance from the top of the box to the concrete in the vertical or horizontal leg is evaluated in Figure 14.6. The precision of either measurement is insufficient. The difference in distance in the vertical leg is only 1 inch as the blocking ratio changes from 0.60 to 1.00.
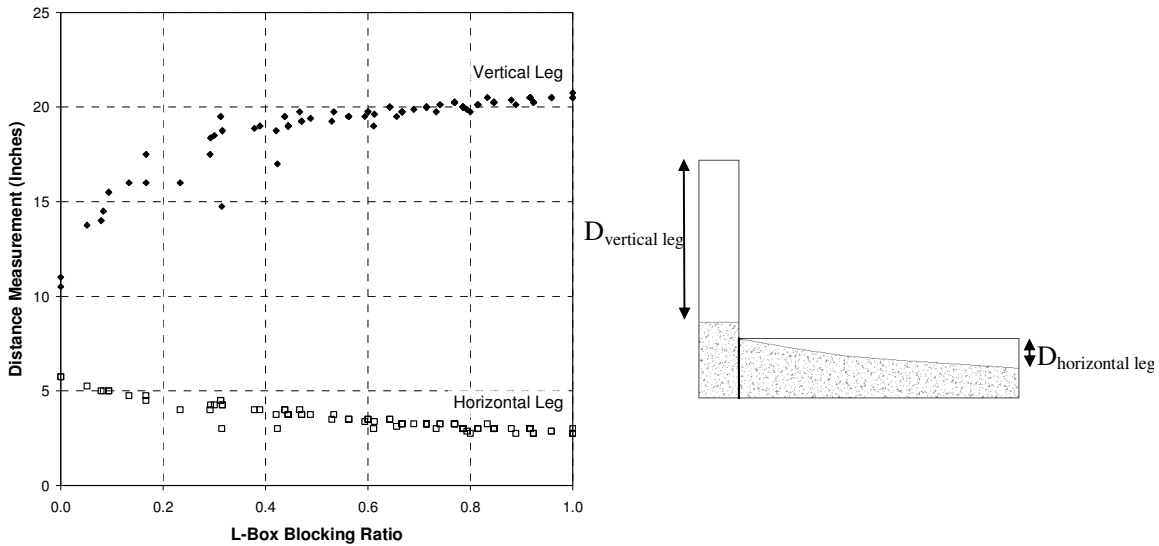
Figure 14.6: Simplified Measurements for L-Box Test

The l-box does reflect field conditions; however, the number of bars through which the concrete must pass is limited. The j-ring has more bars and would likely exhibit less variability from one test to another. The l-box, however, has an advantage over the j-ring in that a larger mass of concrete is available to push concrete through the bars.

14.2.3.2   Advantages and Disadvantages

The advantages of the l-box test include:

- The test provides a visualization of how concrete will flow in the field.
- The amount of mass available to push concrete through the bars is more representative of field conditions than in the j-ring test.
- The relationship between the test results and field performance is better established than for the j-ring test.

The disadvantages of the l-box test include:

- The test does not distinguish between passing ability and filling ability.
- The test apparatus is bulky, difficult to clean, and not well-suited for use in the field.
- The selection of rebar spacing is not well defined.

338

- The determination of blocking ratio requires two measurements and three separate calculations. A single measurement is not possible.

- The volume of concrete required is greater than for the j-ring test.

14.2.3.3   Recommendations

The use of the l-box test is not recommended because the measurement of passing ability is not sufficiently independent of filling ability and because the test is bulky and difficult to clean. The j-ring test is preferred for measuring passing ability. The l-box is preferred to the u-box.

14.2.4 Penetration Apparatus Test

14.2.4.1   Discussion of Test

The penetration apparatus test is a rapid field test for segregation resistance. It was first proposed by Bui (Bui, Akkaya, and Shah 2002; Bui et al. 2002). Variations on the penetration concept—with different penetration heads, concrete specimen sizes, and time sequences—have been proposed. The European Testing SCC project found the sieve stability test to be preferable to the penetration apparatus test for measuring segregation.

The test provides an independent measurement of static stability and does not provide an indication of dynamic stability. Although increasing the slump flow typically increases the susceptibility to segregation, the test does not provide an indication of filling ability or passing ability. The test essentially measures the static yield stress. In fact, a similar penetration test for measuring yield stress was used successfully by Uhlherr et al. (2002) for Carbopol gels and TiO_2 suspensions. The yield stress to stop the descent of the penetration head can be calculated based on the difference between the buoyant force acting upward and the gravitational force acting downward divided by the surface area of the bottom and sides of the cylinder, as shown in Equation (2.2):

$$\tau = \frac{m_{head} - \rho \pi d \left(r_o^{\;2} - r_i^{\;2} \right)}{\pi \left(r_o^2 - r_i^2 \right) + 2 \pi d \left(r_i + r_o \right)} 9.81 \qquad (14.2)$$

where τ is the stress to stop penetration head at given depth (Pa), m_{head} is the mass of the head (kg), ρ is the density of the concrete (kg/m^3), d is the penetration depth (m), and r_o and r_i are

the outer and inner radii of the penetration head (m). The stress to stop segregation is likely lower than that predicted by Equation (2.2) because aggregates must be displaced in order for the penetration head to descend. If resistance to this displacement is provided from specimen boundaries, the stress required for penetration should increase. The test measures the static yield stress—as opposed to the dynamic yield stress—because the shear imposed by the descent of the head is minimal, resulting in negligible breakdown of any build-up in structure due to thixotropy. In addition to the static yield stress, the penetration apparatus test may be further affected by a lack of aggregate particles near the top surface caused by any segregation prior to and during the descent of the penetration head.

The results of the penetration apparatus test were not well correlated to other segregation test methods. As shown in Figure 14.7, there was poor correlation between the column segregation test and the penetration apparatus test measured initially and after 15 minutes. The scatter was too high to select a limiting value below which no segregation occurs without eliminating mixtures that performed well. In contrast El-Chabib and Nehdi (2006) found good correlation between modified versions of the penetration apparatus test and column segregation test while Cussigh, Sonebi, and De Schutter (2003) found good correlation between the penetration apparatus test and the sieve stability test.

The inability of the penetration apparatus to predict segregation resistance is due mainly to the fact that the test measures only one point in time. For segregation resistance, the static yield stress must reach a minimum value quickly to stop the descent of aggregates. The penetration apparatus; however, does not reflect the rate of increase in static yield stress. For instance, a mixture with low static yield stress initially may by sufficiently thixotropic, resulting in a fast increase in static yield stress and minimal segregation. Increased plastic viscosity also reduces the rate at which aggregates settle.

There are variations in the test apparatus and test procedure that are important to interpreting results consistently. The test apparatus can vary significantly. The dimensions and mass of the penetration head can affect results most significantly. The pressure exerted on the concrete, which is a function of the mass, diameter, and thickness of the penetration head—must be carefully matched to the range of yield stresses to be measured. If the pressure is too low, the penetration depth can be too low for reliable measurements. If the pressure is too high, the penetration depth can exceed the height of the penetration head. The concrete specimen size is also important. Short containers can limit the total amount of segregation that can occur. In

narrow containers, the confinement and frictional resistance from the wall surface can reduce the amount of segregation. The use of a slump cone to contain concrete is a reasonable size and is a practical approach to conducting the test. However, leaving concrete in the slump cone for an extended period of time can affect the slump flow measurements due to thixotropy and segregation.
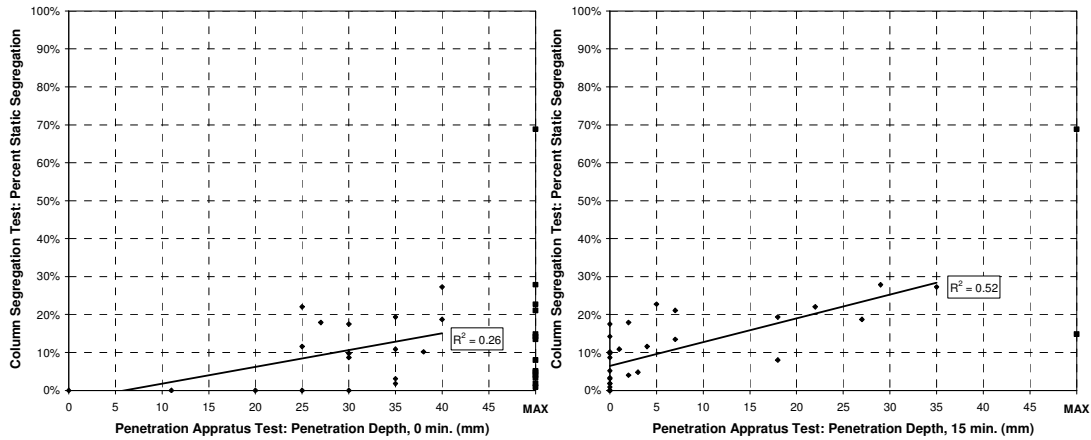
Figure 14.7: Relationship between Column Segregation Test and Penetration Apparatus Test at 0 and 15 Minutes (Koehler et al. 2007)

The test procedure is also crucial because the static yield stress of the concrete can change rapidly. If the test is performed too soon, the effects of thixotropy on increasing the static yield stress and reducing segregation will not be reflecting in test results, resulting in an overestimation of segregation. Even if segregation of coarse aggregate does not occur, the penetration apparatus can descend significantly—namely when the pressure exerted by the penetration head is greater than that exerted by the coarse aggregates. A low initial yield stress does not correspond to segregation if thixotropy, loss of workability, or both increase the static yield stress quickly. If too much time elapses before the cylinder is released, the static yield stress may have increased significantly by that time and prevent the penetration apparatus from descending, even if substantial segregation has already occurred.

14.2.4.2   Advantages and Disadvantages
The advantages of the penetration apparatus test include:
- The test is fast, simple, and easy to perform, such that it could be used as a rapid field acceptance test.

- If used with the slump cone, the specimen size is small.

The disadvantages of the penetration apparatus test include:
- The test results are highly dependent on the amount of time the concrete remains at rest prior to releasing the cylinder.
- The test does not measure dynamic segregation.

14.2.4.3   Recommendations

The penetration apparatus test may be suitable for measuring static segregation if it is better developed. The time sequence for performing the test must be carefully selected. In addition, the dimensions and mass of the penetration head and the concrete specimen size must be well defined.

14.2.5 Sieve Stability Test

14.2.5.1   Discussion of Test

The sieve stability test for segregation resistance has been used mainly in Europe and was recommended by the European Testing SCC project for use as the reference test method for segregation resistance. The sieve stability test measures static segregation and—to some extent—dynamic segregation. When concrete is left undisturbed in the bucket for 15 minutes, any segregation that occurs is due to static segregation. Segregation of coarse aggregate and bleeding lead to more mortar and paste at the top of the specimen, which is then poured onto and passes through a sieve. The amount of mortar passing the sieve depends to some extent on dynamic segregation resistance because viscous, cohesive mortar is less likely to pass through the sieve. Since this evaluation of dynamic segregation is determined after the concrete has remained undisturbed for 15 minutes, it may not reflect the dynamic segregation resistance of the concrete during placement conditions where the concrete is sheared continuously. It is likely that dropping the concrete onto the sieve does not fully breakdown the effects of thixotropy. The indication of dynamic segregation resistance would be more relevant to field conditions if done prior to the 15-minute rest period.

Although the sieve stability test is much simpler to perform than the column segregation test, it is not suitable for use as a rapid field acceptance test because of the amount of time

342

required to perform the test and the need for a balance. The test is simpler than the column segregation test because it does not require separating and cleaning the coarse aggregate. The test requires approximately 20 minutes to perform—including filling the bucket, waiting for the 15-minute rest period, pouring the concrete on the sieve and allowing it to remain there for 2 minutes, and measuring the final mass of material passing the sieve.

The European Testing SCC project preferred the sieve stability test over the column segregation test (rectangular cross section mounted on drop table) because the column segregation test is harder to perform and provides results that are no better than the sieve stability test.

14.2.5.2 Advantages and Disadvantages

The advantages of the sieve stability test include:

- The test provides an independent measurement of segregation resistance.
- The test is simpler to perform than the column segregation test.

The disadvantages of the sieve stability test include:

- The test conditions are not as directly representative of field conditions for static segregation as the column segregation test.
- The test requires a balance.
- The test requires too much time for use as a rapid acceptance test in the field.
- The test does not fully measure dynamic stability.

14.2.5.3 Recommendations

Either the column segregation test or the sieve stability test should be used to measure static segregation resistance. The results of the two tests are well-correlated; however, the sieve stability test is easier to perform. The sieve stability test is not appropriate as a rapid field acceptance test. When using the test in the laboratory to qualify mixture proportions, mixtures should be prepared with the range of water contents and HRWRA dosages expected during production. If these mixtures exhibit adequate segregation resistance and the slump flow test is used in the field to control concrete rheology indirectly, it is not necessary to use the sieve stability test in the field. The possibility of measuring dynamic stability by dropping concrete onto the sieve without the 15-minute rest period should be evaluated further.

14.2.6 Slump Flow Test (with T_{50} and VSI)

14.2.6.1   Discussion of Test

The slump flow test is the most well-known and widely used test for characterizing SCC and is extremely easy and straightforward to perform. The slump flow (yield stress) is the main fundamental difference between SCC and conventionally placed concrete. The slump flow test provides a measure of filling ability. The horizontal spread reflects the ability of the concrete to flow under its own mass (yield stress) while the T_{50} time and VSI provide indications of the plastic viscosity and segregation resistance, respectively. The test does not provide a complete description of filling ability because it does not fully reflect harshness and the ability to fill all corners of the formwork. The test does, however, provide a valuable visualization of concrete flow.

There are variations in the test apparatus, test procedure, and measurement of test results that are important to interpreting results consistently. The test apparatus may vary in the material used for the base plate and the moisture condition of the base plate. A smooth, plastic base plate is typically best. It is particularly important that the plate be level, flat and free of any standing water, all of which can affect results. Any appreciable amount of water not only increases the slump flow but may also reduce the observed stability. A squeegee should be used to remove any standing water.

The main variation in the test procedure is the orientation of the cone—namely inverted or upright. The final spread is the same regardless of the orientation; however, the T_{50} time is greater with the inverted orientation. The inverted orientation is preferred because (1) the larger end of the cone can be more easily filled with less spillage, (2) the mass of concrete in the cone is sufficient to hold the cone down—eliminating the need for a person to stand on the foot pedals of the cone—and (3) the T_{50} is greater and can be measured with increased precision. The test results may also be influenced by the speed with which the concrete is lifted. The 4-inch diameter of the bottom of the cone is sufficiently large such that test results are not typically influenced by passing ability.

The main difference in the measurement of test results involves the determination of T_{50}. In some cases a longer or shorter distance is used for high or low slump flows, respectively. Given that most SCC exhibits slump flow greater than 22 inches (560 mm) and T_{50} greater than

2-3 seconds (inverted orientation), the use of 50 mm is appropriate for the vast majority of SCC mixtures. Using various distances, while technically sound, reduces the simplicity and practicality of the test. Another variation occurs in determining the precise time to stop the T_{50} measurement. If concrete does not flow at the same rate in all directions, which is common, all concrete will not reach the T_{50} line at the same time. Therefore, it is important to specify whether T_{50} should be determined when concrete first touches the T_{50} line or completely reaches the entire T_{50} line.

The meaning of the slump flow test results is well-defined. The slump flow spread reflects the ability of concrete to flow under its own mass and is related to the yield stress. For a given concrete mixture over a wide range of slump flow measurements, the correlation between yield stress and slump flow is high, as shown in Figure 14.8. For the narrower range of slump flow values mainly associated with SCC—namely 22 to 30 inches— and for a wide variety of materials and mixture proportions, the variation in yield stress for a given change in slump flow is very small, such that a strong correlation between the two values cannot be established. Indeed, Figure 14.9 indicates the scatter in the relationship between slump flow and yield stress is high over this narrower range of slump flows. Plastic viscosity also affects the final slump flow. Figure 14.10 indicates that for a constant slump flow, increasing the yield stress requires a lower plastic viscosity.

The T_{50} measurement is well correlated to plastic viscosity (Figure 14.11), particularly when considering the precision of the T_{50} test. This relationship is valid for nearly the full range of slump flows associated with SCC. Determining the plastic viscosity—either directly or indirectly—is particularly important because, with the yield stress relatively unchanged over the range of rheology associated with SCC, the plastic viscosity is often the main factor distinguishing the workability of one mixture from another. Changes in plastic viscosity can directly reflect changes in materials or mixture proportions, making the T_{50} measurement particularly valuable for quality control.

The VSI fails to reflect the segregation resistance fully. Indeed, Figure 14.12 shows the poor level of correlation between VSI and the column segregation test. Elsewhere, Sedran and de Larrard (1999) found that the size of the mortar halo from the slump flow test was not correlated to the amount of segregation. Khayat (1999) and Khayat, Assaad, and Daczko (2004) also found the VSI inadequate for evaluating segregation resistance. The VSI does not reflect static segregation conditions in the field. Concrete mixtures may exhibit instability when

345

observed for VSI determination but quickly improve when left undisturbed due to thixotropy. Conversely, mixtures that exhibit low VSI may exhibit gradual segregation that accumulates over time under static conditions but is not evident on the time scale of the slump flow test. The subjectivity of assigning the VSI also reduces the reliability of the index.
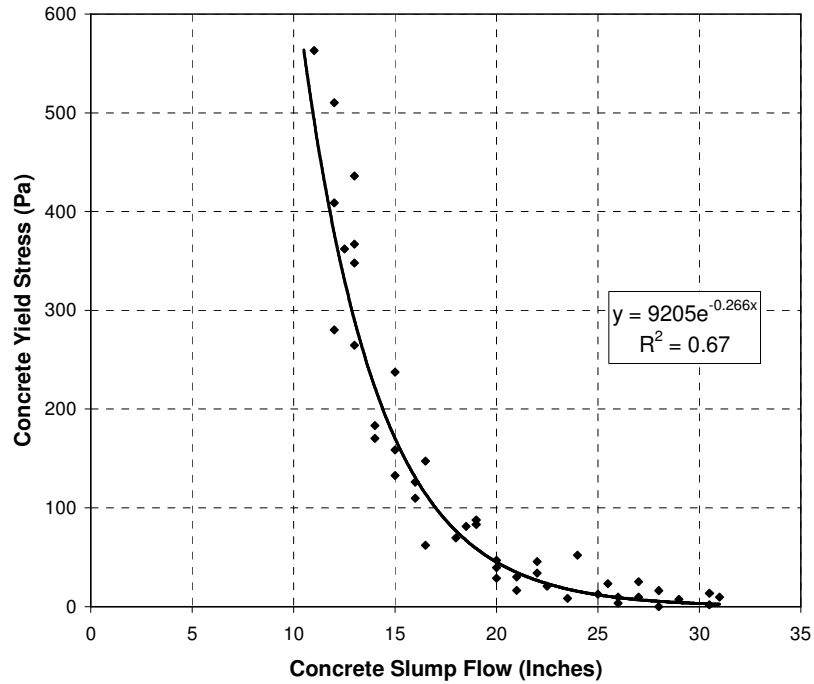
Figure 14.8: Relationship between Slump Flow and Yield Stress for Constant Mixture Proportions (Variable HRWRA Type and Dosage)
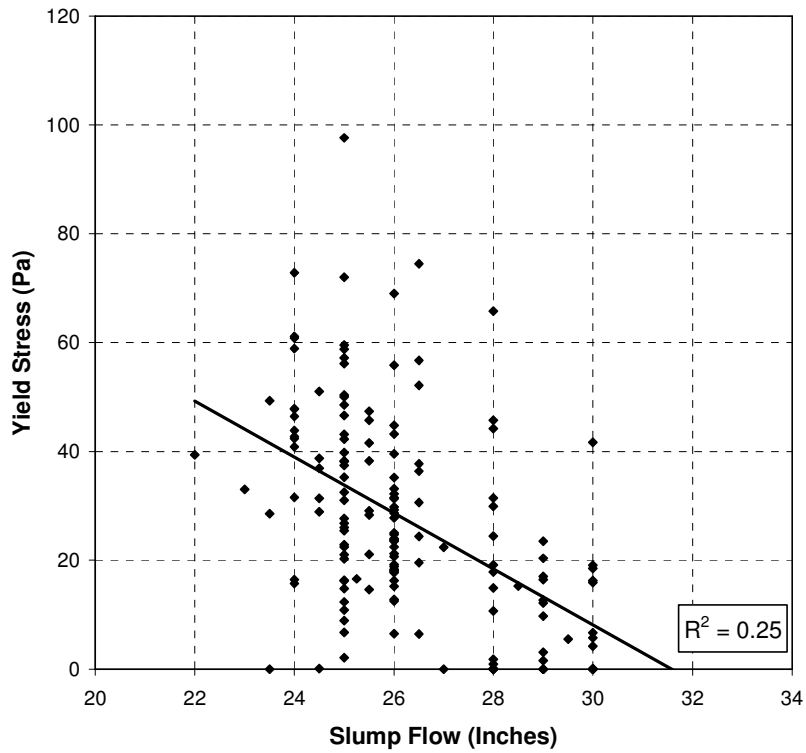
Figure 14.9: Relationship between Slump Flow and Yield Stress for SCC Mixtures (Various Materials and Mixture Materials)
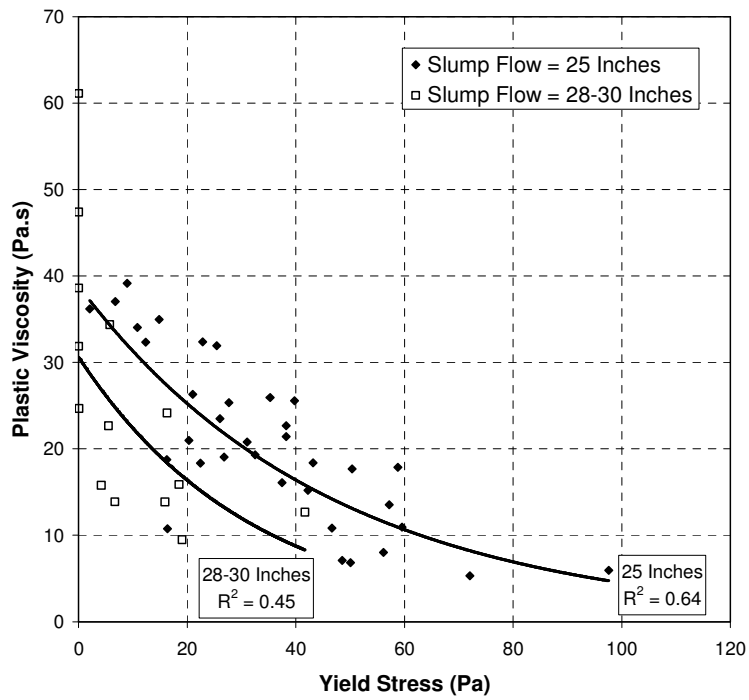
Figure 14.10: Relationship between Yield Stress and Plastic Viscosity at Various Slump Flows

347
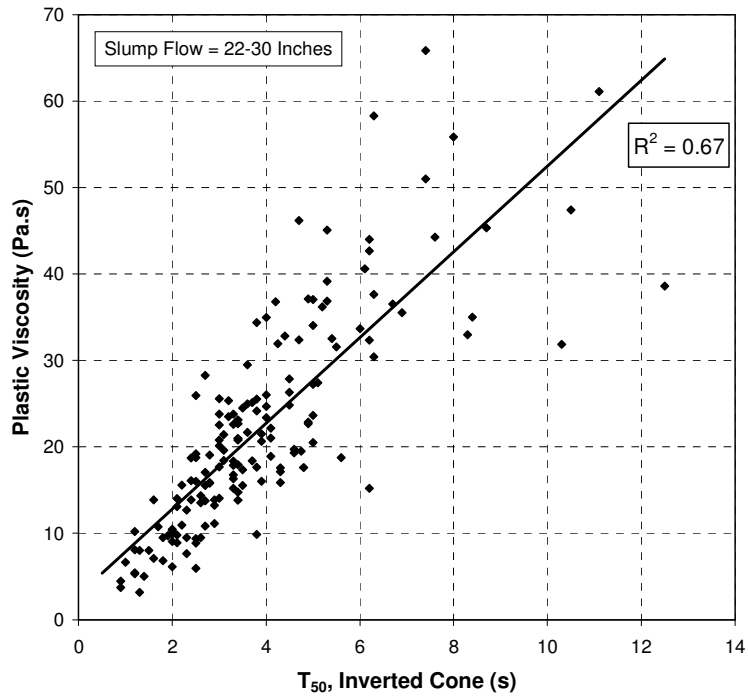
Figure 14.11 Relationship between T_{50} Time (Inverted Cone) and Plastic Viscosity
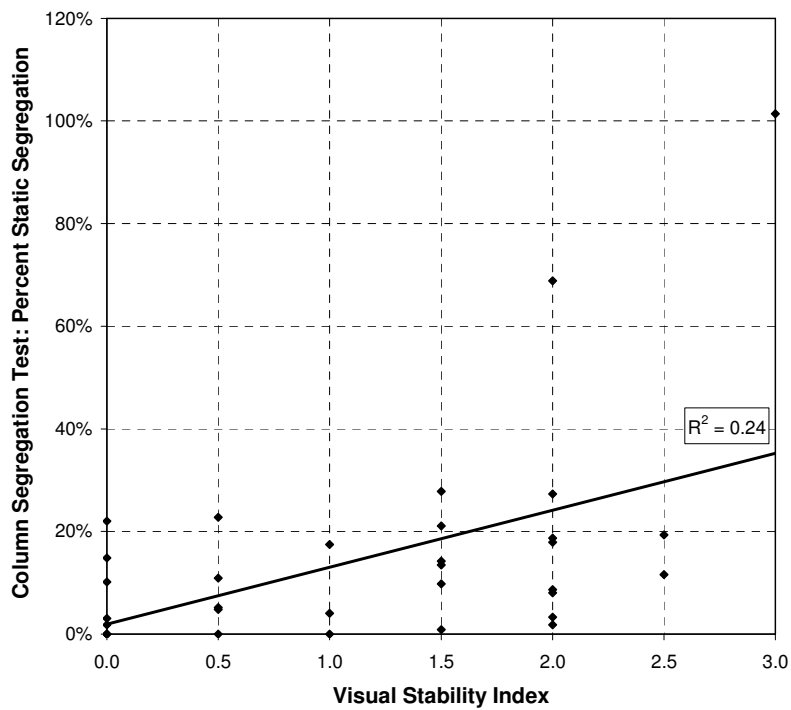
Figure 14.12: Relationship between VSI and Column Segregation Test (Koehler et al. 2007)

14.2.6.2   Advantages and Disadvantages

The advantages of the slump flow test include:

- The test provides an independent measurement of filling ability.
- The test is well-known, widely used, and simple to perform.
- The test is inexpensive and easily portable.
- The specimen size is small.
- The test is robust and repeatable.
- The spread is related to yield stress and T_{50} is related to plastic viscosity.
- The test provides a visualization of concrete flow.

The disadvantages of the slump flow test include:

- The VSI is inadequate for ensuring segregation resistance.
- The test results do not reflect all aspects of filling ability and do not indicate the harshness of mixtures.
- The test must be conducted on a flat base plate with no standing water.

14.2.6.3   Recommendations

The slump flow test is a simple, inexpensive, robust, and effective test for measuring filling ability. The ability of the test to measure indirectly the fundamental rheological properties of yield stress and plastic viscosity is especially valuable. In addition to slump flow, which is related to yield stress, T_{50} should always be measured because it is related to plastic viscosity. The test should always be performed with the cone in the inverted orientation because this orientation makes the test easier to perform and the use of consistent orientation ensures accurate comparisons between tests.

The slump flow test can be used in both the laboratory and field. For many cases, the slump flow test is the only test needed in the field for quality control. The slump flow spread should be used to adjust the HRWRA dosage to ensure the ability of the concrete to flow under its own mass. T_{50} should be used in the laboratory for developing and qualifying mixtures to assess plastic viscosity and should be used in the field to detect unexpected changes in materials and mixture proportions. The VSI can be used to catch cases of severe segregation; however, it

is not reliable as an assurance of adequate segregation resistance. Mixtures with high VSI should be investigated further but not necessarily rejected.

14.2.7 V-Funnel Test

14.2.7.1 Discussion of Test

The v-funnel test measures a single value that is related to filling ability, passing ability, and segregation resistance. Therefore, the test may be suitable as a pass/fail test but cannot provide an independent indication of filling ability, passing ability, or segregation resistance. Low v-funnel times can be associated with good flow properties, but the test provides no information for troubleshooting mixtures with high v-funnel times.

For a homogenous fluid with no segregation, the v-funnel test results have been shown to be a function of yield stress and plastic viscosity (Roussel and Le Roy 2005). By determining yield stress and plastic viscosity, the test provides a measure of filling ability. Since yield stress does not vary over a wide range for SCC, the v-funnel time of self-flowing concretes that can be idealized as homogenous, non-segregating fluids is mainly a function of plastic viscosity. As the size and volume of aggregate increase, the potential for blocking of aggregate across the opening increases. Therefore, the v-funnel is affected by passing ability in some cases. Any segregation that occurs from when the concrete is loaded into the v-funnel until the concrete flows out of the v-funnel increases the v-funnel time. Even if the gate of the v-funnel is opened as soon as practical, it is possible for some segregation to occur.

Figure 14.13 indicates that the relationship between plastic viscosity and v-funnel time is poor for concrete. For v-funnel times less than 10 seconds, a better correlation between v-funnel time and plastic viscosity appears to exist. The scatter is much greater at higher v-funnel times due to any harshness, blocking, or segregation—which increase v-funnel time but do not increase plastic viscosity by a proportionate amount. For mortar, the relationship between v-funnel time and plastic viscosity is better due to the reduced blocking and segregation.

There are variations in the test apparatus, test procedure, and measurement of test results that are important to interpreting results consistently. The test apparatus mainly varies in the dimensions. Alternative shapes are available, such as an o-shaped cross section and the orimet, which consists of a cylinder with a narrowed opening at the bottom. Smaller versions of funnels are available for mortar and paste. Even for the v-shape version for concrete, the dimensions

vary. The test procedure mainly varies in the amount of time from filling the funnel to opening the gate. This period can be lengthened to measure segregation. Whatever period is chosen, it should be consistent for all tests. Care should be taken to load the concrete in a consistent time frame—such as filling quickly with a single bucket of concrete or more gradually with a scoop. The measurement of test results can be reported as the v-funnel time or the average rate of flow. The calculation of average rate of flow is an unnecessary extra step.
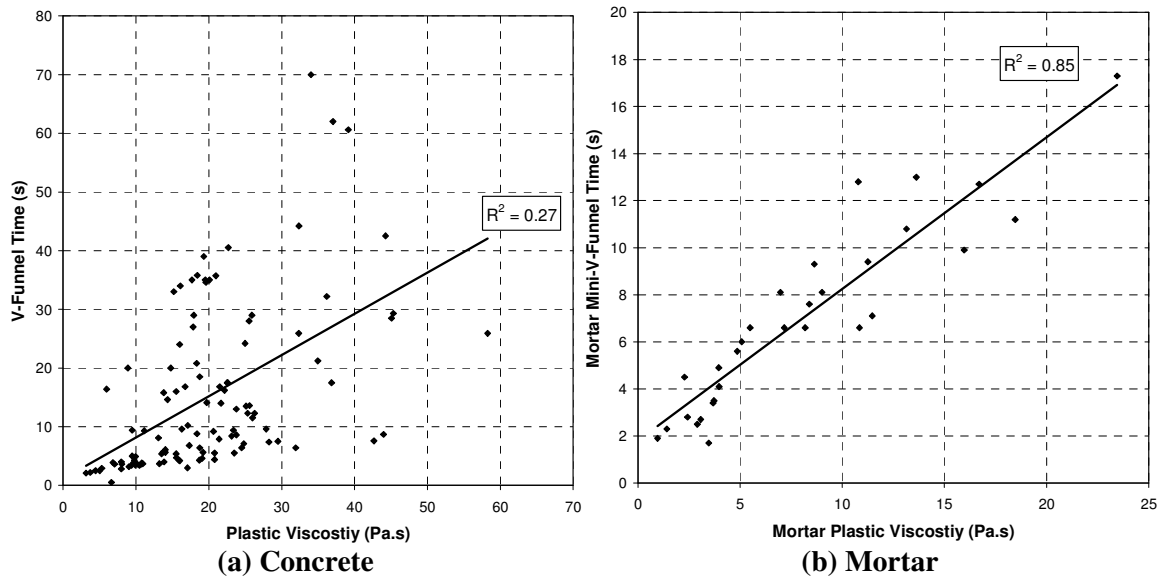
(a) Concrete   (b) Mortar
Figure 14.13: Relationship between Plastic Viscosity and V-Funnel Time

14.2.7.2   Advantages and Disadvantages
The advantages of the v-funnel test include:

- The test is relatively simple to perform and results are expressed in a single value related to filling ability, passing ability, and segregation resistance.
- For paste, mortar, and concrete mixtures that can be idealized as homogenous, non-segregating materials, the results are a function of yield stress and plastic viscosity. For such materials that are also self-flowing (near-zero yield stresses), the results are primarily a function of plastic viscosity.

The disadvantages of the v-funnel test include:

- The test does not provide an independent indication of filling ability, passing ability, or segregation resistance.

351

- The test frame is large, bulky, and must be placed on a level surface.

14.2.7.3   Recommendations

The use of the v-funnel test is not recommended because the results are affected by filling ability, passing ability, and segregation resistance. Although the test does provide indications of each of these three characteristics, it should not be relied upon as conclusive confirmation of any one of these characteristics. The test can be used as a pass/fail test; however, no information is provided to troubleshoot problematic mixtures.

14.3 Conclusions

The following conclusions can be drawn based on the information presented in this chapter:

- In evaluating the workability of SCC, tests should measure filling ability, passing ability, and segregation resistance independently. Such an approach is preferred to pass/fail-type tests that measure multiple aspects of workability. Measuring each property individually provides a more direct insight into the performance of the concrete and allows more effective troubleshooting. These advantages outweigh the need to conduct multiple tests.
- To evaluate the workability of SCC, the slump flow test (with T_{50} and VSI) should be used for filling ability, the j-ring test for passing ability, and the column segregation test or sieve stability test for segregation resistance.
- The sieve stability test is preferred to the column segregation test because it is easier to perform and the results of the two tests are well correlated. The column segregation test, however, is more likely to be used in the US because it has been standardized by ASTM International.
- For quality control measurements in the field, only the slump flow test is needed in most cases. (This recommendation matches that of the European Testing SCC project.) The slump flow spread should be used to adjust HRWRA dosage to achieve proper slump flow for self-flow, T_{50} should be used to measure indirectly plastic viscosity and to detect changes in materials and mixture proportions, and VSI should be used to identify significant segregation.

Chapter 15: Summary, Conclusions, and Recommendations

15.1 Summary

The role of aggregates in self-consolidating concrete was evaluated. In total, 12 fine aggregates, 7 coarse aggregates, and 6 microfines were evaluated. Additionally, a range of cementitious materials and chemical admixtures were evaluated. The objectives of the research were to evaluate the effects of specific aggregate characteristics and mixture proportions on the workability and hardened properties of SCC, to identify favorable aggregate characteristics for SCC, and to develop guidelines for proportioning SCC with any set of aggregates. Prior to commencing work, a thorough literature review was conducted on SCC materials, fresh properties, hardened properties, and mixture proportioning.

Aggregates were characterized to determine grading, shape and angularity, methylene blue value, and packing density. Tests were conducted on paste, mortar, and concrete. Paste measurements were conducted to evaluate the effects of cement, fly ash, microfines, HRWRA, and VMA on rheological properties. Mortar measurements were conducted to evaluate the effects of fine aggregates, microfines, and mixture proportions on workability and hardened properties. Concrete measurements were conducted to evaluate the effects of fine aggregates, coarse aggregates, microfines, and mixture proportions on workability and hardened properties.

Target properties for SCC workability were defined as a function of the application in terms of filling ability, passing ability, segregation resistance, and rheology. Seven workability test methods were evaluated extensively to provide sound, engineering justifications for their use and for the interpretation of their results. Specific tests for filling ability, passing ability, and segregation resistance were recommended.

Based on the results of this research and well-established principles from the literature, a mixture proportioning procedure for SCC was developed. The procedure is based on a consistent, rheology-based framework and was designed and written to be accessible and comprehensible for routine use throughout the industry. In the procedure, concrete is represented as a suspension of aggregates and paste. The three-step procedure consists of selecting the aggregates, paste volume, and paste composition. Detailed recommendations are provided for each step. Aggregates are selected on the basis of grading, maximum size, and shape and angularity. The paste volume is set based on the aggregate characteristics. The paste

composition is established to achieve workability and hardened properties. All required testing is conducted with methods standardized by ASTM International.

15.2 Conclusions

Based on the results of this research project, the following main conclusions can be reached:

- SCC workability should be defined in terms of filling ability, passing ability, and segregation resistance. Rheology can be used to provide additional insights into workability. The main difference between SCC and conventionally placed concrete is the low yield stress (high slump flow) required to achieve self-flow. The plastic viscosity should not be too low, which would result in poor stability, or too high, which would result in reduced placeability. HRWRA is mainly responsible for the reduction in yield stress. Aggregate characteristics, paste volume, and paste composition can be varied to reduce the HRWRA demand for a given slump flow.

- SCC can be idealized as a suspension of aggregates in paste. This approach provides a fundamental, rheology-based framework for evaluating SCC. In this framework, paste is defined as water, air, and all powder finer than approximately 75 μm. The characteristics of the combined aggregates are considered—that is, the maximum aggregate size, grading, and shape and angularity. Workability is a function of the aggregate characteristics, the paste volume, and the rheology of the paste. The rheology of the paste is a function of the volume, grading, and shape and angularity of the powder blend, the volume of water, the volume of air, and the types and dosages of admixtures.

- No single aggregate characteristic is sufficient for predicting SCC workability. Both grading as well as shape and angularity significantly affect SCC workability. There is no universally optimal grading for SCC—the best grading depends on the aggregate and application. In general, the 0.45 power curve results in increased packing density and in consistently low HRWRA demand and plastic viscosity. Coarser gradings also result in low HRWRA demand and plastic viscosity but may be harsh due to a lack of fine particles. Finer gradings result in higher HRWRA demand and plastic viscosity but reduced harshness. In many cases, finer gradings may be preferred. Gap-graded mixtures can result in higher packing density and lower HRWRA demand and plastic viscosity; however, they should be avoided in most cases because they increase the

354

susceptibility to segregation. Increasing the maximum aggregate size is generally favorable for filling ability; however, limitations on maximum aggregate size may be needed to ensure passing ability and segregation resistance. The benefit of increasing the maximum aggregate size is due to the improved grading and wider spread of sizes. In terms of shape and angularity, equidimensional, well-rounded aggregates result in increased packing density and reduced interparticle friction, which result in reduced HRWRA demand, reduced plastic viscosity, and improved passing ability.

- A minimum volume of paste is needed to achieve SCC workability. The minimum paste volume, which should be determined separately for filling ability and passing ability, depends primarily on the aggregate characteristics. The minimum paste volume for filling ability can be estimated based on the volume of voids between compacted aggregates and a visual rating of aggregate shape and angularity. Increasing the paste volume for a given aggregate increases passing ability by reducing the volume of aggregates that must pass through confined spaces and reducing interparticle friction between aggregates. The use of equidimensional, well-rounded aggregates with high packing density allows the paste volume to be reduced, resulting in improved economy and hardened properties.

- Increasing the paste volume beyond the minimum needed to achieve SCC workability results in increased robustness with respect to aggregate properties. Aggregates with poor shape and angularity, poor grading, or both can be accommodated in SCC by increasing the paste volume. Once sufficient paste volume is provided for a given aggregate, the workability can be further improved by adjusting the paste composition.

- Increasing the aggregate packing density generally results in improved SCC workability; however, the maximum packing density may not be optimum. Increasing the packing density reduces the amount of paste needed to fill voids between the aggregates. Additionally, aggregates with favorable shape and angularity not only increase packing density but further improve workability by reducing interparticle friction.

- The effects of aggregate characteristics on hardened properties are mostly indirect. The changes in mixture proportions required to achieve SCC workability for a given aggregate are often more significant than the effects of the aggregate itself. The trends between mixture proportions and hardened properties for conventionally placed concrete are generally applicable to SCC. The modulus of elasticity was reduced with increased

355

paste volume and increased sand-aggregate ratio; however, these effects were small compared to the effects of changing the aggregate stiffness or water-cementitious materials ratio. Shrinkage mainly increased with increased paste volume. SCC hardened properties are typically of good general quality due to the common use of low water-cementitious materials ratios and high dosages of supplementary cementitious materials.

- Microfines can be used successfully in SCC. When proportioning SCC with microfines, the microfines should be included as part of the powder and accounted for as part of the paste volume. The water-powder ratio should be used to evaluate workability and water-cementitious materials ratio should be used to evaluate long-term hardened properties. Microfines should be selected on the basis of grading, shape characteristics, and the presence of clay or other deleterious materials. Grading should be considered in the context of the overall powder grading. Microfines finer than the cementitious materials often result in improved workability. Shape characteristics should be evaluated relative to the shape characteristics of the other powder materials the microfines may be replacing. High clay contents increase HRWRA demand. If sufficient HRWRA is provided to offset the effects of the clays, the workability and hardened properties are typically not adversely affected. The potential for the thaumasite form of sulfate attack should also be evaluated; however, it was not considered in this research.

- SCC workability test methods should independently measure filling ability, passing ability, and segregation resistance. In contrast, pass/fail-type tests are unsuitable because they provide little information for troubleshooting mixtures that fail. The slump flow test should be used for filling ability, the j-ring test for passing ability, and either the column segregation test or sieve stability test for segregation resistance. In the field, it is often only necessary to use the slump flow test.

- Improving the aggregate characteristics can significantly improve the performance and economy of SCC. In many cases, it is likely that the additional costs of selecting higher quality aggregates can be more than offset by benefits such as reductions in the quantities of cementitious materials and admixtures.

15.3 Recommendations for Future Research

The results of the research described in this dissertation can be extended by conducting the following additional research:

- **Field Testing.** Field testing should be conducted to relate laboratory measurements to field performance, to define SCC performance requirements for use in specifications, and to verify the ICAR SCC mixture proportioning procedure with a wider range of materials and applications.

- **Methylene Blue Value Test.** The methylene blue value test should be evaluated further to develop a better understanding of test results and to link test results to field performance.

- **Characterization of Aggregate Shape and Angularity.** At the present time, a visual assessment is the most practical approach to characterizing aggregate shape and angularity. Although this approach is effective, alternative low-cost and practical methods of objectively quantifying aggregate shape and angularity are desirable. Additionally, better characterization methods of the shape and angularity of microfines are needed.

- **Workability Retention.** Although workability retention depends on many factors, the effects of microfines and mixture proportions on workability retention should be evaluated further.

- **Durability of SCC.** In this research, durability was assessed in terms of rapid chloride permeability and abrasion resistance. Testing of a wider range of durability characteristics is needed. In particular, the potential for the thaumasite form of sulfate attack—which is associated with the use of limestone powder in cold, sulfate-rich environments and possibly other conditions—should be evaluated.

- **Relationships between Properties of Paste, Mortar, and Concrete.** The ability to link paste and mortar properties to concrete properties is beneficial because it allows simplified testing on smaller scale specimens and it allows a better understanding of how paste and mortar proportions affect overall concrete properties. Although the relationships between paste, mortar, and concrete properties are complex, further definition of these relationships should be developed.

- **Application of ICAR SCC Mixture Proportioning Procedure to Conventionally Placed Concrete.** The concepts of the ICAR SCC mixture proportioning procedure should be applied to conventionally placed concrete. Aggregate characteristics that result in favorable SCC performance should also be beneficial for conventionally placed concrete mixtures. Although the effects of materials and mixture proportions are

357

typically not as significant for conventionally placed concrete, the volume of conventionally placed concrete is much higher than SCC.

Appendix A: Materials
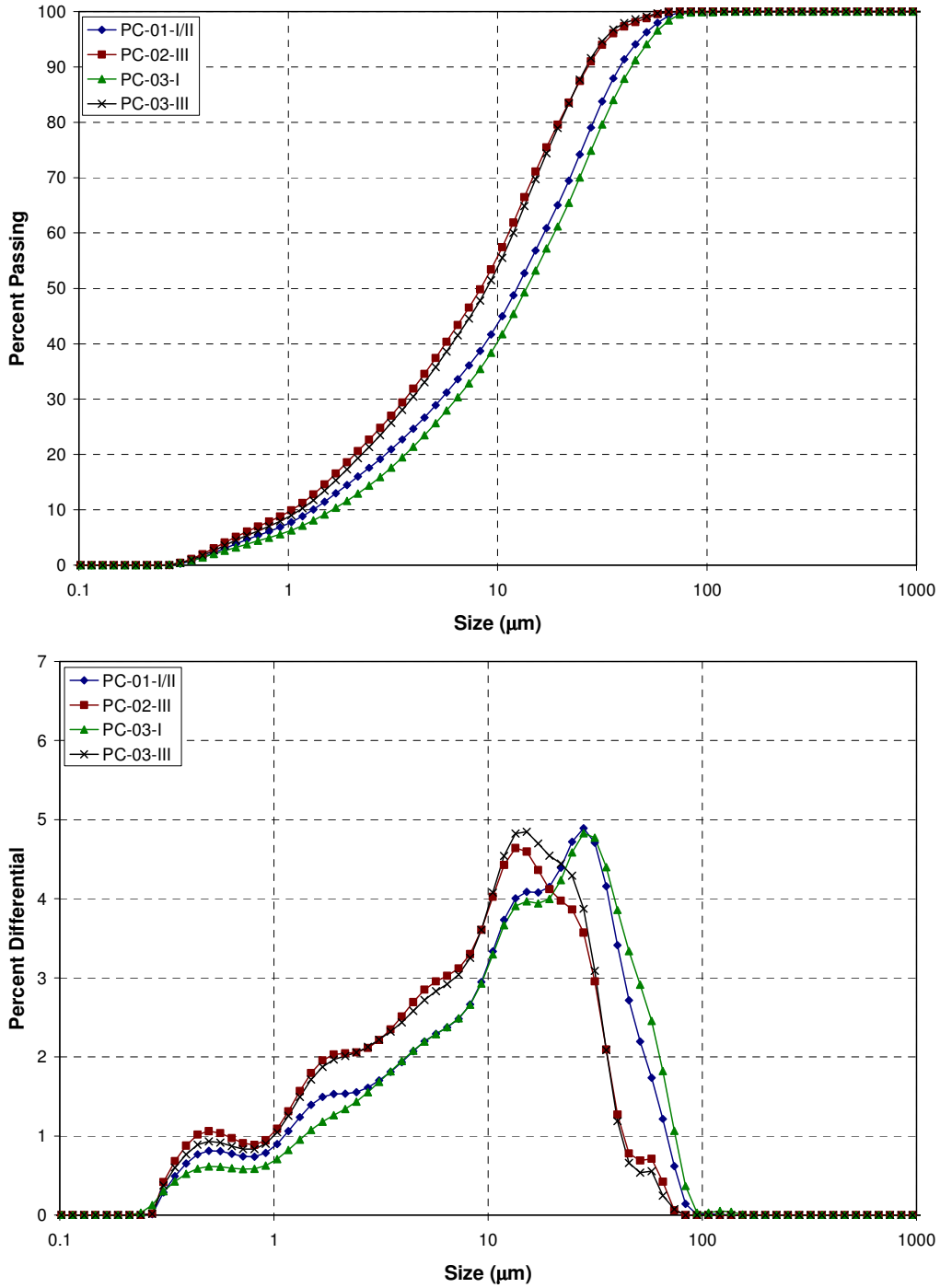
Figure A.1: Laser Diffraction Measurements of Cement
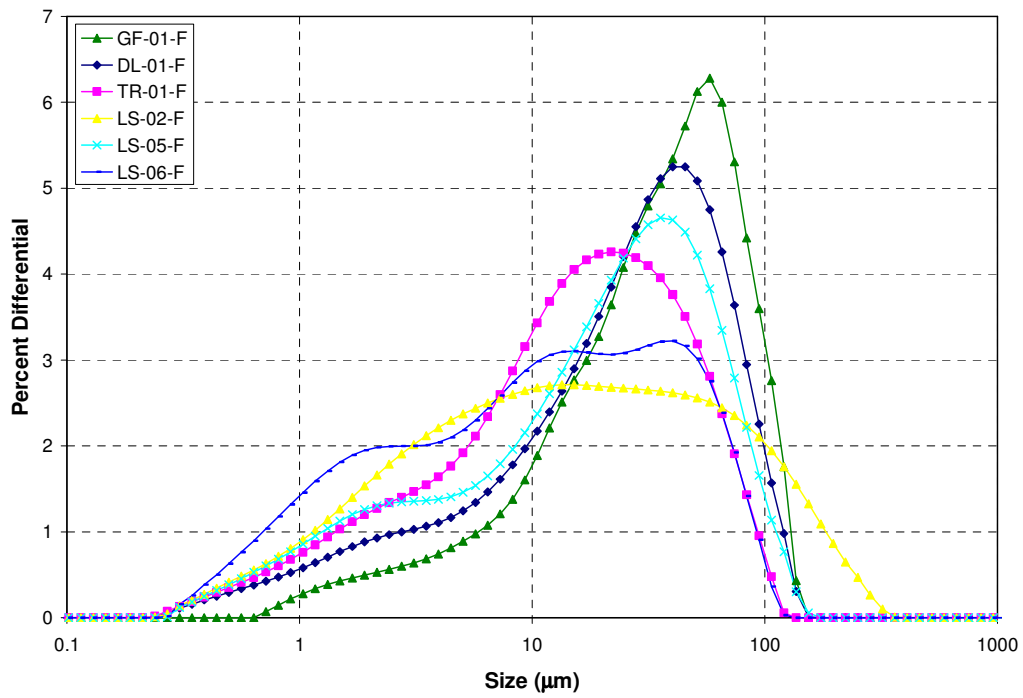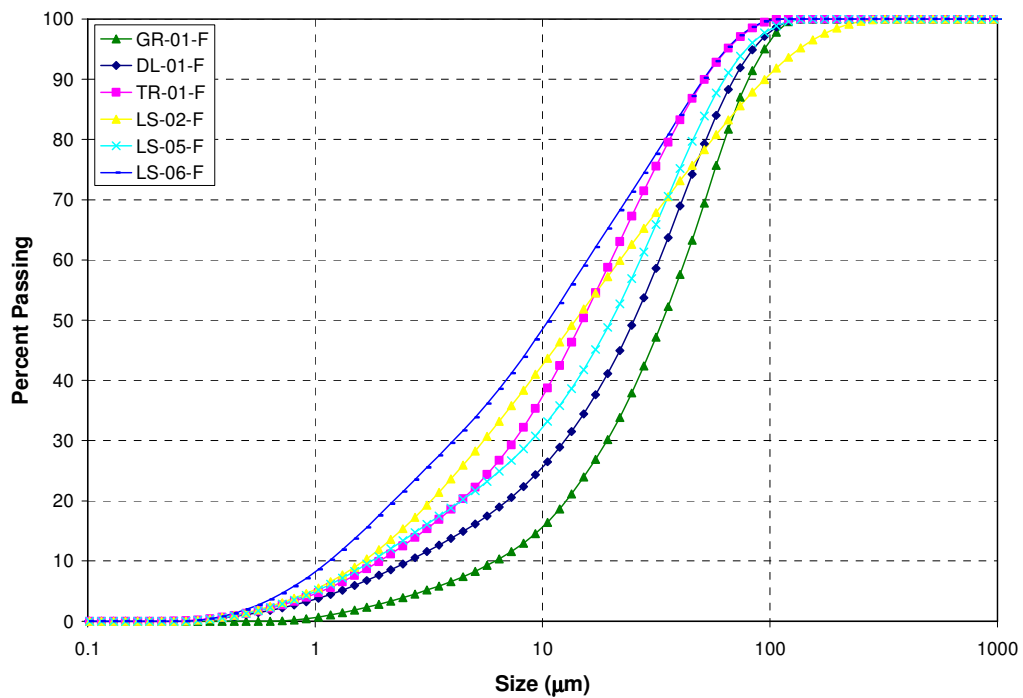
Figure A.2: Laser Diffraction Measurements of Microfines
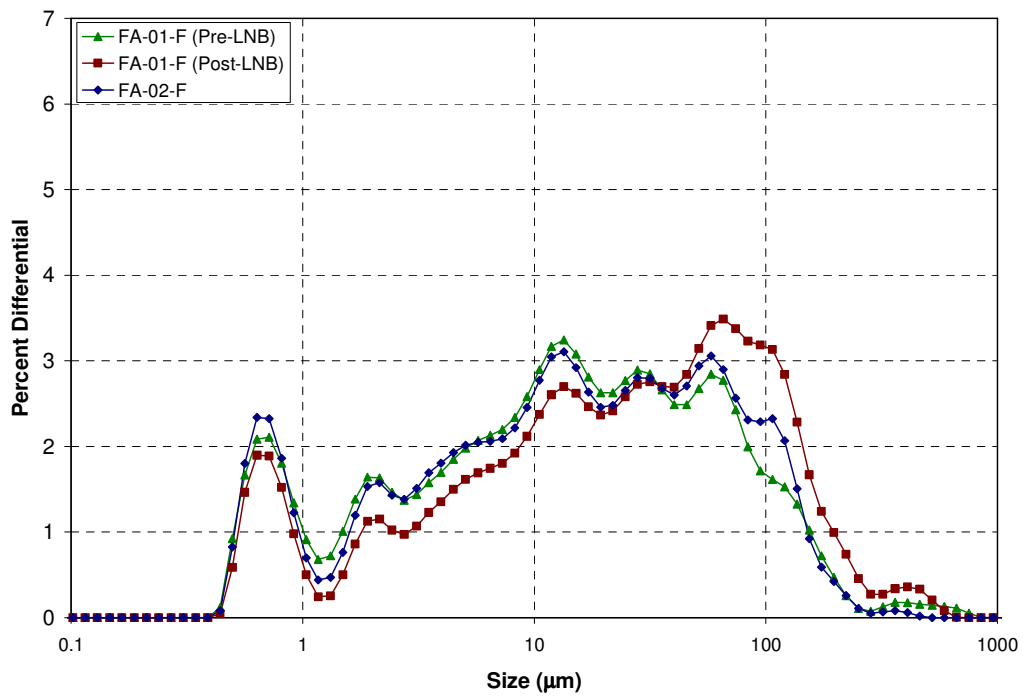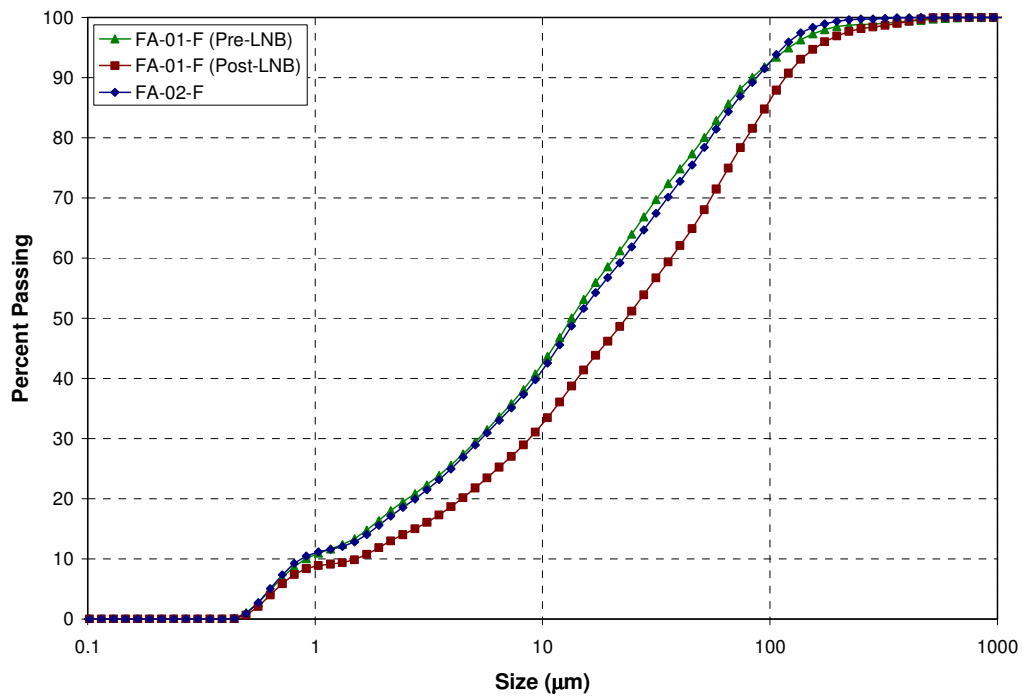
Figure A.3: Laser Diffraction Measurements for Fly Ash

Table A.1 Laser Diffraction Measurements

Material ID	d(0.1)	d(0.5)	d(0.9)	Span	SSA
	(mm)	(mm)	(mm)		(1/µm)
PC-01-I/II	1.31	12.348	38.225	2.990	1.729
PC-02-III	1.042	8.287	26.916	3.122	2.179
PC-03-I	1.626	13.716	43.421	3.047	1.523
PC-03-III	1.142	8.878	26.497	2.856	2.046
GR-01-F	6.205	33.765	80.218	2.192	0.467
DL-01-F	2.573	25.27	69.235	2.638	0.965
TR-01-F	1.922	14.985	51.4	3.302	1.243
LS-02-F	1.632	13.962	94.796	6.673	1.394
LS-05-F	1.771	20.103	62.92	3.042	1.214
LS-06-F	1.152	10.609	50.888	4.688	1.806
FA-01-F (Post-LNB)	1.52	23.354	116.75	4.934	1.347
FA-01-F (Pre-LNB)	0.909	13.383	83.319	6.158	1.729
FA-02-F	0.866	14.136	87.275	6.113	1.706

Table A.2 Cement and Fly Ash Material Properties

	PC-01-I/II	PC-02-III	PC-03-I	PC-03-III	FA-01-F	FA-02-F
Chemical Tests						
Silicon Dioxide (SiO$_2$), %	20.2	20.6	20.70	20.09	52.49	55.11
Aluminum Oxide (Al$_2$O$_3$), %	4.6	4.9	5.11	4.87	21.78	20.42
Iron Oxide (Fe$_2$O$_3$), %	3.1	3.4	1.21	1.87	4.94	8.18
Calcium Oxide (CaO), %	64.9	64.1	64.43	63.43	13.92	9.90
Magnesium Oxide (MgO), %	1.4	0.8	1.21	1.24	2.00	2.72
Sulfur Trioxide (SO$_3$), %	2.8	3.5	3.30	4.34	0.79	0.54
Sodium Oxide (Na$_2$O), %	0.13				0.32	
Potassium Oxide (K$_2$O), %	0.44				0.74	
Total Alkalies (as Na$_2$O$_{eq}$), %	0.42	0.50	0.56	0.54	0.81	
Available Alkalies (as Na$_2$O$_{eq}$), %					0.24	0.46
Limestone, %	3.1					
CaCO$_3$ in Limestone, %	93					
Free Lime, %		1.5				
Insoluble Residue, %	0.19	0.57	0.47	0.10		
C$_3$S, %	61	56.6	59.5	57.79		
C$_2$S, %	12	16.3	14.5	14.02		
C$_3$A, %	7	7.2	11.5	9.73		
C$_4$AF, %	9	10.3	3.7	5.69		
Physical Tests						
Fineness						
Wagner, m^2/kg		264		274		
Blaine, m^2/kg	379	539	358	552		
Setting Time						
Initial (Gilmore), min		110		105		
Final (Gilmore), min		210		148		
Initial (Vicat), min	155		106	63		
Final (Vicat), min			147	101		
Compressive Strength						
1 day, MPa	13.9	24.1		26.8		
3 day, MPa	26.7	32.6		37.5		
7 day, MPa	33.8	39.1		42.9		
28 day, MPa	45.1	46.8		48.8		
Air Content, %	5	6		7.40		
Moisture Content, %					0.26	0.07
False Set, %		73				
Loss on Ignition, %	2.7	2.1	1.59	2.47	1.05	0.11
Amount Retained on #325 Sieve, %		0.9		0.9	27.68	28.92
Specific Gravity					2.33	2.39
Autoclave Soundness, %	0.02	-0.02		0.00	0.07	-0.03
Strength Activity Index (7 day), %					73.6	80
Strength Activity Index (28 day), %					82.0	96
Water Required, %					93.8	96

Appendix B: Test Methods

The workability test methods are described in this appendix as they were performed in the research described in this dissertation.

B.1   Column Segregation Test

Apparatus
1. PVC pipe sections, 8 inches in diameter and 6.5 inches in height, with seals and clips to accept clamps (4). (Alternative: replace 2 middle sections with single 13-inch long section)
2. Spring clamps (12)
3. Base plate (the bottom PVC pipe section is permanently attached to the base plate)
4. Collector plate
5. No. 4 sieve (at least 1, preferably 2)
6. Scoop or bucket to load concrete into column
7. Stopwatch
8. Drying containers or dishes, minimum 5 liters (2)
9. Oven or microwave
10. Balance

Concrete Volume
0.76 ft^3 (21.4 l)
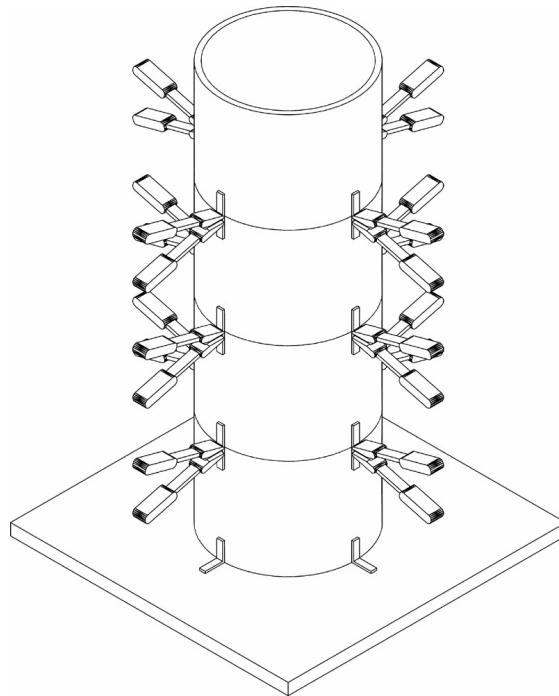
Figure B.1: Column Segregation Test (Collector Plate not Shown)

1. Assemble the PVC pipe sections. Use the clamps to secure each PVC pipe section firmly and to ensure a water-tight seal.
2. Place the assembled apparatus on a firm, level surface.
3. Fill the column with concrete with no external compaction effort.
4. Allow the concrete to remain undisturbed for 15 minutes.
5. Use the collector plate to remove individually each PVC pipe section with the concrete material inside.
6. Individually transfer the contents of the top and bottom pipe section to separate No. 4 sieves. Discard the contents of the middle section(s). Wash each concrete sample over the No. 4 sieve to remove all paste and fine aggregate, leaving behind only clean coarse aggregates on each sieve.
7. Collect the coarse aggregates retained on each sieve in a separate container for each pipe section. Dry each sample in an oven or microwave until it reaches a constant mass.
8. **Measure** the mass of each sample of coarse aggregates.

Results

1. Percent Static Segregation:

$$\text{Percent Static Segregation} = \begin{cases} \dfrac{M_{bottom} - M_{top}}{M_{bottom} + M_{top}} \times 100\% & \text{if } M_{bottom} > M_{top} \\ 0\% & \text{if } M_{bottom} < M_{top} \end{cases}$$

Where: M_{bottom} = mass of aggregate retained on No. 4 sieve from bottom pipe section
M_{top} = mass of aggregate retained on No. 4 sieve from top pipe section.

Notes

1. This test method is standardized as ASTM C 1610.
2. ASTM C 1621 allows aggregates to be dried to saturated-surface dry condition instead of oven-dried. In this case, towels are needed to dry surface moisture from aggregates.

B.2   J-Ring Test

Apparatus
1. J-ring (Figure B.2), 300 mm diameter with 17 equally spaced, 16 mm-diameter reinforcement bars (deformed)
2. Rigid, non-absorbent plate, at least 32 inches square, with concentric circles marked at diameters of 200 mm (8 in.) and 300 mm (12 in.).
3. Slump cone (ASTM C 143)
4. Scoop or bucket to load concrete into slump cone
5. Measuring tape or ruler

Concrete Volume
0.20 ft^3 (5.6 l)

Bar Clear Spacing: 39 mm
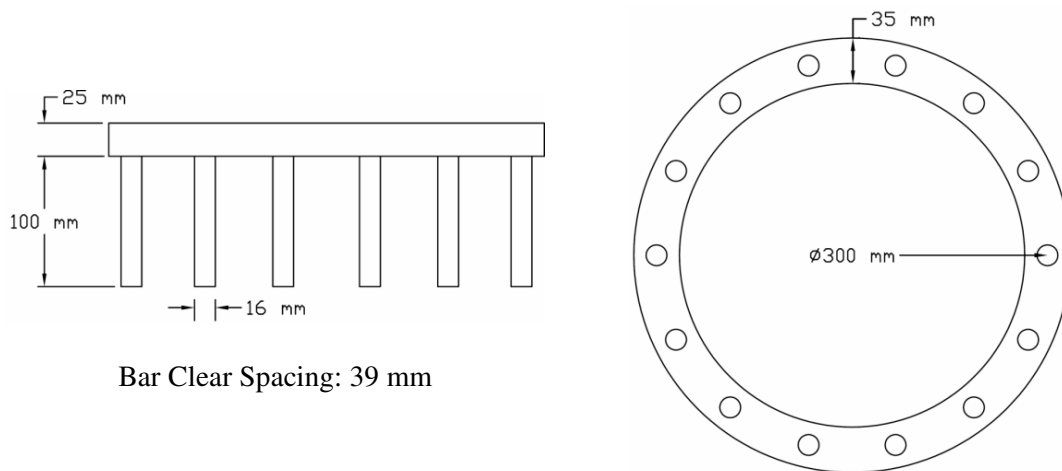
Figure B.2: J-Ring (Bar Spacing Can Vary)

Procedure
1. Attach reinforcement bars on one side of the j-ring to achieve the desired clear spacing between bars.
2. Dampen the slump cone and plate (ensure there is no standing water). Place the plate on firm, level ground. Center the j-ring on the plate (use the 12-inch concentric circle as a guide). Center the slump cone on the plate (use the 8-inch concentric circle as a guide) and hold down firmly.
3. Fill the slump cone with concrete. Do not apply any external compaction effort. Strike off any excess concrete above the top of the slump cone. Remove any concrete on the plate.
4. Remove the slump cone by lifting it vertically upward, being careful not to apply any lateral or torsional motion. Allow the concrete to spread horizontally and cease flowing.
5. **Measure** the height of concrete inside the ring (H_{in}) and outside the ring (H_{out}) at four locations around the ring (See Figure B.3).
6. **Measure** the height of concrete in the center of the ring (H_{center}).
7. **Measure** the final horizontal slump flow in two orthogonal directions.
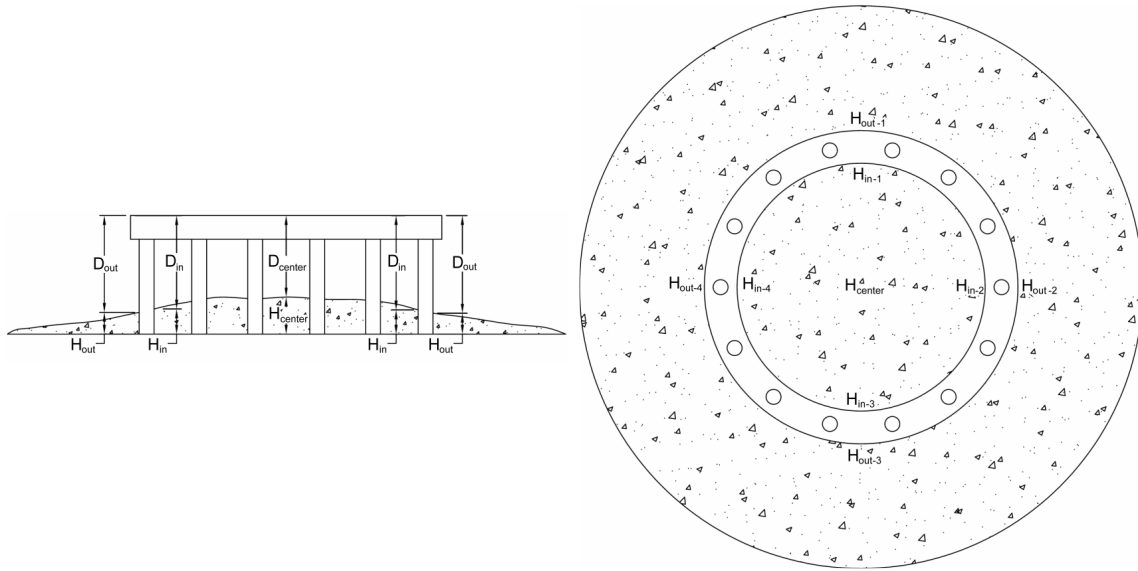
Figure B.3: J-Ring Measurement Locations

Results

1. J-ring Δheight = mean(H_{in}-H_{out}), in inches or mm
2. J-ring test value = 2*median(H_{in}-H_{out})-median(H_{center}-H_{in}), in inches or mm
3. J-ring Δslump flow = (Slump Flow)$_{without\ J\text{-}ring}$ − (Slump Flow)$_{with\ J\text{-}ring}$, in inches or mm

Notes

1. This test method is now standardized as ASTM C 1621.
2. Bar spacing can vary. Changes in bar spacing can be facilitated by threading top of reinforcing bars to screw into tapped holes on top of ring. Different bar spacing can be used on either side of j-ring.
3. For all tests performed in this research, 17 equally spaced, 16-mm diameter deformed reinforcing bars were used. The j-ring in ASTM C 1621 uses 16 equally-spaced 5/8 inch-diameter smooth bars.
4. The ASTM C 1621 test method does not require the slump cone to be used in the inverted orientation.

B.3   L-Box Test

Apparatus
1. L-box (Figure B.4), with 3 equally spaced, 16 mm-diameter, deformed reinforcement bars (clear spacing = 38 mm)
2. Scoop or bucket to load concrete into l-box
3. Stopwatch
4. Measuring tape or ruler

Concrete Volume
0.44 ft^3 (12.6 l)
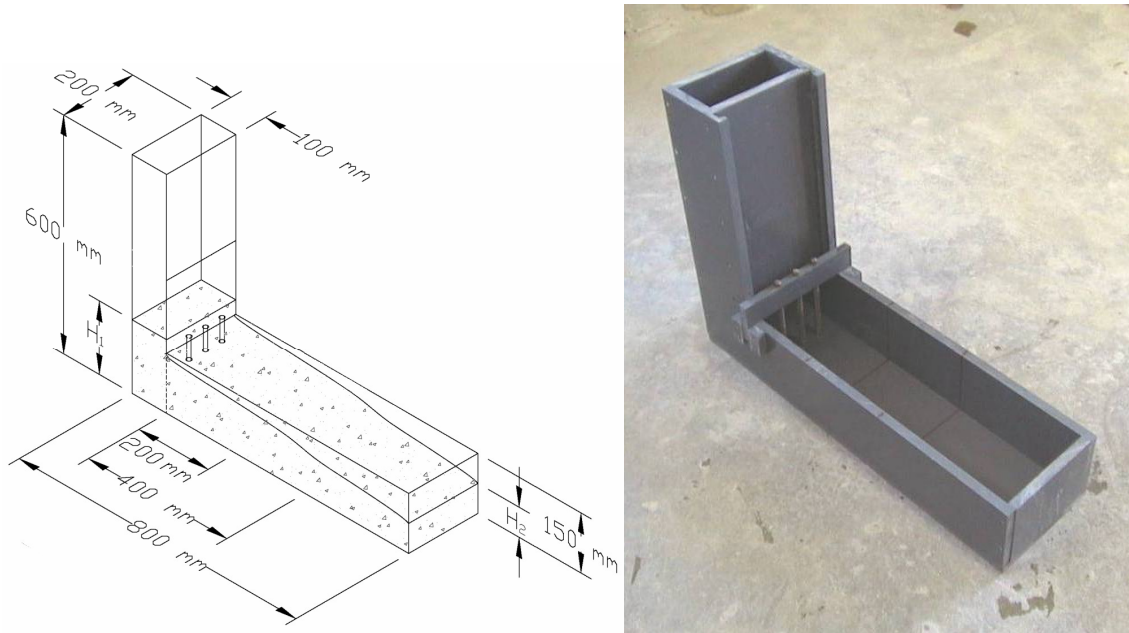
Figure B.4: L-Box Apparatus

Procedure
1. Place the l-box on a firm, level surface. Close the gate.
2. Fill vertical portion of the l-box with concrete. Do not apply any external compaction effort.
3. Allow the concrete to remain undisturbed in the l-box for one minute.
4. Open the gate fully.
5. **Measure** the time for the concrete to reach point marked at 400 mm (T_{40}) down the length of the box.
6. **Measure** the heights H_1 and H_2 at each end of the box (see Figure B.4) after concrete flow has ceased.

Results
1. Time for the concrete to flow to a point 400 mm down the box (T_{40}), in seconds
2. Blocking Ratio = H_2/H_1

B.4   Penetration Apparatus Test

Apparatus
1. Concrete specimen container (e.g. 6x12-inch cylinder, slump cone)
2. Penetration cylinder (aluminum, 45 g)
3. Cylinder positioning apparatus with length scale
4. Stopwatch

Concrete Volume
0.20 ft^3 (5.6 l) for slump cone
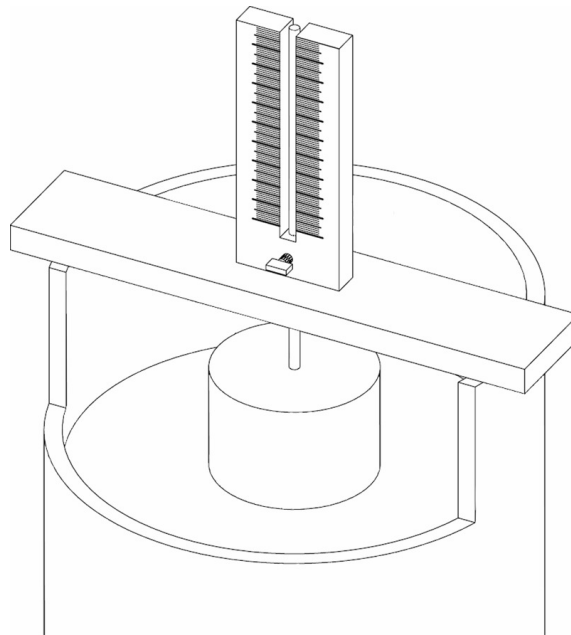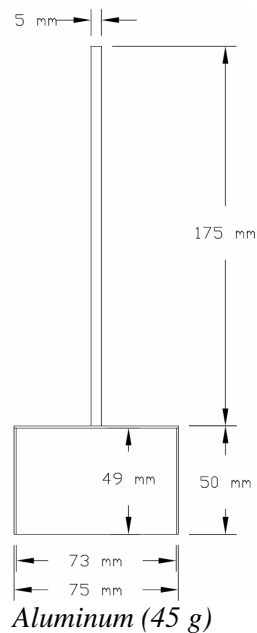
Figure B.5: Penetration Apparatus

Procedure
1. Fill the specimen container with no external compaction effort and ensure top surface of concrete is level.
2. Immediately put the cylinder positioning apparatus into place such that the penetration cylinder is centered above the specimen. Position the bottom of the penetration cylinder just above the top surface of the concrete and tighten the set screw to secure the cylinder in this position.
3. Allow the concrete to remain undisturbed for one minute from the completion of the filling the specimen container.
4. Release the set screw and allow the penetration cylinder to sink into the concrete under its own mass.
5. **Measure** the penetration depth after 30 seconds.
6. OPTIONAL: Repeat the procedure an additional two times.

<u>*Results*</u>
1. Average Penetration Depth

<u>*Notes*</u>
1. For the research described in this dissertation, test was conducted once on each mixture. The specimen container for concrete was an inverted slump cone; however, the test method is not limited to this concrete specimen container.
2. Other sizes of penetration cylinders can be used.

B.5   Sieve Stability Test

Apparatus
1. Container, 10-12 liter capacity, with lid, provide line at 10 liters
2. Balance (accuracy +/- 20g)
3. No. 4 Sieve
4. Pan (the sieve should be easily removed from the pan so as not to cause extra mortar to pass through the pan)
5. Frame to position container 500 mm over sieve
6. Stopwatch

Figure B.6: Sieve Stability Test

Concrete Volume
0.35 ft^3 (10 l)

Procedure
1. Fill the container with 10 +/-0.5 liters of concrete with no external compaction effort. Cover the container.
2. Allow the concrete to remain undisturbed in the container for 15 +/- 0.5 minutes.
3. Place the pan and sieve on the scale. **Measure** the mass of the pan.
4. Pour 4.8 +/- 0.2 kg of concrete from a height of 500 +/- 50 mm onto the sieve. **Measure** the mass of concrete poured onto the sieve.
5. After 2 minutes, remove the sieve. **Measure** the mass of the pan and any mortar that has passed into the pan.

Results
1. Sieved Portion = (Mass$_{pan+passed\ mortar}$-Mass$_{pan}$)/(Mass$_{concrete\ poured\ on\ sieve}$)*100%

B.6 Slump Flow Test

Apparatus
1. Rigid, non-absorbent plate, at least 32 inches square, with concentric circles marked at diameters of 200 mm (8 in.) and 500 mm (20 in.)
2. Slump cone (ASTM C 143)
3. Scoop or bucket to load concrete into slump cone
4. Stopwatch
5. Measuring tape or ruler

Concrete Volume
0.20 ft^3 (5.6 l)
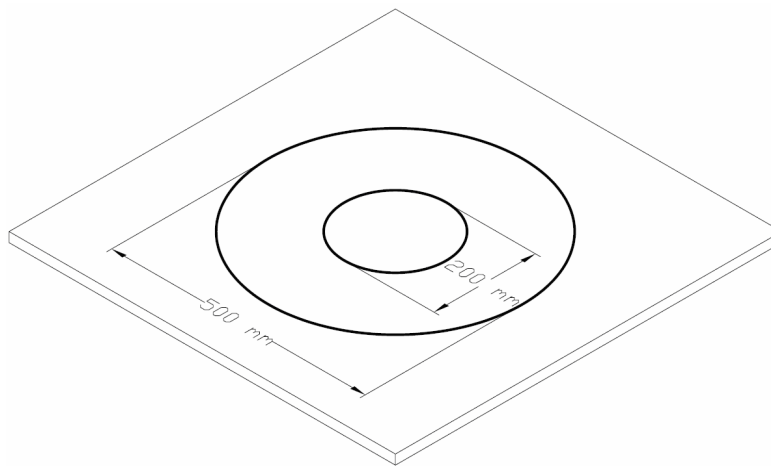
Figure B.7: Slump Flow Plate

Procedure
1. Dampen the slump cone and plate (ensure there is no standing water). Place the plate on firm, level ground. Center the slump cone on the plate (use the 8-inch concentric circle as a guide) and hold down firmly.
2. Fill the slump cone in one lift. Do not apply any external compaction effort. Strike off any excess concrete above the top of the slump cone. Remove any concrete on the plate.
3. Remove the slump cone by lifting it vertically upward, being careful not to apply any lateral or torsional motion.
4. **Measure** the time for the concrete to spread to a diameter of 500 mm (T$_{50}$)
5. **Measure** the final slump flow in two orthogonal directions after the concrete has ceased flowing.
6. **Assign** the visual stability index (VSI) to the nearest 0.5 based on the criteria in Table B.1.

Table B.1: Visual Stability Index Ratings (Daczko 2002)

VSI	Criteria
0	No evidence of segregation in slump flow patty or in mixer drum or wheelbarrow.
1	No mortar halo or aggregate pile in the slump flow patty but some slight bleed or air popping on the surface of the concrete in the mixer drum or wheelbarrow.
2	A slight mortar halo (< 10 mm) and/or aggregate pile in the slump flow patty and highly noticeable bleeding in the mixer drum and wheelbarrow.
3	Clearly segregating by evidence of a large mortar halo (>10 mm) and/or a large aggregate pile in the center of the concrete patty and a thick layer of paste on the surface of the resting concrete in the mixer drum or wheelbarrow.

Results
1. Average slump flow, in inches or mm
2. T_{50}, in seconds
3. Visual stability index

Notes
1. This test method is standardized as ASTM C 1611.
2. The slump cone can be used in the inverted or upright orientation. The inverted orientation is preferred.
3. The visual stability index ratings vary slightly in ASTM C 1611 from Table B.1, which were used for the research described in this dissertation.

B.7   V-Funnel Test

Apparatus
1. V-funnel (Figure B.8)
2. Bucket (minimum capacity = 0.35 ft^3 or 10.0 l)
3. Scoop or bucket to load concrete into v-funnel
4. Stopwatch

Concrete Volume
0.35 ft^3 (10.0 l)
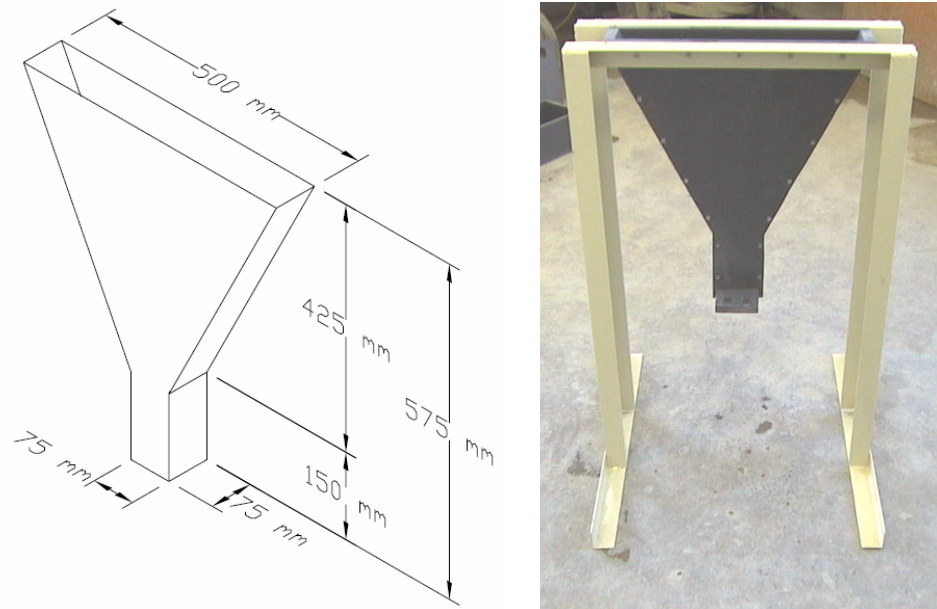
Figure B.8: V-Funnel

Procedure
1. Place the v-funnel frame on firm, level ground. Position the bucket below the opening in the v-funnel.
2. Dampen the inside of the v-funnel. Leave the bottom gate open for sufficient time so that once the gate is closed, water does not drain and collect on the gate.
3. Close the bottom gate.
4. Fill the v-funnel with concrete. Do no apply any external compaction effort. Strike off any excess concrete above the top of the v-funnel.
5. Allow the concrete to remain undisturbed in the v-funnel for one minute.
6. Open the gate of the v-funnel and allow the concrete to flow into the bucket.
7. **Measure** the time from the opening of the gate to the point when light is first visible through the bottom hole.

Optional steps (for v-funnel time after 5 minutes of rest):
8. Close the gate and refill the v-funnel. Do not apply any external compaction effort. Strike off any excess concrete above the top of the v-funnel. It is not necessary to clean the v-funnel for this subsequent test.

374

9. Allow the concrete to remain undisturbed for 5 minutes.
10. Open the gate and allow the concrete to flow into the bucket.
11. **Measure** the time from the opening of the gate to the point when light is first visible through the bottom hole.

Results
1. Standard v-funnel time (T_{std}), in seconds
2. Five-minute v-funnel time ($T_{5\,min}$), in seconds

Notes
1. Only the standard v-funnel time was recorded for the research described in this dissertation.
2. Separate mini-v-funnel used for mortar.

Appendix C: Test Data

Table C.1: Paste Rheology—Comparison of HRWRAs

Mix	HRWRA		w/c	ϕ	Yield Stress	Plastic Viscosity	R^2
	Type	Dosage					
		% cm mass			*Pa*	*Pa.s*	
s1	HRWRA-01	0.1	0.3	0.514	200.00	1.444	0.970
s2	HRWRA-01	0.15	0.3	0.514	20.53	0.683	0.992
s3	HRWRA-01	0.2	0.3	0.514	2.44	0.295	0.998
s4	HRWRA-01	0.25	0.3	0.514	0.68	0.051	0.984
s5	HRWRA-01	0.3	0.3	0.514	0.30	0.025	0.779
s6	HRWRA-01	0.4	0.3	0.514	-0.03	0.018	0.880
s7	HRWRA-03	0.1	0.3	0.514	83.13	0.636	0.962
s8	HRWRA-03	0.15	0.3	0.514	0.36	0.308	0.999
s9	HRWRA-03	0.2	0.3	0.514	0.68	0.026	0.949
s10	HRWRA-03	0.25	0.3	0.514	0.76	0.019	0.781
s11	HRWRA-03	0.3	0.3	0.514	0.35	0.029	0.967
s13	HRWRA-04	0.15	0.3	0.514	59.37	0.589	0.910
s14	HRWRA-04	0.2	0.3	0.514	7.66	0.692	0.997
s15	HRWRA-04	0.25	0.3	0.514	-0.05	0.281	0.991
s16	HRWRA-04	0.3	0.3	0.514	-0.21	0.213	0.995
s12	HRWRA-04	0.35	0.3	0.514	-0.26	0.254	0.982
s17	HRWRA-02	0.1	0.3	0.514	27.69	0.464	0.983
s18	HRWRA-02	0.15	0.3	0.514	0.68	0.087	0.990
s19	HRWRA-02	0.2	0.3	0.514	0.50	0.015	0.611
s20	HRWRA-02	0.25	0.3	0.514	0.62	0.018	0.867
s21	HRWRA-02	0.3	0.3	0.514	0.56	0.031	0.941
s22	HRWRA-05	0.4	0.3	0.514	828.80	-2.990	0.693
s23	HRWRA-05	0.6	0.3	0.514	421.29	-1.575	0.547
s24	HRWRA-05	1.0	0.3	0.514	116.50	-1.580	0.577
s25	HRWRA-05	1.4	0.3	0.514	42.37	-0.616	0.515
s26	HRWRA-05	1.8	0.3	0.514	25.68	-0.145	0.268
s27	HRWRA-02	0.15	0.25	0.559	20.87	0.733	0.996
s28	HRWRA-02	0.15	0.35	0.476	0.30	0.020	0.873
Cement: PC-01-I/II							

Table C.2: Paste Rheology—HRWRA-Cement Interaction

Mix	HRWRA Type	Dosage %m cm	Cement Type	w/c	Yield Stress (Pa)	Plastic Viscosity (Pa.s)	R²
c1			PC-01-I/II	0.4	4.98	0.164	0.989
c2			PC-03-I	0.4	1.81	0.084	0.989
c3			PC-03-III	0.4	55.13	1.192	0.872
c4			PC-02-III	0.4	108.08	0.880	0.903
s3	HRWRA-01	0.002	PC-01-I/II	0.3	2.44	0.295	0.998
s18	HRWRA-02	0.0015	PC-01-I/II	0.3	0.68	0.087	0.990
c5	HRWRA-01	0.002	PC-03-I	0.3	4.24	0.485	0.999
c6	HRWRA-02	0.0015	PC-03-I	0.3	21.15	0.391	0.987
c7	HRWRA-02	0.0015	PC-03-III	0.3	39.33	0.528	0.994
c17	HRWRA-01	0.002	PC-03-III	0.3	119.23	1.35	0.980
c8	HRWRA-01	0.002	PC-02-III	0.3	116.52	0.331	0.872
c9	HRWRA-01	0.004	PC-02-III	0.3	-0.25	0.324	0.996
c10	HRWRA-01	0.006	PC-02-III	0.3	-0.50	0.205	0.993
c11	HRWRA-01	0.007	PC-02-III	0.3	-0.53	0.244	0.991
c12	HRWRA-02	0.0015	PC-02-III	0.3	82.20	0.574	0.937
c13	HRWRA-02	0.003	PC-02-III	0.3	3.31	0.482	0.989
c14	HRWRA-02	0.0035	PC-02-III	0.3	0.05	0.212	0.998
c15	HRWRA-02	0.004	PC-02-III	0.3	1.63	0.769	0.998
c16	HRWRA-02	0.0045	PC-02-III	0.3	-0.22	0.126	0.995

Table C.3: Paste Rheology—Comparison of VMAs

Mix	HRWRA Type	Dosage %m cm	VMA Type	Dosage oz/cwt	w/c	Yield Stress (Pa)	Plastic Viscosity (Pa.s)	R²
v1	HRWRA-02	0.15	VMA-02	0.5	0.3	0.37	0.454	0.999
v2	HRWRA-02	0.15	VMA-02	2.25	0.3	6.15	1.135	0.998
v3	HRWRA-02	0.15	VMA-02	4	0.3	16.37	1.562	0.996
v4	HRWRA-02	0.15	VMA-01	2	0.3	0.68	0.217	0.997
v5	HRWRA-02	0.15	VMA-01	8	0.3	2.41	0.478	0.995
v6	HRWRA-02	0.15	VMA-01	14	0.3	11.18	0.563	0.989
v7	HRWRA-02	0.15	VMA-02	2.25	0.25	151.95	2.528	0.962
v8	HRWRA-02	0.15	VMA-02	2.25	0.35	1.31	0.190	0.994
v9	HRWRA-02	0.15	VMA-01	8	0.25	22.70	0.876	0.995
v10	HRWRA-02	0.15	VMA-01	8	0.35	1.91	0.120	0.988
Cement: PC-01-I/II								

Table C.4: Paste Rheology—Comparison of Fly Ashes

Mix	HRWRA Type	Dosage %m cm	Dosage (ml)	Fly Ash Type	Dosage % Vol	w/c	φ (by vol)	Yield Stress (Pa)	Plastic Viscosity (Pa.s)	R²
f1	HRWRA-02	0.106	0.76	FA-02-F	20	0.316	0.514	1.87	0.174	0.999
f2	HRWRA-02	0.107	0.76	FA-01-F (Post-LNB)	20	0.319	0.514	2.65	0.132	0.962
f3	HRWRA-02	0.105	0.76	FA-01-F (Pre-LNB)	20	0.315	0.514	2.28	0.136	0.988
Cement: PC-01-I/II										

Table C.5: Paste Rheology—Comparison of Aggregate Microfines

Mix	Cement Type	Microfines Type	Dosage % Vol	w/c by mass	w/p by vol	ϕ by vol	Yield Stress Pa	Plastic Viscosity Pa.s	R²
p1	PC-01-I/II	none		0.4	0.4	0.442	4.98	0.164	0.989
constant w/c									
p2	PC-01-I/II	GR-01-F	15	0.4	0.349	0.483	26.16	0.295	0.959
p4	PC-01-I/II	LS-02-F	15	0.4	0.352	0.483	50.75	0.443	0.974
constant solids volume fraction									
p5	PC-01-I/II	GR-01-F	15	0.471	0.410	0.442	5.44	0.150	0.993
p7	PC-01-I/II	LS-02-F	15	0.471	0.413	0.442	6.68	0.227	0.973
effect of cement type									
o1	PC-03-I	none	15	0.4		0.442	1.81	0.084	0.989
o2	PC-03-III	none	15	0.4		0.442	55.13	1.192	0.872
o3	PC-03-I	GR-01-F	15	0.471		0.442	2.34	0.092	0.983
o4	PC-03-III	GR-01-F	15	0.471		0.442	59.42	1.138	0.889
o7	PC-03-I	LS-02-F	15	0.471		0.442	2.46	0.073	0.956
o8	PC-03-III	LS-02-F	15	0.471		0.442	15.02	0.413	0.930

Table C.6: Mortar Mixtures—Effects of Shape Characteristics and Grading

Sand ID	Gradation	Sphericity	L/W	HRWRA Dosage		Slump Flow	T$_{8in}$	V-Funnel Time	Comments
				% cm mass	ml/(l mortar)	inches	s	s	
DO-01-F	As-Rec, (w/o µfines)	1.111	1.520	0.168%	2.60	8.5	5.3	32	severe bleeding; harsh
	As-Rec. (w/ µfines)	1.111	1.520	0.116%	1.80	8.5	4.1	stopped	bleeding; harsh
	0.45 Power Curve	1.106	1.523	0.090%	1.40	9	3.4	6.8	better stability, but still some bubbles and slight bleeding
	Coarse Sand	1.111	1.518	0.155%	2.40	8.5	6.2	11.9	
	Fine Sand	1.099	1.534	0.515%	8.00	7	n/a	10.8	saturation point of HRWRA reached
DL-01-F	As-Rec, (w/o µfines)	--	--	0.193%	3.00	9	4.4	10.5	good stability
	As-Rec. (w/ µfines)	--	--	0.399%	6.20	9	5.2	17	bad stability, viscous
	0.45 Power Curve	--	--	0.174%	2.70	9	5	11.3	bad stability, viscous
	Coarse Sand	--	--	0.161%	2.50	8.75	8.6	22	segregation in mixer, high v-funnel time due to high viscosity
	Fine Sand	--	--	0.277%	4.30	8.75	12	17.3	
LS-01-F	As-Rec, (w/o µfines)	1.144	1.502	0.103%	1.60	9	2.3	4.3	slight segregation
	As-Rec. (w/ µfines)	1.144	1.502	0.168%	2.60	9	1.2	4.3	good stability
	0.45 Power Curve	1.129	1.513	0.129%	2.00	9	2.1	4.7	good stability
	Coarse Sand	1.137	1.504	0.122%	1.90	9	5.4	5.4	good stability, less viscous
	Fine Sand	1.123	1.514	0.155%	2.40	9	2.8	7.2	good stability, viscous
LS-02-F	As-Rec, (w/o µfines)	1.126	1.492	0.077%	1.20	9	3.2	6.5	bubbles, very slight bleeding
	As-Rec. (w/ µfines)	1.126	1.492	0.077%	1.20	9	3	7.2	very good stability, no bubbles
	0.45 Power Curve	1.128	1.488	0.064%	1.00	9	2.2	4.8	bubbles, good stability
	Coarse Sand	1.135	1.483	0.052%	0.80	9	1.5	3.4	good stability, low viscosity
	Fine Sand	1.119	1.502	0.129%	2.00	9	3.6	6.2	bubbles, segregation, slight lump of sand in slump flow bleeding
LS-03-F	As-Rec, (w/o µfines)	1.129	1.546	0.168%	2.60	9	4.5	stopped	harsh mix, slight segregation
	As-Rec. (w/ µfines)	1.129	1.546	0.155%	2.40	9	4.1	68	harsh, sand pile in slump flow, severe bleeding, non-cont. flow in v-funnel
	0.45 Power Curve	1.109	1.549	0.180%	2.80	9	3.7	7.6	much richer mix, no segregation
	Coarse Sand	1.115	1.551	0.155%	2.40	9	3.9	9.1	bleeding less than as-received mixes
	Fine Sand	1.104	1.555	0.309%	4.80	8.5	7.9	8.4	reached saturation point
LS-04-F	As-Rec, (w/o µfines)	1.087	1.484	0.097%	1.50	9	6.5	7.6	viscous, borderline segregation
	As-Rec. (w/ µfines)	1.087	1.484	0.103%	1.60	9	5.5	7.4	viscous, better stability
	0.45 Power Curve	1.099	1.466	0.090%	1.40	9	3.4	6.8	bubbles, bleeding, segregation
	Coarse Sand	1.104	1.458	0.103%	1.60	9	2.7	23.1	bubbles, bleeding, severe segregation, esp. in v-funnel
	Fine Sand	1.092	1.470	0.168%	2.60	9	5	6.9	bubbles, slight segregation
LS-05-F	As-Rec, (w/o µfines)	--	--	0.110%	1.70	9	4.6	6.6	bubbles
	As-Rec. (w/ µfines)	--	--	0.103%	1.60	9	3.5	6.3	bubbles
	0.45 Power Curve	--	--	0.090%	1.40	9	2.2	4.9	
	Coarse Sand	--	--	0.077%	1.20	9	3.3	5.3	bubbles
	Fine Sand	--	--	0.110%	1.70	9	5.2	6.6	bubbles
LS-06-F	As-Rec, (w/o µfines)	--	--	0.084%	1.30	9	1.8	3.3	very low viscosity
	As-Rec. (w/ µfines)	--	--	0.135%	2.10	9	1.5	4.1	higher viscosity
	0.45 Power Curve	--	--	0.084%	1.30	9	1.7	3.6	bubbles
	Coarse Sand	--	--	0.077%	1.20	9	1.9	3.5	bubbles
	Fine Sand	--	--	0.116%	1.80	9	1.6	3.8	
GR-01-F	As-Rec, (w/o µfines)	1.196	1.501	0.541%	8.40	8	15	16.9	reached saturation dosage
	As-Rec. (w/ µfines)	1.196	1.501	0.283%	4.40	9	8.1	12.6	extremely viscous, slight bleeding
	0.45 Power Curve	1.200	1.520	0.090%	1.40	9	6.3	9.4	borderline segregation
	Coarse Sand	1.215	1.500	0.116%	1.80	9	5.7	12.7	extreme bleeding, segregation, non-continuous flow in v-funnel
	Fine Sand	1.173	1.516	0.387%	6.00	9	15	17.4	extremely viscous, starting to segregate and bleed
TR-01-F	As-Rec, (w/o µfines)	1.122	1.508	0.129%	2.00	9	4	5.9	good stability
	As-Rec. (w/ µfines)	1.122	1.508	0.155%	2.40	9	4.2	5.9	good stability
	0.45 Power Curve	1.118	1.512	0.116%	1.80	9	2.9	4.75	
	Coarse Sand	1.123	1.511	0.110%	1.70	9	2.4	3.8	borderline segregation
	Fine Sand	1.118	1.512	0.148%	2.30	9	4.4	7.4	good stability
NA-01-F	As-Rec, (w/o µfines)	1.085	1.452	0.097%	1.50	9	3	4.9	
	As-Rec. (w/ µfines)	1.085	1.452	0.116%	1.80	9	2.9	5.5	good stabilitiy
	0.45 Power Curve	1.086	1.434	0.077%	1.20	9	1.9	3.8	
	Coarse Sand	1.092	1.429	0.077%	1.20	9	1.9	4.1	
	Fine Sand	1.087	1.455	0.097%	1.50	9	2.1	5.3	air bubbles
NA-02-F	As-Rec, (w/o µfines)	1.075	1.453	0.142%	2.20	9.5	1.7	3.7	good stability
	As-Rec. (w/ µfines)	1.075	1.453	0.168%	2.60	9	2	4	slightly more viscous with microfines
	0.45 Power Curve	1.077	1.448	0.129%	2.00	9	1.3	2.9	slightly lower viscosity than other mixes
	Coarse Sand	1.082	1.440	0.103%	1.60	9	1.8	2.8	very good stability
	Fine Sand	1.082	1.440	0.161%	2.50	9.25	1.7	3.5	good stability, workability loss

Table C.7: Mortar Mixtures—Summary of Effects of Shape, Angularity, Texture, and Grading

ID	Particle Size Distribution	HRWRA Dosage		T_{8in}	V-Funnel
		% cm mass	ml/(l mortar)	s	s
Average	As-Rec, (w/o μfines)	0.159%	2.47	4.7	9.3
	As-Rec. (w/ μfines)	0.165%	2.56	3.8	12.9
	0.45 Power Curve	0.110%	1.70	3.0	5.9
	Coarse Sand	0.109%	1.69	3.8	8.9
	Fine Sand	0.214%	3.33	5.6	8.4
Average, no outlier mixes	As-Rec, (w/o μfines)	0.157%	2.44	4.7	7.0
	As-Rec. (w/ μfines)	0.171%	2.65	3.7	7.4
	0.45 Power Curve	0.104%	1.62	2.9	5.7
	Coarse Sand	0.100%	1.55	3.5	8.6
	Fine Sand	0.175%	2.71	5.3	8.2
Standard Deviation	As-Rec, (w/o μfines)	0.126%	1.95	3.7	8.5
	As-Rec. (w/ μfines)	0.091%	1.41	1.9	18.7
	0.45 Power Curve	0.037%	0.58	1.5	2.5
	Coarse Sand	0.035%	0.54	2.2	7.2
	Fine Sand	0.131%	2.03	4.4	4.6
St. Dev., no outlier mixes	As-Rec, (w/o μfines)	0.139%	2.16	4.0	4.1
	As-Rec. (w/ μfines)	0.099%	1.53	2.1	4.2
	0.45 Power Curve	0.033%	0.51	1.6	2.7
	Coarse Sand	0.031%	0.48	2.3	7.9
	Fine Sand	0.090%	1.39	4.5	5.0
Median	As-Rec, (w/o μfines)	0.119%	1.85	4.2	6.5
	As-Rec. (w/ μfines)	0.145%	2.25	3.8	6.3
	0.45 Power Curve	0.090%	1.40	2.6	4.9
	Coarse Sand	0.106%	1.65	3.0	5.4
	Fine Sand	0.158%	2.45	4.4	7.1
Outlier Mixes:DO-01-F, LS-03-F					

Table C.8: Mortar Mixtures—Effects of Microfines (Microfines as Sand)

Micofines ID	Microfines Rate	HRWRA Demand		Slump Flow	T$_{8in}$	V-Funnel Time	28-Day f'$_m$	112-Day Shrinkage	Comments
	% Sand Vol	% cm mass	ml/(l mortar)	inches	s	s	psi	μ-strain	
Control[1]	0	0.077%	1.28	9	4.4	6.6	9928	-610	air bubbles, bleeding
GR-01-F	5	0.090%	1.50	9	4.6	7.4	--	--	bubbles
	10	0.103%	1.71	9.25	3.9	9.4	--	--	viscous, good stability
	15	0.161%	2.68	9	3.8	12.5	11159	-783	viscous, good stability
	20	0.206%	3.42	9	6.4	17.4	--	--	very viscous, good stability
TR-01-F	5	0.103%	1.71	9	3.6	5.2	--	--	bubbles
	10	0.122%	2.03	8.5	4.1	7.5	--	--	bubbles
	15	0.180%	3.00	10	2.8	8.6	11488	-1043	good stability, low yield stress, high viscosity
	20	0.226%	3.75	9	4.2	10.5	--	--	viscous
LS-02-F	5	0.077%	1.28	9	3.2	5.3	--	--	air bubbles
	10	0.090%	1.50	9	2.3	5.7	--	--	
	15	0.116%	1.93	9	3.3	6.3	10952	-837	
	20	0.129%	2.14	9	3.5	7.5	--	--	bubbles, viscous
DL-01-F	5	0.110%	1.82	9	4.8	6	--	--	good stability, no bubbles
	10	0.129%	2.14	9	4.1	7.8	--	--	
	15	0.168%	2.78	9	4.4	8.1	10488	-880	
	20	0.206%	3.42	9	5.4	9.2	--	--	
LS-05-F	5	0.090%	1.50	9	2.8	5.5	--	--	bubbles
	10	0.103%	1.71	9	3.3	7.9	--	--	
	15	0.116%	1.93	9	3.3	7.4	10842	-973	lost workability quickly
	20	0.142%	2.35	9	5.3	9.5	--	--	
LS-06-F	5	0.071%	1.18	9		5.2	--	--	slight segregation, bubbles
	10	0.084%	1.39	9	3.1	5.1	--	--	bubbles
	15	0.090%	1.50	9	3.5	5.1	10395	-917	
	20	0.110%	1.82	9	3.6	5.7	--	--	

1. Control mixture with no microfines, w/cm=0.35

Table C.9: Mortar Mixtures—Effects of Microfines (Microfines as Powder)

Micofines ID	Microfines Rate	HRWRA Demand		Slump Flow	T$_{8in}$	V-Funnel Time	28-Day f'$_m$	112-Day Shrinkage	Comments
	% Sand Vol	% cm mass	ml/(l mortar)	inches	s	s	psi	μ-strain	
Control[1]	0	--	--	--	--	--	5146	-1240	
GR-01-F	15	0.141%	1.50	9	5.5	8	5118	-857	borderline segregation, bleeding
TR-01-F	15	0.212%	2.25	9	4.6	6.2	5860	-1107	borderline segregation, bubbles, bleeding
LS-02-F	15	0.141%	1.50	8.5	6	5.5	4231	-617	very bad segregation, bleeding, bubbles
DL-01-F	15	0.202%	2.14	9	4.4	5.9	4281	-765	bubbles
LS-05-F	15	0.161%	1.71	8.75	4.4	5.7	5213	-733	bubbles, borderline segregation, slight bleeding
LS-06-F	15	0.121%	1.28	9	2	4.3	5236	-795	bubbles, segregation

1. Control mixture with w/cm = 0.57, no HRWRA

Table C.10: Mortar Mixtures—Effects of Microfines (Effect of HRWRA Dosage)

Mix ID	HRWRA Demand		Slump Flow	T$_{8in}$	V-Funnel Time	28-Day f'$_m$	112-Day Shrinkage	Purpose
	% cm mass	ml/(l mortar)	inches	s	s	psi	μ-strain	
HR1	0.083%	1.30	--	--	--	9451	-1063	TR-01-F microfines; effect of HRWRA
HR2	0.138%	2.14	--	--	--	9099	-1005	TR-01-F microfines; effect of HRWRA
HR3	0	0.00	--	--	--	8527	-1007	TR-01-F microfines; effect of HRWRA

Table C.11: Mortar Mixtures—Mixture Proportioning (LS-02-F Fine Aggregate)

Sand: LS-02-F

Mix	PV	FA	$\text{phi}_{\text{paste}}$	w/cm	w/c	w/p	w/cm	w/c	w/p	HRWRA ml/l	HRWRA (% cm)	T_8 s	V-Funnel s	24h f'c psi	28d f'c psi
		Factors		Metrics (mass)			Metric (vol)								
1	0.469	0.062	0.483	0.396	0.422	0.353	1.220	1.328	1.069	1.75	0.113%	5.0	9.5	3743	8797
2	0.469	0.062	0.567	0.277	0.295	0.252	0.853	0.929	0.763	3.33	0.180%	11.2	35.8	7695	11598
3	0.469	0.258	0.483	0.422	0.569	0.374	1.220	1.792	1.069	1.00	0.069%	3.8	4.7	2148	7232
4	0.469	0.258	0.567	0.295	0.398	0.267	0.853	1.253	0.763	2.17	0.125%	6.8	12.3	4171	7690
5	0.581	0.062	0.471	0.396	0.422	0.368	1.220	1.328	1.122	0.83	0.042%	1.0	2.3	3725	8934
6	0.581	0.062	0.557	0.277	0.295	0.261	0.853	0.929	0.795	2.92	0.124%	3.4	7.8	8121	10547
7	0.581	0.258	0.471	0.422	0.569	0.391	1.220	1.792	1.122	0.50	0.027%	0.3	1.7	2249	6736
8	0.581	0.258	0.557	0.295	0.398	0.277	0.853	1.253	0.795	1.33	0.060%	2.7	5.3	4696	10533
9	0.430	0.157	0.530	0.341	0.405	0.302	1.020	1.275	0.886	could not achieve 9-inch mini-slump flow					
10	0.620	0.157	0.511	0.341	0.405	0.322	1.020	1.275	0.956	1.00	0.045%	1.6	2.9	3925	9298
11	0.525	0.000	0.519	0.324	0.324	0.299	1.020	1.020	0.927	1.83	0.093%	2.9	7.9	6488	10636
12	0.525	0.331	0.519	0.361	0.540	0.330	1.020	1.700	0.927	0.75	0.042%	1.8	3.4	2453	7822
13	0.525	0.157	0.448	0.462	0.548	0.419	1.381	1.726	1.234	0.67	0.042%	0.8	2.2	2325	7803
14	0.525	0.157	0.590	0.252	0.299	0.235	0.754	0.943	0.694	3.00	0.139%	5.6	19.2	7439	12467
15	0.525	0.157	0.519	0.341	0.405	0.314	1.020	1.275	0.927	1.25	0.067%	2.2	4.7	4062	10181
16	0.525	0.157	0.519	0.341	0.405	0.314	1.020	1.275	0.927	1.25	0.067%	2.5	5.1	3917	8848
17	0.525	0.157	0.519	0.341	0.405	0.314	1.020	1.275	0.927	1.25	0.067%	2.4	5.0	4149	9461
18	0.525	0.157	0.519	0.341	0.405	0.314	1.020	1.275	0.927	1.33	0.071%	2.5	5.2	4113	10312
19	0.525	0.157	0.519	0.341	0.405	0.314	1.020	1.275	0.927	1.42	0.076%	1.9	4.4	4666	9387
20	0.525	0.157	0.519	0.341	0.405	0.314	1.020	1.275	0.927	1.25	0.067%	2.4	4.4	4109	9526

Table C.12: Mortar Mixtures—Mixture Proportioning (NA-02-F Fine Aggregate)

Sand: NA-02-F

Mix	PV	FA	$\text{phi}_{\text{paste}}$	w/cm	w/c	w/p	w/cm	w/c	w/p	HRWRA ml/l	HRWRA % cm	T_8 s	V-Funnel s	24h f'c psi	28d f'c psi
		Factors		Metrics (mass)			Metric (vol)								
1	0.446	0.081	0.457	0.396	0.422	0.387	1.220	1.328	1.187	1.92	0.124%	2.3	3.9	3690	8627
2	0.446	0.081	0.545	0.277	0.295	0.271	0.853	0.929	0.834	3.67	0.198%	5.3	14.3	7099	11583
3	0.446	0.319	0.457	0.422	0.569	0.412	1.220	1.792	1.187	1.75	0.121%	1.4	2.5	2284	6573
4	0.446	0.319	0.545	0.295	0.398	0.289	0.853	1.253	0.834	3.00	0.173%	3.4	7.8	4620	9593
5	0.564	0.081	0.455	0.396	0.422	0.390	1.220	1.328	1.199	1.17	0.059%	0.8	1.6	3649	8848
6	0.564	0.081	0.543	0.277	0.295	0.273	0.853	0.929	0.841	3.00	0.127%	2.4	6.8	6646	11281
7	0.564	0.319	0.455	0.422	0.569	0.416	1.220	1.792	1.199	0.75	0.041%	0.3	1.3	2014	6698
8	0.564	0.319	0.543	0.295	0.398	0.291	0.853	1.253	0.841	2.00	0.091%	1.4	3.5	4398	10557
9	0.406	0.200	0.502	0.341	0.405	0.333	1.020	1.275	0.990	4.00	0.267%	6.0	7.4	3746	8017
10	0.604	0.200	0.498	0.341	0.405	0.338	1.020	1.275	1.007	1.58	0.071%	0.7	1.9	4110	9099
11	0.505	0.000	0.500	0.324	0.324	0.319	1.020	1.020	1.000	2.67	0.135%	1.9	4.9	5665	10862
12	0.505	0.400	0.500	0.361	0.540	0.354	1.020	1.700	1.000	1.50	0.085%	0.9	1.9	2666	8009
13	0.505	0.200	0.426	0.462	0.548	0.453	1.381	1.726	1.349	1.08	0.068%	0.5	1.3	2243	6865
14	0.505	0.200	0.574	0.252	0.299	0.249	0.754	0.943	0.741	3.83	0.178%	3.1	9.6	7015	12432
15	0.505	0.200	0.500	0.341	0.405	0.336	1.020	1.275	1.000	2.08	0.111%	1.3	3.4	4158	10469
16	0.505	0.200	0.500	0.341	0.405	0.336	1.020	1.275	1.000	2.00	0.107%	1.4	3.6	4289	9971
17	0.505	0.200	0.500	0.341	0.405	0.336	1.020	1.275	1.000	2.08	0.111%	1.5	3.2	3985	9550
18	0.505	0.200	0.500	0.341	0.405	0.336	1.020	1.275	1.000	2.08	0.111%	1.8	3.4	4056	9756
19	0.505	0.200	0.500	0.341	0.405	0.336	1.020	1.275	1.000	1.83	0.098%	1.9	3.8	4091	9638
20	0.505	0.200	0.500	0.341	0.405	0.336	1.020	1.275	1.000	2.08	0.111%	1.7	3.4	4048	9653

Table C.13: Mortar Mixtures—Mixture Proportioning (DL-01-F Fine Aggregate)

Sand: DL-01-F

Mix	Factors PV	FA	phi$_{paste}$	Metrics (mass) w/cm	w/c	w/p	Metric (vol) w/cm	w/c	w/p	HRWRA ml/l	HRWRA (% cm)	T$_8$ s	V-Funnel s	24h f'c psi	28d f'c psi
1	0.541	0.081	0.499	0.519	0.553	0.339	1.602	1.743	1.005	3.75	0.284%	1.8	5.3	3057	8026
2	0.541	0.081	0.557	0.387	0.413	0.268	1.195	1.300	0.795	4.83	0.309%	5.8	17.5	5260	10828
3	0.541	0.319	0.499	0.554	0.747	0.354	1.602	2.352	1.005	3.17	0.256%	2.0	3.7	1639	5592
4	0.541	0.319	0.557	0.413	0.557	0.280	1.195	1.754	0.795	3.83	0.261%	4.1	11.8	3206	8428
5	0.639	0.081	0.461	0.519	0.553	0.391	1.602	1.743	1.170	2.17	0.129%	0.4	1.6	2345	8055
6	0.639	0.081	0.523	0.387	0.413	0.303	1.195	1.300	0.911	3.00	0.151%	1.8	4.2	5249	11929
7	0.639	0.319	0.461	0.554	0.747	0.410	1.602	2.352	1.170	1.50	0.095%	0.6	1.4	1333	5344
8	0.639	0.319	0.523	0.413	0.557	0.319	1.195	1.754	0.911	2.42	0.130%	1.1	3.0	3010	8637
9	0.508	0.200	0.543	0.462	0.548	0.290	1.381	1.726	0.841	5.00	0.394%	5.8	15.1	3272	8411
10	0.672	0.200	0.482	0.462	0.548	0.366	1.381	1.726	1.074	1.83	0.096%	0.9	1.9	2613	7879
11	0.590	0.000	0.508	0.438	0.438	0.319	1.381	1.381	0.967	3.42	0.204%	2.3	5.5	4413	10576
12	0.590	0.400	0.508	0.489	0.731	0.345	1.381	2.302	0.967	2.50	0.167%	1.1	2.5	1583	6397
13	0.590	0.200	0.458	0.595	0.705	0.407	1.778	2.222	1.185	2.25	0.165%	0.8	1.8	1549	5595
14	0.590	0.200	0.559	0.363	0.430	0.270	1.083	1.354	0.788	3.83	0.211%	2.8	7.8	4892	10931
15	0.590	0.200	0.508	0.462	0.548	0.331	1.381	1.726	0.967	3.00	0.189%	1.5	3.5	3035	8275
16	0.590	0.200	0.508	0.462	0.548	0.331	1.381	1.726	0.967	3.17	0.199%	1.7	4.0	3103	8094
17	0.590	0.200	0.508	0.462	0.548	0.331	1.381	1.726	0.967	3.00	0.189%	1.4	3.4	3084	8365
18	0.590	0.200	0.508	0.462	0.548	0.331	1.381	1.726	0.967	3.00	0.189%	1.8	3.8	3126	8414
19	0.590	0.200	0.508	0.462	0.548	0.331	1.381	1.726	0.967	3.00	0.189%	1.3	3.8	3057	7943
20	0.590	0.200	0.508	0.462	0.548	0.331	1.381	1.726	0.967	3.00	0.189%	1.3	3.7	2974	8141

Table C.14: Concrete Mixtures—Fine Aggregates

Mix	Mixture Sand	Gradation	HRWRA Demand	Slump Flow Flow	T$_{50}$	VSI	V-Funnel	Visual Ratings Filling	Passing	Seg.	Sufficient Paste Volume?	J-Ring Δh	S. Flow Diff.	Rheology τ_0	μ	Compressive Strength 24-hr	28-d	Elastic Modulus 28-d	Flexural Strength 28-d	RCP	Drying Shrinkage 112-d
			% cm m	in	s		s	0-3	0-3	0-3		in	in	Pa	Pa.s	psi	psi	ksi	psi	C	μ-strain
F1	DO-01-F	As-Rec	0.103%	23.5	4.6	2.5	14.1	3	3	3	no	1.63	-2.0	28.6	19.7	1902	5833	6099	1068		-357
F2		Standard	0.090%	24.5	3.4	3.0	20.0	3	3	3	no	1.00	-2.0	28.9	14.8	1814	6248	6050	1097		-407
F3	DL-01-F	As-Rec	0.194%	25	5.3	1.5	60.6	1.5	1	0.5	borderline	0.72	-0.5	8.9	39.2	2562	8945	5994	1169	685	-460
F4		Standard	0.129%	24	3.8	2.5	28.0	3	3	0.5	borderline	1.25	-3.0	43.8	25.5	2333	8339	5718	1104	675	-483
F5	GR-01-F	As-Rec	0.103%	25.5	4.5	3.0	7.1	2	0.5	2	no	0.50	0.0	14.6	24.8	1903	6065	5310	853	880	-443
F6		Standard	0.077%	26	3.9	3.0	16.8	2	2	2.5	no	0.69	-1.0	12.5	21.5	2097	6493	5014	900	965	-420
F7	TR-01-F	As-Rec	0.142%	25	4.3	0.5	6.4	0.5	1	0	yes	0.75	-1.5	25.4	31.9	2680	8680	6633	1141	810	-523
F8		Standard	0.116%	24	3.5	0.5	6.8	1.5	1.5	1	yes	1.25	-1.5	46.4	17.3	2196	8316	6271	1017	700	-497
F9	LS-01-F	As-Rec	0.103%	24.5	3.4	1.5	29.0	2	1.5	1.5	borderline	0.91	-1.0	36.9	17.9	2424	8203	5942	1034	735	-433
F10		Standard	0.103%	24.5	3.4	2.0	15.8	2	1	2	borderline	0.69	-0.5	31.3	13.8	2443	8314	5873	1005	775	-450
F11	LS-02-F	As-Rec	0.065%	24	2.5	0.5	4.2	0.5	0.5	0.5	yes	0.41	-1.0	31.6	16.0	2346	8335	5995	1018	870	-450
F12		Standard	0.065%	25.5	2.5	1.0	3.4	1.5	0.5	1	yes	0.25	0.0	28.3	9.4	2259	7950	5927	936	870	-500
F13	LS-03-F	As-Rec	0.194%	23	4.5	3.0	9.6	3	3	1.5	no	1.75	-5.0	33.0	27.9	2072	7070	5369	976	830	-413
F14		Standard	0.129%	25	2.4	2.0	34.0	1.5	1.5	1.5	borderline	1.06	-2.0	37.5	16.1	2156	7747	5711	916	725	-467
F15	LS-04-F	As-Rec	0.103%	25	3	0.0	4.4	0	0	0	yes	0.25	0.0	31.0	20.8	2287	8087	5227	922	1045	-507
F16		Standard	0.077%	24	2.9	0.5	9.3	1	0.5	0.5	yes	0.63	-0.5	61.2	11.1	2016	7400	4920	918	1165	-523
F17	LS-05-F	As-Rec	0.103%	26	2.7	0.5	3.0	0	0	0.5	yes	0.25	0.0	25.0	17.1	2542	9116	6604	1101	760	-525
F18		Standard	0.077%	24	2.6	0.5	9.4	0.5	1	0.5	yes	0.38	0.0	58.9	9.5	2313	8406	6402	1009	720	-463
F19	LS-06-F	As-Rec	0.116%	26	2.6	1.5	14.6	1	1	1.5	borderline	0.88	0.0	33.1	14.3	2126	7955	5372	885	990	-463
F20		Standard	0.090%	25.5	2.1	1.5	20.0	0.5	0.5	1	borderline	0.50	0.0	29.1	8.9	1933	7306	5338	945	1080	-410
F21	NA-01-F	As-Rec	0.103%	26	1.3	0.0	2.8	0	0	0	yes	0.13	-1.0	31.5	8.0	2321	8020	6519	1046	865	-417
F22		Standard	0.090%	26	1.4	0.0	2.5	0.5	0.5	0.5	yes	0.50	0.0	31.3	5.0	2061	7837	6279	1031	825	-480
F23	NA-02-F	As-Rec	0.142%	26.5	0.9	0.0	2.2	0	0	0	yes	0.13	-0.5	52.1	3.7	2126	7694	6589	969	860	-453
F24		Standard	0.103%	26.5	1.3	0.5	2.1	0.5	0	1	yes	0.31	0.0	37.7	3.1	1861	7241	6333	937	815	-477

Table C.15: Concrete Mixtures—Coarse Aggregates

Mix	Sand	Gradation	HRWRA Demand	Slump Flow Flow	T₅₀	VSI	V-Funnel	Filling	Passing	Seg.	Sufficient Paste Volume?	J-Ring Δh	S. Flow Diff.	τ₀	μ	Comp. 24-hr	Comp. 28-d	Elastic Modulus 28-d	Flexural Strength 28-d	RCP	Drying Shrinkage 112-d
			% cm m	in	s		s	0-3	0-3	0-3		in	in	Pa	Pa.s	psi	psi	ksi	psi	C	μ-strain
C1	DO-01-C	As-Rec.	0.065%	25.5	4.0	1.5	9.4	1	1	1.5	no	1.19	-2.5	38.2	23.4	2522	9006	6144	1037	690	-407
C2		Gap	0.065%	24	3.9	1.0	9.2	0.5	1	1	no	1.25	-3.0	47.9	20.6	2513	9019	6109	1018	650	-400
C3		Intermediate	0.071%	25	4.6	2.0	39.0	1	1	1.5	no	0.75	0.0	32.5	19.3	2458	8525	5884	1063	725	-423
C4		0.45	0.071%	25	3.4	1.0	40.5	0.5	1.5	1	no	1.25	-2.5	38.2	22.7	2426	8432	6157	1005	745	-403
C5	NA-02-C	As-Rec.	0.071%	24.5	2.9	0.0	4.0	0	0	0.5	yes	0.25	0.0	38.7	13.8	2260	7763	5653	977	790	-440
C6		Gap	0.065%	26.5	2.0	1.0	3.5	0	0	2	yes	0.25	0.5	74.5	9.9	2201	7726	5950	947	820	-387
C7		Intermediate	0.071%	26.5	2.2	1.0	4.7	0	0.5	1.5	yes	0.63	0.5	24.4	15.6	2233	7829	6104	1050	685	-410
C8		0.45	0.077%	26	2.0	1.0	4.9	0	0	1	yes	0.50	0.5	35.2	10.0	2519	7922	5903	977	700	-430
C9	LS-01-C	As-Rec.	0.084%	26	3.5	1.5	16.0	0.5	0	3	no	0.63	1.0	28.7	15.5	2571	8256	5316	1176	820	-407
C10		Gap	0.065%	26	2.7	0.5	5.7	0	0	1.5	yes	0.56	0.0	69.0	13.7	2333	7968	5231	1011	765	-383
C11		Intermediate	0.071%	26	2.4	0.5	4.3	0	0	1	yes	0.25	1.0	39.6	18.7	2235	7744	5113	979	800	-420
C12		0.45	0.071%	26	3.0	0.5	6.1	0	0.5	1	yes	0.69	-1.0	55.8	14.0	2137	7090	4697	1014	850	-403
C13	LS-02-C	As-Rec.	0.065%	25.3	3.5	0.0	6.4	0.5	0.5	0.5	yes	0.56	-1.0	16.6	24.5	2218	8238	5217	1127	785	-497
C14		Gap	0.065%	26	4.3	1.0	10.2	0	0.5	1	yes	1.00	-1.0	44.8	17.1	2377	8598	5744	1113	830	-513
C15		Intermediate	0.065%	25	3.1	1.0	7.9	0	0.5	0.5	yes	0.69	-0.5	38.2	21.4	2492	8985	5491	1161	780	-530
C16		0.45	0.065%	24	3.3	0.0	9.6	0.5	0.5	0	yes	0.66	-2.0	47.8	16.3	2453	8856	5192	1116	840	-443
C17	LS-03-C	As-Rec.	0.065%	26	3.0	1.0	8.6	0.5	1	1	yes	1.34	-1.5	23.7	23.8	2186	7989	5131	985	935	-643
C18		Gap	0.065%	25.5	3.3	0.5	17.5	0.5	2	0.5	yes	1.25	-3.0	41.5	22.6	2391	7731	5152	961	735	-553
C19		Intermediate	0.065%	24.5	3.9	0.5	24.0	0.5	2	0.5	no	1.50	-2.0	51.0	16.0	2381	7519	4719	944	855	-580
C20		0.45	0.071%	26.5	3.1	0.5	35.8	0.5	1.5	1	borderline	1.16	-2.5	19.5	18.4	2341	7849	4809	985	795	-540
C21	LS-04-C	As-Rec.	0.071%	26	3.8	2.0	no flow	1	1.5	1.5	yes	1.25	-1.0	16.3	17.6	2876	7812	4652	1042	1170	-477
C22		Gap	0.071%	26	3.6	1.5	14.0	0	1	1	yes	1.44	-2.0	12.8	21.7	2407	7371	4631	995	1265	-503
C23		Intermediate	0.065%	24	4.8	1.5	35.0	0.5	0.5	1	yes	1.19	1.0	15.7	19.5	2238	7033	4194	966	1385	-507
C24		0.45	0.071%	26	3.0	1	35.0	1	1	1	yes	1.03	-1.00	18.1	20.1	2286	7300	4463	969	1345	-517
C25	LS-05-C	As-Rec.	0.065%	25	3.3	1.5	27.0	0	1	2	yes	1.19	-2	58.8	17.8	2673	9130	5799	1074	875	-490
C26		Gap	0.065%	25	2.5	1.5	29.0	0	1.5	2	yes	1.19	-1	35.2	25.9	2560	8603	5952	1115	815	-500
C27		Intermediate	0.065%	25	3.0	0.5	35.0	0.5	0.5	1	yes	0.63	-1.5	50.4	17.7	2466	8977	5895	1045	830	-467
C28		0.45	0.071%	25	3.3	1	33.0	1	0.5	1.5	yes	0.75	-1	42.2	15.2	2563	8622	5837	1120	760	-463

Table C.16: Concrete Mixtures—Effects of Aggregates at Various Paste Volumes

Mix	Agg.	Gradation	Paste Vol.	HRWRA Demand	Slump Flow Flow	T₅₀	VSI	V-Funnel	Filling	Passing	Seg.	Sufficient Paste Volume?	J-Ring Δh	S. Flow Diff.	τ₀	μ	Comp. 24-hr	Comp. 28-d	Elastic Modulus 28-d	Flexural Strength 28-d	RCP	Drying Shrinkage 112-d
				% cm m	in.	s		s	0-3	0-3	0-3		in.	in.	Pa	Pa.s	psi	psi	ksi	psi	C	μ-strain
P1	DO-01-C	cont	34.1	0.155%	24.0	8.7	2.0	29.3	2.0	3.0	2.5	no	1.75	-5.0	16.4	45.3	2094	6022	5895	1030	1055	-353
P2	DO-01-C	cont	36.6	0.077%	25.0	5.0	1.0	62.0	1.5	1.5	1.0	no	1.25	-3.0	6.7	37.0	3671	9786	6513	1199	945	-427
P3	DO-01-C	cont	39.0	0.071%	26.0	3.1	1.5	34.6	1.0	1.0	1.5	yes	1.00	-1.0	21.2	19.6	3712	10415	6325	1241	1075	-457
P4	DO-01-C	cont	41.4	0.065%	26.5	2.1	1.5	8.1	0.5	0.5	1.0	yes	0.56	0.0	36.4	13.1	3727	10317	6285	1160	1235	-473
P5	DO-01-C	gap	34.1	0.116%	26.0	5.3	3.0	17.5	3.0	2.0	3.0	no	1.50	-3.0	27.8	36.8	3646	8375	6683	1081	955	-387
P6	DO-01-C	gap	36.6	0.071%	25.0	4.7	0.5	44.2	1.5	2.0	0.5	borderline	1.50	-4.0	22.8	32.4	4184	10172	6662	1206	1135	-420
P7	DO-01-C	gap	39.0	0.060%	25.0	3.2	0.0	12.3	0.5	1.5	0.5	yes	1.44	-3.0	27.7	25.3	4043	10047	6769	1047	965	-473
P8	DO-01-C	gap	41.4	0.060%	25.0	2.2	0.5	3.7	0.0	0.5	1.5	yes	0.69	-1.0	59.6	10.9	4059	9789	6361	1206	1075	-483
P9	DO-01-F		32.7	0.335%	22.0	6.2	3.0	7.6	3.0	3.0	3.0	no	1.75	-9.0	39.4	42.7	1908	6224	6647	874	850	-333
P10	DO-01-F		35.2	0.090%	25.0	6.2	1.0	25.9	2.0	1.5	0.0	no	1.31	-3.5	12.4	32.3	3599	8704	6889	1123	755	-403
P11	DO-01-F		37.7	0.065%	25.0	3.4	1.0	35.7	1.5	1.5	0.5	no	1.19	-3.0	20.3	21.0	3480	8950	6506	1071	870	-443
P12	DO-01-F		40.2	0.077%	26.0	2.3	1.5	5.0	0.0	0.5	1.5	yes	0.38	0.5	24.7	9.5	3654	8376	6333	1123	845	-497
P13	DO-01-F		42.7	0.052%	25.0	1.6	1.0	3.6	0.0	0.0	0.5	yes	0.38	-1.0	48.5	7.1	3292	7932	6466	1094	1125	-560

Table C.17: Concrete Mixtures—Effects of Microfines

Mix	μ-fines	Used As	HRWRA Demand	Slump Flow Flow	T₅₀	VSI	V-Funnel	Filling	Passing	Seg.	J-Ring Δh	S. Flow Diff.	τ₀	μ	Comp. 24-hr	Comp. 28-d	Elastic Modulus 28-d	Flexural Strength 28-d	RCP	Drying Shrinkage 112-d	Abrasion Mass Loss
			oz/yd³	in	s		s	0-3	0-3	0-3	in	in	Pa	Pa.s	psi	psi	ksi	psi	C	μ-strain	g
M1	Control	Aggregate	24	26	1.9	0.0	3.9	0.5	0	0	0.19	0.0	32.2	9.7	2170	8143	5830	1028	765	-477	-5.9
M2		Powder	0													883	4457	4626	842	1470	-437	-7.5
M3	GR-01	Aggregate	38	24	3.6	0.0	7.5	0.5	0.5	0	0.50	-2.0	42.4	29.5	2663	8540	5853	1007	885	-477	-4.2
M4		Powder	28	25	2.8	0.0	4.6	0	0	0	0.25	0.0	26.8	19.1	1108	4860	4746	795	1355	-453	-8.2
M5	TR-01	Aggregate	48	26	2.5	0.0	5.6	0	0	0	0.25	0.0	23.7	19.2	2637	8534	5967	1083	815	-527	-3.3
M6		Powder	36	25.5	2	0.0	3.4	0	0	0.5	0.13	0.5	47.4	10.4	1048	5421	5013	902	1100	-510	-6.4
M7	DL-01	Aggregate	46	24	3.4	0.0	5.5	0	0	0	0.25	0.0	42.7	20.8	2524	8468	5648	1043	770	-527	-4.6
M8		Powder	40	24	2	0.0	3.2	0	0	0	0.50	-0.5	60.8	9.0	998	4941	4708	729	1275	-493	-6.6
M9	LS-02	Aggregate	28	26	2.1	0.0	5.6	0	0	0.5	0.25	-0.5	15.2	14.0	2102	8405	5638	935	770	-493	-5.2
M10		Powder	26	25	1.7	0.5	3.6	0	0	2	0.25	1.0	16.3	10.8	895	5379	5367	748	1300	-450	-6.2
M11	LS-05	Aggregate	32	25	3.2	0.0	5.5	0	0.5	0	0.25	0.0	26.0	23.5	2284	9006	5733	1065	785	-517	-4.2
M12		Powder	26	25	2.7	0.5	3.8	0	0	1.5	0.25	0.5	46.6	10.8	1003	5616	4734	821	1200	-483	-7.3
M13	LS-06	Aggregate	28	24	2.9	0.0	3.7	0	0	0	0.25	-0.5	40.8	13.2	2132	8298	5631	988	830	-527	-4.3
M14		Powder	22	25	1.2	0.5	2.9	0	0	1	0.25	0.5	72.0	5.3	811	4864	4613	850	1330	-537	-6.6

Table C.18: Concrete Mixtures—Effects of Mixture Proportions (Material Set 1)

| Mix | Factors | | | | w/p | HRWRA Demand | Slump Flow | | | V-Funnel | Visual Ratings | | | Sufficient Paste Volume? | J-Ring | | Rheology | | Compressive Strength | | Elastic Modulus 28-d | Flexural Strength 28-d | RCP | Drying Shrinkage 112-d |
| | PV | W/CM | FA | S/A | | | Flow | T$_{50}$ | VSI | | Filling | Passing | Seg. | | Δh | S. Flow Diff. | τ$_0$ | μ | 24-hr | 28-d | | | | |
						% cm m	in.	s		s	0-3	0-3	0-3		in.	in.	Pa	Pa.s	psi	psi	ksi	psi	C	μ-strain
1	40.7	0.380	31.9	0.480	0.991	0.052%	26.5	0.9	1.0	2.5	0.0	0.0	1.0	yes	0.13	0.0	30.6	4.4	2042	7303	5370	913	920	-477
2	32.4	0.380	31.9	0.420	0.970	0.090%	25	3.3	2.0	20.8	2.5	3.0	2.5	no	1.75	-3.0	22.4	18.3	1910	6641	6097	903	615	-290
3	40.5	0.320	31.9	0.420	0.849	0.058%	26	2.7	0.5	5.4	0.0	0.0	1.0	yes	0.38	0.0	23.5	15.5	3163	8479	6431	1061	515	-487
4	32.6	0.320	31.9	0.480	0.814	0.245%	25	5.0	1.5	70.0	1.5	2.0	1.5	yes	1.66	-4.0	10.8	34.0	1859	6226	6162	923	610	-360
5	40.5	0.380	8.1	0.420	1.078	0.060%	26	1.2	0.5	3.6	0.0	0.0	1.0	yes	0.44	-0.5	18.0	8.1	3402	8074	5800	1021	2080	-517
6	32.6	0.380	8.1	0.480	1.028	0.116%	25	5.2	2.0	32.2	2.5	2.5	2.5	no	1.75	-5.0	2.1	36.2	3149	7434	6005	945	2020	-420
7	40.7	0.320	8.1	0.480	0.907	0.077%	26	2.7	0.5	7.4	0.0	0.0	0.5	yes	0.69	-1.0	18.8	28.3	4305	9335	6128	1128	1620	-490
8	32.4	0.320	8.1	0.420	0.887	0.310%	24.5	7.6	2.5	42.5	1.5	3.0	1.0	no	1.75	-4.5	0.1	44.3	3100	8277	6829	1004	1245	-343
9	29.7	0.350	20.0	0.450	0.909	0.439%	23.5	6.3	2.0	25.9	2.0	3.0	1.5	no	1.56	-5.5	0.0	58.3	1243	5992	5933	852	810	-350
10	43.4	0.350	20.0	0.450	0.963	0.049%	26	1.0	0.0	0.5	0.0	0.0	1.5	yes	0.13	0.0	23.9	6.6	2918	7778	6060	988	1000	-477
11	36.6	0.300	20.0	0.450	0.812	0.103%	26.5	5.3	0.5	28.5	0.0	0.5	0.0	yes	0.56	-2.5	6.4	45.1	4762	10189	6472	1129	745	-473
12	36.6	0.400	20.0	0.450	1.069	0.071%	26	2.1	1.0	4.3	0.0	0.5	1.5	yes	0.50	-0.5	19.2	9.8	2483	7620	5874	961	1055	-390
13	36.6	0.350	0.0	0.450	1.003	0.086%	25	4.0	0.5	21.2	0.5	1.5	0.0	yes	1.00	-2.0	14.8	34.9	4395	8936	5930	1096	2070	-443
14	36.6	0.350	40.0	0.450	0.887	0.060%	25	2.5	0.0	6.4	0.5	0.5	0.5	yes	0.75	-1.0	16.2	18.8	2097	7801	5802	903	590	-393
15	36.4	0.350	20.0	0.400	0.950	0.071%	26	3.6	0.5	24.2	0.5	1.5	1.5	yes	1.25	-4.0	17.7	25.0	3187	8844	6173	1106	795	-383
16	36.7	0.350	20.0	0.500	0.932	0.077%	26	3.4	0.5	8.4	0.0	0.5	1.0	yes	0.56	-0.5	6.5	23.1	3315	8560	5909	999	1030	-477
17	36.6	0.350	20.0	0.450	0.941	0.071%	26	3.0	1.0	17.5	0.5	1.0	1.5	yes	0.84	-1.5	22.5	22.5	3504	8584	6333	1049	925	-450
18	36.6	0.350	20.0	0.450	0.941	0.077%	26	3.3	1.0	16.8	0.5	0.5	1.0	yes	0.75	0.0	20.7	16.7	3092	8361	6394	1018	1010	-395
19	36.6	0.350	20.0	0.450	0.941	0.071%	26	4.1	1.0	16.2	0.5	0.5	0.5	yes	0.88	-1.0	18.3	22.1	3256	8723	5990	989	1030	-377
20	36.6	0.350	20.0	0.450	0.941	0.071%	25	3.0	0.0	13.6	0.5	1.0	0.5	yes	0.81	-2.5	39.8	25.6	3357	8496	6123	1021	825	-450
21	36.6	0.350	20.0	0.450	0.941	0.071%	26	3.7	0.0	13.5	0.5	1.0	1.0	yes	0.91	-2.5	29.8	25.1	3078	8574	6112	992	855	-433

Table C.19: Concrete Mixtures—Effects of Mixture Proportions (Material Set 2)

Mix	Cement lb/yd³	Fly Ash lb/yd³	Coarse lb/yd³	Fine lb/yd³	Water lb/yd³	Retarder oz/cwt	Paste Vol %	S/A	w/p	w/cm	w/c	Fly Ash %	HRWRA Demand % cm m	Flow in.	T₅₀ s	VSI s	Jring Δh in.	L-Box Blkng Ratio
1	490.0	210.0	1679.0	1411.1	210.0		29.1	0.458	0.855	0.300	0.429	30	0.373	27	3.3	1.0	2.13	1.00
2	490.0	210.0	1629.9	1369.8	245.0		31.1	0.458	0.997	0.350	0.500	30	0.301	28	1.0	1.5	0.56	0.92
3	490.0	210.0	1580.7	1328.5	280.0		33.2	0.458	1.140	0.400	0.571	30	0.215	23.5	1.0	0.0	1.38	0.44
4	490.0	210.0	1551.2	1303.7	301.0		34.5	0.458	1.225	0.430	0.614	30	0.186	26	1.0	0.5	1.13	0.60
5	560.0	240.0	1475.2	1239.8	320.0		37.7	0.458	1.140	0.400	0.571	30	0.172	26	1.0	0.5	0.13	0.64
6	560.0	240.0	1587.6	1334.3	240.0		32.9	0.458	0.855	0.300	0.429	30	0.373	28.5	2.0	2.0	0.88	0.92
7	560.0	140.0	1591.7	1337.7	280.0		32.7	0.458	1.177	0.400	0.500	20	0.258	26.5	1.5	0.0	0.56	0.44
8	700.0	0.0	1613.7	1356.2	280.0		31.8	0.458	1.260	0.400	0.400	0	0.272	29.5	1.5	1.5	0.69	0.56
9	700.0	0.0	1662.8	1397.5	245.0		29.7	0.458	1.103	0.350	0.350	0	0.358	29	2.0	2.0	0.75	0.17
10	560.0	140.0	1640.9	1379.0	245.0		30.7	0.458	1.030	0.350	0.438	20	0.344	29	1.0	1.0	0.88	
11	700.0	0.0	1613.7	1356.2	280.0		31.8	0.458	1.260	0.400	0.400	0	0.287	28.5	1.0	1.5	0.50	0.42
12	700.0	0.0	1487.6	1481.8	280.0		31.8	0.500	1.260	0.400	0.400	0	0.301	27	1.1	0.5	0.75	0.30
13	700.0	0.0	1785.1	1185.4	280.0		31.8	0.400	1.260	0.400	0.400	0	0.258	30	1.0	1.5		0.08
14	700.0	0.0	1933.8	1037.2	280.0		31.8	0.350	1.260	0.400	0.400	0	0.244	29	1.0	2.0	1.63	0.00
15	700.0	0.0	1785.1	1185.4	280.0		31.8	0.400	1.260	0.400	0.400	0	0.287	29.5	0.5	2.0	1.38	0.29
20	775.0	0.0	1701.4	1129.9	310.0		35.0	0.400	1.260	0.400	0.400	0	0.229	30	0.5	1.5	1.25	0.31
21	850.0	0.0	1617.8	1074.4	340.0		38.2	0.400	1.260	0.400	0.400	0	0.172	27.5	0.5	0.5	1.13	0.39
22	560.0	140.0	1760.7	1169.3	280.0		32.7	0.400	1.177	0.400	0.500	20	0.229	28.5	0.7	1.5	1.38	0.17
23	680.0	170.0	1588.3	1054.8	340.0		39.3	0.400	1.177	0.400	0.500	20	0.143	28	0.5	1.5	1.25	0.44
24	640.0	160.0	1423.5	1418.0	280.0		34.8	0.500	1.030	0.350	0.438	20	0.287	30.5	1.5	1.5	0.00	0.71
25	640.0	160.0	1565.9	1276.2	280.0		34.8	0.450	1.030	0.350	0.438	20	0.258	31	1.0	1.5	0.13	0.77
26	640.0	160.0	1708.2	1134.4	280.0		34.8	0.400	1.030	0.350	0.438	20	0.244	30	1.0	1.0	0.88	0.79
27	640.0	160.0	1475.3	1469.6	240.0		32.4	0.500	0.883	0.300	0.375	20	0.430	29	2.2	0.5	0.25	1.00
28	640.0	160.0	1423.5	1418.0	280.0	3	34.8	0.500	1.030	0.350	0.438	20	0.258	29	1.0	0.5	0.31	0.71
29	640.0	160.0	1565.9	1276.2	280.0	3	34.8	0.450	1.030	0.350	0.438	20	0.229	27.5	1.1	0.0	0.31	0.49
30	640.0	160.0	1708.2	1134.4	280.0	3	34.8	0.400	1.030	0.350	0.438	20	0.215	27.5	1.3	0.0	0.38	0.44
31	640.0	160.0	1423.5	1418.0	280.0		34.8	0.500	1.030	0.350	0.438	20	0.301	30	1.4	1.0	0.63	0.83
32	640.0	160.0	1423.5	1418.0	280.0	4	34.8	0.500	1.030	0.350	0.438	20	0.287	30	1.1	1.0	0.88	0.60
35	640.0	160.0	1423.5	1418.0	280.0	2	34.8	0.500	1.030	0.350	0.438	20	0.287	31	1.1	1.0	0.31	0.92
36	800.0	0.0	1446.7	1441.1	280.0	3	33.7	0.500	1.103	0.350	0.350	0	0.272	26	2.0	0.0	1.19	0.47
37	800.0	0.0	1736.0	1152.9	280.0	3	33.7	0.400	1.103	0.350	0.350	0	0.258	30	1.3	1.0	1.38	0.92
56	700.0	0.0	1551.3	1545.3	231.0	4	28.9	0.500	1.040	0.330	0.330	0	0.459	28	4.6	1.0	1.44	0.64
57	700.0	0.0	1524.1	1518.2	252.0	4	30.1	0.500	1.134	0.360	0.360	0	0.344	27.5	2.2	0.5	0.75	0.77
58	700.0	0.0	1496.9	1491.1	273.0	4	31.4	0.500	1.229	0.390	0.390	0	0.330	27	1.5	0.5	0.38	0.77
59	800.0	0.0	1467.4	1461.7	264.0	4	32.7	0.500	1.040	0.330	0.330	0	0.344	28	1.9	0.5	0.25	0.85
60	900.0	0.0	1383.6	1378.2	297.0	4	36.6	0.500	1.040	0.330	0.330	0	0.287	28	1.3	0.5	0.25	0.85
66	700.0	0.0	1861.5	1236.2	231.0	4	28.9	0.400	1.040	0.330	0.330	0	0.401	28.5	2.0	2.0	1.50	0.38
67	700.0	0.0	1828.9	1214.5	252.0	4	30.1	0.400	1.134	0.360	0.360	0	0.308	27.5	1.9	2.0	1.16	0.13
68	700.0	0.0	1796.2	1192.9	273.0	4	31.4	0.400	1.229	0.390	0.390	0	0.258	26.5	1.0	0.5	0.94	0.08
69	800.0	0.0	1760.9	1169.4	264.0	4	32.7	0.400	1.040	0.330	0.330	0	0.258	27	1.6	0.5	0.94	0.32
70	900.0	0.0	1660.3	1102.6	297.0	4	36.6	0.400	1.040	0.330	0.330	0	0.244	27	1.5	0.5	0.38	0.59
72	935.9	0.0	1667.8	1107.6	280.8	4	36.3	0.400	0.945	0.300	0.300	0	0.258	28	1.6	0.5	0.38	0.44
73	983.7	0.0	1667.8	1107.6	265.6	4	36.3	0.400	0.851	0.270	0.270	0	0.373	28	2.2	0.5	0.63	0.53
75	759.7	0.0	1461.8	1456.2	281.1	4	33.0	0.500	1.166	0.370	0.370	0	0.258	27.5	1.0	1.0	0.31	0.77
76	665.6	166.4	1461.8	1456.2	246.3	4	33.0	0.500	0.871	0.296	0.370	20	0.315	26.5	1.8	0.5	0.50	0.64
77	1000.0	0.0	1559.7	1035.8	330.0	3	40.4	0.400	1.040	0.330	0.330	0	0.201	28.5	1.0	1.0	0.25	0.71
78	622.0	155.5	1461.8	1456.1	264.4	3	33.0	0.500	1.001	0.340	0.425	20	0.258	29	1.8	0.5	0.25	0.79
79	672.1	168.0	1429.1	1423.6	268.8	3	34.5	0.500	0.942	0.320	0.400	20	0.244	28	1.6	0.5	0.63	0.71
80	819.3	0.0	1461.8	1456.2	262.2	3	33.0	0.500	1.008	0.320	0.320	0	0.315	29.5	1.7	1.5	0.13	0.92
81	845.9	0.0	1461.8	1456.2	253.8	3	33.0	0.500	0.945	0.300	0.300	0	0.344	30	2.3	2.0	0.25	0.85
82	886.8	0.0	1429.1	1423.6	266.0	3	34.5	0.500	0.945	0.300	0.300	0	0.315	28.5	2.3	1.5	0.13	0.92
83	641.1	160.3	1461.8	1456.2	256.4	4	33.0	0.500	0.942	0.320	0.400	20	0.272	26.5	2.6	0.0	0.50	0.71
85	724.1	310.3	1570.9	1043.2	289.6	3	40.0	0.400	0.798	0.280	0.400	30	0.201	27.5	1.7	0.5	0.31	0.79
86	666.9	285.8	1649.5	1095.4	266.8	3	37.0	0.400	0.798	0.280	0.400	30	0.229	28	2.5	1.0	0.38	0.85
87	730.6	243.5	1649.5	1095.4	263.0	3	37.0	0.400	0.782	0.270	0.360	25	0.229	28	2.8	1.0	0.38	0.81
88	845.9	0.0	1461.8	1456.2	253.8	3	33.0	0.500	0.945	0.300	0.300	0	0.330	26.5	4.1	0.0	0.69	0.44
89	631.5	221.9	1560.0	1271.4	260.3	4	35.0	0.450	0.880	0.305	0.412	26	0.265	30	1.5	1.5	0.25	0.85
94	617.0	245.9	1560.0	1271.4	254.6	4	35.0	0.450	0.845	0.295	0.413	28.5	0.258	25	2.8	0.0	0.69	0.47
95	645.7	198.4	1560.0	1271.4	265.9	4	35.0	0.450	0.916	0.315	0.412	23.5	0.229	26	2.0	1.0	0.50	0.56
96	623.8	156.0	1461.8	1456.2	257.3	4	33.0	0.500	0.971	0.330	0.413	20	0.272	27	2.2	1.0	0.41	0.71
97	633.3	298.0	1649.5	1095.4	260.8	4	37.0	0.400	0.793	0.280	0.412	32	0.215	28	2.4	0.5	0.41	0.67
100	645.7	238.8	1536.0	1251.9	265.4	4	36.0	0.450	0.863	0.300	0.411	27	0.258	29	1.5	1.0	0.25	0.79
101	665.1	198.7	1536.0	1251.9	276.4	4	36.0	0.450	0.933	0.320	0.416	23	0.229	29.5	1.2	1.5	0.31	0.79

Notes
1. No air entrainment
2. Cement: PC-03-III; Fly Ash: FA-01-F; Coarse: NA-02-C; Fine: NA-02-F; HRWRA-02; RET-01
3. Slump flow test performed with upright cone orientation.

386

Table C.20: Concrete Mixtures—Effects of Alternate Fly Ashes

Mix	Fly Ash ID	Fly Ash Dosage	HRWRA Demand	Slump Flow Flow	T50	VSI	V-Funnel	Visual Ratings Filling	Passing	Seg.	J-Ring Δh	S. Flow Diff.	Rheology τ0	μ	Compressive Strength 24-hr	28-d	Elastic Modulus 28-d	Flexural Strength 28-d	RCP	Drying Shrinkage 112-d
		%	% cm m	in	s		s	0-3	0-3	0-3	in	in	Pa	Pa.s	psi	psi	ksi	psi	C	μ-strain
SC1	FA-01-F	20	0.086%	25.0	4.5	0.5	12.3	0.5	0.5	0.5	0.63	-1.0	21.0	26.3	3211	8669	5995	1034	700	-470
SC2	FA-01-F	30	0.086%	25.5	4	0.5	11.5	0.5	0.5	0.5	0.63	-1.0	21.1	26.0	2568	8235	5976	976	540	-447
SC3	FA-01-F	40	0.086%	26.0	3.3	0.0	13.0	0	0	0	0.47	0.0	43.2	23.8	1876	8070	5834	986	485	-423
SC4	FA-03-C	20	0.077%	25.0	3.7	0.0	8.8	0.5		1	0.75	-2.5	43.2	18.4	3538	9344	6243	1065	1550	-530
SC5	FA-03-C	30	0.077%	25.5	2.8	0.0	4.3	0.5	0.5	0.5	0.63	-1.5	45.7	15.9	2766	9245	6514	1063	1020	-563
SC6	FA-03-C	40	0.071%	25.0	2.6	0.0	5.4	0.5	0.5	0	0.69	-2.0	57.2	13.5	2024	9292	6471	1042	805	-527

Note: Results for FA-02-F obtained from testing for effects of mixture proportions.

Table C.21: Concrete Mixtures—Effects of VMA Dosage

Mix	VMA Dosage	HRWRA Demand	Slump Flow Flow	T50	VSI	V-Funnel	Visual Ratings Filling	Passing	Seg.	J-Ring Δh	S. Flow Diff.	Rheology τ0	μ	a1	b	c	Compressive 24-hr	28-d	Elastic Modulus 28-d	Flexural Strength 28-d	RCP	Drying Shrinkage 112-d
	oz/cwt	% cm m	in	s		s	0-3	0-3	0-3	in	in	Pa	Pa.s				psi	psi	ksi	psi	C	μ-strain
VD1	0	0.077%	26.0	1.9	0.0	3.9	0.5	0	0	0.19	0.0	32.2	9.7	0.159	0.543	0.896	2170	8143	5830	1028	765	-477
VD2	2	0.077%	26.0	1.2	0.0	3.6	0	0	0.5	0.25	0.0	29.3	10.2	-0.037	0.655	0.441	2213	8044	5514	873	765	-467
VD3	8	0.065%	25.0	1.8	0.0	3.9	0	0	0.5	0.13	1.0	50.0	6.8	0.051	0.560	0.418	2104	7488	5377	1014	785	-497
VD4	14	0.065%	25.0	1.5	0.0	4.0	0	0	0	0.25	0.0	56.1	8.0	0.103	0.612	0.490	2046	7850	5392	993	845	-437

1. Parameters a, b, and c based on Herschel-Bulkley model: $T = a + bN^c$

Table C.22: Concrete Mixtures—Effect of VMA on Minimum Paste Volume for Filling Ability

Mix	VMA Dosage	Paste Vol.	HRWRA Demand	Slump Flow Flow	T50	VSI	V-Funnel	Visual Ratings Filling	Passing	Seg.	Sufficient Paste Volume?	J-Ring Δh	S. Flow Diff.	Rheology τ0	μ	Compressive 24-hr	28-d	Elastic Modulus 28-d	Flexural Strength 28-d	RCP	Drying Shrinkage 112-d
	oz/cwt		% cm m	in.	s		s	0-3	0-3	0-3		in.	in.	Pa	Pa.s	psi	psi	ksi	psi	C	μ-strain
VPV1	14.0	32.7	0.361%	23.5	6.2	2.5	8.7	3.0	3.0	3.0	no	1.75	-10.5	49.3	44.0	1625	7275	6371	5554	895	-380
VPV2	14.0	35.2	0.206%	24.0	5.6	2.0	18.5	3.0	2.5	2.5	no	1.47	-3.0	72.8	18.8	2214	6896	6360	6410	1025	-397
VPV3	14.0	37.7	0.142%	25.0	2.5	1.5	16.4	1.5	1.0	1.0	no	0.94	-0.5	97.6	6.0	2600	8258	6683	7533	1025	-450
P9	0.0	32.7	0.335%	22.0	6.2	3.0	7.6	3.0	3.0	3.0	no	1.75	-9.0	39.4	42.7	1908	6224	6647	874	850	-333
P10	0.0	35.2	0.090%	25.0	6.2	1.0	25.9	2.0	1.5	0.0	no	1.31	-3.5	12.4	32.3	3599	8704	6889	1123	755	-403
P11	0.0	37.7	0.065%	25.0	3.4	1.0	35.7	1.5	1.5	0.5	no	1.19	-3.0	20.3	21.0	3480	8950	6506	1071	870	-443
P12	0.0	40.2	0.077%	26.0	2.3	1.5	5.0	0.0	0.5	1.5	yes	0.38	0.5	24.7	9.5	3654	8376	6333	1123	845	-497
P13	0.0	42.7	0.052%	25.0	1.6	1.0	3.6	0.0	0.0	0.5	yes	0.38	-1.0	48.5	7.1	3292	7932	6466	1094	1125	-560

Note: Mixtures P9 to P13 reprinted in this table for convenience.

References

AASHTO TP57-99. "Standard Test Method for Methylene Blue Value of Clays, Mineral Fillers, and Fines," American Association of State Highway Transportation Officials.

ACI Committee 209. (1997). "Prediction of Creep, Shrinkage, and Temperature Effects in Concrete Structures," (ACI 209R-92). American Concrete Institute, Farmington Hills, MI.

ACI Committee 211. (2002). "Standard Practice for Selecting Proportions for Normal, Heavyweight, and Mass Concrete," (ACI 211.1-91). American Concrete Institute, Farmington Hills, MI.

ACI Committee 318. (2005). "Building Code Requirements for Structural Concrete," (ACI 318-05). American Concrete Institute, Farmington Hills, MI.

ACI Committee 363. (1992). "State-of-the-Art Report on High-Strength Concrete," (ACI 363R-92). American Concrete Institute, Farmington Hill, MI.

Abrams, D.A. (1918). "Design of Concrete Mixtures," *Bulletin 1*, Structural Materials Research Laboratory, Lewis Institute, Reprints from Minutes of the Annual Meeting of the Portland Cement Association, New York.

Ahmed, A.E., and El-Kourd, A.A. (1989). "Properties of Concrete Incorporating Natural and Crushed Stone Very Fine Sand," *ACI Materials Journal*, 86(4), 417-424.

Ahn, N. (2000). "An Experimental Study on the Guidelines for Using Higher Contents of Microfines in Portland Cement Concrete," PhD Dissertation, The University of Texas at Austin.

Aitcin, P.-C. (1998). *High Performance Concrete*, New York: E&FN Spon, 591 pp.

Aitcin, P.-C. (1999). "Demystifying Autogenous Shrinkage," *Concrete International*, 21(11), 54-56.

Aitcin, P.-C., and Mehta, P.K. (1990). "Effect of Coarse Aggregate Characteristics on Mechanical Properties of High-Strength Concrete," *ACI Materials Journal*, 87(2), 103-107.

Alexander, M.G., and Milne, T.I. (1995). Influence of Cement Blend and Aggregate Type on Stress-Strain Behavior and Elastic Modulus of Concrete" *ACI Materials Journal*, 92(3), 227-235.

Andersen, P.J., and Johansen, V. (1993). "A Guide to Determining the Optimal Gradation of Concrete Aggregates," (Report SHRP-C-334). National Research Council, Washington, DC.

Andreasen, A.H.M., and Anderson, J. (1929). "The Relation of Grading to Interstitial Voids in Loosely Granular Products (With Some Experiments)," *Kolloid-Z.*, 49, 217-228.

Arrhenius, S. (1917). "The viscosity of solutions," *Biochemical Journal*, 11, 112-133.

Assaad, J., and Khayat, K.H. (2004). "Assessment of Thixotropy of Self-Consolidating Concrete and Concrete-Equivalent-Mortar—Effect of Binder Composition and Content," *ACI Materials Journal*, 101 (5), 400-408.

Assaad, J., Khayat, K.H., and Daczko, J. (2004). "Evaluation of Static Stability of Self-Consolidating Concrete," *ACI Materials Journal*, 101(3), 207-215.

Assaad, J., Khayat, K.H., and Mesbah, H. (2003a). "Assessment of the Thixotropy of Flowable and Self-Consolidating Concrete," *ACI Materials Journal*, 100(2), 99-107.

Assaad, J., Khayat, K.H., and Meshab, H. (2003b). "Variation in Formwork Pressure with Thixotropy of Self-Consolidating Concrete," *ACI Materials Journal*, 100(1), 29-37.

ASTM C 29/C 29M-97. "Standard Test Method for Bulk Density (Unit Weight) and Voids in Aggregate," ASTM International.

ASTM C 33-03. "Standard Specification for Concrete Aggregates," ASTM International.

ASTM C 39/C 29M. "Standard Test Method for Compressive Strength of Cylindrical Concrete Specimens," ASTM International.

ASTM C 78-02. "Standard Test Method for Flexural Strength of Concrete (Using Simple Beam with Third-Point Loading)," ASTM International.

ASTM C 109/C 109M-05. "Standard Test Method for Compressive Strength of Hydraulic Cement Mortars (Using 2-in. or [50-mm] Cube Specimens)," ASTM International.

ASTM C 115-96a. "Standard Test Method for Fineness of Portland Cement by the Turbidimeter," ASTM International.

ASTM C 117-03. "Standard Test Method for Materials Finer than 75μm (No. 200) Sieve in Mineral Aggregates by Washing," ASTM International.

ASTM C 127-04. "Standard Test Method for Density, Relative Density (Specific Gravity), and Absorption of Coarse Aggregate," ASTM International.

ASTM C 128-04a. "Standard Test Method for Density, Relative Density (Specific Gravity), and Absorption of Fine Aggregate," ASTM International.

ASTM C 136-01. "Standard Test Method Sieve Analysis of Fine and Coarse Aggregates," ASTM International.

ASTM C 150-05. "Standard Specification for Portland Cement," ASTM International.

ASTM C 157/C 157M-06. "Standard Method for Length Change of Hardened Hydraulic Cement Mortar and Concrete," ASTM International.

ASTM C 187-04. "Standard Test Method for Normal Consistency of Hydraulic Cement," ASTM International.

ASTM C 191-01. "Standard Test Method for Time of Setting of Hydraulic Cement by Vicat Needle," ASTM International.

ASTM C 204-00. "Standard Test Method for Fineness of Hydraulic Cement by Air Permeability Apparatus," ASTM International.

ASTM C 305-06. "Standard Practice for Mechanical Mixing of Hydraulic Cement Pastes and Mortars of Plastic Consistency." ASTM International.

ASTM C 403/C 403M-99. "Standard Test Method for Time of Setting of Concrete Mixtures by Penetration Resistance," ASTM International.

ASTM C 469-02. "Standard Test Method for Static Modulus of Elasticity and Poisson's Ratio of Concrete in Compression," ASTM International.

ASTM C 494-05a. "Standard Specification for Chemical Admixtures for Concrete," ASTM International.

ASTM C 618-05. "Standard Specification for Coal Fly Ash and Raw or Calcined Natural Pozzolans for Use in Concrete," ASTM International.

ASTM C 944-99. "Standard Test Method for Abrasion Resistance of Concrete or Mortar Surfaces by the Rotating-Cutter Method," ASTM International.

ASTM C 1202-05. "Standard Test Method for Electrical Indication of Concrete's Ability to Resist Chloride Ion Penetration," ASTM International.

ASTM C 1252-03. "Standard Test Methods for Uncompacted Void Content of Fine Aggregate (as Influenced by Particle Shape, Surface Texture, and Grading)," ASTM International.

ASTM C 1610/C 1610M-06. "Standard Test Method for Static Segregation of Self-Consolidating Concrete Using Column Technique," ASTM International.

ASTM C 1611/C 1611M-05. "Standard Test Method for Slump-Flow of Self-Consolidating Concrete," ASTM International.

ASTM C 1621/C1621M-06. "Standard Test Method for Passing Ability of Self-Consolidating Concrete by J-Ring," ASTM International.

ASTM D 471-99. "Standard Test Method for Flat Particles, Elongated Particles, or Flat and Elongated Particles in Coarse Aggregate," ASTM International.

ASTM D 3398-00. "Standard Test Method for Index of Aggregate Shape and Texture," ASTM International.

ASTM D 5821-01. "Standard Test Method for Determining the Percentage of Fractured Particles in Coarse Aggregate," ASTM International.

ASTM E 11-04. "Standard Specification for Wire Clothes and Sieves for Testing Purposes," ASTM International.

Attiogbe, E.K., See, H.T., and Daczko, J.A. (2002). "Engineering properties of self-consolidating concrete," *First North American Conference on the Design and Use of Self-Consolidating Concrete*, Chicago, IL: ACBM, 371-376.

Audenaert, K., Boel, V., and De Schutter, G. (2002) "Durability of self-compacting concrete," *First North American Conference on the Design and Use of Self-Consolidating Concrete*, Chicago, IL: ACBM, 377-383.

Baalbaki, W., Aitcin, P.-C., and Ballivy, G. (1992). "On Predicting Modulus of Elasticity in High-Strength Concrete," *ACI Materials Journal*, 89(5), 517-520.

Baalbaki, W., Benmokrane, B., Chaallal, O., and Aitcin, P.-C. (1991). "Influence of Coarse Aggregate on Elastic Properties of High Performance Concrete," *ACI Materials Journal*, 88(5), 499-503.

Bache, H.H., and Nepper-Christensen, P. (1965). "Observations on Strength and Fracture in Lightweight and Ordinary Concrete. The Structure of Concrete and its Behaviour under Load," *Proceedings of International Conference*, London, 93.

Bager, D.H., Geiker, M.R., and Jensen, R.M. (2001). "Rheology of Self-Compacting Mortars," *Nordic Concrete Research*, 26.

Barnes, H.A. (1997). "Thixotropy—a review," *Journal of Non-Newtonian Fluid Mechanics*, 70, 1-33.

Barnes, H.A., Hutton, J.F., and Walters, K. (1989). *An Introduction to Rheology*, New York: Elsevier.

Barrett, P.J. (1980). "The shape of rock particles, a critical review," *Sedimentology*, 27, 291-303.

Bartos, P.J.M., Sonebi, M., Tamimi, A.K. (Eds.). (2002). "Workability and Rheology of Fresh Concrete: Compendium of Tests," Cachan Cedex, France: RILEM.

Beaupre, D., Mindess, S., and Pigeon, M. (1994). "Rheology of Fresh Shotcrete," P.J.M. Bartos, Ed., *Proceedings, Special Concretes: Workability and Mixing,* Paisley, Scotland: RILEM, 225-235.

Bensted, J. (2003). "Thaumasite-direct, woodfordite and other possible formation routes," *Cement and Concrete Composites*, 25, 873-877.

Bentz, D.P., Jensen, O.M., Hansen, K.K., Olsen, J.F., Stang, H., and Haecker, C.J. (2001). "Influence of cement particle size distribution on early age autogenous strains and stresses in cement-based materials," *Journal of the American Ceramic Society*, 84(1), 129-135.

Berke, N.S., Cornman, C.R., Jeknavorian, A.A., Knight, G.F., Wallevik, O. (2002). "The effective use of superplasticizers and viscosity-modifying agents in self-consolidating concrete," *First North American Conference on the Design and Use of Self-Consolidating Concrete*, Chicago, IL: ACBM, 173-178.

Bigas, J.P., and Gallias, J.L. (2002). "Effect of fine mineral additions on granular packing of cement mixtures," *Magazine of Concrete Research*, 54(3), 155-164.

Bigas, J.P., and Gallias, J.L. (2003). "Single-drop agglomeration of fine mineral admixtures for concrete and water requirement of pastes," *Powder Technology*, 130, 110-115.

Billberg, P. (2000). "Influence of superplasticizers and slag blended cement on the rheology of fine mortar part of concrete," *Nordic Concrete Research*, 24.

Billberg, P. (2002). "Mix design model for self-compacting concrete," *First North American Conference on the Design and Use of Self-Consolidating Concrete*, Chicago, IL: ACBM, 65-70.

Billberg, P., and Osterberg, T. (2001). "Thixotropy of self-compacting concrete," *Proceedings of the Second International Symposium on Self-Compacting Concrete*, Tokyo, Japan, 99-108.

Bissonnette, B., Pascale, P., and Pigeon, M. (1999). "Influence of key parameters on drying shrinkage of cementitious materials," *Cement and Concrete Research*, 29, 1655-1662.

Bittner, J., Gasiorowski, S., and Hrach, F. (2001). "Removing Ammonia from Fly Ash," *Proceedings of the International Ash Utilization Symposium*, Center for Applied Energy Research, University of Kentucky.

Blask, O., and Honert, D. (2003). "The Electrostatic Potential of Highly Filled Cement Suspension Containing Various Superplasticizers," *Seventh CANMET/ACI International Symposium on Superplasticizers and Other Chemical Admixtures in Concrete*, Malhotra, V.M, ed., 87-101.

Bosiljkov, V.B. (2003). "SCC mixes with poorly graded aggregate and high volume of limestone filler," *Cement and Concrete Research*, 33, 1279-1286.

Bouwman, A.M., Bosma, J.C., Vonk, P., Wesseling, J.A., and Frijlink, H.W. (2004). "Which shape factor(s) best describe granules?" *Powder Technology*, 146, 66-72.

Browne, C., Rauch, A.F., Haas, C.T., Kim, H. (2003). "Performance Evaluation of Automated Machines for Measuring Gradation of Aggregates," *Geotechnical Testing Journal*, 26(4), 1-9.

Buchenau, G., and Hillemeier, B. (2003). "Quality-test to prove the flow behavior of SCC on site," *3rd International Symposium on Self-Compacting Concrete*, Reykjavik, Iceland, 84-93.

Bui, V.K., (2002). "Application of minimum paste volume method in designing cost-effect self-consolidating concrete—an experience in New Zealand," *First North American Conference on the Design and Use of Self-Consolidating Concrete*, Chicago, IL: ACBM, 127-132.

Bui, V.K., Akkaya, Y., and Shah, S.P. (2002). "Rheological Model for Self-Consolidating Concrete," *ACI Materials Journal*, 99(6), 549-559.

Bui, V.K., and Montgomery, D. (1999a). "Drying shrinkage of self-compacting concrete containing milled limestone," *Proceedings of the First International RILEM Symposium on Self-Compacting Concrete*, Stockholm, Sweden, 227-238.

Bui, V.K., and Montgomery, D. (1999b). "Mixture proportioning method for self-compacting high performance concrete with minimum paste volume," *Proceedings of the First International RILEM Symposium on Self-Compacting Concrete*, Stockholm, Sweden, 373-384.

Bui, V.K., Montgomery, D., Hinczak, I., Turner, K. (2002). "Rapid test method for segregation resistance of self-compacting concrete," *Cement and Concrete Research*, 32, 1489-1496.

Burge, T.A. (1999). "Multi-component polymer concrete admixtures," *Proceedings of the First International RILEM Symposium on Self-Compacting Concrete*, Stockholm, Sweden, 411-424.

Bury, M.A., and Christensen, B.J. (2002). "Role of innovative chemical admixtures in producing self-consolidating concrete," *First North American Conference on the Design and Use of Self-Consolidating Concrete*, Chicago, IL: ACBM.

Cabrera, J.G., and Hopkins, C.J. (1984). "A modification of the Tattersall two-point apparatus for measuring concrete workability," *Magazine of Concrete Research*, 36(129), 237-240.

Carrasquillo, R.L., Nilson, R.H., and Slate, F.O. (1981). "Properties of High-Strength Concrete Subject to Short-Term Loads," *ACI Journal*, 78(3), 171-178.

Celik, T., and Marar, K. (1996). "Effects of Crushed Stone Dust on Some Properties of Concrete," *Cement and Concrete Research*, 26(7), 1121-1130.

Cerulli, T., Clemente, P., Decio, M., Ferrari, G., Gamba, M., Salvioni, D., and Surico, F. (2003). "A New Superplasticizer for Early High-Strength Development in Cold Climates," *Seventh CANMET/ACI International Symposium on Superplasticizers and Other Chemical Admixtures in Concrete*, Malhotra, V.M, ed., 113-126.

Cetin, A., and Carrasquillo, R.L. (1998). "High Performance Concrete: Influence of Coarse Aggregates on Mechanical Properties," *ACI Materials Journal*, 95(3), 252-261.

Chandan, C., Sivakumar, K., Masad, E., and Fletcher, T. (2004). "Application of Imaging Techniques to Geometry Analysis of Aggregate Particles," *Journal of Computing in Civil Engineering*, 18(1), 75-82.

Chang, P.-K. (2004). "An approach to optimizing mix designs for properties of high-performance concrete," *Cement and Concrete Research*, 34, 623-629.

Chen, Y.-Y., Tsia, C.-T., and Hwang, C.-L. (2003). "The study on mixture proportion of gap-gradation of aggregate for SCC," *3rd International Symposium on Self-Compacting Concrete*, Reykjavik, Iceland, 533-539.

Chetana, R., Tutumluer, E., and Stefanski, J.A. (2001). "Coarse Aggregate Shape and Size Properties Using a New Image Analyzer," *ASTM Journal of Testing and Evaluation*, 29(5), 461-471.

Christensen, B.J., and Ong, F.S. (2005). "The Performance of High-Volume Fly Ash Self-Consolidating Concrete," *Proceedings of SCC-2005*, Chicago, IL: ACBM.

Collepardi, M. (1998). "Admixtures Used to Enhance Placing Characteristics of Concrete," *Cement and Concrete Composites*, 20, 103-112.

Collepardi, M. (1999). "Thaumasite formation and deterioration in historic buildings," *Cement and Concrete Composites*, 21, 147-154.

Collepardi, M. (2003). "Self Compacting Concrete: What Is New?" *Seventh CANMET/ACI International Symposium on Superplasticizers and Other Chemical Admixtures in Concrete*, Malhotra, V.M, ed., 1-16.

Comparet, C., Nonat, A., Pourchet, S., Mosquet, M., and Maitrasse, P. (2003). "The Molecular Parameters and the Effect of Comb-Type Superplasticizers on Self-Compacting Concrete: A Comparison of Comb-Type Superplasticizer Adsorption onto a Basic Calcium Carbonate Medium in the Presence of Sodium Sulphate," *Seventh CANMET/ACI International Symposium on Superplasticizers and Other Chemical Admixtures in Concrete*, Malhotra, V.M, ed., 195-209.

Counto, U.J. (1964). "Effect of the Elastic Modulus of the Aggregate on the Elastic Modulus, Creep, and Creep Recovery of Concrete," *Magazine of Concrete Research*, 16(48), 129-138.

Coussot, P., and Ancey, C. (1999). "Rheophysical classification of concentrated suspensions and granular pastes," *Physical Review E*, 59(4), 4445-4457.

Coussot, P., and Piau, J.-M. (1995). "A large-scale field coaxial cylinder rheometer for the study of the rheology of natural coarse suspensions," *Journal of Rheology*, 39(1), 105-124.

Crammond, N.J. (2003). "The thaumasite form of sulfate attack in the UK," *Cement and Concrete Composites*, 25, 809-818.

Crouch, L.K., and Pearson, J.B. (1995). Neoprene Capping for Static Modulus of Elasticity Testing," *ACI Materials Journal*, 92(6), 643-648.

Cussigh, F., Sonebi, M., and De Schutter, G. (2003). "Project Testing SCC-segregation test methods," *3rd International Symposium on Self-Compacting Concrete*, Reykjavik, Iceland, 311-322.

Cyr, M., and Mouret, M. (2003). "Rheological Characterization of Superplasticized Cement Pastes Containing Mineral Admixtures: Consequences of Self-Compacting Concrete Design," *Seventh CANMET/ACI International Symposium on Superplasticizers and Other Chemical Admixtures in Concrete*, Malhotra, V.M, ed., 241-255.

D'Ambrosia, M.D., Lange, D.A., and Brinks, A.J. (2005). "Restrained shrinkage and creep of self-consolidating concrete," *Proceedings of SCC 2005*, Chicago, IL: ACBM.

Daczko, J.A. (2002). "Stability of Self-Consolidating Concrete—Assumed or Ensured?," *First North American Conference on the Design and Use of Self Consolidating Concrete*, Chicago, IL: ACBM, 249-251.

Daczko, J.A. (2003). "A comparison of passing ability test methods for self-consolidating concrete," *3rd International Symposium on Self-Compacting Concrete*, Reykjavik, Iceland, 335-344.

Day, K.W. (1995). *Concrete Mix Design, Quality Control and Specification*, London: E&FN Spon.

de Larrard, F. (1999a). *Concrete Mixture Proportioning*, London: E&FN Spon.

de Larrard, F. (1999b). "Why Rheology Matters," *Concrete International*, 21(8), 79-81.

de Larrard, F., Hu, C., Sedran, T., Szitkar, J.C., Joly, M., Claux, F., and Derkx, F. (1997). "A New Rheometer for Soft-to-Fluid Fresh Concrete," *ACI Materials Journal*, 94(3), 234-243.

de Schutter, G. (2005). "Guidelines for Testing Fresh Self-Compacting Concrete," Project Report from European Project *Measurement of Properties of Fresh Self-Compacting Concrete*.

Diamond, S. (2003). "Thaumasite in Orange County, Southern California: an inquiry into the effect of low temperature," *Cement and Concrete Composites*, 25, 1161-1164.

Domone, P.L. (2006). "Self-compacting concrete: an analysis of 11 years of case studies," *Cement and Concrete Composites*, 28, 197-208.

Edamatsu, Y., Nishida, N., and Ouchi, M. (1999). "A rational mix-design method for self-compacting concrete considering interaction between coarse aggregate and mortar particles," *Proceedings of the First International RILEM Symposium on Self-Compacting Concrete*, Stockholm, Sweden, 309-320.

Einstein, A. (1906). "Ein neue Bestimmung der Molekuldimension," *Ann. Physik*, 19, 289-306.

Einstein, A. (1911). "Berichtigung zu meiner Arbeit: Eine neue Bestimmung der Molekuldimension," *Ann.Physik*, 34, 591-592.

EFNARC. (2001). "Specification Guidelines for Self-Compacting Concrete," Farnham, UK: European Federation of Producers and Contractors of Specialist Products for Structures.

EFNARC. (2005). "The European Guidelines for Self-Compacting Concrete," Farnham, UK: European Federation of Producers and Contractors of Specialist Products for Structures.

El-Chabib, H., and Nedhi, M. (2006). "Effect of Mixture Design Parameters on Segregation of Self-Consolidating Concrete," *Cement and Concrete Research*, 103(5), 374-383.

Emborg, M., Gurnewald, S., Hedin, C., and Carlsward, J. (2003). "Test Methods for Filling Ability of SCC," *3rd International Symposium on Self-Compacting Concrete*, Reykjavik, Iceland, 323-334.

Erdogan, S.T. (2005). "Determination of Aggregate Shape Properties Using X-Ray Tomographic Methods and the Effect of Shape on Concrete Rheology," PhD Dissertation, The University of Texas at Austin.

Farris, R.J. (1968). "Prediction of the Viscosity of Multimodal Suspensions from Unimodal Viscosity Data," *Transactions of the Society of Rheology*, 12(2), 281-301.

Fernlund, J.M.R. (2005). "Image analysis method for determining 3-D shape of coarse aggregate," *Cement and Concrete Research*, 35, 1629-1637.

Ferraris, C.F. (1999). "Measurement of the Rheological Properties of High Performance Concrete: State of the Art Report," *Journal of Research of the National Institute of Standards and Technology*, 104(5), 461-478.

Ferraris, C.F., and Brower, L.E. (Eds.). (2001). *Comparison of concrete rheometers: International tests at LCPC (Nantes, France) in October 2000*. (NISTIR 6819). Gaithersburg, MD. National Institute of Standards and Technology.

Ferraris, C.F., and Brower, L.E. (Eds.). (2004). *Comparison of concrete rheometers: international tests at MB (Cleveland, Ohio, USA) in May 2003*. (NISTIR 7154). Gaithersburg, MD. National Institute of Standards and Technology.

Ferraris, C.F., Brower, L., Ozyildirim, C., Daczko, J. (2000). "Workability of Self-Compacting Concrete," *International Conference on High Performance Concrete*, Orlando, FL, PCI/FHWA/FIB, 398-407.

Ferraris, C.F., Hackley, V.A., Aviles, A.I., and Buchanan, C.E. (2002). "Analysis of the ASTM Round-Robin Test on Particle-Size Distribution of Portland Cement: Phase I," (NISTIR 6883). National Institute of Standards and Technology, Gaithersburg, MD.

Ferraris, C.F., Obla, K.H., and Hill, R. (2001). "The influence of mineral admixtures on the rheology of cement paste and concrete," *Cement and Concrete Research*, 31, 245-255.

Flatt, R.J., and Houst, Y.F. (2001). "A simplified view on chemical effects perturbing the action of superplasticizers," *Cement and Concrete Research*, 31, 1169-1176.

Fuller, W.B., and Thompson, S.E. (1907). "The Laws of Proportioning Concrete," *Transactions of ASCE*, 59, 67-143.

Garboczi, E.J. (2002). "Three-dimensional mathematical analysis of particle shape using X-ray tomography and spherical harmonics: applications to aggregates used in concrete," *Cement and Concrete Research*, 32, 1621-1638.

Garboczi, E.J., Martys, N.S., Saleh, H.H., Livingston, R.A. (2001). "Acquiring, Analyzing, and Using Complete Three Dimensional Aggregate Shape Information," *Proceedings of the 9th Annual ICAR Symposium*, Austin, TX.

Geiker, M.R., Brandl, M., Thrane, L.N., Bager, D.H., Wallevik, O. (2002). "The effect of measuring procedure on the apparent rheological properties of self-compacting concrete," *Cement and Concrete Research*, 32, 1791-1795.

Ghezal, A.F., and Khayat, K.H. (2003). "Pseudoplastic and thixotropic properties of SCC equivalent mortar made with various admixtures," *Third International Symposium on Self-Consolidating Concrete*, Reykjavik, Iceland, 69-83.

Ghezal, A., and Khayat, K.H. (2001). "Optimization of cost-effective self-consolidating concrete," *Proceedings of the Second International Symposium on Self-Compacting Concrete*, Tokyo, Japan, 329-338.

Ghezal, A.F., and Khayat, K.H. (2002). "Optimizing Self-Consolidating Concrete with Limestone Filler by Using Statistical Factorial Design Methods," *ACI Materials Journal*, 99(3), 264-272.

Gjorv, O. (1998). "Workability: A New Way of Testing," *Concrete International*, 20(9), 57-60.

Golaszewski, J., and Szwabowski, J. (2004). "Influence of superplasticizers on rheological behavior of fresh cement mortars," *Cement and Concrete Research*, 34, 235-248.

Golden, D.M. (2001). "The U.S. Power Industry's Activities to Expand Coal Ash Utilization in Face of Lower Ash Quality," *Proceedings of the Fifth CANMET/ACI International Conference on Recent Advances in Concrete Technology*, Montreal, QC, 267-289.

Goldsworthy, S. (2005). "Manufactured Sands in Portland Cement Concrete—The New Zealand Experience," *Proceedings of the 13th Annual ICAR Symposium*. International Center for Aggregates Research.

Goltermann, P., Johansen, V., and Palbol, L. (1997). "Packing of Aggregates: An Alternative Tool to Determine the Optimal Aggregate Mix," *ACI Materials Journal*, 94(5), 435-443.

Gomes, P.C.C., Gettu, R., Agullo, L., and Bernad, C. (2001). "Experimental optimization of high-strength self-compacting concrete," *Proceedings of the Second International Symposium on Self-Compacting Concrete*, Tokyo, Japan, 377-386.

Haas, C.T., Rauch, A.F., Kim, H., and Browne, C. (2002). "Rapid Test to Establish Grading of Unbound Aggregate Products," (ICAR Report 503-3). Austin, TX: International Center for Aggregate Research.

Hackley, V., and Ferraris, C.F. (2001). *The Use of Nomenclature in Dispersion Science and Technology*. (Special Report 960-3). Gaithersburg, MD: National Institute of Standards and Technology.

Hammer, T.A. (2003). "Cracking susceptibility due to volume changes of self-compacting concrete (SCC)," *Third International Symposium on Self-Consolidating Concrete*, Reykjavik, Iceland, 553-557.

Hanehara, S., and Yamada, K. (1999). "Interaction between cement and chemical admixture from the point of cement hydration, adsorption behavior of admixture, and paste rheology," *Cement and Concrete Research*, 29, 1159-1165.

Hansen, T.C. (1960). "Strenght, Elasticity, and Creep as Related to the Internal Structure of Concrete," *Chemistry of Cement*, Proceedings of the Fourth International Symposium, Monograph 43, V2, Washington, 709-723.

Hashin, Z. (1962). "Elastic Moduli of Heterogeneous Materials," *Journal of Applied Mechanics*, 29(1), 143-150.

Hasholt, M.T., Pade, C., and Winnefield, F. (2005). "A conceptual and mathematical model for the flowability of SCC," *Proceedings of SCC-2005*, Chicago, IL: ACBM.

He, D., and Ekere, N.N. (2001). "Viscosity of concentrated noncolloidal bidisperse systems," *Rheol Acta*, 40, 591-598.

Heirman, G., and Vandewalle, L. (2003). "The influence of fillers on the properties of self-compacting concrete in fresh and hardened state," *Third International Symposium on Self-Consolidating Concrete*, Reykjavik, Iceland, 606-608.

Hirsch, T.J. (1962). "Modulus of Elasticity of Cocnrete Affected by Elastic Moduli of Cement Paste Matrix and Aggregate," *Journal of the American Concrete Instutite*, 59, 427-451.

Ho, D.W.S., Sheinn, A.M.M., Ng, C.C., and Tam, C.T. (2002). "The use of quarry dust for SCC applications," *Cement and Concrete Research*, 32, 505-511.

Honek, T., Hausnerova, B., and Saha, P. (2005). "Relative viscosity models and their application to capillary flow data of highly filled hard-metal carbide powder compounds," *Polymer Composites*, 26(1), 29-36.

Hudson, B. (2002). "Discovering the Lost Aggregate Opportunity: Part 1," *Pit and Quarry*, 95(6), 42-46.

Hudson, B. (2003a). "Discovering the Lost Aggregate Opportunity: Part 2," *Pit and Quarry*, 95(7), 44-45.

Hudson, B. (2003b). "Discovering the Lost Aggregate Opportunity: Part 3," *Pit and Quarry*, 95(8), 54-56.

Hudson, B. (2003c). "Discovering the Lost Aggregate Opportunity: Part 4," *Pit and Quarry*, 95(9), 40-43.

Hudson, B. (2003d). "Discovering the Lost Aggregate Opportunity: Part 5," *Pit and Quarry*, 95(10), 40-42.

Hudson, B. (2003e). "Discovering the Lost Aggregate Opportunity: Part 7," *Pit and Quarry*, 95(12), 42-43.

Hudson, B. (2003f). "Discovering the Lost Aggregate Opportunity: Part 8," *Pit and Quarry*, 96(1), 36-40.

Huo, X.S., Al-Omaishi, N., and Tadros, M.K. (2001). "Creep, Shrinkage, and Modulus of Elasticity of High Performance Concrete," *ACI Materials Journal*, 98(6), 440-449.

Hwang, C.-L., and Chen, Y.-Y. (2002). "The property of self-consolidating concrete designed by densified mixture design algorithm," *First North American Conference on the Design and Use of Self-Consolidating Concrete*, Chicago, IL: ACBM, 121-126.

Hwang, C.-L., and Tsai, C.-T. (2005). "The application of geometry concept to solve algebraic solution in DMDA method," *Second North American Conference on the Design and Use of Self-Consolidating Concrete*, Chicago, IL: ACBM.

Iravani, S. (1996). "Mechanical Properties of High-Strength Concrete," *ACI Materials Journal¸* 93(5), 1-11.

Irassar, E.F., Bonavetti, V.L., Trezza, M.A., and Gonzalez, M.A. (2005). "Thaumasite formation in limestone filler cements exposed to sodium sulphate solution at 20C," *Cement and Concrete Composites*, 27, 77-84.

Jamkar, S.S., and Rao, C.B.K. (2004). "Index of aggregate particle shape and texture of coarse aggregate as a parameter for concrete mix proportioning," *Cement and Concrete Research*, 34, 2021-2027.

JSCE (1999). "Recommendations for Self-Compacting Concrete," (Concrete Engineering Series 31). Japanese Society of Civil Engineers.

Jardine, L.A., Koyata, H., Folliard, K.J., Ou, C.-C., Jachimowicz, F., Chun, B.-W., Jeknavorian, A.A., and Hill, C.L. (2002). Admixture and method for optimizing addition of EO/PO superplasticizer to concrete containing smectite clay-containing aggregates, US Patent 6,352,952.

Jardine, L.A., Koyata, H., Folliard, K.J., Ou, C.-C., Jachimowicz, F., Chun, B.-W., Jeknavorian, A.A., and Hill, C.L. (2003). Admixture for optimizing addition of EO/PO plasticizers, US Patent 6,670,415.

Jeknavorian, A.A., Jardine, L., Ou, C.C., Koyata, H., and Folliard, K. (2003). "Interaction of Superplasticizers with Clay-Bearing Aggregates," *Seventh CANMET/ACI International Symposium on Superplasticizers and Other Chemical Admixtures in Concrete*, Malhotra, V.M, ed., 143-159.

Jensen, O.M., and Hansen, P.F. (2001). "Autogenous deformation and RH change in perspective," *Cement and Concrete Research*, 31(12), 1859-1865.

Johansen, V., and Andersen, P.J. (1991). "Particle Packing and Concrete Properties," *Materials Science of Concrete II*, Skalny, J., and Mindess, S., eds. Westerville, OH: American Ceramic Society, 111-147.

Jossic, L., and Magnin, A. (2001). "Drag and Stability of Objects in a Yield Stress Fluid," *AIChE Journal*, 47(12). 2666-2672.

Kadri, E.H., and Duval, R. (2002). "Effect of Ultrafine Particles on Heat of Hydration of Cement Mortars," *ACI Materials Journal*, 99(2), 138-142.

Kennedy, C.T. (1940). "The Design of Concrete Mixes," *Journal of the American Concrete Institute*, 36, 373-400.

Kennedy, T.W., Huber, G.A., Harrigan, E.T., Cominsky, R.J., Hughes, C.S., Quintus, H.V., and Moulthrop, J.S. (1994). "Superior Performing Asphalt Pavements (Superpave): The Production of the SHRP Asphalt Research Program," (Report SHRP-A-410). National Research Council, Washington, DC.

Khayat, K.H. (1995). "Effects of Antiwashout Admixtures on Fresh Concrete Properties," *ACI Materials Journal*, 92(2), 164-171.

Khayat, K.H. (1996). "Effects of Antiwashout Admixtures on Properties of Hardened Concrete," *ACI Materials Journal*, 93(2), 134-146.

Khayat, K.H. (1998a). "Viscosity-Enhancing Admixtures for Cement Based Materials," *Cement and Concrete Composites*, 20(2-3), 171-188.

Khayat, K.H. (1998b). "Use of Viscosity Modifying Admixture to Reduce Top Bar Effect of Anchor Bars Cast with Fluid Concrete," *ACI Materials Journal*, 95(2), 158-167.

Khayat, K.H. (1999). "Workability, Testing, and Performance of Self-Consolidating Concrete," *ACI Materials Journal*, 96(3), 346-354.

Khayat, K.H. (2000). "Optimization and Performance of Air Entrained Self-Consolidating Concrete," *ACI Materials Journal*, 97(5), 526-535.

Khayat, K.H., and Assaad, J. (2002). "Air Void Stability of Self-Consolidating Concrete," *ACI Materials Journal*, 99(4), 408-416.

Khayat, K.H., Assaad, J., and Daczko, J. (2004). "Comparison of Field-Oriented Test Methods to Assess Dynamic Stability of Self-Consolidating Concrete," *ACI Materials Journal*, 101(2), 168-176.

Khayat, K.H., and Ghezal, A. (2003). "Effect of viscosity-modifying admixture-superplasticizer combination on flow properties of SCC equivalent mortar," *3rd International Symposium on Self-Compacting Concrete*, Reykjavik, Iceland, 369-387.

Khayat, K.H., Ghezal, A., and Hadriche, M.S. (1999). "Utility of statistical models in proportioning self-consolidating concrete," *Proceedings of First International RILEM Symposium on Self-Compacting Concrete*, Stockholm, Sweden, 345-359.

Khayat, K.H., and Guizani, Z. (1997). "Use of Viscosity Modifying Admixture to Enhance Stability of Fluid Concrete," *ACI Materials Journal*, 94(4), 332-340.

Khayat, K.H., Hu, C., and Laye, L.M. (2002). "Importance of Aggregate Packing Density on Workability of Self-Consolidating Concrete," *First North American Conference on the Design and Use of Self-Consolidating Concrete*, Chicago, IL: ACBM, 53-62.

Khayat, K.H., Pavate, T.V., Assaad, J., and Jolicoeur, C. (2003). "Analysis of Variations in Electrical Conductivity to Assess Stability of Cement Based Materials," *ACI Materials Journal*, 100(4), 302-310.

Khayat, K.H., and Yahia, A. (1997). "Effect of Welan Gum-High Range Water Reducer Combinations on Rheology of Cement Grouts," *ACI Materials Journal*, 94(5), 365-372.

Kitano, T., Katakoa, T, and Shirato, T. (1981). "An empirical equation of the relative viscosity of polymer melts filled with various inorganic fillers," *Rheo Acta*, 20, 207-209.

Klug, Y., and Holschemacher, K. (2003). "Comparison of the hardened properties of self-compacting and normal vibrated concrete," *3rd International Symposium on Self-Compacting Concrete*, Reykjavik, Iceland, 596-605.

Koehler, E.P. (2004). "Development of a Portable Rheometer for Fresh Portland Cement Concrete," MS Thesis, The University of Texas at Austin.

Koehler, E.P., Foley, E., Rogers, G., Watanachet, S., Jung, M.J., and Fowler, D.W. (2007). "Mixture Proportioning, Testing, and Early-Age Engineering Properties of Self-Consolidating Concrete for Precast Structural Applications," (Report No. 0-5134-1). *Center for Transportation Research*, Austin, TX.

Kosmatka, S.H., Kerkhoff, B., and Panarese, W.C. (2002) *Design and Control of Concrete Mixtures*, 14th Edition, Portland Cement Associate, Skokie, IL, 372 pp.

Krieger, I.M., and Dougherty, T.J. (1959). "A Mechanism for Non-Newtonian Flow in Suspensions of Rigid Spheres," *Transactions of the Society of Rheology*, 137-152.

Kubo, M., Nakano, M., Aoki, H., Sugano, S., and Ouchi, M. (2001). "The quality control method of self-compacting concrete using testing apparatus for self-compactability evaluation," *Proceedings of the Second International Symposium on Self-Compacting Concrete*, Tokyo, Japan, 555-564.

Kuroiwa, S., Matsuoka, Y., Hayakawa, M., Shindoh, T. (1983). "Application of Super Workable Concrete to Construction of a 20-Story Building," In *SP-140: High Performance Concrete in Severe Environments*, P. Zia, Ed., Detroit, MI: American Concrete Institute, 147-161.

Kwan, A.K.H., Mora, C.F., and Chan, H.C. (1999). "Particle shape analysis of coarse aggregate using digital image processing," *Cement and Concrete Research*, 29, 1403-1410.

Lachemi, M., Hossain, K.M.A., Lambros, V., and Bouzoubaa, N. (2003). "Development of Cost Effective Self-Consolidating Concrete Incorporating Fly Ash, Slag Cement, or Viscosity-Modifying Admixtures," *ACI Materials Journal*, 100(5), 419-425.

Lachemi, M., Hossain, K.M.A., Lambros, V., Nkinamubanzi, P.-C., and Bouzoubaa, N. (2004a). "Performance of new viscosity enhancing admixtures in enhancing the rheological properties of cement paste," *Cement and Concrete Research*, 24, 917-926.

Lachemi, M. Hossain, K.M.A., Lambros, V., Nkinamubanzi, P.-C., and Bouzoubaa, N. (2004b). "Self-consolidating concrete incorporating new viscosity modifying admixtures," *Cement and Concrete Research*, 24, 917-926.

Lane, R.O. (1978). "Abrasion Resistance," *Significance of Tests and Properties of Concrete and Concrete Making Materials*, (STP 169B), Philadelphia: American Society for Testing and Materials, 332-350.

Leivo, M. (1990). "Rheological Modeling of the Compaction Properties of Concrete," H.-J. Wierig, Ed., *Properties of Fresh Concrete, Proc. of the Coll.* RILEM, Chapman and Hall, 277-285.

Li, C.-Z., Feng, N.Q., Li, Y-D., and Chen, R.-J. (2005). "Effects of polyethylene oxide side chains on the performance of polycarboxylate-type water reducers," *Cement and Concrete Research*, 35, 867-873.

Li, L.-S. and Hwang, C.-L. (2003) "The mixture proportion and property of SCC," *3rd International Symposium on Self-Compacting Concrete*, Reykjavik, Iceland, 525-529.

Li, H., Wee, T.H., and Wong, S.F. (2002). "Early-Age Creep and Shrinkage of Blended Cement Concrete," *ACI Materials Journal*, 99(1), 3-10.

Liu, T.C. (1981). "Abrasion Resistance of Concrete," *ACI Materials Journal*, 78(5), 341-350.

Lowke, D., Wiegrink, K.-H., and Schiessl, P. (2003). "A simple and significant segregation test for SCC," *3rd International Symposium on Self-Compacting Concrete*, Reykjavik, Iceland, 356-366.

Macphee, D., and Diamond, S. (2003). "Thaumasite in cementitious materials," *Cement and Concrete Composites*, 25, 805-807.

Malhotra, V.M., and Carette, G.G. (1985). "Performance of Concrete Incorporating Limestone Dust as Partial Replacement for Sand," *ACI Materials Journal*, 82(3), 363-371.

Mansfield, M.L., Douglas, J.F., and Garbozci, E.J. (2001). "Intrinsic viscosity and the electrical polarizability of arbitrarily shaped objects," *Physical Review E*, 64(6), 061401-16.

Martin, D.J. (2002). "Economic impact of SCC in precast applications," *First North American Conference on the Design and Use of Self-Consolidating Concrete*, Chicago, IL: ACBM.

Martys, N.S. (2005). "Study of a dissipative particle dynamics based approach for modeling suspensions," *Journal of Rheology*, 49(2), 401-424.

Marquardt, I., Diederichs, U., and Vala, J. (2002). "Determination of the optimum water content of SCC mixes," *First North American Conference on the Design and Use of Self-Consolidating Concrete*, Chicago, IL: ACBM, 85-92.

Marquardt, I., Vala, J., and Diederichs, U. (2001). "Optimization of self-compacting concrete mixes," *Proceedings of the Second International Symposium on Self-Compacting Concrete*, Tokyo, Japan, 295-302.

Mehta, P.K., and Monteiro, P.J.M. (1993). *Concrete: Structure, Properties and Materials*, Englewood Cliffs, NJ; Prentice Hall, 548 pp.

Midorikawa, T., Pelova, G.I., and Walraven, J.C. (2001). "Application of 'the water layer model' to self-compacting mortar with different size distribution of fine aggregate," *Proceedings of the Second International Symposium on Self-Compacting Concrete*, Tokyo, Japan, 237-246.

Mokhtarzadeh, A., and French, C. (2000). "Mechanical Properties of High-Strength Concrete with Consideration for Precast Applications," *ACI Materials Journal*, 97(2), 136-148.

Mooney, M.J. (1951). "The viscosity of a concentrated suspension of spherical particles," *Journal of Colloid Science*, 6(2), 162-170.

Mora, C.F., Kwan, A.K.H., and Chan, H.C. (1998). "Particle size distribution analysis of coarse aggregate using digital image processing," *Cement and Concrete Research*, 28(6), 921-932.

Mora, C.F., and Kwan, A.K.H. (2000). "Sphericity, shape factor, and convexity measurement of coarse aggregate for concrete using digital image processing," *Cement and Concrete Research*, 30, 351-358.

Mork, J.H. (1996). "A Presentation of the BML Viscometer," P.J.M. Bartos, C.L. Marrs, and D.J. Cleland, Eds., *Production Methods and Workability of Concrete, Proc. of the Conf.* RILEM, E&FN Spon, 369-376.

Mortsell, E., Maage, M., and Smeplass, S. (1996). "A particle-matrix model for prediction of workability of concrete," P.J.M. Bartos, C.L. Marrs, and D.J. Cleland, Eds., *Production Methods and Workability of Concrete, Proc. of the Conf.* RILEM, E&FN Spon, 429-438.

Naito, C., Brunn, G., Parent, G., and Tate, T. (2005). "Comparative Performance of High Early Strength and Self-Consolidating Concrete for Use in Precast Bridge Beam Construction," ATLSS Report 05-03. Lehigh University, Bethlemen, PA.

National Coal Council. (2005). "Opportunities to Expedite the Construction of New Coal-Based Power Plants,"

Nehdi, M., Mindess, S., and Aitcin, P.-C. (1998). "Rheology of high-performance concrete: effect of ultrafine particles," *Cement and Concrete Research*, 28(5), 687-697.

Nehdi, M., El Chabib, H., and El Naggar, M.H. (2001). "Predicting Performance of Self-Compacting Concrete Mixtures Using Artificial Neural Networks," *ACI Materials Journal*, 98(5), 394-401.

Neubauer, C.M., Jennings, H.M., and Garboczi, E.J. (1996). "A three-phase model of the Elastic and Shrinkage Properties of Mortar," *Advanced Cement Based Materials*, 4, 6-20.

Neville, A.M. (1997). "Aggregate Bond and Modulus of Elasticity of Concrete," *ACI Materials Journal*, 94(1), 71-74.

Nielsson, I., and Wallevik, O.H. (2003). "Rheological evaluation of some empirical test methods-preliminary results," *3rd International Symposium on Self-Compacting Concrete*, Reykjavik, Iceland, 59-68.

Nilsen, A.U., and Monteiro, P.J.M. (1993). "Concrete: A three phase material," *Cement and Concrete Research*, 23(1), 147-151.

Nguyen, T.L.H., Roussel, N., Coussot, P. (2006). "Correlation between L-box test and rheological parameters of a homogenous yield stress fluid," *Cement and Concrete Research*, 36, 1789-1796.

Obla, K.H., Hill, R.H., Thomas, M.D.A., Shashiprakash, S.G., and Perebatova, O. (2003). "Properties of Concrete Containing Ultra-Fine Fly Ash," *ACI Materials Journal*, 100(5), 426-433.

Oh, S.G., Noguchi, T., Tomosawa, F. (1999). "Toward mix design for rheology of self-compacting concrete," *Proceedings of the First International RILEM Symposium on Self-Compacting Concrete*, Stockholm, Sweden, 361-372.

Ohno, A., Edamatu, Y., Sugamata, T., and Ouchi, M. (2001). "The mechanism of time dependence for fluidity of high belite cement mortar containing polycarboxylate-based superplasticizer," *Proceedings of the Second International Symposium on Self-Compacting Concrete*, Tokyo, Japan, 169-178.

Okamura, H., and Ouchi, M. (1999). "Self-compacting concrete. Development, present use, and future," *Proceedings of the First International RILEM Symposium on Self-Compacting Concrete*, Stockholm, Sweden, 3-14.

Okamura, H., and Ouchi, M. (2003). "Self-Compacting Concrete," *Journal of Advanced Concrete Technology*, 1(1), 5-15.

Okamura, H., and Ozawa, K. (1995). "Mix Design for Self-Compacting Concrete," *Concrete Library of JSCE*, 25, 107-120.

Oluokun, F.A., Burdette, E.G., and Deatherage, J.H. (1991). "Elastic Modulus, Poisson's Ratio, and Compressive Strength Relationships at Early Ages," *ACI Materials Journal*, 88(1), 3-10.

Ouchi, M. (1999). "Self-Compacting Concrete: Development, Applications, and Investigations," *Nordic Concrete Research*, Publication 23.

Ouchi, M., Hibino, M., and Okamura, H. (1997). "Effect of Superplasticizer on Self-Compactability of Fresh Concrete," *Transportation Research Record 1574*, 37-40.

Ozol, M.A. (1978). "Shape, Surface Texture, Surface Area, and Coatings," *Significance of Tests and Properties of Concrete and Concrete Making Materials*, (STP 169B), Philadelphia: American Society for Testing and Materials, 573-628.

Ozyildirim, C. (2005). "The Virginia Department of Transportation's Early Experience With Self-Consolidating Concrete," *Proceedings of the Transportation Research Board Annual Meeting*.

Park, C.K., Noh, M.H., and Park, T.H. (2005). "Rheological properties of cementitious materials containing mineral admixtures," *Cement and Concrete Research*, 35, 842-849.

Patel, R., Hossain, K.M.A., Shehata, M., Bouzoubaa, N., and Lachemi, M. (2004). "Development of Statistical Models for Mixture Design of High-Volume Fly Ash Self-Consolidating Concrete," *ACI Materials Journal*, 101(4), 294-302.

Pauw, A. (1960). "Static Modulus of Elasticity as Affected by Density," *Journal of the American Concrete Institute*, 32(6), 679-687.

PCI (2003). *Interim Guidelines for the Use of Self-Consolidating Concrete in Precast/Prestressed Concrete Institute Member Plants*, (TR-6-03). Chicago, IL: Precast/Prestressed Concrete Institute.

Pedersen, B., and Mortsell, E. (2001). "Characterization of fillers for SCC," *Proceedings of the Second International Symposium on Self-Compacting Concrete*, Tokyo, Japan, 257-266.

Pera, J., Husson, S. and Guilhot, B. (1999). "Influence of finely ground limestone on cement hydration," *Cement and Concrete Composites*, 21, 99-105.

Persson, B. (2001). "A comparison between mechanical properties of self-compacting concrete and the corresponding properties of normal concrete," *Cement and Concrete Research*, 31, 193-198.

Persson, B. (2003). "Internal frost resistance and salt frost scaling of self-compacting concrete," *Cement and Concrete Research*, 33, 373-379.

Petersen, B.G., and Reknes, K. (2003). "Properties of the concrete matrix of self-compacting concrete with lignosulphonate superplasticizer," *3rd International Symposium on Self-Compacting Concrete*, Reykjavik, Iceland, 395-402.

Petersson, O., Gibbs, J., and Bartos, P. (2003). "Testing-SCC: A European project," *3rd International Symposium on Self-Compacting Concrete*, Reykjavik, Iceland, 299-304.

Petrou, M.F., Wan, B., Gadala-Maria, F., Kolli, V.G., and Harries, K.A. (2000). "Influence of Mortar Rheology on Aggregate Settlement," *ACI Materials Journal*, 97(4), 479-485.

Phyffereon, A., Monty, H., Skaggs, B., Sakata, N., Yanai, S., and Yoshizaki, M. (2002). "Evaluation of the biopolymer, diutan gum, for use in self-compacting concrete," *First North American Conference on the Design and Use of Self-Consolidating Concrete*, Chicago, IL: ACBM, 147-152.

Plank, J., and Hirsch, C. (2003). "Superplasticizer Adsorption on Synthetic Ettringite," *Seventh CANMET/ACI International Symposium on Superplasticizers and Other Chemical Admixtures in Concrete*, Malhotra, V.M, ed., 283-297.

Popovics, S., and Erdey, M. (1970). "Estimate of the Modulus of Elasticity of Concrete-Like Composite Materials," *Materials and Structures*, 3(16), 253-260.

Pons, M.N., Vivier, H., Belaroui, K., Bernard-Michel, B., Cordier, F., Oulhana, D., and Dodds, J.A. (1999). "Particle morphology: from visualization to measurement," *Powder Technology*, 103, 44-57.

Powers, T.C. (1932). "Studies of Workability of Concrete," *Proceedings*, American Concrete Institute, Detroit, 28, 419-488.

Powers, T.C. (1968). *Properties of Fresh Concrete*, New York: John Wiley & Sons, 664 pp.

Quiroga, P.N. (2003). "The Effect of Aggregate Characteristics on the Performance of Portland Cement Concrete," Ph.D. Dissertation, University of Texas at Austin.

Rahman, A.M., and Nehdi, M. (2003). "Effect of Geometry, Gap, and Surface Friction of Test Accessory on Measured Rheological Properties of Cement Paste," *ACI Materials Journal*, 100(4), 331-339.

Reknes, K. (2001). "Particle-matrix model based design of self-compacting concrete with lignosulfonate water reducer," *Proceedings of the Second International Symposium on Self-Compacting Concrete*, Tokyo, Japan, 247-256.

Rols, S., Ambroise, J., and Pera, J. (1999). "Effects of different viscosity agents on the properties of self-compacting concrete," *Cement and Concrete Research*, 29, 261-266.

Roscoe, R. (1952). "The viscosity of suspensions of rigid spheres," *British Journal of Applied Physics*, 3, 267-269.

Roshavelov, T.T. (1999). "Concrete Mixture Proportioning with Optimal Dry Packing," *Proceedings of the First International RILEM Symposium on Self-Compacting Concrete*, Stockholm, Sweden, 385-396.

Roshavelov, T.T. (2002). Concrete mixture proportioning based on rheological approach," *First North American Conference on the Design and Use of Self-Consolidating Concrete*, Chicago, IL: ACBM, 113-119.

Roshavelov, T.T. (2005). "Prediction of fresh concrete behavior based on analytical model for mixture proportioning," *Cement and Concrete Research*, 35, 831-835.

Roussel, N., and Le Roy, R. (2005). "The Marsh cone: a test or rheological apparatus?" *Cement and Concrete Research*, 35, 823-830.

Roussel, N., Stefani, C., and Leroy, R. (2005). "From mini-cone test to Abrams cone test: measurement of cement-based materials yield stress using slump tests," *Cement and Concrete Research*, 35, 817-822.

Roziere, E., Turcry, P., Loukili, A., and Cussigh, F. (2005). "Influence of paste volume, addition content and addition type on shrinkage cracking of self-compacting concrete," *Proceedings of SCC 2005*, ACBM, Chicago, IL.

Saak, A.W. (2000). "Characterizing and Modeling of the Rheology of Cement Paste: With Applications to Self-Flowing Materials," PhD Dissertation, Northwestern University, Evanston, IL.

Saak, A.W., Jennings, H.M., and Shah, S.P. (2001). "New Methodology for Designing Self-Compacting Concrete," *ACI Materials Journal*, 98(6), 429-439.

Sahu, S., Badger, S., and Thaulow, N. (2003). "Mechanism of thaumasite formation in concrete slabs on grade in Southern California," *Cement and Concrete Composites*, 25, 889-897.

Sakai, E., Yamada, K., and Ohta, A. (2003). "Molecular Structure and Dispersion-Adsorption Mechanisms of Comb-Type Superplasticizers Used in Japan," *Journal of Advanced Concrete Technology*, 1(1), 16-25.

Sakata, N., Maruyama, K., and Minami, M. (1996). "Basic properties and effects of welan gum on self-consolidating concrete," *Production Methods and Workability of Concrete*, *Proc. of the Conf.* RILEM, E&FN Spon.

Santhanam, M., Cohen, M.D., and Olek, J. (2001). "Sulfate attack research—whither now?" *Cement and Concrete Research*, 31, 845-851.

Schindler, A.K., Barnes, R.W., Roberts, J.B., and Rodriguez, S. (2007). "Properties of Self-Consolidating Concrete for Prestressed Members," *ACI Materials Journal*, 104(1), 53-61.

Schober, I., and Mader, U. (2003). "Compatibility of Polycarboxylate Superplasticizers with Cements and Cementitious Blends," *Seventh CANMET/ACI International Symposium on Superplasticizers and Other Chemical Admixtures in Concrete*, Malhotra, V.M, ed., 453-468.

Schramm, G. (1994). *A Practical Approach to Rheology and Rheometry*. Karlsruhe, Germany: Haake Rheometers.

Schwartzentruber, A., and Catherine, C. (2000). "Method of the concrete equivalent mortar (CEM) – a new tool to design concrete containing admixture," [in French] *Materials and Structures*, 33(232), 475-482.

Sedran, T., and de Larrard, F. (1999). "Optimization of self-compacting concrete thanks to packing model," *Proceedings of the First International RILEM Symposium on Self-Compacting Concrete*, Stockholm, Sweden, 321-332.

Sedran, T., de Larrard, F., Hourst, F., and Contamines, C. (1996). "Mix design of self-compacting concrete (SCC)," *Proceedings of the Second International Symposium on Self-Compacting Concrete*, Tokyo, Japan, 439-450.

Shadle, R., and Somerville, S. (2002). "The Benefits of Utilizing Fly Ash in Producing Self-Compacting Concrete," *First North American Conference on the Design and Use of Self-Consolidating Concrete*, Chicago, IL: ACBM, 235-241.

Shah, S.P., and Ahmad, S.H. (1985). "Structural Properties of High Strength Concrete and Its Implications for Precast Prestressed Concrete," *Journal of the Prestressed Concrete Institute*, 30(6), 92-119.

Shen, L., Struble, L., and Lange, D. (2005). "Testing static segregation of SCC," *Proceedings of SCC 2005*, ACBM, Chicago, IL.

Shilstone, J.M. (1990). "Concrete Mixture Optimization," *Concrete International*, 12(6), 33-39.

Shilstone, J.M., and Shilstone, J.M. (2002). "Performance-Based Concrete Mixtures and Specifications for Today," *Concrete International*, 24(2), 80-83.

Smeplass, S., and Mortsell, E. (2001). "The particle matrix model applied on SCC" *Proceedings of the Second International Symposium on Self-Compacting Concrete*, Tokyo, Japan, 267-276.

Sonebi, M., Bahadori-Jahromi, A., Bartos, P.J.M. (2003). "Development and optimization of medium strength self-compacting concrete by using pulverized fly ash," *3rd International Symposium on Self-Compacting Concrete*, Reykjavik, Iceland, 514-524.

Sonebi, M. (2004a). "Applications of Statistical Models in Proportioning Medium Strength Self-Consolidating Concrete," *ACI Materials Journal*, 101(5), 339-346.

Sonebi, M. (2004b). "Medium strength self-compacting concrete containing fly ash: Modeling using statistical factorial plans," *Cement and Concrete Research*, 34, 1199-1208.

Stark, D. (2003). "Occurrence of thaumasite in deteriorated concrete," *Cement and Concrete Composites*, 25, 1119-1121.

Stewart, J.G., Norvell, J.K., Juenger, M.C.G., and Fowler, D.W. (2006). "Characterizing Minus No. 200 Fine Aggregate for Performance in Concrete," (ICAR Report 107-1), International Center for Aggregates Research, Austin, TX.

Struble, L., and Sun, G.-K. (1995). "Viscosity of Portland Cement Paste as a Function of Concentration," *Advanced Cement Based Materials*, 2, 62-69.

Struble, L., Szecsy, R., Lei, W.-G., and Sun, G.-K. (1998). "Rheology of Cement Paste and Concrete," *Cement, Concrete, and Aggregates*, 20(2), 269-277.

Su, N., Hus, K.-C., and Chai, H.W. (2001). "A simple mix design method for self-compacting concrete," *Cement and Concrete Research*, 31, 1799-1807.

Su, J.K., Cho, S.W., Yang, C.C., and Huang, R. (2002). "Effect of Sand Ratio on the Elastic Modulus of Self-Compacting Concrete," *Journal of Marine Science and Technology*, 10(1), 8-13.

Suksawang, N., Nassif, H.H., and Najim, H.S. (2005). "Durability of self compacting concrete (SCC) with pozzolanic materials," *Proceedings of SCC 2005*, ACBM, Chicago, IL.

Sugamata, T., Sugiyama, T., and Ohta, A. (2003). "The Effects of a New High-Range Water-Reducing Agent on the Improvement of Rheological Properties," *Seventh CANMET/ACI International Symposium on Superplasticizers and Other Chemical Admixtures in Concrete*, Malhotra, V.M, ed., 343-359.

Svermova, L., Sonebi, M., and Bartos, P.J.M. (2003). "Influence of mix proportions on rheology of cement grouts containing limestone powder," *Cement and Concrete Composites*, 25, 737-749.

Szecsy, R.S. (1997). *Concrete Rheology*, Ph.D. Dissertation, University of Illinois, Champaign-Urbana.

Szecsy, R.S. (2005). "Integration and Application of Self-Compacting Concrete as a Technology into Other Types of Performance Concrete," *Proceedings of SCC 2005*, ACBM, Chicago, IL.

Takada, K., and Walraven, J. (2001). "Influence of mixing efficiency on the properties of flowable cement pastes," *Proceedings of the Second International Symposium on Self-Compacting Concrete*, Tokyo, Japan, 545-554.

Tanaka, K., Sato, K., Watanabe, S., Arima, I., and Suenaga, K. (1993). "Development and Utilization of High Performance Concrete for the Construction of the Akashi Kaikyo Bridge," In *SP-140: High Performance Concrete in Severe Environments*, P. Zia, Ed., Detroit, MI: American Concrete Institute, 147-161.

Tang, C., Yen, T., Chang, C., and Chen, K. (2001). "Optimizing Mixture Proportions for Flowable High Performance Concrete Via Rheology Tests," *ACI Materials Journal*, 98(6), 493-502.

Tattersall, G.H. (1990). "Progress in Measurement of Workability by the Two-Point Test," H.-J. Wierig, Ed., *Properties of Fresh Concrete, Proc of the Coll*. RILEM, Chapman and Hall, 203-212.

Tattersall, G.H. (1991). *Workability and Quality Control of Concrete*. London: E&FN Spon.

Tattersall, G.H., and Bloomer, S.J. (1979). "Further development of the two-point test for workability and extension of its range," *Magazine of Concrete Research*, 31(109), 202-210.

Taylor, M. (2002). "Quantitative measures for shape and size of particles," *Powder Technology*, 124, 94-100.

Tazawa, E., and Miyazawa, S. (1995a). "Experimental study on mechanism of autogenous shrinkage of concrete," *Cement and Concrete Research*, 25(8), 1633-1638.

Tazawa, E., and Miyazawa, S. (1995b). "Influence of cement and admixture on autogenous shrinkage of cement paste," *Cement and Concrete Research*, 25(2), 281-287.

Testing-SCC (2005). "Measurement of properties of fresh self-compacting concrete," Final Report (http://www.civeng.ucl.ac.uk/research/concrete/Testing-SCC/).

Thomas, M.D.A., Rogers, C.A., and Bleszynski, R.F. (2003). "Occurrences of thaumasite in laboratory and field concrete," *Cement and Concrete Composites*, 25, 1045-1050.

Tolppanen, P., Illerstrom, A., and Stephansson, O. (1999). "3-D laser analysis of size, shape and roughness of railway ballast: Research in progress," Proceedings of the Seventh Annual ICAR Symposium, Austin, TX.

Toussaint, F., Juge, C., Laye, J.M., and Pellerin, B. (2001). "Assessment of thixotropic behavior of self-compacting microconcrete," *Proceedings of the Second International Symposium on Self-Compacting Concrete*, Tokyo, Japan, 89-98.

Tragardh, J. (1999). "Microstructural features and related properties of self-compacting concrete," *Proceedings of the First International RILEM Symposium on Self-Compacting Concrete*, Stockholm, Sweden, 175-186.

Tsai, S.C., Botts, D., and Plouff, J. (1992). "Effects of particle properties on the rheology of concentrated noncolloidal suspensions," *Journal of Rheology*, 36(7), 1291-1305.

Tsivilis, S., Chaniotaksi, E., Badogiannis, E., Pahoulas, G., and Ilias, A. (1999). "A study on the parameters affecting the properties of portland limestone cements," *Cement and Concrete Composites*, 21, 107-136.

Turcry, P, and Loukili, A. (2003). "A study of plastic shrinkage of self-compacting concrete," *Third International Symposium on Self-Consolidating Concrete*, Reykjavik, Iceland, 576-585.

Turcry, P., Loukili, A., and Haidar, K., (2002). "Mechanical properties, plastic shrinkage, and free deformations of self-consolidating concrete," *First North American Conference on the Design and Use of Self-Consolidating Concrete*, Chicago, IL: ACBM, 335-340.

Uhlherr, P.H.T., Gou, J., Fang, T.-N., and Tiu, C. (2002) "Static measurement of yield stress using a cylinder penetrometer," *Korea-Australia Rheology Journal*, 14(1), 17-23.

U.S. Department of Energy (2001). "Advanced NO_x Control Technology for Coal-Fired Power Plants," National Energy Technology Program.

Utsi, S. Emborg, M., and Carsward, J. (2003). "Relation between workability parameters and rheological parameters," *3rd International Symposium on Self-Compacting Concrete*, Reykjavik, Iceland, 154-164.

Vachon, M., Kaplan, D., and Fellaki, A. (2002). "A SCC Application with Eccentric Sand," *First North American Conference on the Design and Use of Self-Consolidating Concrete*, Chicago, IL: ACBM, 469-474.

Velten, U., Schober, I., Sulser, U., and Mader, U. (2001). "Blends of polycarboxylate-type superplasticizers in use for concrete admixtures," *Proceedings of the Second International Symposium on Self-Compacting Concrete*, Tokyo, Japan, 187-194.

Vieira, M., and Bettencourt, A. (2003). "Deformability of hardened SCC," *3rd International Symposium on Self-Compacting Concrete*, Reykjavik, Iceland, 637-644.

Vikan, H., and Justnes, H. (2003). "Influence of silica fume on rheology of cement paste," *3rd International Symposium on Self-Compacting Concrete*, Reykjavik, Iceland, 190-201.

Vikan, H., Justnes, H., and Winnefeld, F. (2005). "The importance of cement type on flow resistance of cement paste," *Second North American Conference on the Design and Use of Self-Consolidating Concrete*, Chicago, IL: ACBM.

Wallevik, J.E. (2003). "Computation rheology thixotropic explorations of cement pastes; an introduction," *Third International Symposium on Self-Consolidating Concrete*, Reykjavik, Iceland, 41-48.

Watanabe, T., Nakajima, Y., Ouchi, M., and Yamamoto, K. (2003). "Improvement of the automatic testing apparatus for self-compacting concrete," *3rd International Symposium on Self-Compacting Concrete*, Reykjavik, Iceland, 895-903.

Whorlow, R.W. (1992). *Rheological Techniques*. Chicheser, West Sussex, England: Ellis Horwood Limited.

Xie, Y., Liu, B., Yin, J., and Zhou, S. (2002). "Optimum mix parameters of high-strength self-compacting concrete with ultrapulverized fly ash," *Cement and Concrete Research*, 32, 477-480.

Yahia, A., Tanimura, M., Shimabukuro, A., and Shimoyama, Y. (1999). "Effect of rheological parameters on self-compactability of concrete containing various mineral admixture," *Proceedings of the First International RILEM Symposium on Self-Compacting Concrete*, Stockholm, Sweden, 523-535.

Yahia, A., Tanimura, M., and Shimoyama, Y. (2005). "Rheological properties of highly flowable mortar containing limestone filler-effect of powder content and w/c ratio," *Cement and Concrete Research*, 35, 532-539.

Yamada, K., Takahashi, T., Hanehara, S., and Matsuhisa, M. (2000). Effects of the chemical structure on the properties of polycarboxylate-type superplasticizer," *Cement and Concrete Research*, 30, 197-207.

Yamada, K., Yanagisawa, T., and Hanehara, S. (1999). "Influence of Temperature on the dispersibility of polycarboxylate type superplasticizer for highly fluid concrete," *Proceedings of the First International RILEM Symposium on Self-Compacting Concrete*, Stockholm, Sweden, 437-448.

Yamada, K., Ogawa, S., and Takahashi, T. (2001). "Improvement of the compatibility between cement and superplasticizer by optimizing the chemical structure of the polycarboxylate-type superplasticizer," *Proceedings of the Second International Symposium on Self-Compacting Concrete*, Tokyo, Japan, 159-168.

Yen, T., Tang, C., Chang, C., and Chen, K. (1999). "Flow behavior of high strength high-performance concrete," *Cement and Concrete Composites*, 21(5), 413-424.

Yool, A.I.G., Lees, T.P., and Fried, A. (1998). "Improvements to the methylene blue dye test for harmful clays in aggregates for concrete and mortar," *Cement and Concrete Research*, 28(10), 1417-1428.

Yoshioka, K., Tazawa, E., Kawai, K., and Enohata, T. (2002). "Adsorption characteristics of superplasticizers on cement component minerals," *Cement and Concrete Research*, 32, 1507-1513.

Zhang, M.H., Tam, C.T., Leow, M.P. (2003). "Effect of water-to-cementitious materials ratio and silica fume on the autogenous shrinkage of concrete," *Cement and Concrete Research*, 33(10), 1687-1694.

Zhou, F.P., Lydon, F.D., and Barr, B.I.G. (1995). "Effect of Coarse Aggregate on Elastic Modulus and Compressive Strength of High Performance Concrete," *Cement and Concrete Research*, 25(1), 177-186.

Zhu, W., and Gibbs, J.C. (2005). "Use of different limestone and chalk powders in self-compacting concrete," *Cement and Concrete Research*, 35, 1457-1462.

Zhu, W., Quinn, J, and Bartos, P.J.M. (2001). "Transport properties and durability of self-compacting concrete," *Proceedings of the Second International Symposium on Self-Compacting Concrete*, Tokyo, Japan, 451-458.

Vita

Eric Koehler was born on April 3, 1981, in Charlotte, NC, to Roger and Susan Koehler. He graduated high school from Charlotte Christian School in 1999. He then attended Clemson University, where he graduated *summa cum laude* in 2002 with a Bachelor of Science degree in Civil Engineering. He then entered the University of Texas at Austin, where he received his Master of Science degree in Civil Engineering in 2004 and subsequently began his studies towards a Doctor of Philosophy degree.

Permanent address: 6309 Royal Aberdeen Court, Charlotte, NC 28277

This dissertation was typed by the author.